

Homogeneous Catalysis—II

Homogeneous Catalysis—II

Denis Forster and James F. Roth,
Editors

A symposium co-sponsored
by the Division of Industrial
and Engineering Chemistry
and the Division of
Petroleum Chemistry at the
166th Meeting of the
American Chemical Society,
Chicago, Ill.,
Aug. 27–29, 1973.

Library
American Chemical Society

ADVANCES IN CHEMISTRY SERIES

132

AMERICAN CHEMICAL SOCIETY
WASHINGTON, D. C. 1974



Library of Congress CIP Data

Homogeneous catalysis—II

(Advances in chemistry series, 132)

"A symposium co-sponsored by the Division of Industrial and Engineering Chemistry and the Division of Petroleum Chemistry at the 166th meeting of the American Chemical Society, Chicago, Ill., Aug. 27-29, 1973."

Includes bibliographical references.

1. Catalysis—Congresses.

I. Forster, Denis, 1941- ed. II. Roth, James Frank, 1925- ed. III. American Chemical Society. Division of Industrial and Engineering Chemistry. IV. American Chemical Society. Division of Petroleum Chemistry. V. Title.

QD1.A355 No. 132 [QD505] 540'.8 [541'.395]

74-14896

ISBN 0-8412-0201-X ADCSAJ 132 1-331 (1974)

Copyright © 1974

American Chemical Society

All Rights Reserved

PRINTED IN THE UNITED STATES OF AMERICA

American Chemical Society
Library
1155 16th St., N.W.
Washington, D.C. 20036

In Homogeneous Catalysis—II; Forster, D., et al.;
Advances in Chemistry; American Chemical Society: Washington, DC, 1974.

Advances in Chemistry Series

Robert F. Gould, *Editor*

Advisory Board

Kenneth B. Bischoff

Bernard D. Blaustein

Ellis K. Fields

Edith M. Flanigen

Jesse C. H. Hwa

Phillip C. Kearney

Egon Matijević

Thomas J. Murphy

Robert W. Parry

FOREWORD

ADVANCES IN CHEMISTRY SERIES was founded in 1949 by the American Chemical Society as an outlet for symposia and collections of data in special areas of topical interest that could not be accommodated in the Society's journals. It provides a medium for symposia that would otherwise be fragmented, their papers distributed among several journals or not published at all. Papers are refereed critically according to ACS editorial standards and receive the careful attention and processing characteristic of ACS publications. Papers published in ADVANCES IN CHEMISTRY SERIES are original contributions not published elsewhere in whole or major part and include reports of research as well as reviews since symposia may embrace both types of presentation.

Homogeneous Catalysis—II
ADVANCES IN CHEMISTRY
SERIES No. 132

Errata

The illustrations on pages 159 through 163 do not bear the correct legends. The legend on page 159 goes with the illustration on page 160, the legend on page 160 goes with the illustration on page 161, the legend on page 161 goes with the illustration on page 162, the legend on page 162 goes with the illustration on page 163, and the legend on page 163 goes with the illustration on page 159.

**American Chemical Society
Library**

**1155 16th St., N.W.
Washington, D.C. 20036**

In Homogeneous Catalysis—II; Forster, D., et al.;
Advances in Chemistry; American Chemical Society: Washington, DC, 1974.

PREFACE

The six years since the first ADVANCES IN CHEMISTRY SERIES volume, "Homogeneous Catalysis—Industrial Applications and Implications," (Number 70) have been a period of mushrooming activity in the field. Not only has this activity been marked by the discovery of new types of catalysts and new insights into reaction mechanisms, but several major commercial processes based on homogeneous catalysts have been developed.

The papers in this volume concern results observed in catalytic systems. They span a broad range of catalytic reactions including hydroformylation, hydrocarboxylation, hydrogenation, carbonylation, cyanation, and olefin oxidation. To some extent, the results provide a significant extension of our understanding of previously studied catalysts and catalytic reactions. However, some of the papers are concerned with newer areas of research and feature results of both scientific and potential industrial importance.

Thus transition metal complexes capable of effecting cyanation reactions on aromatic nuclei under mild conditions have been discovered; Cassar *et al.* describe such a catalytic system. The past few years have also seen the discovery of asymmetric catalysis. Asymmetric catalysts contain optically active ligands and, like enzymes, can promote catalytic reactions during which substantial levels of optical activity are introduced into the products. This volume contains examples of asymmetric hydrogenation and asymmetric hydroformylation catalysis in the papers, respectively, by Knowles *et al.* and Pino *et al.*

Finally, there has been intense interest and activity recently in a new area that has sometimes been described as the heterogenization of homogeneous catalysts. Work in this area has generally been directed toward preparing and using various types of solid metal complex catalysts. These consist either of conventional complexes dispersed on porous solid supports or of complexes in which the ligand itself is a solid polymeric moiety. This volume contains several contributions in this area. Candlin and Thomas describe catalysts in which the metal complexes are attached to an inorganic polymer (*e.g.*, metal oxide), and Jurewicz *et al.* form their complexes with organic polymeric ligands. In many cases similar results are obtained with analogous metal complexes in heterogeneous or homogeneous systems. This suggests that the term homogeneous catalysis

which has traditionally been used to describe catalysis by metal complexes is too restrictive and that we need to adopt a more general term for this area of catalysis such as metal complex catalysis.

The interest and activity in metal complex catalysis will continue to be marked by further advances in asymmetric catalysis and catalysis by solid metal complexes as well as in the discovery of new complexes capable of catalytically activating molecules such as hydrocarbons, nitrogen, oxygen, and carbon dioxide in a manner that permits new uses for these abundant materials.

DENIS FORSTER
JAMES F. ROTH

St. Louis, Missouri
March 1974

Some Effects of the Olefinic Structure on the Orientation of the Hydroformylation Reaction

RICHARD LAÏ and EUGENE UCCIANI

Laboratoire de Chimie Organique Appliquée, Université de Provence, 13331 Marseille Cedex 3, France

*The behavior of α,β -unsaturated esters ($-\overset{\text{O}}{\underset{\text{O}}{\text{C}}}=\overset{\text{O}}{\underset{\text{O}}{\text{C}}}-\text{COOR}$) and of alkenylbenzenes ($-\overset{\text{O}}{\underset{\text{O}}{\text{C}}}=\overset{\text{O}}{\underset{\text{O}}{\text{C}}}-\text{C}_6\text{H}_5$) has been studied under hydroformylation conditions with $\text{Co}_2(\text{CO})_8$ and $\text{Rh}/\text{Al}_2\text{O}_3$ as catalysts. The results show that the formation of either aldehydes or saturated products as well as the distribution of isomeric aldehydes depend on: (1) the presence of $-\text{COOR}$ and C_6H_5- groups, (2) the location of the substituents on the double bond, and (3) the nature of catalytic precursors. Furthermore, in rhodium catalysis, the geometry of the double bond in olefinic stereoisomers affects the aldehyde distribution; this allowed us to establish the *cis* character of the addition.*

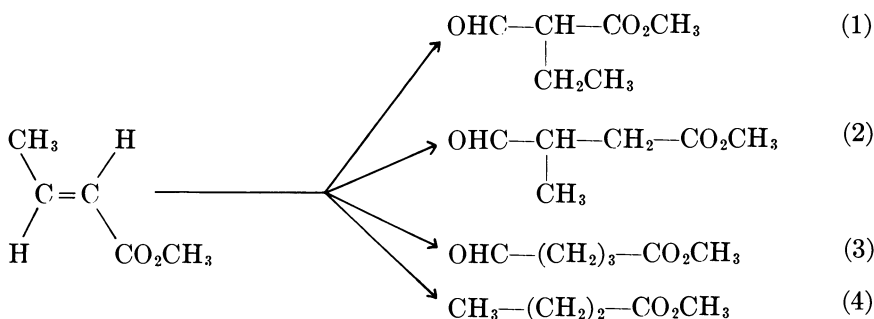
We have studied the hydroformylation reaction using α,β -unsaturated esters and alkenylbenzenes. Our purpose was first to use the oxo process as a synthetic method and then to quantify some phenomena we had observed with these unsaturated compounds. The selectivity of the reaction depends both on the structure of the olefin and on the catalytic precursor (Rh or Co). Rhodium- and cobaltcarbonyls give different results as far as the distribution of isomeric aldehydes and the hydroformylation of conjugated dienes are concerned (1, 2, 3). However few attempts have been made to compare the properties of these two transition metals to explain their different behavior except for Falbe on the hydroformylation of methyl cinnamate and methyl methacrylate (4, 5).

Only a few examples of alkenylbenzene hydroformylation are available. Styrene and α -methylstyrene were reported to lead to hydrogenation as the main reaction when $\text{Co}_2(\text{CO})_8$ was used.

Results

Our preliminary results with α,β -unsaturated esters and alkenylbenzenes follow. In each experiment we have compared the behavior of cobalt and rhodium. Rhodium is more reactive than cobalt, and it was used either alone or in the presence of triphenylphosphine.

Hydroformylation of α,β -Unsaturated Esters. METHYL CROTONATE. Hydroformylation leads to the following four products:



The assays are reported in Table I. The selectivity of the reaction is lower when rhodium rather than cobalt is used, and it is lower still when rhodium is used in the presence of triphenylphosphine. Thus, the catalytic precursor changes the selectivity to the possible isomeric aldehydes markedly. In each case it is possible to obtain one of the three aldehydes in good yields and in a high state of purity.

METHYL 3,3-DIMETHACRYLATE. Hydroformylation of methyl 3,3-dimethacrylate yields only one isomeric aldehyde and the corresponding saturated ester:

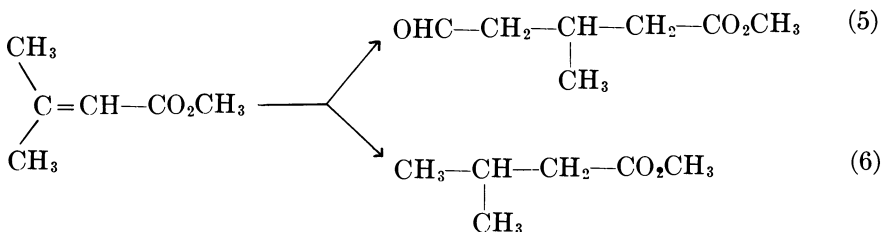


Table II shows that in the presence of $\text{Co}_2(\text{CO})_8$ the selectivity is very high. With rhodium the reaction requires higher metal concentration and temperature; furthermore, whatever the experimental

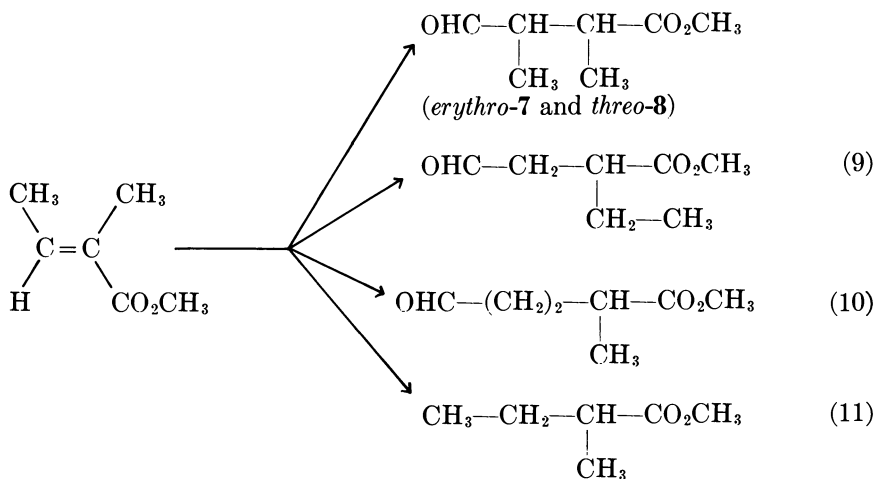
Table I. Hydroformylation of Methyl Crotonate^a

Catalytic Precursor	Reaction Time, min	Olefin Conversion, mole %	Selectivity ^b	Aldehyde Distribution ^c		
				1 ^d	2 ^d	3 ^d
Co ₂ (CO) ₈	125	99.1	94.7	0	21.3	72.6
Rh	160	98.7	68.6	3.2	57.6	7.0
Rh—(C ₆ H ₅) ₃ P	385	100	49.0	47.3	1.7	0

^a Reaction temperature, 120°C.^b Moles of aldehydes per 100 moles of reacted olefin.^c Moles of aldehydes per 100 moles olefin.^d Numbers refer to products of methyl crotonate reaction.

conditions, only hydrogenation of the unsaturated ester occurs, leading to methyl isovalerate.

METHYL TIGLATE [(*E*)-methyl-2-methyl-2-butenoate]. Hydroformylation of methyl tiglate leads to the following compounds:

**Table II. Hydroformylation of Methyl 3,3-Dimethacrylate^a**

Rh conc.: 5×10^{-3} at gram per mole olefin
 (C₆H₅)₃P conc.: 1×10^{-1} mole per mole olefin

Catalytic Precursor	Reaction Temp, °C	Reaction Time min	Olefin Conversion, mole %	Selectivity ^a	Aldehyde Distribution 5
Co ₂ (CO) ₈	120	150	100	94	94
Rh	150	150	100	0	0
Rh—(C ₆ H ₅) ₃ P	150	270	100	0	0

^a Moles of aldehyde per 100 moles of reacted olefin.

Table III shows that the selectivity is higher with rhodium than with cobalt in contrast to the case with methyl crotonate and methyl 3,3-dimethacrylate. Isomer selectivity is weak with $\text{Co}_2(\text{CO})_8$, and the two isomeric aldehydes (9 and 10) are formed in nearly the same proportions. Aldehydes 7 and 8 are formed in very low yields but in the same proportions. With rhodium, 9 is the main product (38.9%) while 10 represents only 17.4% of the yield: the threo and the erythro diastereoisomers occur in 23.4 and 8.4% yields, respectively.

Table III. Hydroformylation of Methyl Tiglate

Reaction temp: 120°C

Catalytic Precursor	Reaction Time, min	Olefin Conversion, mole %	Selectivity ^a	Aldehyde Distribution			
				7	8	9	10
$\text{Co}_2(\text{CO})_8$	460	98.2	49.5	0.5	0.5	18.9	28.7
Rh	530	92.7	95.0	8.4	23.4	38.9	17.4

^a Moles of aldehyde per 100 moles of reacted olefin.

METHYL CINNAMATE. Using lower temperature and pressure than those used by Falbe (5) (to avoid lactone formation) the selectivity of the reaction toward aldehydes and hydrogenated products was comparable with his.

Methyl cinnamate leads to methyl dihydrocinnamate (12) and methyl 3-phenyl-3-formylpropanoate (13):

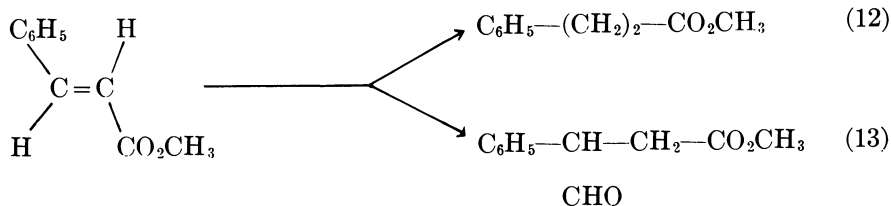


Table IV. Hydroformylation of Methyl Cinnamate

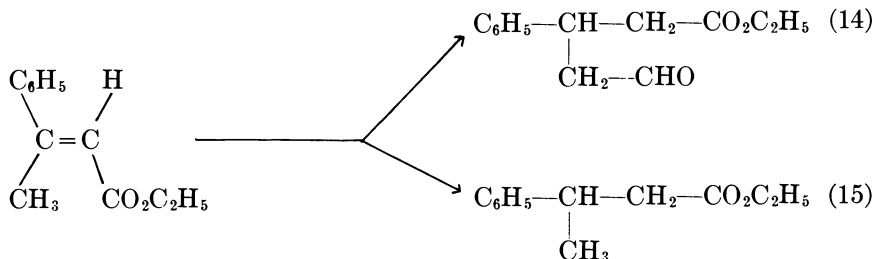
Reaction temp: 120°C

Catalytic Precursor	Reaction Time, min	Olefin Conversion, mole %	Selectivity ^a	Aldehyde Distribution
				13
$\text{Co}_2(\text{CO})_8$	405	88.1	33.4	29.4
Rh	320	100	75.3	75.3
$\text{Rh}-(\text{C}_6\text{H}_5)_3\text{P}$	375	100	60.8	60.8

^a Moles of aldehyde per 100 moles of reacted olefin.

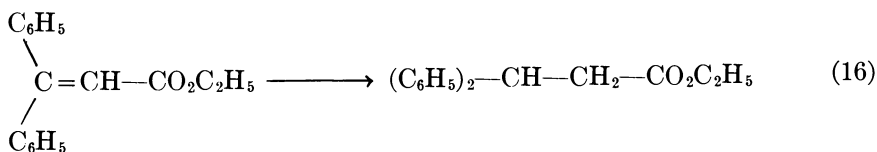
Data reported in Table IV show that with this ester, the selectivity of the reaction is lower with cobalt than with rhodium as in the case of methyl tiglate.

ETHYL 3-PHENYL-2-BUTENOATE. This ester leads only to one aldehyde and to the corresponding saturated ester:



Hydrogenation is the main reaction with $\text{Co}_2(\text{CO})_8$ (82%) as well as with rhodium (87%) (Table V).

ETHYL 3,3-DIPHENYL-2-PROPENOATE. In the presence of either $\text{Co}_2(\text{CO})_8$ or rhodium this ester leads only to the hydrogenated product (16):



Hydroformylation of Alkenylbenzenes. ALLYL BENZENE, *trans*- AND *cis*-PROPENYL BENZENE. Hydroformylation of these three isomeric alkenylbenzenes leads to propylbenzene (17) and to these aldehydes (18, 19, 20) (6, 7, 8):

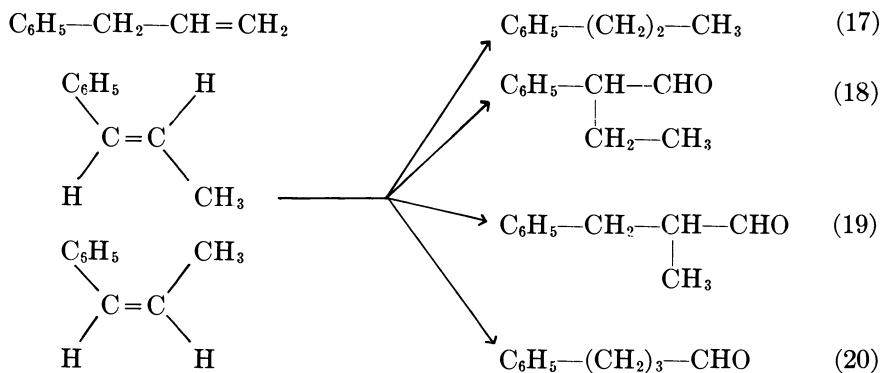


Table V. Hydroformylation of Ethyl 3-Phenyl-2-butenate

Catalytic Precursor	Reaction temp: 145°C			
	Reaction Time, min	Olefin Conversion, mole %	Selectivity ^a	Aldehyde Distribution 14
Co ₂ (CO) ₈	65	100	17.8	17.8
Rh	125	100	12.7	12.7

^a Moles of aldehyde per 100 moles of reacted olefin.

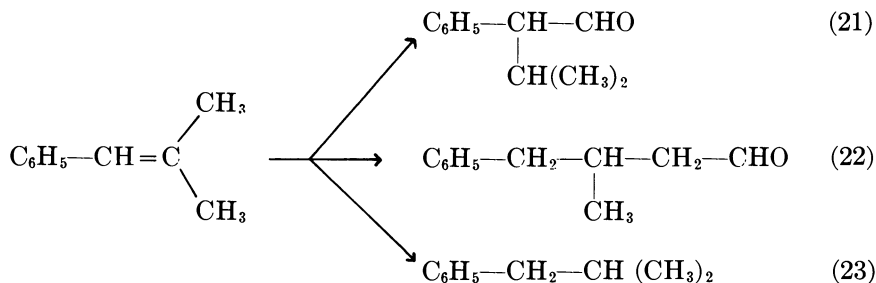
Table VI shows that regardless of the starting isomeric olefin, selectivity is lower with Co₂(CO)₈ than with rhodium; this is especially true when the starting isomer is conjugated. Moreover, when hydroformylation is done with Co₂(CO)₈, two aromatic ring effects are observed:

(a) orientation of the addition which places the CHO group on the α carbon with respect to the ring, and

(b) destabilization of σ complexes in the α position which explains the high propylbenzene ratios.

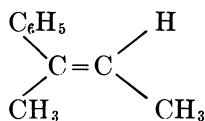
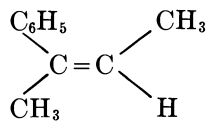
When rhodium is used, this ring effect is very important only with *trans*-propenylbenzene, and it becomes even more important when triphenylphosphine is added to rhodium.

1-PHENYL-2-METHYLPROPENE. Hydroformylation of this alkenylbenzene leads to two isomeric aldehydes and a saturated aromatic hydrocarbon:



The data of Table VII show that the selectivity is poor with Co₂(CO)₈ and very high with rhodium. Aldehyde distribution shows an important orientation effect on the α carbon with respect to the ring. When rhodium is used, isomerization towards the methyl group is much more extensive than with propenylbenzene. When triphenylphosphine is used, isomer selectivity is essentially unchanged. In the presence of Co and Rh, reaction rates are lower than with propenylbenzenes; this effect can be attributed to steric hindrance of the *gem*-dimethyl group.

HYDROFORMYLATION OF PHENYLBUTENES. In this section we present results on the hydroformylation of both (*E*)- and (*Z*)-2-phenyl-2-butenes,

(*E*)(*Z*)

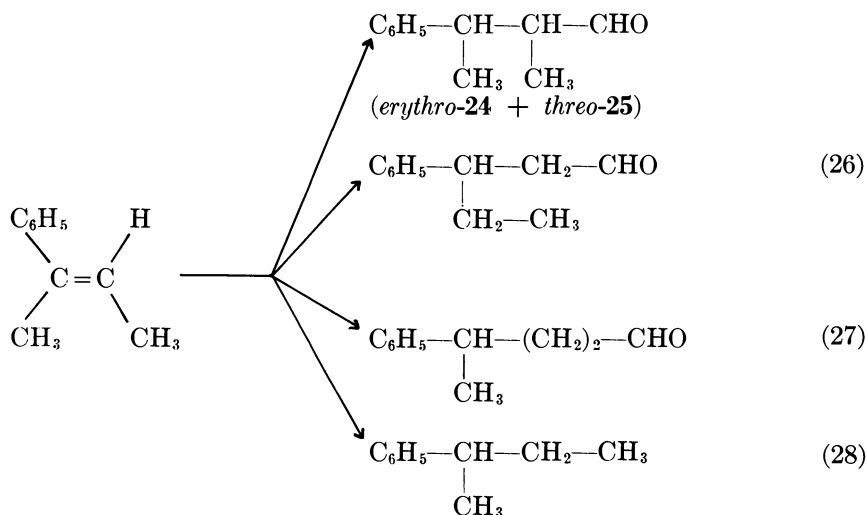
and those of the two isomers obtained when the double bond shifts on either methyl group, α -ethylstyrene, $\text{C}_6\text{H}_5-\text{C}=\text{CH}_2$, and 3-phenyl-1-



butene, $\text{C}_6\text{H}_5-\text{CH}(\text{CH}_3)-\text{CH}=\text{CH}_2$.



(*E*)-2-phenyl-2-butene. Hydroformylation of this alkenylbenzene leads to four aldehydes (two of them diastereoisomers) and to the following saturated hydrocarbons:



The results in Table VIII show that the selectivity with $\text{Co}_2(\text{CO})_8$, although higher than that obtained with 1-phenyl-2-methylpropene, is still very low. The aldehyde distribution is comparable with that for methyl tiglate. The main isomeric aldehyde is 27, and the erythro and threo diastereoisomers are formed in the same proportions. With rhodium the selectivity is very high, and the main aldehydes are 26 and 27. Twice as much threo isomer as erythro isomer is produced (14.2 and 8.4%).

Table VI. Hydroformylation of Allylbenzene

Reaction temp: $\text{Co}_2(\text{CO})_8$: 110°C

Olefin	Catalytic Precursor	Reaction Time, min	Olefin Conversion, mole %
Allylbenzene	$\text{Co}_2(\text{CO})_8$	240	98.1
	Rh	80	99.0
<i>trans</i> -Propenylbenzene	$\text{Co}_2(\text{CO})_8$	480	83.8
	Rh	150	100
	$\text{Rh}-(\text{C}_6\text{H}_5)_3\text{P}$	70	94.5
<i>cis</i> -Propenylbenzene	$\text{Co}_2(\text{CO})_8$	720	100
	Rh	170	97.0
	$\text{Rh}-(\text{C}_6\text{H}_5)_3\text{P}$	340	88.3

^a Moles of aldehyde per 100 moles of reacted olefin.

To determine whether this isomer distribution was the result of epimerization, hydroformylation of (*Z*)-2-phenyl-2-butene was studied.

(*Z*)-2-Phenyl-2-butene. (*Z*)-2-phenyl-2-butene is not as stable as its (*E*) isomer. When $\text{Co}_2(\text{CO})_8$ is used, results are the same with the (*E*) stereoisomer. However, when rhodium is used, isomer selectivity changes (Table VIII). The main isomeric aldehyde is the erythro diastereoisomer which represents 33.9% of the whole mixture. Aldehyde 27 is formed in nearly the same ratio (32.9%) while 6.8% and 4.4% of aldehyde 26 and the threo diastereoisomer are formed.

α -Ethylstyrene. Hydroformylation of α -ethylstyrene with $\text{Co}_2(\text{CO})_8$ leads to nearly the same results as with both the (*E*) and (*Z*) stereoisomers of 2-phenyl-2-butene (Table VIII) However, in contrast to the (*Z*)- and (*E*)-2-phenyl-2-butenes, the main aldehyde is 26 when rhodium is used. Its formation can be explained in terms of an addition of CHO group to the starting double bond, and isomerization leading to 27 is very low. With rhodium the threo diastereoisomer is slightly more important than the erythro.

Table VII. Hydroformylation of 1-Phenyl-2-Methylpropene

Reaction temp: 120°C

Catalytic Precursor	Reaction Time, min	Olefin Conversion, mole %	Selectivity ^a	Aldehyde Distribution	
				21	22
$\text{Co}_2(\text{CO})_8$	510	100	16.1	8.5	7.6
Rh	440	91.0	92.7	53.1	31.3
$\text{Rh}-(\text{C}_6\text{H}_5)_3\text{P}$	540	84.4	95.7	55.2	25.6

^a Moles of aldehyde per 100 moles of reacted olefin.

and of *trans*- and *cis*-Propenylbenzene— Rh and Rh — (C₆H₅)₃P: 90°C

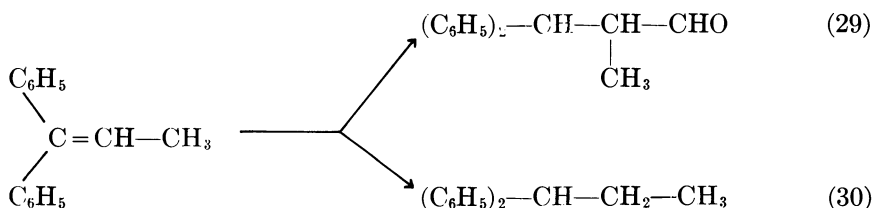
Selectivity ^a	Aldehyde Distribution		
	18	19	20
78.3	13.6	9.7	53.6
97.4	13.2	36.3	46.9
52.0	30.0	2.0	11.6
94.3	67.9	24.5	1.9
92.2	80.3	11.9	0
41.5	28.3	2.5	10.7
98.6	54.1	39.8	1.7
99.5	56.7	30.2	1.0

3-Phenyl-1-butene. With Co₂(CO)₈, hydroformylation of this alkenylbenzene, as with allylbenzene, yields little hydrogenation product (Table VIII).

Thus, at 110°C, the least branched aldehyde **27** is the main product (69.5%). Only 9% of aldehyde **26** is found, and an erythro-to-threo ratio slightly favors the erythro isomer.

With rhodium, aldehyde **27** is also the main isomeric aldehyde, but no aldehyde **26** is formed. Furthermore, slightly more erythro than threo isomer is formed. Thus, hydroformylation on β carbon is different for allylbenzene and for 3-phenyl-1-butene. The lower yield of 3-phenyl-2-methylbutanal is very likely the result of steric hindrance from the methyl group on the α carbon.

1,1-DIPHENYLPROPENE. Hydroformylation with this olefin leads to only two compounds (**29**, **30**):



At 120° and at 160°C with Co₂(CO)₈, only hydrogenation occurs. For a suitable reaction rate with rhodium, 160°C and 0.6% Rh are required. Under those conditions, hydrogenation is extensive (33%), and aldehyde **29** is partially reduced to the corresponding alcohol. (This is the only example of extensive reduction of aldehydes to alcohols. In all other cases only traces of alcohols were detected either with cobalt or with rhodium.)

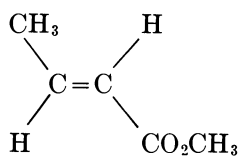
Table VIII. Hydroformylation

Olefin	Catalytic Precursor	Reaction Temp, °C	Reaction Time, min	Olefin Conversion, mole %
<i>(E)</i> -2-Phenyl-2-butene	Co ₂ (CO) ₈ Rh	120	425	99.0
			520	91.8
<i>(Z)</i> -2-Phenyl-2-butene	Co ₂ (CO) ₈ Rh	120	465	99.0
			465	82.0
α -Ethylstyrene	Co ₂ (CO) ₈ Rh	120	465	100
			505	86.0
3-Phenyl-1-butene	Co ₂ (CO) ₈ Rh	110	375	100
		90	310	91.5

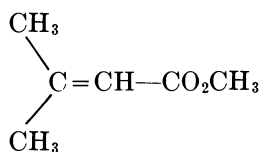
^a Moles of aldehyde per 100 moles of reacted olefin.

Discussion

α,β -Unsaturated Esters. The results show clearly that the ester group determines the selectivity of the reaction according to the catalyst used. With cobalt as the catalytic precursor, selectivity decreases in the following order:

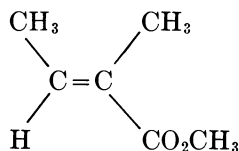


(94.7)

 \gg 

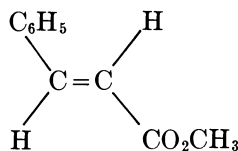
(94.0)

>



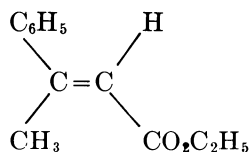
(49.5)

>



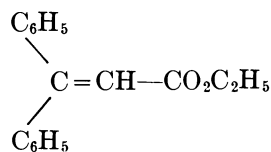
(33.4)

>



(17.8)

>

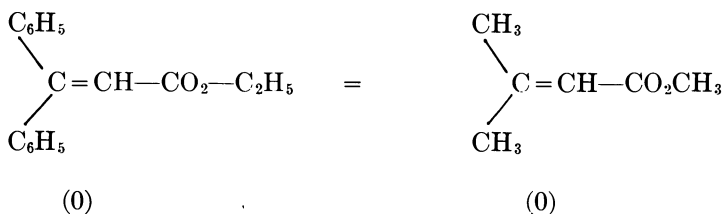
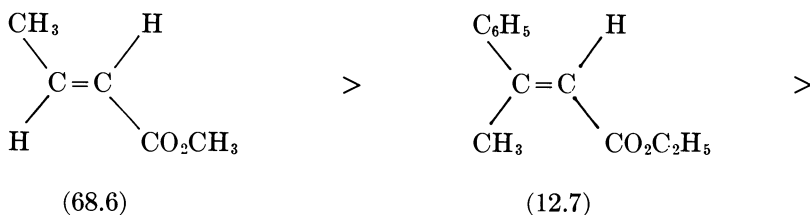
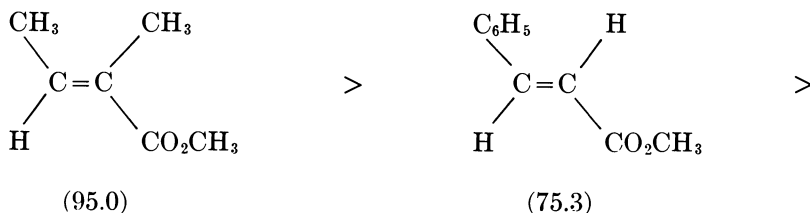


(0)

of Phenylbutenes

Selectivity ^a	Aldehyde Distribution			
	24	25	26	27
27.6	0.4	0.3	10.1	16.5
96.9	7.4	14.2	41.8	25.6
25.9	0.4	0.3	9.7	15.2
95.1	33.9	4.4	6.8	32.9
25.0	0.2	0.2	10.3	14.3
84.5	1.8	3.3	63.5	4.1
80.7	1.4	0.9	9.0	69.5
98.1	10.4	6.6	0	72.8

With rhodium, selectivity decreases in the following order:

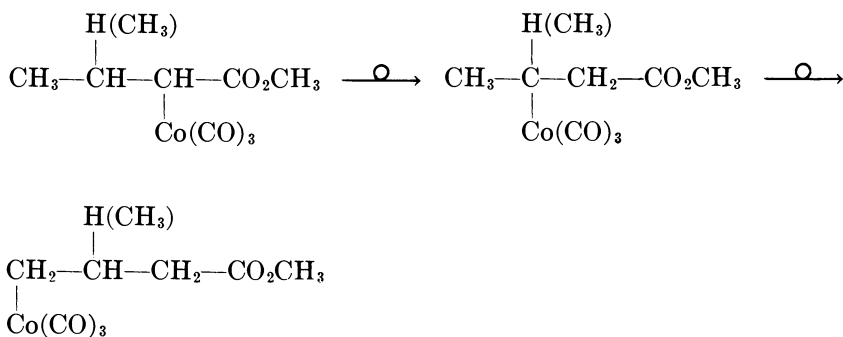


When cobalt is used, the selectivity with aliphatic esters is higher when the α carbon is unsubstituted (methyl crotonate, methyl 3,3-dimethylacrylate) than when it is substituted—*e.g.*, methyl tiglate.

The influence of the ester selectivity is even more pronounced when a phenyl group is present on the β carbon; selectivity decreases further

when this carbon is substituted by both a phenyl and an alkyl group (methyl-3-phenyl-2-butenate), and it is at its lowest point when the β carbon bears two phenyl groups. The observed differences in selectivity can be explained in terms of the relative stabilities of the alkylcobalt-carbonyl intermediates. The stability of these intermediates decreases markedly with carbon structure ramification. If one considers the σ complex obtained from the cobaltcarbonyl and the substrate, three possible pathways exist: (1) a CO insertion to give the aldehyde, (2) isomerization, and (3) hydrogenolysis.

One might expect one of these reactions to prevail according to the alkylcobaltcarbonyl structure on the one hand and according to the reaction conditions on the other hand. For example, for methyl crotonate and methyl 3,3-dimethacrylate, rapid isomerization gives a new alkylcobaltcarbonyl:

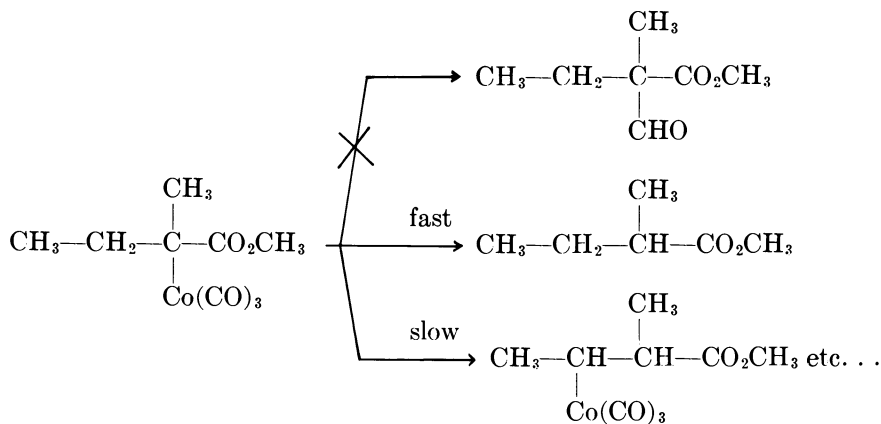
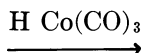
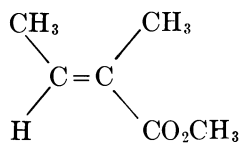


With methyl tiglate, the extent of hydrogenolysis could be explained by the formation of a *tert*-alkylcobaltcarbonyl which cannot insert CO and which apparently undergoes hydrogenolysis faster than isomerization (*see top of next page*).

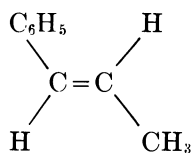
With α,β -unsaturated aromatic esters, the aromatic nucleus seems to destabilize the alkylcobaltcarbonyl, thus favoring hydrogenolysis rather than CO insertion or isomerization.

The reactions catalyzed by rhodium are quite different from those with cobalt. For example, the results with methyl 3,3-dimethacrylate indicate a destabilizing effect of the ester group, leading mainly to hydrogenolysis since isomerization occurs less readily with rhodium than with cobalt. Moreover, the nature and the position of the substituents seem to have little influence on the alkylrhodiumcarbonyl stability. This attenuates the effect of the ester group, as shown by the results with methyl tiglate, methyl cinnamate, and ethyl 3-phenyl-2-butenate.

Alkenylbenzenes. With $\text{Co}_2(\text{CO})_8$, whatever the structure of the alkenylbenzene, when the double bond is conjugated with the aromatic

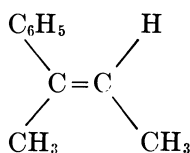


ring, selectivity is always low. Under our experimental conditions, it follows the order:



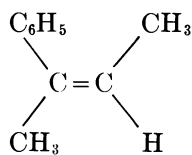
(52.0)

>



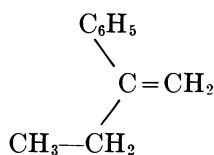
(27.6)

>>



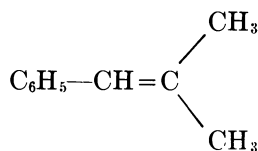
(25.9)

>>



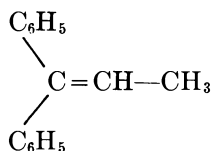
(25.0)

>



(16.1)

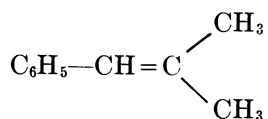
>



(0)

In the presence of $\text{Co}_2(\text{CO})_8$, selectivity seems to depend on the number and relative position of the double bond substituents as well as on the reaction temperature. As is usually the case with $\text{Co}_2(\text{CO})_8$, hydroformylation leads mainly to the least branched aldehydes when the carbon α to the ring bears two substituents. However, when this carbon is monosubstituted, the ring effect becomes more important and CO insertion occurs on the benzylic position.

With Rh, the phenomena are strikingly different since the aromatic ring does not influence the selectivity which is always very high, no matter what olefinic structure (except for 1,1-diphenylpropene). Isomer selectivity depends on several factors, mainly the structure and the stereochemistry of the alkenylbenzene. With conjugated alkenylbenzenes, addition of the CHO group occurs preferentially on the α carbon when the α and β carbons are monosubstituted. When the β carbon is disubstituted, because of steric requirements, hydroformylation is less selective and occurs on both the α and γ carbon:



Thus, it is not the isopropenyl structure alone which prevents hydroformylation with methyl 3,3-dimethacrylate but the occurrence of both the isopropenyl structure and the $-\text{COOCH}_3$ group.

When the α carbon is disubstituted, hydroformylation occurs on the β carbon if it is unsubstituted. When this carbon is monosubstituted, selectivity depends on stereochemistry, and addition occurs on both the β carbon and the alkyl groups attached to the double bond.

With nonconjugated alkenylbenzenes such as $\text{C}_6\text{H}_5-\text{CH}_2-\text{CH}=\text{CH}_2$ and $\text{C}_6\text{H}_5-\text{CH}(\text{CH}_3)-\text{CH}=\text{CH}_2$, isomer selectivity is a function of substitu-



tion; the reaction shows more selectivity when the α carbon is substituted, and hydroformylation leads to the addition of CHO group on the ω carbon.

Effect of the Stereochemistry. With rhodium, the geometry of molecules such as (*E*)- and (*Z*)-2-phenyl-2-butenes influences both the distribution of diastereoisomers formed by addition of CHO group on the β carbon and the distribution of aldehydic isomers. Depending on the starting (*E*) or (*Z*) stereoisomer, one of the two diastereoisomers predominates; this implies some degree of stereospecificity in the hydroformylation reaction. On the other hand, when $\text{Co}_2(\text{CO})_8$ is used, no stereospecificity in the hydroformylation reaction is observed. It is thus possible to get information about the stereochemistry of the hydro-

formylation with rhodium. The relative distributions of threo and erythro diastereoisomers that we obtained from either (*E*) or (*Z*) stereoisomers showed that the hydroformylation proceeds by cis addition. It is also apparent that the degree of cis addition is higher from the (*Z*) than the (*E*) isomer, despite (*Z*)'s lower thermodynamic stability. This phenomenon can be attributed to the relative stability of reaction intermediates which depend on the olefinic structure. The fact that with $\text{Co}_2(\text{CO})_8$ we do not find any stereospecificity does not mean that the addition is not a cis addition; with olefins in which isomerization is impossible, it was possible to determine that the hydroformylation proceeds by a cis addition (9, 10).

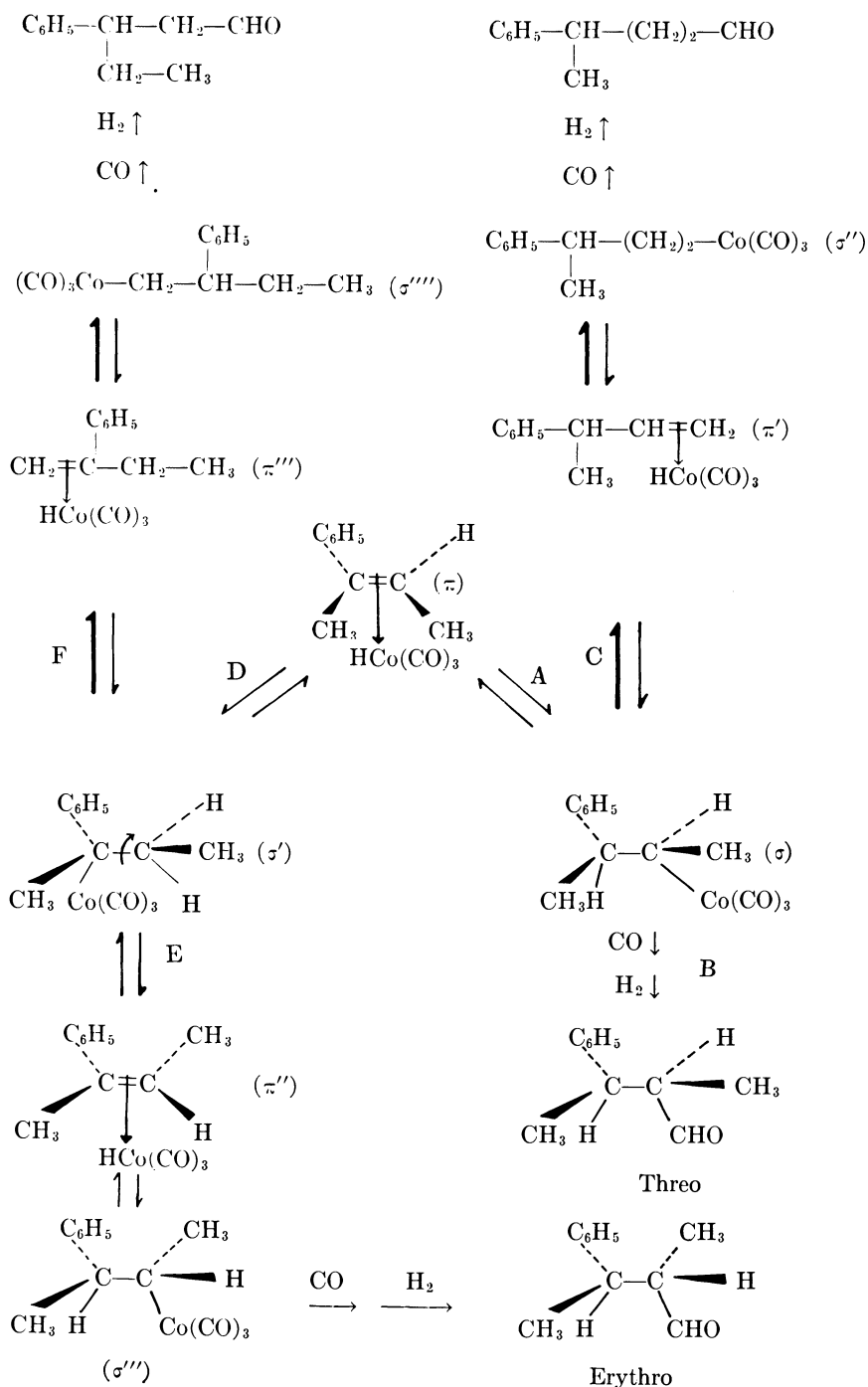
The other feature of hydroformylation of (*E*)- and (*Z*)-2-phenyl-2-butenes concerns the distribution of aldehydic isomers 26 and 27. With $\text{Co}_2(\text{CO})_8$, whatever the stereochemistry of the olefin, the distribution of these two aldehydes is exactly the same. On the other hand, with $\text{Rh}/\text{Al}_2\text{O}_3$ the reaction is more or less oriented towards the formation of one of the aldehydic isomers. Moreover, the phenomenon is more striking with (*Z*) than with (*E*) stereoisomer.

To explain the different behavior of cobalt- and rhodiumcarbonyls, one might consider their respective isomerization abilities. With $\text{Co}_2(\text{CO})_8$ as a catalytic precursor, we can postulate, as generally admitted, that a very fast conversion from π to σ complexes occurs (σ or σ') as shown in Scheme 1 for (*E*)-2-phenyl-2-butene.

The σ complex (σ) obtained by cis addition of the cobaltcarbonyl hydride (path A) can either lead to the expected threo aldehyde (path B) or isomerize through a new π complex (π') path C, to give aldehyde 27. The other possible σ complex (σ') obtained by the cobaltcarbonyl hydride addition (path D) must isomerize to undergo a CO insertion. It can do this through a π complex (π'') (path E) to give as a final product the erythro aldehyde or through a π complex (π''') (path F) leading to aldehyde 26.

The same reaction scheme can be written for (*Z*)-2-phenyl-2-butene, except that paths B and E would lead to erythro and threo aldehydes. In cobalt catalysis this isomerization could explain both the lack of stereospecificity and the lack of influence of the stereochemistry of the starting olefin on the distribution of aldehydes 26 and 27. This hypothesis agrees well with results with α -ethylstyrene. On the other hand, when rhodium is used, extensive isomerization occurs less readily probably because of a better stability of alkyl- and acylrhodium carbonyls, and one can thus achieve a high degree of stereospecificity.

However, the different isomer selectivity toward aldehydes 26 and 27 obtained from (*E*)- and (*Z*)-2-phenyl-2-butenes is difficult to explain.



Scheme I

It is conceivable that depending on the geometry of the olefin, the orientation of the rhodiumcarbonyl hydride addition could be different. This possibility could also account for the results of the hydroformylation of *cis*- and *trans*-propenylbenzene.

Conclusion

This work shows clearly that hydroformylation remains a privileged way to prepare aldehydes which are difficult to obtain otherwise. The proper choice of catalytic precursor is difficult *a priori* since a complete understanding of the role played by functional groups or geometric structure on the substrate is not known. Only this knowledge will allow one to predict correctly the results of a catalyzed hydroformylation.

The points that we established are:

(1) The *cis* addition character of the hydroformylation catalyzed by rhodium,

(2) the direct influence of substrate geometry on the aldehyde isomeric distribution.

Work is underway to arrive at a better understanding of the reaction from a mechanistic point of view.

Experimental

General Hydroformylation Procedure. All runs were performed in the absence of solvent in a 125-ml Prolabo autoclave under 160 bars total pressure (1 H₂/1 CO), as measured at room temperature. Most assays were carried out with 1×10^{-2} mole Co₂(CO)₈ or 1×10^{-3} atm-Rh and 2×10^{-2} mole (C₆H₅)₃P if required, per mole of olefin.

The reaction was allowed to proceed until no significant pressure drop occurred. After rapid cooling, the gases were vented, and the reaction mixture was analyzed. Each run was repeated at least twice.

CHEMICALS. Co₂(CO)₈ was prepared according to Wender (11). Rh/Al₂O₃, (C₆H₅)₃P, allylbenzene, and *trans*-propenylbenzene were reagent grade commercial products. The following α,β -unsaturated esters were prepared from the corresponding commercial acids by esterification with methanol, HCl: methyl 3,3-dimethacrylate, crotonate, tiglate, and cinnamate. (1) Ethyl 3-phenyl-2-butenate and 3,3-diphenyl-2-propenoate were prepared by the Reformatsky condensation followed by dehydration. (2) 1-Phenyl-2-methylpropene, (*E*)-2-phenyl-2-butene, and 1,1-diphenylpropene were synthesized by condensation of the Grignard reagent and the suitable carbonyl compound, followed by dehydration.

(3) (Z)-2-Phenyl-2-butene, α -ethylstyrene, *cis*-propenylbenzene, and 3-phenyl-1-butene were obtained by the Wittig reaction.

ANALYSIS. Reaction mixtures were analyzed with an Intersmat IGC-15 gas chromatograph.

Products were identified either by gas chromatography using authentic samples or from NMR, infrared, and mass spectrometric data of pure products after preparative gas chromatography using a A-700 Varian Autoprep gas chromatograph.

Literature Cited

1. Wakamatsu, H., *Nippon Kagaku Zasshi* (1964) **85**, (3) 227.
2. Veryard, K. J., British Patent **801,734**.
3. Fell, B., Rupilius, W., *Tetrahedron Lett.* (1969) **32**, 2721.
4. Falbe, J., Huppel, N., Korte, F., *Chem. Ber.* (1964) **97**, 863.
5. Falbe, J., Huppel, N., *Brennstoff. Chem.* (1967) **48**, 46.
6. Lai, R., Ucciani, E., *Compt. Rend. Ser. C.* (1971) **273**, 1368.
7. *Ibid.* (1972) **275**, 1033.
8. *Ibid.* (1973) **276**, 425.
9. Beal, P. F., Rebenstorf, M. A., Pike, J. E., *J. Amer. Chem. Soc.* (1959) **81**, 1231.
10. Rosenthal, A., *Advan. Carbohyd. Chem.* (1968) **23**, 60.
11. Wender, I., Sternberg, H. W., Metlin, S., Orchin, M., *Inorg. Synth.* (1957) **V**, 190.

RECEIVED July 30, 1973.

New Hydroformylation Technology with Cobalt Carbonyls

R. KUMMER, H. J. NIENBURG, H. HOHENSCHUTZ, and
M. STROHMEYER

BASF, Ludwigshafen, Germany

In the classical oxo process the catalyst cobalt carbonyl is formed in situ by introducing divalent cobalt into the reactor. High temperature is required for this catalyst formation that gives a mixture of aldehydes and alcohols containing only 60–70% of linear product. A new BASF process using cobalt carbonyl hydride shows improved selectivity and efficient catalyst recovery. The catalyst is prepared by passing an aqueous solution of cobalt salt over a promoter and extracting the catalyst from the water phase with olefin. The olefin is then hydroformylated at low temperatures (90°–120°C) to yield 72–80% of linear aldehydes. The catalyst is recovered by mixing the product with air in an aqueous solution of cobalt formate.

The hydroformylation reaction or oxo synthesis has been used on an industrial scale for 30 years, and during this time it has developed into one of the most important homogeneously-catalyzed technical processes (1). A variety of technical processes have been developed to prepare the real catalyst cobalt tetracarbonyl hydride from its inactive precursors, e.g., a cobalt salt or metallic cobalt, to separate the dissolved cobalt carbonyl catalyst from the reaction products (decobaltation) and to recycle it to the oxo reactor. The efficiency of each step is of great economical importance to the total process. Therefore many patents and papers have been published concerning the problem of making the catalyst cycle as simple as possible. Another important problem in the oxo synthesis is the formation of undesired branched isomers. Many efforts have been made to keep the yield of these by-products at a minimum.

All technical processes now in operation offer at best a satisfactory solution to only one of these two problems. Processes with a simple and

efficient catalyst cycle, especially those which recycle an aqueous solution of a cobalt salt after decobaltation by oxidation with air, require relatively high reaction temperatures to form the catalyst *in situ* from the cobalt salt. These high reaction temperatures increase the yield of the less desirable branched reaction products, and in the case of long chain olefins an inseparable mixture of aldehydes and alcohols is obtained. Other technical processes yielding predominantly straight chain products use a cobalt compound soluble in an organic solvent or a cobalt carbonyl catalyst modified by phosphines. The number of steps required and the loss of modifier through oxidation add to the cost of the process. The phosphine process which produces primarily alcohols is therefore less suited for technical purposes if aldehydes are desired.

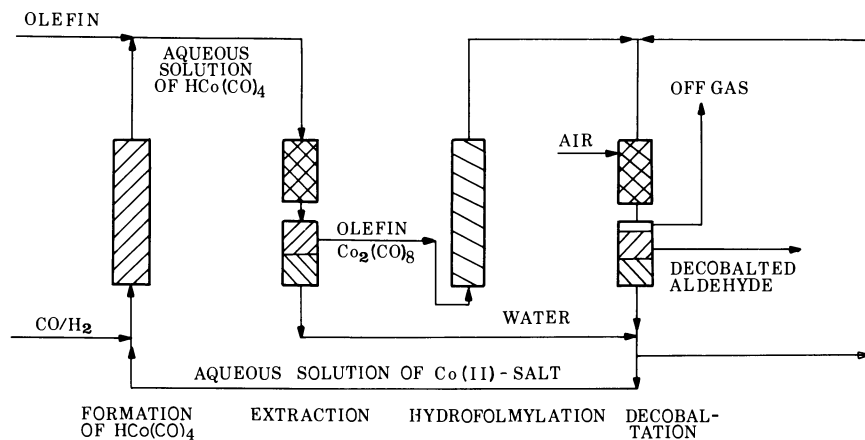
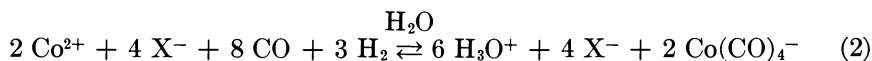


Figure 1. Flow sheet of new oxo process

In recent years BASF has developed an effective method which uses a simple and very economical catalyst cycle to produce predominantly straight chain aldehydes. An important feature of the new process (Figure 1) is a small separate reactor to prepare the cobalt carbonyl catalyst from an aqueous solution of cobalt salt outside the hydroformylation reactor. Extracting the catalyst with the olefin from the aqueous solution gives a homogeneous solution of cobalt carbonyls in the hydrocarbon for use in the oxo reaction. The oxo reaction itself is carried out in the absence of water or any additional solvent permitting low reaction temperatures and thus improving the yield of straight chain aldehydes. Finally the catalyst is removed quantitatively by mixing air with the reaction product in the presence of an aqueous solution of cobalt formate. Two phases separate with the cobalt catalyst remaining entirely in the aqueous phase. The aqueous phase containing the cobalt salt is recycled to the carbonyl regeneration reactor.

The Four Main Steps of the New Process

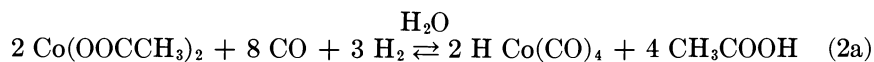
Step 1: Formation of the Active Cobalt Carbonyl Catalyst. Many efforts have been made (2, 3, 4) to prepare carbonyl catalyst by treating metallic cobalt or cobalt compounds at high temperatures (150°–200°C) and pressures with carbon monoxide and hydrogen (Reactions 1 and 2).



Even at 180°C, however, Reaction 2 proceeds very slowly and decomposition to metallic cobalt (Reaction 1) is significant. The use of a palladium catalyst to promote Reaction 2 has recently (5) been suggested, but it is economically less suitable.

A number of simple and inexpensive materials catalytically promote the cobalt–carbonylation (Reaction 2) in aqueous solution. These include ion-exchange resins, zeolites, or special types of activated carbon. Formation of the active catalyst in a separate reactor is thus economically feasible. The mechanism of this catalysis has not yet been elucidated and seems to differ for each promoter mentioned. After an induction period during which the cobalt fed to the reactor is partially retained by the promoter, fully active materials have absorbed cobalt carbonyl anion $\text{Co}(\text{CO})_4^-$ (ion exchange resins), Co^{2+} cation (zeolites), or a mixture of Co^{2+} , cobalt carbonyl hydride, and cluster-type cobalt carbonyls (activated carbon). This can be shown by analytical studies (extraction, titration, and IR studies) of active material withdrawn from the reactor.

Figure 2 shows the influence of temperature on the reaction time of a 70% conversion of Co^{2+} in Reaction 2a.



A 70% conversion of Co^{2+} to $\text{HCo}(\text{CO})_4$, which means a 1:2 ratio of Co^{2+} to $\text{Co}(\text{CO})_4^-$ or formation of the compound $\text{Co}[\text{Co}(\text{CO})_4]_2$ is sufficient to carry out the next step of the process.

Step 2: Extraction of the Catalyst from the Aqueous Solution. It is not feasible technically to charge the aqueous solution of cobalt carbonyl hydride directly into the hydroformylation reactor because two phases may form, especially with the long chain olefins. The most direct and most efficient way to eliminate water while permitting full use of the carbonyl catalyst is to extract it from the water phase with the olefin intended for hydroformylation. The extraction is carried out between

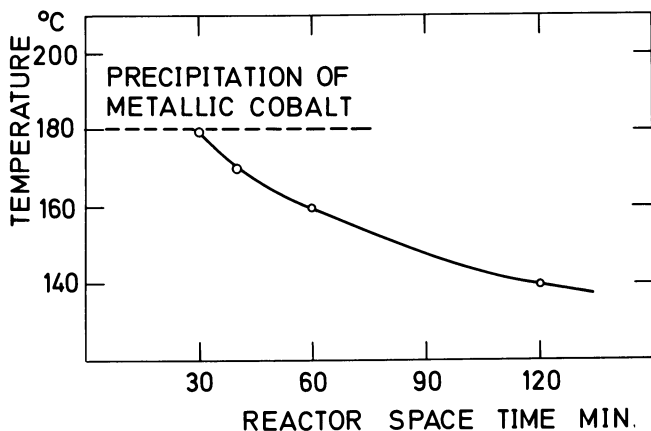
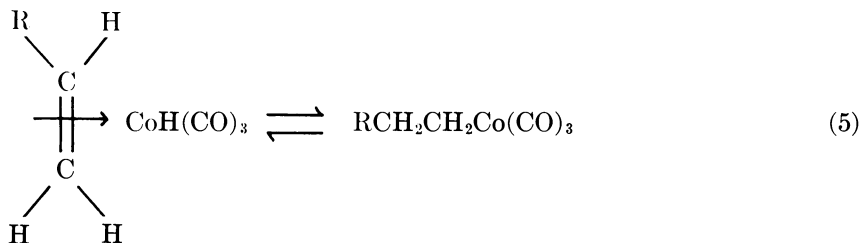
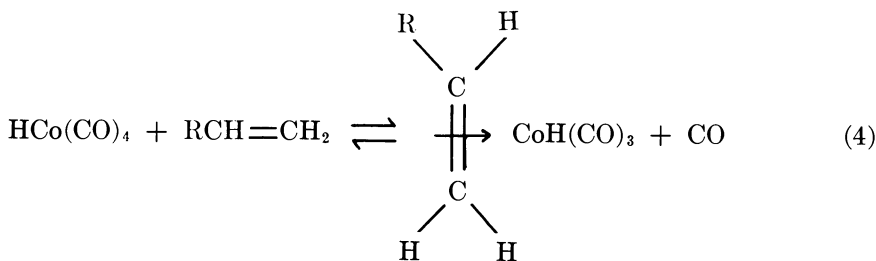
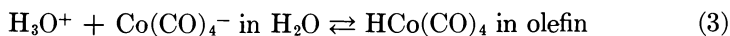
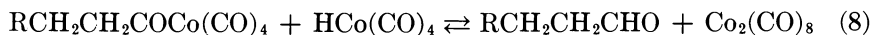
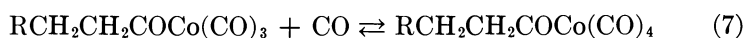


Figure 2. Influence of temperature on reactor space time for 70% conversion of an aqueous solution of cobalt acetate (1% Co^{2+}); activated carbon as promoter, 280 atm, $\text{CO}:\text{H}_2 = 1:1$

20°–100°C and a total pressure of 1–300 atm (the pressure of the hydroformylation reaction), depending on the reactivity of the olefin. After the cobalt carbonyl hydride has passed from the aqueous phase into the organic phase (Reaction 3), stoichiometric hydroformylation (6, 7, 8) takes place (Reactions 4–8).





After extraction the catalyst remains in the olefin phase as shown by IR analysis either as an acyl complex, as dicobalt octacarbonyl, or (at low CO pressure) as tetracobalt dodecacarbonyl.

The extraction may be carried out in a countercurrent or concurrent extraction column. If there is sufficient mixing of the two phases, a very short contact time even for long chain olefins is adequate to ensure complete transfer of the catalyst from the aqueous phase into the olefin.

After extraction the two phases are separated and the olefin phase containing the active catalyst is fed to the hydroformylation reactor.

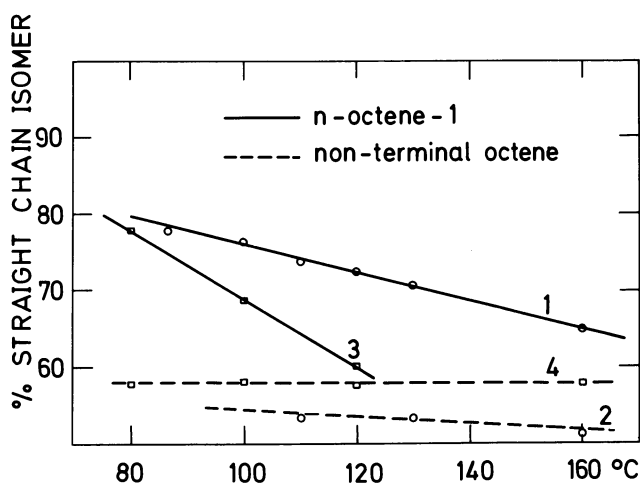


Figure 3. Isomer distribution in the hydroformylation of octene; total pressure 280 atm, curve 1,2, $\text{CO}:\text{H}_2 = 1:1$, curve 3,4, $\text{CO}:\text{H}_2 = 1:3$

Step 3: Hydroformylation with Pre-Formed Homogeneous Catalyst.

The goal is to improve the ratio of straight chain to branched chain products (n : iso ratio) and to keep the hydrogenation of olefin to paraffin and aldehyde to alcohol as low as possible.

All hydroformylation experiments were performed in a continuously operated reactor. The concentration of the catalyst was varied from 0.1 to 0.4 wt % to keep olefin conversion at the same level (80–90%) for all reaction temperatures. The total pressure for all experiments was 280 atm, and n -octene was used as typical straight chain olefin of medium chain length.

Improvement in the isomer distribution can be achieved by lowering the hydroformylation temperature from the range 150°–170°C, now used industrially, to 100°C. Figure 3 shows an almost constant 2% increase in yield of straight chain products for each 10° decrease in reaction temperature. This increase becomes even more pronounced (4–5%) at higher hydrogen partial pressure ($\text{CO}:\text{H}_2 = 1:3$).

An increase in hydrogen partial pressure increases reaction velocity (9, 10); thus it could be desirable to use a higher ratio of $\text{H}_2:\text{CO}$ than the usual 1:1.

Figure 3 also shows the isomer distribution resulting from the hydroformylation of a mixture of straight chain octenes with predominantly internal double bond (2% 1-octene, 37% 2-octene, 36% 3-octene, and 23% 4-octene). In this case the n:iso ratio did not change for the range of temperatures examined. The conclusion is that increased rate of olefin isomerization to 1-octene resulting from increased temperature or higher hydrogen partial pressure is compensated for by a decrease in the n:iso ratio. Therefore no advantage can be seen in hydroformylating internal olefins using a low-temperature process.

Another important economic problem in industrial processes concerns losses through side reactions, especially the hydrogenation of starting material to paraffin and the conversion of aldehydes to alcohols.

Figure 4 shows the effect of temperature and partial pressure variations on the product yield from the hydrogenation of octene. Equimolar

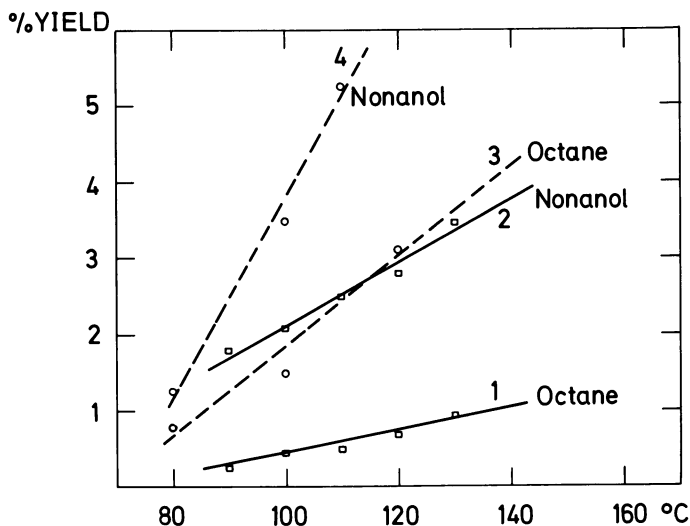


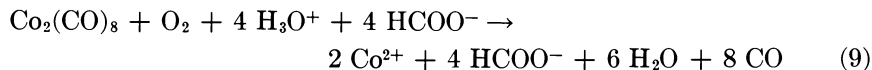
Figure 4. Influence of temperature on hydrogenation of olefin and aldehyde; total pressure 280 atm, curve 1,2, $\text{CO}:\text{H}_2 = 1:1$, curve 3,4, $\text{CO}:\text{H}_2 = 1:3$

amounts of CO and H₂ give less than 1% direct hydrogenation below 130°C, but even lower temperatures (80°–100°C) are required to reduce the alcohol formed to 2%. The results compare favorably with the more than 5% of paraffin and 10% of alcohol produced in older industrial processes using reaction temperatures above 150°C. Though the decrease in the rate of hydrogenation is substantially greater with the 3:1 H₂ to CO mixture than that with the 1:1 mixture, the curves in Figure 4 show that more than 2% alcohol and 1% paraffin are obtained at reaction temperatures above 85°C.

Another side reaction of hydroformylation is formate ester formation (11). The 4% yield of formates did not change in the temperature range examined or with lower CO partial pressure.

Reaction products obtained by low-temperature hydroformylation (100°–120°C) of linear α -olefins with an equimolar amount of CO and H₂ at 280 atm were (%): aldehyde, 94 \pm 1 (n:iso ratio 2, 56 to 3, 16); formate, 4 \pm 0.5; alcohol, 2 \pm 0.5. Furthermore, 1% of the olefin feed is hydrogenated to paraffin and 2–3% is converted to high boiling products (aldols, ketones, and acetals).

Step 4: Decobaltation of the Reaction Product. The product of the hydroformylation reactor containing the catalyst as a mixture of cobalt carbonyl hydride and dicobalt octacarbonyl is fed to the decobalting section. Mixing the product at 120°C and 10 atm with a dilute formic acid/cobalt formate solution in the presence of air decomposes the catalyst (Reaction 9) (12).



The reaction conditions ensure that all cobalt catalyst remains in the aqueous phase and that only Co²⁺-compounds that are soluble in water are formed. The aqueous phase, after dilution with the water from the extraction section (Figure 1), is recycled partially to the decobalting tube and partially to the catalyst formation section where the active catalyst is regenerated.

Summary

The five important advantages of the new process are then:

1. The process has an absolutely closed catalyst cycle; no losses occur during the cycle. The catalyst always remains in liquid phase eliminating the handling of solid materials.

2. Only air is needed as an auxiliary chemical. Waste streams which might cause a pollution problem or effect the commercial feasibility are excluded.

3. No water or any organic solvent is fed to the hydroformylation reactor.

4. The catalyst is always fed as the true active cobalt carbonyl catalyst to the reactor, and its concentration in the reactor may be varied within a wide range.

5. Carrying out the hydroformylation reactions at low temperatures significantly improves the yield of straight chain aldehydes and reduces losses by olefin hydrogenation.

Literature Cited

1. Falbe, J., "Carbon Monoxide in Organic Synthesis," Springer-Verlag, Berlin, 1970.
2. Nienburg, H. J., Hauber, H., Hagen, W., German Patent **843,848** (7-14-1952, appl. 7-1-1950).
3. Nienburg, H. J., Hauber, H., Hagen, W., German Patent **849,103** (9-11-1952, appl. 8-1-1950).
4. Mertzweiler, J. K., Smith, W. M., U.S. Patent **2,725,401** (11-29-1955, appl. 11-19-1948).
5. Usami, S., Nishimura, K., Koyama, T., Fukushi, S., *Bull. Chem. Soc. Jap.* (1969) **42**, 2966.
6. Heck, R. F., Breslow, D. S., *J. Amer. Chem. Soc.* (1961) **83**, 4023.
7. Karapinka, G. L., Orchin, M., *J. Org. Chem.* (1961) **26**, 4187.
8. Rupilius, W., Orchin, M., *J. Org. Chem.* (1972) **37**, 936.
9. Martin, A. R., *Chem. Ind. (London)* (1954) 1536.
10. Natta, G., Ercoli, R., Castellano, S., *Chim. Ind. Milan* (1955) **37**, 6.
11. Marko, L., Szabo, P., *Chemische Technik* (1961) **13**, 482.
12. Moell, H., Eckert, E., Kerber, H., Appl, M., Hohenschutz, H., Walz, H. (BASF), German Patent **1,272,911** (7-18-68, appl. 4-5-66).

RECEIVED July 20, 1973.

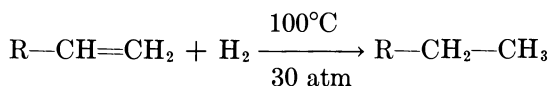
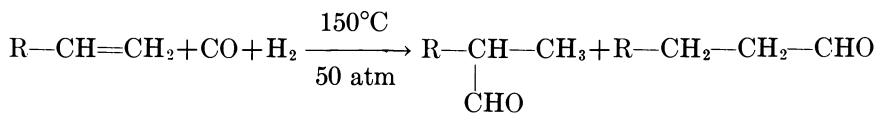
Homogeneous Hydrogenation of Ketones Catalyzed by Cobalt Carbonyl Phosphine Complexes

LA'SZLO MARKÓ, BA'LINT HEIL and SA'NDOR VASTAG

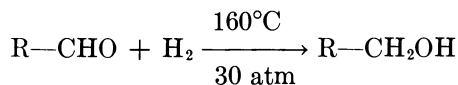
Veszprém University of Chemical Engineering, Veszprém, Hungary

Cobalt carbonyl complexes substituted by tertiary phosphines catalyze the hydrogenation of ketones at 200°C and 150–250 atm. The catalyst is formed in situ from $\text{Co}_2(\text{CO})_8$ and the phosphine(L) added separately to the starting mixture. According to IR spectra $\text{Co}_2(\text{CO})_6\text{L}_2$, $\text{CoH}(\text{CO})_3\text{L}$, and $\text{CoH}(\text{CO})_2\text{L}_2$ are the main cobalt carbonyl species present during the reaction. Trialkylphosphines were more suitable than phosphines with aryl groups. Best results were achieved with P:Co ratios of 2:1. Carbon monoxide retarded hydrogenation whereas tertiary amines like NEt_3 had no significant effect. Consecutive hydrogenation of the secondary alcohol to the corresponding hydrocarbon was usually less than 2%. No measurable asymmetric induction was observed if PRR'R'' type phosphines were used.

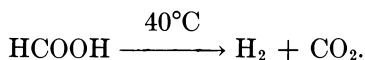
Cobalt carbonyl derivatives containing tertiary phosphines show a variety of catalytic properties. These complexes are useful as catalysts for hydroformylation (1) and hydrogenation (2) of olefins



hydrogenation of aldehydes (3)



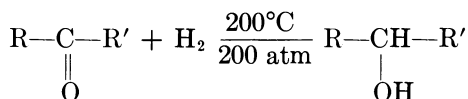
and the decomposition of formic acid (4)



Hydrido carbonyl phosphine complexes of the general formula $\text{CoH}(\text{CO})_n(\text{PR}_3)_{4-n}$ are regarded as the catalysts in these reactions. The active species are probably hydrido complexes with lower coordination numbers formed by the loss of carbon monoxide or phosphine from these precursors.

Few reports on the homogeneous hydrogenation of ketones (5, 6, 7, 8, 9, 10) have been published, and none have been developed into a useful general procedure.

We have found that these tertiary phosphine-substituted cobalt carbonyls are useful as catalysts for the hydrogenation of ketones too.



The catalysts are formed *in situ* from $\text{Co}_2(\text{CO})_8$, and the phosphine is added separately to the starting reaction mixture. IR spectra of samples taken from the reaction mixture show three types of complexes present (3, 11):

Table I. IR Bands of Reaction Products

<i>Complex</i>	<i>Characteristic Strong CO Bands, cm⁻¹</i>	<i>Remarks</i>
$\text{CoH}(\text{CO})_3(\text{PR}_3)$	2050, 1970	main species in samples taken from the autoclave at reaction temperature
$\text{CoH}(\text{CO})_2(\text{PR}_3)_2$	1905	
$\text{Co}_2(\text{CO})_6(\text{PR}_3)_2$	1955	main species in the reaction product cooled under pressure to 20°C

Compared with the analogous hydrogenation of aldehydes, the reaction requires somewhat more drastic conditions (about 200°C and 6 hrs), but the temperature is still within the stability range of the cobalt carbonyl phosphine complexes containing tertiary alkyl phosphines as ligands. If aryl phosphines are used, a more or less pronounced decomposition of the carbonyl complexes can be observed (as indicated by the IR

spectra of the reaction mixture and by the formation of a precipitate) which is also reflected by the diminished yields of the hydrogenation reaction. This may be seen in Table II.

Table II. Effect of Phosphine Structure on the Hydrogenation of Acetophenone^a

<i>Phosphine</i>	<i>Yield of α-phenyl-ethanol, %</i>
PEt ₃	87
PBu ₃	96
P(C ₆ H ₁₁) ₃	67
PMePrPh	77
PEt ₂ Ph	62
PMePh(CH ₂ Ph)	49
P(CH ₂ Ph) ₃	36
PPh ₃	18

^a Reaction conditions: 200°, 6 hrs, 150–250 atm p_{H_2} , 1 mole % Co₂(CO)₈, P:Co = 2:1, solvent hexane.

Best results were achieved with P:Co ratios between 1:1 and 3:1, therefore a 2:1 ratio was used in most experiments. Larger amounts of phosphine significantly inhibited the activity of the catalyst, and no hydrogenation was observed without phosphines (*see* Table III). Carbon monoxide retarded hydrogenation even in small concentrations (< 5 p_{CO}) (*see* Table IV).

Table III. Effect of P:Co Ratio on the Hydrogenation of Acetophenone^a

<i>PBu₃:Co₂(CO)₈</i>	<i>Yield of α-Phenyl-ethanol, %</i>
0:1	—
2:1	90
3:1	94
4:1	96
6:1	92
20:1	36

^a Reaction conditions: 200°, 6 hrs, 150–250 atm p_{H_2} , 1 mole % Co₂(CO)₈, solvent hexane.

Tetrahydrothiophene, added in a S:Co = 2.5:1 ratio diminished the reaction rate to about 1/6 its original value. Tertiary amines such as NEt₃ have no significant effect and thus permit the hydrogenation of nitrogen containing ketones.

Under optimum conditions, secondary alcohol yields between 60–99% were achieved with rather different types of ketones (*see* Table V). Subsequent hydrogenation of the secondary alcohol to the corresponding hydrocarbon was small, usually below 2%. This compares favorably

Table IV. Effect of p_{CO} on the Hydrogenation of Acetophenone^a

Initial p_{CO} , atm	Yield of α -Phenyl-ethanol, %
0	96
2	77
3	66
5	48

^a Reaction conditions: 200°, 6 hrs, 150–250 atm p_{H_2} , 1 mole % $\text{Co}_2(\text{CO})_8$, 4 mole % PBu_3 , solvent hexane.

Table V. Hydrogenation of Different Ketones^a

Ketone	Alcohol	Yield, %
Acetone	2-Propanol	95
Methyl ethyl ketone	2-Butanol	99
Acetophenone	α -Phenylethyl alcohol	96
Benzophenone ^b	Benzhydrol	68
Cyclohexanone	Cyclohexanol	94
4- <i>tert</i> -Butylcyclohexanone	<i>cis</i> -4- <i>tert</i> -Butylcyclohexanol	44
	<i>trans</i> -4- <i>tert</i> -Butylcyclohexanol	44
Menthone ^c	Menthol	40
	Isomenthol	25
	Neomenthol	16
	Neoisomenthol	15
Ethyl acetoacetate	Ethyl-3-hydroxybutyrate	94
5-Diethylamino-2-pentanone	5-Diethylamino-2-pentanol	90

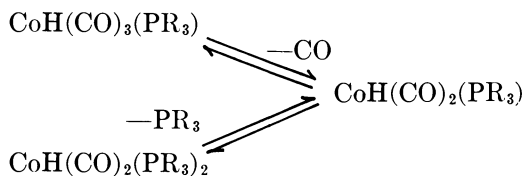
^a Reactions were carried out at 200° and 150–250 atm p_{H_2} with 1 mole % $\text{Co}_2(\text{CO})_8$ + 4 mole % PBu_3 in hexane as solvent. Reaction times 6 hrs.

^b Solvent ethanol, 2 mole % $\text{Co}_2(\text{CO})_8$ + 8 mole % PBu_3 .

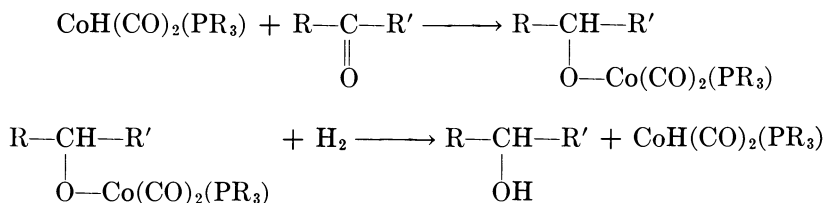
^c Mixture of 86% menthone and 14% isomenthone. Solvent toluene.

with the results obtained with $\text{CoH}(\text{CO})_4$ as catalyst where hydrogenolysis was often the main reaction if aromatic ketones were hydrogenated (5).

No detailed investigation of the reaction mechanism (kinetic measurements, etc.) was performed. The actual catalyst is probably the coordinatively unsaturated $\text{CoH}(\text{CO})_2(\text{PR}_3)$ species which may be formed by the loss of one ligand from both hydrido carbonyl phosphine complexes present in the reaction mixture:



This follows the inhibiting effect of tetrahydrothiophene, excess CO, and PR_3 . The catalytic cycle may then proceed analogously to that supposed in similar reactions:



Using chiral phosphines as catalyst components, asymmetric induction may be expected if $\text{R} \neq \text{R}'$. This assumption was tested with acetophenone as substrate ($\text{R} = \text{Ph}$, $\text{R}' = \text{Me}$) and two different optically active tertiary phosphines as ligands: (*S*)-(+)-PMePrPh and (*S*)-(–)-PMePh(CH_2Ph). Only insignificant optical activity of the product was achieved in both cases (optical yields below 1%). High reaction temperature and/or the low coordination number of the intermediate complexes (lack of steric factors) may be the cause of this negative result.

Experimental

Experiments were performed in a 125 ml stainless steel rocking autoclave. $\text{Co}_2(\text{CO})_8$ (12), (*S*)-(+)-PMePrPh (13, 14) and (*S*)-(–)-PMePh(CH_2Ph) (13, 14) were prepared according to published methods, all other reagents were laboratory grade chemicals.

One-tenth mole ketone, 0.001 mole $\text{Co}_2(\text{CO})_8$, 0.004 mole phosphine, and the quantity of hexane necessary to bring the reaction mixture to 40 grams total weight were measured into the autoclave which was then flushed and pressured to 170 atm with dihydrogen. Pressure rose during heating to 240–270 atm and dropped according to the reaction rate; repressuring was only necessary if larger quantities of substrates were used. In some experiments samples were taken from the autoclave during the reaction.

The cobalt carbonyl phosphine complexes dissolved in the samples, and the products were detected by IR. Ketones, alcohols, and other organic components were determined after distillation (to eliminate cobalt) by GLC.

Literature Cited

1. Slauch, L. H., Mullineaux, R. D., *J. Organometal. Chem.* (1968) **13**, 469.
2. Ferrari, G. F., Andreetta, A., Pregaglia, G. F., Ugo, R., *J. Organometal. Chem.* (1972) **43**, 213.
3. Pregaglia, G. F., Andreetta, A., Ferrari, G. F., Ugo, R., *J. Organometal. Chem.* (1971) **30**, 387.
4. Marangoni, A., Andreetta, A., Ferrari, G. F., Pregaglia, G. F., *Chim. Ind. Milano* (1970) **52**, 862.
5. Wender, I. *et al.*, *J. Amer. Chem. Soc.* (1951) **73**, 2656.
6. Bressan, C., Broggi, R., *Chim. Ind. Milan* (1968) **50**, 1194.
7. Pregaglia, G., Castelli, R., French Patent **1,509,863** (1968).
8. Schrock, R. R., Osborn, J. A., *Chem. Commun.* (1970) 567.

9. Markó, L., Szabó, P., Laky, J., Hungarian Patent **157,605** (1971).
10. Bonvicini, P., Levi, A., Modena, G., Scorrano, G., *Chem. Commun.* (1972) 1188.
11. Piacenti, E., Bianchi, M., Benedetti, E., *Chim. Ind. Milan* (1967) **49**, 245.
12. Szabó, P., Markó, L., Bor, G., *Chem. Tech. Leipzig* (1961) **13**, 549.
13. Korpium, O., Lewis, R. A., Chickos, J., Mislow, K., *J. Amer. Chem. Soc.* (1968) **90**, 4842.
14. Naumann, K., Zon, G., Mislow, K., *J. Amer. Chem. Soc.* (1969) **91**, 7012.

RECEIVED August 20, 1973.

Palladium(II) Acetate-Catalyzed Reactions of Olefins in Acetic Acid

P. M. HENRY and R. N. PANDEY

University of Guelph, Guelph, Ontario, Canada N1G 2W1

Sodium or lithium acetate converts trimeric palladium(II) acetate ($Pd_3(OAc)_6$) first to dimer $M_2Pd_2(OAc)_6$ ($M = Na$ or Li) and then to monomer, $M_2Pd(OAc)_4$. Surprisingly, equilibrium is not instantaneous. Formation of olefin π complexes from the dimer involved a fast replacement of a terminal acetate by olefin to give a dimeric π complex and a slow reaction involving breaking of acetate bridges by olefin to give monomeric π complexes. Studies of vinyl ester exchange showed that $M_2Pd_2(OAc)_6$ is the most active catalytic species, $Pd_3(OAc)_6$ is next, and $M_2Pd(OAc)_4$ is inactive. Allylic ester exchange showed that dimeric π complex is the catalytically active species while monomeric π complex is inactive. Several metal oxidants were found to change the products of oxidation of ethylene from vinyl acetate to 1,2-disubstituted alkanes.

Homogeneous catalysis has made considerable progress in the past decade. Even so there is still uncertainty as to the detailed mechanism of many catalytic reactions. This is particularly true of Pd(II) catalysis. The advances in organic synthesis by Pd(II) catalytic chemistry have been impressive; a recent review (1) of two volumes had few references before 1963. However the advances have mainly been in synthetic chemistry, and relatively little effort has been expended on studies of mechanism in this chemistry. To fill this gap we have undertaken a systematic study of the basic mechanisms of Pd(II) catalysis. Some choice of the many catalytic reactions available for study had to be made. For several reasons the reactions chosen for initial study were olefin oxidation and exchange reactions of vinylic and allylic esters and chlorides. Work has concentrated on the $PdCl_2$ -NaCl or LiCl systems in

acetic acid and has recently been reviewed (2). The next system chosen for study was chloride-free palladium(II) acetate system in acetic acid which has been under investigation in these laboratories for the past year and a half. The acetate system has many interesting features not found in the chloride system. Below is a summary of the previous studies on the chloride containing system which relate to the studies on the chloride free system.

The Palladium(II) Chloride System in Acetic Acid-Equilibria

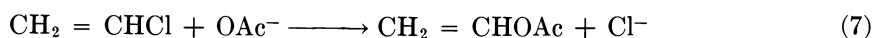
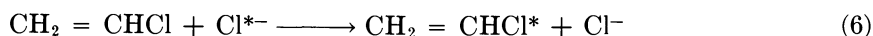
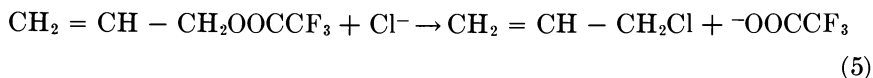
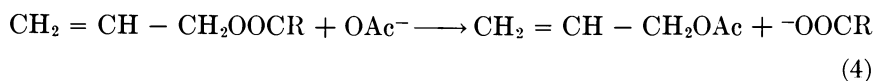
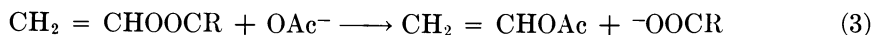
To interpret the kinetics in any metal ion-catalyzed reaction, it is necessary to know the equilibria present in the system. A molecular weight and spectral study indicated the following two equilibria are



operative where K_1 has a value of $0.1M^{-1}$ and K_D has a value of $2.6M^{-1}$ at 25°C . The rate of equilibration in this system is instantaneous.

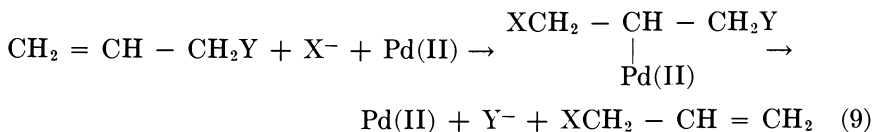
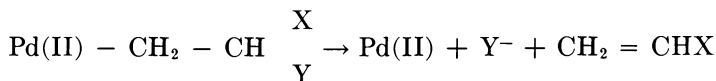
Exchange

The following exchanges have been studied in the Pd(II)chloride-chloride containing system.

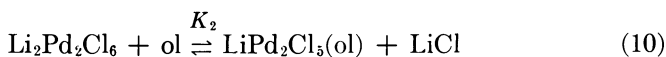


These studies, plus analogy with other Pd(II) chemistry (3), leave little doubt that the general mechanism for these exchanges involves addition of acetate (acetoxy-palladation) or chloride (chloro-palladation) followed by elimination of acetate (deacetoxy-palladation) or chloride

(dechloropalladation). The schemes for vinyl and allylic exchange are given by Equations 8 and 9 (X or $Y = \text{Cl}^-$, $^-\text{OOCR}$, or OAc^-).



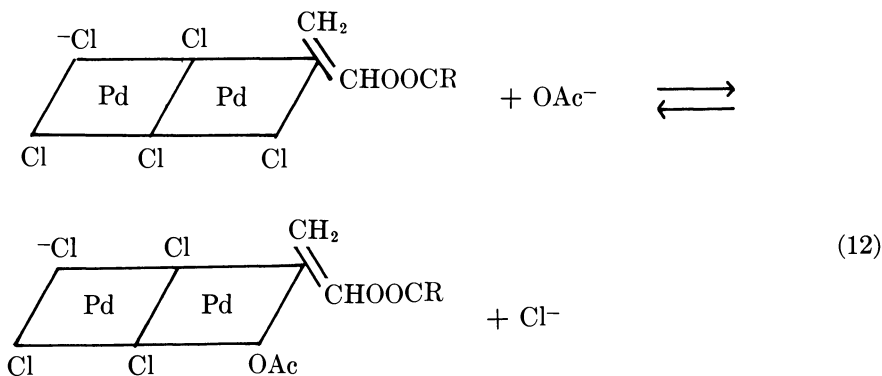
The detailed mechanism by which these additions and eliminations occur is of interest. The rate expression in all cases is consistent with the first step of the exchange being the formation of a dimeric π complex according to Equation 10 (ol = vinyl or allylic ester or chloride). π com-



plex formation is apparently required to activate the olefin for attack of nucleophile. Now monomeric π complex can be formed *via* Equation 11, and as shall be discussed later, in some exchanges the formation of



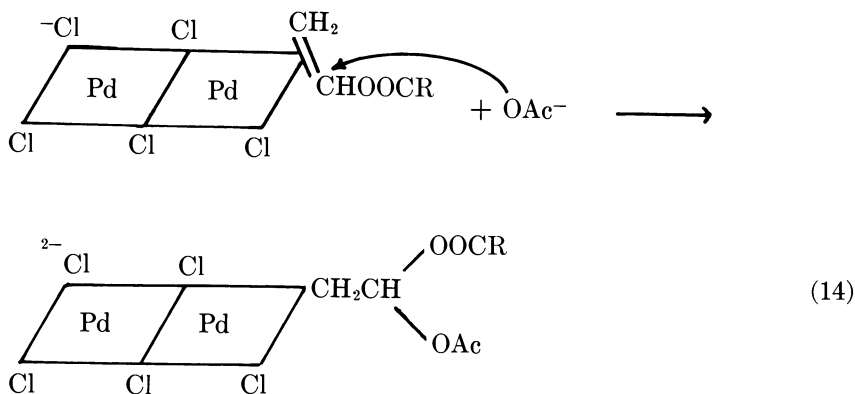
monomeric π complex predominates over dimeric π complex formation. However the monomeric π complex is completely unreactive. This lack of reactivity is believed to result from electrostatic factors.



The next step in the reaction sequence must involve attack of acetate or chloride to give the Pd(II) σ -bonded carbon intermediate. First consider the case of acetate using vinyl ester exchange as an example. If acetate were attacking from the coordination sphere, it must enter the coordination sphere by means of the equilibrium shown in Equation 12. What would the rate expression for this route be? First the equilibria shown in Equation 10 would require a $[\text{Li}_2\text{Pd}_2\text{Cl}_6][\text{C}_2\text{H}_3\text{OOCR}]/[\text{LiCl}]$ term in the rate expression while Equation 12 would require a $[\text{LiOAc}]/[\text{LiCl}]$ term so the complete rate expression would be that given by Equation 13. Actually the rate expression contained a $[\text{LiCl}]$ term to the first power,

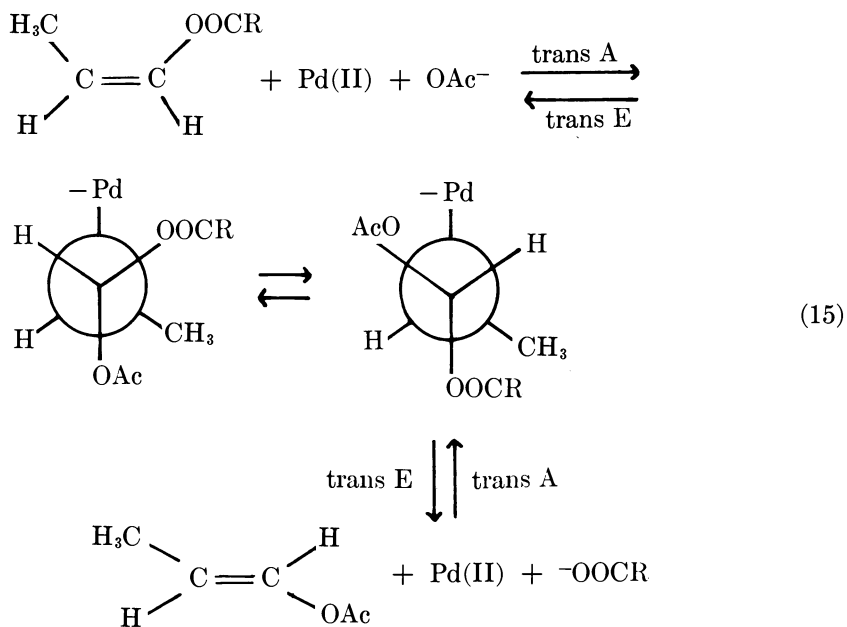
$$\text{rate} = \frac{k[\text{Li}_2\text{Pd}_2\text{Cl}_6][\text{C}_2\text{H}_3\text{OOCR}][\text{LiOAc}]}{[\text{LiCl}]^2} \quad (13)$$

indicating the equilibrium represented by Equation 12 is not taking place. This also indicates that attack of acetate is taking place from outside the coordination sphere. A Reaction 14-type of attack implies

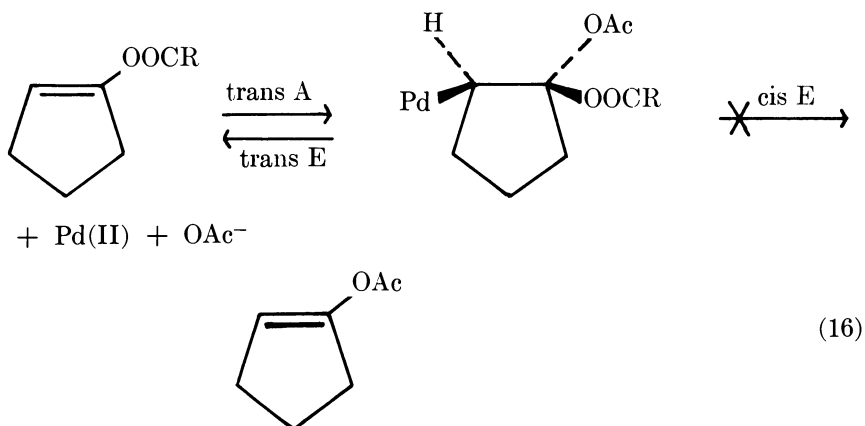


stereospecific *trans* stereochemistry. Results on the exchange of *cis*- and *trans*-1-propen-1-yl esters with acetic acid confirmed that acetoxy-palladation (and thus deacetoxy-palladation by the principle of microscopic reversibility) is a stereospecific process. The result with *cis* ester is shown in Equation 15 (A = addition; E = elimination). Thus stereospecific addition-elimination requires that isomerization occur every time there is exchange. This is the observed result.

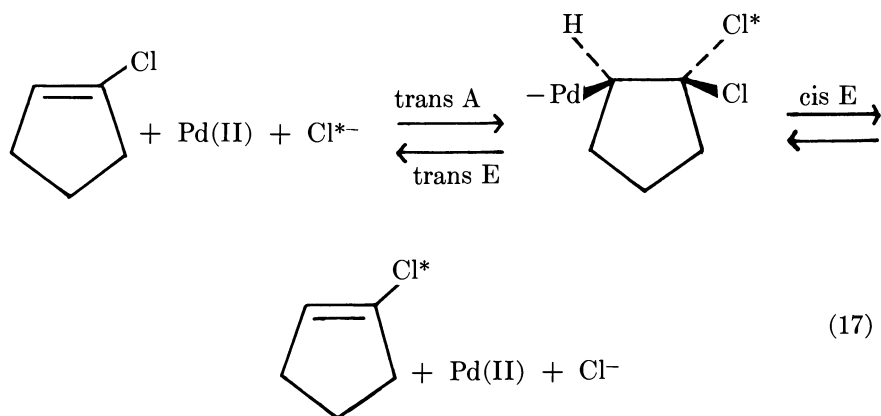
Further evidence that acetoxy-palladation is stereospecific is provided by the fact that cyclic esters such as 1-cyclopenten-1-yl ester do not exchange. As shown by Equation 16, stereospecific addition-elimination would not permit exchange.



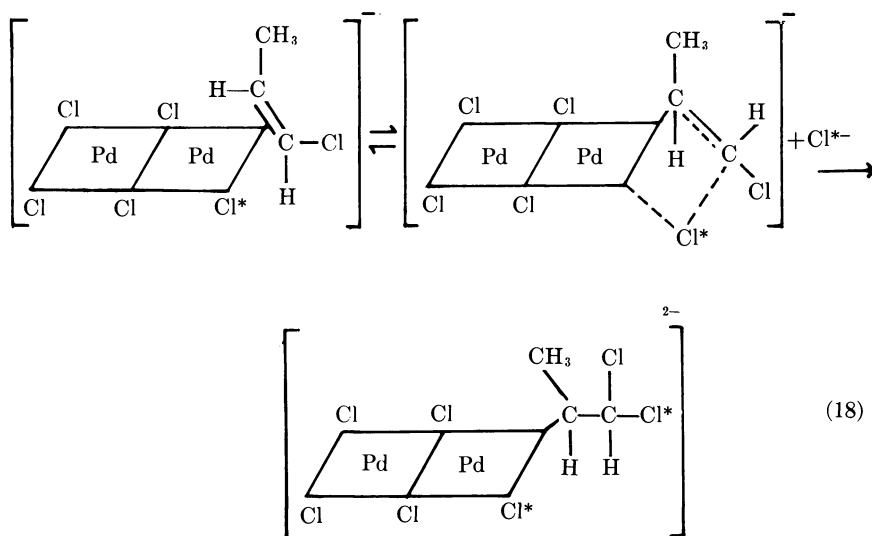
Chloropalladation is somewhat different. Acetate does not attack cis because it is believed that chloride is much more strongly complexed to Pd(II) than acetate, and thus, acetate cannot get in the coordination sphere to attack cis. Chloride is already in the coordination sphere and thus in position for cis attack. Chloride might also be expected to attack trans from outside the coordination sphere as does acetate. For these reasons, chloropalladation may not be as stereospecific a process as acetoxy-palladation; in fact, this is the case. For example 1-chlorocyclo-



pentene exchanges at a fair rate. As shown by Equation 17, this result indicates non-stereospecific addition-elimination.



An interesting feature brought out by kinetic studies of chloride exchange is that *cis* addition does not occur unless chloride is available to fill the incipient coordination site. This shows itself as a $[LiCl]$ term in the numerator of the rate expression. The scheme for *cis* chloropalladation is shown in Equation 18.



The final result of interest in the exchange studies is the inhibition of allylic ester exchange (Equation 4) by the allylic esters themselves. Both the starting allylic ester, as well as the allylic acetate product, readily formed monomeric π -complex according to Equation 19. Since

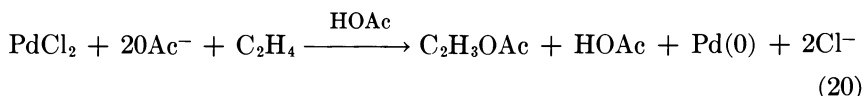
this monomeric π complex was unreactive, it served to decrease the rate of exchange. The tendency to form monomeric π complexes according to Equation 19 is much greater than the tendency to form reactive dimeric



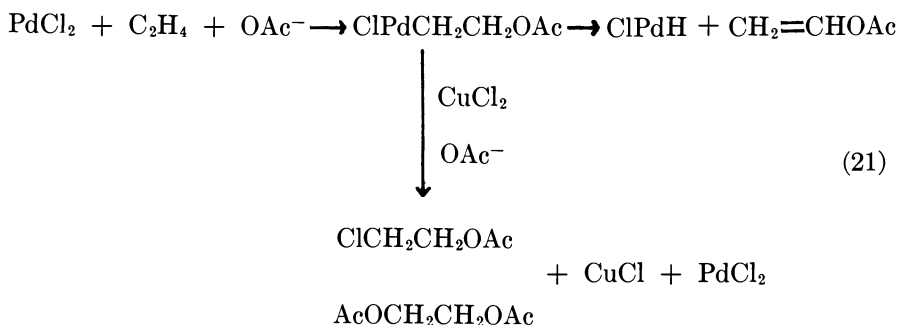
complexes (Equation 10). For that reason formation constants for formation of dimeric π complexes could not be measured. This inhibition was not noted in the case of vinylic ester exchange because vinylic esters have a much lesser tendency to form π complexes than do allylic esters.

Oxidation

Palladium(II) chloride alone in acetic acid oxidizes olefins to unsaturated esters. For instance ethylene is oxidized to vinyl acetate. Reaction 20 almost certainly proceeds by way of a Pd(II) σ -bonded

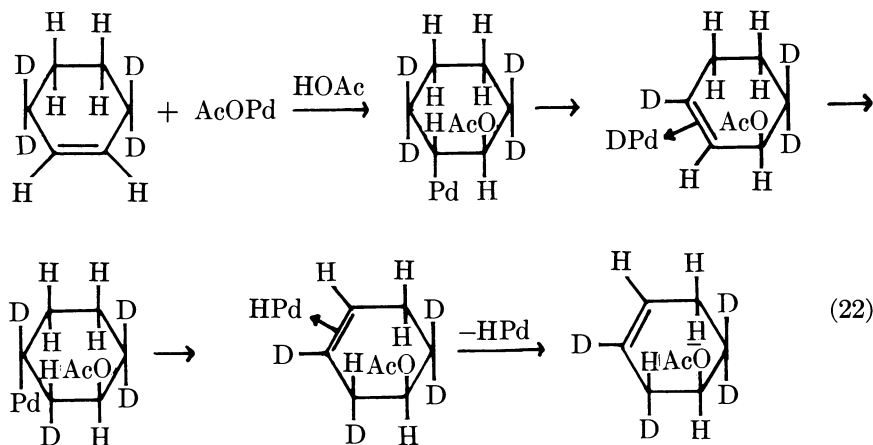


intermediate analogous to that shown in Equation 8 (3). An interesting variation of this reaction occurs when CuCl_2 is added to the system. The product distributions change from entirely unsaturated esters to mixtures of unsaturated esters and disubstituted alkanes (4), and at high CuCl_2 concentrations the only products are the alkanes. It is believed that the alkanes arise from reaction of the Pd(II) σ -bonded intermediate with CuCl_2 . The reaction scheme for ethylene is given by Equation 21. Note



that if the intermediate is not captured by CuCl_2 , it decomposes to Pd(II) hydride. The hydride is unstable and decomposes to Pd(O) and HCl. In the absence of CuCl_2 the entire reaction, of course, proceeds by this path.

Very little work has been carried out on the kinetics of the PdCl_2 only system. This is probably because of the slowness of the reaction. A stereochemical study using 3,3,6,6-cyclohexene- d_4 , however, provided evidence for *trans*-acetoxypalladation in this system (5). For example the reaction scheme for formation of 3-cyclohexen-1-yl acetate is shown in Equation 22 (from Ref. 5). This scheme involves *trans*-acetoxypalladation and *cis*-Pd(II)-H (D) eliminations and additions. This agrees with the exchange kinetics which also suggest *trans*-acetoxypalladation.



A kinetic study (6) of the oxidation of ethylene in the PdCl_2 - CuCl_2 indicated the reaction was first order in $[\text{PdCl}_2]$ and $[\text{CuCl}_2]$ supporting a scheme with interaction between a Pd(II) species and CuCl_2 . Stereochemical studies (5) indicate that both unsaturated esters and disubstituted alkanes arise from a common intermediate, supporting the scheme given by Equation 21.

$\text{Pd}(\text{OAc})_2$ System in Acetic Acid

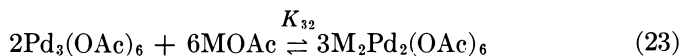
This system is worthy of study because the chloride system studies give us several possibilities for predicting the reaction paths. First, in the acetate containing system acetate is both a ligand and a reactant, so different stereochemical results are possible if the mechanistic interpretations in the chloride system are correct. Thus, in the acetate system addition of acetate could occur *cis* as well as *trans*. Second, many reactions, such as olefin oxidation, occur more readily in this system (7, 8). Third, peculiar results (*see* Oxidation) which require explanation have already been reported for this system. Finally, acetate is likely to be quite

different from chloride as a bridging ligand. The equilibria between the various Pd(II) species present in the two systems will thus probably be quite different. As discussed below this last expectation was realized.

Equilibrium between Pd(OAc)₂ and NaOAc or LiOAc

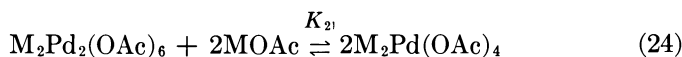
In the absence of added acetate, molecular weight measurements showed the palladium(II) acetate existed in the form of trimer, Pd₃(OAc)₆.

The reaction of the trimer with acetate was measured spectrally. The reaction was measurably slow at 25°C with half-lives on the order of hours. The equilibrium was first determined on solutions which had been allowed to stand for sufficient time (at least 12 hrs) to completely equilibrate. Isosbestic points in the initial region of acetate concentration suggested that two Pd(II) species were present in this region. The only equilibrium which satisfied the data was conversion of trimer to dimer. (M = Na or Li).



The conversion to dimer was complete at *ca.* 0.2M NaOAc and 0.5M LiOAc. The value of K_{32} for NaOAc is $7.8 \times 10^4 M^{-5}$ while that for LiOAc is $1.76 \times 10^2 M^{-5}$.

Further addition of acetate caused another series of spectral changes which could best be interpreted as conversion of dimer to monomer. This reaction was also slow. Studies on fully equilibrated solutions in the



NaOAc system gave a K_{21} of $7.6 \times 10^{-4} M^{-1}$.

The kinetics of the slow conversion of trimer to dimer was studied in detail. The reaction had the following rate expression:

$$\text{rate} = (k_1 + k_2 [\text{MOAc}])[\text{Pd}_3(\text{OAc})_6] \quad (25)$$

This simple expression is consistent with the slow step of the reaction being the breaking of one of the six acetate bridges by acetate or acetic acid. The subsequent decomposition to dimer is fast.

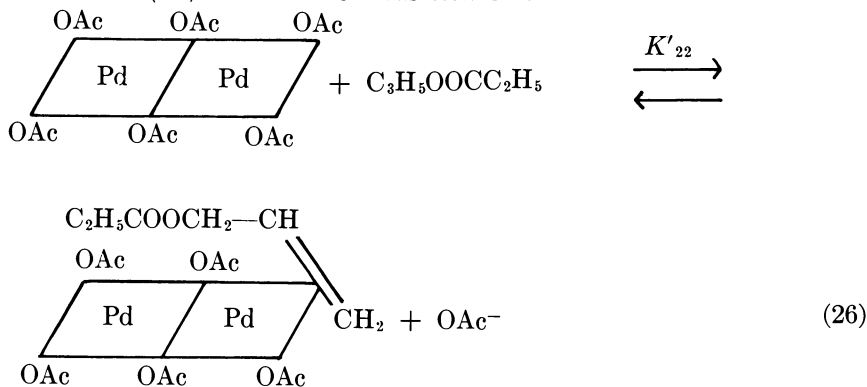
In comparison with the previous studies in the chloride system the acetate equilibria are considerably more complicated. An extra equilibrium is present in the acetate system, and the rate of attainment of equilibration is slow.

Olefin π Complex Formation

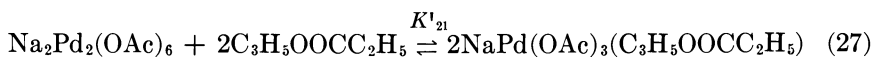
Since the reaction of Pd(II) species with acetate is slow, we might predict the reactions of olefins with the Pd(II) species to give the intermediate π complexes which are also slow. However, this is only partially true.

In the chloride-containing system, two types of equilibria were detected; the formation of unreactive monomeric π complex *via* Equation 19 and the formation of reactive dimeric π complex *via* Equation 10. In the case where complexing could be detected (allylic ester exchange) the monomeric π complex is so predominant that the dimeric π complex formation could not be detected.

Olefin complexing in the acetate system was studied in the region of acetate concentration in which the dimer is the predominant species. Addition of olefins (allylic esters, styrene, or 3,3,3-trimethylpropene) causes two series of spectral changes. First there is a rapid change followed by a much slower change taking place over hours. Studies on completely equilibrated solutions using allyl propionate as olefin indicated complexing was complete at an olefin concentration of 0.4M when the total Pd(II) concentration was 0.0128M.



The fast equilibrium could be studied at short reaction times at which the second equilibrium did not interfere. Treatment of the spectral data by standard procedures indicated the fast equilibrium is the formation of dimeric π complex. Studies on fully equilibrated solutions showed that the slow equilibrium is the formation of monomeric π complex. The value of K'_{22} in Equation 26 is 0.17 while the value for K'_{21} in Equation 27 is 16.5. These constants are such that in fully equilibrated solutions the concentration of monomeric π complex is much higher than that of dimeric π complex. The chloride system has the same effect, but both



equilibrations were so rapid that dimeric π complex formation was not detected.

Vinyl Ester Exchange

The kinetics of vinyl ester exchange (Equation 3) was studied using vinyl propionate as reactant. The runs were carried out on solutions which had been allowed to stand until complete equilibration of all Pd(II) species had been achieved. At a given palladium(II) acetate concentration the rate of exchange first increased sharply with increasing [NaOAc] until a maximum was reached at 0.2M [NaOAc]. With further increase in [NaOAc], the rate gradually decreased. A plot of the data is given in Figure 1. Using the value K_{32} and K_{21} in Equations 23 and 24, respectively, it can be shown that the initial increase in rate results from conversion of $\text{Pd}_3(\text{OAc})_6$ to more reactive $\text{Na}_2\text{Pd}_2(\text{OAc})_6$. The gradual decrease in rate at higher [NaOAc] results from conversion of $\text{Na}_2\text{Pd}_2(\text{OAc})_6$ to unreactive $\text{Na}_2\text{Pd}(\text{OAc})_4$. The complete rate expression is

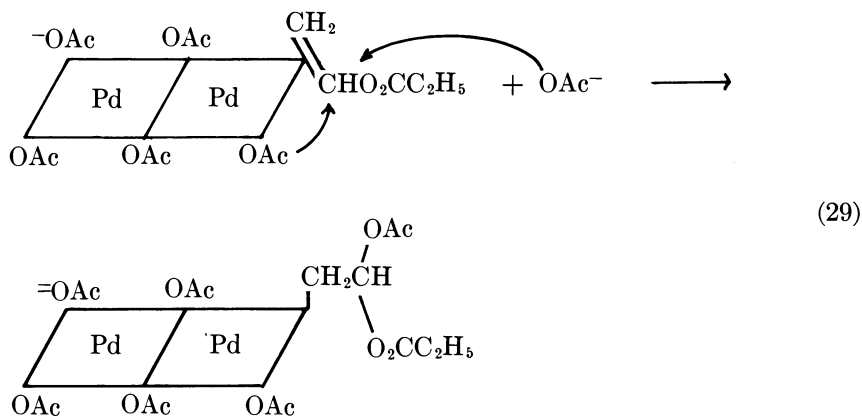
$$\text{rate} = (k_t[\text{Pd}_3(\text{OAc})_6] + k_d[\text{Na}_2\text{Pd}_2(\text{OAc})_6])[\text{C}_2\text{H}_3\text{OOC}_2\text{H}_5] \quad (28)$$

given by Equation 28 where k_t is $0.045 \text{ M}^{-1}\text{sec}^{-1}$ and $k_d = 0.102 \text{ M}^{-1}\text{sec}^{-1}$ at 25° .

Stereochemical studies were carried out using *cis*- and *trans*-1-propen-1-yl propionate. It was found that each of these esters exchanged to give mixtures of *cis*- and *trans*-1-propen-1-yl acetates. As shown by Equation 15, this result is unexpected if acetoxy-palladation were a stereospecific process. Further evidence was provided by the fact that 1-cyclopenten-1-yl propionate exchanged to give the corresponding acetate. Again, as shown by Equation 16, this result is unexpected if acetoxy-palladation were stereospecific.

Acetate must thus be capable of attacking from both inside and outside the coordination sphere as shown in Equation 29.

The rate equation (Equation 28) must be examined in light of this mode of addition. The first point to note is that the expression does not contain an acetate term since formation of the reactive dimeric π complex by a pre-equilibrium analogous to Equation 26 would introduce a $1/[\text{NaOAc}]$ term in the rate expression. Now this term must be cancelled by a catalytic term in [NaOAc] in the numerator of the rate expression. It is easy to see that attack of acetate from outside the coordination sphere would cause this [NaOAc] term in the rate expression but for *cis* addition the need for this term is not so obvious. However the situation is exactly analogous to the chloride exchange for chloride in the chloride



containing system (Equation 6). Here the rate expression and stereochemical results were analogous. The need for a chloride term in the rate expression for *cis*-chloropalladation was attributed to the need for chloride to fill the incipient vacant coordination site on Pd(II). The scheme is given in Equation 18. An exactly analogous route must be operative for *cis*-acetoxypalladation.

Allyl Propionate Exchange

The allyl propionate exchange (Equation 4) also involves acetoxy-palladation, and thus its kinetic behavior might be expected to parallel that for vinyl propionate exchange. In its general features it is, in fact, very similar to vinyl ester exchange. The rate profile with sodium acetate concentration is of the same form as Figure 1.

However the one important difference is that allyl propionate is much better at π -complex formation than is vinyl propionate. Thus the vinyl propionate kinetics in the chloride containing system do not exhibit inhibition by vinyl propionate. On the other hand allyl propionate strongly inhibits its own exchange because it forms appreciable amounts of unreactive monomeric π complex according to Equation 11. Inhibition in the acetate system is more complicated because the equilibrium to form unreactive monomeric π complex (Equation 27) is slow. Thus, initially only the reactive dimeric π complex is formed (Equation 26). However as the exchange proceeds, more of the monomeric π complex is formed, and the rate of exchange gradually decreases.

Olefin Oxidation

Olefin oxidation in the chloride free system is of particular interest because of several observations. First product distributions are different

from those found for olefin oxidation by palladium(II) chloride (9). For instance the product distributions with cyclohexene are somewhat different in the chloride free media than in the chloride containing media.

The product distributions and their change with acetate concentration is also of interest. A study of the initial product distributions with various terminal and internal olefins provided strong evidence for an acetoxy-palladation step followed by a Pd(II) hydride elimination (7).

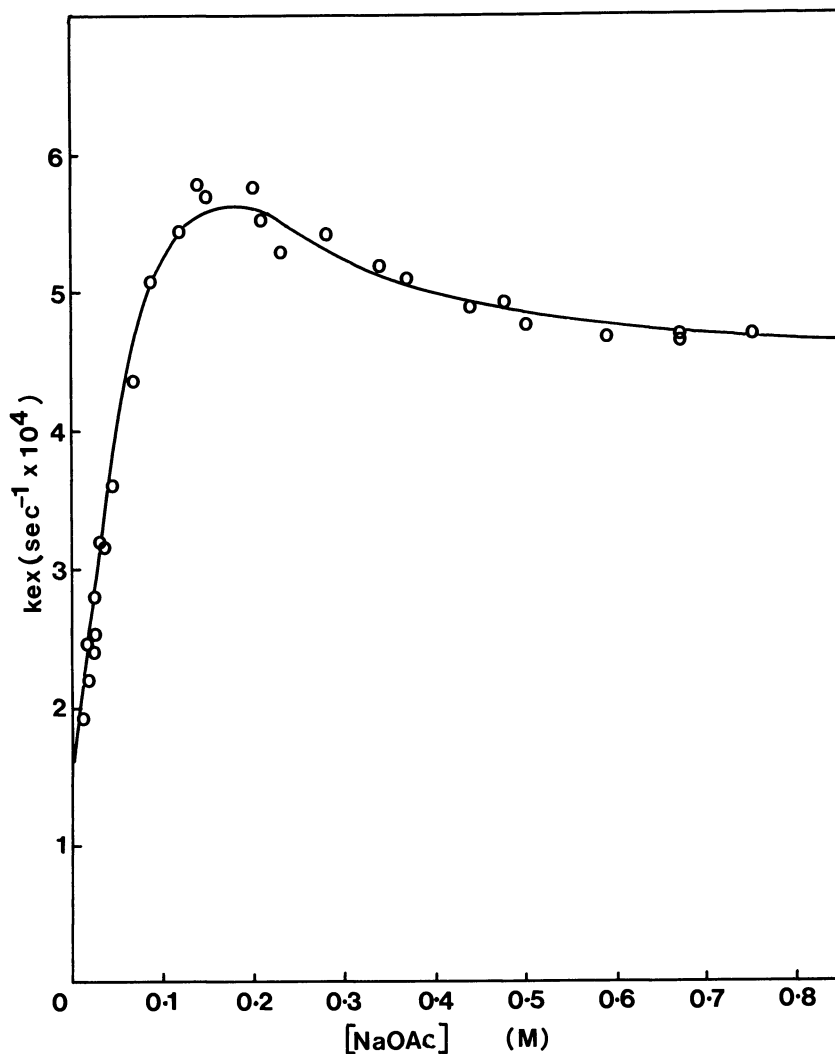
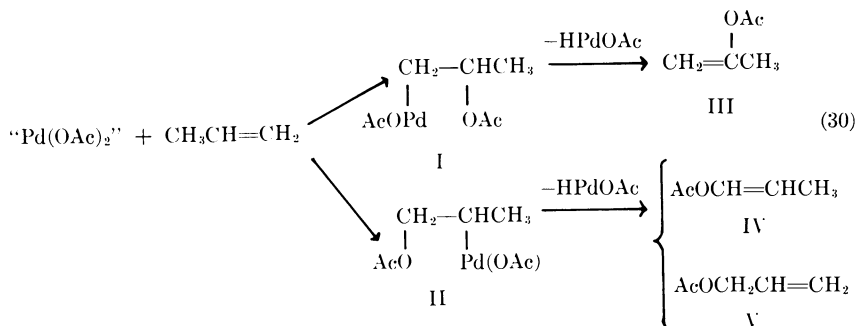


Figure 1. Plot of calculated (—) and experimental (O) rate constant for exchange of vinyl propionate (k_{ex}) vs. the concentration of NaOAc at 25°C; total [Pd(II)] = 0.0128M

The scheme for propylene is given in Equation 30. "Pd(OAc)₂" means the state of aggregation is unknown.



It has been reported that the product distributions change with added acetate in both the chloride containing (10) and chloride free media (10, 11, 12). In one report (12) in the absence of added acetate the product consisted of 96% isopropenyl acetate, III. At [NaOAc] = 0.88 molar, III made up only 10% of the product, the other 90% being the allyl acetate, V.

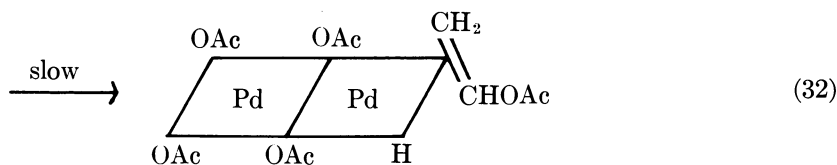
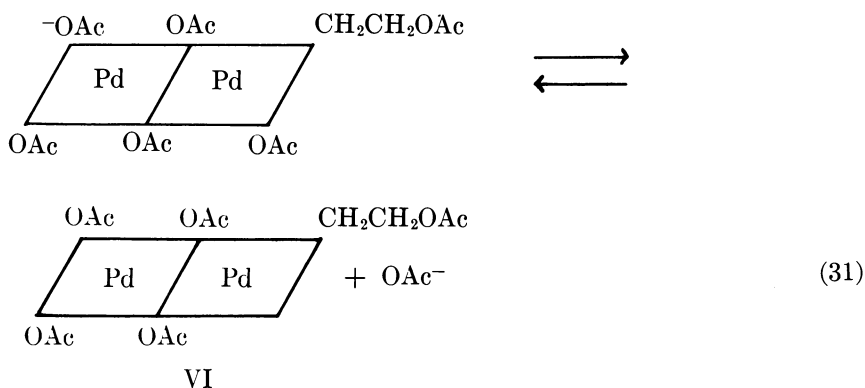
Finally a kinetic study of the oxidation of ethylene by palladium(II) acetate gave a rate-[NaOAc] profile similar to Figure 1 which could also be interpreted as conversion of less reactive trimer to more reactive dimer. However at [NaOAc] > 0.2M the decrease in rate with increase in [NaOAc] is much greater than that shown in Figure 1 and corresponds to a 1/[NaOAc] term in the rate expression for reaction of dimer. This difference in rate expression between exchange and olefin oxidation could have very interesting mechanistic implications. For instance, the added acetate inhibition term could result from the need for a vacant coordination site on the Pd(II) before hydride elimination can occur. The scheme is shown in Equations 31 and 32.

The acetate inhibition would result from the equilibrium shown in Equation 31. This scheme has analogy in the exchange of vinyl chloride with acetate (Equation 7) in the chloride containing media (13). It was found that chloride was not eliminated from the intermediate (Equation 8, X = OAc; Y = Cl) until a vacant coordination site was present on the Pd(II).

This scheme could also explain the changes in product distributions at different [NaOAc] (Equation 30). Thus if I is the intermediate formed by kinetic control at low [NaOAc], when HPdOAc elimination is rapid, III would be expected to be the main product. However at higher [NaOAc], at which HPdOAc elimination is much slower, I and II will have an opportunity to reach an equilibrium distribution for which II

may be the intermediate present in largest amounts. Thus V could then become the predominant product.

The kinetics of the oxidation of styrene and 3,3,3-trimethylpropene are presently under investigation to see if they follow the kinetics reported by the earlier workers for ethylene. These studies are quite complicated because they must take into account the π -complex equilibria discussed previously and which the earlier workers did not consider. Preliminary results indicate that the initial increase in rate with increasing [NaOAc] found for exchange (Figure 1) is also operative for oxidation. However the shape of the rate [NaOAc] profile at higher [NaOAc] is uncertain.



Finally it was mentioned that the $\text{PdCl}_2\text{-CuCl}_2$ combined oxidation to give disubstituted alkenes (Equation 21) did not operate in chloride free media. A further study of this type of oxidation by Pd(II) plus other oxidants indicated that a number of other oxidants can replace CuCl_2 (14). These include $\text{K}_2\text{Cr}_2\text{O}_7$, $\text{Pb}(\text{OAc})_4$, NaNO_3 , NaNO_2 , $\text{Tl}(\text{OAc})_3$, and AuCl_4^- . Some of these, such as $\text{Pb}(\text{OAc})_4$, $\text{K}_2\text{Cr}_2\text{O}_7$, and $\text{Tl}(\text{OAc})_3$ give the oxidation in the absence of chloride. The main product obtained in most chloride free systems is ethylene glycol diacetate but in some cases appreciable quantities of monoacetate and ethylidene diacetate were formed.

Oxidations which did not give the reaction at 25°C include $\text{Fe}(\text{OAc})_3$, KMnO_4 , MoCl_5 , and MoOCl_4 . Certainly more work is required before this type of reaction will be understood.

Acknowledgment

The authors thank J. E. McCaskie for communicating some of his results before their publication in thesis form.

Literature Cited

1. Maitlis, P. M., "The Organic Chemistry of Palladium," Vols. I & II, Academic, New York, 1971.
2. Henry, P. M., *Accounts Chem. Res.* (1973) **6**, 16.
3. Henry, P. M., *Trans. N.Y. Acad. Sci.* (1973) **33**, 41.
4. Henry, P. M., *J. Org. Chem.* (1967) **32**, 2575.
5. Henry, P. M., *J. Amer. Chem. Soc.* (1972) **94**, 7305.
6. Clark, D., Hayden, P., Smith, R. D., *Amer. Chem. Soc., Div. Petrol. Chem., Prepr.* **14** (2), B10 (Minneapolis, April 1969).
7. Kitching, W., Rappoport, Z., Winstein, S., Young, W. G., *J. Amer. Chem. Soc.* (1966) **88**, 2054.
8. Moiseev, I. I., Belov, A. P., Igoshin, V. A., Syrkin, Ya K., *Dokl. Akad. Nauk. SSSR* (1967) **173**, 863.
9. Brown, R. G., Davidson, J. M., Triggs, C., *Amer. Chem. Soc., Div. Petrol. Chem., Prepr.* **14** (2), B23 (Minneapolis, April 1969).
10. Schultz, R. G., *ADVAN. CHEM. SER.* (1968) **70**, 97.
11. Clark, D., Hayden, P., Smith, R. D., *Discuss. Faraday Soc.* (1968) **45**, 98.
12. McCaskie, J. E., Ph.D. Thesis, University of California, Los Angeles (1971).
13. Henry, P. M., *J. Amer. Chem. Soc.* (1972) **94**, 7311.
14. Henry, P. M., *J. Org. Chem.* (1973) **38**, 1681.

RECEIVED July 30, 1973. Work was supported by the National Research Council of Canada.

Kinetics and Mechanism in the Homogeneous Oxidation of Hexenes Catalyzed by Palladium Acetate

ROBERT G. BROWN and JOHN 'M. DAVIDSON*

Department of Chemical Engineering, Pembroke St., Cambridge, England

1-Hexene (I) reacts with Pd(OAc)₂ in HOAc at 25°C yielding first Pd₃(1,2,3-h³-C₆H₁₁)₂(OAc)₄ and then Pd₂(1,2,3-h³-C₆H₁₁)₂(OAc)₂. cis-2-Hexene (II) forms similar complexes. 1-Hexene I reduces Pd₃(OAc)₆ with formation of 1-hexen-2-yl acetate, 2-hexanone, etc. and isomerizes to 2-hexenes. With Pd₃(OAc)₆, I is oxidized by O₂ to esters as before. Small amounts of hexenols and hexenones are formed by free radical reactions. Under conditions of catalytic oxidation the yield of 2-hexenes is 1.4 times that of oxidized products suggesting sequential reactions. 3,3-Dimethyl-1-butene is similarly oxidized by O₂ to 3,3-dimethyl-1-buten-2-yl acetate. The yield is 50% of that expected on O₂ consumption. Palladium acetate also catalyzes the oxidation of II to hexenols and allylic esters, etc. Oxidation of II is slow and inhibited by quinol. Empirical rate laws are given.

By virtue of their industrial applications two of the most important Cl-Pd(II) catalyzed olefin oxidation reactions (1) are the oxidation of ethylene in water (2) and in acetic acid (3). In both cases the reaction of a π complex appears to be rate determining. Although kinetic studies give interesting information about the nature of palladium-containing species and about the nucleophilic character of the reaction, other questions remain unresolved. In the Wacker reaction, tracer studies using C₂D₄ show that a deuterium shift affords CD₃CDO, but the

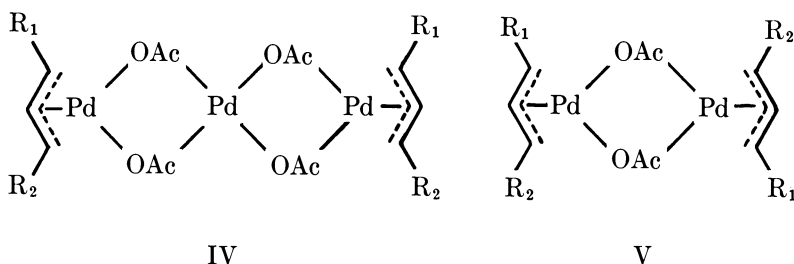
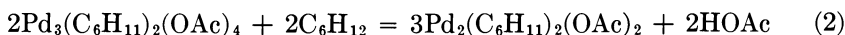
* Present address: Department of Chemical Engineering, School of Engineering Science, University of Edinburgh, Edinburgh, Scotland EH9-3JL.

mechanism of the decomposition of the organopalladium intermediate to acetaldehyde is still not known nor is the mechanism of the so-called regeneration step known which may conceivably involve the oxidation species derived from Pd(0), Pd(I) (5), or PdH⁺ (6). Copper(II), which is used as a co-catalyst, promotes glycol derivative formation in the decomposition of the organometallic intermediates (3). Very little attention has been given to the role of oxygen. It is often assumed that it serves only to reform the palladium(II) catalyst species. Our purpose has been to seek reactions to study the "catalyst regeneration" and oxygen reactivity in these systems.

A number of investigators have studied the oxidation of higher olefins such as *n*-hexenes (7, 8, 9) and *n*-octenes (8). In some cases copper(II) chloride was used as the oxidant with palladium(II) as catalyst while in other systems palladium acetate was used as a stoichiometric oxidizing agent rather than as a catalyst. There is general agreement (8, 9, 10) that in the oxidation of α -olefins addition of palladium acetate to the double bond follows the Markovnikov rule, leading to 1-alken-2-yl acetates as the major products. Sodium acetate promotes the formation of allylic esters which are also the principal oxidation products of internal olefins. Our preliminary studies (11, 12) show that palladium acetate catalyzes the oxidation of higher olefins in acetic acid under mild conditions (25°C, 1 atm O₂) even in the absence of Cu²⁺ and Cl⁻ ions that might have some co-catalytic action. It seems that consistent rate data for palladium acetate-catalyzed reactions can be obtained only after rigorous attention to the purity of the reagents, especially the catalyst which may contain traces of cyanide ion (13) or oxyanions of nitrogen (14) (*see* Experimental). We report data for the catalytic oxidation of 1-hexene (I), *cis*-2-hexene (II), and 3,3-dimethyl-1-butene (III) and compare them with the known reactivity of cyclohexene (15). Mechanistic interpretation is incomplete, but the rate laws reveal striking differences in the reactivities of the various olefins. Thus the familiar oxypalladation-deoxypalladation mechanism substantially accounts for the reactions of the α -olefins of types I and III whereas type II is oxidized mainly *via* a free radical route. Although III displays conventional chemistry as far as its oxidation product is concerned, the overall stoichiometry is unusual and probably indicates a complex type of catalyst regeneration. The rate laws depend on the types of palladium complex formed by the olefin. Allylic complexes are formed very readily (1, 16), and they are more significant in terms of overall kinetics than suspected until now. The allylic moiety is generally stable, but the exception appears to be 1,2,3-*h*³-cyclohexenylpalladium, where decomposition provides the route to allylic oxidation.

Formation of Complexes and Stoichiometric Oxidation

Palladium acetate has a trimeric ring structure (17) which is necessarily cleaved if a complex is formed. Both the α -olefin I and the internal olefin II follow a similar path in reacting with $\text{Pd}_3(\text{OAc})_6$ to form trinuclear 1,2,3- and 2,3,4-*h*³-hexenylpalladium complexes, $\text{Pd}_3(\text{C}_6\text{H}_{11})_2(\text{OAc})_4$ (IVa and IVb, respectively) (Reaction 1). At 25°C in acetic acid this reaction is complete within 6 hrs, and if oxygen is absent, a second reaction follows in which the corresponding dimeric 1,2,3- and 2,3,4-*h*³-hexenyl complexes $\text{Pd}_2(\text{C}_6\text{H}_{11})_2(\text{OAc})_2$ (Va and Vb, respectively) appear (Reaction 2).



IVa and Va have $\text{R}_1 = \text{H}$, $\text{R}_2 = \text{C}_3\text{H}_7$

IVb and Vb have $\text{R}_1 = \text{CH}_3$, $\text{R}_2 = \text{C}_2\text{H}_5$

The complexes were characterized by elemental analysis, molecular weight, quantitative hydrogenation, and NMR. All were fluxional (IVa and b have 10 isomers including optical isomers) but gave characteristic first-order NMR spectra in the fast exchange limit at 60°C in CDCl_3 , *e.g.*, Va had a double-triplet centered at $\tau = 4.82$ and doublets at $\tau = 6.40$ and 7.44, and IVa was similar but incompletely coalesced. In view of the singlet resonance from the acetate group in the trinuclear complexes, it is assumed that the structure is the simple linear one shown in IV. However this spectrum could arise through exchange in a more complex structure. Few useful assignments could be made in the IR spectra of these complexes, but the following strong bands allowed semiquantitative analysis of mixtures of solids recovered from reaction solutions: $\text{Pd}_3(\text{OAc})_6$, 1600, 700; IVa and b, 1560, 700; Va and b, 1560, 675 cm^{-1} . Presumably the trihapto-allylic complexes are formed directly from π -olefin complexes by loss of acetic acid. In general trihapto-alkenylpalladium complexes are less readily prepared from straight chain olefins than from

branched ones (16), and this may be attributable to the occurrence of intractable mixtures of various polynuclear species.

It is now possible to understand the curious phenomenon whereby the reaction of palladium acetate with I *in vacuo* first rapidly produces a metal precipitate and then slows at about 20% conversion and finally stops with much of the palladium(II) unreacted. These stages in the reaction correspond to oxidation first by $\text{Pd}_3(\text{OAc})_6$ and then by IVa with ultimate formation of the inert species Va. A complex mixture of hexenyl acetates is formed in the oxidation of which the major constituent 1-hexen-2-yl acetate (VI) is 0.68 mole fraction of the whole mixture. Overall the mixture is closely similar to that obtained in the catalytic reactions of O_2 described later, suggesting that the same active palladium-containing species is involved. Much of I is isomerized to a 5:1 mixture of *trans*- and *cis*-2-hexene (85% at 6 hrs) with only 3% each of the 3-hexene isomers. This aspect of the selectivity problem in which only one shift of the double bond takes place is also reproduced in the catalytic reaction, but oxygen suppresses the rate of isomerization relative to oxidation.

cis-2-Hexene undergoes the same Reactions 1 and 2 as does I and at about the same rate. The important difference is that the oxidation of II by any of the palladium(II) species is extremely slow (4% conversion to allylic hexenyl esters after seven days), and the olefin is not isomerized at all. If VI is derived from I by acetoxy-palladation followed by elimination of HPdOAc as proposed by Kitching *et al.* for 1-butene (10), the corresponding addition-elimination mechanism must be very slow for the internal olefin, and it is not surprising that the rate of an alternative type of catalytic oxidation is much faster in the presence of oxygen.

Catalytic Oxidation of 1-Hexene

Palladium acetate gives catalyst solutions that are stable and active for many days at 25°C under 1 atm of oxygen. Figure 1 shows curves of oxygen consumption in the catalytic oxidation of I using quinol to inhibit free radical reactions. There are two distinct regimes of reaction—*viz.*, an initial fast stage lasting up to 6 hrs and a second slower steady state which persists to high conversion of olefin. IR analysis of the complexes in solution shows that the onset of the steady state corresponds to complete formation of IVa and that some $\text{Pd}_3(\text{OAc})_6$ is present in the first stage. When IVa was introduced as the catalyst at the outset, the steady state was attained immediately without a fast stage (Figure 1). Under conditions of catalytic oxidation the inactive dimeric complex

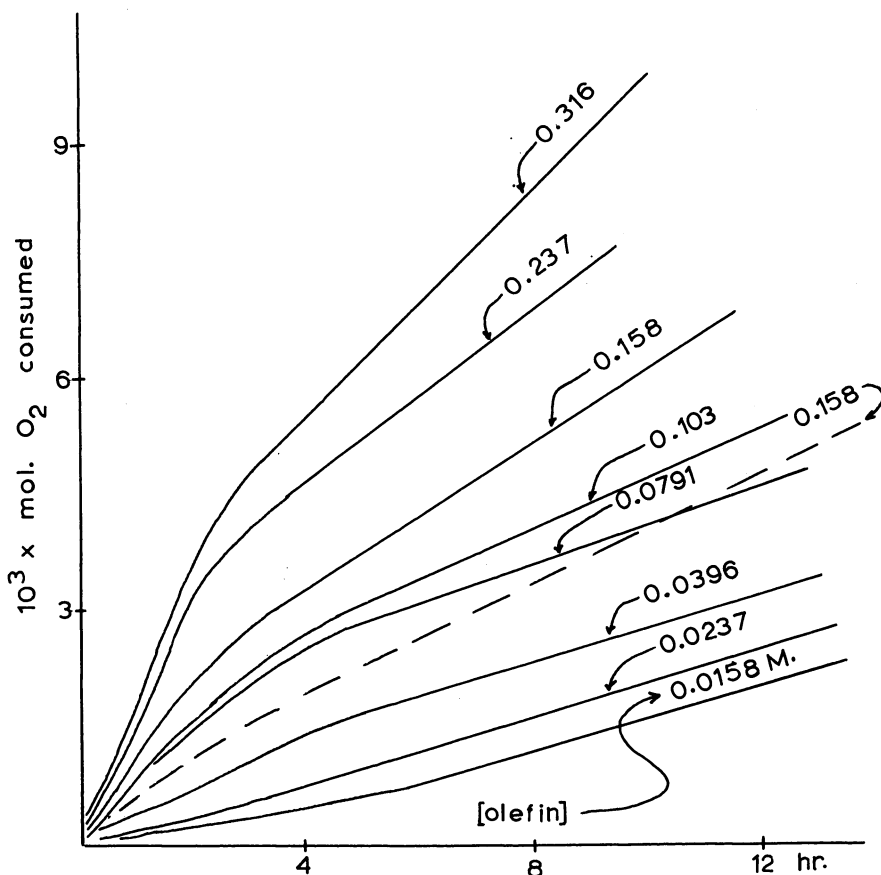


Figure 1. Catalytic oxidation of 1-hexene

— $[Pd_2(OAc)_6] = 0.00163M$, - - - - $[Pd_2(C_6H_{11})_2(OAc)_6] = 0.00163M$, $[quinol] = 4.4 \times 10^{-3}M$, $P_{O_2} = 803, 9 \text{ mm Hg}$

Va is formed very slowly, and even after 144 hrs about 80% of the palladium was present as IVa.

Material balances and product analyses were experimentally difficult as they involved a large number of products. Details are given in the Experimental Section, and a typical run is shown in Figure 2. The reactions went to high conversion in the absence of quinol. Using the number of moles of oxygen consumed as a measure and assuming a four-electron oxidation, the dotted line represents the theoretical amount of olefin consumed and converted into hexenyl esters and 2-hexanone. The recovery of hexenes was quite good, but the poor yield of oxidized products reflects the difficulty of separating the esters using a wet method and fractional distillation at low pressure. The form of these curves

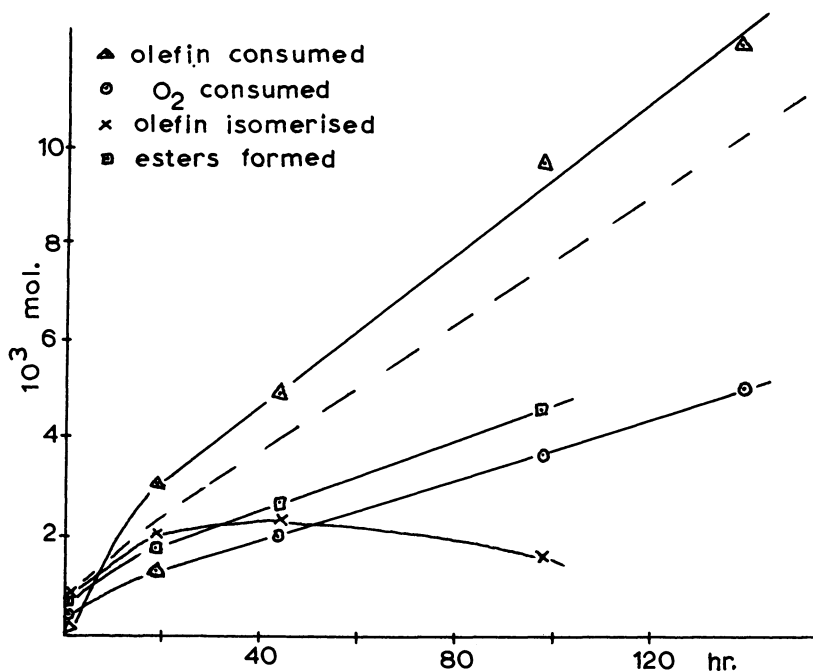


Figure 2. Catalytic oxidation of 1-hexene

Material balance of reactants and products: 60 ml acetic acid; 0.00224 mole $[Pd_4(OAc)_6]$ 0.016 mole 1-hexene

invariably follows that of the oxygen uptake curve as, also, does that of the formation of *cis*- and *trans*-2-hexene. Figure 2 shows that the latter falls away at high conversion presumably because of oxidation of 2-hexene, but at low conversion the relationship between rate of oxidation and rate of isomerization is almost linear (Table I). About 1.4 moles of 2-hexene are produced compared with the theoretical number of moles of oxidation product.

Table I. Stoichiometry of the Oxidation and Isomerization of 1-Hexene^a

	Yields			
	4 hrs	20 hrs	48 hrs	94 hrs
$10^5 \times$ Moles O ₂ consumed	17.4	45.5	73.1	116.0
$10^5 \times$ Moles 2-hexene formed	65.5	119.0	178.0	234.0
$\frac{\text{Moles 2-hexene}}{2 \times \text{moles O}_2}$	1.9	1.3	1.2	1.0

^a 1-Hexene, 0.022 mole; Pd(OAc)₂, 0.000237 mole; HOAc, 60ml.

The analysis of oxidation products from a typical run is given in Table II. Consistent results were obtained for the mole fractions among the various oxidized products despite the unsatisfactory material balances. In the GLC analysis it was not possible to separate *cis* and *trans* isomers except in the case of 2-hexen-2-yl acetate. One minor peak was a composite of three esters. The major product was VI, the mole fraction of which was 0.62 at 10% conversion and 0.27 at 85% conversion. However blank experiments showed that VI is decomposed slowly by palladium acetate yielding 2-hexanone which together with the unchanged ester constitutes a fraction of the products that decreases only slowly during runs (from 0.71 to 0.65). Of the minor components only the mole fraction of 1-hexen-3-yl acetate changes significantly with conversion perhaps because it may be derived from 2-hexene produced in the system by isomerization. Small yields of hexenols and hexenones were obtained. These products were assumed to result from a palladium-catalyzed free radical reaction since they were not present when quinol was used as an inhibitor. Overall, the selectivity changed remarkably little during runs and was the same during the initial fast stage and the steady state. The unusual selectivity in isomerization of I was similarly constant, giving very little 3-hexene and a high *trans* to *cis* ratio of 5.3 to 6.8 for 2-hexene.

Table II. Mole Fractions of Oxidized Products

Product	Yields				
	1 hr	19 hrs	44 hrs	98 hrs	139 hrs
1-Hexen-2-yl acetate	0.62	0.52	0.47	0.34	0.27
<i>trans</i> -2-Hexen-2-yl acetate	} 0.03	0.04	0.04	0.04	0.04
3-Hexen-2-yl acetate					
2-Hexen-3-yl acetate					
<i>cis</i> -2-Hexen-2-yl acetate	0.10	0.09	0.08	0.07	0.08
2-Hexen-1-yl acetate	0.08	0.10	0.10	0.08	0.09
3-Hexen-1-yl acetate	—	0.01	0.01	0.01	0.01
1-Hexen-3-yl acetate	0.02	0.06	0.06	0.06	0.06
2-Hexanone	0.09	0.11	0.15	0.32	0.38
3-Hexanone	—	—	—	—	0.01
Hexenols & hexenones	0.06	0.05	0.08	0.07	0.07

Kinetic data for the oxidation of I were obtained at 25°C using solutions containing palladium acetate (0.00105–0.00382*M*), I (0.0158–0.316*M*), and quinol (4.4×10^{-5} *M*). The oxygen pressure was varied from 474 to 1234 mm Hg. A group of runs is shown in Figure 1. Since the rate data were obtained at essentially constant concentration of the reactants, catalyst plots of $\log(\text{rate})$ vs. $\log[\text{I}]$, $\log[\text{Pd}(\text{OAc})_2]$, or $\log(P_{\text{O}_2})$ gave reaction orders. Consumption of oxygen is almost linear

with time during the first 2–3 hrs. Approximate values of initial rates were obtained as well as the steady rates. The former proved to be independent of P_{O_2} and nearly first order (0.9) in I with 0.00163M catalyst. However, the apparent order in catalyst concentration (less than 1) was not constant, presumably reflecting the different ratios of the various species present at different concentrations. The most useful data were obtained after 4 hrs when the steady rate had been attained (Figure 1). In particular at rather low concentrations of I (0.0158–0.0791M) the rate was independent of olefin concentration, the rate law being:

$$-\frac{d[O_2]}{dt} = k_{obs}[Pd_3(OAc)_6]^{1.18}(p_{O_2})^{1.09}$$

At higher concentrations of olefin the rate increased rapidly. The simplest type of complexity that could account for this behavior might lead to a two-term rate law. Crude analysis of the data suggests that there may be a term which is nearly second order in olefin while being very low or zero order in catalyst and oxygen concentrations. The addition of a mixture of preformed hexenyl esters to the reaction mixture had no effect on the rate.

Catalytic Oxidation of 3,3-Dimethyl-1-butene

The olefin 3,3-dimethyl-1-butene (III) was studied since it gave almost exclusively the expected product 3,3-dimethyl-1-buten-2-yl acetate (VII) with only traces of ketone or 3,3-dimethyl-1-buten-1-yl acetate. With a single product the test of material balance was simplified since it was possible to run a blank on the wet separation and then check the yield of VII by isotope dilution using $(CH_3)_3CC(OCOCD_3)=CH_2$. Experiments with III are not complicated by isomerization or allylic palladium complex formation and are unlikely to involve free radical reactions.

Figure 3 shows a group of runs carried out at 0.158M olefin. The duplicate runs at 0.00163M palladium acetate concentration show that an increase in P_{O_2} has no effect on the rate. The reaction has an induction period, indicating that $Pd_3(OAc)_6$ itself is not an active catalyst. After onset of the reaction the palladium acetate may be recovered, but it is then mixed with a pale yellow complex that could not be crystallized. IR analysis shows the presence of an ester-type acetate presumably from a trihapto-allylic complex (16), thus showing that some 1,3-diene may have been formed. If oxygen acted as a four-electron acceptor, the yield of ester was 49.0% by direct GLC determination and 44.1% by isotope dilution followed by mass spectrographic analysis.

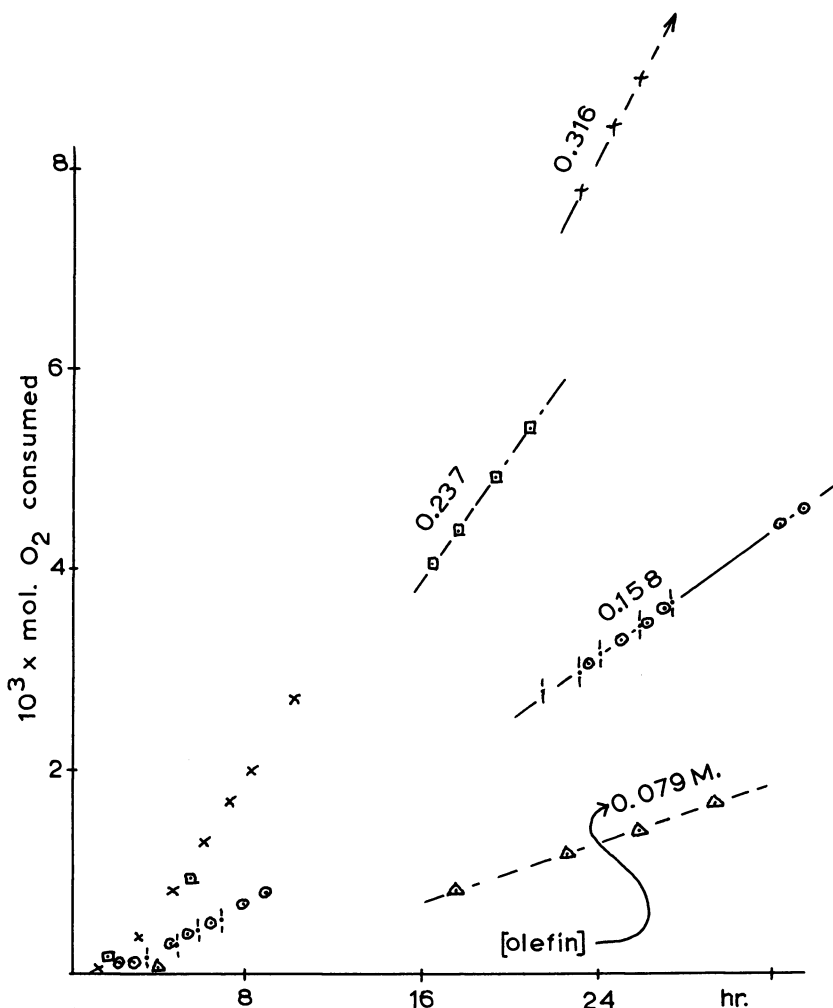


Figure 3. Catalytic oxidation of 3,3-dimethyl-1-butene

$\Delta/\square \times [Pd_3(OAc)_6] = 0.00163M, P_{O_2} = 804 \text{ mm Hg};$
 $\circ [Pd_3(OAc)_6] = 0.00163M, P_{O_2} = 1122 \text{ mm Hg}$

Catalytic Oxidation of *cis*-2-Hexene

The oxidation of *cis*-2-hexene (II) catalyzed by palladium acetate proceeds after an induction period of 2–4 hrs shown in Figure 4. Using 0.00163M palladium acetate total inhibition of reaction was observed with $1.08 \times 10^{-5}M$ quinol. 2,4,6-tri(*tert*-Butyl)phenol ($5.60 \times 10^{-5}M$) only showed the reaction without total inhibition. The formation of the allylic complex IVb proceeds in a similar way to the reaction of I, and it is the major species in the catalyst solutions. The formation of unsatu-

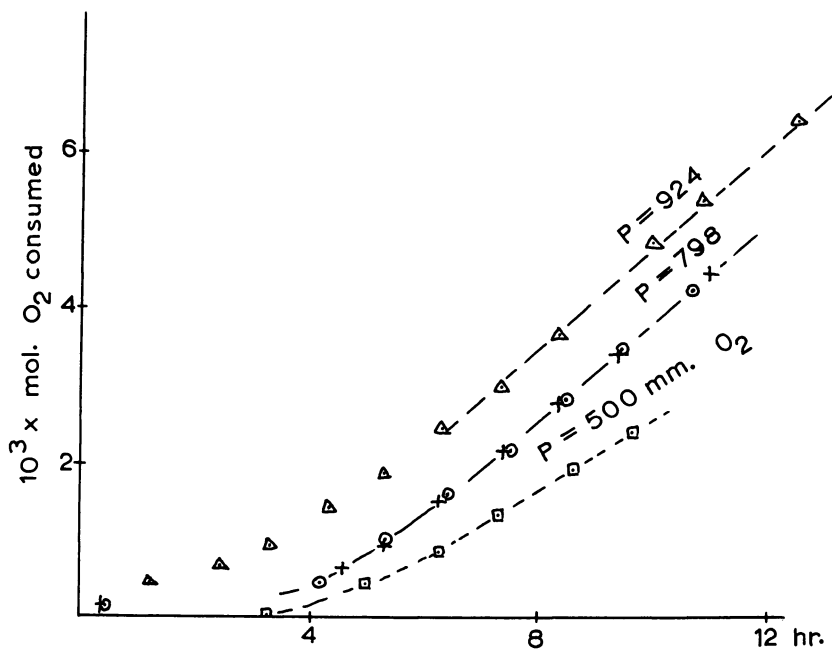


Figure 4. Catalytic oxidation of *cis*-2-hexene

$[Pd_3(OAc)_6] = 0.00162M$, $[cis\text{-}2\text{-hexene}] = 0.316M$

rated ketones and alcohols was much enhanced compared with I, amounting to a mole fraction of 0.34 of the oxidation products. The major products were 1-hexen-3-yl acetate (mole fraction 0.24), 3-hexen-2-yl acetate (mole fraction *ca.* 0.18) and 2-hexen-1-yl acetate (mole fraction 0.05) together with small amounts of the vinylic ester, 2-hexen-2-yl acetate, the homoallylic esters 4-hexen-2-yl acetate and 3-hexen-1-yl acetate, and saturated ketones. *cis*-2-Hexene did not isomerize. After the induction period the rate of O₂ consumption was linear with time at least up to 30 hrs with good reproducibility. Reaction orders obtained from $\log(\text{rate})$ vs. $\log(\text{concentration})$ plots indicated complex kinetics with a rate law of the form that can arise from a free radical reaction.

$$-\frac{d[O_2]}{dt} = k_{obs}[Pd_3(OAc)_6]^{0.26}[cis\text{-}2\text{-hexene}]^{0.68}(p_{O_2})^{0.66}$$

Oxidation by Benzoquinone

Benzoquinone has been used as an alternative oxidizing agent to oxygen in the oxidation of olefins catalyzed by palladium acetate (I). Presumably it has the same role as a regenerating agent in oxidizing some

palladium-containing reduced species. 1-Hexene was oxidized to the same mixture of hexenyl acetates as with O₂ and in the same proportions. As expected, hexenols and hexenones were not formed. For II, oxidation was barely detectable. This is consistent with the mechanism *via* addition-elimination being, at best, very slow and with the existence of an alternative route in the reaction with O₂.

Discussion

In the oxidation of I, catalytic activity is associated with Pd₃(OAc)₆ and IVa but not with Va. The trihapto-hexenylpalladium complexes are stable with respect to solvolysis and reduction of the palladium(II). Therefore the allylic palladium group is not an intermediate in the formation of esters. The mixture of reaction products is highly complicated, yet selectivity is the same in both the fast and the steady reaction stages. This suggests that the active catalytic species is the same in both stages and is most likely monomeric palladium(II). The results may be rationalized in terms of elementary steps (formation of complexes, displacement, oxypalladation, and reversible elimination of palladium hydride) discussed previously in different contexts by Kitching *et al.* (10), Cramer (18), and others (1). Figure 5 shows the reactions of I and indicates the origin of the important products. Geometric isomerism has been ignored. One striking feature of the catalytic reaction is that approximately one (actually *ca.* 1.4) molecule of 2-hexene is produced for each molecule of I that has been oxidized. This contrasts with the reaction *in vacuo* where a small amount of palladium hydride causes extensive isomerization. For this reason the heavy arrows in Figure 5 indicate a coupled sequence of reactions that would produce this result. Reactions 1, 2, and 3 are accepted as the mode of oxidation of α -olefins, *i.e.*, formation of a π complex followed by oxypalladation in the Markovnikov sense and then elimination of palladium hydride to give VIII. The hydrido-palladium complex VIII may then undergo an associative substitution (Reaction 4) because of the large excess of olefin; thus allowing isomerization of I by an addition-elimination sequence (Reactions 5 and 6). Apparently the resultant 2-hexene complex IX does not isomerize further to 3-hexene. Also, substitution of I in IX to give XI, Reaction 8, is unfavored under oxidizing conditions since it would lead to extensive isomerization as it does *in vacuo*. We conclude that IX is the type of complex that reacts with oxygen in the regeneration step (Reaction 7) and that the process may or may not involve prior dissociation to give a hydridopalladium species that is not complexed by a double bond. The mechanism in Figure 5 contains certain implications concerning the reactivity of the hydridopalladium complex of the vinylic ester, VIII. This

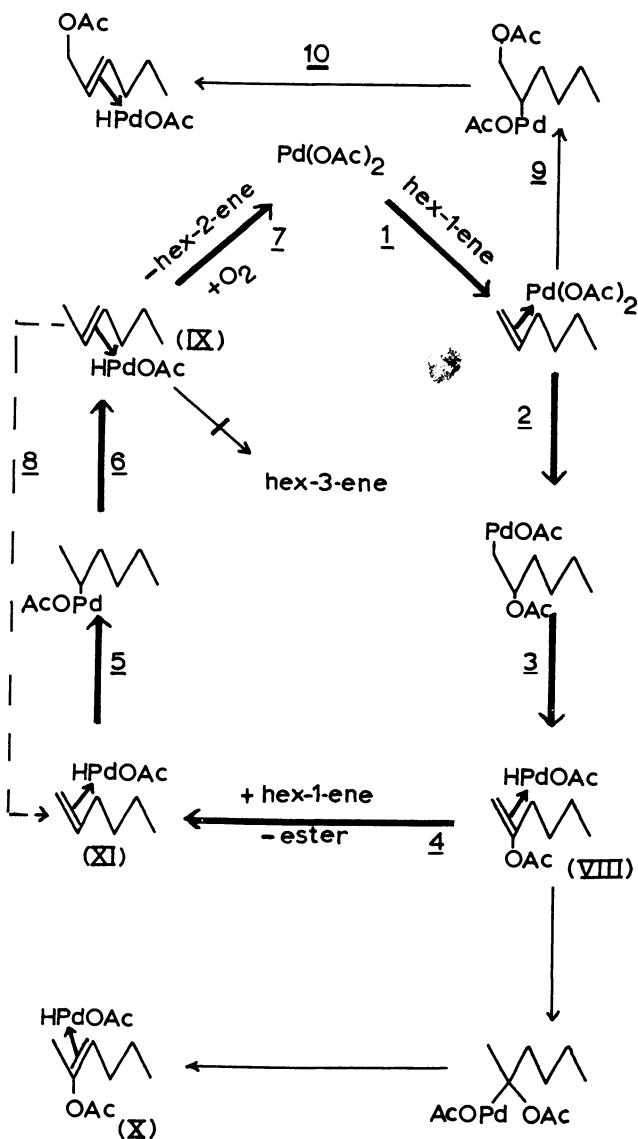


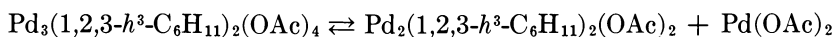
Figure 5. Reactions of 1-hexene

species must be more stable towards dissociation, substitution, or oxidation than the 2-hexene complex, IX, thus allowing isomerization first to X and then to a complex of the allylic ester 3-hexen-2-yl acetate. Supporting the suggested stability of π -hexenyl acetate complexes, palladium(II) complexes of unsaturated acetates may be isolated from solution in the reaction of cyclohexene (15). The mole fraction of 1-hexen-2-yl

acetate among the oxidation products obtained by oxidation of I with palladium acetate *in vacuo* is almost as high (0.58) as in the catalytic reactions. This seems to exclude the direct oxidation of VIII by oxygen as the regeneration step; otherwise a more marked effect on the selectivity in isomerization is expected.

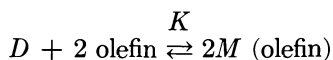
The oxypalladation reaction of I takes place partly in the anti-Markovnikov direction (Reaction 9) leading to 2-hexen-1-yl acetate *via* Reaction 10. Subsequently an allylic shift (19) can generate 1-hexen-3-yl acetate.

The most difficult problem in the selectivity between the various reactions is the way in which oxygen inhibits formation of Va, although it is expected that oxygen is involved only after further steps in the sequence. Perhaps palladium acetate monomer and Va arise by the following equilibrium process:



The reverse reaction is readily demonstrated, and if a relatively high concentration of palladium acetate is maintained by the regeneration process in the catalytic oxidation, this would inhibit formation of the dimer Va.

In the reactions of III, some of the inherent complexities of the *n*-hexene systems are removed because of the structure of the olefin. The induction period shows that $\text{Pd}_3(\text{OAc})_6$ is not catalytically active while the rate law suggests that a dimeric species (D) predominates in solution. If the latter reacts with the olefin III in an equilibrium step to form a monomeric σ complex, M (olefin), the rate-determining reaction of the latter would give the correct rate law.



$$\text{Rate} = kK^{1/2}[D]^{1/2}[\text{olefin}]$$

During the initial stages of the reaction of I and before it is converted into IVa, a similar kinetic scheme may apply.

As expected, the reaction of complexed III proceeds with high stereoselectivity. Oxypalladation followed by elimination of a hydride of palladium should yield $\text{HPd}(\text{OAc})((\text{CH}_3)_3\text{CC}(\text{OAc})=\text{CH}_2)$. Oxidation of the hydridopalladium species to a hydroperoxide is an attractive possibility as the first step in catalyst regeneration. For *n*-hexenes which have

allylic reactivity, any peroxide generated this way could react further with the olefin to yield the observed hexenols and hexenones. However, the stoichiometry of the reaction of III with oxygen indicates that the hydrido complex of 3,3-dimethyl-1-buten-2-yl acetate apparently reacts further to generate another oxidation product prior to the eventual reformation of palladium acetate.

In the reaction of I in the steady stage, when the concentration of olefin is low, the slow step involves oxygen. In effect there must be a chain reaction because formation of a complex, addition and elimination reactions, and other possible steps must precede the rate-determining step. Thus the isolatable complexes may be involved only in initiation steps that produce a more reactive palladium species.

For II, the induction period action of inhibitors and kinetic complexity all point to a free radical oxidation. This is not to say that the addition-elimination mechanism does not occur, but it must be slow and even in the absence of O_2 is blocked by the formation of stable allylic complexes. Since cyclohexene is also an internal olefin, one might expect similar reactivity to II. This is not the case in chloride-free media since cyclohexenylpalladium acetate complexes are unstable and decompose to 2-cyclohexen-1-yl acetate (14, 15).

Experimental

Materials. Palladium acetate was prepared by oxidizing palladium black in acetic acid by O_2 or by nitric acid (20). Material from nitric acid oxidation was crystallized five times or more before use, or more often, was purified by the following procedure. Finely powdered palladium acetate was made into a paste with sulfuric acid and digested at 140° – $150^{\circ}C$ for 30 min. Palladium(II) was thus converted into palladium sulfate, and crucial impurities were destroyed. Palladium sulfate was dissolved in water. After the sulfuric acid was neutralized, the addition of excess acetic acid precipitated purified palladium acetate. Oxidizable impurities were removed from acetic acid by repeated fractionation from CrO_3 and $KMnO_4$ solutions. Olefins were treated with alumina before use to remove peroxides. The reproducibility of the rate data was used as a test of the purity of reagents since the results were erratic when inadequate precautions had been taken.

Reactions of Palladium Acetate. Appropriate reagents were sealed into evacuated tubes after degassing by a freeze-and-melt technique. These tubes were left on a shaking machine at 18° – $23^{\circ}C$ for the full reaction time. Catalytic runs were done at $25 \pm 0.01^{\circ}C$. For accurate kinetic studies a glass reaction vessel (75 ml) equipped with magnetic stirrer and containing 40 ml of solution was used. The vessel was connected to a manometer containing acetic acid, one arm of which was constructed from the calibrated section of a buret. As oxygen was consumed (usually at a rate of *ca.* 0.5 ml/hr), acetic acid was run into the reference arm of the manometer from a reservoir to restore the level.

The reservoir was connected to a 2-liter bulb to render the change in volume and pressure on the reference side of the manometer negligible. The construction was of glass with Rotaflow taps that facilitated total immersion in the thermostat. The system could be pressurized with pure O₂ in the range 500–2000 mm Hg, variations during runs being less than 0.3%.

Analyses. Samples of reaction mixtures were frozen and sublimed into the vacuum line (10⁻⁶ mm Hg). The vapor was passed through a wide-bore U-trap at -45°C which collected acetic acid and volatile oxidation products and allowed any unreacted hexenes to pass. After further fractional condensation the hexene was transferred to a graduated tube to measure the volume and was finally analyzed by GLC using a 12 meter × 6 mm column packed with polypropylene glycol LB-550-X on Chromosorb W. The sublimation residue was analyzed by IR spectroscopy while the acetic acid condensate was subjected to a wet separation (5, 15) to recover the oxidation products for GLC analysis.

Acknowledgments

R.G.B. thanks the Science Research Council for a Research Studentship.

Literature Cited

1. Maitlis, P. M., "The Organic Chemistry of Palladium," vol. 2, Academic, New York, 1971.
2. Aguilo, A., *Advan. Organometal. Chem.* (1967) **5**, 321.
3. Clark, D., Hayden, P., Smith, R. D., *Discuss. Faraday Soc.* (1968) **46**, 99.
4. Henry, P. M., *J. Amer. Chem. Soc.* (1964) **86**, 3246.
5. Davidson, J. M., Triggs, C., *J. Chem. Soc. (A)* (1969) 1324.
6. Halpern, J., *Chem. Eng. News* (1966) **44**, 66.
7. Levanda, O. G., Moiseev, I. I., *Zhur. Obs. Khim.* (1968) **4**, 1533.
8. Matsuda, T., Mitsuyasu, T., Nakamura, Y., *Kogyo Kagaku Zasshi* (1969) **72**, 1751.
9. Schultz, R. G., Gross, D. E., *ADVAN. CHEM. SER.* (1968) **70**, 197.
10. Kitching, W., Rappoport, Z., Winstein, S., Young, W. G., *J. Amer. Chem. Soc.* (1966) **88**, 2054.
11. Brown, R. G., Davidson, J. M., Triggs, C., *Amer. Chem. Soc. Div. Petrol. Chem., Prepr.* (1966) **14**, 66.
12. Brown, R. G., Davidson, J. M., *Chem. Commun.* (1972) 642.
13. Braithwaite, B., Wright, D., *Chem. Commun.* (1969) 1329.
14. Wolfe, S., Campbell, P. G. C., *J. Amer. Chem. Soc.* (1971) **93**, 1497, 1499.
15. Brown, R. G., Davidson, J. M., *J. Chem. Soc. (A)* (1971) 1321.
16. Powell, J., "M.T.P. International Review of Science," Inorganic Chemistry, Chapter 7, Series 1, vol. 6, Butterworths, London, 1972.
17. Skapski, A. C., Smart, M. L., *Chem. Commun.* (1970) 658.
18. Cramer, R., Lindsey, R. V., *J. Amer. Chem. Soc.* (1966) **88**, 3534.
19. Henry, P. M., *J. Amer. Chem. Soc.* (1972) **94**, 5200.
20. Stephenson, T. A., Morehouse, S. M., Powell, A. R., Heffer, J. P., Wilkinson, G., *J. Chem. Soc.* (1965) 3632.

RECEIVED July 30, 1973.

6

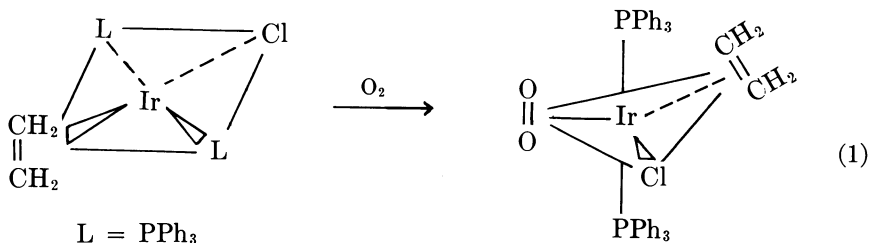
Oxidation of Olefins in the Presence of Transition Metal Complexes

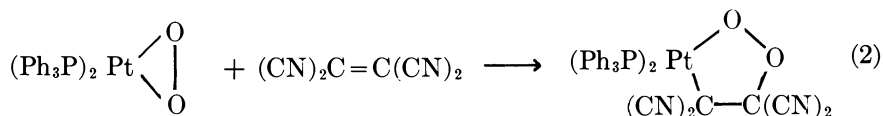
JAMES E. LYONS

Corporate Research Department, Sun Oil Co., P.O. Box 426,
Marcus Hook, Pa. 19061

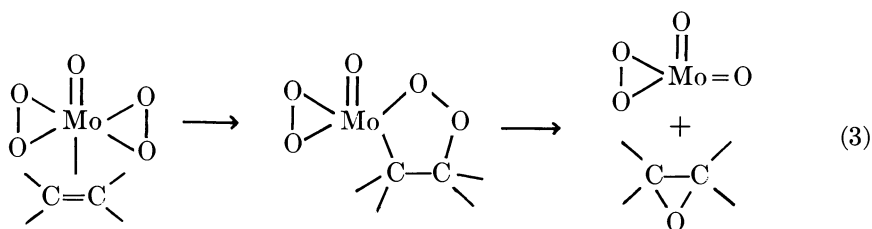
With certain metal complexes the product profile resulting from olefin oxidation differs greatly from that of classical autoxidation. Reactions carried out in the presence of certain metal complexes are highly selective in forming one product or a single set of products. When group VIII metal complexes are used, α,β unsaturated alcohols and ketones predominate. With molybdenum, epoxides are formed in high yield; with vanadium complexes, epoxy alcohols are formed. The oxidation of substituted olefins by the complexes which we studied proceeds via an allylic hydroperoxide intermediate. The observed products are a function of the selective decomposition of the allylic hydroperoxide by the metal complex. In the decomposition of allylic hydroperoxides the products obtained with a given complex parallel the results of oxidation.

Many transition metal complexes react reversibly with molecular oxygen (1, 2) and with olefins (3, 4, 5). van Gaal *et al.* (6) recently prepared a group VIII metal complex which contains both oxygen and an olefin in the coordination sphere (Reaction 1).





In several instances oxygen is transferred to the olefin within the coordination sphere of the metal. Ugo (7) reported, for example, that the dioxygen complex, $(\text{Ph}_3\text{P})_2\text{PtO}_2$, reacts with tetracyanoethylene to form a cyclic complex (Reaction 2). Mimoun *et al.* (8) found that molybdenum complexes of the general formula $[\text{Mo}(\text{O}_2)_2\text{O}]\text{L}_1\text{L}_2$ react with an olefin to give an epoxide in high yield. A cyclic complex was postulated as a likely reaction intermediate (Reaction 3). Dudley and Read (9)



recently isolated methyl ketones from the oxidation of 1-olefins in the presence of several rhodium(I) complexes. These authors propose a mechanism in which an epoxide is formed by transfer of oxygen to the olefin within the coordination sphere of the metal (Reaction 4) (9). The resulting epoxide may rearrange to a methyl ketone while coordinated to the rhodium center (9).

Synthetic interest in the oxidation of olefins in the presence of oxygen-carrying transition metal complexes has been stimulated by the possi-

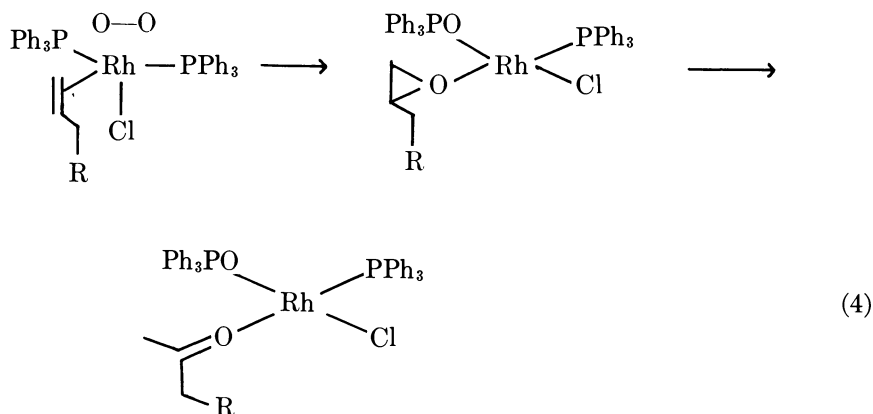


Table I. Oxidation of Tetramethylethylene^a in

<i>Metal Complex</i>	<i>Radical Inhibitor</i>
None ^d	None
[RhCl(CO)(Ph ₃ P) ₂]	None
[RhCl(CO)(Ph ₃ P) ₂]	HQ ^e
[IrCl(CO)(Ph ₃ P) ₂]	None
[IrCl(CO)(Ph ₃ P) ₂]	HQ ^e
[RuCl ₂ (Ph ₃ P) ₃]	None
[RuCl ₂ (Ph ₃ P) ₃]	HQ ^e
[C ₅ H ₅ Mo(CO) ₃] ₂	None
[C ₅ H ₅ Mo(CO) ₃] ₂	HQ ^e
[C ₅ H ₅ V(CO) ₄] ^f	None
[C ₅ H ₅ V(CO) ₄]	HQ ^e

^a Oxygen bubbled through 12 ml of TME containing 8×10^{-5} mole metal complex for 4 hrs at 50°C.

^b Conversions, mole %, of TME to the indicated products.

^c Unidentified high-boiling by-products were also formed in 2.8% yield.

bility of novel oxidation pathways like those in Reactions 2, 3, and 4. Commercial interest in olefin oxidation is a result of the value and utility of the products—alcohols, acids, carbonyl compounds, epoxides, etc. Classical radical initiated autoxidation of an olefin is usually unselective and yields various oxidation products (10). It is, however, desirable and often imperative that oxidation be selective to be economically attractive. Specific oxidizing agents may be used to effect a selective transformation, but they are costly. Catalytic air-oxidation is a viable alternative to stoichiometric reactions, and several processes are in commercial operation. Transition metal complexes can catalyze selective reactions of various small molecules with olefins (11). It is of interest, therefore, whether novel homogeneous transition metal-catalyzed reactions will occur between oxygen and olefins which will result in the selective formation of oxidation products that could not be produced in high yield by conventional autoxidation techniques.

This paper presents the results of an investigation of the oxidation of substituted olefins in the presence of hydrocarbon-soluble transition metal complexes. Results indicate that the initial interaction of oxygen with the olefin probably does not occur within the coordination sphere of the metal. The best interpretation appears to be autoxidation of the olefin, initiated either by the metal or by metal catalyzed decomposition of peroxidic impurities. The initial product of an olefin having allylic hydrogens is an allylic hydroperoxide species; this is usually the case in radical initiated autoxidations. Nonetheless, with some metal complexes the product profile differs markedly from that observed when radical initiators are used. In the presence of several complexes, oxidation is

the Presence of Transition Metal Complexes

Acetone	Yield of Products, % ^b				Unreacted TME, % ^c
	I	II	III	IV	
—	2	0.5	2	—	92
4	25	22	10	—	34
0.5	3	5	2	—	88
3	20	15	9	—	47
0.3	3	3	1	—	92
3.5	20	21	—	—	52
0.4	3	2	—	—	93
1	19	12.5	—	—	62
—	—	—	—	—	100
—	14	1	—	14	67
—	—	—	—	—	100

^d Reaction run in the presence of 4×10^{-4} mole of azobisisobutyronitrile.

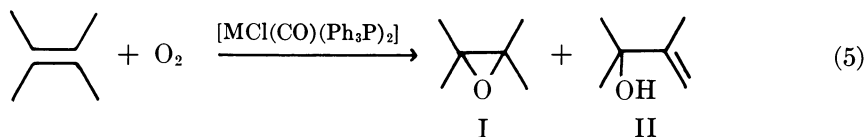
^e Hydroquinone present in 3.3 mole %.

^f Reaction ran for 6 hrs at 50°C.

quite selective. This is the result of the selective nature of the metal catalyzed reactions of the allylic hydroperoxide which is initially formed. Although evidence of new pathways for the activation of molecular oxygen *via* coordination catalysis was not found, the increased ability to control the products by selective reaction of hydroperoxide intermediates may ultimately prove valuable from a synthetic standpoint.

Results and Discussion

Oxidation of Tetramethylethylene. Tetramethylethylene, TME, was an excellent model olefin since it was rapidly and selectively oxidized in the presence of many transition metal complexes (12). Oxidation of TME in the presence of the group VIII metal complexes: $[\text{MCl}(\text{CO})(\text{Ph}_3\text{P})_2]$ ($\text{M} = \text{Rh}, \text{Ir}$) at 50°C gave two major products: 2,3-dimethyl-2,3-epoxybutane, I, and 2,3-dimethyl-3-hydroxy-1-butene, II (Reaction 5). Reaction mixtures were homogeneous with no observable deposits of insoluble materials. Little oxidation occurred under these conditions in the absence of the metal complexes, but low yields of I and II were obtained in the presence of a radical initiator (Table I). Reactions were severely inhibited by hydroquinone. The ruthenium(II) complex, $[\text{RuCl}_2(\text{Ph}_3\text{P})_3]_2$, also promoted efficient oxidation of TME yielding I



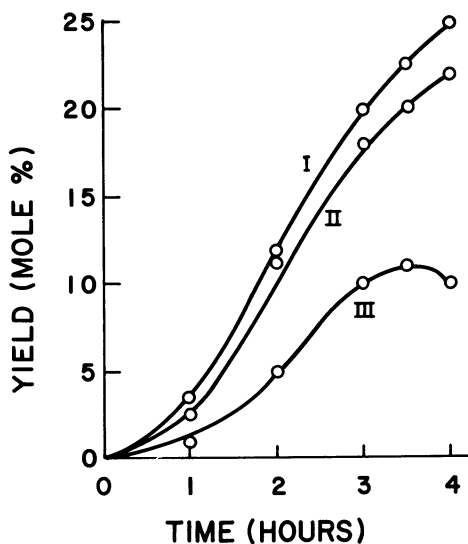
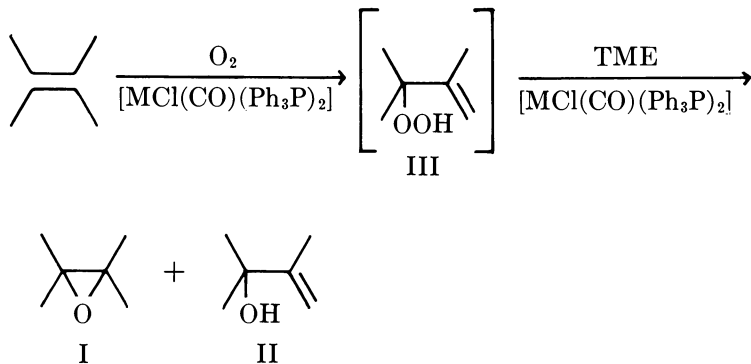


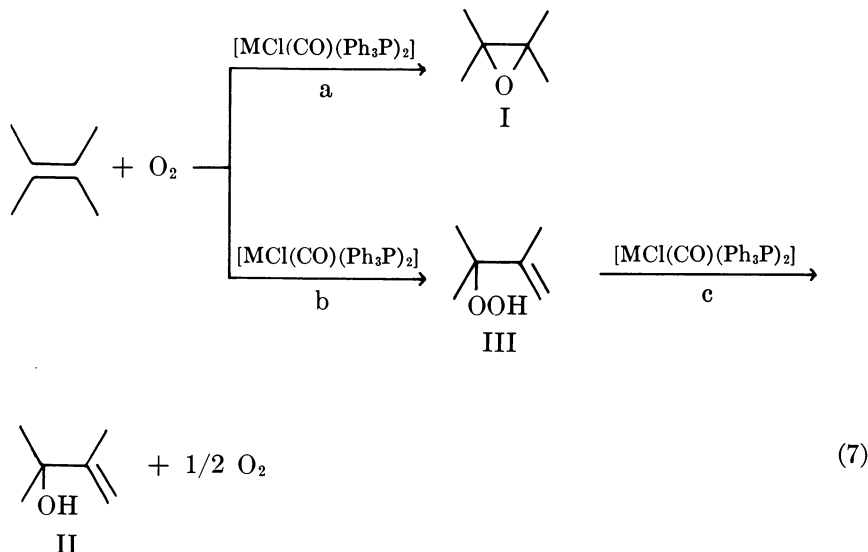
Figure 1. Oxidation of TME (120 ml) in the presence of $[\text{RhCl}(\text{CO})(\text{Ph}_3\text{P})_2]$ (8×10^{-4} mole) at 50°C

and II as the principal products. However, the mixture was dark and cloudy throughout the reaction. Results are included in Table I.

The allylic hydroperoxide, 2,3-dimethyl-3-hydroperoxy-1-butene, III, was detected during the oxidation of TME in the presence of $[\text{MCl}(\text{CO})(\text{Ph}_3\text{P})_2]$ ($\text{M} = \text{Rh}, \text{Ir}$) and reached a maximum yield of 11% after 3.5 hours when the rhodium complex was used (Figure 1). James and Ochiai (13) have cited spectral evidence for hydroperoxide intermediates, and Fusi *et al.* (14) obtained evidence which supports the intermediacy of an allylic hydroperoxide during cyclohexene oxidation in the presence of metal complexes. The allylic hydroperoxide (III) which is formed during the oxidation of TME in the presence of $[\text{MCl}(\text{CO})(\text{Ph}_3\text{P})_2]$



may be a reaction intermediate. It is also probable that III reacts with TME to give the stable oxidation products I and II (Reaction 6). Alternatively, the epoxide, I, might be formed *via* a direct oxidation, and II could be the result of metal-catalyzed decomposition of a hydroperoxide to the corresponding alcohol (Reaction 7).



Indeed, the rhodium(I) and iridium(I) complexes can catalytically decompose a hydroperoxide in a manner similar to Reaction 7c (12). Toluene solutions of *tert*-butyl hydroperoxide readily decompose at room temperature in the presence of $[\text{MCl}(\text{CO})(\text{Ph}_3\text{P})_2]$ ($\text{M} = \text{Rh}, \text{Ir}$) with the liberation of oxygen and the formation of *tert*-butyl alcohol (Table II). However, when the $[\text{MCl}(\text{CO})(\text{Ph}_3\text{P})_2]$ -catalyzed reaction of *tert*-butyl hydroperoxide was carried out in TME rather than toluene, little oxygen evolved, and the products were I and *tert*-butyl alcohol (Reaction 8; Table II). No observable epoxidation of TME occurred under similar conditions in the absence of the catalyst. Thus, the $[\text{MCl}(\text{CO})(\text{Ph}_3\text{P})_2]$ -catalyzed reaction of an alkyl hydroperoxide follows a different course in TME than in the absence of olefin, giving strong support to the occurrence of Reaction 6 during TME oxidation. These findings alone, however, do not rule out the existence of Reaction 7C as a competitive pathway. In fact, when the allylic hydroperoxide, III, was treated with $[\text{RhCl}(\text{CO})(\text{Ph}_3\text{P})_2]$ in excess TME, the ratio of products was: $\text{I}/\text{II} = 0.5$. Thus, much of the allylic alcohol, II, formed during TME oxidation may arise *via* Reaction 7c.

Since the oxidation reactions (Table I) are inhibited by hydroquinone, a radical pathway probably exists for the formation of III

Table II. Reactions of *tert*-Butyl Hydroperoxide in the Presence of Transition Metal Complexes^a

Metal Complex	Medium	Yield of Products, % ^b		Unreacted <i>tert</i> -Butyl Hydroperoxide, %
		<i>tert</i> -Butyl Alcohol	I	
[RhCl(CO)(Ph ₃ P) ₂]	Toluene	14	—	85
[RhCl(CO)(Ph ₃ P) ₂]	TME	25	26	71
[IrCl(CO)(Ph ₃ P) ₂]	Toluene	46	—	53
[IrCl(CO)(Ph ₃ P) ₂]	TME	50	42	34
[C ₅ H ₅ Mo(CO) ₃] ₂ ^c	Toluene	41	—	59
[C ₅ H ₅ Mo(CO) ₃] ₂ ^c	TME	58	60	40
[C ₅ H ₅ V(CO) ₄] ^d	Toluene	92	—	—
[C ₅ H ₅ V(CO) ₄] ^d	TME	90	—	—
[C ₅ H ₅ V(CO) ₄] ^{d,e}	TME	39	13	57
[C ₅ H ₅ V(CO) ₄] ^{d,f}	II	92	^g	—

^a *tert*-Butyl hydroperoxide (0.01 mole) was added dropwise over 5 min to 0.08 mmole of the complex (unless otherwise noted) in 0.1 mole TME or toluene at 25°C, and the mixture was stirred for 1 hr.

^b Conversions, mole %, based on *tert*-butyl hydroperoxide.

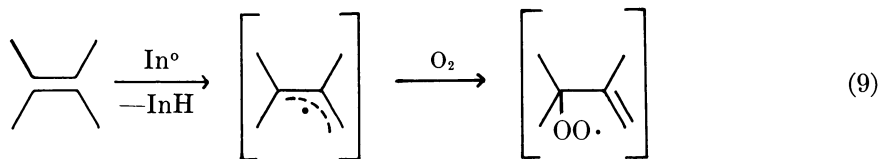
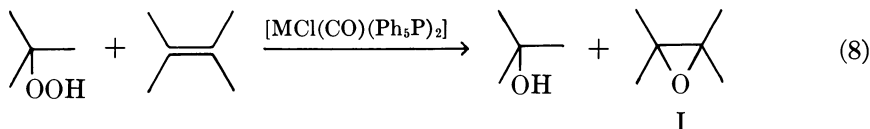
^c 0.12 mmole.

^d 0.16 mmole.

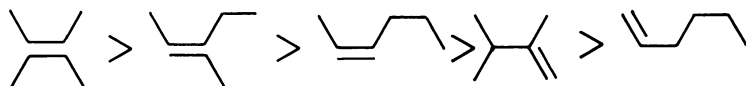
^e Catalytic species generated *in situ* by adding 1 mmole of *tert*-butyl hydroperoxide 5 min prior to reaction.

^f Reaction carried out at 50°C.

^g IV formed in 90% yield.



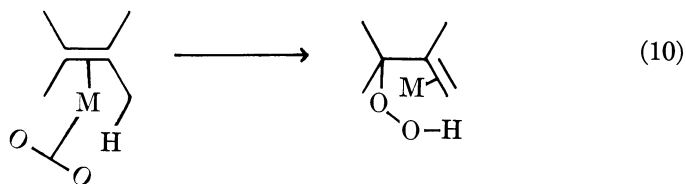
(Reaction 9) (15). We also found that the ease with which olefins are oxidized in the presence of [MCl(CO)(Ph₃P)₂] (M = Rh, Ir) increases with the degree of substitution (12). Reactivity follows the order:



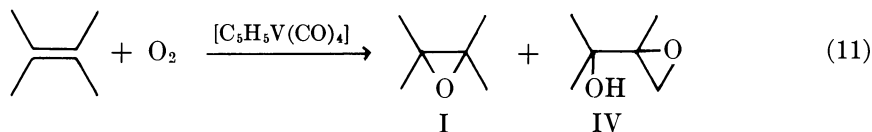
If a pathway which involved metal ion activation followed by oxygen transfer in the coordination sphere (Reaction 10) were operative, olefin reactivity would be expected to parallel the coordinative ability of the

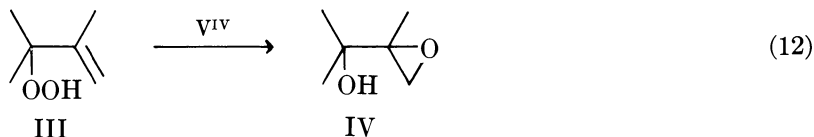
olefin in most other metal catalyzed reactions. The reactivity series above holds for both the formation of III and the epoxidation of TME using *tert*-butyl hydroperoxide. Our data do not allow us to distinguish between initiation by the metal center and initiation by radical species present owing to metal catalyzed decomposition of trace impurities. While neither Reaction 9 nor 10 may adequately represent the true mechanistic pathway, TME oxidation in the presence of the rhodium(I) and iridium(I) complexes clearly exhibits characteristics which are more similar to radical initiated oxidation than to coordination catalysis.

Acetylacetonate complexes of molybdenum and vanadium, known catalysts for olefin epoxidation (16, 17), were unsuitable for TME oxidation at 50°C. No observable reaction occurred after 4-hour periods with these complexes. Both $[\text{C}_5\text{H}_5\text{Mo}(\text{CO})_3]_2$ and $[\text{C}_5\text{H}_5\text{V}(\text{CO})_4]$, however, were quite active under these conditions. When TME was oxidized in the presence of $[\text{C}_5\text{H}_5\text{Mo}(\text{CO})_3]_2$, I and II were the major products. The allylic hydroperoxide, III, was not observed during this reaction presumably because of efficient epoxidation of TME catalyzed by the molybdenum complex. The molybdenum complex catalyzes the decomposition of *tert*-butyl hydroperoxide at room temperature in a manner analogous to the group VIII metal complexes. This complex also catalyzes the epoxidation of the olefin under mild conditions (Table II). During TME oxidation in the presence of $[\text{C}_5\text{H}_5\text{Mo}(\text{CO})_3]_2$, considerably higher yields of the epoxide, I, were formed than of the allylic alcohol, II. Again it appears that Reaction 6 is not the only pathway for epoxide formation during TME oxidation under mild conditions.

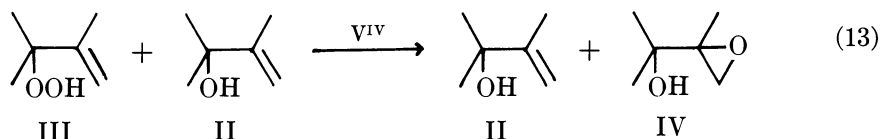


When TME was oxidized in the presence of $[\text{C}_5\text{H}_5\text{V}(\text{CO})_4]$, again only two major products were formed. Here, however, one product was different from previous reactions. The products were I and 1,2-epoxy-2,3-dimethyl-3-hydroxybutane (IV) (Reaction 11). Very little allylic alcohol, II, was formed, and the allylic hydroperoxide, III, did not accumulate during this reaction. Allison *et al.* (18) have shown that an allylic

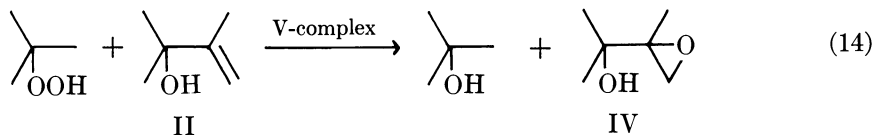




hydroperoxide will yield an epoxyol when treated with vanadylacetylacetonate (Reaction 12). These authors and others (19) considered this reaction to be a rearrangement of the allylic hydroperoxide. At least one other pathway should be considered for this reaction—*i.e.*, the epoxidation of II by III during the oxidation (Reaction 13).



To probe hydroperoxide reactivity in these systems we studied the reaction of *tert*-butyl hydroperoxide in the presence of $[\text{C}_5\text{H}_5\text{V}(\text{CO})_4]$. In contrast to the rhodium(I) and molybdenum complexes, $[\text{C}_5\text{H}_5\text{V}(\text{CO})_4]$ catalyzed the rapid decomposition of *tert*-butyl hydroperoxide to oxygen and *tert*-butyl alcohol in both toluene and TME (Table II). When reaction was done by adding the hydroperoxide rapidly to the vanadium complex in TME, no epoxide (I) was produced. However, when the TME solution of $[\text{C}_5\text{H}_5\text{V}(\text{CO})_4]$ was treated with a small amount (2–3 times the molar quantity of vanadium complex) of *tert*-butyl hydroperoxide at room temperature, a species was formed *in situ* which could catalyze the epoxidation of TME. Subsequent addition of *tert*-butyl hydroperoxide gave I in 13% yield (Table II). This vanadium complex also could catalyze the epoxidation of the allylic alcohol (II) to give *tert*-butyl alcohol and IV (Reaction 14). Reaction 14 was nearly quantitative, and the reaction rate was considerably faster than with TME.



The existence of a facile epoxidation of II at a more rapid rate than that of TME is of interest in relation to a possible intermolecular pathway for formation of an epoxy alcohol from an allylic hydroperoxide during olefin oxidation. When a solution of II (0.01 mole) in TME (0.09 mole) was treated with *tert*-butyl hydroperoxide (0.01 mole) in the presence of

the oxidized vanadium complex at 50°C, IV was formed almost exclusively (98%). Thus a small amount of II formed during oxidation in the presence of the vanadium complex could be epoxidized, preferentially by III, in the presence of excess TME to give high yields of IV (Reaction 13). The allylic alcohol, II, once formed is not depleted by reaction with III to give IV (Reaction 13).

When the allylic hydroperoxide, III, was treated with vanadium(IV) (*i.e.*, vanadylacetylacetonate), it was rapidly converted to IV in 85% yield. Low yields (5-10%) of II, however, accompanied this product. Thus, II is probably an intermediate in the formation of IV from III in this case as well. Although it seems likely that an intermolecular epoxidation pathway exists for the formation of IV, concurrent intramolecular rearrangement has not yet been ruled out.

The behavior of the low valent vanadium complex, $[\text{C}_5\text{H}_5\text{V}(\text{CO})_4]$, is quite different from that of the vanadium(IV) complexes: $[\text{VO}(\text{acac})_2]$ and $[(\text{C}_5\text{H}_5)_2\text{VCl}_2]$. Neither vanadylacetylacetonate nor bis(cyclopentadienyl)dichlorovanadium(IV) could rapidly initiate TME oxidation at 50°C. The vanadium(IV) complexes, however, catalyze the epoxidation of unsaturated molecules by hydroperoxides. The difference in valence state is probably responsible for the marked difference in behavior of the vanadium complexes. During the early stages of the reaction of an olefin with oxygen in the presence of $[\text{C}_5\text{H}_5\text{V}(\text{CO})_4]$, the low valent vanadium complex may be oxidized while rapidly decomposing traces of hydroperoxide with the probable generation of radical species. In this way it can initiate olefin oxidation. Once in a more stable, higher oxidation state, the vanadium complex can catalyze the epoxidation of unsaturated molecules. The ease with which vanadium complexes catalyze epoxidation of allylic alcohols by hydroperoxides has been reported by others (20) and is discussed below.

Despite its inability to initiate oxidation, $[(\text{C}_5\text{H}_5)_2\text{VCl}_2]$ can be used in combination with the group VIII metal complexes: $[\text{RhCl}(\text{CO})(\text{Ph}_3\text{P})_2]$, $[\text{IrCl}(\text{CO})(\text{Ph}_3\text{P})_2]$, and $[\text{RuCl}_2(\text{Ph}_3\text{P})_3]_2$ at 50°C (Table III). The function of the group VIII metal complex is to initiate formation of an allylic hydroperoxide which is converted to stable oxidation products by subsequent reactions catalyzed by the group VIII complex or the vanadium complex. The major products of the reaction are I and IV (Table III). Although $[(\text{C}_5\text{H}_5)_2\text{VCl}_2]$ could be used effectively in this manner, vanadylacetylacetonate could not be used at 50°C. This complex seemed to inhibit the activity of the group VIII complexes, and no reaction was observed after four hours. However, Allison *et al.* (18) found that in the presence of efficient radical initiators and hydroperoxides, the vanadylacetylacetonates could catalyze epoxy alcohol formation during reactions of oxygen with several olefins.

Table III. Oxidation of TME in the Presence of Group VIII Complexes and $[(C_5H_5)_2VCl_2]^a$

Group VIII Complex	Yield of Products, % ^b				Unreacted TME, % ^c
	Acetone	I	II	IV	
$[RhCl(CO)(Ph_3P)_2]$	2	17	1.5	16	57
$[IrCl(CO)(Ph_3P)_2]$	3	19	2.5	16	54
$[RuCl_2(Ph_3P)_3]$	—	18	7.0	13	53

^a Oxygen bubbled through 12 ml of TME containing 9×10^{-5} mole group VIII metal complex and 2.4×10^{-4} mole $[(C_5H_5)_2VCl_2]$ for 4 hrs at 50°C.

^b Conversions, mole % of TME to the indicated products.

^c Unidentified high boiling by-products also formed in 5-10% yield.

Oxidation of Cyclohexene. Much has been learned in recent years about the nature of olefin oxidation in the presence of metal salts and complexes by studying cyclohexene as the olefinic substrate (21). In an early investigation, Chalk and Smith (22) found that the oxidation of cyclohexene in the presence of transition metal ions exhibits free radical chain character. Kurkov *et al.* (23) showed that an oxygen-carrying rhodium(I) phosphine complex behaves in a similar manner. Gould and Rado (24) studied the oxidation of cyclohexene in the presence of acetylacetonate complexes of transition metals; they demonstrated that the distributions of volatile products closely follow the patterns observed for the decomposition of cyclohexenyl hydroperoxide in the presence of the same metal compounds. Several of the results of this study are summarized in Table IV. Although the reactions were not particularly selective, there was a noticeable change in product profile between the group VIII metal complexes and reactions run in the presence of molybdenum and vanadium complexes. Fusi *et al.* (14) studied the oxidation of cyclohexene in the presence of various oxygen-carrying group VIII metal phosphine complexes; they concluded that an allylic hydroperoxide was the reaction intermediate in these cases as well.

Table IV. Oxidation of Cyclohexene Catalyzed

Complex	% Conv.	Hydroperoxide
$Co(acac)_3$	5.27	5.55
$Fe(acac)_3$	5.15	5.38
$MoO_2(acac)_2$	8.23	0.17
$VO(acac)_3$	5.99	0.33

^a Data from Gould and Rado (24).

While there are differences in mechanistic detail, studies by others (13, 25) substantiate the existence of allylic hydroperoxides as intermediates in the homogeneous, transition-metal promoted oxidation of cyclohexene.

We studied the oxidation of cyclohexene at 70°C in the presence of cyclopentadienylcarbonyl complexes of several transition metals. As with the acetylacetonates, the metal center was the determining factor in the product distribution. The decomposition of cyclohexenyl hydroperoxide by the metal complexes in cyclohexene gave insight into the nature of the reaction. With iron and molybdenum complexes the product profile from hydroperoxide decomposition paralleled that observed in olefin oxidation. When vanadium complexes were used, this was not the case. Variance in product distribution between the cyclopentadienylcarbonyl metal-promoted oxidations as a function of the metal center were more pronounced than with the acetylacetonates. Results are summarized in Table V.

The oxidation of cyclohexene in the presence of the iron complex, $[\text{C}_5\text{H}_5\text{Fe}(\text{CO})_2]_2$ gave rise to two major stable oxidation products at low conversion: 2-cyclohexene-1-ol, VII, and 2-cyclohexene-1-one, VIII. A minor amount of cyclohexene oxide, VI, was also formed together with some non-volatile residue. At higher conversions the relative amount of VIII increased substantially. A similar product profile resulted from oxidations done in the presence of various group VIII metal complexes (*i.e.*, $\text{Fe}(\text{acac})_2$, CoCl_2 , CoBr_2 , $[\text{CoCl}_2(\text{Ph}_3\text{P})_2]$, $[\text{RuCl}_2(\text{Ph}_3\text{P})_3]$, and others) (11, 19, 21, 23). This product distribution did not vary substantially with the metal center nor with the ligand system about the metal in these cases and was similar to that obtained when cyclohexene was oxidized in the presence of the radical initiator, azobisisobutyronitrile. We can conclude, therefore, that the oxidation of cyclohexene in the presence of $[\text{C}_5\text{H}_5\text{Fe}(\text{CO})_2]_2$ is most probably radical initiated and that the decomposition of the intermediate cyclohexenyl hydroperoxide, V, also follows the normal course of radical-initiated decomposition. Indeed, the reaction was severely inhibited by ionol or hydroquinone.

by Metal Acetylacetonates at 70°C^a

<i>Products, mmole</i>			
<i>(VII)</i>	<i>(VIII)</i>	<i>(VI)</i>	<i>Residue</i>
1.55	2.09	0.20	1.14
0.93	1.68	0.35	0.35
3.71	3.90	4.11	1.55
4.11	2.49	4.20	—

Table V. Oxidation of Cyclohexene in the Presence

<i>Metal Complex</i>	<i>Reaction Time, hr</i>	<i>Unreacted Cyclohexene, %</i>
$[\text{C}_5\text{H}_5\text{Fe}(\text{CO})_2]_2$	3	84.0
$[\text{C}_5\text{H}_5\text{Mo}(\text{CO})_3]_2$	3	80.0
$[\text{C}_5\text{H}_5\text{V}(\text{CO})_4]$	5	81.7

^a Oxygen bubbled through 12 ml of cyclohexene containing 1.6×10^{-4} mole metal complex for 4 hrs at 70°C.

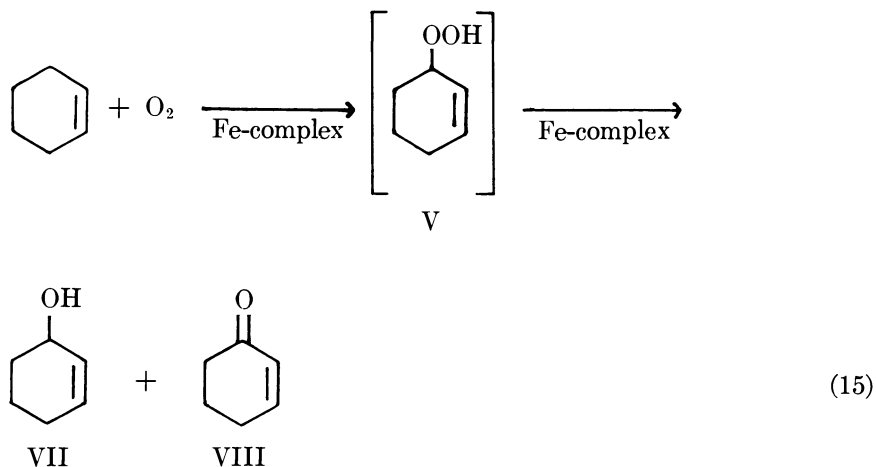
Furthermore, decomposition of a cyclohexene solution of V in the presence of $[\text{C}_5\text{H}_5\text{Fe}(\text{CO})_2]_2$ at 70°C gave VII and VIII as the major products (Table VI). Reaction 15, therefore, represents the predominant course of the oxidation of cyclohexene in the presence of cyclopentadienyldicarbonyl iron dimer.

Table VI. Reactions of a Cyclohexene Solution of Cyclohexenyl Hydroperoxide in the Presence of Cyclopentadienylmetalcarbonyl Complexes^a

<i>Metal Complex</i>	<i>Products, mmole^b</i>				
	<i>V</i>	<i>VI</i>	<i>VII</i>	<i>VIII</i>	<i>IX</i>
$[\text{C}_5\text{H}_5\text{Fe}(\text{CO})_2]_2$	1.2	0.4	2.4	2.8	—
$[\text{C}_5\text{H}_5\text{Mo}(\text{CO})_3]_2$	—	8.4	7.0	—	0.5
$[\text{C}_5\text{H}_5\text{V}(\text{CO})_4]$	—	3.6	7.2	0.8	trace

^a Cyclohexenyl hydroperoxide, 8.0 mmole, in 10 ml of cyclohexene was added to 0.20 mmole of the metal complex and heated with stirring under nitrogen at 70°C for 2 hrs.

^b The quantity (mmole) of the designated products in the solution after 2 hrs reaction.

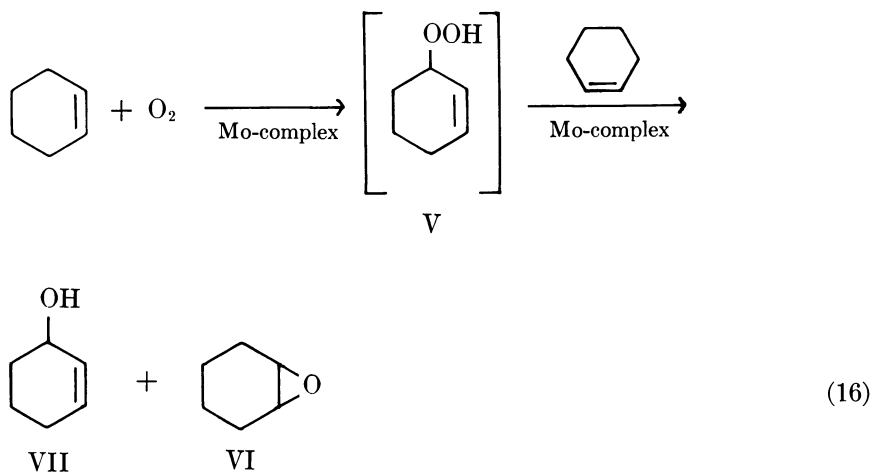


of Cyclopentadienylmetalcarbonyl Complexes^a

<i>Products, mole %^b</i>					
V	VI	VII	VIII	IX	Residue
1.2	1.1	5.0	6.8	—	0.9
0.2	7.5	7.8	1.7	—	3.0
0.3	4.1	2.2	1.0	8.2	2.8

^b Conversions, mole %, of TME to the indicated products.

Cyclohexene oxidation in the presence of the molybdenum complex, $[\text{C}_5\text{H}_5\text{Mo}(\text{CO})_3]_2$, gave two major products at low conversion: VI and VII nearly 1:1 mole ratio, Table V. The ketone, VIII, was formed in very low yield in contrast to oxidations using the iron complex. This reaction is far more selective than the oxidation of cyclohexene in the presence of $\text{MoO}_2(\text{acac})_2$ reported by Gould and Rado (24). When a cyclohexene solution of V was exposed to $[\text{C}_5\text{H}_5\text{Mo}(\text{CO})_3]_2$ at 70°C, VI and VII were formed in approximately equimolar amounts (Table VI). These data show that the molybdenum complex efficiently catalyzes the epoxidation of cyclohexene by V before the allylic hydroperoxide decomposes substantially. Reaction 16 represents the predominant course of cyclohexene oxidation in the presence of cyclopentadienyltricarbonyl molybdenum dimer.



Cyclohexene oxidation in the presence of the vanadium complex, $[\text{C}_5\text{H}_5\text{V}(\text{CO})_4]$, gave a product distribution which differed greatly from that observed with either the iron or the molybdenum complex. The major product, 1,2-epoxy-3-hydroxycyclohexane, IX, was not formed with the iron or molybdenum complexes. The epoxy alcohol, IX, represented

Table VII. Reaction of a Cyclohexene Solution of Cyclohexenyl

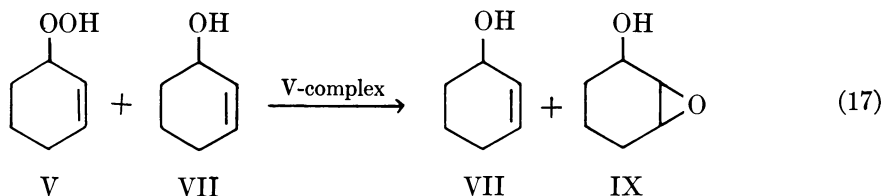
<i>Added Olefin</i>	<i>Time, hrs</i>	<i>T, °C</i>
None ^c	2	70
VII	3	70
II	3	25
VII + II (1:1)	3	25

^a Cyclohexenyl hydroperoxide, 8.0 mmoles, in 10 ml of cyclohexene was added to 0.20 mmole of the metal complex in 0.5 ml of the olefin and stirred under nitrogen at the specified times and temperatures.

^b The quantity (mmole) of the designated products in the solution after the 2 hrs reaction.

more than 50% of the volatile products at 20% conversion. Smaller amounts of VI, VII, and VIII were produced as well (Table V). It is interesting that IX was not reported as a product of cyclohexene oxidation in the presence of vanadylacetylacetonate (24). Allison *et al.* has shown that epoxy alcohols are produced when several allylic hydroperoxides are treated with vanadylacetylacetonate (18). This reaction was considered to be an example of a vanadium-catalyzed rearrangement of an allylic hydroperoxide (18, 19).

When we added a cyclohexene solution of cyclohexenyl hydroperoxide, V, to catalytic quantities of $[C_5H_5V(CO)_4]$ at room temperature, an exothermic reaction occurred with rapid liberation of oxygen (Table VI). The major product was 2-cyclohexene-1-ol, VII. Smaller amounts of VI were formed, and only traces ($< 0.2\%$) of the epoxy alcohol, IX, were detected. This result was consistent with the observation of Gould and Rado concerning the decomposition of V in the presence of $VO(acac)_2$ at 70°C. Decomposition of V in the presence of $[(C_5H_5)_2VCl_2]$ followed the same course as with $[C_5H_5V(CO)_4]$; however, reaction occurred much more slowly at room temperature.



From these results it seems that the epoxy alcohol, IX, does not arise *via* an intramolecular vanadium-catalyzed rearrangement of cyclohexenyl hydroperoxide, V. An alternative pathway is an intermolecular epoxidation reaction between the allylic hydroperoxide, V, and the allylic alcohol which is formed during the oxidation (Reaction 17). We found that IX was produced from reaction of V with VII in the presence of $[C_5H_5V-$

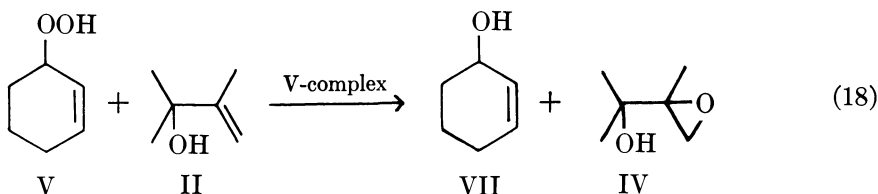
Hydroperoxide with Other Olefins in the Presence of $[\text{C}_5\text{H}_5\text{V}(\text{CO})_4]^a$

<i>Products, mmole^b</i>					
IV	V	VI	VII	VIII	IX
—	—	3.6	7.2	0.8	trace
—	3.9	—	^d	—	4.0
6.2	—	—	6.0	—	—
5.8	—	—	^d	—	trace

^c The solution of cyclohexenyl hydroperoxide in cyclohexene was added directly to the metal complex in this case.

^d Olefin VII is present in excess.

(CO)₄]. Furthermore, when V was contacted with the vanadium complex in the presence of the more reactive allylic alcohol, II, the predominant product was IV (Reaction 18). Results are summarized in Table VII.



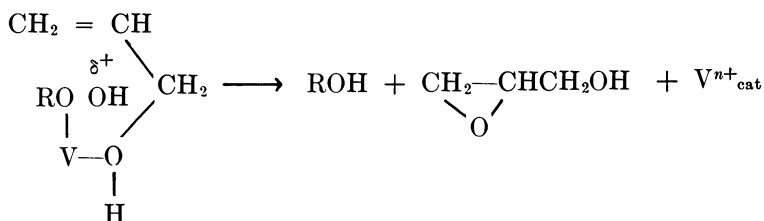
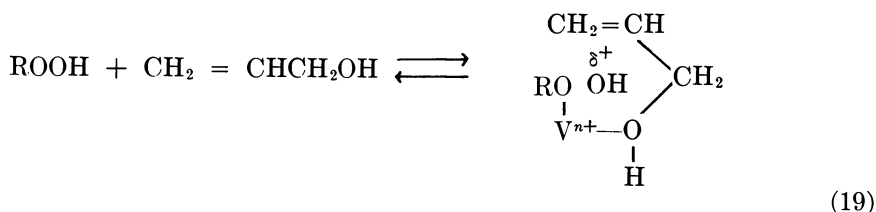
These observations suggest the existence of an intermolecular pathway for the epoxy alcohol formation during TME and cyclohexene oxidation in the presence of $[\text{C}_5\text{H}_5\text{V}(\text{CO})_4]$. The allylic alcohol necessary for intermolecular epoxidation could be formed by radical decomposition of the allylic hydroperoxide during the initiation step. For the epoxy alcohol to be the predominant product, the allylic alcohol which is formed in low yield in these reactions must react far more rapidly with the intermediate hydroperoxide than does the surrounding olefin. We have studied the reaction of *tert*-butyl hydroperoxide with olefins and with the corresponding allylic alcohols and find that this is the case (Table VIII). In the presence of both $[(\text{C}_5\text{H}_5)_2\text{VCl}_2]$ and $[\text{C}_5\text{H}_5\text{V}(\text{CO})_4]$, allylic alcohols were epoxidized much faster than the corresponding simple olefin (Table VIII). Sheng and Zajacek (20) reported the same trend during the VO(acac)₂-catalyzed epoxidation of unsaturated substrates. The mechanism offered by these authors (Reaction 19) involves the coordination of the allylic alcohol to the vanadium center in such a way as to bring the olefinic center close to the hydroperoxidic oxygen (20). This would enhance the rate-determining oxygen transfer step and thus explain the rapid rates of epoxidation of allylic alcohols in the presence of vanadium complexes. Presumably this effect would not be observed when the softer molybdenum complexes are used since they would preferentially

Table VIII. Reaction of *tert*-Butyl Hydroperoxide

Olefin	Reaction Time, hrs	Temperature, °C	<i>tert</i> -Butyl Alcohol
TME	2	50	50
II	2	50	92
TME (90%) + II (10%)	3	50	99
Cyclohexene	2	70	78
VII	2	70	99
Cyclohexene (90%) + VII (10%)	3	70	98

^a After generating the active catalytic species, 0.01 mole *tert*-butyl alcohol was added to 0.1 mole of the olefin containing 2.0×10^{-4} mole of catalyst and stirred under nitrogen for the designated time at the temperature shown.

coordinate the simple olefins. Thus, given a choice between excess olefin and a small amount of allylic alcohol, the molybdenum complex would catalyze olefin epoxidation. These arguments (20) seem to explain quite well the observed differences in product distribution between the vanadium and molybdenum promoted oxidation of TME and cyclohexene (Table V).



Thus, depending on the metal complex used, cyclohexene oxidation can occur *via* one or more of at least three major pathways, as shown in Reaction 20: path A, radical initiated decomposition of cyclohexenyl hydroperoxide; path B, metal catalyzed epoxidation of the olefin; and path C, metal catalyzed epoxidation of an allylic alcohol. Ugo found that path B becomes more pronounced when molybdenum complexes are used to modify the oxidation of cyclohexene in the presence of group

with Olefins in the Presence of $[\text{C}_5\text{H}_5\text{V}(\text{CO})_4]^a$

<i>I</i>	Products, mole % ^b			Unreacted <i>tert</i> -Butyl Hydro- peroxide, %
	<i>IV</i>	<i>VI</i>	<i>IX</i>	
24	—	—	—	50
—	90	—	—	—
0.5	97	—	—	—
—	—	61	—	8
—	—	—	88	—
—	—	28	59	—

^b Conversions, mole %, based on *tert*-butyl hydroperoxide.

VIII metal complexes (27). Since each path has a unique product, the yield of this product gives an estimate of the selectivity of the complex in catalyzing the reaction by each pathway. The iron complex, $[\text{C}_5\text{H}_5\text{Fe}(\text{CO})_2]_2$, seems highly selective for path A whereas the molybdenum complex, $[\text{C}_5\text{H}_5\text{Mo}(\text{CO})_3]_2$, is greater than 80% selective for path B, with the remainder proceeding *via* A. The vanadium complex, $[\text{C}_5\text{H}_5\text{V}(\text{CO})_4]$, exhibits products of all three pathways in the approximate ratio: A/B/C \cong 10/30/60.

As with TME oxidation, the vanadium(IV) complex, $[(\text{C}_5\text{H}_5)_2\text{VCl}_2]$, did not readily initiate cyclohexene oxidation. This complex, however, is an efficient catalyst for allylic alcohol epoxidation. The ability of the vanadium complex to initiate oxidation seems to be a function of its

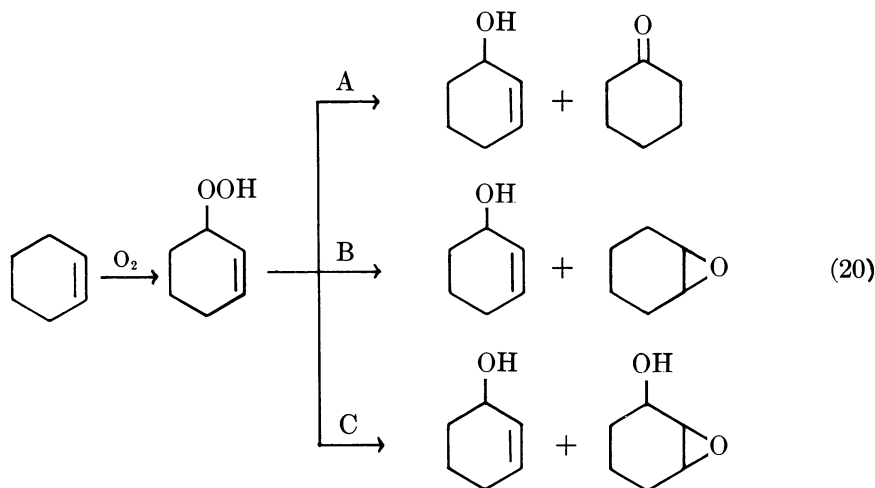


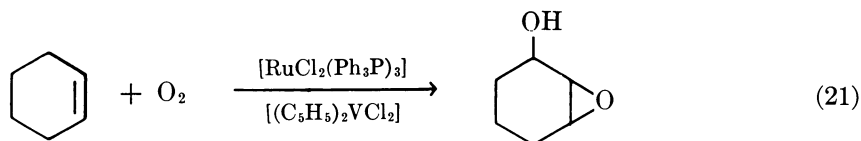
Table IX. Oxidation^a of Styrene in

<i>Metal Complex</i>	<i>Radical Initiator^c</i>	<i>Radical Inhibitor^d</i>	<i>Time, hrs</i>	<i>Conversion, %</i>
			6.0	1
	AIBN		6.0	50
	AIBN	IONOL	6.0	0
IrCl(CO)(Ph ₃ P) ₂			6.0	60
IrCl(CO)(Ph ₃ P) ₂		IONOL	6.0	0
IrH(CO)(Ph ₃ P) ₃			6.0	45
RhCl(CO)(Ph ₃ P) ₂			5.0	59
RhCl(CO)(Ph ₃ P) ₂		IONOL	5.0	0
RuCl ₂ (Ph ₃ P) ₃			3.5	54
RuCl ₂ (Ph ₃) ₃ P ₃		IONOL	3.5	0
OsBr ₂ (Ph ₃ P) ₃			6.0	80

^a Data from Lyons and Turner (31).

^b Oxygen bubbled through a solution of 6 ml styrene in 6 ml toluene containing 0.04 g of metal complex with stirring at 75°C. At the time designated above, volatile materials were collected by vacuum transfer at 0.1 mm from the reaction flask. A gummy residue (10–30% by weight of total product) was left behind. The volatile fraction contained toluene and 70–90% by weight of total reaction product which was analyzed by GLPC.

valence state. The vanadium(I) complex, [C₅H₅V(CO)₄], is an efficient initiator whereas the vanadium(IV) complex is not. This suggests that the process of initiation involves the oxidation of the vanadium complex to a higher valence state where it functions as an epoxidation catalyst once the radical chains have been initiated. As with TME, the epoxy alcohol may be formed during cyclohexene oxidation in the presence of [(C₅H₅)₂VCl₂] if an initiator is also present (*see* Reaction 21). Thus,



mixed-metal systems such as Ru(II)–V(IV) and Ru(II)–V(III) may be used, but selectivities are usually inferior to those obtained with [C₅H₅V(CO)₄] alone. This is the result of competing decomposition of V by the group VIII metal complex.

Oxidation of Styrene. Until now we have considered only olefins which have allylic hydrogen available for radical abstraction. Most of the evidence in these systems suggests the formation of allylic hydroperoxides and their subsequent reaction to form stable oxidation products in the presence of various transition metal complexes. It has not been necessary to postulate novel catalytic activation of oxygen to explain our

the Presence of Metal Complexes^b

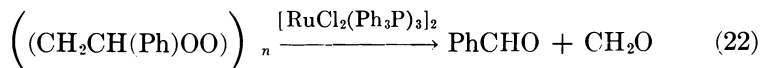
<i>Product Selectivity, %</i>				
<i>Benzaldehyde</i>	<i>Formaldehyde^e</i>	<i>Acetophenone</i>	<i>Styrene Oxide</i>	<i>Polymer</i>
1	—	—	—	—
31	35	—	—	33 ^f
—	—	—	—	—
40	40	2	3	15
—	—	—	—	—
41	32	2	10	15
44	18	4	23	11
—	—	—	—	—
43	16	2	26	13
—	—	—	—	—
41	14	5	24	14

^c 0.04 gram.^d 0.10 gram.^e Sum of formaldehyde which distilled and paraformaldehyde which sublimed from reaction mixture.^f Approximately 50% styrene polyperoxide.

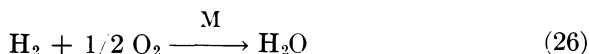
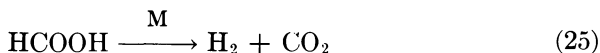
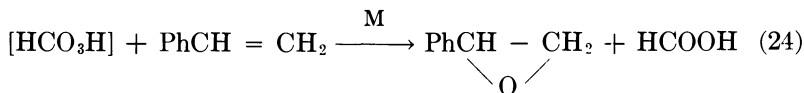
results. Takao and co-workers (28, 29, 30) studied the oxidation of styrene in the presence of group VIII metal complexes including $[\text{IrCl}(\text{CO})(\text{Ph}_3\text{P})_2]$ and $[\text{RhCl}(\text{CO})(\text{Ph}_3\text{P})_2]$. These authors suggest a mechanistic path which involves coordination of molecular oxygen with the metal center, resulting in an increased oxygen–oxygen bond length and enhanced reactivity with styrene in the coordination sphere of the metal (29). This is an interesting possibility since styrene—an olefin with no allylic hydrogen for radical abstraction—might undergo catalytic oxidation under mild conditions *via* a non-radical path in the presence of complexes which react reversibly with both oxygen and olefins.

In work reported elsewhere (31) we have shown that the oxidation of styrene under mild conditions is promoted by many group VIII metal complexes. The product profile depends on the nature of the metal center and often differs from that observed when radical initiators are used (Table IX). Substantial quantities of styrene oxide are found in some cases but not in others (31). The epoxide which is formed, however, seems to arise *via* the co-oxidation of styrene and formaldehyde which is formed by oxidative cleavage of the double bond. Formaldehyde may be oxidized to performic acid or formylperoxy radicals which are efficient epoxidizing agents. Reactions of styrene with oxygen in the presence of group VIII complexes exhibit induction periods and are severely retarded by radical inhibitors (31). Thus, the initial step in the oxidation of styrene in the presence of the Ir(I), Rh(I), Ru(II), and Os(II) com-

plexes which we studied seems to be radical initiated oxidative cleavage of the double bond (32). In the presence of AIBN, styrene polyperoxide is formed (33). The metal complex efficiently cleaved the polyperoxide to give benzaldehyde and formaldehyde (Reaction 22). The substantially



higher epoxide yields which accompany some of these reactions are probably the result of subsequent epoxidations (Reaction 24) which may be subject to metal catalysis. Although formic acid is not a product of this



reaction, it is decomposed to hydrogen and CO_2 by group VIII metal salts and complexes (Reaction 25) (34). Furthermore, hydrogen and oxygen form water under these conditions (Reaction 26) (35). Both water and CO_2 were by-products of styrene oxidation in the presence of $[\text{RuCl}_2(\text{Ph}_3\text{P})_3]_2$. Although there is much evidence to support a radical mechanism for the oxidation of styrene, one cannot rule out competing metal ion activation mechanism.

Conclusions

The oxidation of substituted olefins occurs readily under mild conditions in the presence of transition metal complexes. Although the catalytic metal ion activation and transfer of oxygen to an olefin selectively are attractive goals, this does not seem to be the usual manner in which reaction occurs. Nonetheless, interesting products arise in high yields from these reactions which are not generally found during classical autoxidation. The metal usually exerts its most profound effect during oxidation by catalyzing transformations of hydroperoxide formed *in situ* to several types of oxygenated species. Within the scope of these reactions lies the potential for the selective catalytic synthesis of useful oxygen-containing monomers.

Experimental

Infrared spectra were determined using Perkin-Elmer infrared spectrophotometers models 137-B and 21. NMR spectra were run using Varian T-60 and A-60 spectrometers. Gas chromatographic analyses were done on a Hewlett-Packard model 5750B instrument. Fractional distillations were performed on a Nester-Faust 18-inch semimicro spinning band column equipped with a stainless steel band.

Materials. Olefinic hydrocarbons of at least 99% purity were obtained from Chemical Samples Co., distilled under nitrogen, and then passed through freshly activated silica gel under nitrogen before use. The complexes $[\text{RhCl}(\text{CO})(\text{Ph}_3\text{P})_2]$, $[\text{IrCl}(\text{CO})(\text{Ph}_3\text{P})_2]$, $[(\text{C}_5\text{H}_5)_2\text{VCl}_2]$, $[\text{C}_5\text{H}_5\text{V}(\text{CO})_4]$, $[\text{C}_5\text{H}_5\text{Mo}(\text{CO})_3]_2$, and $[\text{C}_5\text{H}_5\text{Fe}(\text{CO})_2]_2$ were obtained from Strem Chemical Co. The complex $\text{VO}(\text{acac})_2$ was obtained from Ventron Corp., Alpha Products. The complex $[\text{RuCl}_2(\text{Ph}_3\text{P})_3]$ was prepared according to the method of Wilkinson (36). *tert*-Butyl hydroperoxide (92% by titration) was purchased from Lucidol. Oxygen cylinders were obtained from Linde Air Products Co.

Oxidation of TME in the Presence of Metal Complexes. Oxygen was bubbled (1.5 liters/hr) through 12.0 ml of TME containing 8×10^{-5} mole of metal complex for 4 hrs at 50°C. Liquid was returned to the reaction flask by an efficient micro dry ice condenser. A small amount of liquid (~ 0.5 ml) was carried by the gas stream into a -78°C trap and was returned to the reaction flask at the end of the run. After 4 hrs the volatile reaction products were immediately flash evaporated away from the catalyst and 0.3–0.6 gram of a viscous liquid which did not distil by gentle warming at 0.01 mm. The vacuum-transferred reaction mixture was then analyzed by GLPC using a 6 ft \times 0.125 inch column packed with 10% silicone UC-W98 on 80–100 mesh Chromosorb W (Hewlett-Packard) and an injection port temperature under 200°C. It was established using pure standards that little or no decomposition of reaction products occurred during GLPC analysis of product mixtures. I, II, and IV were unaffected by column conditions while a small amount of decomposition of III occurred in the injection port. For this reason, III was also analyzed titrimetrically [iodometric method (34)], and the results agreed to within $\pm 1\%$ of the GLPC value. Compounds I, bp 90.5°C , n_{D}^{20} 1.4014 [lit. (35) n_{D}^{20} 1.4010], $> 99.5\%$ GLPC purity, and II, bp 117°C , n_{D}^{20} 1.4316 [lit. (35) n_{D}^{20} 1.4312], $> 99\%$ GLPC purity were obtained by spinning band distillation of a run using $[\text{RhCl}(\text{CO})(\text{Ph}_3\text{P})_2]$ 10 times the size of those reported above and were identified by comparison of their IR, NMR, and mass spectra with those of authentic samples. Pure III, n_{D}^{20} 1.4432 [lit. (35) n_{D}^{20} 1.4428] was obtained by preparative GLPC and identified by comparison of IR and NMR spectra with those of an authentic sample. Compound IV was obtained in $> 99\%$ purity by preparative GLPC and identified by comparison of its NMR spectrum with that given in the literature (36). IV showed absorptions at 1645 and 2225 $\text{m}\mu$ in the near IR (terminal hydrogens of the epoxy group) and a major fragmentation ion $m/e = 59$ caused by fission of the 2,3-C-C bond. Spectral data for I, II, III, and IV were identical with those reported in the literature (34, 36, 37). When the reaction was run under conditions identical to those above in the *absence* of a metal complex or

an initiator, less than 2% of oxidation products was observed (GLPC) after 4 hrs.

Inhibition by Hydroquinone. Reactions were done under conditions identical with the above in TME which contained 3.3 mole % hydroquinone.

Reactions of *tert*-Butylhydroperoxide in the Presence of Metal Complexes. *tert*-Butylhydroperoxide (0.01 mole) was added dropwise over a 5 min period to 8×10^{-5} mole of $[\text{MCl}(\text{CO})(\text{Ph}_3\text{P})_2]$ ($\text{M} = \text{Rh}, \text{Ir}$); to 1.2×10^{-4} mole of $[\text{C}_5\text{H}_5\text{Mo}(\text{CO})_3]_2$; or to 1.6×10^{-4} mole of $[\text{C}_5\text{H}_5\text{V}(\text{CO})_4]$ in 0.1 mole of TME or toluene at 25°C, and the mixture was stirred for 1 hr under nitrogen. The volatile products were immediately vacuum transferred from the catalyst and analyzed by GLPC (Table II). Little or no organic residue remained. In the case of $[\text{C}_5\text{H}_5\text{V}(\text{CO})_4]$, if 1 mmole of *tert*-butyl hydroperoxide were added slowly to the complex in TME and stirred for 5–10 min before adding 0.09 mole of *tert*-butyl hydroperoxide, the mixture changed from red to orange and I was formed in 13% yield (Table II). If the entire 0.01 mole of *tert*-butyl hydroperoxide were added rapidly to the complex in TME, an exothermic reaction occurred with oxygen evolution, the solution darkened, and I was not observed.

Oxidation of TME in the Presence of Mixed-Metal Systems. Oxygen was bubbled (1.5 l/hr) through 12.0 ml of TME containing 9×10^{-5} mole of one of the group VIII metal complexes: $[\text{IrCl}(\text{CO})(\text{Ph}_3\text{P})_2]$, $[\text{RhCl}(\text{CO})(\text{Ph}_3\text{P})_2]$, or $[\text{RuCl}_2(\text{Ph}_3\text{P})_3]$ and 2.4×10^{-4} mole of $[(\text{C}_5\text{H}_5)_2\text{VCl}_2]$ for 4 hrs at 50°C. The products (I, II, III, and IV) (Table III) were analyzed as described above. Very low yields of III were formed during reaction in the presence of the vanadium complex. At no time did the yield of III exceed 3% in any of these cases.

Reaction of III in the Presence of $[\text{RhCl}(\text{CO})(\text{Ph}_3\text{P})_2]$. Compound III, 0.10 gram, was added to $[\text{RhCl}(\text{CO})(\text{Ph}_3\text{P})_2]$, 0.01 gram, in 1.0 ml of TME, and the mixture was stirred at 50°C for 1 hr under nitrogen. After the reaction mixture was vacuum transferred from the catalyst, it was analyzed by GLPC for total product composition and iodometrically as a check on III. After 1 hr the conversion of III to products was 81%. Products formed were I, (27%), and II (53%). Yields were based on *tert*-butyl hydroperoxide.

Reaction of III in the Presence of $\text{VO}(\text{acac})_2$. Compound III, 99%, 0.17 mmole, was added to 0.18 ml of benzene containing 1.1×10^{-3} mmole, of $\text{VO}(\text{acac})_2$ and the solution was stirred at room temperature for 1 hr. Analysis in the usual manner showed that 94–97% of the allylic hydroperoxide, III, had been converted. The products were IV (85%), II (8%), and small amounts of unidentified materials having long GLPC retention times. A duplicate experiment gave IV (83%) and II (13%) after 1.1 hrs.

Oxidation of Cyclohexene in the Presence of Cyclopentadienyltricyclopentadienyl Metal Complexes. Oxygen was bubbled (1.5 liters/hr) through 12 ml of cyclohexene containing 2.5×10^{-4} mole metal complex for 4 hrs at 70°C. $[\text{C}_5\text{H}_5\text{Fe}(\text{CO})_2]_2$ and $[\text{C}_5\text{H}_5\text{Mo}(\text{CO})_3]_2$ gave orange solutions whereas $[\text{C}_5\text{H}_5\text{V}(\text{CO})_4]$ gave a clear, pale amber solution. Liquid was returned to the flask by an efficient condensing system operating at -20°C . A small amount of liquid (~ 0.5 ml) was carried by the gas

stream into a -78°C trap and was returned to the reaction flask at the end of the run. After 4 hrs the volatile reaction products were immediately flash evaporated from the catalyst and 0.3–0.7 gram of a viscous liquid which did not distil by warming to 80°C at 0.01 mm. This residue was assumed to be largely a dimeric peroxide (41), and its mole percentage was calculated on this basis. The vacuum-transferred reaction mixture was then analyzed iodometrically for cyclohexenyl hydroperoxide. With vanadium and molybdenum complexes practically no hydroperoxide was found (less than 0.3% in each case based on starting cyclohexene). The vacuum-transferred reaction mixtures were then analyzed by GLPC using a 6 ft \times 0.125 inch column packed with 10% silicone UC-W98 on 80–100 mesh Chromasorb W (Hewlett Packard). It was established using pure standards that little or no decomposition of the stable oxidation products (VI, VII, VIII, or IX) occurred during GLPC analysis of product mixtures. With the iron complex, hydroperoxide concentration was greater (1.2 mole %), and it was decomposed with triphenylphosphine (41) before analysis by GLPC. Compounds VI, VII, and VIII were obtained by preparative GLPC and were identified by comparison of their GLPC retention times with those of authentic samples and by comparison of their IR and NMR spectra with commercial samples. Compound IX, bp $96^{\circ}\text{--}98^{\circ}\text{C}/10$ mm, n_{D}^{20} 1.4865, lit. (39) bp $100^{\circ}\text{C}/12$ mm n_{D}^{20} 1.4867; lit. (40) bp $100^{\circ}\text{--}102^{\circ}\text{C}/13$ mm n_{D}^{20} 1.4861, was obtained by a spinning band distillation of a run 10 times the size of those above in which the complex $[\text{C}_5\text{H}_5\text{V}(\text{CO})_4]$ was used. No attempt was made to separate the cis and trans isomers of IX nor did they separate under GLPC analysis. Further identification was made by comparing GLPC retention time with authentic IX prepared by epoxidation of VII using $\text{VO}(\text{acac})_2$ as the catalyst and *tert*-butyl hydroperoxide as the epoxidizing agent. Infrared and NMR spectra were in complete agreement with literature data (42, 43) for IX.

Metal Catalyzed Reactions of a Cyclohexene Solution of Cyclohexenyl Hydroperoxide, V. Solutions of cyclohexenyl hydroperoxide in cyclohexene were prepared by the methods of Gould and Rado (24) and Van Sickle *et al.* (41). In either case a solution approximately 0.7–0.8M in cyclohexenyl hydroperoxide is obtained (24, 41). Smaller concentrations of VI ($\sim 0.01\text{M}$), VII (0.09M), and VIII (0.06M) are also present in solution (24, 41). A solution of cyclohexenyl hydroperoxide (8.0 mmoles by iodometric titration) in 10 ml of cyclohexene was rapidly added to 0.20 mmole of the metal complex and heated with stirring under nitrogen at 70°C for 2 hrs. Metal complexes used were: $[\text{C}_5\text{H}_5\text{Fe}(\text{CO})_2]_2$, $[\text{C}_5\text{H}_5\text{Mo}(\text{CO})_3]_2$, and $[\text{C}_5\text{H}_5\text{V}(\text{CO})_4]$. The reaction mixture was then quickly vacuum transferred at $80^{\circ}\text{C}/0.01$ mm. Little or no residue remained. Yields in mmoles of the products in solution were obtained by GLPC analysis of the vacuum transferred reaction mixtures. Correction was made for the amount of the product initially present (24, 41). Results are listed in Table VI.

Reaction of Cyclohexenyl Hydroperoxide With Allylic Alcohols. Cyclohexenyl hydroperoxide, 8.0 mmoles, in 10 ml of cyclohexene (*see above*) was added to 0.20 mmole of $[\text{C}_5\text{H}_5\text{V}(\text{CO})_4]$ in 0.50 ml of VII and stirred for 3 hrs at 70°C . Then the reaction mixture was vacuum transferred and analyzed as in previous runs. Iodometric titration of the

solution showed 3.9 mmoles of unreacted hydroperoxide while GLPC analysis showed that 4.0 mmoles of IX was produced.

Cyclohexenyl hydroperoxide, 8.0 mmoles, in 10 ml of cyclohexene was added to 0.2 mmole $[\text{C}_5\text{H}_5\text{V}(\text{CO})_4]$ in 0.50 ml of II and stirred for 3 hrs at 70°C. The hydroperoxide was completely converted, and GLPC analysis showed equimolar amounts of VI (6.2 mmoles) and VII (6.0 mmoles) produced.

Cyclohexenyl hydroperoxide, 8.0 mmoles, in 10 ml of cyclohexene was added to 0.2 mmole $[\text{C}_5\text{H}_5\text{V}(\text{CO})_4]$ in a solution of 0.25 ml of II and 0.25 ml of VII; the mixture stirred at room temperature for 3 hrs. The crossover product, IV, (5.8 mmoles) was formed almost exclusively with only a trace (< 0.1 mmole) of product formed having a GLPC retention time identical to IX.

Reaction of *tert*-Butyl Hydroperoxide with Olefins in the Presence of $[\text{C}_5\text{H}_5\text{V}(\text{CO})_4]$. A more active catalyst for epoxidation can be generated *in situ* from the complex: $[\text{C}_5\text{H}_5\text{V}(\text{CO})_4]$, by adding a small amount of *tert*-butyl hydroperoxide (1×10^{-3} mole) to 0.1 mole of the olefin containing (4×10^{-4} mole) of the vanadium complex and stirring 5–10 min. The solution turns from red to light orange, and more hydroperoxide can now be added without rapid decomposition.

After generating the active catalytic species, 0.1 mole *tert*-butyl alcohol was added to 0.1 mole of the olefin containing 4×10^{-4} mole of catalyst, and the mixture was stirred under nitrogen. Thus, TME, II, and a 90/10 mixture (vol %) of TME and II were each allowed to react with *tert*-butyl hydroperoxide at 50°C. Similarly, cyclohexene, VIII, and a 90/10 mixture of cyclohexene and VII were each allowed to react with *tert*-butyl hydroperoxide at 70°C. Product work-up and analysis are identical to previous runs (GLPC and iodometric titration). Results are listed in Table VIII.

Acknowledgment

The author thanks John O. Turner, who collaborated with him in early studies of the group VIII metal catalyzed oxidation of TME and styrene, Caroline Link for technical assistance, and Arthur Brown for iodometric titrations and experimental assistance.

Literature Cited

1. Valentine, J. S., *Chem. Rev.* (1973) **73**, 235.
2. Choy, V. J., O'Connor, C. J., *Coord. Chem. Rev.* (1973) **9**, 145.
3. Hartley, F. R., *Angew. Chem. Int. Ed. Engl.* (1972) **11**, 596.
4. Biellman, J. F., Hemmer, H., Levisalles, J., "The Chemistry of Alkenes," Vol. 2, Chap. 5, Interscience, New York, 1970.
5. Hartley, F. R., *Chem. Rev.* (1969) **69**, 799.
6. van Gaal, H., Cuppers, G., van der Ent, A., *Chem. Commun.* **1970**, 1694.
7. Ugo, R., *Engelhard Tech. Bull.* (1970) **11**, 45.
8. Mimoun, H., Seree de Roch, I., Sajus, L., *Tetrahedron* **1970**, 37.
9. Dudley, C., Read, G., *Tetrahedron Lett.* **1972**, 5273.
10. Van Sickle, D., Mayo, F., Arluck, R., Szy, M., *J. Amer. Chem. Soc.* (1967) **89**, 967.

11. "Transition Metals in Homogeneous Catalysis," G. N. Shrauzer, Ed., Marcel Dekker, New York, 1971.
12. Lyons, J., Turner, J., *J. Org. Chem.* (1972) **37**, 2881.
13. James, B., Ochiai, E., *Can. J. Chem.* (1970) **49**, 975.
14. Fusi, A., Ugo, R., Fox, F., Pasini, A., Cenini, S., *J. Organometal. Chem.* (1971) **26**, 417.
15. Howard, J., Ingold, K., *Can. J. Chem.* (1967) **45**, 793.
16. Indictor, N., Brill, W., *J. Org. Chem.* (1965) **30**, 2074.
17. Sheng, N., Zajacek, J., *ADVAN. CHEM. SER.* (1968) **76**, 418.
18. Allison, K., Johnson, P., Foster, G., Sparke, M., *Ind. Eng. Chem., Prod. Res. Develop.* (1966) **5**, 166.
19. Jachberger, T., Miller, D., Herman, F., Indictor, N., *J. Org. Chem.* (1971) **26**, 4078.
20. Sheng, N., Zajacek, J., *J. Org. Chem.* (1970) **35**, 1839.
21. Collman, J. P., Kubota, M., Hosking, J., *J. Amer. Chem. Soc.* (1967) **89**, 4811.
22. Chalk, A., Smith, J., *Trans. Faraday Soc.* (1957) **53**, 1214.
23. Kurkov, V., Pasky, J., Lavigne, J., *J. Amer. Chem. Soc.* (1968) **90**, 4744.
24. Gould, E., Rado, M., *J. Catal.* (1969) **13**, 238.
25. Baldwin, J., Swallow, J., *Angew. Chem.* (1969) **81**, 571.
26. Cenini, S., Fusi, A., Capparella, G., *J. Inorg. Nucl. Chem.* (1971) **33**, 3579.
27. Ugo, R., private communication.
28. Takao, K., Fujiwara, Y., Imanaka, T., Teranishi, S., *Bull. Chem. Soc. Jap.* (1970) **43**, 1153.
29. Takao, K., Wayaku, M., Fujiwara, Y., Imanaka, T., Teranishi, S., *Bull. Chem. Soc. Jap.* (1970) **43**, 3898.
30. *Ibid.* (1972) **45**, 1505.
31. Lyons, J., Turner, J., *Tetrahedron Letters* **1972**, 2903.
32. Sheldon, R., *Chem. Commun.* **1971**, 788.
33. Miller, A., Mayo, F., *J. Amer. Chem. Soc.* (1956) **78**, 1017.
34. Coffey, R., *Chem. Commun.* **1967**, 923.
35. Vaska, L., Tadros, M., *J. Amer. Chem. Soc.* (1971) **93**, 7099.
36. Hallman, P., McGarvey, B., Wilkinson, G., *J. Chem. Soc. A* **1968**, 3143.
37. Silbert, L., Swern, D., *Anal. Chem.* (1958) **30**, 385.
38. Foote, C., Wexler, S., *J. Amer. Chem. Soc.* (1964) **86**, 3879.
39. Pierre, J., Chaulemps, P., Arnaud, P., Gey, C., *Chim. Anal. (Paris)* (1968) **50**, 494.
40. Bartlett, P., Mendenhall, G., *J. Amer. Chem. Soc.* (1970) **92**, 210.
41. Van Sickle, D., Mayo, F., Arluck, R., *J. Amer. Chem. Soc.* (1965) **87**, 4824.
42. Henbest, H., Wilson, R., *J. Chem. Soc.* **1957**, 1958.
43. Chamberlain, P., Roberts, M., Whitman, G., *J. Chem. Soc. (B)* **1970**, 1374.

RECEIVED August 20, 1973.

Synthesis and Reactions of Palladium–Carbon Sigma-Bonded Complexes

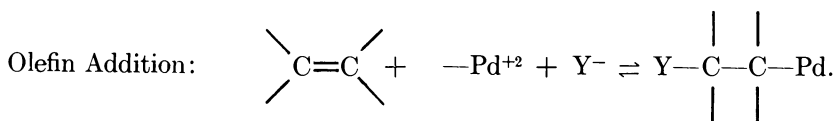
J. K. STILLE, L. F. HINES, R. W. FRIES, P. K. WONG,
D. E. JAMES, and K. LAU

University of Iowa, Iowa City, Iowa 52242

Complexes containing carbon–palladium sigma bonds can be stereospecifically synthesized by the addition reactions of palladium(II) and a nucleophile across an olefin by the oxidative addition of an alkyl halide to palladium(0) and by the exchange reaction of palladium(II) with an organomercurial. When carbon monoxide is present, these reactions provide stereospecific catalytic syntheses of carboxylic esters by insertion of carbon monoxide into the carbon–palladium sigma bond with retention of configuration at carbon. Halogens and acid halides also cleave carbon–palladium sigma bonds, in some cases stereospecifically.

In most organic syntheses involving palladium, palladium–carbon sigma bonds are involved at some stage in the reaction pathway (1). Two important types of reactions which take place in organo-palladium syntheses are oxidative additions to palladium(0) and addition of palladium(II) complexes across olefins as well as the respective reverse (elimination) reactions. In both these reactions, carbon–palladium sigma bonds are made and broken:

Oxidative Addition: $RX + Pd \rightleftharpoons R-Pd-X$



Such reactions become especially valuable if they are stereospecific or stereoselective, if they can be carried out to give compounds not readily available by other means, or if they are practical in the laboratory and/or

economical by virtue of their development into a catalytic process. In most cases, however, the stereochemistry of these reactions cannot be determined readily since the carbon-palladium sigma-bonded complexes are unstable. Furthermore, a knowledge of the stereochemistry of the reactions of carbon-palladium sigma bonds requires a prior knowledge of the steric nature of the carbon attached to palladium.

Formation of Carbon-Palladium Sigma Bonds

Palladium(II)-Nucleophile Addition across Olefins. Adding palladium complexes to olefins, either in the presence of an external nucleophile or a ligand which is attached to palladium, produces a palladium-carbon sigma-bonded complex which is not usually isolated in the case of monoolefins. Instead it decomposes and in doing so oxidizes the olefin to an organic carbonyl compound or a vinyl compound, exchanges a substituent group on the olefin, isomerizes the double bond, arylates (alkylates) the olefin, or carboxylates the olefin (2, 3).

In the case of certain diolefins, the palladium-carbon sigma-bonded complexes can be isolated and the stereochemistry of the addition with a variety of nucleophiles is trans (4, 5, 6). The stereochemistry of the addition-elimination reactions in the case of the monoolefins, because of the instability of the intermediate sigma-bonded complex, is not clear. It has been argued (7, 8, 9) that the chelating diolefins are atypical, and the stereochemical results cannot be extended to monoolefins since approach of an external nucleophile from the cis side presents steric problems. The trans stereochemistry has also been attributed either to the inability of the chelating diolefins to rotate 90° from the position perpendicular to the square plane of the metal complex to a position which would favor cis addition by metal and a ligand attached to it (10), or to the fact that methanol (nucleophile) does not coordinate to the metal prior to addition (11). In the Wacker Process, the kinetics of oxidation of olefins suggest, but do not require, the cis hydroxypalladation of olefins (12, 13, 14). The acetoxypalladation of a simple monoolefin, cyclohexene, proceeds by trans addition (15, 16).

The addition-elimination reaction of olefins presents a dichotomy of mechanistic results in that many of the reactions are consistent with either a cis addition, cis elimination or trans addition, trans elimination, and in others, either a cis addition followed by a trans elimination or *vice versa*. Furthermore, in some cases predominately Markovnikov addition is observed, and in others anti-Markovnikov is observed.

Most of these mechanistic differences with simple olefins can be rationalized by considering two types of addends or nucleophiles; those which are coordinated to palladium transferring directly from palladium

Table I. Catalytic Carbonylation Products^b

Olefin	Methyl 3-Methoxy-2-Butanecarboxylate			
	Time, hrs	% Yield	% Threo	% Erythro
<i>cis</i> -2-Butene	2	1.4	100	0
	8	6.7	100	0
	100	33	87	13
<i>trans</i> -2-Butene	2	0.7	0	100
	8	1.9	0	100
	100	19	40	60
<i>cis</i> -2-Butene ^d	100	0	—	—
<i>trans</i> -2-Butene ^d	100	0	—	—

^a 50 mmole olefin, 2.8 mmole PdCl₂, 100 mmole CuCl₂, 75 ml methanol, 2 atm CO at 28°C.

^b % Yield ± 1%, determined by GLC and based on olefin. Isomer distribution ± 1%

to an olefin carbon and those which are solvated but not coordinated, forming a bond with carbon by external nucleophilic attack. An inspection of the literature reveals that those addition–elimination reactions in which the addend or nucleophile can be considered to be coordinated to palladium just prior to reaction proceeded by *cis* addition, anti-Markovnikov, and *cis* elimination. Those addition–elimination reactions in which the nucleophile can be considered to be solvated and uncoordinated proceed by *trans* addition, Markovnikov, and *trans* elimination.

One approach to the problem of determining the stereochemistry of the unstable palladium–carbon sigma-bonded intermediate is its trapping by replacement of the palladium with some other group by a reaction that takes place at least competitively with elimination. The carbonylation of such intermediates proceeds more rapidly than the elimination, and it proceeds with 100% retention of configuration at the carbon bearing the palladium (17, 18).

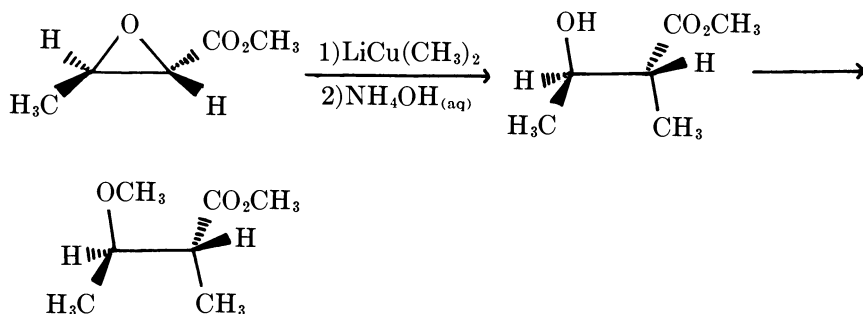
The carbonylation of both *cis*- and *trans*-2-butene in methanol in the presence of a palladium catalyst and copper(II) has demonstrated the stereochemistry of this oxymetallation of simple monoolefins (19). In the initial stages of the reaction, stereospecific *trans* methoxypalladation is observed, yielding exclusively the *threo*- and *erythro*-β-methoxy esters, respectively (Table I). In the later stages of the reaction *cis*–*trans* isomerization of both butenes becomes increasingly important such that *trans* methoxypalladation to the *cis*–*trans* mixtures yield both *erythro* and *threo* products. The rate of methoxypalladation of *cis*-2-butene is approximately three times faster than that of the *trans* isomer.

The *erythro* and *threo* isomers were identified by the independent synthesis of *threo*-methyl 3-methoxy-2-butanecarboxylate (20).

of *cis*- and *trans*-2-Butene^a

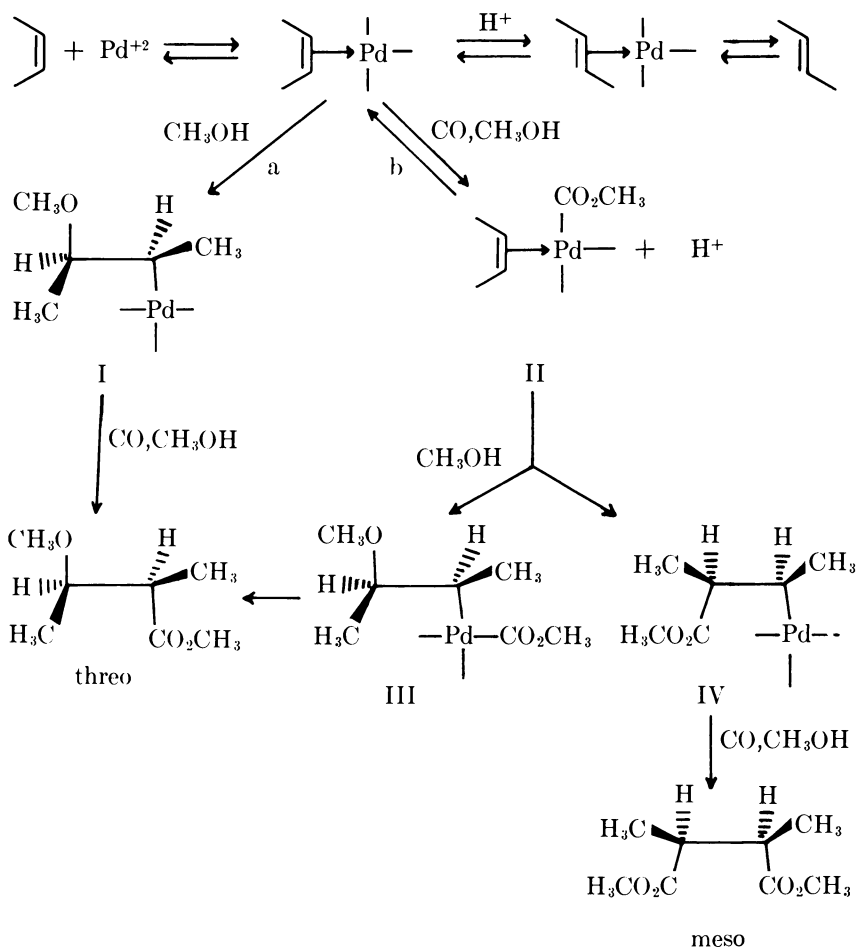
Products ^b				
Dimethyl 2,3-Butanedicarboxylate			Olefin Isomerization	
% Yield	% <i>d,l</i> ^c	% <i>Meso</i> ^c	% <i>Cis</i>	% <i>Trans</i>
—	—	—	100	0
—	—	—	85	15
1	60	40	23	77
—	—	—	0	100
—	—	—	5	95
1	100	0	20	80
3	0	100	100	0
20	100	0	0	100

determined by GLC.

^c Identified by hydrolysis to the corresponding acids (21).^d 100 mmole of sodium acetate added to the reaction mixture.

Substituted succinic esters are formed coincidentally with the methoxy esters, although in relatively smaller amounts. *cis*-2-Butene gives a mixture of diesters, meso and *d,l*-pair, while *trans*-2-butene yields only the *d,l* enantiomers. By the addition of sodium acetate, conditions which preclude prior isomerization of the olefins are obtained; the diesters are the exclusive products, and the dicarbonylation is stereospecifically *cis*. The carbonylation of *trans*-2-butene, which is at least seven times faster than that of the *cis* isomer, gives exclusively the *d,l*-succinic ester while *cis*-2-butene gives only the meso diastereomer. These results are consistent with the mechanism shown for *cis*-2-butene (19) (see top of next page).

Several aspects of this mechanism deserve comment. The *cis*-*trans* isomerization reaction appears to be acid catalyzed as isomerization does not occur in the early stages of the reaction or under buffered (sodium acetate) conditions. The *threo*- β -methoxy ester could be readily obtained from the carbonylation of the intermediate product I resulting from *trans*



methoxypalladation of the *cis*-2-butene. The olefin palladium carboxylate complex II is a plausible common intermediate to both the β -methoxy ester and the diester. Trans attack of uncoordinated methanol solvent could give the sigma-bonded complex III which undergoes carbon monoxide insertion and reaction with methanol also to give the *threo*- β -methoxy ester. Alternatively, II may undergo a *cis* addition of palladium and coordinated carboxylate to yield the sigma-bonded complex IV, carbonylation of which gives the observed *meso* diester.

The faster rate of the conversion of *cis*-2-butene to β -methoxy ester relative to *trans*-2-butene is consistent with this mechanism which requires formation of a more stable π complex for the *cis* isomer (22) and greater relief of steric repulsion in the transition state for the *trans* addition to a *cis* olefin. By contrast, *cis* addition of coordinated carboxylate

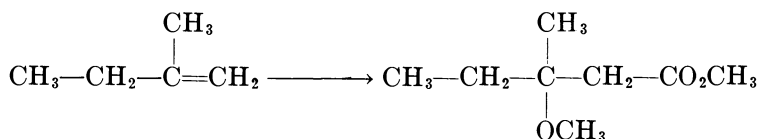
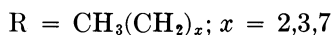
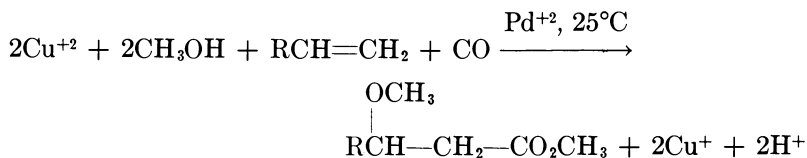
ligand and palladium to *cis*-2-butene to form diester requires a transition state generating greater steric crowding than that observed for the *trans* isomer.

The relative rate data, showing that the rate of methoxypalladation is greater for the *cis* isomer while the rate of carbomethoxypalladation is greater for the *trans* isomer, also suggests that IV is not an intermediate in the formation of both β -methoxy ester and diester products. Although S_N2 displacement of palladium by nucleophile has been demonstrated in acetic acid systems (15, 16) and postulated for alcoholic systems (23), it is clear that β -methoxy ester and diester products are best explained by two distinctly different intermediates arising from the rate-determining step (formation of the Pd-C sigma-bonded complex).

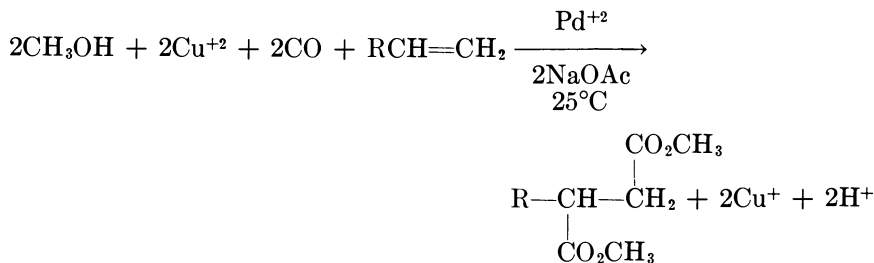
The affect of added acetate to this system is quite remarkable in that it can change the course of the reaction completely, and either β -methoxy ester or diester can be obtained at will. Several explanations are possible. If path a and b each are exclusively responsible for the formation of β -methoxy ester and diester, respectively, sodium acetate may enhance the formation of intermediate II by base catalysis. Also, acetate ion may influence the rates of the reactions occurring by the different pathways by coordination to palladium, thereby changing the structures of the intermediate complexes and thus their activity.

The synthesis of succinic acid derivatives, β -alkoxy esters, and α,β -unsaturated esters from olefins by palladium catalyzed carbonylation reactions in alcohol have been reported (24, 25, 26, 27), but full experimental details of the syntheses are incomplete and in most cases the yields of β -alkoxy ester and diester products are low. A similar reaction employing stoichiometric amounts of palladium(II) has also been reported (28). In order to explore the scope of this reaction for the syntheses of β -alkoxy esters and succinic acid derivatives, representative cyclic and acyclic olefins were carbonylated under these same conditions (Table I). The reactions were carried out in methanol at room temperature using catalytic amounts of palladium(II) chloride and stoichiometric amounts of copper(II) chloride under 2 atm of carbon monoxide. The methoxypalladation reaction of 1-pentene affords a good conversion (55%) of olefin to methyl 3-methoxyhexanoate, the product of Markovnikov addition. In the carbonylation of other 1-olefins, β -methoxy methyl esters were obtained in high yields; however, substitution of a methyl group on the double bond reduced the yield of ester markedly. For example, the carbonylation of 2-methyl-1-butene afforded < 10% yield of methyl 3-methyl-3-methoxypentanoate. This suggests that unsubstituted 1-olefins may be preferentially carbonylated in the presence of substituted 1-olefins or internal olefins. The reactivities of the olefins fall in the order: $RCH=CH_2 > cis-RCH=CHR > trans-RCH=CHR >$

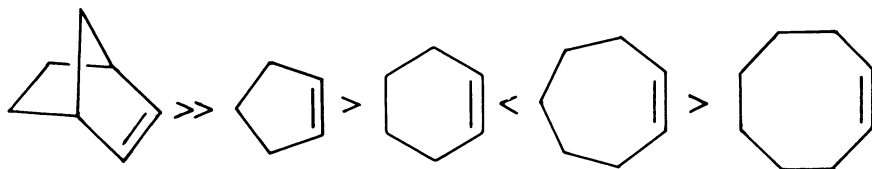
$R_2C=CH_2$. When greater than stoichiometric amounts of copper(II) were added to the reaction, quantitative yields of the β -methoxy ester could be obtained.



As in the case of *cis*- and *trans*-2-butenes, added sodium acetate completely alters the reaction path, and only diesters are obtained from 1-olefins.



Under the standard reaction conditions (no sodium acetate), the cyclic olefins tested afforded predominantly diesters with the exception of cyclohexene which gave a low yield of β -methoxy ester (Table II). In each case, the cycloalkane 1,2- and 1,3-dicarboxylic esters obtained were the *cis* isomers. The relative rates of diester formation show the



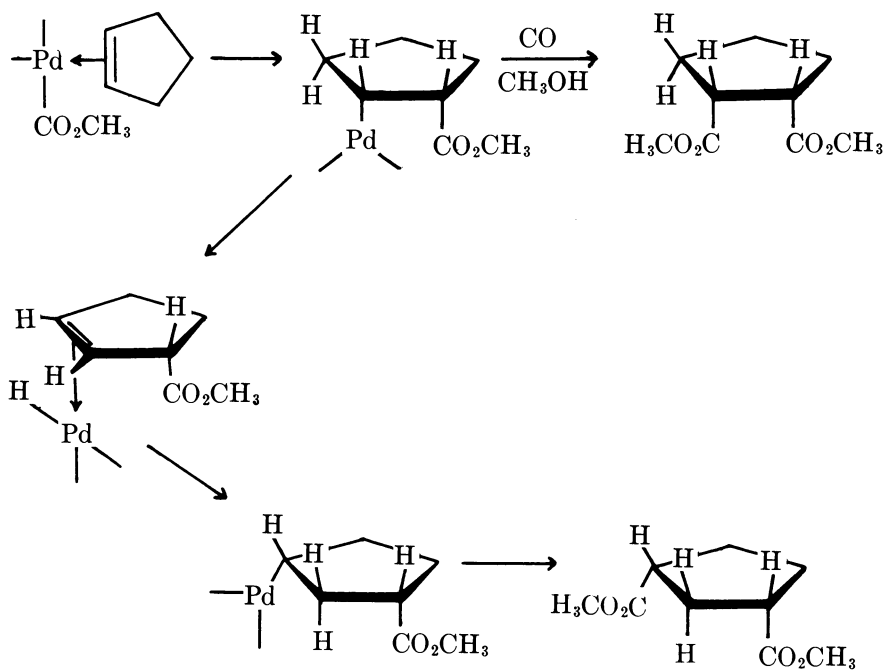
same order as that established for hydroformylation (29) and hydroboration by disiamylborane (30). These results are also consistent with *cis* addition to a double bond where the rate of the reaction is influenced

Table II. Carbonylation of Cyclic Olefins

<i>Olefin</i>	<i>Products</i>	<i>Product Ratio</i>		<i>Conversion, %</i>
		<i>2 atm CO</i>	<i>15 atm CO</i>	
Norbornene	dimethyl <i>exo-cis</i> -norbornane-2,3-dicarboxylate	—	—	82
Cyclopentene	dimethyl <i>cis</i> -1,2-cyclopentane-dicarboxylate	1	1.5	60
	dimethyl <i>cis</i> -1,3-cyclopentane-dicarboxylate	4	1	
Cyclohexene	methyl <i>trans</i> -2-methoxycyclohexanecarboxylate	—	—	17
Cycloheptene	dimethyl <i>cis</i> -1,2-cycloheptane-dicarboxylate	1	4	58
	dimethyl <i>cis</i> -1,3-cycloheptane-dicarboxylate	1.9	1	
Cyclooctene	dimethyl <i>cis</i> -1,2-cyclooctane-dicarboxylate	9	—	<10
	dimethyl <i>cis</i> -1,3-cyclooctane-dicarboxylate	1	—	
	methyl <i>trans</i> -2-methoxycyclooctanecarboxylate	trace	—	

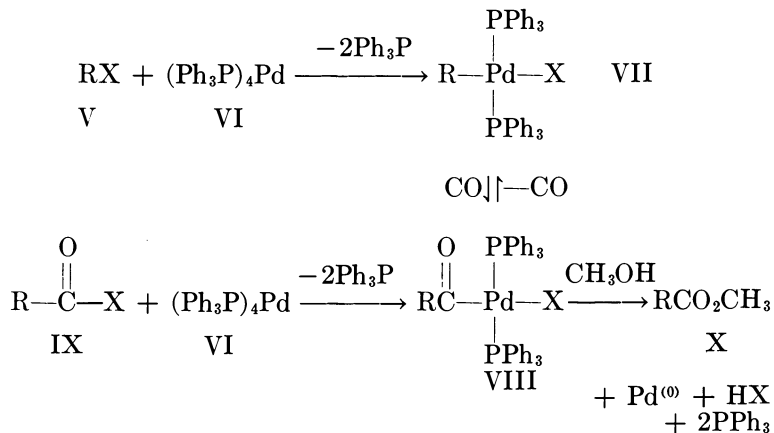
by the magnitude of the internal strain of the olefin. The influence of internal strain is also reflected in the type of product formed. While the strained olefins give predominately diester, unstrained cyclohexene behaves more like 2-butene in yielding methyl *trans*-2-methoxycyclohexanecarboxylate. Increasing the carbon monoxide pressure has the effect of increasing the amount of 1,2-diester at the expense of the 1,3-diester. These results are consistent with a mechanism in which the carboxymethyl-palladium *cis* 1,2-addition intermediate is formed first and can rearrange *via* a palladium hydride elimination and readdition before carbonylation to give the 1,3-diester. Increasing the carbon monoxide pressure increases the rate at which the 1,2-addition intermediate is trapped, effectively reducing the rearranged product (*see* top of next page).

Oxidative Addition of Alkyl Halides to Palladium(0). The stereochemistry of the oxidative addition (31) of alkyl halides to the transition metals of group VIII can provide information as to which of the many possible mechanisms are operative. The addition of alkyl halides to d^8 -iridium complexes has been reported to proceed with retention (32), inversion (33), and racemization (34, 35) *via* a free radical mechanism at the asymmetric carbon center. The kinetics of this reaction are consistent with nucleophilic displacement by iridium on carbon (36). Oxi-



dative addition of alkyl halides to d^8 -cobalt has also been reported to occur with inversion of configuration at carbon (37).

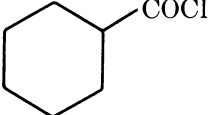
Tetrakis(triphenylphosphine)palladium(0) (VI) is regarded as coordinatively saturated yet it is potentially unsaturated since it undergoes dissociation in solution thereby allowing oxidative addition to take place. A new convenient method for preparing VI (38) in addition to the fact that it readily undergoes oxidative addition (39, 40, 41, 42, 43, 44) make this reaction attractive for studying the stereochemistry of the process.



The oxidative addition is quite general with alkyl, allyl, benzyl, vinyl, and aryl halides as well as with acyl halides to afford the palladium(II) complex VII. The *trans*-bis(triphenylphosphine)alkylpalladium halides can also be carbonylated in an insertion reaction to give the corresponding acyl complexes, the stereochemistry of which (17, 18) proceeds with retention of configuration at the carbon bonded to palladium. The acyl complex also can be formed from the addition of the corresponding acid halide to tetrakis(triphenylphosphine)palladium(0).

Various alkyl and acyl halides have been reported (39, 40, 41, 42, 43, 44) to undergo addition to tetrakis(triphenylphosphine)palladium(0). In addition, the analogous reaction with the halides listed in Table III has been carried out.

Table III. Halides Used in Addition Reactions

<i>RX</i> Type Structure V	<i>RCOX</i> Type Structure IX
a $C_6H_5CH_2Cl$	a $C_6H_5CH_2COCl$
b $CH_2=CH-CH_2Cl$ (sigma-complex)	
c $CH_3CH_2-\overset{\overset{CH_3}{ }}{CH}-Br$	c $CH_3CH_2-\overset{\overset{CH_3}{ }}{CH}-COBr$
d $C_6H_5-\overset{\overset{CF_3}{ }}{CH}-Cl$	d $C_6H_5-\overset{\overset{CF_3}{ }}{CH}-COCl$
e $C_6H_5-C(CH_3)_2CH_2Cl$	e $C_6H_5C(CH_3)_2CH_2COCl$
	f $(CH_3)_3C-COCl$
	g $C_6H_5-\overset{\overset{C(CH_3)_3}{ }}{CH}-COCl$
	h 

In each case the alkyl complex VII formed from RX could be converted to the acyl complex VIII which was identical to a sample of VIII prepared by the addition of the acid halide (RCOX) to VI. Complex VIII could be decomposed in methanol to afford the methyl ester of the acid. Analytically pure compounds were obtained in most cases.

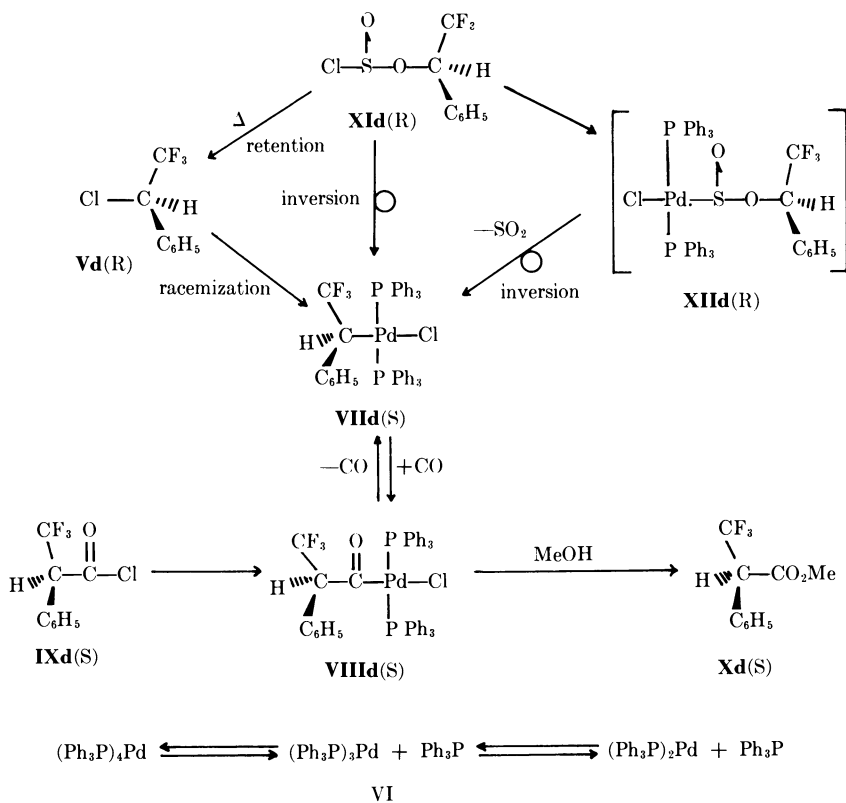
The reaction of compound Vc afforded a comparatively stable complex considering the fact that it contains a hydrogen β to the palladium and therefore can decompose by a β elimination of palladium hydride. Evidently, the triphenylphosphine ligands in this complex provide some added degree of stability toward this decomposition pathway.

The addition of the acid halide to VI does not involve R and thus will not affect the configuration of an optically active R group. The stereochemistry of the conversion of VII to VIII proceeds with retention of configuration at R (*vide supra*) and thus the stereochemistry of two of the links in the cycle—at least in one direction—is known. Optically active 1-phenyl-2,2,2-trifluoroethanol (45) was stereospecifically converted to the corresponding chloride Vd which has the advantage that it contains no β hydrogens and that the product of its oxidative addition to palladium(0) cannot decompose *via* palladium hydride elimination. Optically active 2-phenyl-3,3,3-trifluoropropionic acid (46) was converted to the corresponding acid chloride IXd with thionyl chloride; hydrolysis of a portion of the acid chloride gave back the starting acid without any loss of optical activity. Since oxidative addition of the acid chloride IXd to tetrakis(triphenylphosphine)palladium(0) does not involve the chiral center, it therefore provides the acyl complex VIIIId of known geometry. Further, complex VIIIId, which had a strong carbonyl absorption at 1675 cm^{-1} , was converted by the reaction with methanol to ester (46) of the same absolute configuration as the acid.

When the addition of optically active Vd to tetrakis(triphenylphosphine)palladium(0) was carried out, a stable complex VIIc was obtained which exhibited no rotation; essentially the reaction proceeded with racemization.

Optically active 1-phenyl-2,2,2-trifluoroethanol was also converted to its chlorosulfite ester, XIId, by reaction with thionyl chloride. When XIId was added to VI, the stable complex VIIIId was also obtained which exhibited a sign of rotation opposite to that of the starting chloride Vd and chlorosulfite ester, XIId. Treatment of a slurry of VIIId in ether or acetone with carbon monoxide afforded complex VIIIId containing a strong carbonyl absorption (1675 cm^{-1} , CHCl_3) with an absolute rotation larger than that of VIIId, but of the same sign. Complex VIIIId was identical to that obtained from acid chloride IXd of the opposite configuration. Thus the oxidative addition of the chlorosulfite ester XIId to the d^{10} palladium complex proceeded with net inversion of configuration at carbon. Tetrakis(triphenylphosphine)palladium(0) (47) dissociates in solution to tris- and bis(triphenylphosphine)palladium(0) (47) and apparently can act as a nucleophile in the displacement of halogen from aryl halides since the substitution of + sigma groups on the ring facilitates these oxidative additions (42). Direct nucleophilic displacement of

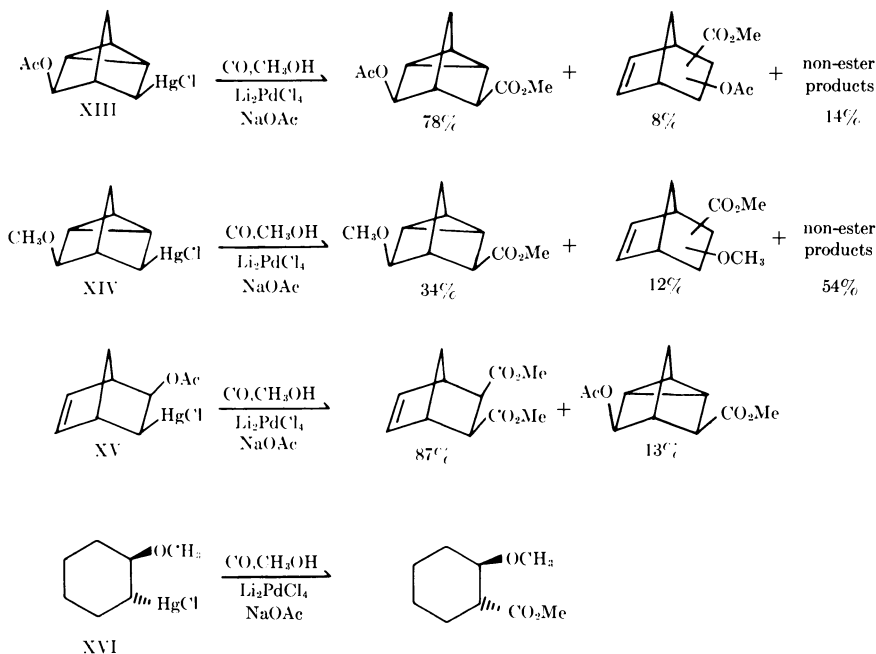
chloride from Vd, however, would be expected to proceed with inversion of configuration at the asymmetric carbon to afford an optically active complex VIIId. Prior solvolysis of Vd probably does not take place to yield the trifluoromethyl phenyl carbonium ion and subsequently racemic VIIId since both the chlorosulfite ester, XIId, and the tosylate of 1-phenyl-2,2,2-trifluoroethanol are unusually resistant to solvolysis. The oxidative addition of alkyl chlorides to palladium(0) most probably takes place by a free radical mechanism. Recently, the oxidative addition product of optically active ethyl- α -bromopropionate to bis(*tert*-butyl-isonitrile)palladium(0) was isolated, but the complex was racemic (48). Racemization was attributed to a β elimination and readdition, a mechanism which does not appear to be likely in light of the results obtained with Vd.



The reaction of the chlorosulfite ester XIId with palladium(0) may take place by direct nucleophilic displacement of the chlorosulfite group at carbon by palladium or *via* an intermediate sulfite complex XIIId. The direct nucleophilic displacement would be expected to take place with inversion of configuration. The reaction of the chlorosulfite ester to afford

XIId does not involve the chiral center, so if the reaction takes place by this pathway, the migration of the alkyl group from sulfur to palladium (with the concomitant or subsequent loss of sulfur dioxide) must take place with inversion of configuration at carbon. Inversion of configuration at carbon has been observed in the reverse-type reaction, the sulfur dioxide insertion into a carbon-iron sigma bond (49). Nucleophilic displacement at carbon in compounds of type XIId is unusually difficult, so the reaction *via* the sulfite intermediate XIId would appear to be more likely. Conversion of the tosylate of 1-phenyl-2,2,2-trifluoroethanol to the corresponding chloride, a reaction which takes place in the presence of tetra-(*n*-butyl)ammonium chloride with inversion of configuration at carbon, requires 100°C for 24 hrs in dimethylsulfoxide.

Palladium Exchange Reactions with Alkyl Mercury Compounds. A third possible method of stereospecific synthesis of palladium-carbon sigma-bonded complexes involves the reaction of alkylmercury chlorides of known configuration with palladium chloride. This reaction is known to produce an olefin as a result of β -palladium hydride elimination from the intermediate palladium-carbon sigma-bonded complex through the exchange of palladium for mercury (50, 51). Trapping the unstable palladium intermediate, again by carbonylation, gives some information concerning the stereochemistry of this palladium-mercury exchange reaction (52). The reaction has been carried out with mercurials of types



XIII–XVI in methanol by adding a palladium catalyst under 1 atm of carbon monoxide.

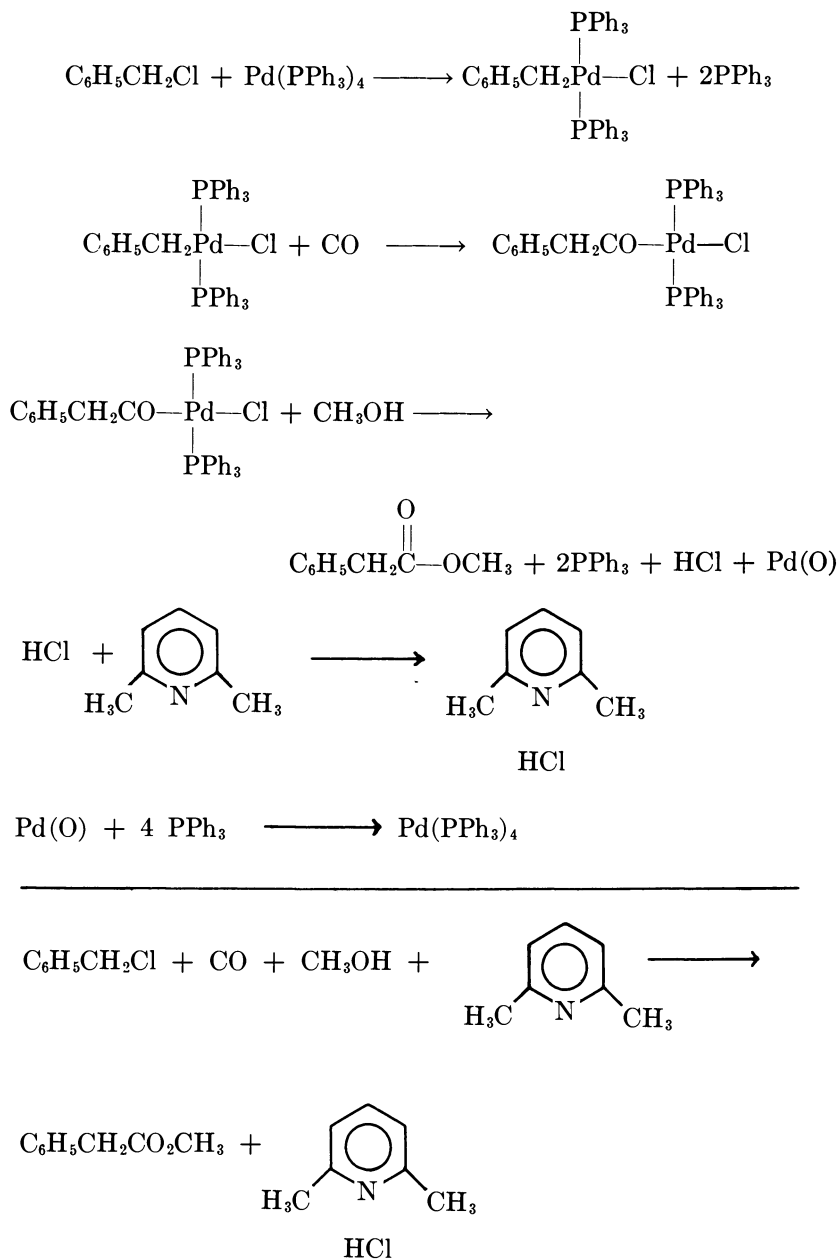
These results show that the palladium exchange reaction takes place predominately with retention of configuration at the carbon bearing the mercury.

Reactions of Carbon–Palladium Sigma Bonds

Carbon Monoxide Insertion. The reactions of carbon–palladium sigma-bonds discussed above have been useful in elucidating the configuration of organopalladium compounds since the insertion proceeds with complete retention of configuration. This reaction would be much more valuable if the oxidative addition and carbonylation reaction could be made to be catalytic with respect to palladium. When the acyl complex VIII containing palladium in the +2 oxidation state is formed in the presence of methanol, the corresponding methyl ester of the acid is obtained, producing palladium(0). In other reagents, palladium(0) precipitates. In this case, however, molar amounts of triphenylphosphine are present to regenerate VI. In other reactions in which palladium(0) is a product, triphenylphosphite in the reaction effectively coordinates with palladium keeping it in solution (53). Removing HX from the reaction mixture is essential to recycling the tetrakis(phosphine)palladium catalyst, however (54). By the addition of 2,6-lutidine, a base which is a poor nucleophile, benzyl chloride can be converted to methyl phenylacetate with a twentyfold turnover of palladium catalyst (*see* p. 104).

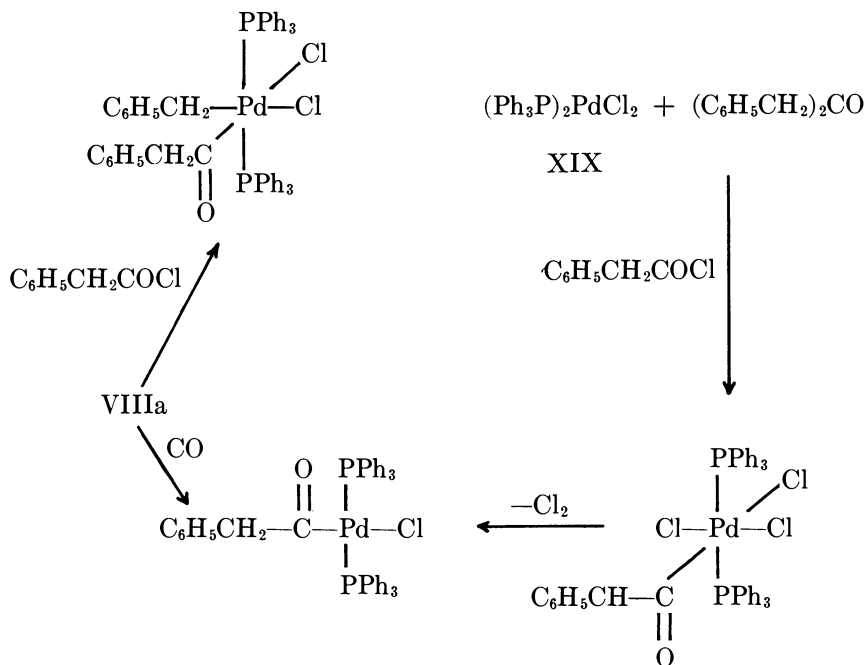
Reactions with Acyl Halides. The palladium–carbon bond in alkyl VII and acyl VIII complexes also can be broken by acyl and alkyl halides, respectively, to give ketones (55). The reaction of the benzyl complex VIIa with acetyl chloride in the presence of 2,6-lutidine provided good yield of methyl benzyl ketone, XVII. In the absence of the base, lower yields (26%) were obtained. Surprisingly, a similar reaction between the benzyl complex and an excess of phenylacetyl chloride afforded a 156% yield of dibenzyl ketone, XVIII, based on the starting benzyl complex (*see* bottom of p. 105).

The facts that the phenylacetyl complex VIIIa also undergoes a reaction with phenylacetyl chloride under identical experimental conditions to yield dibenzyl ketone, XVIII (218% with respect to VIIIa), and that XVII was also obtained from the reaction of phenylacetyl chloride with dichlorobis(triphenylphosphine)palladium(0), XIX, implicate XIX in the catalytic cycle. The palladium(II) complex XIX does indeed catalyze the conversion of an acyl halide to the corresponding symmetrical ketone (123% with respect to XIX). The palladium(IV) structures are only

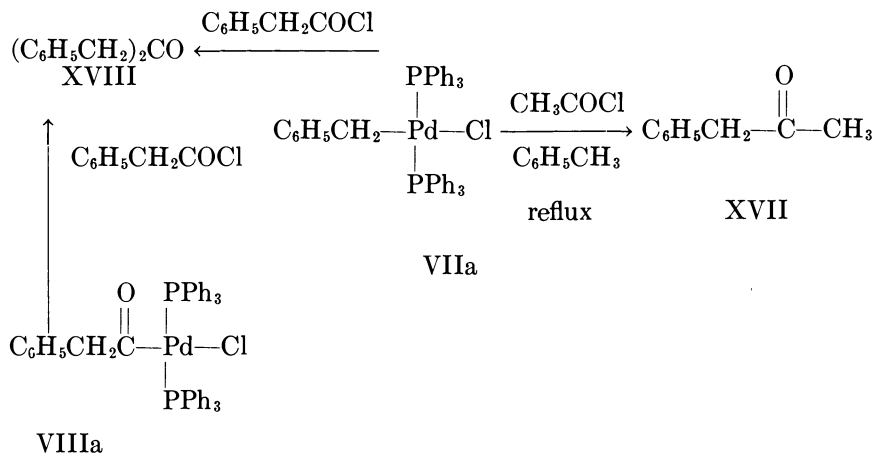


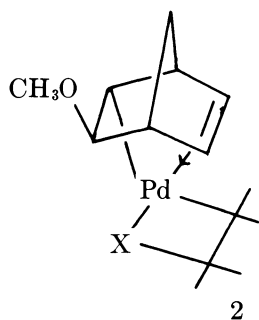
postulated intermediates; alternate mechanisms include a concerted, four-centered transition leading from VIIIa to XIX (*see* top of next page).

Reactions with Halogens. Bromination and chlorination of the noricyclic complex XXa proceed (56) with retention of configuration at

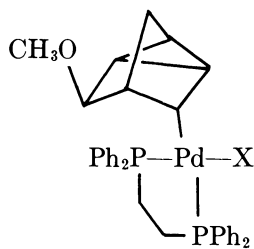


the carbon bearing the palladium. The mechanism of the reaction, especially with regard to radical or ion attack and whether there is prior coordination to palladium, is unknown. In order to test the generality of this stereochemistry and learn more about the mechanism of halogen cleavage, the halogenation reaction of complexes XX–XXII was investigated.

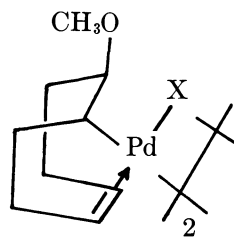




XX

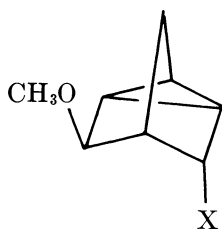


XXI

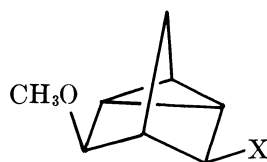


XXII

The halogenation of compounds XX and XXI in methylene chloride afforded a mixture of 3-*exo*-methoxy-5-halonortricylenes in all cases (Table IV and V).



XXIIIa



XXIIIb

Table IV. Halogenation of Methoxynorbornenyl Complex^a

Complex	Halogen	T, °C	% Cl (<i>endo/exo</i>)	% Br (<i>endo/exo</i>)
XX				
Cl	Cl ₂	25	100 (83/17)	—
Cl	Cl ₂	-78	100 (84/16)	—
Br	Br ₂	25	—	100 (82/18)
Br	Br ₂	-78	—	100 (87/13)
Cl	Br ₂	25	22 (70/30) ^b	78 (80/20) ^b
Br	Cl ₂	-78	77 (75/25) ^b	23 (70/30) ^b

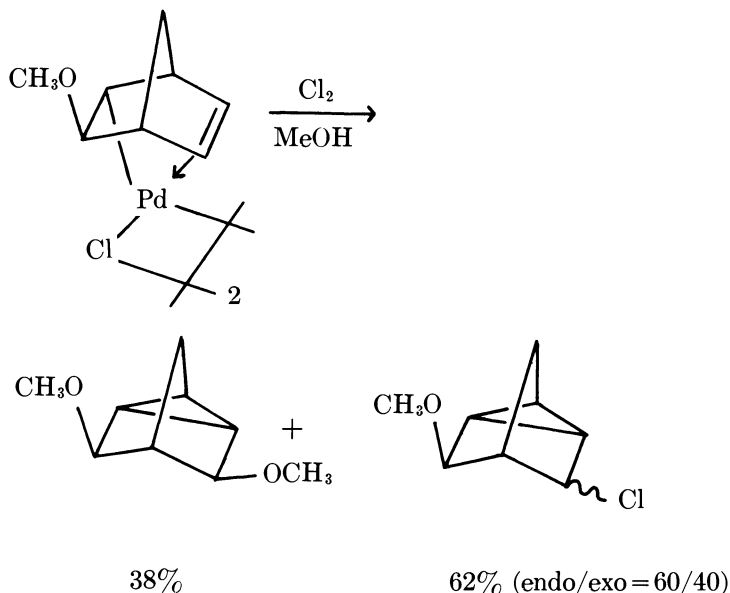
^a Results reproducible within ±3%.

^b Error ±5%.

Table V. Halogenation of Methoxynortricyclenyl Complex

Complex XXI	Halogen	T, °C	XXIII (<i>endo/exo</i>)
Cl	Cl ₂	25	91/9
Cl	Cl ₂	-78	96/4
Br	Br ₂	25	84/16
Br	Br ₂	-78	88/12

When the chlorination of XXa was carried out in methanol, the following products were obtained.

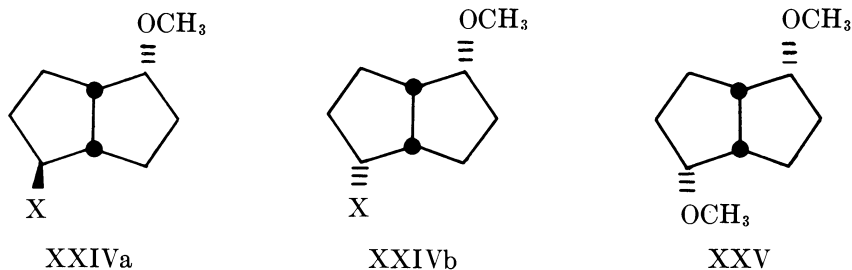


Also, in the halogenation of XXb with cyanogen bromide the predominate product was the nortricyclic bromide (XXIIIa and b, X = Br); the treatment of XXIa with iodine monochloride yields the *endo*-nortricyclic iodide (XXIIIa, X = I). Thus the mechanism appears to involve attack of a positive halogen with predominate retention of configuration at carbon.

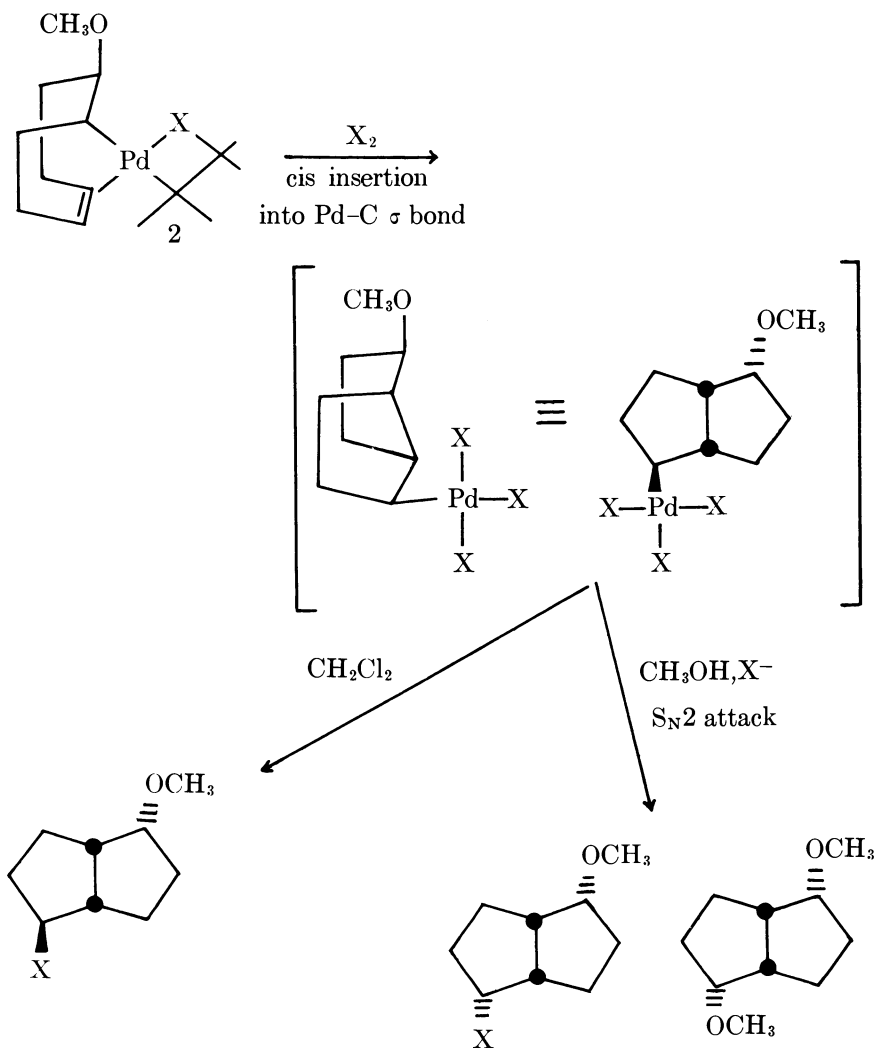
Table VI. Halogenation of Methoxycyclooctenyl Complex

Complex XXII	Halogen	Solvent	% XXIV (<i>exo/endo</i>)	% XXV
Cl	Cl ₂	CH ₂ Cl ₂	100 (72/28)	—
	Cl ₂	CH ₃ OH	77 (17/83)	23
	Cl ₂	CH ₃ OH, LiCl	98 (14/86)	2
Br	Br ₂	CH ₂ Cl ₂	100 (95/5)	—
	Br ₂	CH ₃ OH	58 (45/55)	42
	Br ₂	CH ₃ OH, NaBr	100 (10/90)	—

Halogenation of complex XXII afforded a mixture of 2-*endo*-methoxy-6-halo-*cis*-bicyclo[3.3.0]octane epimers, XXIVa and XXIVb (Table VI). In methanol, 2,6-*endo,endo*-dimethoxy-*cis*-bicyclo[3.3.0]octane, XXV, was obtained in addition to XXIV. The presence of halide ions suppressed the formation of XXII and favored that of XXIVb. Control experiments showed that both XXIV and XXV were primary products and did not



arise from nucleophilic attack at XXII. The structures XXIVa, XXIVb, and XXV were established by independent syntheses.



The results can be rationalized in terms of an oxidative addition-reductive elimination mechanism as illustrated with XXII. A similar mechanism has been proposed for the acid cleavage of Pt(II)-C sigma bond (57, 58).

Literature Cited

1. Tsuji, J., *Fortschr. Chem. Forsch.* (1972) **28**, 41.
2. Maitlis, P. M., "The Organic Chemistry of Palladium," Academic, New York (1971).
3. Henry, P. M., *Accounts Chem. Res.* (1973) **6**, 16.
4. Stille, J. K., Morgan, R. A., *J. Amer. Chem. Soc.* (1966) **88**, 5135.
5. Panattoni, C., Bombieri, G., Forsellini, E., Crociani, B., Belluco, U., *Chem. Commun.* (1969) 187.
6. Stille, J. K., Fox, D. B., *J. Amer. Chem. Soc.* (1970) **92**, 1274.
7. Heck, R. F., *Fortschr. Chem. Forsch.* (1971) **16**, 221.
8. Henry, P. M., *ADVAN. CHEM. SER.* (1968) **70**, 151; *Amer. Chem. Soc., Div. Petrol. Chem., Prepr.*, **14**, F17, New York, 1969.
9. Green, M., Hancock, R. I., *J. Chem. Soc. A* (1967) 2054.
10. Shaw, B. L., *Chem. Commun.* (1968) 464; *Amer. Chem. Soc., Div. Petrol. Chem., Prepr.*, **14**, F17, New York, 1969.
11. Hartley, F. R., *Nature London* (1969) **223**, 615.
12. Henry, P. M., *ADVAN. CHEM. SER.* (1968) **70**, 126-154.
13. Henry, P. M., *J. Amer. Chem. Soc.* (1964) **86**, 3246.
14. *Ibid.*, (1966) **88**, 1595.
15. Henry, P. M., Ward, G. A., *J. Amer. Chem. Soc.* (1971) **93**, 1494.
16. *Ibid.*, (1972) **94**, 7305.
17. Stille, J. K., Hines, L. F., *J. Amer. Chem. Soc.* (1970) **92**, 1798.
18. Hines, L. F., Stille, J. K., *J. Amer. Chem. Soc.* (1972) **94**, 485.
19. Stille, J. K., James, D. E., Hines, L. F., *J. Amer. Chem. Soc.* (1973) **95**, 5062.
20. Herr, R. W., Wieland, D. M., Johnson, C. R., *J. Amer. Chem. Soc.* (1970) **92**, 3813.
21. Linstead, R. P., Whalley, M., *J. Chem. Soc.* (1954) 3722.
22. Hartley, F. R., *Chem. Rev.* (1973) **73**, 163.
23. Kaliya, O. L., Tomkin, O. N., Mekhryakova, N. G., Flid, R. M., *Dokl. Akad. Nauk. SSSR* (1971) **199**, 706.
24. Fenton, D. M., U.S. Patent 3,397,226 (1968); *Chem. Abs.* (1968) **69**, 66919n.
25. Tsuji, J., Takahashi, H., Japanese Patent 15,165 (1968); *Chem. Abs.* (1969) **70**, 67653d.
26. Biale, G., U.S. Patent 3,530,168 (1970).
27. Fenton, D. M., Steinwand, P. J., *J. Org. Chem.* (1972) **37**, 2034.
28. Heck, R. F., *J. Amer. Chem. Soc.* (1972) **94**, 2712.
29. Wendel, I., Metlin, S., Ergun, E., Sternberg, H. W., Greenfeld, H., *J. Amer. Chem. Soc.* (1956) **78**, 5401.
30. Brown, H. C., "Hydroboration," pp. 198-202, W. A. Benjamin, Inc., New York, 1962.
31. Collman, J. P., *Accounts Chem. Res.* (1968) **1**, 136.
32. Pearson, R. G., Muir, W. R., *J. Amer. Chem. Soc.* (1970) **92**, 5519.
33. Labinger, J. A., Braus, R. J., Dolphin, D., Osborn, J. A., *Chem. Commun.* (1970) 612.
34. Bradley, J. S., Connor, D. E., Dolphin, D., Labinger, J. A., Osborn, J. A., *J. Amer. Chem. Soc.* (1972) **94**, 4043.

35. Jensen, F. R., Knickel, B., *J. Amer. Chem. Soc.* (1971) **93**, 6339.
36. Chock, P. B., Halpern, J., *J. Amer. Chem. Soc.* (1966) **88**, 3511.
37. Jensen, F. R., Madan, V., Buchanan, D. H., *J. Amer. Chem. Soc.* (1970) **92**, 1414.
38. Coulson, D. R., *Inorg. Syn.* (1972) **13**, 121.
39. Fitton, P., Johnson, M. P., McKeon, J. E., *Chem. Commun.* (1968) 6.
40. Fitton, P., McKeon, J. E., *Chem. Commun.* (1968) 4.
41. Fitton, P., McKeon, J. E., Ream, B. C., *Chem. Commun.* (1969) 370.
42. Fitton, P., Rick, E. A., *J. Organometal. Chem.* (1971) **28**, 287.
43. Rosevear, D. T., Stone, F. G. A., *J. Chem. Soc. A* (1968) 164.
44. Mukhedkar, A. J., Green, M., Stone, F. G. A., *J. Chem. Soc. A* (1969) 3023.
45. Peters, H. M., Feigel, D. M., Mosher, H. S., *J. Org. Chem.* (1968) **33**, 4245.
46. Aaron, C., Dull, D., Schmiegl, J. L., Jaeger, D., Ohashi, Y., Mosher, H. S., *J. Org. Chem.* (1967) **32**, 2797.
47. Fischer, E. O., Werner, H., *Chem. Ber.* (1962) **95**, 703.
48. Otsuka, S., Nakamura, A., Yoshida, T., Naruto, M., Ataka, K., *J. Amer. Chem. Soc.* (1973) **95**, 3180.
49. Whitesides, G. M., Boschetto, D. J., *J. Amer. Chem. Soc.* (1971) **93**, 1529.
50. Moiseev, I. I., Vargaftik, M. N., *Dokl. Akad. Nauk SSSR* (1966) **166**, 81.
51. Heck, R. F., *J. Amer. Chem. Soc.* (1968) **90**, 5518.
52. Henry, P. M., *Tetrahedron Lett.* (1968) 2285.
53. Brown, E. S., Rick, E. A., *Amer. Chem. Soc., Div. Petrol. Chem., Prepr.*, **14**, B29 (Minneapolis, 1969).
54. Kudo, K., Hidai, M., Murayama, T., Uchida, Y., *Chem. Commun.* (1970) 1701.
55. Carturan, G., Graziani, M., Ros, R., Belluco, U., *J. Chem. Soc., Dalton Trans.* (1972) 262.
56. Coulson, D. R., *J. Amer. Chem. Soc.* (1969) **91**, 200.
57. Belluco, U., Croatto, U., Uguagliati, D., Pietropaolo, R., *Inorg. Chem.* (1967) **6**, 718.
58. Belluco, U., Giustiniani, M., Graziani, M., *J. Amer. Chem. Soc.* (1967) **89**, 6494.

RECEIVED July 30, 1973. Work partially supported by the Petroleum Research Fund.

The Use of Oxidized Rhodium Complexes in Catalytic Reactions

ROBERT L. AUGUSTINE, REGIS J. PELLET, JAN F. VAN PEPPEN, and JOHN P. MAYER

Seton Hall University, South Orange, N. J. 07079

Oxygen containing rhodium complexes reduced in the presence of a variety of ligands can be made to produce mixed ligand complexes which are capable of catalyzing olefin hydrogenation. In such reactions catalyzed by these mixed ligand complexes both reaction rate and product stereochemistry are dependent on the nature of the added ligand.

In determining the scope and utility of the homogeneous hydrogenation catalyst, $(\phi_3\text{P})_3\text{RhCl}$ (**1**) (*1*), the addition of small amounts of oxygen or hydrogen peroxide resulted in a marked increase in the rate of olefin hydrogenation (*2, 3*). It was further shown that oxygen in benzene-ethanol solutions of **1** is responsible for the double bond isomerization which takes place along with olefin hydrogenation over **1** in this mixed solvent system (*3*). In an attempt to clarify the role of oxygen in these reactions, **1** was treated with oxygen in a number of solvents, and the oxidized complexes that formed were isolated and characterized (*4, 5*).

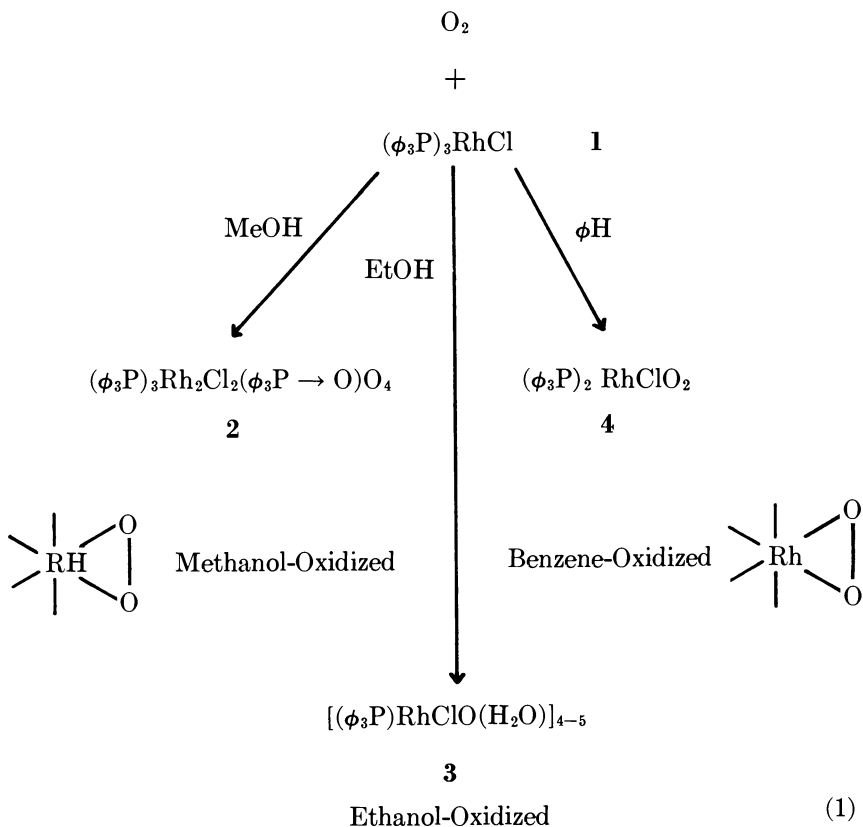
In methanol the initial gas uptake was quite rapid with 1.5–1.8 moles of oxygen absorbed per mole of **1**. The oxidized product (*see 2* in Reaction 1) precipitated and was isolated by filtration and washed thoroughly with ether. The IR spectrum of **2** had strong absorption bands at 850 (dioxygen ligand) (*6, 7*) and 1120 cm^{-1} (triphenylphosphine oxide) (*8*). X-ray analysis established a Rh:P:Cl ratio in **2** of 1:2:1. These data along with the elemental analyses and molecular weight determinations indicated the formula, $\text{Rh}_2(\phi_3\text{P})_3(\phi_3\text{P} \rightarrow \text{O})\text{O}_4\text{Cl}_2$ for **2** (*4*).

In ethanol the amount of oxygen consumed was greater than in methanol with an average of 3.3 moles of oxygen taken up per mole of **1**. The soluble oxidized complex thus formed, **3**, was isolated by evaporating the solvent and washing the residue thoroughly with ether. The IR spectrum of **3** had no absorption band at 850 cm^{-1} but did have one at

1550 cm^{-1} (complexed water) (9). The formula $[\text{Rh}(\phi_3\text{P})(\text{H}_2\text{O})\text{OCl}]_{4-5}$ has been proposed for 3 (4). In dry benzene one mole of oxygen was absorbed and a third oxide, 4, was formed. This species had a dioxygen ligand (strong 850 cm^{-1} absorption band in the IR spectrum), no phosphine oxide ligand, and a proposed molecular formula of $\text{Rh}(\phi_3\text{P})_2\text{O}_2\text{Cl}$ (5). The oxidation reactions are summarized in Reaction 1. In the following discussion the methanol-oxidized, ethanol-oxidized, and benzene-oxidized species will be referred to respectively as 2, 3, and 4.

The ethanol-oxidized material, 3, could be reduced to give a fair hydrogenation catalyst (10) but a much better catalyst was obtained by hydrogenating 3 in the presence of an equivalent of triphenylphosphine (6). These oxidized species, 2, 3, and 4, were used to prepare series of mixed ligand complexes and thus made available catalyst systems in which reactivity and selectivity can be carefully controlled.

In some preliminary work, 3 was hydrogenated in the presence of a number of ligands, and the resulting solutions were used for the hydrogenation of 1-heptene. Rate data for these reactions are given in Table I.

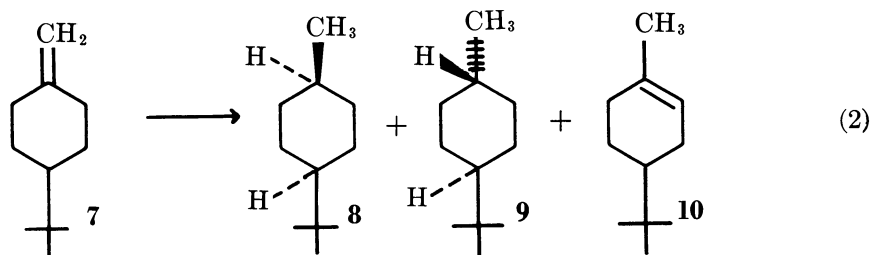


As these data indicate, even those ligands known to have an adverse effect on homogeneous olefin hydrogenation over analogs of 1, *i.e.*, $n\text{-Bu}_3\text{P}$ and pyridine, give better catalysts for this reaction than that obtained from the hydrogenation of 3 in the absence of any added ligand. Furthermore when no ligand was present the use of reduced 3 in olefin hydrogenation gave rise to extensive double bond isomerization which was not observed with any of the ligands listed in Table I.

Table I. Effect of Added Ligand on the Rate of 1-Heptene Hydrogenations over Reduced 3

Ligand	Relative Rate
—	1.0
$\phi_3\text{P}$	6.4
$\phi_3\text{As}$	3.2
$n\text{-Bu}_3\text{P}$	2.3
Pyridine	1.2

Since the product stereochemistry obtained on hydrogenation of substituted cyclohexenes and methylenecyclohexanes was very useful in the comparison and mechanistic determinations of both heterogeneous (11) and homogeneous (12) catalysts, it was decided to use the *cis* (8)/*trans* (9) ratio obtained from the hydrogenation of 4-*tert*-butylmethylenecyclohexane (7) (TBMC) as a probe for comparing the various catalysts prepared from 2, 3, and 4.



The hydrogenation of 7 over the catalyst prepared by the reduction of 3 in the absence of any added ligand gave a *cis*/*trans* product ratio of 4.0. In addition, a rather large amount of the endo olefin, 10, was also formed. When the catalyst was prepared by the reduction of 3 in the presence of triphenylphosphine (6), a saturated isomer ratio of 2.0 was observed with no double bond isomerization. The same product stereochemistry and lack of double bond isomerization was also found using pre-hydrogenated 1 in the reduction of 7 (3). Thus, one might assume that the catalytic species in these latter two reactions are quite similar, if not identical.

These results gave some support to the premise that mixed ligand complexes could be prepared from these oxidized rhodium complexes. Because of the supposed polymeric nature of **3** and the difficulty encountered in determining the nature of the oxygen function present in this species, more attention was devoted to studying the reactions of **2** and **4**, in both of which the nature of the oxygen function has been established.

The hydrogenation of **2** occurred reasonably well in benzene-ethanol to give a rather poor catalyst for the hydrogenation of 1-heptene. The reduction of **2** in the presence of **6** gave a catalyst which was almost twice as reactive for this hydrogenation (Table II). In both cases though, double bond isomerization occurred almost as rapidly as did hydrogenation of **7** over these reduced **2** catalysts. But in this case, the catalyst prepared from **2** in the absence of **6** was almost completely unreactive, presumably because of the increased bulk of the olefin (Table III).

Table II. Hydrogenation of 1-Heptene over Reduced **2**

<i>Ligand</i>	<i>Rate of H₂ Uptake ml/min./mmole</i>	<i>Heptane, %</i>	<i>2-Heptene, %</i>
None	5.4	45	31
$\phi_3\text{P}$	9.0	53	31

Hydrogen is not necessary for the reduction of the oxide which can be accomplished merely by stirring **2** in benzene-ethanol for two days under nitrogen. A black solution was thus obtained which was a poor catalyst for the hydrogenation of TBMC (**7**). A cis/trans product ratio of 3.0 was obtained from this reaction. When **2** was reduced in the presence of **6** the catalyst formed was about 10 times more reactive for the

Table III. Hydrogenation of TBMC over Reduced **2**

<i>Added Ligand</i>	<i>Reducing Agent</i>	<i>ml H₂/min/ mmole Rh</i>	<i>% 7</i>	<i>% 10</i>	<i>% 8 & 9</i>	<i>C/T</i>
—	H ₂ -Ethanol	3.85	23	11	66	1.9
$\phi_3\text{P}$	H ₂ -Ethanol	71	66	15	19	2.2
—	Ethanol	0.63	19	20	61	3.0
$\phi_3\text{P}$	Ethanol	7.46	17	47	36	2.5

hydrogenation of **7**. In both of these reactions a large amount of the isomerized olefin, **10**, was formed. The catalytic species formed in these reactions are still unidentified but the fact that they promote extensive double bond isomerization and give product stereochemistry ratios greater than 2.0 show that they differ from those formed using **1** as the catalyst in hydrogenations.

When **2** was heated for a short time under nitrogen with amines or amides, dark solids or oils were formed. These reactive mixtures, which

are soluble in benzene or benzene-ethanol, were used directly as catalysts for olefin hydrogenation. Alternately, the catalytic species was isolated by washing with ether to remove excess amine or amide.

In these reactions triphenylphosphine was liberated, and the IR spectrum of the product showed that the dioxygen ligand was no longer present (absence of the strong 850 cm^{-1} bond). X-ray analyses showed a Rh:P:Cl ratio of 1:1:1 in these products. The presence of amine or amide ligands in the catalytic species was verified by IR, PMR, and elemental analysis. Despite this instrumental and analytical data, no reasonable formula can be proposed for any of these species.

The rates of hydrogenation of 1-heptene over a number of catalysts prepared from **2** and a variety of amines and amides are listed in Table IV. The activity of these catalysts is clearly related to the degree of substitution on the nitrogen atom of the amine or amide used in their preparation. This is most obvious by comparing Run 5 with Run 6 and Run 9 with Run 10.

Table IV. 1-Heptene Hydrogenations Using Amine or Amide Treated 2

Run	Amine or Amide	Method of Work-up	ml H ₂ /min/mmole Rh
1	Ephedrine	used as is	74
2		used as is ^a	31
3		ether wash	71
4		HCl wash	0
5	Dimethyl formamide	ether wash	54
6	N-Methyl Acetamide		17
7	α-Methylbenzylamine	used as is	12
8		HCl wash	0
9	Triethanolamine	used as is	67
10	Diethanolamine		23

^aExposed to air during heating.

A difference in reaction selectivity is also observed between that complex obtained from **2** and triethanolamine (TEA) and that from diethanolamine (DEA). That catalyst obtained from **2** and TEA is capable of hydrogenating TMBC (**7**), albeit very slowly, but that obtained from DEA is inactive in this reaction (Table V).

The formation of a rather efficient asymmetric catalyst from py₃RhCl₃, sodium borohydride, and (–)-1-phenethylformamide (**13**) led us to pos-

Table V. TBMC Hydrogenations over Amine Treated 2

Amine	ml H ₂ /min/mmole Rh	% 7	% 10	% 8 & 9	C/T
TEA	2.3	77	7.5	15.5	5.1
DEA	No Rxn	—	19	81	5.1

tulate that a similar type of catalyst could be prepared by the reaction of **2** with (–)-ephedrine or (+)- α -methylbenzylamine. Hydrogenation of atropic and itaconic acids over these catalysts, however, gave products with no significant optical activity.

At this stage the investigation shifted to a study of the benzene-oxidized species **4**. In benzene alone, **4**, as well as **2**, was inactive for olefin hydrogenation. In the presence of ethanol, however, a reactive catalyst was obtained. When **4** was stirred in benzene–ethanol under hydrogen for about two hours, a dark solution was formed which slowly catalyzed the hydrogenation of TBMC (**7**). The cis/trans ratio of the saturated products obtained from this hydrogenation was 2.0. Less than 10% of the isomerized olefin, **10**, was formed. Evaporating the solution and washing the residue gave a material, **11**, which from x-ray spectroscopy had a Rh:P:Cl ratio of 1:1:1. This was considered a good species to use for the introduction of one equivalent of a ligand other than triphenylphosphine into a catalytically active species. It was necessary to first determine what effect rhodium complexes containing other ligands would have on the hydrogenation of **7**.

Previous work has shown that the electronic characteristics of the benzene substituent in triarylphosphine chlororhodium complexes have a marked influence on the rate of olefin hydrogenation catalyzed by these compounds. Thus, in the hydrogenation of cyclohexene using L_3RhCl the rate decreased as $L = \text{tri-}p\text{-methoxyphenylphosphine} > \text{triphenylphosphine} > \text{tri-}p\text{-fluorophenylphosphine}$ (**14**). In the hydrogenation of 1-hexene with catalysts prepared by treating dicyclooctene rhodium chloride with 2.2–2.5 equivalents of substituted triarylphosphines, the substituent effect on the rate was $p\text{-methoxy} > p\text{-methyl} \gg p\text{-chloro}$ (**15**). No mention could be found of any product stereochemistry studies using this type of catalyst.

The rate and product stereochemistry data obtained from the hydrogenation of TBMC (**7**) over a series of bisphosphine complexes prepared from dicyclooctene rhodium chloride (**1**) are shown in Figures 1 and 2. The product stereochemistry data (Figure 2) shows that the cis/trans ratio is dependent on the electronic character of the ligand and permits the use of this ratio to evaluate the effect of an added ligand in a mixed ligand complex. In contrast to the previously reported rate data, however, the tri- p -methoxyphenylphosphine complex was slower than the tri- p -tolylphosphine in the present work (Figure 1). In the present case all of the reaction rates were zero order in olefin while a first order relationship was noted when **1** and analogous compounds were used in olefin hydrogenation (**1**). The reasons for these discrepancies are not known, but two explanations are possible. First, the olefins used previously were 1-hexene and cyclohexene while a more complex olefin, **7**, was used here.

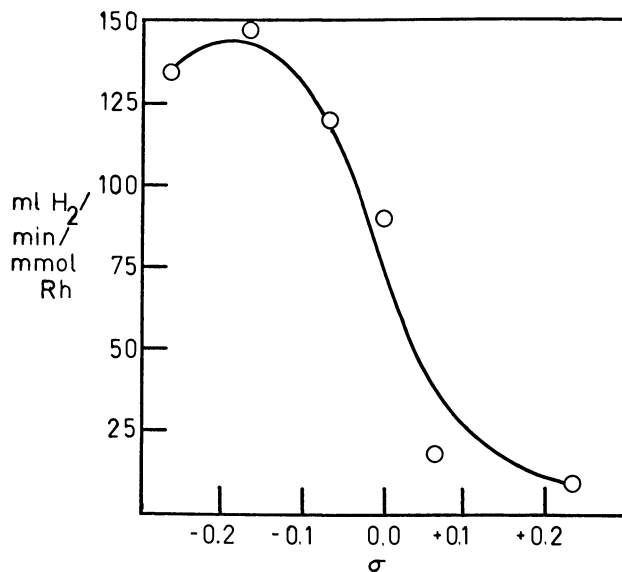


Figure 1. The effect of substituents on the rate of hydrogenation of TBMC (7) using L_2RhCl

$L = (S-\phi)_3P$, $S = p-OCH_3$ ($\sigma = -0.27$), $p-CH_3$ ($\sigma = -0.17$), $m-CH_3$ ($\sigma = -0.07$), H ($\sigma = 0.0$), $p-F$ ($\sigma = +0.06$), and $p-Cl$ ($\sigma = +0.23$)

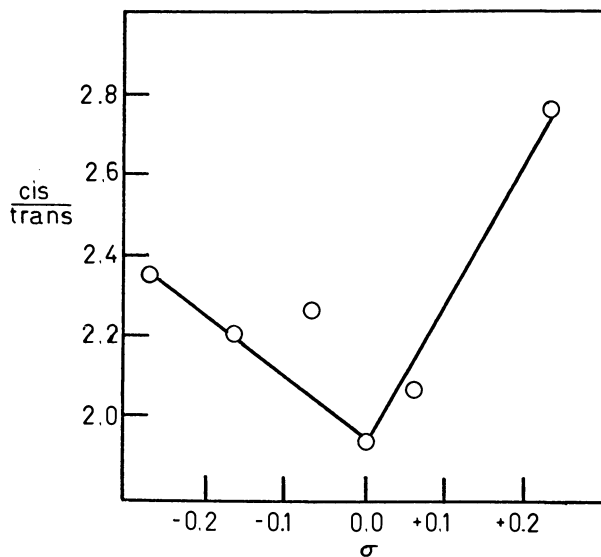


Figure 2. The effect of substituents on the product stereochemistry 8/9 ratio from hydrogenation of TBMC (7) using L_2RhCl ; $L = (S-\phi)_3P$

If subtle steric factors are operative they would be more likely to show up with 7 than with the more simple olefins. Second, the previous work used a benzene solvent and phosphine: rhodium ratios of 2.4 to 3 while benzene-ethanol and ratios of 2.0 were used here. While further work in this area is obviously indicated, the reaction conditions used were the same as those to be used in those hydrogenations using the mixed ligand complexes prepared from 4. Thus, the data presented in Figures 1 and 2 can serve as meaningful references in evaluating and comparing the mixed ligand complexes.

As previously mentioned, the monophosphine complex, 11, prepared by stirring 4 in benzene-ethanol under hydrogen was considered the logical material to use in preparing the desired mixed ligand complexes. Thus, one equivalent each of a number of triarylsubstituted phosphines was added to a benzene-ethanol solution of 11, and the resulting mixtures were used to hydrogenate TBMC. As with the bisphosphine complexes, in every case in this series the reaction rate was zero order in olefin. The rate and product stereochemistry data from this series of reactions are given in Figures 3 and 4. The data show changes in reaction rate similar to but less pronounced than shown in Figure 1. Further, the added ligand has no apparent effect on the stereochemistry of the products. X-ray analysis of the washed residue obtained from the tri-*p*-chlorophenylphosphine reaction showed that only about 0.25 equivalent of the substituted

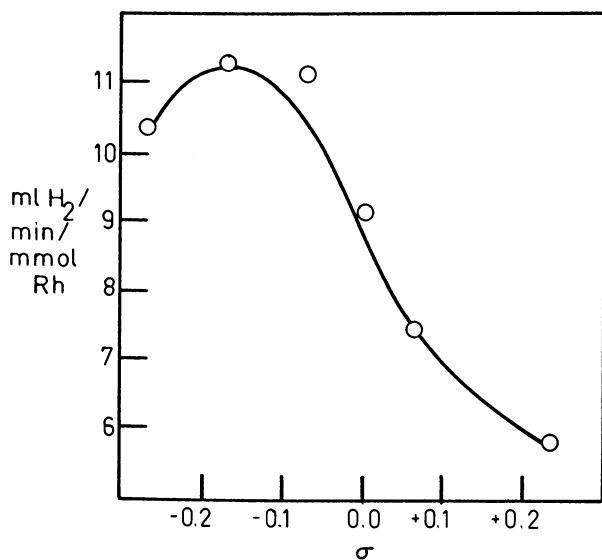


Figure 3. The effect of substituents on the rate of hydrogenation of TBMC (7) using solutions obtained by reducing 4 in benzene-ethanol under hydrogen and adding an equivalent of $(S-\phi)_3P$

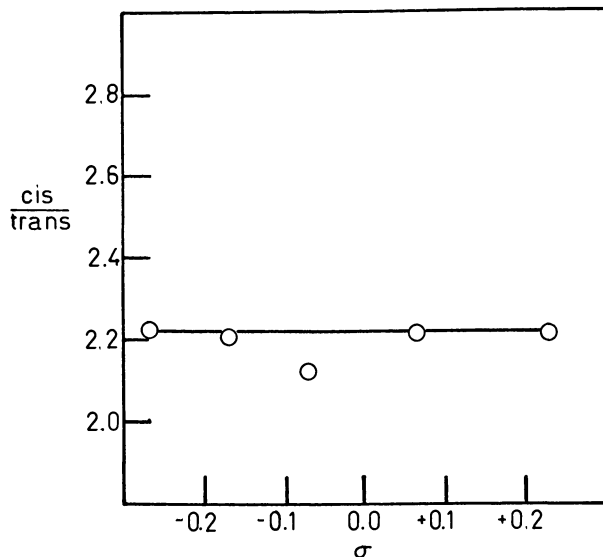


Figure 4. The effect of substituents on the product stereochemistry ratio from the hydrogenations of **7** using hydrogen reduced **4** with $(S-\phi)_3P$

phosphine was incorporated into the catalyst. PMR analysis of the washed residue from the tri-*p*-methoxyphenylphosphine run gave the same indication. Thus, the species (presumably a Rh(III) dihydride), initially formed from **4**, hydrogen, and ethanol while apparently coordinatively unsaturated, does not react readily with the added ligand. The observed fractional incorporation indicates the presence of at least two species in the reaction mixture. The slight changes depicted in Figures 3 and 4 are probably attributable to the presence of a small amount of a mixed ligand species in the reaction mixture.

As with **2**, hydrogen was not necessary to reduce **4** but this reaction could take place readily under nitrogen in benzene-ethanol. Examination of the IR spectra of aliquots taken from this reaction showed the 850 cm^{-1} band (dioxygen ligand) decreased very rapidly, and after a few hours, a new band at 1976 cm^{-1} (complexed carbonyl) began to appear. Evidently the ethanol reacts rapidly with the dioxygen ligand to give acetaldehyde which is subsequently decarbonylated. X-ray analysis of the isolated carbonyl complex showed a 2:3:2 ratio for Rh, P, and Cl.

When the reduction was repeated in the presence of one equivalent of triphenylphosphine, aliquots taken for IR analyses gave comparable spectral changes. In this reaction, a precipitate, identified as $[(\phi_3P)_2\text{-RhCl}]_2$ (**12**) (*I*), was formed toward the end of the reaction, and the carbonyl species which was formed was identified as the known (*I*) $(\phi_3P)_2\text{CORhCl}$ (**13**). The catalytic activity of the reduction mixture

increased as the dioxygen function decreased and peaked before extensive carbonyl complex formation was observed (5). A correlation of the catalyst activity toward hydrogenation of 7 and the strengths of the 850 and 1986 cm^{-1} (carbonyl) bands is shown in Figure 5.

The formation of both 12 and 13 during the reduction of 4 in the presence of triphenylphosphine indicated not only that one-half of an equivalent of the added phosphine was taken up, but also that the intermediate formed is the bisphosphine complex, $(\phi_3\text{P})_2\text{RhCl}$, proposed as the reactive intermediate in hydrogenation runs using 1 as the catalyst (1). This assumption is further supported by the fact that the product stereochemistry (*cis/trans* = 2.0) and lack of double bond isomerization observed on hydrogenation of 7 with this reaction mixture corresponds directly with the data obtained on hydrogenation of 7 using pre-hydrogenated 1 (3). When the reduction of 4 was repeated in the presence of tri-*p*-tolylphosphine, the carbonyl complex formed was isolated and shown by PMR spectroscopy to contain 1.5 equivalents of triphenylphosphine and 0.5 equivalent of the tri-*p*-tolylphosphine, as expected.

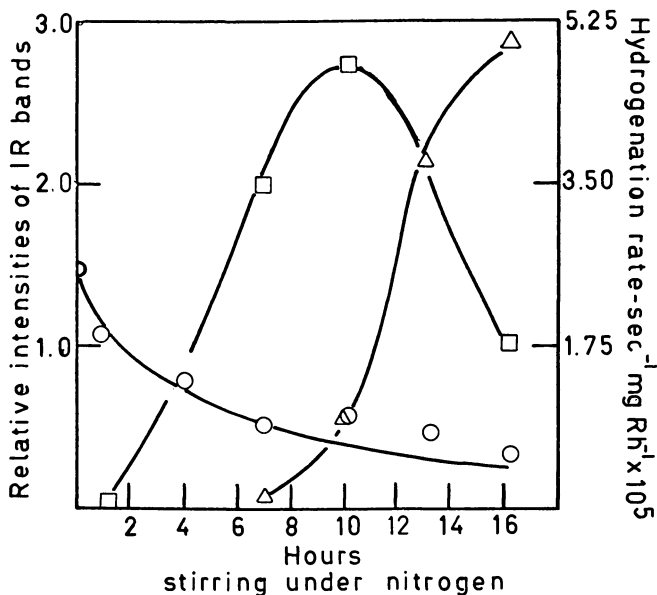


Figure 5. Correlation between the hydrogenation rate and IR intensities of aliquots taken in the reduction of 4 in the presence of triphenylphosphine: ○ = relative intensity of 850 cm^{-1} band; △ = relative intensity of 1986 cm^{-1} band; □ = hydrogenation rate in $\text{sec}^{-1} \text{mg Rh}^{-1} \times 10^5$

The reduction of 4 was run in the presence of a series of aryl substituted phosphines. Hydrogenation profiles similar to that shown in Figure 5 were obtained. The rates of hydrogenation of 7 using aliquots

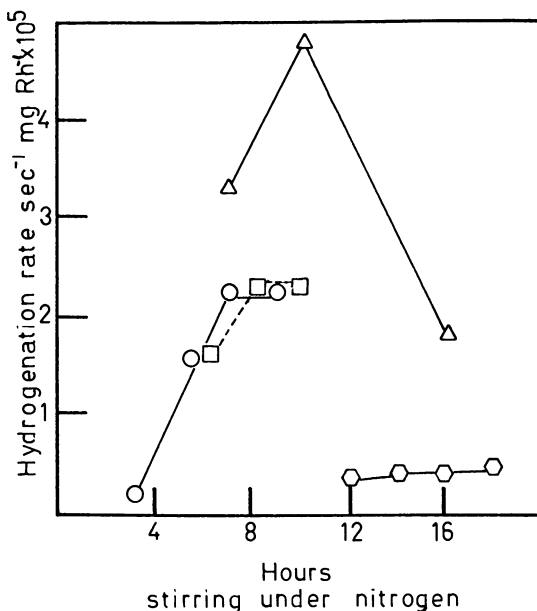


Figure 6. Rates of hydrogenation of 7 using aliquots taken from benzene-ethanol solutions of 4 stirred under nitrogen in the presence of one equivalent of $(S-\phi)_3P$; ○, $S = p-OCH_3$; □, $S = p-CH_3$; △, $S = H$; ◯, $S = p-Cl$

taken from several reduction runs are shown in Figure 6. Because of the differing rates at which the various catalytically inactive substituted carbonyl complexes were formed, it was difficult to determine the true hydrogenation rates of the catalytic intermediates formed in these reductions. Thus, any comparisons with the rate data shown in Figure 6 are meaningless. As with the Wilkinson catalyst and its analogues, the hydrogenation rates in this series were first order in olefin. The product stereochemistry data shown in Figure 7 show a slight, but real, change similar to that depicted in Figure 2.

On the basis of these data a series of mixed ligand catalysts has been prepared by this procedure. It is also apparent from this work that care must be taken to determine how best to treat the oxidized complexes to permit the incorporation of the added ligand. If this problem is solved with each of the oxidized species, a broad spectrum of catalytically active materials will become available.

Experimental

The hydrogen used in this work was passed through an Engelhard Deoxo-Puridryer before use. Prepurified nitrogen was used. The oxidized complexes were prepared as described (4, 5) as was the TBMC (16, 17).

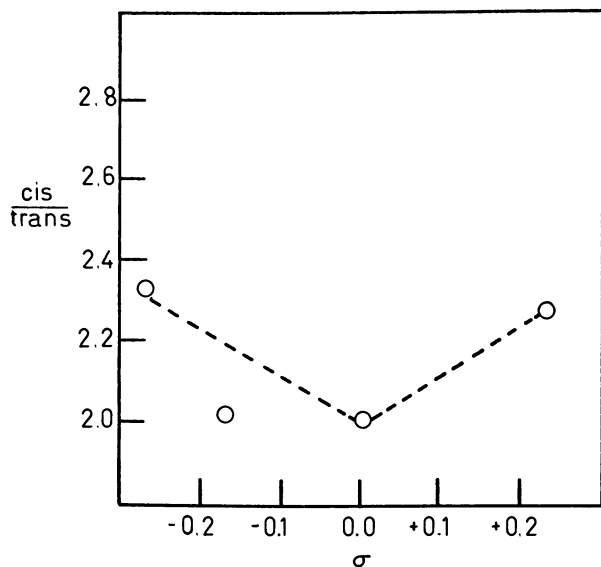


Figure 7. Effect of substituents on the product stereochemistry ratio obtained from the hydrogenation of **7** over $Rh_2(\phi_3P)_3(L_3P)Cl_2$; $L = (S-\phi)_3P$

The solvents were degassed immediately before use. The hydrogenations were run at atmospheric pressure and 25°C using the apparatus and procedure described previously (3). X-ray data were obtained using a General Electric XRD 5 spectrometer equipped with an EDT crystal and a SPG 4 detector under helium. Rhodium was determined using the $L_{\alpha 1}$ band (62.97°), phosphorus the $K_{\alpha 1}$ band (88.72°), and chlorine the K_{α} band (64.98°). The instrument was calibrated using known mixtures of rhodium oxide, triphenylphosphine, and chloroanthracene as well as an authentic sample of $(\phi_3P)_3RhCl$. IR spectra were obtained using a Beckmann IR10 spectrophotometer. The spectra were taken as mulls on KBr plates. NMR spectra were obtained using a Varian A 60A spectrometer. GLC analyses were run as described (3).

The Reaction of 2 with Amines or Amides. Two hundred mg of **2** was placed, under nitrogen, in a double Schlenk tube fitted with a reflux condenser and septum adapter. The amine or amide (5 ml) was added, and the mixture was placed in an oil bath preheated to 200°C. After the mixture turned black it was heated for an additional 20 min, cooled, and passed through the filter disc. This solution can be used directly for hydrogenation, or ether can be added to produce a black precipitate. The ether washed precipitate can also be used in olefin hydrogenations.

The Reduction of 2. Complex **2** (32.0 mg, 0.0457 mmole) was placed either with or without an equivalent (12 mg) of triphenylphosphine in a round-bottom flask under an inert atmosphere. A 1:1 benzene-ethanol mixture (20 ml) was added, and the resultant mixture stirred under hydrogen or nitrogen until complete solution was effected (2–48 hrs). Aliquots of these solutions were used directly for olefin hydrogenation.

The Reduction of 4 under Hydrogen. A mixture of 215.4 mg of 4 in 172 ml of 1:1 benzene-ethanol was stirred for 2 hrs under hydrogen giving a black solution. Aliquots containing 0.0487 mmole of Rh (27 ml) were taken and added to flasks each containing 0.0487 mmole of one of the various aryl-substituted phosphines used in this study. These solutions were then stirred under hydrogen for an additional 8 hrs and frozen in liquid nitrogen until used. In the olefin hydrogenation, 9 ml of the thawed solution was presaturated with hydrogen in the reactor for 20 min before the olefin (80 μ l) was injected. The triarylphosphines used were tri-*p*-methoxyphenylphosphine ($\sigma = -0.27$), tri-*p*-tolylphosphine ($\sigma = -0.17$), tri-*m*-tolylphosphine ($\sigma = -0.07$), triphenylphosphine ($\sigma = 0$), tri-*p*-(fluorophenyl)phosphine ($\sigma = 0.06$), and tri-*p*-chlorophenylphosphine ($\sigma = 0.23$).

Under Nitrogen. A 1.8×10^{-3} mM solution of 4 in 1:1 benzene-ethanol was stirred under nitrogen in the presence of one equivalent of the added ligand. Aliquots were taken periodically and frozen in liquid nitrogen until they could be used further. After thawing, the solutions were centrifuged, and the supernatant was used for IR or hydrogenation studies. For the olefin hydrogenations, 10 ml of this solution was presaturated with hydrogen for 15 min in the reactor before the olefin was injected. In every instance a small amount of the supernatant was evaporated to determine the amount of dissolved material present.

Literature Cited

1. Osborn, J. A., Jardine, F. H., Young, J. F., Wilkinson, G., *J. Chem. Soc. (A)* (1966) 1711.
2. vanBekum, H., vanRantwijk, F., van der Putte, T., *Tetrahedron Lett.* (1969) 1.
3. Augustine, R. L., Van Peppen, J. F., *J. Amer. Oil Chem. Soc.* (1970) 47, 478.
4. Augustine, R. L., Van Peppen, J. F., *Chem. Commun.* (1970) 497.
5. Augustine, R. L., Pellet, R. J., unpublished data.
6. Vaska, L., *Science* (1963) 140, 809.
7. Valentine, J. S., *Chem. Revs.* (1973) 73, 235.
8. Cotton, F. A., Barnes, R. D., Bannister, E., *J. Chem. Soc.* (1960) 2199.
9. Rundle, R. E., Nakamoto, K., Richardson, J. W., *J. Chem. Phys.* (1955) 23, 2450.
10. Augustine, R. L., Van Peppen, J. F., *Chem. Commun.* (1970) 571.
11. Siegel, S., *Advan. Catal.* (1966) 16, 123.
12. Siegel, S., Ohrt, D. W., *Tetrahedron Lett.* (1972) 5155.
13. Abley, P., McQuillin, F. J., *Chem. Commun.* (1969) 477.
14. Montelatici, S., van der Ent, A., Osborn, J. A., Wilkinson, G., *J. Chem. Soc. (A)* (1968) 1054.
15. Horner, L., Bathe, H., Siegel, H., *Tetrahedron Lett.* (1968) 4023.
16. Wittig, G., Schoellkopf, U., *Org. Synth.* (1960) 40, 66.
17. Greenwald, R., Chaykovsky, M., Corey, E. J., *J. Org. Chem.* (1963) 28, 1128.

RECEIVED August 20, 1973.

The Influence of Potentially Bridging Groups in Homogeneous Hydrogenation with Rhodium Complexes: A Study of para-Dimethylamino-Substituted Phenylphosphine Metal Complexes

R. B. KING and C. R. BENNETT

University of Georgia, Athens, Ga. 30602

Some studies are reported on the homogeneous hydrogenation of cyclohexene with rhodium(I) chloride catalysts of the composition $[(p\text{-Me}_2\text{NC}_6\text{H}_4)_x\text{P}(\text{C}_6\text{H}_5)_{3-x}]_n\text{RhCl}$ ($x = 1, 2, \text{ or } 3; n = 1, 2, \text{ or } 3$) generated by room temperature reactions of the cyclooctene complex $[(\text{C}_8\text{H}_{14})_2\text{RhCl}]_2$ with the appropriate triarylphosphine. In some cases, the rates of these hydrogenations are inhibited by excess hydrogen concentration. This inhibitory effect of excess hydrogen concentration increases with increasing p-dimethylamino substitution in the ligands. The rhodium(I) chloride catalysts containing the p-dimethylaminophenyl phosphines $(p\text{-Me}_2\text{-NC}_6\text{H}_4)_x\text{P}(\text{C}_6\text{H}_5)_{3-x}$ ($x = 2 \text{ and } 3$) had optimum activity for homogeneous hydrogenations at ligand:rhodium ratios of around 1.5 rather than 2, suggesting coordination of some of the dimethylamino nitrogen atoms as well as the trivalent phosphorus atoms to the rhodium in the catalysts.

A landmark in the developing homogeneous hydrogenation catalysts was the discovery by Coffey (1) and by Osborn *et al.* (2) of the high activity of tris(triphenylphosphine)rhodium(I) chloride as a homogeneous hydrogenation catalyst. Since then, intensive effort (2, 3, 4, 5, 6, 7) has been devoted to the mechanisms of catalytic hydrogenations catalyzed by rhodium(I) complexes with the ultimate objective of improving the activity and selectivity of homogeneous catalysts based on rhodium(I) and related complexes.

One approach in studying the triarylphosphine rhodium(I) derivatives as hydrogenation catalysts has been to modify the structure of the triarylphosphine by introducing substituents into the aromatic ring (3). Until now such studies have been limited to innocuous substituents such as *p*-methoxy and *p*-fluoro which could have significant electronic effects on the benzenoid ring but which would not affect the mechanism by complexing directly with the rhodium atom. Such work (3) showed that electron-releasing substituents like *p*-methoxy increased the catalytic activity of the triarylphosphine rhodium(I) halides whereas electron-withdrawing substituents such as *p*-fluoro decreased the catalytic activity of the rhodium complex.

The enhancement of the catalytic activity of triarylphosphine rhodium(I) halides by introducing the electron-releasing *p*-methoxy group suggested the possibility of preparing extremely active hydrogenation catalysts by using the very strongly electron-releasing *p*-dimethylamino group as a substituent in the triarylphosphine ligands of the rhodium(I) halide complexes. The *p*-dimethylamino group, however, had the possible complication of complexing directly with the rhodium(I) atom, thereby blocking some of the coordination sites needed to activate the hydrogen and/or the olefin to effect the desired catalysis. To evaluate whether the *p*-dimethylamino group would enhance the catalytic activity of triarylphosphine rhodium(I) complexes through its strong electron-releasing characteristics or inhibit the catalytic activity of these rhodium(I) complexes by coordinating with the rhodium atom, we prepared rhodium(I) complexes of the type $[(p\text{-Me}_2\text{NC}_6\text{H}_4)_x\text{P}(\text{C}_6\text{H}_5)_{3-x}]_n\text{RhCl}$ ($x = 1, 2, \text{ or } 3; n = 1, 2, \text{ or } 3$) and studied their catalytic activity for the homogeneous hydrogenation of cyclohexene. The problems associated with the isolation of pure rhodium(I) complexes of this type were circumvented by generating these complexes in solution from the cyclooctene-rhodium(I) complex $[(\text{C}_8\text{H}_{14})_2\text{RhCl}]_2$ and the desired quantity of the tertiary phosphine $(p\text{-Me}_2\text{NC}_6\text{H}_4)_x\text{P}(\text{C}_6\text{H}_5)_{3-x}$. This paper describes some novel effects of the hydrogen pressure, the olefin concentration, the ligand-metal ratio, and the number of *p*-dimethylamino substituents on the rates of homogeneous hydrogenation of cyclohexene catalyzed by this series of rhodium(I) complexes.

Experimental

Preparation of Ligands. Tris(*p*-dimethylaminophenyl)phosphine (abbreviated as L^3) and diphenyl(*p*-dimethylaminophenyl)phosphine (abbreviated as L^1) were prepared by König's method (8). To prepare tris(*p*-dimethylaminophenyl)phosphine, a mixture of 30 ml of pyridine, 15 ml of phosphorus trichloride, and 30 ml of *N,N*-dimethylaniline was boiled under reflux for 8 hrs. The resulting green solution was acidified, filtered, and excess starting materials were removed by steam distillation.

The resulting dark solid mass was dissolved in ethanol, filtered, and re-crystallized several times from ethanol to give 7.03 grams (22% yield) of white tris(*p*-dimethylaminophenyl)phosphine, mp 305°C (lit. (8) mp 308°–310°C). The ligand diphenyl(*p*-dimethylaminophenyl)phosphine, mp 147°–149°C (lit. (9) 152°–153°C) was prepared in 10% yield by a similar procedure using diphenylchlorophosphine instead of phosphorus trichloride.

This method was not suitable to prepare phenylbis(*p*-dimethylaminophenyl)phosphine (abbreviated as L^2). This ligand was prepared in 23% yield by the method of Venanzi and co-workers (10) using the reaction of the lithium derivative from *p*-bromo-*N,N*-dimethylaniline with phenyldichlorophosphine.

Preparation of the Cyclooctene Complex $[(C_8H_{14})_2RhCl]_2$ (11). A nitrogen-saturated mixture of 1.0 gram (3.8 mmoles) of rhodium trichloride trihydrate, 3.0 ml (23 mmoles) of cyclooctene, and 30 ml of absolute ethanol was allowed to stand at room temperature for several days. The precipitate of $[(C_8H_{14})_2RhCl]_2$ which gradually separated was removed by filtration, washed several times with small portions of ethanol, and dried. After drying at 50°–60°C at 0.1 mm Hg for two days, a sample was analyzed and calculated for $C_{16}H_{28}Cl_2Rh_2$: C, 53.6; H, 7.8%; found: C, 52.6; H, 7.9%.

Kinetic Measurements. The hydrogenation experiments were run in a water-jacketed two-neck reaction vessel attached to a standard atmospheric pressure hydrogenation apparatus equipped with a gas buret. The temperature of the reaction mixture was held constant by circulating water from a constant temperature bath (controlled to $\pm 0.4^\circ$) through the jacket of the reaction vessel. The neck of the reaction vessel not connected to the hydrogenation apparatus was used to introduce substances into the reaction mixture against a counterflow of hydrogen. The reaction mixture was agitated with a magnetic stirrer at maximum speed which in the cylindrical reaction vessel produced a vortex that vigorously mixed the gas and solvent. Rate was followed by volumetric consumption of hydrogen at constant pressure.

The required amount of the tertiary phosphine ligand and 100 ml of benzene was introduced into the cylindrical reaction vessel. The solution was then saturated with hydrogen by repeating four times, with constant stirring—a sequence consisting of evacuation and refill with hydrogen. The $[(C_8H_{14})_2RhCl]_2$ was then added through the free neck in a counter-current of hydrogen. The mixture was then stirred for 30 to 90 min to allow time to generate the tertiary phosphine rhodium(I) catalyst and to hydrogenate any liberated cyclooctene. Decomposition was not observed at this time. After this equilibration period, 10 ml of substrate solution was injected through a septum cap placed on the free neck. The uptake of hydrogen was then followed volumetrically. To ensure constant volumes in each reaction, the substrate solution of cyclohexene (redistilled over calcium hydride) and hexane was held to 10 ml. Kinetic measurements were made before 5% of the total cyclohexene had been consumed.

A useful experimental technique arising from this work permits us to follow changes in the hydrogenation rate with decreases in the hydrogen concentration. When the gas buret has been emptied by reaction of the

hydrogen with the cyclohexene, the pressure in the apparatus can be lowered by lowering the mercury leveling bulb of the buret. The reaction is then monitored at a constant lower total pressure. Since the conditions are nearly identical for any particular reaction mixture, comparable rates can be obtained with this technique.

The experimental results were put into a least squares program directly. There was seldom more than 1% variation from linearity for each run. The slope, which corresponds to the rate in ml/min, was then converted as necessary for further interpretation. The linearity of these initial rate determinations show that there is no apparent product inhibition over this narrow range.

Table I. Effect of Hydrogen Pressure on the Rate of Hydrogenation

Ligand ^a	Temperature, °C	Hydrogen Pressure, mm	Rate in Moles/Liter-Sec × 10 ⁻⁵
L ⁰	37.2	402	0.15
		502	0.25
		602	0.35
L ¹	36.5	349	0.038
		399	0.039
		449	0.043
		499	0.044
		549	0.044
		599	0.035
L ²	40.1	454	0.0095
		494	0.011
		545	0.012
		595	0.011
L ³	36.1	348	0.088
		400	0.13
		450	0.15
		500	0.13
		550	0.079
		600	0.041

^a See the text for an explanation of these abbreviations. These experiments were all conducted at 0.714M cyclohexene concentration and with a 2:1 ligand:rhodium ratio.

Results

To clarify the mechanism of the homogeneous hydrogenation of cyclohexene with tertiary phosphine rhodium(I) complexes, the effects of the following variables on the rate of hydrogenation were examined: (1) hydrogen pressure (Table I); (2) cyclohexene concentration (Table II); and (3) ligand-rhodium ratio (Table III). In addition, determining the effect of *p*-dimethylamino substitution in the triarylphosphines on the rate of hydrogenation allows evaluation of the relative importance of the electron-releasing and coordination position-blocking tendencies of the *p*-dimethylamino group.

Table II. Effect of Cyclohexene Concentration on the Rate of Hydrogenation

<i>Ligand</i> ^a	<i>Temperature</i> °C	<i>Cyclohexene Concentration</i> , M	<i>Rate in Moles/Liter-Sec</i> × 10 ⁻⁵
L ⁰	27.2	0.532	0.043
	27.1	0.714	0.048
	26.2	0.893	0.047
	27.1	1.06	0.045
L ¹	28.3	0.532	0.0090
	27.8	0.80	0.0079
	27.0	1.06	0.010
	26.6	1.332	0.0090
L ¹	30.9	0.621	0.010
	31.0	0.714	0.013
	30.8	0.80	0.016
	31.0	0.893	0.019
L ¹	38.4	0.444	0.17
	39.4	0.621	0.19
	37.9	0.80	0.17
L ²	42.8	0.267	0.29
	42.7	0.319	0.28
	42.9	0.444	0.34
	43.6	0.532	0.32
	43.1	0.621	0.32
L ³	27.6	0.267	0.018
	28.0	0.80	0.034
	27.0	1.06	0.037
	27.1	1.33	0.043
L ³	31.4	0.532	0.009
	31.5	0.621	0.012
	30.8	0.714	0.015
	30.9	0.80	0.017
L ³	36.0	0.621	0.012
	36.1	0.80	0.016
	35.9	0.893	0.020

^a See the text for an explanation of these abbreviations. The experiments were all conducted at 600mm hydrogen pressure and with a 2:1 ligand:rhodium ratio.

Wilkinson and co-workers (3) showed that the maximum activity of the tertiary phosphine rhodium(I) chloride catalysts occurred at a ligand:rhodium ratio of about 2. This ratio was used in the systems studied for the effects of hydrogen pressure (Table I). In the triphenylphosphine system (abbreviated as L⁰), the rate of hydrogenation increased with pressure in the accessible pressure range, in accord with previous observations (2) by Wilkinson and co-workers. However, with the *p*-dimethylamino substituted tertiary phosphines L¹ and L² the rates of hydrogenation were essentially independent of the hydrogen pressure within the experimental errors. For tris(*p*-dimethylaminophenyl)phos-

phine, the rate of hydrogenation decreased when the hydrogen pressure increased above 500 mm. These observations are the first indication that excess hydrogen pressure can inhibit the rhodium(I) catalyzed hydrogenation of olefins. The inhibitory effect of excess hydrogen pressure seems to increase with increasing *p*-dimethylamino substitution of the triarylphosphine ligand.

To measure the effect of cyclohexene concentration on the rate of the rhodium(I) catalyzed hydrogenation, a separate reaction mixture had to be prepared for the rate determination at each cyclohexene concentration. Reproducibility of the data in Table II was not determined. In some cases, the reaction rate increased with cyclohexene concentration as was found by Wilkinson and co-workers (2). However, in a few cases the reaction rate was nearly independent of the cyclohexene concentration. This could arise from superimposition of inhibitory behavior of excess cyclohexene with the increase demonstrated for other cases.

The measurements of the effect of the ligand-rhodium ratio on the rate of hydrogenation listed in Table III show that for the *p*-dimethylaminophenyl phosphines the optimum ligand-rhodium ratio is not 2, as with the triarylphosphines studied by Wilkinson and co-workers (3). With the *p*-dimethylamino substituted tertiary phosphines L² and L³ the

Table III. Effect of Ligand-Rhodium Ratio on the Rate of Hydrogenation

Ligand ^a	Temperature, °C	Hydrogen Pressure, mm	Ligand-Rhodium Ratio	Rate in Moles/Liter-Sec × 10 ⁻⁵
L ⁰	36.6	549	1	0.042
	36.5	545	1.5	0.095
	37.2	552	2	0.15
	36.6	539	2.4	0.06
	36.7	~545	2.6	~0.04
	36.9	~550	3	~0.023
	L ¹	36.6	607	1
36.8		598	1.5	0.006
36.5		599	2	0.035
36.4		600	2.5	0.064
36.9		604	3	0.01
L ²	36.6	603	1	0.037
	36.4	599	1.5	0.042
	36.1	598	2	0.004
	37.0	598	2.5	0.0036
L ³	36.7	594	1	0.05
	36.6	599	1.5	0.094
	36.8	603	2	0.008
	36.2	598	2.5	0.008

^a See the text for an explanation of these abbreviations. These experiments were all conducted at 0.714*M* cyclohexene concentration.

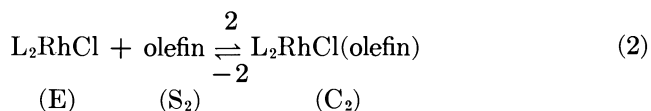
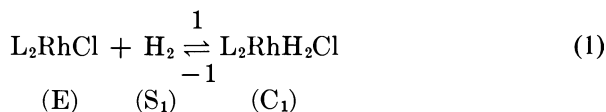
rates of hydrogenation in systems with a ligand–rhodium ratio of 2 are only about 10% of the rates of hydrogenation in equivalent systems with a ligand–rhodium ratio of 1.5. This suggests that the coordination of the nitrogen atoms of the dimethylamino substituent to the rhodium atom is significant in these systems. Addition of sufficient ligand L^2 or L^3 to give what appears from the triphenylphosphine experiments to be the optimum phosphorus–rhodium ratio of 2 introduces sufficient *p*-dimethylamino substituents to inhibit the reaction drastically by blocking needed sites on the catalyst by coordination with the rhodium atom.

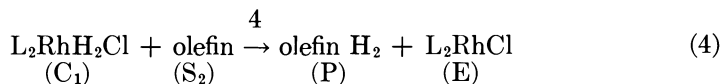
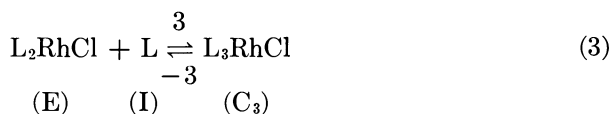
The most obvious conclusion from this work is that the introduction of *p*-dimethylamino substituents into the triarylphosphine ligands in the rhodium(I) halide complexes does not result in an unusually active homogeneous hydrogenation catalyst although the catalytic activity of the triarylphosphine–rhodium(I) chloride system is maintained. We have not yet evaluated whether the *p*-dimethylamino substituents modify the selectivity of the rhodium(I) halide hydrogenation catalysts in any way. It is apparent, however, that the mechanistic complexities introduced into the system by the presence of a potentially strongly coordinating *p*-dimethylamino group preclude meaningful detailed quantitative treatment of the data obtained in this work. Nevertheless, the results permit discussion of some of the more probable mechanisms of the homogeneous hydrogenation of olefins catalyzed by the triarylphosphine–rhodium(I) complexes.

Discussion

The homogeneous hydrogenation systems discussed in this paper may be treated as analogues of enzyme systems with the rhodium catalyst as the enzyme (E), hydrogen (S_1) and cyclohexene (S_2) as the substrates, and excess ligand or other donor site as the inhibitor (I). The well-established mathematical operations of enzyme kinetics (12) can then be used to derive rate equations for various possible mechanisms.

The following equations represent the essential features of the mechanism used by Wilkinson and co-workers (2, 3) with the added explicit expression of inhibition by excess tertiary phosphine ligand:



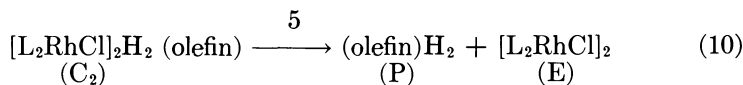
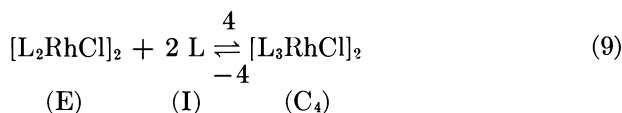
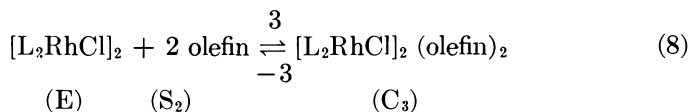
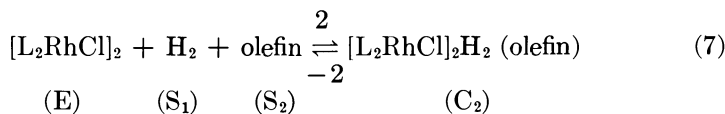
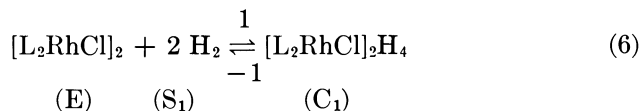


Equation 5 is then obtained for this mechanism:

$$\text{rate} = \frac{dP}{dt} = k_4 C_1 S_2 = \frac{k_4 K_1 S_1 S_2 E_t}{1 + K_1 S_1 + K_2 S_2 + K_3 I} \quad (5)$$

In this equation, k_4 is the rate constant for Reaction 4 (product formation) above, K_1 , K_2 , and K_3 are the equilibrium constants for the corresponding equilibria given above, and E_t is the total rhodium concentration.

This rate equation does not account for our observations of inhibition by excess hydrogen nor possibly excess olefin since the powers of the S_1 and S_2 terms in the denominator are less than or equal to the powers of S_1 and S_2 in the numerator. To accommodate these features, we prefer the mechanism summarized below:



In this mechanism, the catalytically active rhodium(I) derivative is a bimetallic compound thereby providing active sites on two adjacent rhodium atoms. The methods of enzyme kinetics (12) yield the following rate equation for this bimetallic mechanism:

$$\text{rate} = \frac{dP}{dt} = k_5 C_2 = \frac{k_5 K_2 S_1 S_2 E_t}{1 + K_1 S_1^2 + K_2 S_1 S_2 + K_3 S_2^2 + K_4 I^2} \quad (11)$$

The quadratic terms in the denominator are consistent with our observation of inhibition by excess hydrogen and possibly excess cyclohexene. The amount of inhibition by excesses of hydrogen and cyclohexene will depend on the magnitudes of K_1 and K_3 , respectively.

A further advantage of the bimetallic mechanism suggested above is that a bimetallic complex of the type $[L_2RhCl]_2$, which is proposed as the active catalyst, has been isolated in the case of triphenylphosphine (*i.e.* $L = (C_6H_5)_3P$) from the decomposition of $[(C_6H_5)_3P]_3RhCl$. The observed (2) reactivity of $[L_2RhCl]_2$ ($L = (C_6H_5)_3P$) toward oxygen and carbon monoxide makes plausible the postulated reactivity of $[L_2RhCl]_2$ toward hydrogen and olefins which is an essential part of the proposed bimetallic mechanism.

Despite the work presented, no definitive mechanism for the homogeneous hydrogenation of olefins with triarylphosphinerhodium(I) halide catalysts is postulated here. However the experimental observations of inhibition by excess hydrogen and possibly excess olefin are inconsistent with the previously postulated mechanisms (2, 3) involving monometallic active species. The analysis presented suggests that a mechanism involving bimetallic intermediates with the metal sites in reasonable proximity can account for all presently available experimental observations.

Acknowledgment

We acknowledge many helpful discussions with J. F. Garst.

Literature Cited

1. Coffey, R. S., British Patent 1,121,642 (February 18, 1965).
2. Osborn, J. A., Jardine, F. H., Young, J. F., Wilkinson, G., *J. Chem. Soc. A* (1966) 1711.
3. Montelatici, S., van der Ent, A., Osborn, J. A., Wilkinson, G., *J. Chem. Soc. A* (1968) 1054.
4. O'Connor, C., Wilkinson, G., *Tetrahedron Lett.* (1969) 1375.
5. Candlin, J. P., Oldham, A. R., *Discuss. Faraday Soc.* (1968) 60.
6. Augustine, R. L., van Peppen, M. F., *Chem. Commun.* (1970) 571.
7. van Bekkum, H., van Rantwijk, F., van de Putte, T., *Tetrahedron Lett.* (1969) 1.
8. König, E., Friedrich, H., *Ann.* (1934) 509, 138.
9. Trippett, S., Walker, D. M., *J. Chem. Soc.* (1961) 2130.
10. Fritz, H. P., Gorden, I. R., Schwarzhans, K. E., Venanzi, L. M., *J. Chem. Soc.* (1965) 5210.
11. Porri, L., Lionetti, A., Allegra, G., Immirzi, A., *Chem. Commun.* (1965) 336.
12. Reiner, J. M., "Behavior of Enzyme Systems," 2nd ed., van Nostrand Reinhold, New York, 1969.

RECEIVED July 30, 1973. This work was supported by the Air Force Office of Scientific Research under Grants AF-AFOSR-68-1435 and AF-AFOSR-71-2000. Abstracted in part from the doctoral dissertation of C. R. Bennett, University of Georgia, 1973.

The Hydrogenation of 1-Hexene Catalyzed by Solutions of Hydridotetrakis(Triphenylphosphine)Rhodium(I)

JES HJORTKJAER

Technical University of Denmark; Bygning 227; Dk 2800 Lyngby; Denmark

The hydrogenation of 1-hexene catalyzed by solutions of $HRh(PPh_3)_4$ in benzene was found to follow the rate expression:

$$r = k_a \cdot C_A \cdot C_S \cdot C_{H_2} + k_b \cdot C_B \cdot C_S \cdot C_{H_2}$$

where k_a and k_b are rate constants, C_A and C_B are the concentrations of $HRh(PPh_3)_2$ and $HRh(PPh_3)_4$, C_S is the alkene concentration, and C_{H_2} is the hydrogen concentration. A mechanism for the catalytic reaction is proposed and related to the rate expression. The temperature dependence of the reaction rate is referred to a shift in the equilibrium between the catalytically active complexes. The hydrogenation of 1-hexene was accompanied by isomerization to 2- and 3-hexenes, and the high selectivity for the hydrogenation of the terminal alkene is attributed to a difference in complexity constants.

Based on several kinetic investigations on hydrogenations catalyzed by transition metal complexes conducted over the last few years, certain general requirements must be fulfilled if a complex is to form an effective homogeneous catalyst in solution (*see Ref. 1*). One condition is that the catalytically active complex must be coordinatively unsaturated; another that M–H or M–C bonds must be present in the complex.

Some notable examples of these rules are tris(triphenylphosphine)-halogenorhodium(I) studied by Osborn *et al.* (2) and hydridocarbonyl-tris(triphenylphosphine)rhodium(I) reported by O'Connor *et al.* (3). A common feature of these two complexes is that the coordinative unsaturation is caused by dissociation of phosphines and that M–H bonds

are formed by oxidative addition of hydrogen. The kinetic investigations indicate that the oxidative addition of hydrogen is the rate determining step in the catalytic cycle.

It might be possible to make a more active catalyst (per mole complex dissolved per unit volume of solvent) either by increasing the tendency towards the formation of coordinatively unsaturated complexes in solution or by increasing the rate constant of the rate determining step, *i.e.*, the oxidative addition of hydrogen.

Collman (4) has reported that both these effects may be obtained by increasing the electron density around the central metal atom.

Another possibility is to change the steric factors. Thus, Shaw *et al.* (5) have shown that, with respect to transition metal complexes, there is a relationship between the tendency toward hydride formation and the bulkiness of the phosphine ligands so that larger phosphines increase the tendency toward the formation of hydride. This may be explained by the fact that the hydride anion is the smallest conceivable ligand, and thus for purely steric reasons hydride formation is facilitated when the other ligands are very large.

In rhodium-phosphine complexes an increase of the electron density is possible either by para substitution with electron-donor substituents on the aryl groups of triphenylphosphine or by replacing phenyl-phosphine by alkyl-phosphine. However, investigations made by Montelatici *et al.* (6) on the activity of rhodium complexes with alkyl-phosphines instead of phenyl-phosphines, which have a higher electron density, show an activity decrease. This is explained by the greater basicity of alkyl-phosphines promoting reassociation in the presence of hydrogen and consequently a decrease of the concentration of coordinatively unsaturated complexes. Para substitution in phenylphosphines with $-\text{OCH}_3$ leads to an increase in activity of approximately 50%. Another possibility is to replace CO by PPh_3 . In $\text{HRh}(\text{CO})(\text{PPh}_3)_3$ the electron density is reduced by π -back-donation to the carbonyl group. Accordingly, replacing CO by the less demanding π -acid ligand PPh_3 increases the electron density. The steric effect also contributes to the desired increase since PPh_3 is more bulky than CO.

This makes it easy to predict that solutions of $\text{HRh}(\text{PPh}_3)_4$ are more active catalysts than solutions of $\text{HRh}(\text{CO})(\text{PPh}_3)_3$, either because the concentration of coordinatively unsaturated complexes increases or because the rate constant of the oxidative addition of hydrogen increases. A kinetic investigation of the hydrogenation of hexene catalyzed by solutions of hydridotetrakis(triphenylphosphine)rhodium(I) is reported here.

Experimental

Preparation of Catalyst. Hydridotetrakis(triphenylphosphine)rhodium(I) was prepared by Ahmad's *et al.* method (7). The complex was identified by the melting point in air. The kinetic measurements showed that the catalytic activity decreased with time (by less than 25% in 14 days) even when the complex was kept under vacuum or nitrogen. However, all kinetic experiments reported here were made within 2–3 days after the synthesis of the complex.

Kinetic Experiments. The hydrogenation of alkene was followed by measuring the pressure as a function of time in a constant volume apparatus. The reactor was a 250 ml flask surrounded by a jacket through which thermostated water was pumped. The flask was connected to a vacuum pump, a pressure transducer, a Hg-manometer, a N₂-source, and a H₂-source *via* a condenser. Limitation of the reaction rate because of transport restrictions from the gas phase to the liquid phase was avoided by magnetic stirring. Immediately above the reaction flask a small glass

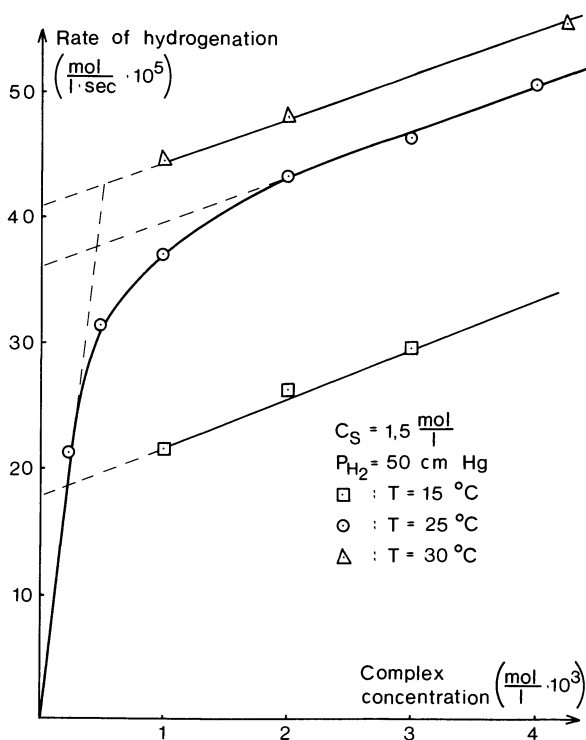


Figure 1. Rate of hydrogenation vs. complex concentration

jar for the catalyst was placed. The jar could be rotated from outside so that the catalyst would fall down into the reaction flask. The total volume of the system was approximately 600 ml.

Procedure. Hexene (Phillips Petroleum, pure grade, 99%) was dried over sodium and filtered through a layer of Al_2O_3 (Merck, Aktivitätsstufe I) to remove peroxides. The alkene was dissolved in benzene (Baker analyzed) dried over sodium, and the reaction mixture was transferred to the reactor. The complex was placed in the jar and the system was closed. To remove all air dissolved in the liquid phase, the system was evacuated and flushed with hydrogen purified for possible O_2 by passing a deoxo catalyst (palladium), under a pressure of 10 atm, and then passing a molecular sieve to remove H_2O 3 to 5 times under stirring. Adjustments permitted stabilization of the pressure in 1–2 min where the reaction rate was to be measured.

When no observable changes of pressure were observed (equilibrium), the catalyst was added by rotating the glass jar. The catalyst dissolved in 10–30 sec, depending on olefin and catalyst concentrations. The pressure drop was recorded as a function of time by the pressure transducer and a recorder. The reaction rate was determined by measuring the slope of the tangent to the curve of the pressure drop at the point corresponding to the desired H_2 -partial pressure and the vapor pressure of the reaction mixture. The variation between two independent rate determinations at the same conditions was always less than 10% of the absolute value.

Molecular weight determinations were carried out osmotically on a Hitachi Perkin Elmer model 115 molecular weight apparatus with the complex dissolved in benzene and at 38°C (the lowest possible temperature). The isomerization was followed by GLC analysis (Perkin Elmer model 11, Squalane column). The desired amount of the complex was placed in a reaction flask which was then flushed with N_2 . Benzene and 1-hexene which had been degassed by refluxing over sodium in an N_2 -atmosphere, were injected through a membrane attached to the flask. Samples were removed through the membrane and injected immediately into the gas chromatograph.

Results

Dependence on Complex Concentrations. The rate of hydrogenation was measured as a function of complex concentration at 15° , 25° , and 30°C . The initial concentration of 1-hexene was 1.5M, and the partial pressure of hydrogen was 50 cm Hg. The data are shown in Figure 1.

Figure 1 indicates that the reaction rate, as a function of complex concentration in this temperature range and a complex concentration above approximately $1.0 \times 10^{-3}\text{M}$, may be described by the equation:

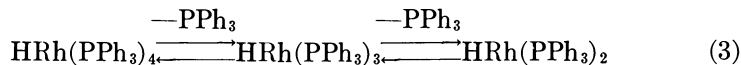
$$r = k_b \cdot C_{A_0} + K \quad (1)$$

where k_b is a rate constant independent of temperature, C_{A_0} is the initial complex concentration, and K is a temperature dependent constant. The few measurements made at complex concentrations below $1.0 \times 10^{-3}\text{M}$ and at 25°C indicate the rate expression:

$$r = k_a \cdot C_{A_0} \quad (2)$$

where $k_a \simeq 24 \times k_b$.

These results may be interpreted by assuming that actually there are two catalytically active complexes. At low concentrations and/or relative high temperature, the catalyst is $\text{HRh}(\text{PPh}_3)_2$, presupposing that the equilibria



lies to the right, but at higher complex concentrations and/or lower temperatures the equilibria shift toward $\text{HRh}(\text{PPh}_3)_3$ so that the catalytic activity is primarily from $\text{HRh}(\text{PPh}_3)_3$.

Table I. Complex Molecular Weights in Benzene at 38°C

Complex Concentration, 10^3M	Molecular Weight
0.5	374
1.0	400
3.0	420
10.0	430

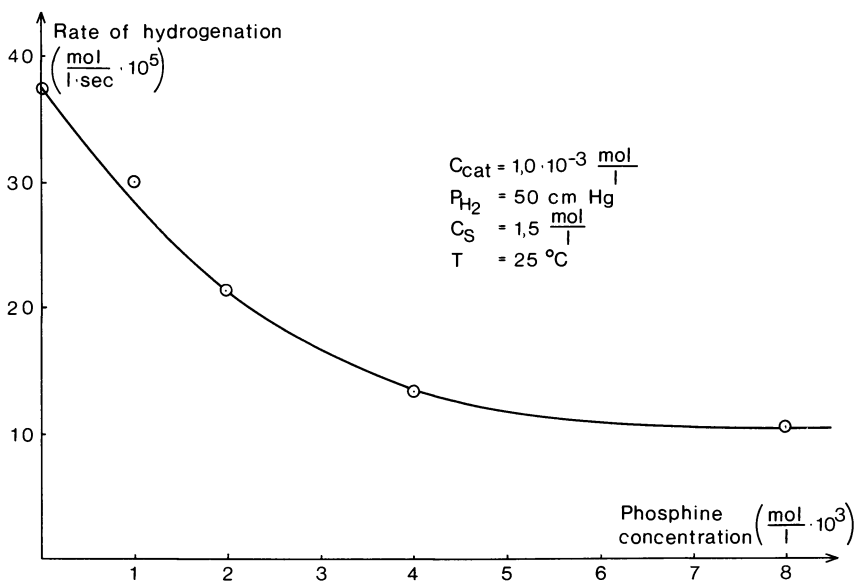


Figure 2. Rate of hydrogenation vs. phosphine concentration

These assumptions are confirmed by molecular weight determinations (Table I) which show that extensive dissociation of the complex occurs in benzene.

The data imply that at 38°C the dissociation to $\text{HRh}(\text{PPh}_3)_2$ is almost complete, even at a complex concentration of 10^{-2}M .

The rate of hydrogenation as a function of the concentration of PPh_3 supports these assumptions. The rate was measured at a fixed complex concentration of $10^{-3}M$, and the results in Figure 2 indicate that Reaction 3 shifts from $\text{HRh}(\text{PPh}_3)_2$ toward the less active $\text{HRh}(\text{PPh}_3)_3$ when the concentration of PPh_3 is increased. The rate then is expressed as

$$r = k_a [\text{HRh}(\text{PPh}_3)_2] + k_b [\text{HRh}(\text{PPh}_3)_3] \quad (4)$$

where k_a and k_b are rate constants which are independent of temperature, the temperature dependence of the catalytic reaction must arise from a shift in the equilibrium between the catalytically active complexes.

Dependence on Hydrogen Pressure. The dependence on hydrogen pressure is linear (Figure 3). The rate of hydrogenation was measured

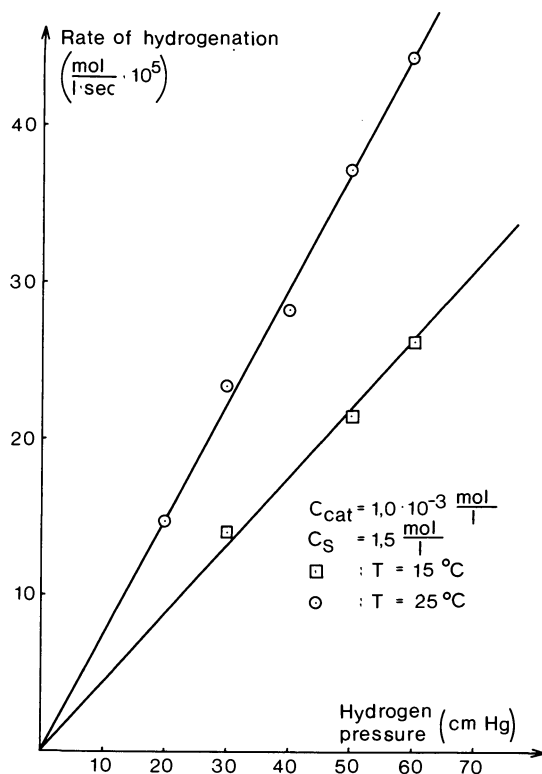


Figure 3. Rate of hydrogenation vs. hydrogen pressure

at 15° and 25°C with a complex concentration of $10^{-3}M$ and an initial 1-hexene concentration of 1.5M. Assuming that the concentration of hydrogen in the liquid phase is proportional to the partial pressure of hydrogen, the rate expression becomes:

$$r = k \cdot C_{\text{H}_2} \quad (5)$$

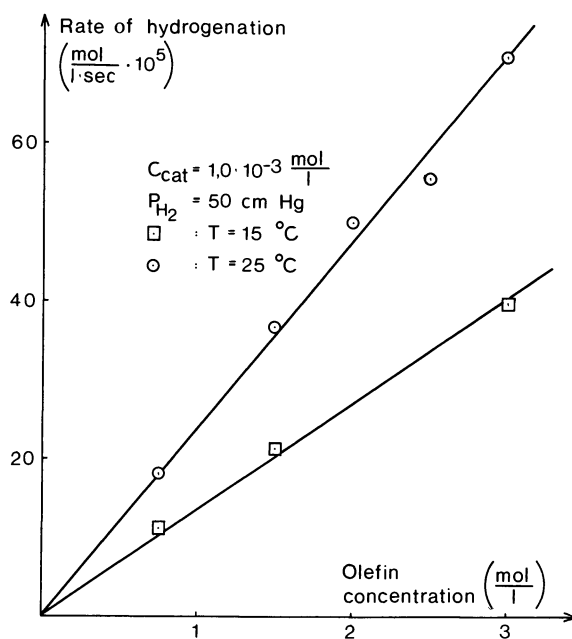


Figure 4. Rate of hydrogenation vs. olefin concentration

Dependence on Olefin Concentration. At 15° and 25°C, a complex concentration of $10^{-3}M$ and a hydrogen pressure of 50 cm Hg, the dependence of hydrogenation rate on the olefin concentration was also linear (Figure 4), implying the rate expression:

$$r = k \cdot C_S \quad (6)$$

Isomerization. The hydrogenation is accompanied by substantial isomerization; indeed at higher catalyst concentrations the isomerization is rapid. After an almost complete hydrogenation with a complex concentration of $4 \times 10^{-3}M$ and $1.5M$ as initial 1-hexene concentration, a GLC analysis of the reaction mixture indicates a composition of 1-hexene, 0.8; hexane, 48.0; *cis*- and *trans*-2-hexene, 42.8; *cis*- and *trans*-3-hexene, 8.4%. The measurements of isomerization alone (Figure 5) indicate that the reaction rate is strongly correlated with the complex concentration and less so with the initial 1-hexene concentration.

Selectivity. The hydrogenation of 2-hexene was very slow, making it difficult to obtain reproducible measurements of the rate at a complex concentration of $10^{-3}M$ and an initial 2-hexene concentration of $1.5M$, but the rate was less than 2% of that for 1-hexene under the same conditions. This rate of reaction is of the same order of magnitude as the rate expected following the isomerization of 2-hexene to 1-hexene since the

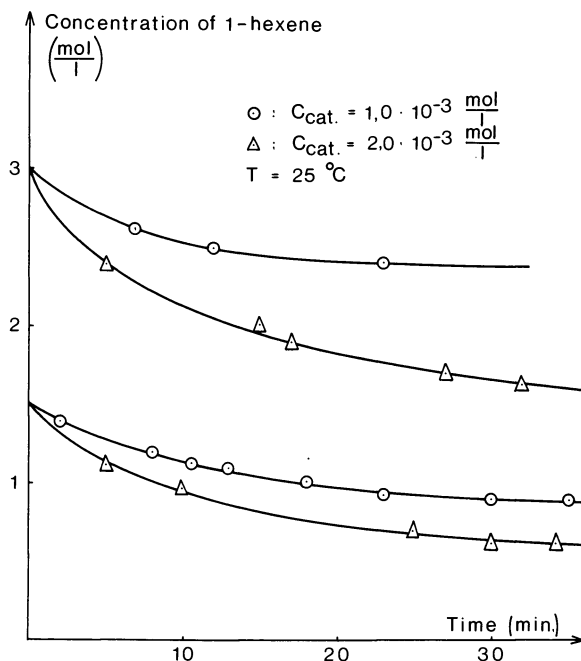
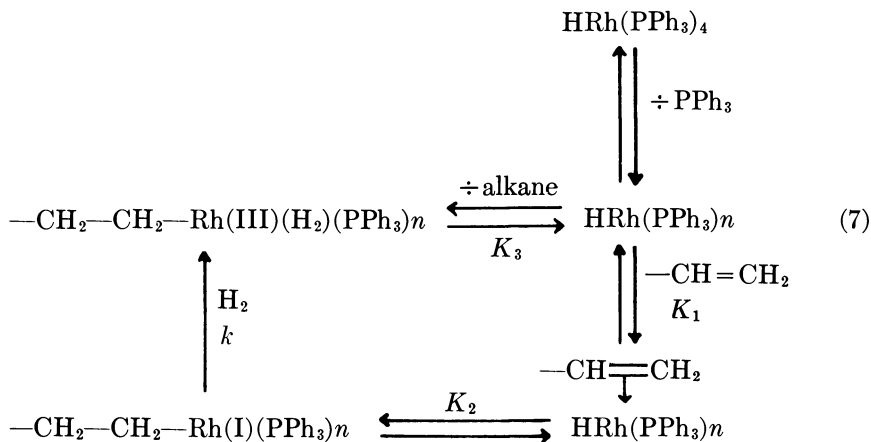


Figure 5. Concentration of 1-hexene vs. time

equilibrium mixture at 25°C consists of 1–2% 1-hexene (8). Thus, no direct hydrogenation of 2-hexene seems to occur. Furthermore, the hydrogenation of 1-hexene was not influenced by adding 2-hexene since no decrease or increase in reaction rate could be detected even upon change in reaction medium by adding 0.5, 1.0, and 1.5M 2-hexene to the initial benzene mixture with a concentration of 1.5M of 1-hexene.



Kinetic Isotope Effect. The reaction rate under standard conditions (complex concentration $10^{-3}M$, $C_S = 1.5M$ 1-hexene, $P_{D_2} = 50$ cm Hg, $T = 25^\circ C$) with deuterium was $33.3 \times 10^{-5}M/sec$ and with hydrogen it was $37.4 \times 10^{-5}M/sec$, producing a positive isotope effect of $k'_H/k'_D = 1.12$.

Discussion

Kinetics. Since the hydrogenation of 1-hexene is accompanied by isomerization to the internal olefin, the catalytic cycle involves an alkyl intermediate which must be formed by inserting the coordinated 1-alkene. Reaction 7 proposes a mechanism for the hydrogenation:

Here n is 2 or 3 with the two hydrogenation cycles running in parallel. In this cycle the oxidative addition of hydrogen is the most probable rate determining step which suggests a rate expression:

$$r = \frac{k \cdot K_1 \cdot K_2 \cdot C_S \cdot C_{H_2} \cdot C_A}{1 + K_1 \cdot C_S + K_1 K_2 \cdot C_S + \frac{C_{alk}}{K_3}} \quad (8)$$

where k is the rate constant for the rate determining step, K_1 , K_2 , and K_3 are equilibrium constants, C_S is the alkene concentration, C_{H_2} is the hydrogen concentration, C_A is the complex concentration, and C_{alk} is the concentration of alkane. Assuming that K_3 is large and K_1 is small (but finite), Equation 8 reduces to:

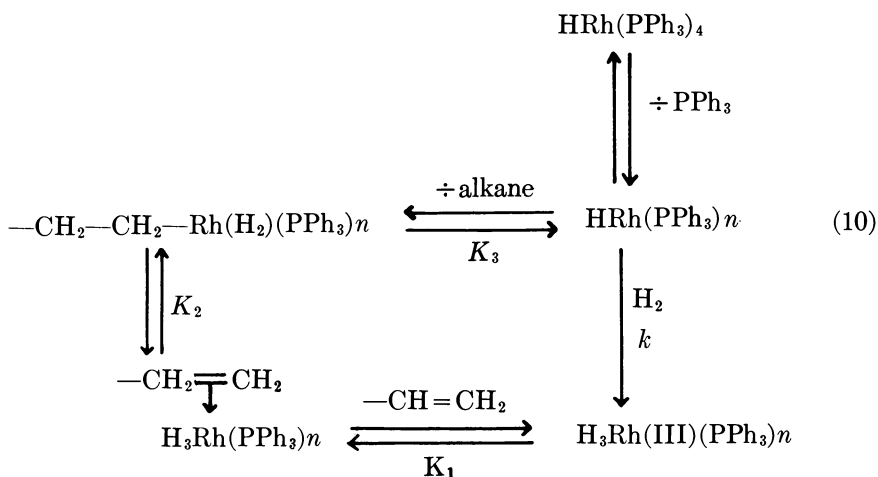
$$r = k \cdot K_1 K_2 \cdot C_S \cdot C_{H_2} \cdot C_A, \quad (9)$$

which agrees with the experimental results. Another possible mechanism involving an alkyl intermediate is seen at the top of the next page. Maintaining the assumption that the oxidative addition of hydrogen is rate determining, this mechanism leads to the rate expression:

$$r = \frac{k \cdot K_1 K_2 K_3 \cdot C_S \cdot C_{H_2} \cdot C_A}{C_{alk} \left(1 + K_1 C_S + K_1 K_2 C_S + \frac{K_1 K_2 K_3 \cdot C_S}{C_{alk}} \right)} \quad (11)$$

which does not agree with the experimental results. If the coordination of the olefin is assumed to be the rate determining step, the rate expression becomes:

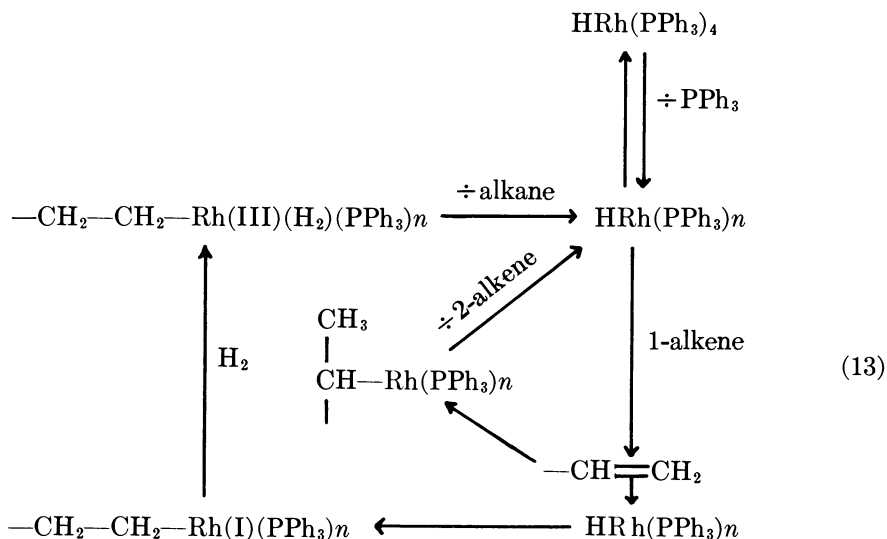
$$r = \frac{k \cdot K_1 \cdot C_{H_2} \cdot C_S \cdot C_A}{1 + K_1 C_{H_2} + \frac{C_{alk}}{K_2 K_3} + \frac{C_{alk}}{K_3}} \quad (12)$$



which can be brought into agreement with the experimental results if K_1 is small and K_3 is large. This mechanism involves a trihydrido complex which cannot be coordinatively unsaturated unless n is 2.

Thus, it must be concluded that the former mechanism of Reaction 7 is the most probable and that the oxidative addition of hydrogen is rate determining.

Selectivity. The insertion of the coordinated 1-alkene creating an alkyl intermediate may proceed either by Markownikoff or anti-Markownikoff addition, but only Markownikoff addition can lead to isomerization. A mechanism which describes both hydrogenation and isomerization may thus be expressed:



Since the hydrogenation of 1-alkene is accompanied by an extensive isomerization, the hindrance toward the formation of an intermediate secondary alkyl does not explain the high selectivity for the hydrogenation of the terminal olefin as it does for $\text{HRh}(\text{CO})(\text{PPh}_3)_3$ (3). The greater instability of the secondary alkyl intermediate toward the elimination of olefin and the formation of metal hydride compared with the instability of the *n*-alkyl intermediate provides a more probable explanation. It is assumed that the complexity constant for the formation of the intermediate olefin complex is significantly smaller for the internal olefin than for the terminal olefin. This assumption is confirmed by the observation that the rate of hydrogenation of 1-hexene is not decreased by addition of 2-hexene which would lead to poisoning of the catalyst by 2-hexene blocking some of the vacant sites if the complexity constants were of the same order of magnitude.

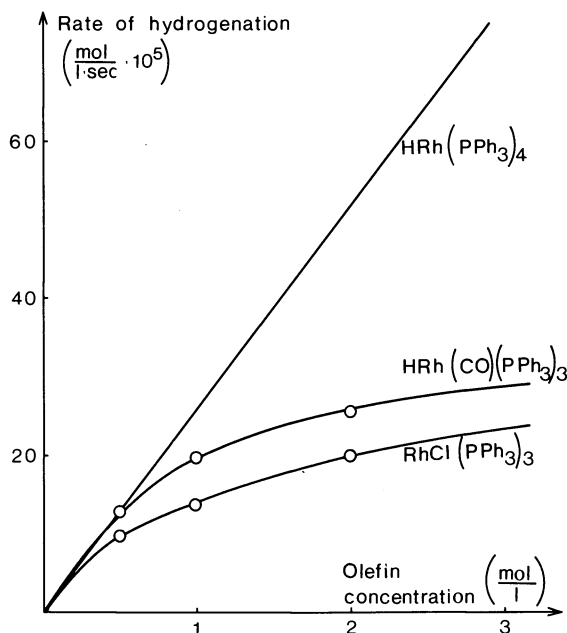


Figure 6. Rate of hydrogenation vs. olefin concentration

Activity. Because of the linear dependence on the olefin concentration, the hydrogenation rate is larger with $\text{HRh}(\text{PPh}_3)_4$ than with $\text{HRh}(\text{CO})(\text{PPh}_3)_3$ at olefin concentration above about 0.5M (Figure 6). The linear dependence also implies that K_1 for the olefin coordination is smaller for $\text{HRh}(\text{PPh}_3)_4$ than for $\text{HRh}(\text{CO})(\text{PPh}_3)_3$. Thus, the greater activity must be attributed to an increased rate constant for the oxidative addition of hydrogen or/and to an increased concentration of the cata-

lytically most active complex $\text{HRh}(\text{PPh}_3)_2$. Both of these effects are achieved by substituting CO by PPh_3 to increase the electron density. Absolute values for the concentration of the catalytically active complexes are unknown, and the rate constants for the oxidative addition of hydrogen are inseparable in the experimental rate expression making it difficult to determine the more important of the two effects.

Literature Cited

1. Ugo, R., *Chim. Ind. Milan* (1969) **51**(12), 1319-31.
2. Osborn, J. A., Jardine, F. H., Young, J. F., Wilkinson, G., *J. Chem. Soc. A* (1966) 1711-32.
3. O'Connor, C., Wilkinson, G., *J. Chem. Soc. A* (1968) 2665-2671.
4. Collmann, J. P., *Accounts Chem. Res.* (1968) **1**(5), 136-43.
5. Shaw, B. L., Cheney, A. J., Duff, J. M., Gill, D., Maun, B. E., Masters, C., Slade, R. M., Stainbank, R. E., "Symposium on Chemistry of Hydroformylation and Related Reactions," Veszpren, Hungary, 1972.
6. Montelatici, A. van der Ernt, Osborn, J. A., Wilkinson, G., *J. Chem. Soc. A* (1968) 1054-8.
7. Ahmad, N., Robinson, S. D., Vitteley, M. F., *J. Chem. Soc., Dalton* (1972) 843.
8. Farkes, A., "Physical Chemistry of the Hydrocarbons," Academic, New York, 1950.

RECEIVED August 20, 1973.

Hydrocarboxylation of Polyunsaturated Fatty Acids and Esters with a Palladium Chloride–Triphenylphosphine Complex Catalyst

E. N. FRANKEL, F. L. THOMAS, and W. K. ROHWEDDER

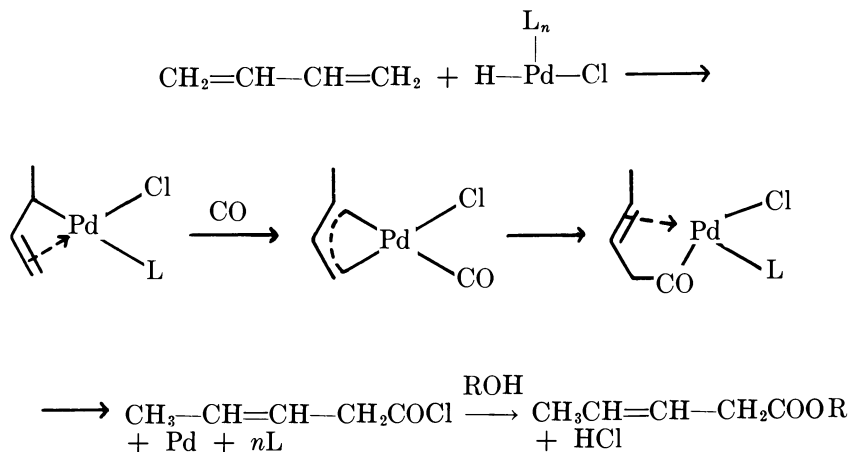
Northern Regional Research Laboratory, Agricultural Research Service,
U.S. Department of Agriculture, Peoria, Ill. 61604

A mixture of palladium chloride and triphenylphosphine effectively catalyzes carboxylation of linoleic and linolenic acids and their methyl esters with water at 110°–140°C and carbon monoxide at 4000 psig. The main products are 1,3- and 1,4-dicarboxy acids from dienes and tricarboxy acids from trienes. Other products include unsaturated monocarboxy and dicarboxy acids, carbomethoxy esters, and substituted α,β -unsaturated cyclic ketones. The mechanism postulated for dicarboxylation involves cyclic unsaturated acyl–PdCl–Ph₃P complexes. These intermediates control double bond isomerization and the position of the second carboxyl group. This mechanism is consistent with our finding of double bond isomerization in polyenes and not in monoenes. A 1,3-hydrogen shift process for double bond isomerization in polyenes is also consistent with the data.

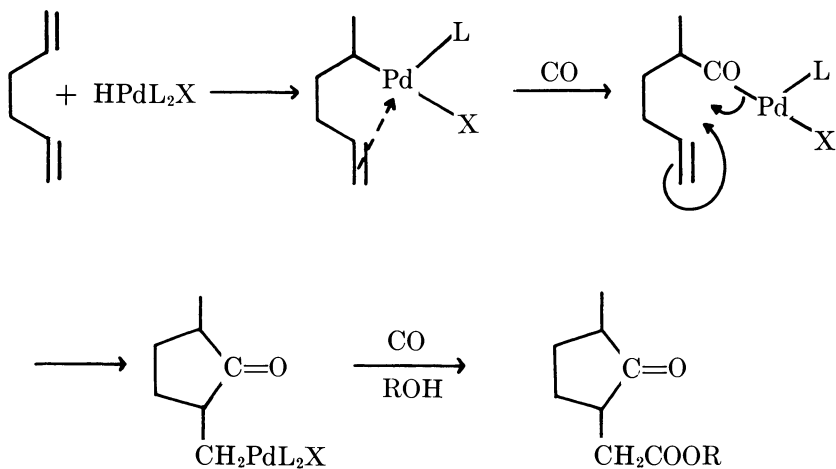
The catalytic reactions of olefins with CO and Pd compounds have received much attention lately (1, 2, 3, 4, 5). Carbonylation of olefins with various Pd catalysts produces carboxy acids with water (hydrocarboxylation) and carboxy esters with alcohol (carboalkoxylation). The two main catalyst systems include PdCl₂ in nonaqueous solvents containing HCl (6, 7) and Pd complexes, such as (Ph₃P)₂PdCl₂, which are more active in the presence of HCl (8). In the PdCl₂ system, alkyl halides are important products at higher HCl concentrations and with higher olefins.

Carbonylation of 1,3-dienes with PdCl₂ gives β,γ -unsaturated esters (9, 10, 11, 12). Butadiene is carboalkoxylated catalytically to form ethyl 3-pentenoate with either PdCl₂ and ethanol (9, 10) or with (Ph₃P)₂PdCl₂ in ethanol containing 10% HCl (8). Tsuji and Ohno (13) propose a mechanism with butadiene that involves the conversion of a PdCl–butenyl

π - σ complex to an acyl PdCl-butenyl π - σ complex through an unsymmetrical π -allyl complex intermediate and that undergoes CO insertion at the less hindered carbon of the complex. An acyl chloride is formed which then reacts with alcohol to give the ester.



In the carbonylation of unconjugated dienes the nature of the products is influenced by reaction conditions. With Pd halides in ethanol at 100°C and 97 atm CO, 1,5-cyclooctadiene is successively carbonylated to the unsaturated monoester and then to the saturated diester (11). With $(\text{Ph}_3\text{P})_2\text{PdCl}_2$ in ethanol-HCl and 300–700 atm CO, the monoester is produced selectively at 60°C and the diester at 100°C (8). Finally, with $(\text{Bu}_3\text{P})_2\text{PdI}_2$ in THF at 150°C and 1000 atm CO, 1,5-cyclooctadiene undergoes transannular addition of CO to give a cyclic ketone in 40–45% yield (14, 15). The mechanism proposed involves a σ - π -cyclooctenyl



PdLX complex undergoing insertion of the coordinated double bond into the σ -Pd-carbon bond to form a Pd-alkyl intermediate. With 1,4-pentadiene and 1,5-hexadiene, cyclic keto esters are formed in MeOH and a similar cyclic mechanism is suggested involving insertion of the coordinated double bond into the acyl Pd complex intermediate (16). Although CO pressures of 1000 atm were used, these cyclic ketones were produced also at 250 atm in the presence of *p*-toluene sulfonic acid, but no details were reported.

Pathways involving alkyl-acyl rearrangements are proposed to explain the carbonylation of σ -bonded alkoxy complexes (17). The stereochemistry of the products indicates that the ester group replaces Pd with retention of configuration at the carbon to which Pd is σ -bonded. In all these studies with unconjugated dienes the nature of carbonylation products to be expected is clearly influenced by the geometry of the intermediate Pd complexes.

Depending on the reaction conditions, *trans,trans,cis*-1,5,9-cyclododecatriene forms mono- and diesters with either PdCl₂ or with Pd-on-carbon with HCl-ethanol at 100°C and 100 atm CO (18). Lack of triester formation is attributed to steric hindrance in the diester that would prevent Pd complex formation with the last *cis* or *trans* double bond. However, mono-, di-, and triesters are produced from 1,5,9-cyclododecatriene with (Ph₃P)₂PdCl₂ in HCl-ethanol at 50°-100°C and 300 atm CO (8). One *trans* double bond reacts first; then the *cis* double bond reacts. The Ph₃P ligands in this system would be expected to stabilize the catalyst. In the absence of Ph₃P, the PdCl₂ catalyst in alcoholic solution would be reduced to metal at the higher temperatures required for triester formation. In these studies with cyclic polyolefins, the relative positions of carboxy acid substituents have not been established. So far as we know, no work has been reported on the carboxylation of acyclic triunsaturated compounds. Double bond isomerization in polyolefins catalyzed by Pd complexes under various carbonylation conditions influences the position of the carboxy acid substituents. This problem has not received much attention and, generally, the mechanism of Pd-catalyzed double bond isomerization remains confused (3, 4).

We previously reported that a mixture of PdCl₂ and excess Ph₃P catalyzes the carboxylation of oleic acid with H₂O and CO to produce 9(10)-carboxyoctadecanoic acid selectively in high yields (85-99%) (19). Carboalkoxylation of methyl oleate with MeOH and CO is also achieved with this catalytic system but in lower yield (76%). One of the catalyst species formed *in situ* was characterized as (Ph₃P)₂PdCl₂. Excess Ph₃P not only provides a stabilizing ligand but also prevents double bond isomerization and byproduct formation which was demonstrated in another related system with Rh-Ph₃P catalyst for the selective

hydroformylation of oleic acid (20). We now report an extension of these studies on the catalytic hydrocarboxylation of polyunsaturated fatty acids and esters with the $\text{PdCl}_2\text{-Ph}_3\text{P}$ system. We followed the course of hydrocarboxylation and determined the nature of the carboxy acids formed to gain insight into some of the factors affecting product distribution.

Experimental

Materials. The catalyst, PdCl_2 (Fisher Scientific, dry, purified grade) and Ph_3P (Strem Chemicals) were used as purchased. Methyl linoleate, alkali-conjugated methyl linoleate (*cis,trans*-9,11- and 10,12-octadecadienoate), and methyl linolenate were prepared as before (21).

Hydrocarboxylations. A 300-ml Hasteloy Magnedash autoclave (Autoclave Engineers) was charged with a mixture of 0.1 mole fatty acid or methyl ester, 1 to 2 mole % PdCl_2 , 4 to 8 mole % Ph_3P , 0.11 to 0.21 mole H_2O in acetone solution (100 ml). Hydrocarboxylations were run at temperatures ranging from 110° to 140°C and initial CO pressure of 2500 psig. In all runs, the final CO pressure was adjusted to 4000 psig when the reaction temperature was reached. The hydrocarboxylations were followed by sequential GLC (22) with a JXR silicone column. For these analyses the solvent in the reaction mixtures was removed under reduced pressure, and the carboxy acids were converted to methyl esters with diazomethane in diethyl ether solution.

Separations. Final products from hydrocarboxylations were first filtered, and the solvent was removed under vacuum. The soluble Pd catalyst, together with carboxy esters and neutral products, was sepa-

Table I. Hydrocarboxylation of Polyunsaturated

Run No.	Substrates	PdCl_2^a , Mole %	Temperature, °C	Time (t), hrs
1 ^c	Linoleic acid	1	120	12
2	Linoleic acid	1	140	6
3	Methyl linoleate	1	110	12
4 ^c	Methyl linoleate	1	120	12
5	Methyl linoleate	2	120	8
6	Methyl linoleate	1	140	6
7 ^c	Methyl linoleate	2	140	4
8 ^c	Conjugated methyl linoleate (<i>cis, trans</i>)	2	140	12
9	Linolenic acid	1	140	6
10	Methyl linolenate	2	110	10
11 ^c	Methyl linolenate	2	120	12
12	Methyl linolenate	2	140	4

^a $\text{PdCl}_2\text{:Ph}_3\text{P}$ mole ratio 1:4.

^b Conjugated dienes are mixtures of *cis,trans* and *trans,trans* isomers.

rated by diethyl ether extraction of the Na salts (yields 10–12%). The carboxy acid products were then regenerated by acidifying the salts with HCl and extracting with diethyl ether. The purified carboxy acids were methylated with diazomethane and fractionated by silicic acid column chromatography (23). Mono-, di-, and tricarbomethoxy esters were isolated by eluting successively with mixtures of 10:90, 15:85, and 25:75 diethyl ether:petroleum ether.

The ether extract containing the catalyst and neutral products was fractionally distilled (130°–160°C at 0.01 mm Hg). The soluble catalyst was concentrated in the pot residues. The distillation fractions were then chromatographed through a silicic acid column. Monoesters and cyclic ketones were eluted successively with 5:95 and 10:90 diethyl ether:petroleum ether, and more polar material was eluted with 15:85 diethyl ether:petroleum ether followed by pure diethyl ether.

Products from Methyl Linoleate

Methyl Carboxyoctadecenoate (1). The product of Run 6 in Table I was characterized as the carbomethoxy ester by GLC and thin-layer chromatography (TLC) (20). Other analyses: IR (neat and CS₂) 1740 (ester C=O) and 965 cm⁻¹ (trans C=C; per cent isolated trans estimated as methyl elaidate, 40.4%); mass spectrum (23) (70 eV) *m/e* (fragment, relative intensity) 354 (M, 8.72), 322 (M - OCH₃ - H, 35.99), 294 (M - COOCH₃ - H, 100.00). Analysis calculated for C₂₁H₃₈O₄: C, 71.14; H, 10.80%; found: C, 70.49; H, 10.86%.

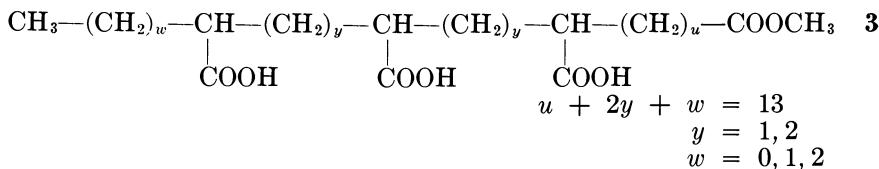
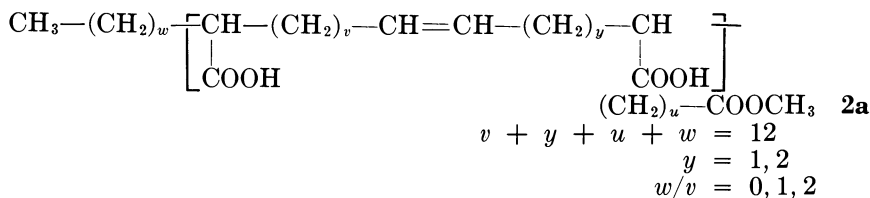
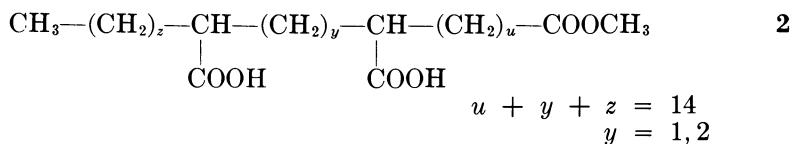
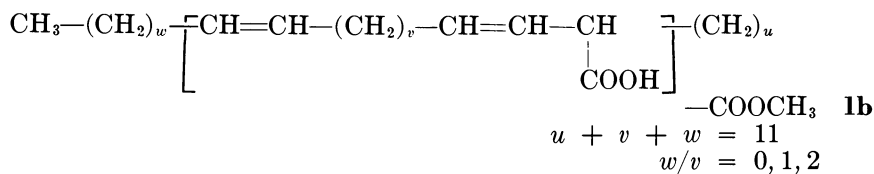
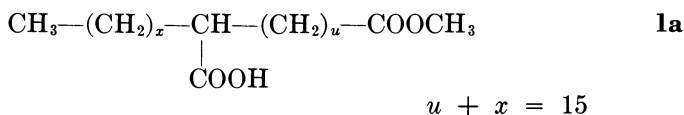
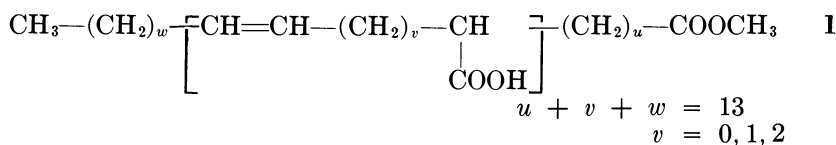
Fatty Acids and Esters Catalyzed by PdCl₂-Ph₃P

GLC Analysis, % at time (t)

Fatty Esters		Carboxy Acids				
Diene	Con-jugated ^b	Mono	Di	Tri	Keto	Others
0.6	0.2	17.2	77.4	0.0	3.6	1.0
0.3	0.2	10.5	80.8	0.0	1.6	6.6
8.2	9.8	34.6	38.9	0.0	3.7	4.8
0.5	1.4	23.8	65.0	0.0	1.2	8.1
0.0	0.0	6.3	77.2	0.0	9.4	7.1
1.2	3.4	23.6	55.1	0.0	5.9	10.8
0.0	0.0	5.2	75.5	0.0	7.8	11.5
0.0	1.2	9.7	78.1	0.0	6.4	4.6
0.0	0.0	1.6	28.6	50.4	12.4	7.0
0.0	8.9	12.1	40.0	21.0	12.1	5.9
0.0	0.0	1.8	36.0	51.5	10.3	0.4
0.0	1.0	1.5	25.5	53.2	10.9	7.9

^c See rate curves in the figures.

Brackets in the following structures indicate more than one isomer having the position of the COOH and CH=CH interchanged.



Methyl Carboxyoctadecanoate (1a). This was prepared by selective hydrogenation of the carbon-carbon double bond of **1** (as the methyl ester) with Pd-on-charcoal + FeCl₂ (**24**). The methyl ester of **1a** had the same chromatographic behavior (GLC and TLC) as methyl 9(10)-carbomethoxyoctadecanoate (**20**), and its IR spectrum showed no band for isolated trans double bond at 965 cm⁻¹. The mass spectrum showed two main isomers: 10- and 12-carbomethoxyoctadecanoate; *m/e* (fragment, relative intensity) 325 (M - OCH₃ + H, 25.19), 297 (M - COOCH₃ + H, 29.24). Isomeric composition based on previous fragmentation studies (**21**) is given in Table II.

Methyl Dicarboxyoctadecanoate (2). This compound was characterized as the dicarbomethoxy ester chromatographically (GLC and TLC) (9) and by other analyses: mass spectrum, m/e (fragment, relative intensity) 383 ($M - OCH_3 + H$, 43.25), 354 ($M - COOCH_3 - H$, 16.11),

323 ($354 - OCH_3$, 20.33), 174 (1,4-diester $MeOOC-\overset{|}{CH}-(CH_2)_2-\overset{|}{CH}-$

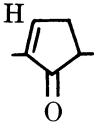
$COOMe$, 33.96), 160 (1,3-diester $MeOOC-\overset{|}{CH}-CH_2-\overset{|}{CH}-COOMe$, 53.93). Isomeric composition is given in Table II based on previous mass spectral studies (21). Analysis calculated for $C_{23}H_{42}O_6$: C, 66.63; H, 10.21%; found: C, 66.61; H, 10.16%.

2(5)-Pentyl-5(2)-carbomethoxyoctyl-2-cyclopentenone and 2(5)-Hexyl-5(2)-carbomethoxyheptyl-2-cyclopentenone (4). These cyclic ketones constitute about 35% (estimated by GLC) of the neutral diethyl ether extract of the salts and amount to 4.6% of the final reaction mixture of carboxylated linoleate. Analyses by GLC (JXR column) show one peak of retention time of 1.06 relative to that of 1; TLC (silica gel G, diethyl ether-petroleum ether, 1:3) R_f 3.74 compared with 5.04 for 2; IR (neat) 1740 (ester $C=O$), 1700 and 1630 cm^{-1} ($C=C-C=O$); UV max

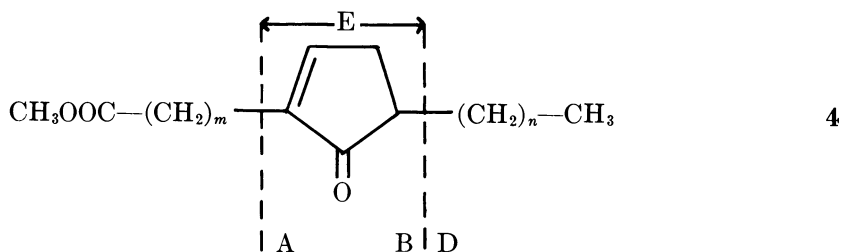
Table II. Mass Spectral Analyses of Mono- and Dicarboxy Acids^a

Branch Carbon No.	Hydrocarboxylated Fatty Esters, relative %			
	Methyl Linoleate		Conjugated Linoleate,	Methyl Linolenate,
	Run 6	Run 7	Run 8	Run 10
Monocarboxy				
9	—	—	11.6	5.4
10	45.6	—	17.4	30.1
11	4.9	—	18.3	1.9
12	36.0	—	20.1	8.3
13	8.3	—	18.1	7.8
14	5.2	—	14.5	1.9
15	—	—	—	37.1
16	—	—	—	7.5
1,3-Dicarboxy				
8,10	—	—	19.8	—
9,11	2.6	3.6	24.3	—
10,12	37.6	35.5	24.8	—
11,13	22.9	21.2	20.7	—
1,4-Dicarboxy				
8,11	—	2.2	3.6	—
9,12	22.9	21.8	3.8	—
10,13	14.0	13.0	3.0	—
11,14	—	2.7	—	—

^a As methyl esters; monocarboxy products were first hydrogenated (21).

(isooctane) 222 nm (ϵ 73,700); NMR (CCl_4) δ 7.09 s, 1,  , 3.79

(s, 3, OCH_3), 2.22 (t, 2, $\text{CH}_2\text{—C=O}$), 2.12 (d, 2, ring $\text{—CH}_2\text{—}$), 1.32 [m, 20, $(\text{CH}_2)_n + \text{CH}$], 0.90 ppm (m, 3, CH_3). High resolution mass spectrum results appear in Table III.



$m, n = 7, 5$ or $8, 4$

Table III. Mass Spectrum Results for 4

m/e	Fragments (m, n)		Elemental Structure	Relative Intensity
	(7,5)	(8,4)		
322 ^a	M		$\text{C}_{20}\text{H}_{34}\text{O}_3$	22.82
291	M - OCH_3		$\text{C}_{19}\text{H}_{31}\text{O}_2$	24.86
252	B + 1		$\text{C}_{15}\text{H}_{24}\text{O}_3$	21.22
238	B + 1		$\text{C}_{14}\text{H}_{22}\text{O}_3$	27.64
220	M - D - $\text{OCH}_3 - 1$		$\text{C}_{14}\text{H}_{20}\text{O}_2$	45.24
206	M - D - $\text{OCH}_3 - 1$		$\text{C}_{13}\text{H}_{18}\text{O}_2$	60.19
166	A + 1		$\text{C}_{11}\text{H}_{18}\text{O}$	100.00
152	A + 1		$\text{C}_{10}\text{H}_{16}\text{O}$	85.34
96	E + 16		$\text{C}_6\text{H}_8\text{O}$	73.40
95	E + 15		$\text{C}_6\text{H}_7\text{O}$	57.49

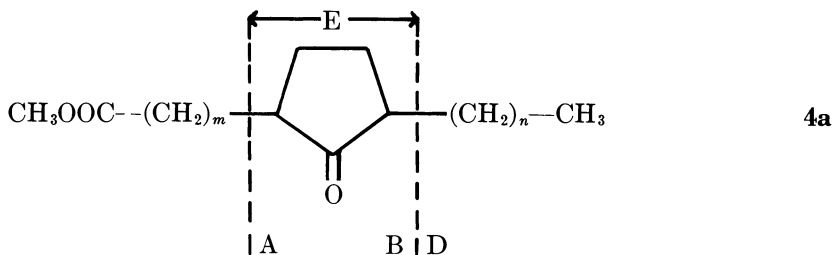
^a M^+ , m/e measured, 322.2522; calculated for $\text{C}_{20}\text{H}_{34}\text{O}_3$, 322.2507.

Analysis calculated for $\text{C}_{20}\text{H}_{34}\text{O}_3$: C, 74.49; H, 10.63%; found: C, 73.74; H, 10.53%.

After hydrogenation of the carbon-carbon double bond with Pd-on-carbon + FeCl_2 (24), compound 4a gave the following analyses: IR bands at 1700 and 1630 cm^{-1} (because of C=C—C=O) were replaced by a band overlapping with the ester carboxyl band (1740 cm^{-1}); NMR at 7.09 ppm (because of ring C=CH) disappeared, and resonance at 2.0 ppm (because of ring CH_2) increased in relative area from 2 to 4 H. The mass spectrum of 4a (hydrogenated ketone) confirms the fragmentation

Table IV. Mass Spectrum Results for 4a

m/e	Fragments (m,n)		Relative Intensity
	(7,5)	(8,4)	
324		M	4.39
293		M - OCH ₃	13.29
254		B + 1	8.77
240	B + 1		10.91
222		M - D - OCH ₃ - 1	13.79
208	M - D - OCH ₃ - 1		19.87
168	A + 1		26.97
154		A + 1	26.90
84		E + 2	100.00



$$m, n = 7, 5 \text{ or } 8, 4$$

scheme assigned to 4 (nonhydrogenated ketone), as shown in Table IV. Before hydrogenation, fragment E in 4 increased in mass by one methylene group, apparently to form a more stable 6-carbon ion. However after hydrogenation, fragment E in 4a gave rise to the base peak and established the size of the pentanone ring. Analysis calculated for C₂₀H₃₆O₃: C, 74.02; H, 11.18%; found: C, 73.32; H, 11.03%.

Methyl Carbomethoxyoctadecenoate. This methyl ester of 1 was isolated directly from the neutral diethyl ether extract fraction of the salts in approximate yield of 10% and identified by mass spectrometry; *m/e* (fragment) 354 (M), 322 (M - OCH₃ - H), 294 (M - COOCH₃ - H); after hydrogenation of the carbon-carbon double bond, *m/e* (fragment) 325 (M - OCH₃), 297 (M - COOCH₃), 283 (297 - CH₂-COOCH₃).

Products from Conjugated Methyl Linoleate

Methyl Carboxyoctadecenoate. The product from Run 8, Table I, was characterized as 1 by GLC, TLC, IR, and mass spectral analyses; *m/e* (fragment, relative intensity) 354 (M, 4.96), 322 (M - OCH₃ - H, 73.74), 294 (M - COOCH₃ - H, 46.49). Mass spectral analysis of the

hydrogenated derivative of **1** (**1a**) showed the carboxy branch to be scattered between carbon-9 and carbon-14 (Table II). Analysis found: C, 71.01; H, 11.34%.

Methyl Dicarboxyoctadecanoate. This was characterized as **2** by GLC, TLC, and mass spectral analyses. Mass spectrum: m/e (fragment, relative intensity) 383 (M - OCH₃, 86.59), 354 (M - COOCH₃ - H, 34.15), 323 (354 - OCH₃ - H, 14.24), 174 (1,4-diester, 32.23), 160 (1,3-diester, 100.00). Isomeric composition is given in Table II. Analysis found: C, 66.96; H, 10.28%.

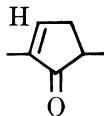
Products from Methyl Linolenate

Methyl Carboxy Acids (1, 1b) and Dicarboxy Acids (2, 2a). These were more difficult to purify chromatographically as the carbomethoxy esters than the corresponding products from linoleate. Analyses by GLC indicated 90–92% purity for these fractions. They were characterized functionally by comparison of their GLC, TLC, and mass spectra with those of **1** and **2** and with those of the corresponding derivatives from hydroformylated methyl linolenate (**2I**). The mass spectrum of the monocarboxy acids from Run 10 (Table I) shows that they consist of carboxyoctadecadienoate (**1b**): m/e (fragment, relative intensity) 352 (M, 8.39), 320 (M - OCH₃ - H, 72.73), 292 (M - COOCH₃ - H, 58.63). The hydrogenated derivative of **1b** (**1a**) has the carboxy branch located mainly on carbon-10 and carbon-15 positions (Table II). The monocarboxy acids from Run 11 (Table I) are a mixture of carboxyoctadecenoate (**1**) and carboxyoctadecadienoate (**1b**): m/e (fragment, relative intensity) 354 (M for **1**, 11.64), 352 (M for **1b**, 6.66), 322 (M - OCH₃ - H for **1**, 46.34), 320 (M - OCH₃ - H for **1b**, 26.82), 294 (M - COOCH₃ - H for **1**, 100.00), 292 (M - COOCH₃ - H for **1b**, 18.73). The monocarboxy acids from Run 12 (Table I) consist of **1**: m/e (relative intensity) 354 (11.70), 322 (60.13), 294 (100.00). The dicarboxy acids from Run 11 (Table I) consist of dicarboxyoctadecenoate **2a**: m/e (fragment, relative intensity) 412 (M, 17.14), 380 (M - OCH₃ - H, 76.97), 352 (M - COOCH₃ + H, 29.20), 320 (352 - OCH₃ - H, 100.00). The dicarboxy acids from the same run consist of dicarboxyoctadecanoate (**2**): m/e (fragment, relative intensity) 383 (M - OCH₃ - H, 29.02), 354 (M - COOCH₃ - H, 12.42), 323 (354 - OCH₃, 15.23), 174 (1,4-diester, 18.75), 160 (1,3-diester, 21.66).

Methyl Tricarboxyoctadecanoate, 3. The product from Run 12, Table I, was characterized functionally by comparing GLC, TLC, and mass spectra of corresponding derivatives from hydroformylated methyl linolenate (**2I**). Mass spectrum: m/e (fragment, relative intensity) 472

(M, 0.85), 441 (M - OCH₃, 26.87), 409 (441 - OCH₃ - H, 33.42), 174 (1,4-diester fragment, 11.69), 160 (1,3-diester fragment, 19.12).

2(5)-Alkyl-5(2)-carbomethoxyalkyl-2-cyclopentenone. This was characterized functionally as **4** by GLC, TLC, IR, and other analyses: UV max (isooctane) 222 nm (ϵ 93,700); NMR (CCl₄) δ 7.06 s, 1,



, 3.56 (s, 3, OCH₃), 2.20 (t, 2, CH₂-C=O), 2.06 (d, 2, ring

CH₂), 1.26 [m, 20, (CH₂)_n + CH], 1.05 t, 1.5, CH₃-C , 0.90

(m, 1.5, CH₃); mass spectrum showed the same fragmentation scheme as that of **4** from linoleate except for the appearance of two new peaks at *m/e* 124 and 110 which can be attributed to ring fragments 95 + CH₂CH₃ and 95 + CH₃, respectively. This evidence confirms in part NMR data (triplet peak at δ 1.05 ppm) indicating that a significant portion of the cyclopentenone ring has either ethyl or methyl substituents. Mass spectrum, *m/e* (relative intensity): 322 (16.40), 291 (15.95), 252 (5.54), 238 (16.76), 220 (15.56), 124 (49.55), 110 (100.00), 206 (42.72), 166 (63.86), 152 (28.44), 96 (63.27), 95 (84.11). Analysis found: C, 74.04; H, 10.49%.

Results and Discussion

Hydrocarboxylations were catalyzed by a mixture of PdCl₂ and Ph₃P which proved to be more effective than preformed (Ph₃P)₂PdCl₂ (**19**). Effective carboxylation of diene and triene fatty acids and esters with a 0.1 mole excess of water was achieved with 1 and 2 mole % PdCl₂ + 4 and 8 mole % Ph₃P at 110°–140°C and 4000 psi CO in acetone solution (Table I). The main products were mono- and dicarboxy acids from dienes and di- and tricarboxy acids from trienes. Yields of dicarboxy acids from dienes were as high as 76 to 81%. Monocarboxy acids were formed in higher amounts at low temperatures and catalyst concentrations. Tricarboxy acids from trienes ranged from 50 to 53%. GLC analyses showed the formation of conjugated fatty esters in the partially carboxylated substrates. Small but significant amounts of a cyclic ketone was also formed along with other unidentified byproducts.

Because conjugated fatty esters are potential intermediates, alkali-conjugated methyl linoleate [mixture of mainly *cis,trans*-(9,11- and 10,12)-octadecadienoate] was catalytically hydrocarboxylated. Under comparable conditions, these conjugated dienes were more difficult to

hydrocarboxylate than methyl linoleate, but the ultimate product distribution was functionally the same (Table I, Runs 7 and 8).

The course of hydrocarboxylation was studied further by sequential analyses of reaction mixtures and by detailed characterization of the purified carboxy acid products. Figure 1 plots kinetic runs with linoleic acid and methyl linoleate at 120°C. Analysis by GLC shows the rapid disappearance of diene followed successively by initial conjugation of the diene system, monocarboxylation, and then dicarboxylation. Cyclic ketones and other unidentified materials (not shown) are formed in minor amounts. Conjugated dienes (mixture of *cis,trans* and *trans,trans*) peak at 1 hr and then rapidly disappear. Monocarboxy acids peak around 6–8 hrs and disappear at later stages of the reaction. At 140°C, the carboxylation follows the same course (Figure 2A). Formation of conjugated dienes reach a maximum around 0.5 hr. Monocarboxy acids peak around 1 hr, decrease, and then level at 3–4 hrs.

Catalytic carboxylation of *cis,trans* conjugated linoleate is accompanied by initial thermal isomerization to *trans,trans*-conjugated dienes which reach a peak concentration around 1 hr (Figure 2B). A small but significant amount of nonconjugated diene reaches a maximum of 3% around 4 hrs. Mono- and dicarboxylation of conjugated dienes follow

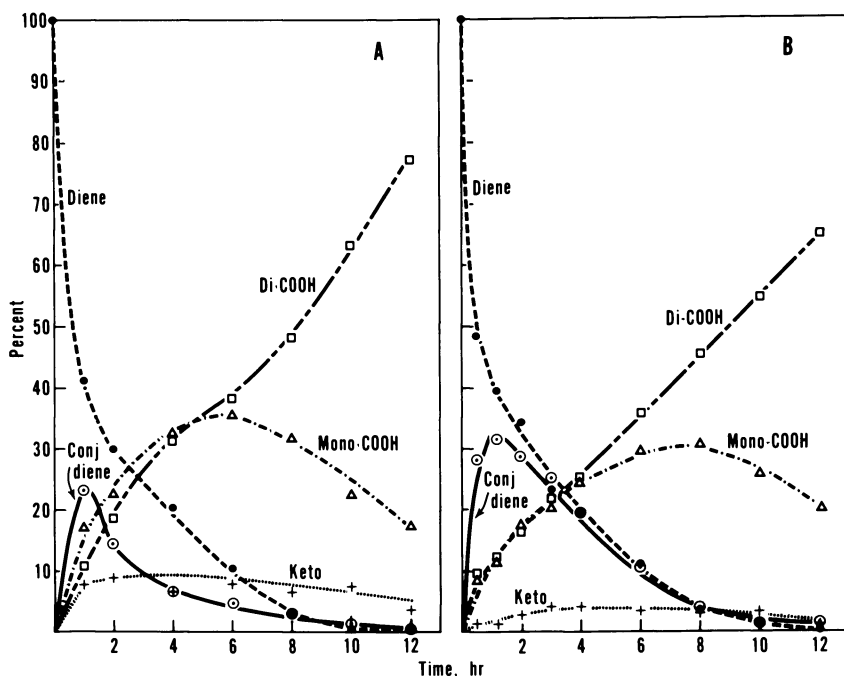


Figure 1. Rate curves for hydrocarboxylation with $\text{PdCl}_2\text{-Ph}_3\text{P}$ at 120°C, 4000 psi CO: (A) Linoleic acid (Run 1, Table I); (B) Methyl linoleate (Run 4)

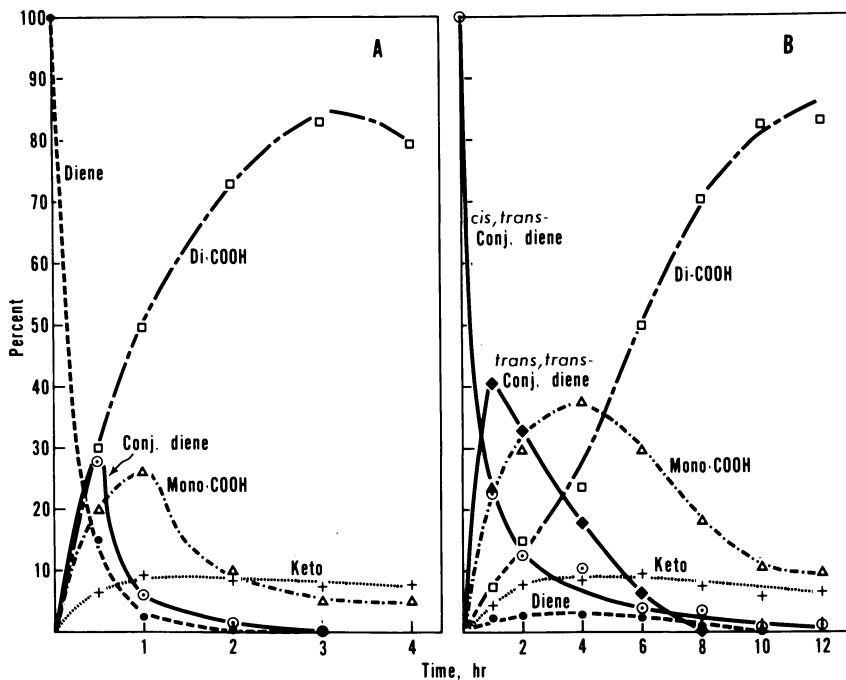


Figure 2. Rate curves for hydrocarboxylation with $\text{PdCl}_2\text{-Ph}_3\text{P}$ at 140°C , 4000 psi CO: (A) Methyl linoleate (Run 7); (B) Conjugated methyl linoleate (Run 8)

the same course as methyl linoleate. Maximum conversion to dicarboxy acids is approximately 83%.

Further characterization showed that the monocarboxy acids from both linoleate and its conjugated diene isomers are unsaturated. These unsaturated carboxy acids to a great extent are carboxylated further. However the GLC and kinetic results indicate that a small amount becomes saturated at 140°C (5 to 10%). Conversion to dicarboxy acids reaches a maximum (75–83%) because of the formation of these saturated monocarboxy acids and byproducts.

To elucidate further the reaction sequence, competitive catalytic carboxylation was studied with mixtures of methyl linoleate and conjugated linoleate. At 120°C methyl linoleate carboxylates initially more rapidly than conjugated linoleate (Figure 3). With this mixture, monocarboxy acids are formed in larger amounts than the dicarboxy acids.

Product characterization provides further insight on the course of diene carboxylation. The monocarboxy acids were identified as methyl carboxyoctadecenoate (1) from chromatographic, IR, mass spectral, and selective hydrogenation studies. The double bond of 1 from carboxylated linoleate is 40% trans in configuration (IR), and its carboxy group is located mainly on carbon-10 and -12 positions (Table II). In contrast,

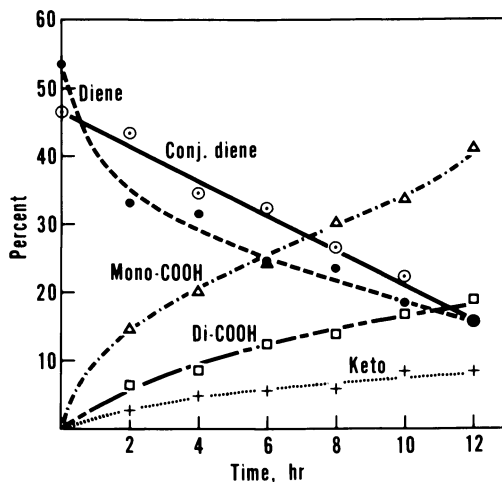


Figure 3. Competitive hydrocarboxylation of a mixture of methyl linoleate and conjugated linoleate (same conditions as Runs 1 and 4 in Figure 1)

compound 1 from carboxylated conjugated linoleate has its carboxy group distributed between the carbon-9 and carbon-14 positions.

The dicarboxy acids from the diene substrates were characterized functionally by chromatographic, elemental, and mass spectral analyses as 2. The dicarbomethoxy esters from carboxylated linoleate consist mainly of the 1,3-disubstituted 10,12- and 11,13-isomers, and 1,4-disubstituted 9,12- and 10,13-isomers (Table II). The 1,3-dicarboxy acids (8,10; 9,11; 10,12; and 11,13) are the principal products of conjugated linoleate. Therefore, the 1,3-dicarboxy acids identified in the products of linoleate can arise from the conjugation process $1,4\text{-diene} \rightarrow 1,3\text{-diene}$.

Kinetic and product studies provide clear evidence for equilibrium between linoleate and conjugated dienes. Carboxylation of both 1,4- and 1,3-diene systems produce carboxyoctadecenoate (1) as the initial product. Carboxylation of 1 produces 1,3- and 1,4-dicarboxyoctadecanoate (2). The 1,3-dicarboxy acids could also arise from double bond isomerization in a Pd complex intermediate of 1. Our results can be explained by a reaction sequence involving both 1,4- and 1,3-diene $\text{PdCl}(\text{Ph}_3\text{P})_n$ complex intermediates (Figure 4).

The conjugation process $1,4\text{-diene} \rightarrow 1,3\text{-diene}$ goes by interconversion of π -Pd complexes I and III *via* the intermediate π -allyl-Pd hydride complex II and involves 1,3-hydrogen shifts. Conversion of *cis,trans* to the thermodynamically favored *trans,trans*-conjugated dienes occurs, but both of these isomers would be carboxylated the same way. CO insertion *via* a Pd carbonyl hydride (allyl or olefin) intermediate gives unsatu-

rated acyl Pd complexes IV, V, and VI. Complex V is a common intermediate arising from both 1,4- and 1,3-diene complexes I and III, and it influences the product distribution from both diene substrates. Complexes IV and VI affect the respective products from linoleate and conjugated linoleate. Carboxy-octadecenoate isomers (11-, 12-, and 13-) **1** are derived either directly from IV, V, and VI or after double bond isomerization from VII, VIII, and X. Further carboxylation to the dicarboxy-octadecanoate isomers (9,11-; 9,12-; 10,12-; 10,13-; 11,13-) **2** involves complexes V, VII, VIII, and IX. The 12-carboxy acid and 10,12-dicarboxy acid are predominant products from linoleate, and they come from complexes V and VIII which, presumably, are the most favorable for CO insertion. The same scheme can be written for the carboxylation of the 9-10 double bond in linoleate and conjugated linoleate. Hydrocarboxylation of (9-, 10-, 11-) acyl-PdCl(Ph₃P)_n-12-octadecenoate complex intermediates (IV', V', and VI') leads to the formation of 9-, 10-, and 11-carboxy-octadecenoate and of the same dicarboxy acids as in Figure 4. The 10-carboxy acid and 10,12-dicarboxy acid predominating from lino-

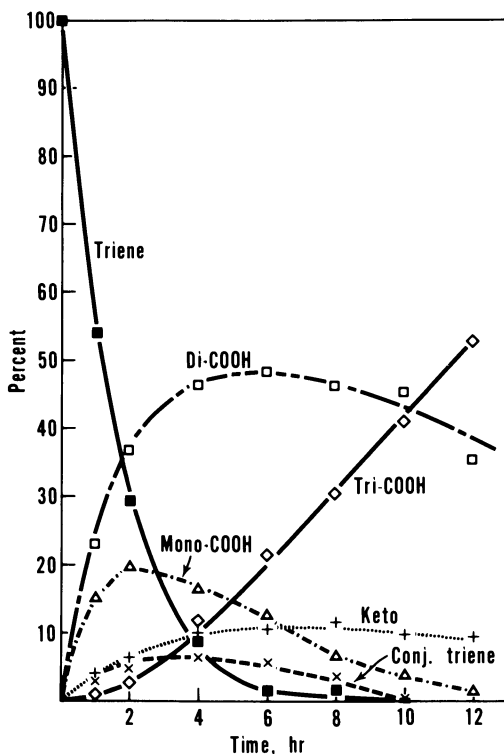


Figure 4. Reaction sequence of linoleate and conjugated linoleate carboxylation by palladium chloride-phosphine catalysis

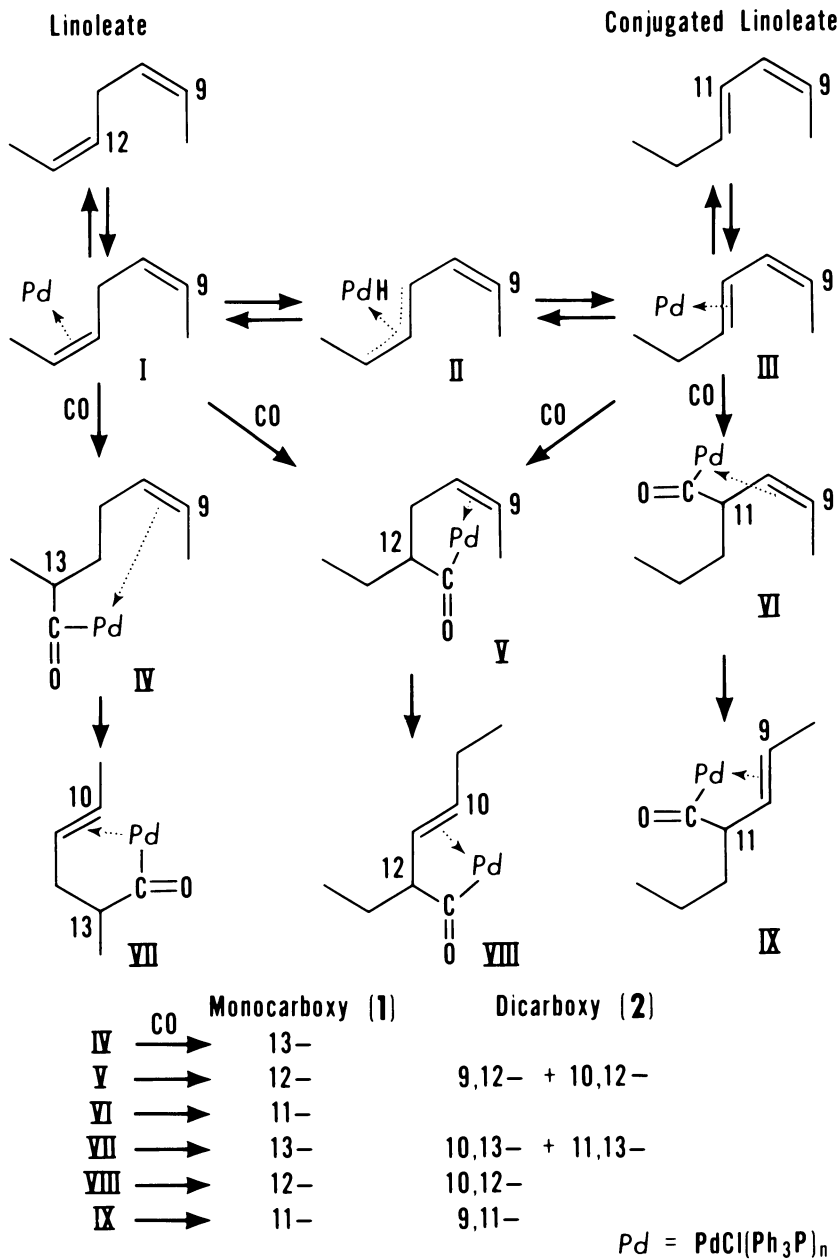


Figure 5. Reactions of carboxy-acyl-PdCl(Ph₃P)_n intermediates

leate are derived from intermediates V' and VIII', 10-acyl-PdCl(Ph₃P)_n-12- and 11-octadecenoate.

Dicarboxylation would involve reaction of complexes V, VII, VIII, and IX with H₂O to produce carboxy-PdCl(Ph₃P)_n intermediates (X) which undergo another CO insertion *via* a Pd carbonyl hydride intermediate. The resulting carboxy-acyl-PdCl(Ph₃P)_n intermediates (XI) are cleaved with H₂O to give the dicarboxy acids and HPdCl(Ph₃P)_n (Figure 5).

This dicarboxylation pathway has common features with that which we previously proposed for the dihydroformylation of methyl linoleate catalyzed by a Rh-Ph₃P system (21). The contrasting feature is the formation of the π -allyl complex intermediate II promoting significant interconversion of 1,4- and 1,3-Pd complexes I and III. This ease of double bond isomerization characteristic of Pd complex catalysts (3, 4) would account for the greater concentration of 1,3-dicarboxy acids produced by the Pd-Ph₃P hydrocarboxylation system than the corresponding diformyls produced by the Rh-Ph₃P hydroformylation system (21). An isomerization process alternate to that depicted in Figure 4 involves 1,2-hydrogen shifts by Pd-hydride addition and elimination through successive Pd- π -olefin and Pd- σ -alkyl complexes (3, 4, 25). However, such a mechanism would promote the formation of 1,2- and 1,5-dicarboxy acids not found among the hydrocarboxylation products. The 1,2-hydrogen shift scheme would also result in isomerization of the double bond in oleic acid during hydrocarboxylation with PdCl₂-Ph₃P. This expected result is, however, inconsistent with our finding (19).

A significant portion of the neutral ethyl ether extract from the salts of carboxylated methyl linoleate consists of α,β -unsaturated cyclic ketones. This material is produced in small but significant amounts (4-10%) (Table I) from the carboxylation of polyunsaturates but not from the corresponding monounsaturated fatty acids and esters (19). These α,β -unsaturated cyclic ketones were identified spectroscopically (IR, UV, and NMR) as 4. This structural assignment was firmly established by mass spectral analyses before and after hydrogenation of the carbon-carbon double bond.

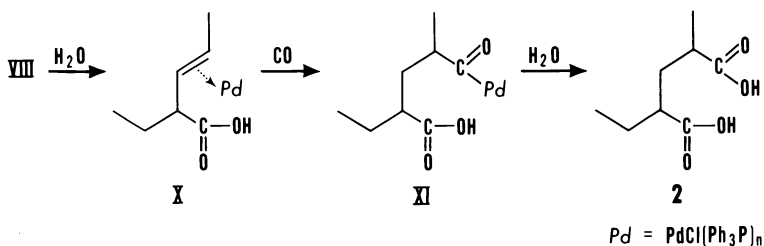


Figure 6. Formation of cyclic ketones based on cyclic mechanism

Of mechanistic interest is the question of whether these cyclic ketones come directly from conjugated diene intermediates or from PdCl_2 complexes of carboxyoctadecenoates. Yields of cyclic ketones **4** are actually of the same order of magnitude from linoleate as from its conjugated diene isomers (Runs 7 and 8, Table I). Studies were also made to determine if yields of cyclic ketones can be influenced by the amount of H_2O used. However, in experiments using no added H_2O and one-tenth the stoichiometric amount of H_2O , only 10 and 8% ketones and conversions (diene disappearance) of only 58 and 78% were obtained, respectively.

The results are consistent with a cyclic mechanism involving unsaturated acyl Pd complexes **V** and **VII** followed by double bond isomeriza-

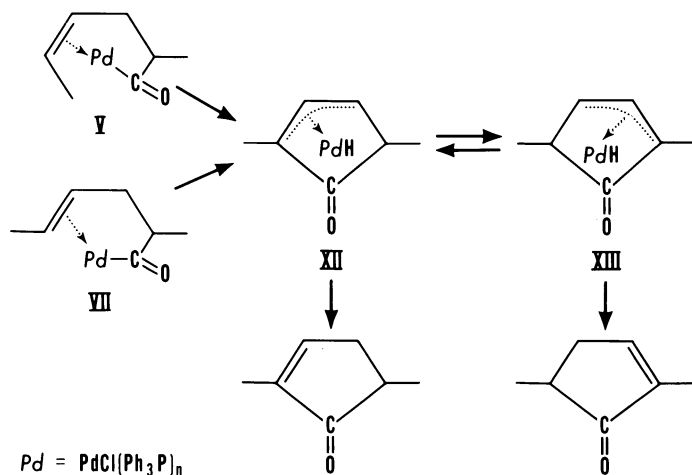


Figure 7. Alternate exocyclic mechanism for cyclic keto carboxy acid formation

tion *via* cyclic acyl Pd hydride allyl complexes **XII** and **XIII** (Figure 6). The isomerization depicted in this scheme places the double bond in **4** on either side of the keto group. Our evidence, however, has not established the position of this double bond.

An alternate exocyclic allylic complex of type **XIV** could produce a cyclic keto carboxy acid, **5** (Figure 7).

Formation of a keto ester of type **5** has already been reported in the carbonylation of 1,5-hexadiene (**16**), albeit under rather high CO pressures. Our evidence cannot exclude the formation of cyclic keto carboxy acids such as **5**. This type of material may be included in tail fractions, obtained in small amounts (1–10%) from carboxylated linoleate, of higher chromatographic polarity than the dicarboxy acids. These partially purified polar fractions showed in their IR spectra a charac-

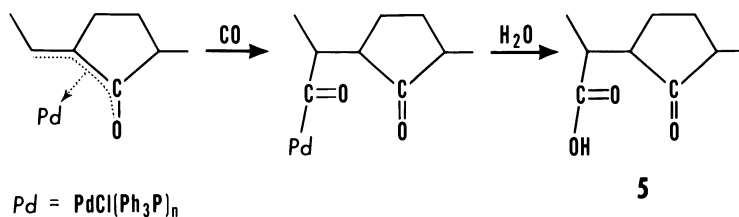


Figure 8. Rate curves for hydrocarboxylation of methyl linolenate with PdCl₂-Ph₃P at 120°C, 4000 psi CO (Run 11)

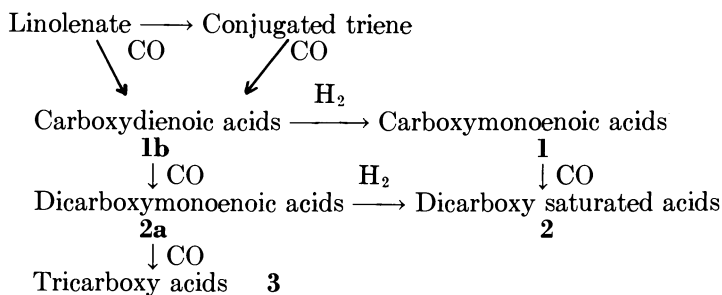
teristic carbonyl band at 1770 cm⁻¹ which may suggest also enol-lactones of the type reported from the carbonylation of unconjugated dienes (14, 15).

The methyl ester of carboxyoctadecenoate **1** was also identified (about 10% by GLC) in the neutral ether extract from the salts of carboxylated linoleate. Apparently some methanol is formed from H₂O and CO under the conditions of hydrocarboxylation, and esterification of the monocarboxy acids occurs to a small extent. Double bond hydrogenation is another minor side reaction observed. Small amounts of carboxyoctadecanoate **1a** detected in final hydrocarboxylation mixtures would arise from H₂ produced by the water-gas reaction (CO + H₂O = CO₂ + H₂).

Figure 8 shows kinetic data on the catalytic hydrocarboxylation of methyl linolenate. There is initial conjugation of the triene system. Monocarboxy acids formed as initial products peak after 2 hrs and disappear almost completely. The dicarboxy acids are important intermediates and carboxylate further to give tricarboxy acids. The conversion to tricarboxy acids at 140°C does not exceed 50 to 53% (Runs 9 and 11, Table I). Cyclic ketones are formed as in linoleate in small but significant amounts.

The monocarboxy acids from linolenate hydrocarboxylated at 110°C (Run 10, Table I) were characterized as carboxyoctadecadienoate **1b** (chromatography, IR, mass spectrum) with the carboxy group located mainly on carbon-10 and -15 positions (Table II). At 120°C (Run 11, Table I), the monocarboxy acids consisted of a mixture of monoenoic acid **1** and dienoic acid **1b**. At 140°C **1b** is hydrogenated to **1** (Run 12, Table I). The cyclic keto product from linolenate (Run 12) proved to have the same structure as **4**, but a significant portion of the cyclopentenone has either ethyl (NMR and mass spectrum) or methyl (mass spectrum) substituents. This structure is expected from cyclization at the 12,15-diene system of linolenate. The formation of this disubstituted pentenone product involves hydrogenation of one carbon-carbon double bond during hydrocarboxylation. The di- and tricarboxy acids of linolenate were characterized as **2**, **2a**, and **3**, but some polar impurities proved difficult to remove from the chromatographic fractions. The posi-

tion of the carboxy acid substituents in these products could not be established reliably because of these impurities and because of the multitude of isomers. However, 1,3- and 1,4-disubstitution predominated as indicated by diester fragments of m/e 160 ($\text{MeOOC}-\underset{\text{|}}{\text{CH}}-\text{CH}_2-\underset{\text{|}}{\text{CH}}-\text{COOMe}$) and m/e 174 [$\text{MeOOC}-\underset{\text{|}}{\text{CH}}-(\text{CH}_2)_2-\underset{\text{|}}{\text{CH}}-\text{COOMe}$] (21). The kinetic and characterization results support a sequence of consecutive reactions (Reaction 1).



Reaction 1

The hydrogenation steps in this scheme account for the lower yields of tricarboxy acids from linolenate compared with the dicarboxy acids from linoleate.

Conclusions

Hydrocarboxylation of polyunsaturated fatty acids with $\text{PdCl}_2\text{-Ph}_3\text{P}$ is more complex than that of oleic acid (19). Polycarboxylation is accompanied by significant double bond isomerization, some hydrogenation, cyclic ketone formation, and the production of other byproducts as yet unidentified. Cyclic ketone formation is observed under much lower CO pressures than previously reported with α,ω -dienes (14, 15, 16). The 1,3-dicarboxy acids are important products of both linoleate and linolenate. Tricarboxy acids are the principal products of linolenate. The greater complexity of these carboxylation products than those made with the $\text{Rh-Ph}_3\text{P}$ hydroformylation system (21) are attributable to the double-bond isomerization activity of the $\text{PdCl}_2\text{-Ph}_3\text{P}$ catalyst. In contrast to monoenes, double bond isomerization in polyenes is initially favored over polycarboxylation. The finding of double bond isomerization in polyenes and not in monoenes requires that unsaturated PdCl complex intermediates are significant in determining the course of carboxylation. A 1,3-hydrogen shift mechanism for double bond isomerization is consistent with the product distribution observed.

Acknowledgments

We are grateful to R. L. Reichert, W. L. Everhart, C. A. Glass, C. E. McGrew, and J. M. Snyder.

Literature Cited

1. Hartley, F. R., *Chem. Rev.* (1969) **6**, 799.
2. Hüttel, R., *Synthesis* (1970) 225.
3. Maitlis, P. M., "The Organic Chemistry of Palladium," Vol. II, "Catalytic Reactions," pp. 18, 128, Academic, New York, 1971.
4. Stern, E. W., *Catalysis* (1968) **1**, 73.
5. Tsuji, J., *Advan. Org. Chem.* (1969) **6**, 109.
6. Tsuji, J., Morikawa, M., Kiji, J., *Tetrahedron Lett.* (1963) 1437.
7. Tsuji, J., Ohno, K., Kajimoto, T., *Tetrahedron Lett.* (1965) 3969.
8. Bittler, K., v. Kutepow, N., Neubauer, D., Reis, H., *Angew. Chem. Int. Ed. Engl.* (1968) **7**, 329.
9. Hosaka, S., Tsuji, J., *Tetrahedron* (1971) **27**, 3821.
10. Tsuji, J., Hosaka, S., *J. Amer. Chem. Soc.* (1965) **87**, 4075.
11. Tsuji, J., Hosaka, S., Kiji, T., Susuki, T., *Bull. Chem. Soc. Jap.* (1966) **39**, 141.
12. Tsuji, J., Kiji, J., Hosaka, S., *Tetrahedron Lett.* (1964) 605.
13. Tsuji, J., Ohno, K., *ADVAN. CHEM. SER.* (1968) **70**, 155.
14. Brewis, S., Hughes, P. R., *Chem. Commun.* (1966) 6.
15. *Ibid.*, (1967) 71.
16. Brewis, S., Hughes, P. R., *Chem. Commun.* (1965) 489.
17. Hines, L. F., Stille, J. K., *J. Amer. Chem. Soc.* (1972) **94**, 485.
18. Tsuji, J., Nogi, T., *Bull. Chem. Soc. Jap.* (1966) **39**, 146.
19. Frankel, E. N., Thomas, F. L., *J. Amer. Oil Chem. Soc.* (1973) **50**, 39.
20. Frankel, E. N., *J. Amer. Oil Chem. Soc.* (1971) **48**, 248.
21. Frankel, E. N., Thomas, F. L., Rohwedder, W. K., *Ind. Eng. Chem., Prod. Res. Develop.* (1973) **12**, 47.
22. Frankel, E. N., Thomas, F. L., *J. Amer. Oil Chem. Soc.* (1972) **49**, 10.
23. Frankel, E. N., Metlin, S., Rohwedder, W. K., Wender, I., *J. Amer. Oil Chem. Soc.* (1969) **46**, 133.
24. Rylander, P. N., Himelstein, N., *Engelhard Ind. Tech. Bull.* (1964) **4** (4), 131.
25. Chalk, A. J., Harrod, J. F., *Advan. Organometal. Chem.* (1968) **6**, 119.

RECEIVED July 30, 1973. Naming firms or trade products does not imply that they are endorsed or recommended by the Department of Agriculture over other firms or similar products not mentioned.

Amine Carbonylation Catalyzed by Ruthenium Complexes under Mild Conditions

G. L. REMPEL and W. K. TEO

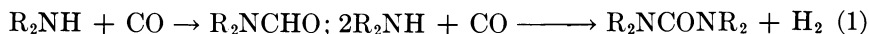
University of Waterloo, Waterloo, Ontario, Canada

B. R. JAMES and D. V. PLACKETT

University of British Columbia, Vancouver, British Columbia, Canada

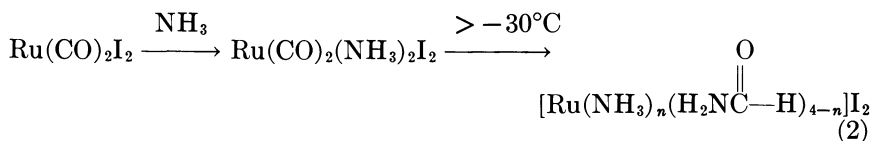
The ruthenium carbonyl complexes $[Ru(CO)_2(OCOCH_3)]_n$, $Ru_3(CO)_{12}$, and a new one, tentatively formulated $[HRu(CO)_3]_n$, homogeneously catalyze the carbonylation of cyclic secondary amines under mild conditions (1 atm, 75°C) to give exclusively the N-formyl products. The acetate polymer dissolves in amines to give $[Ru(CO)_2(OCOCH_3)(amine)]_2$ dimers. Kinetic studies on piperidine carbonylation catalyzed by the acetate polymer (in neat amine) and the hydride polymer (in toluene-amine solutions) indicate that a monomeric tricarbonyl species is involved in the mechanism in each case.

The carbonylation of amines to give substituted formamides and ureas (Reaction 1) has been reviewed by Rosenthal and Wender (1). Cobalt, nickel, and manganese carbonyls have been used fairly exten-



sively as catalysts under severe temperatures and pressures, and the use of rhodium carbonyls under similar conditions has also been noted (2). The mechanisms of these reactions are not well understood.

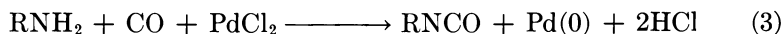
Hieber and Heusinger (3) reported an interesting reaction in which a liquid ammonia solution of ruthenium carbonyl iodide decomposed above -30°C to produce free and coordinated formamide:



Since many ruthenium species, including amines, are readily carbonylated using carbon monoxide under mild conditions (4, 5), there seemed a good probability that effective ruthenium catalysts could be found for amine carbonylation under mild conditions. Product selectivity, a problem at more severe conditions, should also improve.

This paper summarizes our efforts to date and is concerned primarily with kinetic and mechanistic studies on the catalytic carbonylation of piperidine to *N*-formyl product using a ruthenium(I)-bridged acetate dicarbonyl polymer $[\text{Ru}(\text{CO})_2(\text{OCOCH}_3)]_n$ (6, 7) and a less well-characterized polymeric hydridocarbonyl $[\text{HRu}(\text{CO})_3]_n$ (7). Kealy and Benson (8) noted the formation of *N*-cyclohexylformamide when carbonylating cyclohexylamine in the presence of allene using $\text{Ru}_2(\text{CO})_9$ [now known (9) to be $\text{Ru}_3(\text{CO})_{12}$] at high temperature and pressure.

The use of ruthenium salts to produce isocyanates from amines and CO has been patented by Stern and Spector (10). This likely corresponds to the more well-documented palladium(II) chloride reaction which occurs stoichiometrically under mild conditions according to Reaction 3 (10, 11).



However, Tsuji and Iwamoto (12) reported that a PdCl_2 reaction at more severe conditions gives rise to ureas, formamides, and oxamides *via* a metal-catalyzed process.

Kinetic studies on catalytic amine carbonylation reactions are scarce, although Brackman (13) has reported kinetics on a copper(I)-copper(II) catalyzed production of ureas from cyclic secondary amines using carbon monoxide-oxygen mixtures at ambient conditions. Saegusa and coworkers (14) used cuprous salts and other group IB and IIB metal compounds to carbonylate piperidine to *N*-formylpiperidine under more severe conditions. We have published (15) a brief report involving some of the studies described in this paper.

Experimental

Materials. Ruthenium trichloride was obtained as the soluble trihydrate from Johnson Matthey Ltd. Treatment of aqueous acetic acid-acetate solutions of the trichloride with 1 atm CO at 80°C for about 10 hrs gives almost quantitative yields of the tricarbonyl dimer

$[\text{Ru}(\text{CO})_3(\text{OCOCH}_3)]_2$ (7) which decomposes rapidly in the absence of carbon monoxide into the polymeric acetate dicarbonyl $[\text{Ru}(\text{CO})_2(\text{OCOCH}_3)]_n$ (1). These bridged acetate carbonyl complexes are the same as those synthesized by Crooks and coworkers (6) by treating $\text{Ru}_3(\text{CO})_{12}$ with glacial acetic acid. Compound 1 dissolves in amines to yield the complexes $[\text{Ru}(\text{CO})_2(\text{OCOCH}_3)(\text{amine})]_2$ which are readily precipitated by addition of water; these compounds analyze satisfactorily and show three strong $\nu(\text{CO})$ IR bands in the 1920–2030 cm^{-1} region. The following data were obtained, for example, for the piperidine complex 2: C, 35.64; H, 4.60; N, 4.82. $\text{C}_9\text{H}_{14}\text{NO}_4\text{Ru}$ requires C, 35.90; H, 4.65; N, 4.65; $\nu(\text{CO})$ observed at 2025, 1970, and 1935 cm^{-1} . A dimeric pyridine complex was made previously in a similar way (6), and by comparison the cyclic secondary amine complexes that we have isolated are formulated also as dimers. Treatment of an aqueous solution of $\text{RuCl}_3 \cdot 3\text{H}_2\text{O}$ with 1 atm CO at 80°C for several days leads to precipitation of a purple–brown polymeric solid and a clear, colorless filtrate (7). Washing the solid with benzene removes small amounts of $\text{Ru}_3(\text{CO})_{12}$ and $\text{H}_4\text{Ru}_4(\text{CO})_{12}$ (16). The remaining solid after drying under vacuum contains no chloride and analyzes for a hydridocarbonyl $[\text{HRu}(\text{CO})_3]_n$, 3, obtained in about 80% yield. Found: C, 18.97; H, 0.50; Ru, 54.97; O (by difference) 25.74. $\text{C}_3\text{HO}_3\text{Ru}$ requires C, 19.36; H, 0.54; Ru, 54.31; O, 25.79. The IR (Nujol) shows a broad band centered at about 2000 cm^{-1} . The polymer is insoluble in organic solvents but dissolves to some extent in liquid amines (*see* Results) and phosphines. Spectroscopic studies on such solutions have not yet yielded evidence for the presence of a hydride. [High field ^1H NMR signals have now been detected in methyldiphenylphosphine solutions.]

Amines and the *N*-formyl derivatives were obtained at 98–99% purity from Aldrich Chemicals and were used without further purification. Carbon monoxide was a Matheson C.P. grade product.

Kinetics. Kinetic measurements were made by following CO uptake at constant pressure using the apparatus and procedure described earlier (17). The Ru catalyst concentration used was in the range $(0.6\text{--}6.0) \times 10^{-2}\text{M}$. Total pressures up to 1 atm and CO partial pressures from 55–590 mm were used. The CO solubility in pure piperidine was $6.5 \times 10^{-3}\text{M}$ atm^{-1} at 21°C and $5.8 \times 10^{-3}\text{M}$ atm^{-1} at 75°C, Henry's law being obeyed at least up to 1 atm; the solubility in toluene was similar ($5.7 \times 10^{-3}\text{M}$ atm^{-1} at both 21° and 75°C). The solubility in a toluene–piperidine mixture (1:1 by vol), $5.5 \times 10^{-3}\text{M}$ atm^{-1} at 75°C was only slightly less than those in the pure solvents. The vapor pressures of piperidine and toluene differ by only about 15–20 mm between 50°–75°C, that of piperidine being the greater (18). Vapor pressure measurements on the solvent mixtures showed that Raoult's Law was obeyed approximately, and the partial CO pressures over toluene–piperidine solutions could be readily estimated. For practical purposes, the partial pressure of piperidine–toluene mixtures, 2.0–10.1M (neat) in piperidine could be taken as that of pure piperidine.

Product Analysis. The *N*-formyl products were identified by GLC using a Hewlett Packard model 5780 Unit fitted with a flame ionization detector and a column of Pennwalt 223 on 80/100 GasChrom R (Applied Science Labs.).

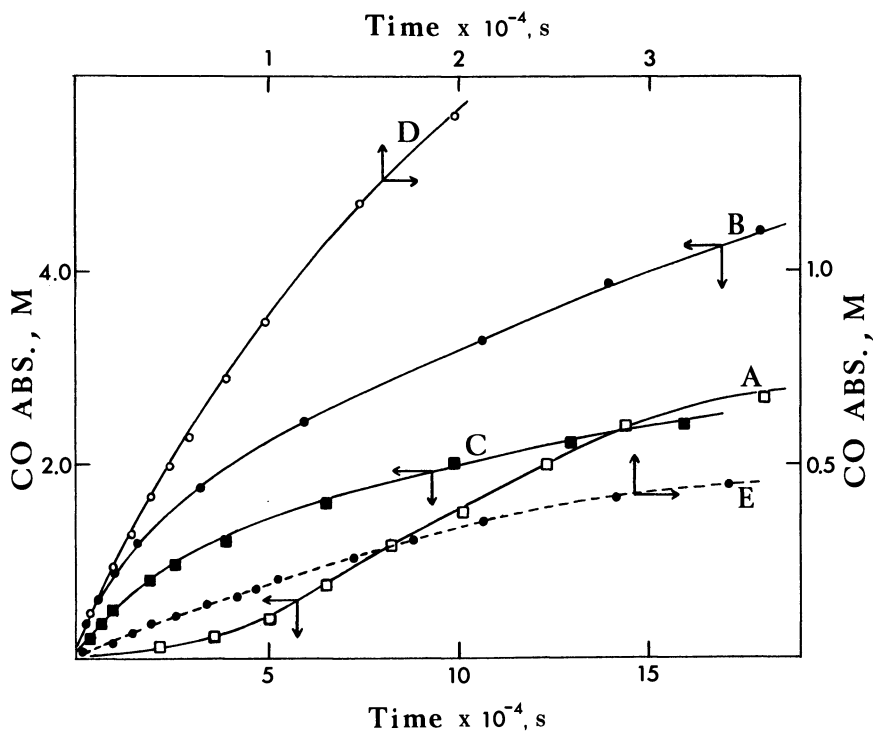


Figure 1. Gas uptake plots for the catalytic carbonylation of neat amines at 1 atm

A. $[\text{Ru}(\text{CO})_2(\text{OCOCH}_3)_n]$, piperidine, 75°C , 0.03M Ru, B. $[\text{HRu}(\text{CO})_3]_n$, piperidine, 75°C , 0.035M Ru, C. $[\text{HRu}(\text{CO})_3]_n$, piperidine, 71°C , 0.022M Ru, D. $[\text{HRu}(\text{CO})_3]_n$, pyrrolidine, 75°C , 0.022M Ru, E. $[\text{HRu}(\text{CO})_3]_n$, morpholine, 75°C , 0.022M Ru

Results

The $[\text{Ru}(\text{CO})_2(\text{OCOCH}_3)_n]$ (1) and $[\text{Ru}(\text{CO})_2(\text{OCOCH}_3)-(\text{amine})]_2$ (2) Catalysts. Compound 1 dissolves in amines to give yellow solutions. These were then subjected to 1 atm CO at about 75°C , and the reaction was monitored by following the CO absorption. Figure 1 (curve A) shows an uptake curve for the piperidine system at the conditions noted. The curve shows an initial autocatalytic region; a maximum rate is reached after about 20 hrs, then the rate slowly decreases after about 30 hrs. The sole product was *N*-formylpiperidine (30% after 70 hrs), and the total gas consumption corresponded to this conversion. The maximum rates (*see* Table I) showed a first-order dependence on CO up to 1 atm total pressure. The Ru dependence is not linear and, in fact, analyzes well for a half-order dependence (Figure 2). The morpholine and pyrrolidine systems behaved similarly but showed lower and higher reactivities, respectively (Table I). Pyridine and aniline solu-

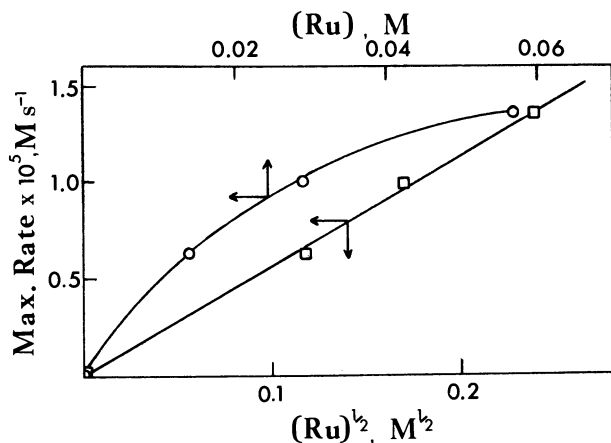


Figure 2. $[\text{Ru}(\text{CO})_2(\text{OCOCH}_3)]_n$ -catalyzed carbonylation of piperidine; ruthenium dependence at 1 atm, 75°C , neat amine

tions of **1** were essentially unreactive toward CO at 75°C and 1 atm; diethylamine solutions reacted slowly at 40°C , this being an upper practical limit because of the lower boiling point of the amine.

Adding small amounts of water to the systems catalyzed by **1** results in an initially faster rate; no autocatalysis is observed, but the catalytic activity falls off as the solutions darken, and conversions to *N*-formyl products are low (<5%) after 50 hrs. These systems are more complex chemically than the anhydrous systems.

The dimeric $[\text{Ru}(\text{CO})_2(\text{OCOCH}_3)(\text{pip})]_2$ complex (**2**) may be used at the appropriate ruthenium molarities to reproduce exactly the uptake plots observed with the polymeric catalyst. Solution IR measurements in regions of maximum activity for both **1**- and **2**-catalyzed systems showed the presence of the amine dimers which could be readily precipitated at any stage of the catalytic carbonylation by adding water.

Adding *N*-formyl product (and other amides such as *N,N*-dimethylacetamide) decreases the carbonylation rate, and thus accumulation of product slowly poisons the catalyst. The rate for the piperidine system (Table I) after 70 hrs decreased to $0.4 \times 10^{-5} \text{M sec}^{-1}$, and at this stage about 100 moles of amine were carbonylated per mole of ruthenium. Amine solutions of the dimers are quite stable at 75°C for long periods *in vacuo* or under argon, and there is no trace of *N*-formylamine.

Although the catalysts are formally Ru(I) d^7 systems, the dimers are diamagnetic in the solid state, and this must be accounted for by metal-metal interaction. Following Crooks and coworkers (6), we formulate the complexes as having Structure I. ESR analyses on samples of the reacting solutions in the region of maximum activity have given no signals at either liquid nitrogen or room temperature.

Table I. Carbonylation of Amines^a

<i>Amine</i>	<i>Catalyst^b</i>	<i>% Conversion to N-formylamine</i>	<i>Maximum rate × 10⁵Msec⁻¹</i>
<i>Primary Amine</i>			
aniline	1 or 3	—	^{c, d}
cyclohexylamine	3	1(10 hrs)	1.57 ^d
<i>n</i> -octylamine	3	—	0.52 ^{d, e}
<i>Secondary Amine</i>			
diethylamine	3	—	0.30 ^{d, f}
di- <i>n</i> -butylamine	3	—	0.24 ^d
dibenzylamine	3	—	0.04 ^d
hexamethyleneimine	3	33(45 hrs)	5.80
morpholine	1	6(20 hrs)	0.40
	3	14(48 hrs)	1.30
piperidine	1 or 2	15(30 hrs), 30(70 hrs)	1.0
	3	32(55 hrs)	10.4
	4	45(65 hrs)	7.2
	5	25(200 hrs)	0.55 ^g
pyrrolidine	1	35(35 hrs)	7.4
	3	34(48 hrs)	11.5
<i>Tertiary Amine</i>			
pyridine	1 or 3	—	^c

^a At 75°C, 1 atm total pressure, 5 ml amine. [Ru] = 3 × 10⁻²M for the bridged acetate complexes and Ru₃(CO)₁₂, [Ru] = 2.2 × 10⁻²M for [HRu(CO)₃]_n.

^b **1** [Ru(CO)₂(OAc)]_n; **2** [Ru(CO)₂(OAc)(pip)]₂; **3** [HRu(CO)₃]_n; **4** Ru₃(CO)₁₂; **5** [Ru₃O(OAc)₆(H₂O)₃][OAc].

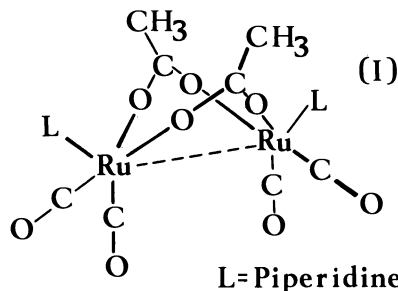
^c No carbonylation observed.

^d Catalyst **3** sparingly soluble.

^e Carbonylation ceased after 1000 sec.

^f At 50°C.

^g 10% H₂O added.



The [HRu(CO)₃]_n (3) Catalyst. The systems were investigated in a manner similar to that described for the acetate catalysts. Figure 1 (curves B-E) shows some representative CO uptake plots by yellow solutions of **3** dissolved in various amines at the conditions noted. No autocatalysis is observed; the initial rates, which are readily measured

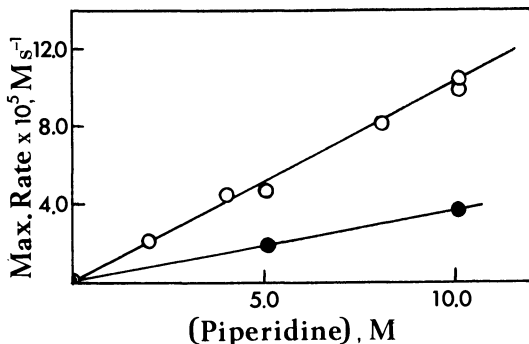


Figure 3. $[\text{HRu}(\text{CO})_3]_n$ -catalyzed carbonylation of piperidine; amine dependence at 75°C , 0.022M Ru in toluene-piperidine solutions. \circ , 490 mm CO; \bullet , 100 mm CO.

since they remain constant for at least 1 hr, subsequently decrease gradually over long times. The only products detected were the *N*-formylamines which again slowly poisoned the catalyst. The kinetics of the piperidine system were investigated using the initial rates. Compound 3 was also soluble in toluene-piperidine mixtures, and this enabled us to demonstrate that the reaction is first order in amine (Figure 3). The CO dependence was more complex than for the acetate-catalyzed system and was first order at lower concentration, but it approached zero order at partial pressures above 0.5 atm (Figure 4). The Ru dependence was first order at least up to $3 \times 10^{-2}\text{M}$ in conditions of both zero- and first-order CO dependence (Figure 5). The carbonylation rates were also studied from 50° – 80°C at 1 atm total pressure where the reaction is

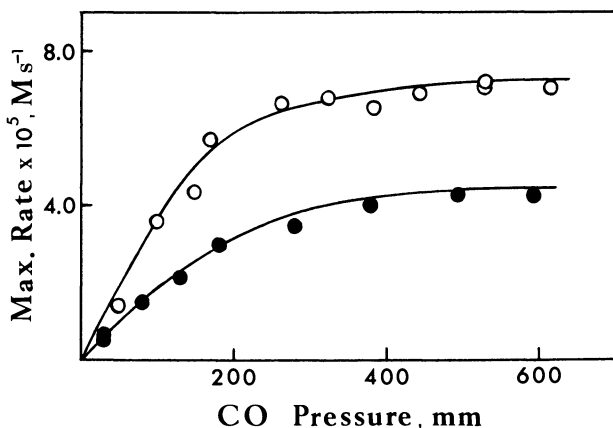


Figure 4. $[\text{HRu}(\text{CO})_3]_n$ -catalyzed carbonylation of piperidine, CO dependence for neat amine solutions. \circ , 71°C , 0.022M Ru; \bullet , 75°C , 0.012M Ru.

Table II. Temperature Dependence for $[\text{HRu}(\text{CO})_3]_n$ -Catalyzed Carbonylation of Piperidine^a

Temperature, °C	Max rate $\times 10^5 \text{ M sec}^{-1}$	$k' \times 10^3 \text{ M}^{-1}\text{sec}^{-1}$
50	1.17	0.05
60	3.52	0.16
65	4.16	0.19
71	7.02	0.32
75	10.4	0.48
80	12.1	0.55

^a $[\text{Ru}] = 2.2 \times 10^{-2} \text{ M}$, 1 atm total pressure, neat piperidine (10.1M).

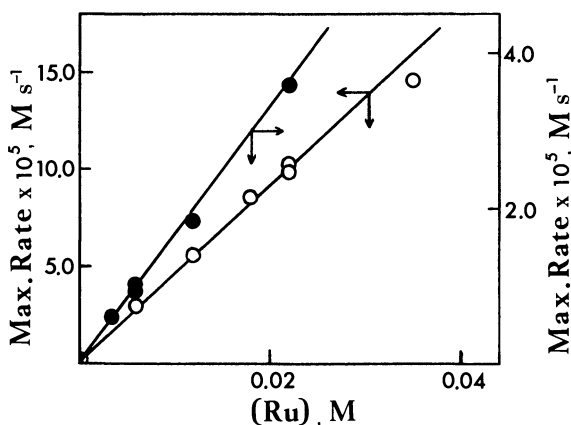
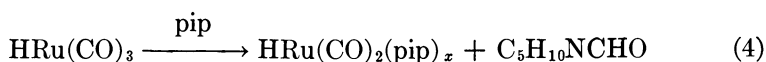


Figure 5. $[\text{HRu}(\text{CO})_3]_n$ -catalyzed carbonylation of piperidine, Ru dependence at 75°C in neat amine. O, 490 mm CO; ●, 100 mm CO.

independent of CO pressure (Table II). The initial carbonylation rates and some per cent conversions of a number of amines are summarized in Table I for the conditions noted.

We have not been able to isolate any pure carbonylamine complexes from amine solutions of $[\text{HRu}(\text{CO})_3]_n$ although a crude yellow product isolated from piperidine solutions gives an IR spectrum in the CO region (three bands at 2025, 1975, and 1940 cm^{-1}) remarkably similar to that of $[\text{Ru}(\text{CO})_2(\text{OCOCH}_3)(\text{pip})]_2$. Interestingly, no net gas evolution is observed on dissolution of the hydridocarbonyl in piperidine under argon at 80°C; but analysis of this system after 12 hrs shows the production of *N*-formylpiperidine. Two experiments have shown that about 0.7 mole of the carbonylated product is formed per mole of Ru. This suggests that one mole of CO is consumed in a stoichiometric reaction and that the piperidine product is a dicarbonyl. For example,



The IR of the isolated crude complex also indicates some free formyl-piperidine, and chemical analyses are consistent with 80% $\text{HRu}(\text{CO})_2\text{-(pip)} + 20\% \text{C}_5\text{H}_{10}\text{NCHO}$.

Attempts to locate a hydride ligand in the range $\tau 10\text{--}30$ by NMR measurements of amine solutions of **3** have been unsuccessful although a limitation is the relatively low solubility ($<0.1\text{M}$) of the complex; exchange with the amine hydrogens could also be occurring. As in the acetate systems, ESR studies have failed to detect any paramagnetic species.

Other Ruthenium Catalysts. $\text{Ru}_3(\text{CO})_{12}$ readily dissolved in piperidine to give a solution effective for catalytic carbonylation of the amine. The uptake plots resemble those shown in Figure 1 (curves B–E), and the maximum rate given in Table I refers to the initial rate. Attempts to characterize the ruthenium complexes formed from reaction of the dodecacarbonyl with amines have been unsuccessful.

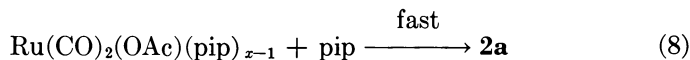
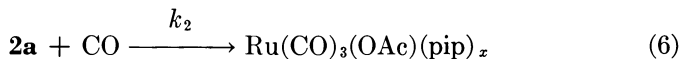
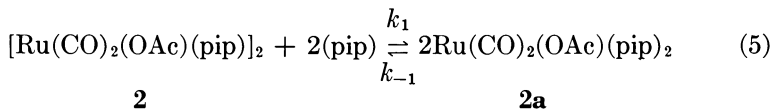
The oxotriruthenium cluster complex $[\text{Ru}_3\text{O}(\text{OCOCH}_3)_6(\text{H}_2\text{O})_3][\text{OCOCH}_3]$ which we had used as ruthenium(II) acetate (**19**), can be used as a catalyst, but small amounts of water are necessary for solubility, and long reaction times are required for reasonable conversions at mild conditions (Table I).

Discussion

The results show that a number of ruthenium carbonyl complexes are effective for the catalytic carbonylation of secondary cyclic amines at mild conditions. Exclusive formation of *N*-formylamines occurs, and no isocyanates or coupling products such as ureas or oxamides have been detected. Noncyclic secondary and primary amines and pyridine (a tertiary amine) are not effectively carbonylated. There appears to be a general increase in the reactivity of the amines with increasing basicity (**20**): pyrrolidine (pK_a at $25^\circ\text{C} = 11.27 >$ piperidine (11.12) $>$ hexamethyleneimine (11.07) $>$ morpholine (8.39). Brackman (**13**) has stressed the importance of high basicity and the stereochemistry of the amines showing high reactivity in copper-catalyzed systems. The latter factor manifests itself in the reluctance of the amines to occupy more than two coordination sites on the cupric ion. In some of the hydridocarbonyl systems, low activity must also result in part from the low catalyst solubility (Table I).

The bridged-acetate catalyst system is reasonably well characterized in that the $[\text{Ru}(\text{CO})_2(\text{OCOCH}_3)(\text{amine})]_2$ complexes are present and can be recovered at any stage throughout the reaction. Further, it is clear from the blank reaction that the dimers are precursors to the true catalyst which must be formed *via* interaction with further carbon monoxide. The

observations and limited kinetic data may be interpreted in terms of the mechanisms outlined in Reactions 5–8, OAc = OCOCH₃:

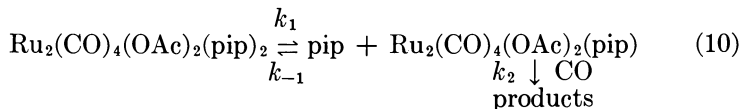


The autocatalytic region could be associated with the buildup of a steady-state concentration of an active monomer **2a** from the dimer **2**. The spectroscopic evidence indicates that the concentration of **2a** remains low, that is, $k_{-1} > k_1$. Writing $K_1 = k_1/k_{-1}$ yields the rate law shown in Equation 9 for the region of maximum activity where Ru_T refers to the total ruthenium calculated as monomer. The observed kinetics are con-

$$\frac{-d[\text{CO}]}{dt} = k_2(K_1/2)^{1/2}[\text{Ru}_T]^{1/2}[\text{pip}][\text{CO}] \quad (9)$$

sistent with such a rate law although the piperidine dependence has not been established. The data of Figure 2 using this rate law give a $k_2K_1^{1/2}$ value of $2.7 \times 10^{-3} M^{-3/2} \text{sec}^{-1}$ at 75°C.

Crooks and coworkers (6) have done molecular weight measurements in solution and noted that ligand dissociation (L) is sometimes observed with complexes of the type $\text{Ru}_2(\text{CO})_4(\text{RCO}_2)_2\text{L}_2$ although details were not reported. A mechanism based on such predissociation of L in neat L (Equation 10) implies a dimer as the active catalyst and will always lead to a first-order dependence on added ruthenium, and thus such a mechanism does not appear to operate.



$[\text{HRu}(\text{CO})_3]_n$ is an interesting complex and has potential for a number of catalytic carbonylation reactions. However, the evidence for the presence of hydrogen is based mainly on chemical analysis which consistently shows the small hydrogen content. The stoichiometric carbonylation according to Reaction 4 and the IR of the crude carbonyl are

consistent with the presence of a tricarbonyl in the starting polymer and, based on analogy with the acetate-bridged-tricarbonyl $[\text{Ru}(\text{CO})_3(\text{OCOCH}_3)_2]_2$, -dicarbonyl-polymer $[\text{Ru}(\text{CO})_2(\text{OCOCH}_3)]_n$, and -dicarbonyl-amine $[\text{Ru}(\text{CO})_2(\text{OCOCH}_3)(\text{pip})]_2$, we consider that the hydrides probably replace the acetate groups and are present as bridging ligands although we have been unable to detect these by IR. The hydridocarbonyl cluster complex $[\text{HRu}(\text{CO})_3]_4$ exists as a tetrahedral arrangement of ruthenium atoms with edge-bridging hydrogen atoms, and weak IR bands assigned to $\nu(\text{Ru-H-Ru})$ have sometimes been observed for this compound (16, 21, 22, 23). The complex we have isolated is quite different from this and related $\text{H}_2\text{Ru}_4(\text{CO})_{13}$ complexes (22, 23). Possible isomers for the $\text{H}_4\text{Ru}_4(\text{CO})_{12}$ and $\text{H}_2\text{Ru}_4(\text{CO})_{13}$ clusters have been discussed (21, 22, 23).

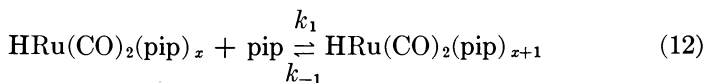
Reaction 4 shows that the ruthenium center with three coordinated carbonyls can transfer one such ligand to the piperidine (presumably coordinated). The mechanism suggested for the acetate complex includes exactly analogous steps (Reactions 6 and 7). The kinetics for the hydride-catalyzed system, however, are quite different and show a first-order dependence in Ru and a more complex dependence on CO (Figure 4). Further, no autocatalysis is evident.

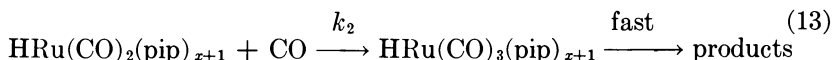
The rate law for the hydride-catalyzed system can be written as $-d[\text{CO}]/dt = k'[\text{Ru}_T][\text{pip}]$, where k' is a pseudo-second-order rate constant which includes the CO dependence. A mechanism which incorporates slow steps corresponding to Reactions 5 and 6 will lead to a rate law of the kind shown in Equation 11 which satisfies all the

$$\frac{-d[\text{CO}]}{dt} = \frac{k_1 k_2 [\text{dimer}][\text{pip}][\text{CO}]}{k_{-1}[\text{monomer}] + k_2[\text{CO}]} \quad (11)$$

dependencies at high $[\text{CO}]$ (when Reaction 5 becomes rate determining). However, at low $[\text{CO}]$ (when Reaction 6 becomes rate determining) a less than first order on Ru is predicted; this is not observed (Figure 5); alternatively at low $[\text{CO}]$ a first order in Ru can result if Reaction 5 lies well to the right, but then the kinetics should become independent of piperidine, which was not observed (Figure 3).

The mechanism suggested for the acetate systems (Reactions 5–8) may be readily modified to account for the observed kinetics if the complex corresponding to 2 at the conditions of the kinetic study is monomeric in solution, and it seems reasonable that hydride bridges would be cleaved in the piperidine solvent. For example,





This gives a rate law $k'[\text{Ru}_T][\text{pip}]$ where

$$k' = k_1 k_2 [\text{CO}] / (k_{-1} + k_2 [\text{CO}]) \quad (14)$$

Rearranging gives

$$\frac{1}{k'} = \frac{k_{-1}}{k_1 k_2 [\text{CO}]} + \frac{1}{k_1} \quad (15)$$

Figure 6 shows a plot of $(k')^{-1}$ vs. $[\text{CO}]^{-1}$ for the two sets of data in Figure 4. Good linear plots result, and the intercept and slope for the data at 75°C give $k_1 = 5.3 \times 10^{-4} \text{M}^{-1} \text{sec}^{-1}$ and $k_2/k_{-1} = 500$.

An alternative mechanism which accounts equally well for the kinetics involves a pre-equilibrium reaction with CO:

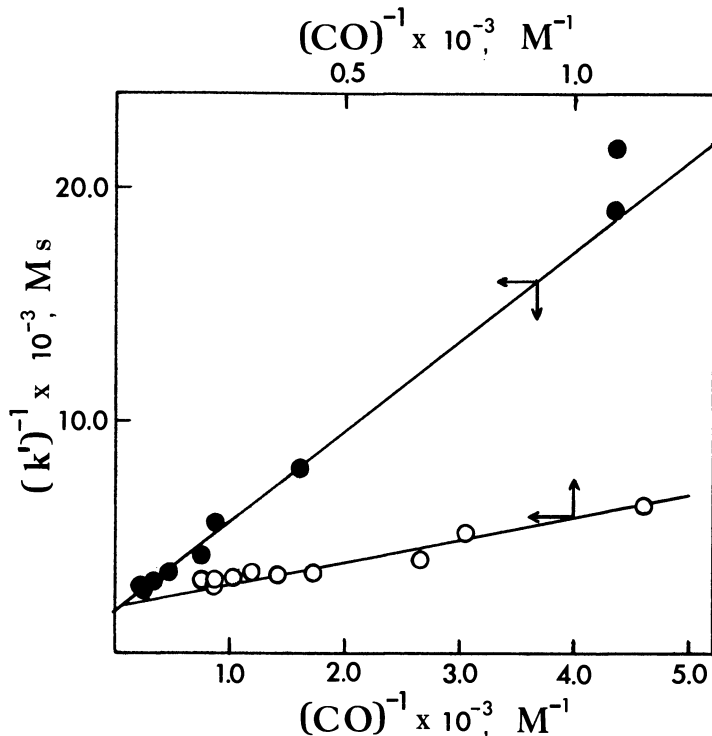
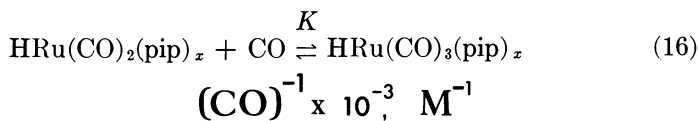
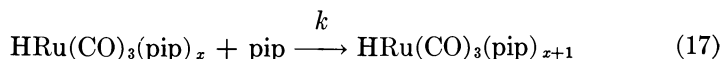


Figure 6. $[\text{HRu}(\text{CO})_3]_n$ -catalyzed carbonylation of piperidine. Analysis of the data of Figure 4 according to Equations 15 or 20.



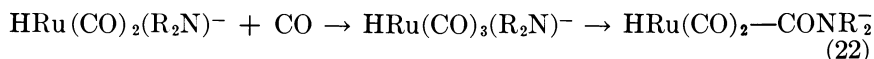
This mechanism gives the rate law

$$-d[\text{CO}]/dt = kK[\text{Ru}_T][\text{pip}][\text{CO}]/(1 + K[\text{CO}]) \quad (19)$$

$$\text{i.e., } k' = kK[\text{CO}]/(1 + K[\text{CO}]) \quad (20)$$

The same analysis as discussed above (Figure 6) gives the value of $5.3 \times 10^{-4} M^{-1} \text{sec}^{-1}$ to k and 500 to K at 75°C . We have no evidence for the existence of Equilibrium 16 although the K value implies that the reaction should be observable.

Thus we tend to favor the mechanism outlined in Reactions 12 and 13 (followed by Reactions 7 and 8). The mechanisms as presented do not indicate how the *N*-formyl product is formed although formation of a Ru-CO-N moiety at some stage seems essential; metal-assisted hydride shifts are a possibility. An alternative role of the attacking piperidine in Reaction 12 or 17 could be that of a proton acceptor as discussed by others (1, 13). For example, a plausible scheme would be the following: (writing R_2 for C_5H_{10})



Reaction 21 for a tricarbonyl species could correspondingly be written instead of Reaction 17. The formation of carbamoyl complexes ($M\text{—CONR}_2$) by the reaction of amines with metal carbonyls, especially cationic ones, has been reviewed by Angelici (24). Further studies are in progress.

The temperature studies (Table II) were carried out under conditions approaching a zero-order dependence on CO—*i.e.*, when $k' \approx k_1$ (or k) (Equations 14, 20). The k' data give a very good Arrhenius plot and yield the activation parameters $\Delta H^\ddagger = 17.5 \pm 0.7$ kcal/mole, $\Delta S^\ddagger = -11 \pm 2$ eu. In terms of Reactions 12 or 17 the negative entropy of activation seems reasonable for a ligand association reaction; the activation energy appears somewhat high but could be related to steric prob-

lems associated with the addition of the bulky piperidine ligand. The ΔH^\ddagger value seems compatible with a rate-determining reaction such as Reaction 21 although such ionization reactions commonly have much larger negative entropies of activation (25).

The stoichiometric carbonylation observed using $[\text{HRu}(\text{CO})_3]_n$ and the proposed catalytic schemes all involve tricarbonyl species as the active catalyst; the relatively high activity of $\text{Ru}_3(\text{CO})_{12}$ is consistent with this. The relative activity of the complexes for piperidine carbonylation is $[\text{HRu}(\text{CO})_3]_n \approx \text{Ru}_3(\text{CO})_{12} > [\text{Ru}(\text{CO})_2(\text{OCOME})]_n$. The major cause of the decrease in carbonylation rates is the accumulation of formyl product although the decrease in amine concentration is also a contributing factor. This catalyst poisoning is likely attributable to complexation to the ruthenium, presumably *via* the carbonyl grouping as commonly found for formamide ligands (26). The product could compete with either amine or CO for a metal coordination site.

Acknowledgment

We thank Johnson Matthey Ltd. for loan of the ruthenium.

Literature Cited

1. Rosenthal, A., Wender, I., "Organic Synthesis *via* Metal Carbonyls," I. Wender and P. Pino, Eds., Vol. 1, p. 405, Interscience, New York, 1968.
2. Durand, D., Lassau, C., *Tetrahedron Lett.* (1969) 2329.
3. Hieber, W., Heusinger, H., *J. Inorg. Nucl. Chem.* (1957) **4**, 179.
4. Allen, A. D., Eliades, T., Harris, R. O., Reinsalu, P., *Can. J. Chem.* (1969) **47**, 1605.
5. James, B. R., *Inorg. Chim. Acta Rev.* (1970) **4**, 73.
6. Crooks, G. R., Johnson, B. F. G., Lewis, J., Williams, I. G., Gamlen, G., *J. Chem. Soc. A* (1969) 2761.
7. James, B. R., Rempel, G. L., *Chem. Ind. (London)* (1971) 1036.
8. Kealy, T. J., Benson, R. E., *J. Org. Chem.* (1961) **26**, 3126.
9. Corey, E. R., Dahl, L. F., *J. Amer. Chem. Soc.* (1961) **83**, 2203.
10. Stern, E. W., Spector, M. L., U.S. Patent **3,405,156** (1968).
11. Stern, E. W., Spector, M. L., *J. Org. Chem.* (1966) **31**, 596.
12. Tsuji, J., Iwamoto, N., *Chem. Commun.* (1966) 380.
13. Brackman, W., *Discuss. Faraday Soc.* (1968) **46**, 122.
14. Saegusa, T., Kobayashi, S., Hirota, K., Ito, Y., *Bull. Chem. Soc. Jap.* (1969) **42**, 2610.
15. Byerley, J. J., Rempel, G. L., Takebe, N., James, B. R., *Chem. Commun.* (1971) 1482.
16. Kaesz, H. D., Knox, S. A. R., Koepke, J. W., Saillant, R. B., *Chem. Commun.* (1971) 477.
17. James, B. R., Rempel, G. L., *Can. J. Chem.* (1966) **44**, 233.
18. "Handbook of Chemistry and Physics," 50th ed., pp. D153-155, Chemical Rubber Co., Cleveland, Ohio, 1970.
19. Cotton, F. A., Norman, J. G., Spencer, A., Wilkinson, G., *Chem. Commun.* (1971) 967.

20. Perrin, D. D., "Dissociation Constants of Organic Bases in Aqueous Solution," Butterworths, London, 1965.
21. Knox, S. A. R., Kaesz, H. D., *J. Amer. Chem. Soc.* (1971) **93**, 4594.
22. Johnson, B. F. G., Johnson, R. D., Lewis, J., Robinson, B. H., Wilkinson, G., *J. Chem. Soc. A* (1968) 2856.
23. Johnson, B. F. G., Lewis, J., Williams, I. G., *J. Chem. Soc. A* (1970) 901.
24. Angelici, R. J., *Accounts Chem. Res.* (1972) **5**, 335.
25. Frost, A. A., Pearson, R. G., "Kinetics and Mechanism," p. 137, Wiley, New York, 1963.
26. Bull, W. E., Madan, S. K., Willis, J. E., *Inorg. Chem.* (1963) **2**, 303.

RECEIVED August 20, 1973. Work was supported by the National Research Council of Canada, the University of Waterloo, and the University of British Columbia.

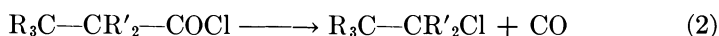
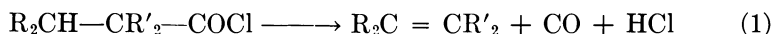
Rhodium Catalyzed Decarbonylations

J. K. STILLE, M. T. REGAN, R. W. FRIES, F. HUANG, and T. McCARLEY

University of Iowa, Iowa City, Iowa 52242

The kinetics of the chlorotris(triphenylphosphine)rhodium promoted decarbonylation of para-substituted benzoyl chlorides and phenylacetyl chlorides have been carried out by following the rearrangement reactions of the pure acyl-rhodium complexes and the decomposition reactions of the pure aryl- or benzylrhodium complexes. The small Hammett ρ -values along with very low entropies of activation for both the rearrangement and the decomposition steps indicate that there is little change in polarity or development of charge in the transition state and that there is little added restriction or disorder in proceeding from the acyl or aryl/benzyl complexes to their respective transition states. Although decarbonylation of optically active 2-phenyl-3,3,3-trifluoropropionyl chloride gives racemic product chloride, the decarbonylations of erythro- and threo-2,3-diphenylbutanoyl chlorides give exclusively trans- and cis-methylstilbene, respectively. The olefin forming reaction prefers Saytzeff elimination.

The decarbonylation reaction utilizing chlorotris(triphenylphosphine)-rhodium(I) is a potentially useful method for converting acid chlorides to olefins or alkyl chlorides. Acid chlorides which contain a β hydrogen produce olefins (Reaction 1) while an alkyl chloride is the product when no β hydrogen is present (1, 2, 3, 4, 5, 6) (Reaction 2).

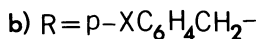
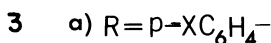
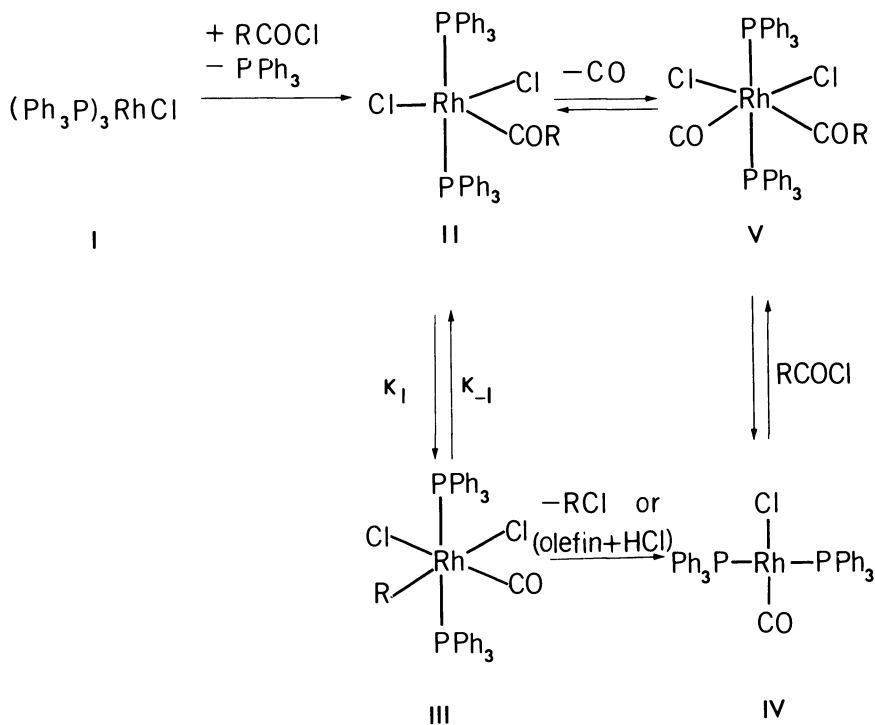


The mechanism that has been proposed for the decarbonylation of acid chlorides by chlorotris(triphenylphosphine)rhodium(I) involves acyl- and alkyl- or arylrhodium complexes (2). Three of the intermediates in the catalytic cycle, II, III, and IV (*see* Reaction 3), can be isolated in this unique reaction. Both acyl complexes (II) and alkyl

complexes (III) (7) decompose to yield the expected decarbonylation products (1, 2).

Kinetics

Complexes of the type IIa,b and IIIa,b (Reaction 3) were synthesized, and the substituent effects and activation parameters were measured for both the acyl-alkyl rearrangement (II \rightarrow III) and the loss of organic halide (III \rightarrow IV). (IIa and b, X = NO₂, Cl, H, OCH₃; IIIa, X = Cl, H, CH₃, OCH₃; IIIb, X = NO₂, Cl.) The acyl complexes (II) are monomeric as shown by molecular weight studies. The alkyl complexes (III) have the structure shown in which the chlorides are neither trans to the phosphine ligands nor trans to each other as shown by their far IR spectra (7, 8). The chlorines in the complexes become scrambled during the rearrangement as demonstrated by the fact that the decompo-



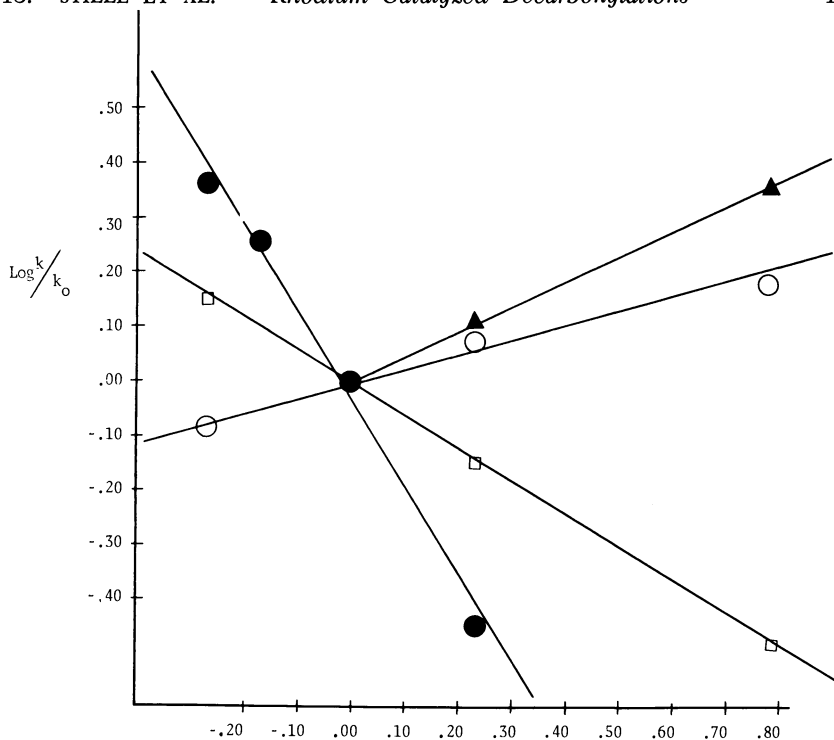


Figure 1. Hammett plots

○ Rearrangement of benzoyl complexes, IIa ($R = p - XC_6H_4$) to phenyl complexes, IIIa ($R = p - XC_6H_4$). ● Loss of *para*-substituted chlorobenzenes from phenyl complexes, IIIa ($R = p - XC_6H_4$). □ Rearrangement of phenylacetyl complexes, IIb ($R = p - XC_6H_4CH_2$) to benzyl complexes, IIIb ($R = p - XC_6H_4CH_2$). ▲ Loss of *para*-substituted benzyl chlorides from benzyl complexes, IIIb ($R = p - XC_6H_4CH_2$).

sition of complexes IIa ($X = H$) and IIb ($X = CH_3$) formed from chlorotris(triphenylphosphine)rhodium (I) containing ^{36}Cl gave chloro-carbonylbis(triphenylphosphine)rhodium (IV) containing about one third of the original amount of ^{36}Cl . The benzyl complexes IIIb were the most unstable in the series, and only the *p*-nitro- and *p*-chloro-substituted complexes could be isolated.

The rearrangement of complexes IIa to IIIa is first order in the disappearance of the acyl complex (IIa), is irreversible, and shows that electron withdrawing groups enhance the rate of rearrangement (Figure 1, Table I). By contrast, the rearrangement of the phenylacetyl complexes (IIb) to the benzyl complexes (IIIb) is reversible, and the forward reaction shows a negative ρ . The magnitude of the ρ -values, 0.265 and -0.612 for the rearrangements of complexes IIa and b to IIIa and b, respectively, are low enough to fall in the range observed for reactions involving radical intermediates; the sign of ρ indicates the type of charge imbalance, however small, in the transition state.

Table I. Summary of Kinetics

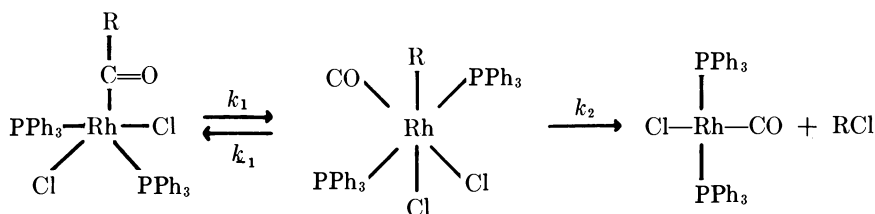
First Order Rate Constant ($10^4 k \text{ sec}^{-1}$) at 25°C

<i>R</i>	k_1	k_{-1}	k_2
<i>p</i> -ClC ₆ H ₄	5.27	0.0	0.59
<i>p</i> -ClC ₆ H ₄ CH ₂	0.50	6.84	9.59

<i>R</i>	$\rho(k_1)$	$\rho(k_2)$
<i>p</i> -XC ₆ H ₄	0.265	-1.64
<i>p</i> -XC ₆ H ₄ CH ₂	-0.612	0.452

<i>R</i>	(k_1)		(k_2)	
	ΔH^\ddagger	ΔS^\ddagger	ΔH^\ddagger	ΔS^\ddagger
<i>p</i> -ClC ₆ H ₄	22.8	2.1	25.9	9.0
<i>p</i> -ClC ₆ H ₄ CH ₂	21.3	-6.8	20.5	-3.6

The decomposition of the phenyl complexes IIIa to chlorobenzenes and IV is first order and irreversible. Triphenylphosphine retards the rate of this decomposition, indicating that the decomposition pathway involves prior dissociation of triphenylphosphine from IIIa. The benzyl complexes IIIb decompose both by rearrangement to IIb and to the benzyl chlorides plus IV. The conversion of IIIb to IV is irreversible, but it is not retarded by added triphenylphosphine. The ρ values for the decomposition of the phenyl complexes IIIa and the benzyl complexes IIIb are also opposite in sign but low enough to fall in the range observed for radical reactions.

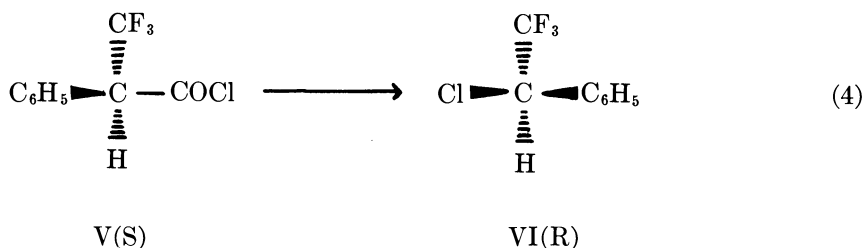


The entropies of activation are small, and for $R = p\text{-ClC}_6\text{H}_4\text{CH}_2$, negative entropies of activation are observed in both steps whereas positive entropies are observed in the same steps for $R = p\text{-ClC}_6\text{H}_4$. The small entropies and the radical character of ρ for the rearrangement of II to III suggests a tight radical pair complex with little change in restriction in going to the transition state. The relatively larger entropy of activation (9.0 eu) for the conversion of the *p*-chlorophenyl complex

(IIIa) to IV is expected for a reaction proceeding by a dissociative mechanism.

Stereochemistry

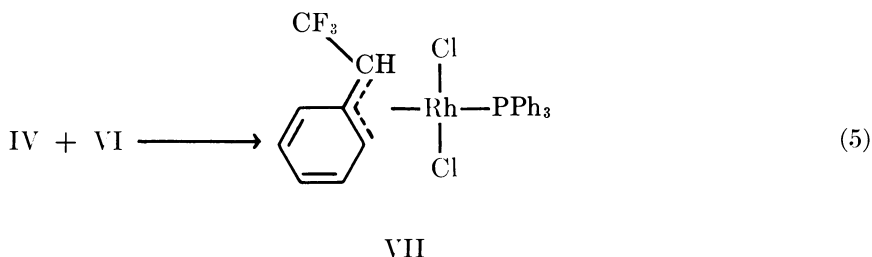
The decarbonylation of chiral aldehydes to alkanes by chlorotris-(triphenylphosphine)rhodium(I) proceeds (9) with retention of configuration. An intramolecular reaction was observed, and a tight radical pair mechanism was proposed to account for the stereospecificity. Since our kinetic results also suggested a tight radical pair mechanism for the conversion of phenylacetyl halides to benzyl halides *via* IIb and IIIb, the decarbonylation of an optically active acyl halide was undertaken. Decarbonylation of (*R*)- α -trifluoromethylphenylacetyl chloride (V), prepared from the optically active acid by its reaction with thionyl chloride (10), was carried out by prior isolation of the corresponding optically active acyl complex of the type IIb. Decomposition of the complex in refluxing benzene or toluene gave 1-phenyl-2,2,2-trifluoroethyl chloride (VI) which was racemic (Reaction 4). When V (*R*) was allowed to react with I *in situ* in refluxing benzene, toluene, or acetonitrile, chloride VI, obtained in a 71% yield, was also racemic. Optically active



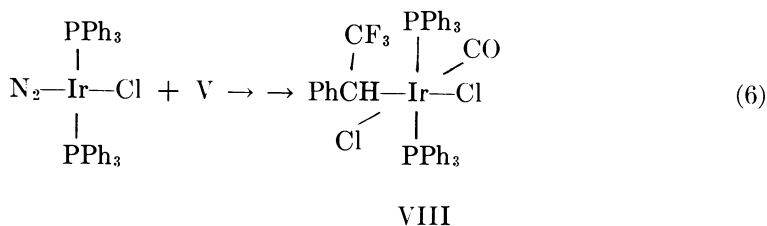
VI, obtained from stereospecific reactions of the corresponding optically active alcohol (11) with thionyl chloride, phosphorus pentachloride, etc., was not racemized under any of the reaction conditions. Monitoring the carbonyl absorption frequencies in the IR during these decarbonylations showed that the transformations II \rightarrow III \rightarrow IV took place during the conversion of V to racemic VI. Thus rearrangement or decomposition or both could be responsible for the racemization.

Although optically active chloride is not racemized under the reaction conditions, and it will not add to IV (reverse reaction) to afford a complex of the type IIIb, under forcing conditions (high temperature and/or long reaction times) the π -benzyl complex (VII in Reaction 5) is obtained which results in a loss of chirality.

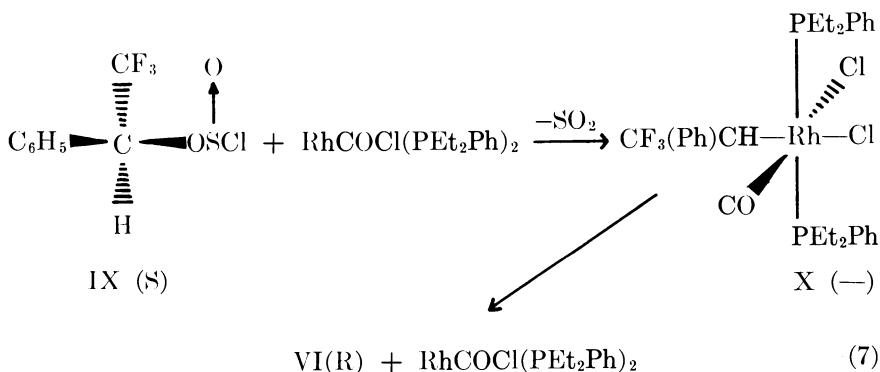
Since it has been observed that the rearrangement of complexes of the type IIb to IIIb is reversible, this step may be responsible for the racemization by a process of attrition on each reversal. The isostructural



d^6 iridium complex can be obtained from the addition of acid chloride to d^8 chlorodinitrogenbis(triphenylphosphine)iridium. When the acid chloride has no β hydrogens, the reaction stops at the alkyl complex (12). Treatment of the optically active acid chloride V with chlorodinitrogenbis(triphenylphosphine)iridium gave the chiral-isostructural iridium complex VIII, although low optical activity ($[\alpha]_{25}^{D} = -5.8^\circ$) was observed (Reaction 6). This is possibly an indication that racemization can take place during the rearrangement step.



Direct addition of VI to chlorocarbonylbis(phosphine)rhodium complexes containing more basic phosphine ligands to yield optically active complexes of the type III did not occur. An optically active benzylrhodium complex (X) was obtained, however, by adding (*S*)- α -trifluoromethylbenzylchlorosulfite (IX) to chlorocarbonylbis(diethylphenylphosphine)rhodium.



phine)rhodium(I). The benzyl complex (X), which had a negative sign of rotation, could be thermally decomposed to afford the optically active chloride VI(R). Thus, the reaction proceeding in two steps (*see* Reaction 7) takes place with one inversion and one retention of configuration at carbon with a net 62% inversion. The assignment of stereochemistry to the individual steps is open to question. The racemization in the decarbonylation of optically active α -trifluoromethylphenylacetyl chloride probably occurs in the acyl to alkyl rearrangement step.

In an attempt to resolve this question of stereochemistry and also to determine whether or not the decarbonylation of an acid chloride containing a β hydrogen takes place stereospecifically, *erythro*-(XI) and *threo*-2,3-diphenylbutanoyl chlorides (XII), obtained by the reaction of the known acids (13, 14) with oxalyl chloride, were synthesized. The reaction of these acid chlorides (*see* Reaction 8) with chlorotris(triphenylphosphine)rhodium gave the corresponding acyl complexes of type IIB [R = C₆H₅CH(CH₃)CH(C₆H₅)]. Decarbonylation of the *erythro*-acyl complex in benzene at 30°C gave a 90% yield of *trans*- α -methylstilbene while decarbonylation of the *threo*-acyl complex under similar reaction

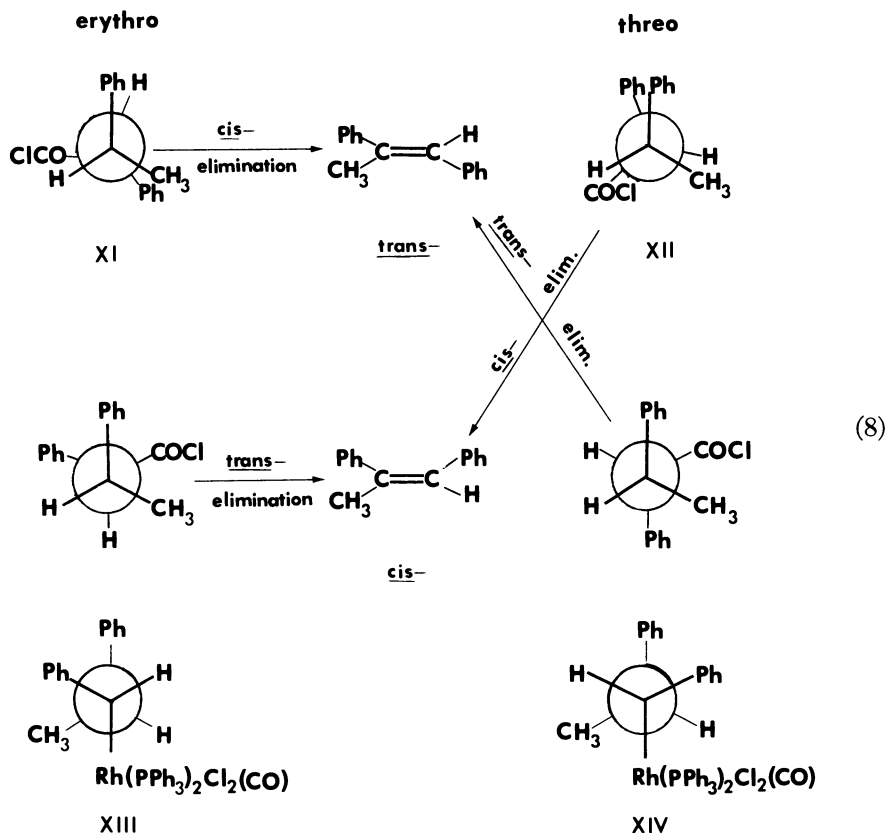


Table II. Decarbonylation of Acid Chlorides with

<i>Acid Chloride</i>	<i>Primary H-abst.</i>	<i>Secondary H-abst.</i>
$\text{CH}_3(\text{CH}_2)_4\text{COCl} \longrightarrow$	—	$\text{CH}(\text{CH}_2)_2\text{CH}=\text{CH}_2$ 96%
$\begin{array}{c} \text{CH}_3 \\ \\ \text{CH}_3(\text{CH}_2)_2\text{CH}-\text{COCl} \end{array} \longrightarrow \text{CH}_3(\text{CH}_2)_2\text{CH}=\text{CH}_2$	30% (1)	$\text{CH}_3\text{CH}_2\text{CH}=\text{CHCH}_3$ cis- and trans- 70% (3.5)
$\begin{array}{c} \text{CH}_3 \\ \\ \text{CH}_3(\text{CH}_2)_2-\text{C}-\text{COCl} \\ \\ \text{CH}_3 \end{array} \longrightarrow \begin{array}{c} \text{CH}_3 \\ \\ \text{CH}_3(\text{CH}_2)_2-\text{C}=\text{CH}_2 \end{array}$	49% (1)	$\begin{array}{c} \text{CH}_3 \\ \\ \text{CH}_3\text{CH}_2\text{CH}=\text{C}-\text{CH}_3 \end{array}$ 47% (3)
$\begin{array}{c} \text{CH}_3 \\ \\ \text{CH}_3-\text{CH}-\text{CH}-\text{CH}_2-\text{CH}_3 \\ \\ \text{COCl} \end{array} \longrightarrow$	—	$\begin{array}{c} \text{CH}_3 \\ \\ \text{CH}_3\text{CHCH}=\text{CHCH}_3 \end{array}$ cis- and trans- 46% (1)
$\begin{array}{c} \text{CH}_3 \quad \text{CH}_3 \\ \quad \\ \text{CH}_3-\text{CH}-\text{CH}-\text{COCl} \end{array} \longrightarrow \begin{array}{c} \text{CH}_3 \\ \\ \text{CH}_3-\text{CH}-\text{CH}=\text{CH}_2 \end{array}$	12.4% (1)	—

^a The statistically corrected ratios appear in parentheses.

conditions resulted in a 90% yield of α -methylstilbenes, 90% of which was the cis isomer and 10% of which was the trans isomer. The elimination, therefore, takes place stereospecifically with overall cis elimination occurring. Thus, in the decarbonylation of both erythro and threo acid chlorides, either the acyl-alkyl rearrangement and the β -hydride elimination occur stereospecifically or a concerted stereospecific cis elimination occurs. If the two-step process is followed, these results are consistent either with retention of configuration during the acyl-to-alkyl rearrangement (II \rightarrow III) to afford an alkyl complex (XIII from the erythro isomer) followed by a cis- β -hydrogen elimination or by inversion of configuration during this rearrangement to give alkyl complex (XIV from the erythro isomer) followed by a trans elimination. The same arguments apply to the threo isomer in which either retention cis elimination or inversion trans elimination explain the results. For the two-step mechanism, the retention cis elimination pathway would be favored on the basis of the retention observed in the decarbonylation of aldehydes with rhodium (9) as well as the evidence for cis metal hydride elimination (15, 16, 17) and

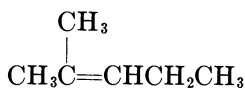
trans-(Ph₃P)₂Rh(CO)Cl in Benzonitrile^a

Tertiary H-abst.

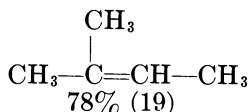
—

—

—

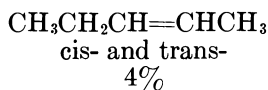


44% (2)

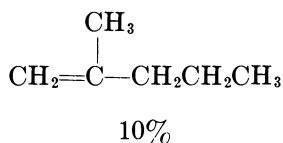
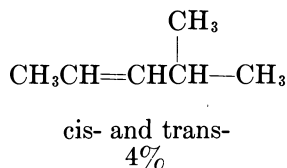


78% (19)

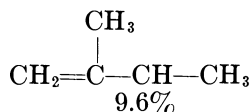
Other



—



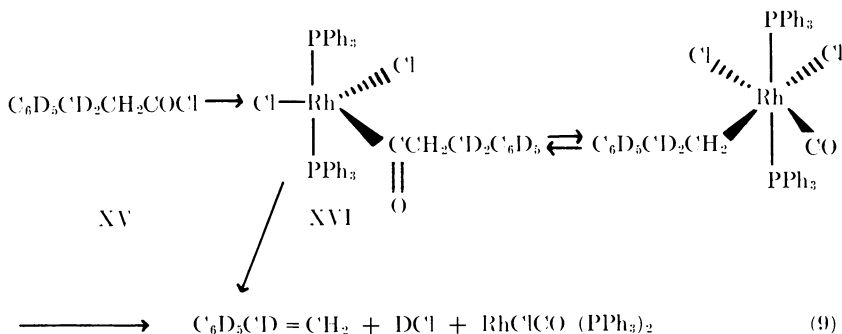
10%



9.6%

retention in acyl-alkyl rearrangements (or the reverse reaction, carbonyl insertion) (18, 19, 20) in other systems.

Acyl complex XVI was prepared from 3-perdeuteriophenyl-3,3-dideuteriopropionyl chloride (XV), and its rate of decarbonylation (Reaction 9) along with that of the undeuteriated complex was measured at 80°C. The rate constants ($K_H = 3.34 \times 10^{-5}$, $K_D = 4.75 \times 10^{-6}$) show a primary deuterium isotope effect of 7.04. These results are also consistent with



either the concerted *cis* elimination or decomposition of the alkyl complex which occurs with the elimination of HCl (DCl) as the rate-determining steps. In the decarbonylation of the *erythro*- (XI) and *threo*-2,3-diphenylbutanoyl chlorides (XII), intermediate alkyl complexes of the types XIII and XIV could be detected by IR although only in very small concentrations. This is still consistent with a rate-determining step involving the conversion of XIII or XIV to stilbenes with the elimination of HCl since an equilibrium between phenylacyl (II) and benzyl complexes (III) is established and lies in favor of the phenylacyl species (II).

Direction of Elimination: Hofmann vs. Saytzeff. In a study designed to determine the selectivity for the direction of elimination in the decarbonylation of acid chlorides containing β hydrogens, several branched acid chlorides were synthesized having primary, secondary, and tertiary β hydrogens in which there were internally available two choices of types of hydrogens (primary vs. secondary, primary vs. tertiary, and secondary vs. tertiary). The reactions were carried out in the presence of added triphenylphosphine which, when present in a molar ratio of 10:1 over the chlorocarbonylbis(triphenylphosphine)rhodium (IV) catalyst, suppressed the isomerization of the product 1-pentene to 2-pentene obtained from the decarbonylation of hexanoyl chloride. In addition, the reaction was carried out such that the olefins and hydrogen chloride were removed from the reaction mixture as soon as they were formed and the evolved hydrogen chloride was neutralized. In this way, the decarbonylation of hexanoyl chloride gave a 96:4 ratio of 1- to 2-pentene while decarbonylation without the added triphenylphosphine gave a 66:34 ratio. Decarbonylation of hexanoyl chloride with stoichiometric amounts of chlorotris(triphenylphosphine)rhodium showed a greater tendency to isomerize the olefin under the reaction conditions tested for IV. The results of these decarbonylations (Table II) show the tendency towards the Saytzeff elimination in that secondary hydrogen abstraction is preferred over primary (3:1) and tertiary over secondary or primary.

Acknowledgments

We thank W. Bahatti for his help in the early stages of a portion of this research.

Literature Cited

1. Ohno, K., Tsuji, J., *J. Amer. Chem. Soc.* (1968) **90**, 99.
2. Baird, M. C., Mague, J. T., Osborn, J. A., Wilkinson, G., *J. Chem. Soc. A* (1967) 1347.
3. Blum, J., Kraus, S., Pickholtz, Y., *J. Organometal. Chem.* (1971) **33**, 227.
4. Blum, J., Oppenheimer, E., Bergmann, E. D., *J. Amer. Chem. Soc.* (1967) **89**, 2338.

5. Tsuji, J., Ohno, K., *Tetrahedron Lett.* (1966) 4713.
6. Tsuji, J., Ohno, K., *J. Amer. Chem. Soc.* (1966) **88**, 3452.
7. Deeming, A. J., Shaw, B. L., *J. Chem. Soc. A* (1969) 597.
8. Brookes, P. R., Shaw, B. L., *J. Chem. Soc. A* (1967) 1079.
9. Walborsky, H. M., Allen, L. E., *J. Amer. Chem. Soc.* (1968) **93**, 5466.
10. Peters, H. M., Feigel, D. M., Mosher, H. S., *J. Org. Chem.* (1968) **33**, 4242.
11. Aaron, C., Dull, D., Schmiegl, J. L., Jaeger, D., Ohashi, Y., Mosher, H. S., *J. Org. Chem.* (1967) **32**, 2797.
12. Kubota, M., Blake, D. M., *J. Amer. Chem. Soc.* (1971) **93**, 1368.
13. Hauser, C. R., Lednicer, D., Brasen, W. R., *J. Amer. Chem. Soc.* (1958) **80**, 4345.
14. Hauser, C. R., Brasen, W. R., *J. Amer. Chem. Soc.* (1956) **78**, 494.
15. Heck, R. F., *J. Amer. Chem. Soc.* (1969) **91**, 6707.
16. Shaw, B. L., *Chem. Commun.* (1968) 464.
17. Henry, P. M., *J. Amer. Chem. Soc.* (1972) **94**, 7305.
18. Johnson, R. W., Pearson, R. G., *Chem. Commun.* (1970) 986.
19. Whitesides, G. M., Boschetto, D. J., *J. Amer. Chem. Soc.* (1969) **91**, 4313.
20. Hines, L. F., Stille, J. K., *J. Amer. Chem. Soc.* (1972) **94**, 485.
21. Carturan, G., Graziani, M., Ros, R., Belluco, U., *J. Chem. Soc. Dalton* (1972) 262.

RECEIVED August 20, 1973. This research was supported in part by the Petroleum Research Fund administered by the American Chemical Society. M.R. and R.F. were supported by NSF Traineeships during part of this graduate study.

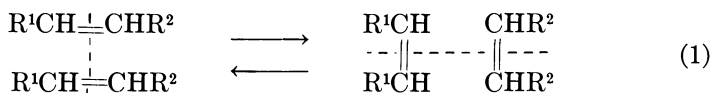
Olefin Disproportionation Catalysts

WILLIAM B. HUGHES

Phillips Petroleum Co., Bartlesville, Okla. 74004

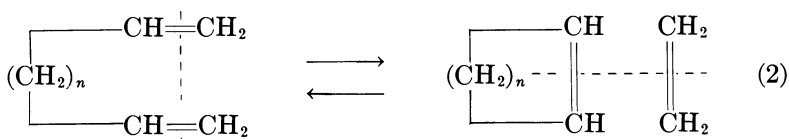
An important class of homogeneous olefin disproportionation catalysts is derived from the Group VIa metal nitrosyl complexes, $MX_2(NO)_2L_2$, and organoaluminum compounds. Study of the IR spectra of the complexes during catalyst formation, the effectiveness of other cocatalysts such as $AlCl_3$, Bu_4Sn , and $LiAlH_4$, the effect on catalytic activity of changes in X (Cl, Br, I), M (Cr, Mo, W), and L (PPh_3 , $OPPh_3$, $AsPh_3$, C_5H_5N) and of the substitution of CO for NO have led to the proposal of a sequence of catalyst-formation reactions. Important steps are removal of the nitrosyl groups and complexation of organoaluminum to the halide ligands. Investigation of some structurally and electronically similar ruthenium complexes and of a series of oxo metal complexes showed that ligands which impart catalytic activity to one metal will not, in general, activate another metal.

Olefin disproportionation or metathesis is a transition-metal catalyzed reaction involving the interchange of alkylidene units between olefins (Reaction 1) (1, 2, 3, 4).

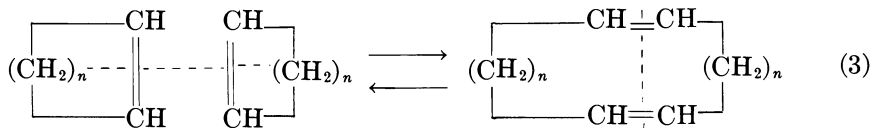


Both 2H and ^{14}C labeling experiments have shown that the reaction proceeds *via* the cleavage and reformation of the double bonds, *i.e.*, it is a transalkylidenation process (5, 6, 7). The reaction is reversible, essentially thermoneutral, and attains a thermodynamic equilibrium typified by a statistical distribution of the alkylidene moieties.

All types of olefins can serve as substrates. Suitable acyclic olefins include ethylene, terminal and internal monoenes up to and including tetrasubstituted-double bonds, and aryl-substituted olefins. With dienes (and polyenes) an additional, intramolecular reaction pathway becomes available which leads to cyclic olefins (Reaction 2).



With cyclic olefins as the reactants, disproportionation results in ring enlargement leading to the formation of macrocyclics and, ultimately, polymeric materials, *i.e.*, polyalkenamers (Reaction 3).



Although in general functionally-substituted olefins are unreactive, the disproportionation of acrylonitrile with propylene and of certain unsaturated fatty acid esters have been recently reported (8, 9). The disproportionation of acetylenes has been observed over heterogeneous catalysts (10).

Both heterogeneous and homogeneous disproportionation catalysts are known. All contain a transition metal component with derivatives of Mo, W, and Re being the most important. Heterogeneous catalysts are generally metal oxides deposited on a support such as silica or alumina (1, 4). Homogeneous catalysts in general require a non-transition metal derivative as cocatalyst (2, 3).

The mechanism of the disproportionation reaction is currently receiving attention. Two basic pathways have been suggested. The first proposes the concerted transformation *via* a symmetrical intermediate, variously described as quasi-cyclobutane (11), tetramethylene (12), etc., of one pair of olefins into another. The second mechanism postulates a nonconcerted process involving metallocyclopentane intermediates (13). Experimental evidence for both mechanisms has been presented, but the issue is still unresolved.

Industrial applications of the disproportionation process have been limited. Shawinigan Chemicals Ltd., Montreal, uses the reaction to convert propylene into polymerization-grade ethylene and high-purity butenes on a commercial scale. Stereokautschukwerke GmbH, Dormagen, West Germany, is bringing on stream a 50,000 metric-ton-a-year plant for producing *trans*-1,5-poly-pentenamer by the ring-cleavage polymerization of cyclopentene. Phillips Petroleum currently has in operation a multi-purpose disproportionation pilot plant producing 500,000 lbs per year of neohexene *via* the ethylene cleavage of diisobutylene. The unit can also produce the α,ω -dienes, 1,9-decadiene, and 1,13-tetradecadiene by the disproportionation of ethylene with cyclooctene and cyclododecene, respectively.

The variety of transformations possible and the availability of both soluble and supported catalysts should make the industrial future of olefin disproportionation a bright one.

Previous reports from these laboratories have described a family of homogeneous disproportionation catalysts derived from molybdenum and tungsten nitrosyl complexes and organoaluminum compounds (14, 15). Studies of the stereochemistry and kinetics of the disproportionation of 2-pentene using these catalysts have also been reported (16, 17). The present report describes a more detailed study of the homogeneous catalysts derived from molybdenum nitrosyl complexes. Various methods of catalyst generation, the effect on catalytic activity of varying the ancillary ligands and of substituting CO for NO, and the IR spectra of catalyst solutions were investigated. The effect on activity of substituting chromium and tungsten for molybdenum in these complexes was also studied. Selected complexes, both nitrosyl and non-nitrosyl, of other transition metals were briefly investigated. The ultimate goal of these studies was to elucidate the actual catalytic species, such knowledge being prerequisite to conclusions about the reaction mechanism and to the tailoring of catalysts for specific applications.

Experimental

All reactions involving catalyst preparations were carried out under an atmosphere of prepurified nitrogen or argon in previously dried equipment. IR spectra were obtained on a Perkin-Elmer model 621 or model 257 spectrometer. The IR cells were of the sealed cavity type ($\sim 100\mu$) with Teflon stoppers. Four types of cell window materials were used: As_2S_3 , KBr, Irtran 2, and Ge metal. The spacers were Teflon except for the KBr cell in which lead was used. Analyses were performed by Phillips Research Division.

The 2-pentene (Phillips pure grade) was purified by distillation from CaH_2 and passage through a column of activated (4 hrs at $540^\circ C$) MgO . Chlorobenzene and CH_2Cl_2 were distilled from CaH_2 or (CH_2Cl_2) passed through activated alumina. The solvents were degassed by sparging with argon for 1 hr.

The molybdenum and tungsten complexes of the type $MX_2(NO)_2L_2$ (with $X = Cl$ or Br) were prepared by the method of Cotton and Johnson in which $[MoX_2(NO)_2]_n$ is treated with the appropriate ligand, L (18, 19). The iodo derivatives have been prepared previously by halogen exchange with $[MoBr_2(NO)_2]_n$ followed by treatment with L (19). The exchange can be effected equally well in the $MoCl_2(NO)_2L_2$ complexes by heating (50° – $60^\circ C$) with KI in acetone for several hours. This procedure is somewhat simpler to conduct since $[MoBr_2(NO)_2]_n$ is air and moisture sensitive whereas the L_2 -derivatives are not. The following complexes were prepared by literature methods as cited: $MoCl(CO)_2(NO)(bipy)$ (20), $Mo(CO)_4(bipy)$ (21), $RuCl_2(CO)_2(PPh_3)_2$ (22), $RuCl(CO)(NO)(PPh_3)_2$ (23), $RuCl_3(NO)(PPh_3)_2$ (24), $CrCl_2(NO)_2(OPPh_3)_2$ (25), $NbOCl_3(PPh_3)_2$ (26), $MoOCl_3(OPPh_3)_2$ (27), $ReOCl_3(PPh_3)_2$

(28), $\text{MoOCl}_3(\text{PPh}_3)_2$ (29), and $\text{OsOCl}_3(\text{PPh}_3)_2$ (30). All other materials were commercial reagent materials and used as received.

The general experimental procedure was to allow the metal complex and cocatalyst to react for *ca.* 1 hr in chlorobenzene and then 2-pentene was added. Both the catalyst formation reaction and the olefin reaction were run at room temperature. The experiments in which AlCl_3 , LiAlH_4 , NaBH_4 , and Bu_4Sn were used contained 0.15 gram (0.2 mmole) $\text{MoCl}_2(\text{NO})_2(\text{PPh}_3)_2$, 10 cc of PhCl , 2 cc of 2-pentene, and 1.0 mmole of the cocatalyst. The experiments in Tables I, II, IV, and VI utilized 0.25 mmole of the metal complex, 20 cc of PhCl , 1 cc of a 1M PhCl solution of methylaluminum sesquichloride (MASC), and 3 cc of 2-pentene. The experiments of Table III employed 0.2 mmole of the molybdenum complex, 10 cc of PhCl , 0.8 cc of the MASC solution, and 2 cc of 2-pentene. The experiments of Table V used 0.2 mmole of the molybdenum or ruthenium complex, 10 cc of PhCl , 1 cc of the MASC solution, and 2 cc of 2-pentene. For the IR studies, the catalyst was generated from 0.2 mmole of $\text{MoCl}_2(\text{NO})_2(\text{PPh}_3)_2$ and 0.8 mmole of MASC in 11 cc of CH_2Cl_2 and allowed to react with 2 cc of 2-pentene. For the IR studies of the $\text{MoCl}_2(\text{NO})_2(4\text{-Etpy})_2$ -derived catalyst, 0.2 mmole of the complex, 0.4 mmole of MASC, and 20 cc of CH_2Cl_2 were used.

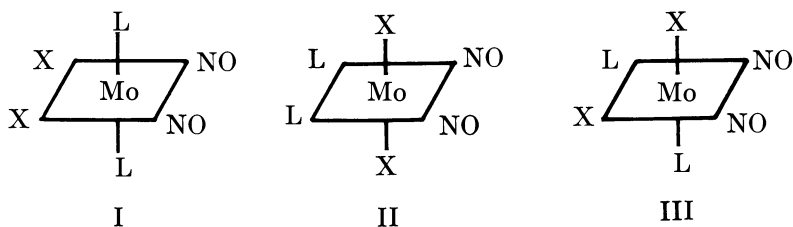
The reaction mixtures were analyzed by GLPC on either a Carbowax 20M or adipate-sebacate column using a Hewlett-Packard model 5750 chromatograph equipped with a flame ionization detector.

Results

Molybdenum Nitrosyl Complexes. The molybdenum nitrosyl complexes which serve as disproportionation catalyst precursors are of the general type $\text{MoX}_2(\text{NO})_2\text{L}_2$ where X is a halogen and L is a neutral, π -bonding ligand. The complexes are light to dark green (except for the iodo derivatives which are purple), diamagnetic, nonelectrolytic solids. They were first reported by Cotton and Johnson (18, 19) and by Canziani, *et al.* (31).

Although it is not certain that a definitive relationship exists between the configuration of the starting complex and the derived catalyst, information about the stereochemistry of the nitrosyl complexes appeared desirable. For all ligands, L and X, examined to date at least two N-O stretching vibrations are observed in the IR spectrum suggesting that the NO groups are *cis*. Assuming this is the case, three isomers are possible (I-III).

Two Mo-Cl stretching vibrations in the far IR and virtual coupling of the methyl protons in the NMR spectrum led to the conclusion that the diphenylmethylphosphine complex ($\text{X} = \text{Cl}$, $\text{L} = \text{PPh}_2\text{CH}_3$) possessed configuration I (32). The similarity of the IR spectrum of the corresponding triphenylphosphine derivative suggested it had the same structure (32). More direct evidence for the configuration of the PPh_3 complex was provided by its 25 MHz proton-decoupled ^{13}C NMR spec-



trum. The substituted, ortho, and meta carbons of the phenyl groups appeared as triplets at δ 130.4, 134.3, and 128.5 ppm (relative to Me_4Si), respectively, with $|J_{\text{cp}} + J_{\text{cp}'}| = 40.4, 9, \text{ and } 10 \text{ Hz}$. Such virtual coupling of the aryl carbons has been associated with trans triphenylphosphine ligands (33). A recent single crystal x-ray diffraction study by Visscher and Caulton has confirmed configuration I for $\text{MoCl}_2(\text{NO})_2(\text{PPh}_3)_2$ (34).

We have prepared the triphenylphosphine complex (as did Visscher and Caulton) by the method of Cotton and Johnson (18, 19), and we have consistently obtained material which melts with decomposition in the range $202^\circ\text{--}205^\circ\text{C}$. This decomposition point is some 50°C lower than that reported in Ref. 18. The reason for this discrepancy is not clear since the materials are presumably the same isomer.

The polymeric nitrosyl $[\text{MoCl}_2(\text{NO})_2]_n$ (from $\text{Mo}(\text{CO})_6$ and NOCl) dissolves in ethanol to give a clear, green solution which presumably contains $\text{MoCl}_2(\text{NO})_2(\text{EtOH})_2$ previously prepared by Canziani, *et al.*, by treatment of $\text{Mo}(\text{CO})_6$ with $\text{HCl}(\text{g})$ and NO in ethanol (31). Addition of Ph_3P to the solution precipitates $\text{MoCl}_2(\text{NO})_2(\text{PPh}_3)_2$ which from IR data (ν_{NO} and $\nu_{\text{Mo-Cl}}$) is also isomer I.

In contrast to the triphenylphosphine derivative, the triphenylphosphine oxide complex ($\text{X} = \text{Cl}$, $\text{L} = \text{OPPh}_3$) shows only one band in the Mo-Cl stretching region at 306 cm^{-1} . This suggests that it has configuration II. The 2,2'-bipyridine complex $\text{MoCl}_2(\text{NO})_2(\text{bipy})$ contains two absorptions at 1772 and 1650 cm^{-1} (CsI) in the N-O stretching region and two $\nu_{\text{Mo-Cl}}$ bands at 318 and 292 cm^{-1} (Nujol). Since the bipyridine is constrained to occupy cis coordination sites, the IR data suggest structure III for this complex. The pyridine complex ($\text{X} = \text{Cl}$, $\text{L} = \text{C}_5\text{H}_5\text{N}$) as originally isolated from the reaction of $[\text{MoCl}_2(\text{NO})_2]_n$ and pyridine in benzene (where the complex precipitates as formed) showed two $\nu_{\text{N-O}}$ bands at 1772 and 1660 cm^{-1} (CsI) and one strong band at 316 cm^{-1} accompanied by a weak band at 287 cm^{-1} ($\nu_{\text{Mo-Cl}}$). Rapid recrystallization from CH_2Cl_2 caused a third band in the N-O stretching region at $\sim 1648 \text{ cm}^{-1}$ and an increase in intensity of the 287 cm^{-1} band (CsI). The IR spectrum of the complex recovered from CH_2Cl_2 after standing overnight now contained $\nu_{\text{N-O}}$ at 1772 and 1648 cm^{-1} and a further enhancement of the 287 cm^{-1} band relative to the 316 cm^{-1} band (CsI). These results indicate that the pyridine complex is originally structure II but slowly

isomerizes to structure III in solution (the choice of III over I is based on the similarity in frequency of the N–O and Mo–Cl stretching vibrations to the bipy complex).

In addition to their stereochemistry the question of the oxidation state of the molybdenum in the $\text{MoX}_2(\text{NO})_2\text{L}_2$ complexes is germane to speculation about the subsequent organoaluminum activation step. The unique ability of nitric oxide to bond to a transition metal as linear NO^+ or bent NO^- makes the (formal) oxidation state of the metal ambiguous. The observed N–O stretching frequencies in the IR spectra of the complexes fall in the range traditionally assigned to NO^+ . On this basis, the complexes have been formulated as $\text{Mo}(0)$ derivatives (18, 19). However, the reliability of ν_{NO} as a criterion of bond type has recently been questioned (35). We have used x-ray photoelectron spectroscopy (ESCA) as an alternate technique for evaluating the nature of the Mo–NO bond. ESCA studies of $\text{MoCl}_2(\text{NO})_2(\text{PPh}_3)_2$ (36) clearly indicate that the NO^+ formalism is inappropriate. The Mo 3*d* electron binding energies are greater than those in the related Mo(II) complex $\text{MoCl}_2(\text{CO})_3(\text{PPh}_3)_2$. This implies extensive back-donation of metal *d* electrons into π^*_{NO} orbitals resulting in a partial negative charge on the NO groups. This finding is corroborated by the x-ray diffraction study which found the Mo–N–O bonds nonlinear (average angle Mo–N–O = 163°) (34).

IR Studies of Catalyst Formation. Treatment of the molybdenum nitrosyl complexes with an organoaluminum reagent (in the absence of olefin) produces significant changes in the N–O stretching region of the IR spectrum. Mixing of $(\text{CH}_3)_3\text{Al}_2\text{Cl}_3$ and $\text{MoCl}_2(\text{NO})_2(\text{PPh}_3)_2$ in CH_2Cl_2 (or PhCl) results in an immediate color change from green to orange-brown. After reacting for ½ hr at room temperature, the solution (CH_2Cl_2) had become more brown. Samples of the reaction were loaded into a Ge metal and KBr cell, and 2-pentene was added to the remaining solution. The IR spectra of the solution samples (recorded *ca.* 5 min after sampling) showed the complete absence of the strong N–O absorptions at 1790 and 1676 cm^{-1} . No new bands were detected in the region of 4000–600 cm^{-1} either with or without the use of a CH_2Cl_2 blank. Concurrently, samples of the reaction mixture were analyzed by GLPC. These showed a 10.5% conversion to 2-butene and 3-hexene 5 min after olefin addition and a 43.6% conversion after 30 min.

A more detailed picture of the interaction of the molybdenum complex and organoaluminum reagent was provided by an IR study of the $\text{MoCl}_2(\text{NO})_2(4\text{-Etpy})_2/(\text{CH}_3)_3\text{Al}_2\text{Cl}_3$ system. Catalyst formation appears to be slower in this case as evidenced by the gradual development of the typical brown coloration. Figure 1-A shows the strong symmetric and asymmetric stretching vibrations of the *cis* nitrosyl ligands in $\text{MoCl}_2(\text{NO})_2(4\text{-Etpy})_2$ in CH_2Cl_2 solution (As_2S_3 cell). Figure 1-B depicts

the same region 6 min after treatment of the complex with $(\text{CH}_3)_3\text{Al}_2\text{Cl}_3$. The $\nu_{\text{N-O}}$ bands have been shifted to higher frequency by 33 and 47 cm^{-1} , respectively. The remainder of Figure 1 reveals two phenomena. First, the gradual disappearance of the bands in Figure 1-B accompanied by the appearance of two new bands at slightly lower frequency. Second, there is an overall diminution in intensity of the absorptions in the $\nu_{\text{N-O}}$ region. It is true that the intensities of the new $\nu_{\text{N-O}}$ bands need not be as great as the original bands, but other experiments showed that these bands essentially disappeared. The presence of residual absorptions in the present case is probably a result of the low MASC/Mo complex ratio ($\sim 2:1$) resulting in incomplete reaction. Similar results were obtained with $\text{MoCl}_2(\text{NO})_2(\text{py})_2$ and EtAlCl_2 in chlorobenzene.

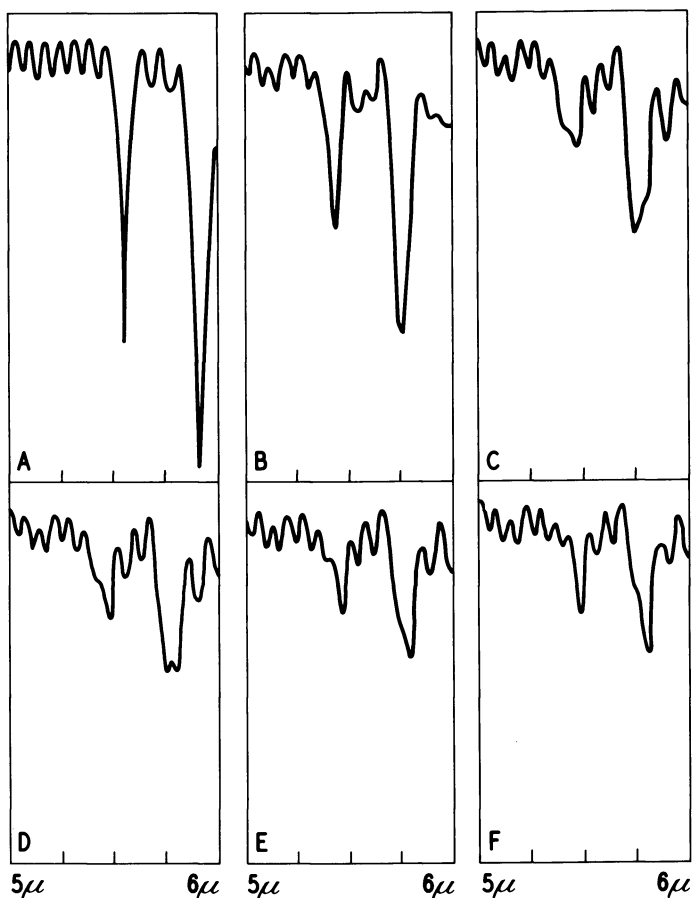


Figure 1. IR spectra of $\text{MoCl}_2(\text{NO})_2(4\text{-Etpy})_2$ in CH_2Cl_2 : (A) complex alone, (B) 6 min after $(\text{CH}_3)_3\text{Al}_2\text{Cl}_3$ added, (C) after 16 min, (D) after 25 min, (E) after 52 min, and (F) after 91 min

Alternate Methods of Catalyst Generation. In our original studies (15, 17) of soluble olefin disproportionation catalysts derived from molybdenum nitrosyl complexes, organoaluminum compounds were used as cocatalysts. Alkyl dihalide, dialkyl monohalide, and alkyl sesquichloride derivatives were all suitable activators although the selectivity and activity of the derived catalyst varied with the type of aluminum compound used. Triethylaluminum did not give catalytically active preparations (37).

As an aid to understanding the role of organoaluminum reagents in catalyst genesis we have investigated some alternate methods of activation. First, AlCl_3 , LiAlH_4 , NaBH_4 , and Bu_4Sn were investigated as cocatalysts. The molybdenum component was $\text{MoCl}_2(\text{NO})_2(\text{PPh}_3)_2$, the solvent chlorobenzene, and the substrate 2-pentene (48% trans, 52% cis). The molybdenum complex and cocatalyst were allowed to react for 1 hr at room temperature prior to olefin addition. After a 3-hr reaction period, only the AlCl_3 system exhibited disproportionation activity having reached the equilibrium conversion (50%) to 2-butene and 3-hexene. The cis/trans ratios for the C_4 , C_5 , and C_6 olefins were also near their equilibrium values. In the remaining reactions, the 2-pentene was completely unchanged. No reaction was observed after 16 hrs. *tert*-BuLi and Et_2Mg do not give catalysts (37). A catalytically active system was also obtained from $\text{MoCl}_2(\text{NO})_2(\text{OPPh}_3)_2$ and AlCl_3 . In this case, the activity was lower with the conversion being only 13% in 3 hrs.

The AlCl_3 system exhibits a high level of activity in the present example. However, this reaction has been carried out a number of times and in some cases slight or no activity was observed. In such cases a dark red solution was obtained compared with a green solution in the present case. At the moment we speculate that the AlCl_3 -derived catalyst is very sensitive to impurities in the system and that small amounts of air or moisture may be responsible for the observed differences. Whatever the reason, the fact remains that AlCl_3 can give a disproportionation catalyst of high activity.

In addition to the use of other cocatalysts, we attempted to generate a catalyst from $\text{MoCl}_2(\text{NO})_2(\text{PPh}_3)_2$ by photolysis. Irradiation of the complex in chlorobenzene in a quartz reactor using an unfiltered high-pressure mercury lamp in the presence of 2-pentene gave no observable disproportionation. Irradiation of the complex alone followed by olefin addition and continued irradiation likewise gave no reaction. During the course of the photolysis the solution changed from green to gold, and a brown solid was recovered upon removal of the PhCl. This material was not characterized, but an IR spectrum indicated the absence of the original nitrosyl absorptions and the presence of a new band at 1727 cm^{-1} ($\nu_{\text{N-O}}?$).

Table I. Effect of Anionic Ligands on Activity of $\text{MoX}_2(\text{NO})_2\text{L}_2$ -Derived Disproportionation Catalysts

$\text{MoX}_2(\text{NO})_2\text{L}_2$	ν_{NO}^a , cm^{-1}	Disproportionation of 2-Pentene, %
L = Ph_3P , X = Cl	1790, 1676	39 in 0.5 hr
	X = Br	35 in 0.5 hr
	X = I	13 in 0.5 hr
L = Ph_3As , X = Cl	1789, 1672 ^b	16 in 1 hr
	X = Br	11 in 1 hr
	X = I	<1 in 1 hr

^a In CHCl_3 .^b Weaker bands at 1775, 1653 cm^{-1} .

Ligand Effects. An indirect probe into the nature of the catalytic species derived from $\text{MoX}_2(\text{NO})_2\text{L}_2$ complexes is to study the effect on catalytic activity of varying the ligands of the complex. We first investigated the effect of variation in the anionic ligands for two series where L = PPh_3 and L = AsPh_3 . The per cent disproportionation (50% is maximum) for the complexes using $(\text{CH}_3)_3\text{Al}_2\text{Cl}_3$ as cocatalyst in chlorobenzene is shown in Table I along with $\nu_{\text{N-O}}$ for the complexes. For both series, the catalytic activity is in the order Cl > Br > I although the difference between the chloro and bromo derivatives is small. This order is not paralleled by the N–O stretching frequencies which show little variation with change in halogen ligand. The Cl– Ph_3As derivative showed two weaker $\nu_{\text{N-O}}$ bands at lower frequency indicating the presence of another isomer.

Table II. Effect of π -Bonding Ligands on Activity of $\text{MoCl}_2(\text{NO})_2\text{L}_2$ -Derived Disproportionation Catalysts

L in $\text{MoCl}_2(\text{NO})_2\text{L}_2$	ν_{NO}^a , cm^{-1}	Disproportionation of 2-Pentene, %
4-Et ₃ py	1792, 1690	50 in 15 min
$\text{Ph}_3\text{P}\text{O}$	1788, 1670	50 in 15 min
Ph_3P	1790, 1676	33 in 15 min
Ph_3As	1789, 1672 ^b	16 in 60 min

^a In CHCl_3 .^b Weaker bands at 1775, 1653 cm^{-1} .

The effect on catalytic activity of varying the π -bonding ligands for a series of chloro complexes was also studied. The cocatalyst was $(\text{CH}_3)_3\text{Al}_2\text{Cl}_3$, and the solvent was PhCl. The results are displayed in Table II along with $\nu_{\text{N-O}}$ for the complexes.

Only with the Ph_3As derivative does catalytic activity fall off appreciably. As with the halogen series, ν_{NO} shows little variation with L and no obvious correlation with catalytic activity.

To gain further insight into the effect of various ligands on catalytic activity, the series of molybdenum complexes in Table III was investigated. Methylaluminum sesquichloride was the cocatalyst and the solvent was chlorobenzene.

The reactions using the three NO-containing complexes all showed equilibrium conversion to 2-butene and 3-hexene in 1 hr. The cis/trans ratios for all olefins were also at their equilibrium values (the initial 2-pentene was 48% trans, 52% cis). With the complex $\text{Mo}(\text{CO})_4(\text{bipy})$ there was observable disproportionation although the conversion was quite small. Some double-bond isomerization was observed with this system (1.2% 1-pentene present). The last complex of Table III also gave a trace of disproportionation, some double-bond isomerization (1.6% 1-pentene), and cis/trans isomerization (equilibrium ratio of cis/trans 2-pentene).

Thermal activation of $\text{MoCl}(\text{CO})_2(\text{NO})(\text{bipy})$ was attempted. Heating the complex in chlorobenzene in the presence of 2-pentene up to 7 hrs at 55°–90°C both in a closed and open (to facilitate escape of CO) system did not result in disproportionation or other observable reaction.

Table III. Effect of Various Ligands on Activity of Molybdenum Disproportionation Catalysts

Complex	$\nu_{\text{CO}}^a, \text{cm}^{-1}$	$\nu_{\text{NO}}^a, \text{cm}^{-1}$	Disproportionation of 2-Pentene ^b , %
$\text{Mo}(\text{CO})_4(\text{bipy})$	2014,1911, 1882,1830 ^c	—	<1
$\text{MoCl}(\text{CO})_2(\text{NO})(\text{bipy})$	2038,1941	1643	50
$\text{MoCl}_2(\text{NO})_2(\text{bipy})$	—	1792,1690	50
$\text{MoCl}_2(\text{NO})_2(\text{py})_2$	—	1800,1693, 1676sh	50
$\text{MoCl}_2(\text{CO})_3(\text{PPh}_3)_2$	2045,1952,1903 ^d	—	<1

^a In CHCl_3 .

^b 1 hr reaction.

^c Ref. 21.

^d In Nujol, Ref. 38.

Complexes of Other Metals. Having studied in detail catalysts derived from molybdenum nitrosyl complexes, it was interesting to investigate the effect on catalytic activity of substituting other transition metals in both nitrosyl derivatives and in other related complexes.

Comparison of the Group VIa metals in the same type of complexes as studied above was possible in the series $\text{MCl}_2(\text{NO})_2(\text{OPPh}_3)_2$ ($\text{M} = \text{Cr}, \text{Mo}, \text{W}$). A further comparison of molybdenum and tungsten could be made in the complexes $\text{MCl}_2(\text{NO})_2(\text{PPh}_3)_2$ ($\text{M} = \text{Mo}, \text{W}$). Nitrosyl stretching frequencies for the complexes and a comparison of the derived catalysts using $(\text{CH}_3)_3\text{Al}_2\text{Cl}_3$ in PhCl are shown in Table IV.

Table IV. Effect of Varying Group VIa Metal on Activity of Disproportionation Catalysts

Complex	$\nu_{\text{NO}}, \text{cm}^{-1}$	Disproportionation of 2-Pentene, %
$\text{CrCl}_2(\text{NO})_2(\text{OPPh}_3)_2$	1841,1699 ^a	none observed
$\text{MoCl}_2(\text{NO})_2(\text{OPPh}_3)_2$	1779,1656 ^b	50 in 15 min
$\text{WCl}_2(\text{NO})_2(\text{OPPh}_3)_2$	1737,1620 ^b	<1 in 5 hrs
$\text{MoCl}_2(\text{NO})_2(\text{PPh}_3)_2$	1790,1676 ^c	35 in 90 min
$\text{WCl}_2(\text{NO})_2(\text{PPh}_3)_2$	1770,1661 ^d	10 in 90 min

^a In Nujol.^b In Csl.^c In CHCl_3 .^d In CH_2Cl_2 .

The variation in catalytic activity is striking and follows the trend in N–O stretching frequencies. Although no disproportionation was observed for the chromium complex in Table IV, systems displaying slight activity have been obtained. Thus, the complex $\text{Cr}(\text{CO})_4(\text{PPh}_3)_2$ with EtAlCl_2 in PhCl gave 3% disproportionation of 2-pentene in 72 hrs.

Ruthenium Complexes. It was of interest to know if a non-Group VIa transition metal in a similar ligand environment could be substituted for molybdenum. The ruthenium complexes listed in Table V appeared to be suitable for such studies since they are isoelectronic with the molybdenum nitrosyl complexes (both of the xenon configuration). Moreover, $\text{RuCl}_2(\text{CO})_2(\text{PPh}_3)_2$ has the same type of stereochemistry as $\text{MoCl}_2(\text{NO})_2(\text{PPh}_3)_2$, *i.e.*, the carbonyl and chloride ligands are *cis* and the triphenylphosphine groups are *trans* (39). The frequencies for the metal–chlorine stretching vibrations are very similar for the two complexes being 300, 275 and 304, 287 cm^{-1} for Ru and Mo, respectively.

The ruthenium complexes were tested for disproportionation activity using $(\text{CH}_3)_3\text{Al}_2\text{Cl}_3$ as cocatalyst, PhCl as solvent, and 2-pentene as substrate. The results, along with that obtained for $\text{MoCl}_2(\text{NO})_2(\text{PPh}_3)_2$ under the same conditions, are summarized in Table V.

Table V. Disproportionation Activity of Ruthenium Complexes

Complex	$\nu_{\text{CO}}^a, \text{cm}^{-1}$	$\nu_{\text{NO}}^a, \text{cm}^{-1}$	Disproportionation of 2-Pentene ^b , %
$\text{RuCl}_2(\text{CO})_2(\text{PPh}_3)_2$	2058,1985 ^c	—	trace
$\text{RuCl}(\text{CO})(\text{NO})(\text{PPh}_3)_2$	1925 ^d	1592 ^d	trace
$\text{RuCl}_3(\text{NO})(\text{PPh}_3)_2$	—	1877 ^e	trace
$\text{MoCl}_2(\text{NO})_2(\text{PPh}_3)_2$	—	1793,1672	50

^a In Nujol.^b 1 hr reaction.^c Ref. 39.^d Ref. 23.^e Ref. 24.

None of the ruthenium complexes gave greater than trace amounts of disproportionation. Both of the nitrosyl-containing ruthenium derivatives showed some double-bond isomerization activity with 1-2% 1-pentene being observed.

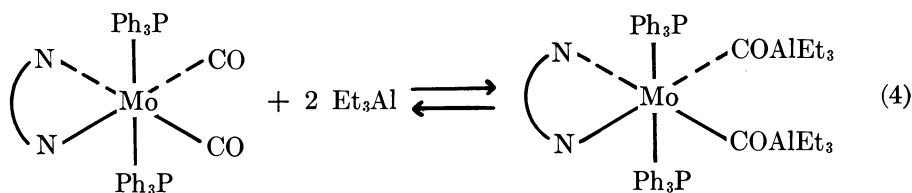
Oxo Complexes. Rhenium oxo complexes $\text{ReOX}_3(\text{PPh}_3)_2$ ($X = \text{Cl}, \text{Br}$) in combination with organoaluminum reagents display moderate activity for olefin disproportionation (40). The availability of a homologous series of the above type of oxo complex spanning several transition metal groups prompted us to investigate the effect on catalytic activity of varying the metal within a periodic series. The reactions were conducted in PhCl using $(\text{CH}_3)_3\text{Al}_2\text{Cl}_3$ as cocatalyst and 2-pentene as substrate. Of the complexes $\text{MOCl}_3(\text{PPh}_3)_2$ ($M = \text{Mo}, \text{Re}, \text{Os}$) and $\text{MOCl}_3(\text{OPPh}_3)_2$ ($M = \text{Nb}, \text{Mo}$), only the rhenium derivative exhibited significant catalytic activity (6% disproportionation in 1.5 hrs). Trace activity was found for the Os-PPh_3 and Mo-OPPh_3 complexes. Also the analogous bromo rhenium complex was less active than the chloro paralleling the behavior of the molybdenum nitrosyl complexes.

Discussion

The IR studies of catalyst formation allow several conclusions. First, the results obtained from the $\text{MoCl}_2(\text{NO})_2(\text{PPh}_3)_2/(\text{CH}_3)_3\text{Al}_2\text{Cl}_3$ system reveal that a solution shown to be catalytically active lacks the two strong N-O stretching bands present in the original complex or any new bands which could be attributed to a metal-complexed nitrosyl group. This indicates that NO is not present as a ligand in the catalytic species. It has been suggested that soluble catalysts derived from transition metal nitrosyl complexes owe their effectiveness to a facile linear-to-bent tautomerism of the M-N-O bonds which induces favorable structural and/or electronic changes in the complex (41). Such behavior does not appear to be the case for olefin disproportionation catalysts derived from molybdenum nitrosyl complexes.

Second, the results obtained from the $\text{MoCl}_2(\text{NO})_2(4\text{-Etpy})_2/(\text{CH}_3)_3\text{Al}_2\text{Cl}_3$ system indicate that the interaction of organoaluminum and complex occurs in several stages. A rapid, initial step in which the ν_{NO} bands are shifted to higher frequency is followed by a slower step in which the first-formed species is converted to a second nitrosyl species with ν_{NO} bands at lower frequencies and a final step in which the NO groups are lost from the molybdenum.

Although the ultimate fate of the nitrosyl ligands has not been established, a reasonable pathway for their removal can be postulated based on our IR data and recent literature results. Shriver *et al.* (42) have found that organoaluminum species will complex with the oxygen of metal-coordinated carbonyl groups. For example, the six-coordinate



molybdenum derivative $\text{Mo}(\text{CO})_2(\text{phen})(\text{PPh}_3)_2$ reacts with Et_3Al as shown in Reaction 4 where $\overset{\text{n}}{\text{N N}} = \text{phen}$.

The above molybdenum complex is the first case in which diadduct formation has been observed. As ligands, CO and NO are similar in many respects, so it is reasonable that the latter would also be capable of complexing with an organoaluminum species. Indeed, IR evidence has been presented that the terminal nitrosyl ligands in $(\pi\text{-C}_5\text{H}_5)\text{CrCl}(\text{NO})_2$ act as Lewis bases toward the organolanthanides $(\text{C}_5\text{H}_5)_2\text{Ln}$ ($\text{Ln} = \text{Sm}, \text{Er}, \text{Yb}$) (43). The high electron density on the NO groups in $\text{MoCl}_2(\text{NO})_2(\text{PPh}_3)_2$ as revealed by the ESCA studies would facilitate electrophilic attack by $\text{R}_x\text{AlCl}_{3-x}$.

Complexing the Lewis acid with CO or NO in the above cases results in shifts of ν_{CO} and ν_{NO} to lower frequencies. As discussed above, mixing $\text{MoCl}_2(\text{NO})_2(4\text{-Etpy})_2$ with $(\text{CH}_3)_3\text{Al}_2\text{Cl}_3$ shifts the ν_{NO} bands to higher frequencies followed by the appearance of new bands at lower frequencies. An interpretation is that initially, the organoaluminum complexes with the chloride ligands resulting in inductive withdrawal of electron density from the NO groups making them more NO^+ in character and thus of higher stretching frequency. Following this, attack by $(\text{CH}_3)_3\text{Al}_2\text{Cl}_3$ on the oxygen atoms of the NO ligands produces the new bands at lower frequency. Complexing the organoaluminum with the NO ligands tends to weaken the Mo–N bonds resulting in the loss of the NO groups from the coordination sphere of the molybdenum.

In addition to removal of the nitrosyl groups, a feasible role of the organoaluminum reagent in catalyst generation from $\text{MoX}_2(\text{NO})_2\text{L}_2$ complexes is replacement of the halide ligands with alkyl groups. In a subsequent step, loss of R_2 could result in reduction of the molybdenum or loss of olefin could yield a hydride complex. The fact that AlCl_3 alone gives an active catalyst free of any organometallic component and that the potential alkylating agents *tert*-BuLi, Et_2Mg , and Bu_4Sn and the hydridic reagents NaBH_4 and LiAlH_4 fail to give a catalyst mitigate against alkylation with or without subsequent reduction or hydride formation.

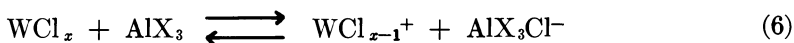
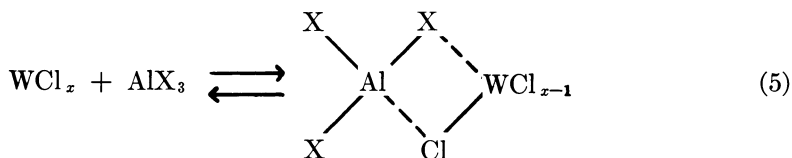
Indirect evidence for this conclusion lies in the fact that as the alkylating/reducing power of the organoaluminum is increased, the extent of olefin double-bond isomerization accompanying disproportionation

becomes greater (15), indicative that the concentration of another catalytic species is increasing.

Additional evidence that reduction is not the role of R_xAlCl_{3-x} in catalyst formation is provided by the observation that the complexes $[Bu_4N][Mo(CO)_5X]$ and $[R_4N][Mo(CO)_5COR']$, in which the molybdenum is in a low oxidation state, require an organoaluminum reagent for catalytic activity (44, 45). In these examples, the function of the organoaluminum is most likely the removal of CO ligands to make available sites for olefin coordination. Molybdenum hexacarbonyl alone is reported to be a disproportionation catalyst; in this case expulsion of the CO groups is attained thermally at 98°C (46).

Based on our experiments, only aluminum-containing reagents are suitable cocatalysts for catalyst formation from $MoX_2(NO)_2L_2$. This suggests that an aluminum moiety is part of the catalytic species.

Evidence has been presented that an aluminum species is involved in the disproportionation catalyst derived from WCl_6 and $BuLi$. Thus, activity is increased at least 100-fold by the addition of an equimolar amount of $AlCl_3$ or $AlBr_3$ (47). An active catalyst can be obtained from WCl_4 or WCl_6 with $AlCl_3$ alone (2). The role of the AlX_3 is perhaps association with the tungsten *via* μ -chloride bonding (Reaction 5) and/or removal of chloride ligands by an acid-base equilibrium (Reaction 6) to form the active sites (2, 47).



The latter process is probably responsible for the observed disproportionation activity of $MoCl_4$ and $AlCl_3$ (48). It has also been suggested that a non-transition metal, *e.g.*, Al is a constituent of the catalyst derived from WCl_6 and $LiAlH_4$ or $NaBH_4$ although in this case hydrogen or alkyl bridges were postulated (49).

We believe removing the nitrosyl groups produces the necessary sites for olefin coordination in the $MoX_2(NO)_2L_2$ catalyst systems. If aluminum is present in these catalysts, it is most likely through an interaction of the type shown in Reaction 5.

The nature of both the halide ligands X and the π -bonding ligands L affect the activity of the catalysts derived from $MoX_2(NO)_2L_2$ complexes

(Tables I and II). If both halide ligands were removed by the organoaluminum cocatalyst, the resulting catalytic species would be the same for the three halogens and should exhibit comparable activity. A possible explanation for the difference in activity between the chloro and bromo *vs.* iodo complex is that catalyst formation requires a significantly different time period for $X = I$. This was tested by allowing the iodo complex to react with MASC for $\frac{1}{2}$ hr and $1\frac{1}{2}$ hrs in addition to the 1 hr of Table I. Essentially the same catalytic activity was found in all cases. The effect of X may be attributed to an intrinsic difference in rate because of electronic factors which seems unlikely in view of the negligible effect X has on ν_{NO} or to differences in solubility of the catalyst. If a halogen-bridged species is present, such an explanation would be reasonable. The extremely dark color of the iodo system makes it difficult to fully assess the homogeneity of the reaction.

The presence of the ligands L is not essential for catalytic activity. The polymeric $[MoCl_2(NO)_2]_n$ in $PhCl$ with MASC gave a 24% conversion of 1-pentene to 4-octene in 1 hr at 0° – $5^\circ C$. However, a considerable quantity of polymeric material was apparently formed as only 23% of the unreacted 1-pentene was recovered. A comparable reaction using $MoCl_2(NO)_2(PPh_3)_2/MASC$ contained 48% 4-octene and 48% 1-pentene. Apparently the π -bonding ligands affect the selectivity of the derived catalyst. This can be explained in terms of their effect on the R_xAlCl_{3-x} activation step—in the absence of L a much greater percentage of the complex is converted to alkyl/hydride species which catalyze polymerization.

The variation in catalytic activity observed for changes in both X and L does not correlate with the $N-O$ stretching frequencies of the complexes. Different complex geometries for $L = Ph_3P, Ph_3PO,$ and py were noted above and could have an effect on the activity of the derived catalyst. Although further work in this area is required before definitive conclusions about the relationship between catalytic activity and the ligands of the complex can be reached, our results would suggest that some or all of these ligands remain attached to the molybdenum in its active form.

Comparison of the five complexes of Table III allow some more general conclusions about the effects of ligands. The two dichloro, dinitrosyl complexes are, of course, of the general type discussed above. The remaining complexes are isoelectronic and likewise coordinatively saturated and, with the exception of the last entry, six-coordinate. The results show that the simultaneous presence of both a chloride and a nitrosyl ligand greatly enhances catalytic activity. It would also appear that two of each of these ligands is not essential although one of the CO groups in $MoCl(CO)_2(NO)(bipy)$ could react in the same manner as a NO group (*see*

above). No major change in catalytic activity was produced by a chelating, π -bonding ligand as shown by the complexes $\text{MoCl}_2(\text{NO})_2(\text{bipy})$ and $\text{MoCl}_2(\text{NO})_2(\text{py})_2$ (Table III). However, shorter reaction times would be necessary to ascertain any minor differences in activity.

The complex $\text{MoCl}_2(\text{CO})_3(\text{PPh}_3)_2$ is the carbonyl equivalent of $\text{MoCl}_2(\text{NO})_2(\text{PPh}_3)_2$. Its very low activity indicates that CO cannot be completely substituted for NO. The values of ν_{CO} for the complex are very similar to those in $\text{MoCl}(\text{CO})_2(\text{NO})(\text{bipy})$ indicating that the extent of back-donation to the CO ligands is similar in the two complexes. The tungsten analogue $\text{WCl}_2(\text{CO})_3(\text{PPh}_3)_2$ has been reported to give good activity with 2-pentene after treatment with EtAlCl_2 in chlorobenzene (50).

The report that $\text{Mo}(\text{CO})_6$ could be activated for olefin disproportionation by thermal expulsion of CO (46) prompted us to use the dicarbonyl derivative of Table III in a similar manner. No activity was achieved by this technique. Photochemical activation of $\text{MoCl}_2(\text{NO})_2(\text{PPh}_3)_2$ was also unsuccessful.

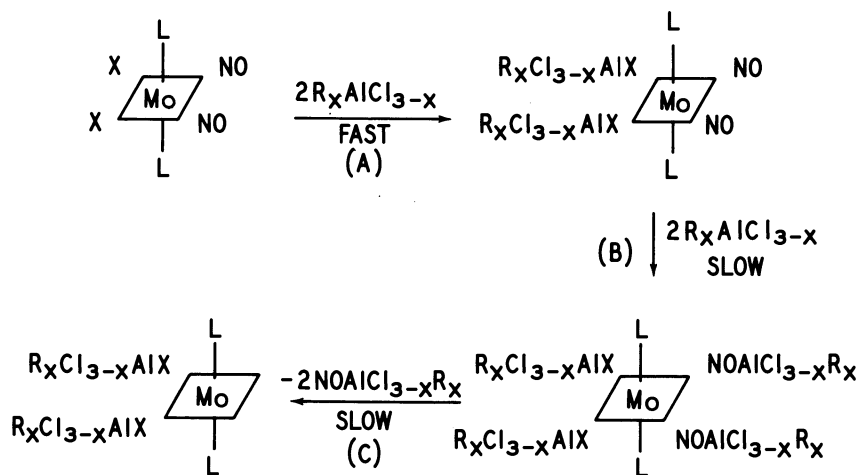
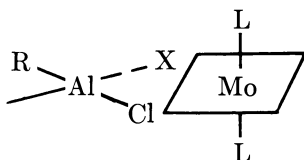


Figure 2. Reactions leading to catalyst generation in $\text{MoX}_2(\text{NO})_2\text{L}_2/\text{R}_x\text{AlCl}_{3-x}$ systems

In previous work, kinetic studies of the system $\text{MoCl}_2(\text{NO})_2(\text{py})_2/\text{EtAlCl}_2$ indicated a 4–5:1 ratio of organoaluminum to molybdenum complex gave maximum catalyst concentration (17). Stereochemical studies supported a mechanism in which the two reactant olefins occupy cis positions about the metal (16). From these results and those of the present paper, the sequence of catalyst-formation reactions shown in Figure 2 can be inferred for the $\text{MoX}_2(\text{NO})_2\text{L}_2/\text{R}_x\text{AlCl}_{3-x}$ systems. The geometry of the $\text{MoCl}_2(\text{NO})_2(\text{PPh}_3)_2$ complex is used to illustrate.

Evidence for the various steps in Figure 2 has been discussed in detail above. Some additional general comments about the scheme can be made. Complexation of R_xAlCl_{3-x} with the halide ligands (A), attack of the organoaluminum on the NO groups (B), and loss of the nitrosyl moieties (C) as shown occur synchronously for the two members of each pair of ligands. Reactions (A)-(C) could, however, themselves occur stepwise. Each of the two chloride ligands is shown coordinated to a R_xAlCl_{3-x} molecule. This point is not clear and a bridged species of the type shown below could be involved. Complexation of the olefins occurs at the cis sites vacated by the nitrosyl ligands.



The present studies and previous work (15) have established the order of catalytic activity for olefin disproportionation among the Group VIa metals as $Mo > W \gg Cr$. Although chromium derivatives yield poor disproportionation catalysts, the same complexes form good catalysts for the polymerization of simple olefins after reacting with organoaluminum reagents. For example, 1 mmole of $CrCl_2(NO)_2(OPPh_3)_2$ with MASC gave 16 grams of polyethylene in 1 hr at $30^\circ-35^\circ C$ (51). Thus, chromium nitrosyl complexes with organoaluminum compounds yield soluble polymerization catalysts whereas the molybdenum and tungsten analogues form disproportionation catalysts. This variation in behavior of homogeneous Group VIa catalysts parallels the behavior of heterogeneous catalysts of these metals as shown in Table VI.

Despite the difference in the type of ligands between the homogeneous and heterogeneous catalysts, similar energies and ordering of metal orbitals are achieved so that upon coordination of an olefin(s) a similar transformation occurs.

Table VI. Comparison of Catalytic Behavior of Group VIa Metals

<i>Catalyst</i>	<i>Reaction</i>
Heterogeneous	
CrO_3/Al_2O_3	Polymerization (C_2H_4)
$MO_3/Al_2O_3^a$	Disproportionation
Homogeneous	
$CrCl_2(NO)_2(OPPh_3)_2/(CH_3)_3Al_2Cl_3$	Polymerization (C_2H_4)
$MCl_2(NO)_2(OPPh_3)_2/(CH_3)_3Al_2Cl_3^a$	Disproportionation

^a M = Mo or W.

The difference in behavior of Cr compared with Mo and W may result from the mode of interaction between the metal complex and the organoaluminum reagent. As shown in Figure 2, catalyst formation from $\text{MoX}_2(\text{NO})_2\text{L}_2$ complexes (and the tungsten analogues as well) involves complexation of $\text{R}_x\text{AlCl}_{3-x}$ with the halide ligands. With the chromium complex, alkyl-halogen interchange may occur instead. The resulting Cr-alkyl bond could, through elimination of olefin, generate a Cr-H bond which would serve as a site for polymerization. The comparatively high N-O stretching frequency in the chromium derivative of Table IV indicates substantially greater NO^+ character to the nitrosyl groups. This would discourage attack by the electrophilic organoaluminum reagent on the NO ligands which is an essential step in catalyst generation.

Such a rationale would not apply to the difference in activity between molybdenum and tungsten. The values of ν_{NO} for the tungsten complexes are lower than those for the molybdenum analogues indicating increased back-donation to the nitrosyl groups in the former. Differences in metal orbital energies as reflected in the ν_{NO} data may be factors in determining catalytic activity.

The results of the study of ruthenium complexes given in Table V indicate that the presence of similar ligands in a similar configuration does not impart catalytic activity to a metal of another group in the same transition series as molybdenum. The very low activity of $\text{RuCl}_2(\text{CO})_2(\text{PPh}_3)_2$ is not surprising, however, in view of the failure of $\text{MoCl}_2(\text{CO})_3(\text{PPh}_3)_2$ to give an active catalyst. IR data indicates that for analogous complexes, both ν_{CO} and ν_{NO} occur at higher frequencies in the ruthenium derivatives compared with those of molybdenum. Thus, in $\text{MoCl}_2(\text{CO})_2(\text{PPh}_3)_2$ the C-O stretching vibrations are found at 1960 and 1890 cm^{-1} vs. 2058 and 1985 cm^{-1} for the Ru counterpart (however, the Mo complex is probably dimeric (38)). The molybdenum complex corresponding to $\text{RuCl}_3(\text{NO})(\text{PPh}_3)_2$ is not known, but for the analogous bipyridine derivatives ν_{NO} occurs at 1886 (1879) and 1705 cm^{-1} for ruthenium (52) and molybdenum (53), respectively. These results indicate greater back-donation of metal electrons to the π -bonding ligands (CO or NO) in the molybdenum complexes. Whether this implied difference in electronic properties of the two metals is responsible, either through a rate difference within similar catalyst molecules or through a lower catalyst concentration arising from a dichotomy in the organoaluminum reaction, for the low activity of the ruthenium complexes is not known.

The results for the series of oxo derivatives reinforce the conclusion drawn from the work with ruthenium and the Group VIa metals; the particular set of ligands which impart catalytic activity to one transition metal will not, in general, impart comparable activity (or even behavior) to another metal either within the same periodic group or

periodic series. In discussions of the effects of various ligands it must be borne in mind that the observed differences in relative activities may not necessarily be the result solely of intrinsic differences in similar catalytic species but may also be influenced by such factors as rates of catalyst formation, selectivities to catalytic species, and rates of catalyst decomposition.

It has been reported that ReCl_5 , when allowed to react with Et_3Al in the presence of appropriate amounts of oxygen, yields a disproportionation catalyst (54). It is possible that a ReOCl_3 species is formed and is responsible for the observed activity.

Literature Cited

1. Bailey, G. C., *Catal. Rev.* (1969) **3**, 37.
2. Calderon, N., *Accounts Chem. Res.* (1972) **5**, 127.
3. Hughes, W. B., *Organometal. Chem. Synth.* (1972) **1**, 341.
4. Banks, R. L., *Fortsch. Chem. Forsch.* (1972) **25**, 39.
5. Calderon, N., Ofstead, E. A., Ward, J. P., Judy, W. A., Scott, K. W., *J. Amer. Chem. Soc.* (1968) **90**, 4133.
6. Mol, J. C., Moulijn, J. A., Boelhouwer, C., *Chem. Commun.* (1968) 633.
7. Clark, A., Cook, C., *J. Catal.* (1969) **15**, 420.
8. Foster, G., German Patent **2063150** (1971); *Chem. Abstr.* (1971) **75**, 63172.
9. van Dam, P. B., Mittelmeijer, M. C., Boelhouwer, C., *Chem. Commun.* (1972) 1221.
10. Pennella, F., Banks, R. A., Bailey, G. C., *Chem. Commun.* (1968) 1548.
11. Bradshaw, C. P. C., Howman, E. J., Turner, L., *J. Catal.* (1967) **7**, 269.
12. Lewandos, G. S., Pettit, R., *Tetrahedron Lett.* (1971) 789.
13. Grubbs, R. H., Brunck, T. K., *J. Amer. Chem. Soc.* (1972) **94**, 2538.
14. Zuech, E. A., *Chem. Commun.* (1968) 1182.
15. Zuech, E. A., Hughes, W. B., Kubicek, D. H., Kittleman, E. T., *J. Amer. Chem. Soc.* (1970) **92**, 528.
16. Hughes, W. B., *Chem. Commun.* (1969) 431.
17. Hughes, W. B., *J. Amer. Chem. Soc.* (1970) **92**, 532.
18. Cotton, F. A., Johnson, B. F. G., *Inorg. Chem.* (1964) **3**, 1609.
19. Johnson, B. F. G., *J. Chem. Soc. A* (1967) 475.
20. Robinson, W. R., Swanson, M. E., *J. Organometal. Chem.* (1972) **35**, 315.
21. Stiddard, M. H. B., *J. Chem. Soc.* (1962) 4712.
22. Stephenson, T. A., Wilkinson, G., *J. Inorg. Nucl. Chem.* (1966) **28**, 945.
23. Laing, K. R., Roper, W. R., *J. Chem. Soc. A* (1970) 2149.
24. Levison, J. J., Robinson, S. D., *J. Chem. Soc. A* (1970) 2947.
25. Beck, W., Lottes, K., *Chem. Ber.* (1963) **96**, 1046.
26. Brown, D., Easey, J. F., du Preez, J. G. H., *J. Chem. Soc. A* (1966) 258.
27. Horner, S. M., Tyree, Jr., S. Y., *Inorg. Chem.* (1962) **1**, 122.
28. Chatt, J., Rowe, G. A., *J. Chem. Soc.* (1962) 4019.
29. Edwards, D. A., *J. Inorg. Nucl. Chem.* (1965) **27**, 303.
30. Chatt, J., Falk, C. D., Leigh, G. J., Paske, R. J., *J. Chem. Soc. A* (1969) 2288.
31. Canziani, F., Sartorella, U., Cariati, F., *Ann. Chim. Rome* (1964) **54**, 1354.
32. Hughes, W. B., Zuech, E. A., *Inorg. Chem.* (1973) **12**, 471.
33. Mann, B. E., Shaw, B. L., Stainbank, R. E., *Chem. Commun.* (1972) 151.
34. Visscher, M. O., Caulton, K. G., *J. Amer. Chem. Soc.* (1972) **94**, 5923.
35. Mingos, D. M. P., Ibers, J. A., *Inorg. Chem.* (1971) **10**, 1479.

36. Hughes, W. B., Baldwin, B. A., *Inorg. Chem.* (1974) **13**, 1531.
37. Zuech, E. A., unpublished data.
38. Colton, R., Tomkins, I. B., *Aust. J. Chem.* (1966) **19**, 1143.
39. Fahey, D. R., *J. Org. Chem.* (1973) **38**, 80.
40. Hughes, W. B., Zuech, E. A., Kittleman, E. T., Kubicek, D. H., *XXIII IUPAC Congr., Macromolec. Prepr.*, Vol. II (1971) 1063.
41. Collman, J. P., Hoffman, N. W., Morris, D. E., *J. Amer. Chem. Soc.* (1969) **91**, 5659.
42. Shriver, D. F., Alich, M., *Inorg. Chem.* (1972) **11**, 2984.
43. Crease, A. E., Legzdins, P., *Chem. Commun.* (1972) 268.
44. Doyle, G., German Patent **2047270** (1971).
45. Kroll, W. R., Doyle, G., *Chem. Commun.* (1971) 839.
46. Lewandos, G. S., Pettit, R., *J. Amer. Chem. Soc.* (1971) **93**, 7087.
47. Wang, J-L, Menapace, H. R., Brown, M., *J. Catal.* (1972) **26**, 455.
48. Singleton, D. M., U.S. Patent **3,530,196** (1970).
49. Chatt, J., Haines, R. J., Leigh, G. J., *Chem. Commun.* (1972) 1202.
50. Bencze, L., Marko, L., *J. Organometal. Chem.* (1971) **28**, 271.
51. Zuech, E. A., *J. Polym. Sci.: Polym. Chem. Ed.* (1972) **10**, 3665.
52. Fairy, M. B., Irving, R. J., *J. Chem. Soc. A* (1966) 475.
53. Davis, R., Johnson, B. F. G., Al-Obaidi, K. H., *J. Chem. Soc. Dalton* (1972) 508.
54. Uchida, Y., Hidai, M., Tatsumi, T., *Bull. Chem. Soc. Jap.* (1972) **45**, 1158.

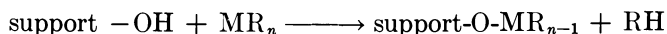
RECEIVED September 27, 1973.

Supported Organometallic Catalysts

J. P. CANDLIN and H. THOMAS

Imperial Chemical Industries Ltd., Corporate Lab., P.O. Box 11, The Heath, Runcorn, Cheshire, England

Many moisture sensitive organometallic compounds react with the surface hydroxyl groups of silica and alumina. The general reaction is



where M = Ti, Zr, Nb, Cr, Mo, W and R = π -allyl ($-\text{C}_3\text{H}_5$) and benzyl. The stoichiometry of the reaction with support surfaces has been studied by volumetric measurements of propene evolution and GLC estimation of toluene. ESR studies of supported tetra- π -allylniobium indicate that the organometallic compound may be attached to the support by one or more chemical bonds. IR spectroscopic evidence for interaction of ethylene with the supported zirconium polymerization system is presented. The catalytic activity of these organometallic compounds in ethylene polymerization and olefin disproportionation is greatly enhanced when they are chemically attached to inorganic oxide supports.

The heterogenizing of homogeneous catalysts by interaction with a solid support material is a recent development in catalytic studies (1, 2, 3). Not only does this facilitate separation of catalyst from products, but in some cases heterogenizing increases the activity and/or selectivity of a particular reaction (4). An early example of this approach is the Merrifield synthesis of polypeptides in which an organic polymeric support is used (5, 6). This technique has been extended to include organic polymers containing donor groups such as substituted tertiary phosphines, tertiary nitrogen, and cyclopentadienyl ligands which are capable of complexing transition metal centers (7, 8, 9, 10, 11, 12). Such com-

plexed metal derivatives have been used as heterogeneous catalysts for carbonylation, hydrogenation, and dimerization of olefins.

Inorganic supports are less prevalent (13, 14). An elegant technique for heterogenizing catalytic gas/liquid reaction systems has been developed in which the catalyst is dissolved in a high boiling solvent and the mixture is adsorbed into the pores of an inorganic oxide matrix. The resulting material looks like a dry solid and has been used to catalyze many gas-phase reactions (15, 16). This technique has been called multiphase catalysis. No interaction of the catalytic species or the reactant with the support is envisaged. An advantage of this method is that the homogeneous reaction can be translated into a gas/solid reaction system, the chemistry being essentially similar for both systems.

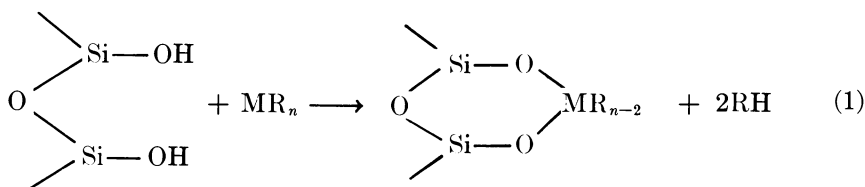
Another approach using inorganic supports is to make a heterogeneous system by using the known chemistry of the support surface and of the homogeneous catalyst. The chemistry of acidic oxides, *e.g.*, SiO_2 , Al_2O_3 , TiO_2 , which contain surface hydroxyl groups, has been well documented, and many reactions with simple molecules have been reported (16, 17, 18). In many examples these involve the reaction of the surface hydroxyl group with water sensitive compounds, either in the vapor phase or in a dry solvent by slurring (2, 3).

The pretreatment of the oxide support determines the nature and concentration of the reactive species on the surface. For example, two distinct types of surface hydroxyl sites have been reported on fully hydroxylated silica surfaces (20). These sites are distributed as 1,4 single surface hydroxyls (type A sites) and $\sim 3,2$ interacting hydroxyl groups arranged in pairs (1,6-type B sites) per 100 Å^2 of silica surface. On heating, the silica type B sites are progressively removed, and at 500°C virtually all type B sites are eliminated to form surface siloxane bridges, Si-O-Si (type S sites). The type A site concentration, however, remains constant up to $\sim 600^\circ\text{C}$. Similar studies have been reported in the literature for alumina (21) and titania (22) although the surface cannot be as precisely defined for these as for silica.

The reaction of water sensitive compounds with alumina surfaces is complicated not only by the multiplicity of the surface hydroxyl groups but also by the Lewis acid centers which can give a strong physical adsorption of the compound without chemical reaction.

Many organometallic compounds are moisture sensitive, a particularly important class from the catalytic viewpoint being transition metal hydrocarbyl derivatives (M^+R_n). These compounds have been used as catalysts for or have been postulated as catalytic intermediates in many olefin reactions such as polymerization, oligomerization, and olefin disproportionation (23). Recent work has shown that compounds containing

hydrocarbyl ligands which possess no β -hydrogen [and hence cannot decompose by olefin elimination (24, 25)] possess sufficient thermal stability to make them accessible for use at ambient temperatures without impairing their catalytic activity. Notable in this class are transition metal π -allyl, $M(\text{CH}_2=\text{CH}=\text{CH}_2)_n$, benzyl, $M(\text{CH}_2\text{C}_6\text{H}_5)_n$, and trimethylsilylmethyl, $M(\text{CH}_2\text{Si}(\text{CH}_3)_3)_n$ compounds. Early transition metal derivatives containing these ligands, for example, $\text{Zr}(\text{benzyl})_4$, $\text{Nb}(\pi\text{-allyl})_4$, $\text{Mo}_2(\pi\text{-allyl})_4$, are extremely moisture sensitive, and solutions of these compounds in inert solvents such as toluene or pentane react with the surface hydroxyl groups of acidic oxides (2). This reaction is envisaged as follows:



Since many of these compounds are strongly colored and react instantly with oxide surfaces, the accessible surface hydroxyl concentration can be estimated by visually titrating a known amount of dried support with the metal hydrocarbyl solution until the supernatant liquid remains colored.

There is evidence in the literature that many of these transition metal derivatives, when chemically bonded or grafted onto an inorganic oxide surface, possess catalytic activity for olefin reactions far greater than that observed when the organometallic compound is used in a homogeneous manner (26). In some examples, catalytic activity was promoted when the original compound had none (3, 27).

The reactions chosen for study in this work were olefin polymerization and olefin disproportionation. Catalysts for the former reaction are, in the majority of cases, metal derivatives of Groups IVB–VIB whereas compounds of molybdenum, tungsten, and rhenium are recognized as catalysts for olefin disproportionation.

We report here a study of Zr, Nb, Cr, and Mo hydrocarbyl compounds grafted onto oxide supports as potential olefin polymerization catalysts and oxide-supported Mo and W π -allyl derivatives in olefin disproportionation catalyses. The interaction of these compounds with silica and alumina supports has been examined using ESR and IR, analyses to define the catalytic materials that result. Finally, we consider why chemical support of these organometallic compounds confers on them an enhanced catalytic activity.

Experimental

All manipulations involving either the preparation of the metal hydrocarbyl compounds or their examination were made with the complete exclusion of oxygen and water.

Metal Hydrocarbyl Compounds. Tetra- π -allyl compounds of zirconium, niobium, tungsten, tris- π -allylchromium, and tetrabenzylzirconium were prepared by methods analogous to those described in the literature (28, 29, 30) while the molybdenum allyls were prepared by both established (28, 31) and novel routes (32, 33). All the compounds are oxygen- and moisture-sensitive, and the preparations and all experiments were carried out in flamed, vacuum-degassed glassware under an atmosphere of dry, oxygen-free nitrogen. All solvents were dried over sodium wire and deoxygenated before use. Allylmagnesium chloride and bromide solutions in diethyl ether were prepared from the corresponding allyl halide (34). Lithium allyl was prepared by the reaction of lithium metal and allylphenyl ether at -15°C in diethyl ether solvent (35) and estimated by established methods (36).

Tetra- π -allylzirconium, $\text{Zr}(\pi\text{-C}_3\text{H}_5)_4$. Anhydrous ZrCl_4 (Alfa Inorganics) was added for 4 hrs to a stirred $(\text{C}_2\text{H}_5)_2\text{O}$ solution containing 4.4 equivalents $\text{C}_3\text{H}_5\text{MgBr}$ at -30°C , and stirring was continued for 20 hrs at the same temperature. The $(\text{C}_2\text{H}_5)_2\text{O}$ solvent was removed *in vacuo* at -40°C , and the resulting red solid was extracted with pentane at -40°C . The deep red extract was filtered through kieselguhr at the same temperature. Upon concentration and cooling to -80°C , dark red needle-like crystals were obtained from the extract, the IR spectrum of which (Figure 1) is consistent with published data (37). Pentane solutions of $\text{Zr}(\pi\text{-allyl})_4$ are stable for several months at -40°C . Typical yields for this reaction are 50–60%.

Tetra- π -allylniobium, $\text{Nb}(\pi\text{-C}_3\text{H}_5)_4$. This was prepared similarly to $\text{Zr}(\pi\text{-allyl})_4$, starting from anhydrous NbCl_5 (Johnson–Matthey) and 5.5 equivalents of $\text{C}_3\text{H}_5\text{MgCl}$ solution. Temperature control of the reaction and product work-up were similar. The final pentane extract was

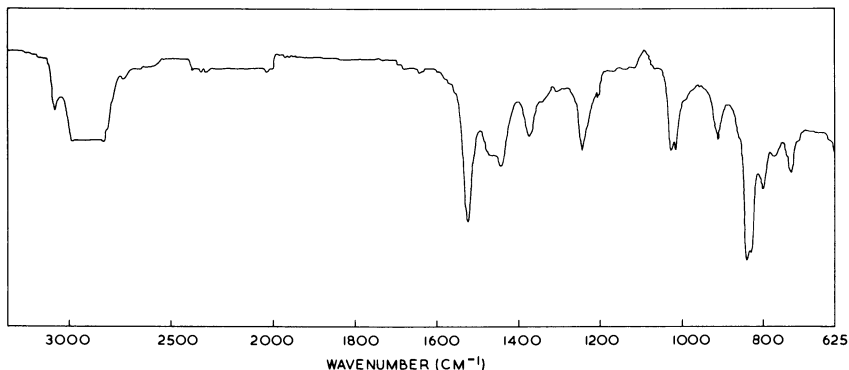


Figure 1. IR spectrum of $\text{Zr}(\pi\text{-allyl})_4$ in hexane compensated for solvent

dark green and yielded small green-black crystals identified by IR spectroscopy as $\text{Nb}(\pi\text{-allyl})_4$ (37).

Tris- π -allylchromium, $\text{Cr}(\pi\text{-C}_3\text{H}_5)_3$. Powdered $\text{CrCl}_3 \cdot 3\text{THF}$ was added to 3.5 equivalents of $\text{C}_3\text{H}_5\text{MgCl}$ in $(\text{C}_2\text{H}_5)_2\text{O}$ solution at -20°C . Evaporation of the ether solution at -20°C yields a dark colored solid which on extraction with pentane at -20°C yielded a blood red solution identified by IR as $\text{Cr}(\pi\text{-allyl})_3$ (Figure 2) (38).

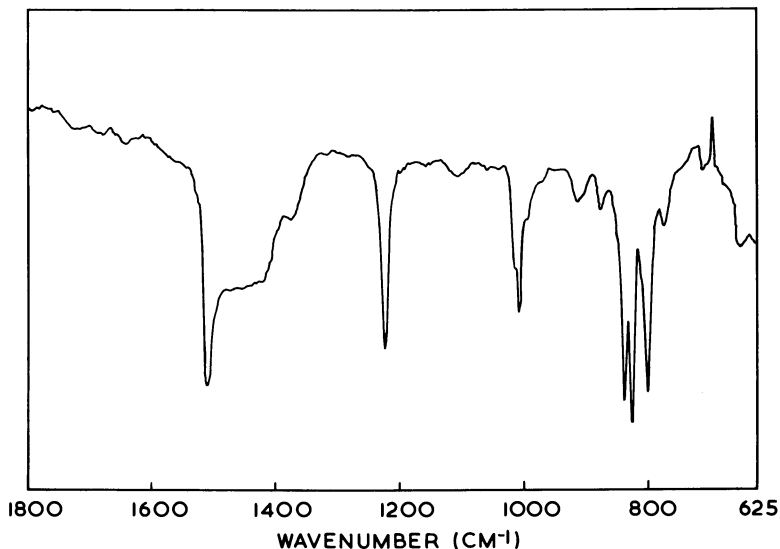


Figure 2. IR spectrum of $\text{Cr}(\pi\text{-allyl})_3$ in pentane compensated for solvent

Tetrabenzylzirconium, $\text{Zr}(\text{CH}_2\text{C}_6\text{H}_5)_4$. This was prepared by methods described in the literature (39, 40, 41, 42, 43).

Tetra- π -allyltungsten, $\text{W}(\pi\text{-C}_3\text{H}_5)_4$. Anhydrous WCl_6 (Alfa Inorganics) was added for 3 hrs to a stirred $(\text{C}_2\text{H}_5)_2\text{O}$ solution containing 6.5 equivalents of $\text{C}_3\text{H}_5\text{MgCl}$ at room temperature. The resulting brown suspension was stirred for 2 hrs. The ether was removed *in vacuo* at ambient temperature, the dark brown residue was extracted with pentane, and the pale brown extract was filtered through kieselguhr. The extract was concentrated at room temperature and cooled to yield small pale brown crystals which were purified by sublimation at $70^\circ\text{--}75^\circ\text{C}$ at 0.1 mm Hg. IR (Figure 3) and PMR (Figure 4) spectra are consistent with those reported (38) for pure $\text{W}(\pi\text{-allyl})_4$. Overall yields in this experiment were of the order of 10%.

A modification of this synthesis in which WCl_6 was added to a stirred THF solution of $\text{C}_3\text{H}_5\text{MgCl}$ at 60°C resulted in 30% overall yields of $\text{W}(\pi\text{-allyl})_4$. Similar yields were also obtained from the reaction between WCl_6 and 6.5 equivalents of LiC_3H_5 in Et_2O at room temperature by a procedure analogous to that described above.

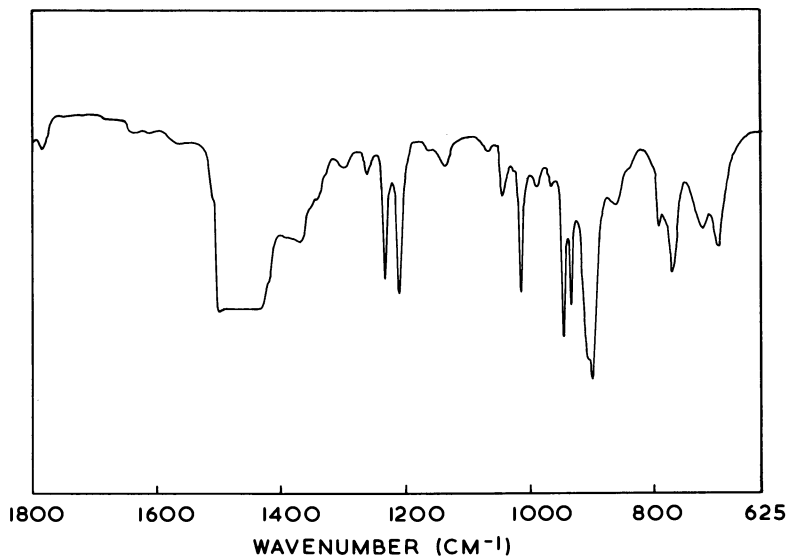


Figure 3. IR spectrum of $W(\pi\text{-allyl})_3$ in pentane compensated for solvent

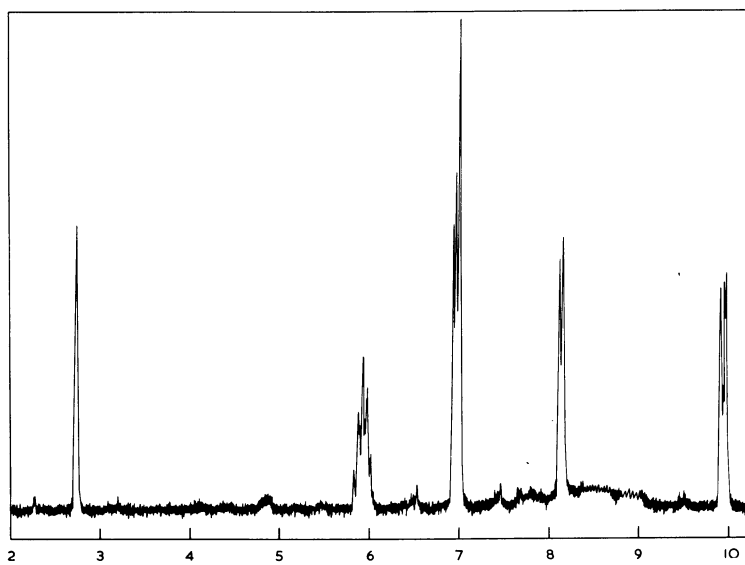


Figure 4. 220 MHz PMR spectrum of $W(\pi\text{-allyl})_3$ in perdeuterobenzene

Tetra- π -allylmolybdenum, $\text{Mo}(\pi\text{-C}_3\text{H}_5)_4$, and *Tetra- π -allyldimolybdenum*, $\text{Mo}_2(\pi\text{-C}_3\text{H}_5)_4$. These compounds were initially prepared by a method similar to those described in the literature (31, 38). Anhydrous MoCl_5 (Climax Molybdenum Co.) was added for 4 hrs to a stirred $(\text{C}_2\text{H}_5)_2\text{O}$ solution containing 5.5 equivalents of $\text{C}_3\text{H}_5\text{MgCl}$ at room temperature, and stirring was continued for 2 hrs. The $(\text{C}_2\text{H}_5)_2\text{O}$ was removed *in vacuo*, and a dark green solid was extracted with pentane. The deep green colored solution was quickly filtered through kieselguhr, concentrated and cooled to -80°C when dark green crystals separated out. IR analysis showed the pentane mother liquor to be rich in $\text{Mo}(\pi\text{-allyl})_4$ and the green crystals to be mainly $\text{Mo}_2(\pi\text{-allyl})_4$. The green crystals were further purified by repeated recrystallization from the minimum amount of pentane at -80°C to give a final product of pure $\text{Mo}_2(\pi\text{-allyl})_4$, as shown by IR and PMR. The original mother liquor, after repeated concentration and cooling to -80°C to remove $\text{Mo}_2(\pi\text{-allyl})_4$, was evaporated to dryness, and the residue was sublimed at 60°C and 0.01 mm Hg. The pale green sublimate was dissolved in pentane to yield a pale green solution of mainly $\text{Mo}(\pi\text{-allyl})_4$ contaminated with some $\text{Mo}_2(\pi\text{-allyl})_4$, shown by IR. Exposure of the pale green solution to air resulted in selective decomposition of $\text{Mo}_2(\pi\text{-allyl})_4$ with the formation of a brown precipitate and a pale yellow supernatant liquor from which a pale yellow product was obtained by evaporation. This was purified by sublimation at 60°C and 0.01 mm Hg to give pale yellow crystals of pure $\text{Mo}(\pi\text{-allyl})_4$, as shown by chemical, IR (Figure 5), and PMR (Figure 6) analyses.

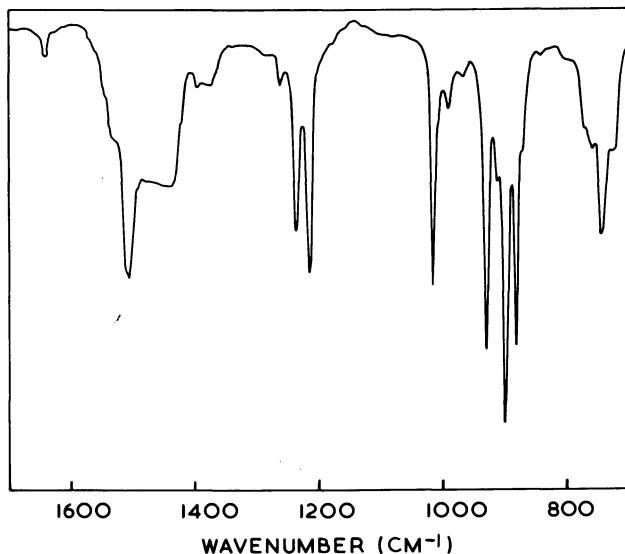


Figure 5. IR spectrum of $\text{Mo}(\pi\text{-allyl})_4$ in pentane compensated for solvent

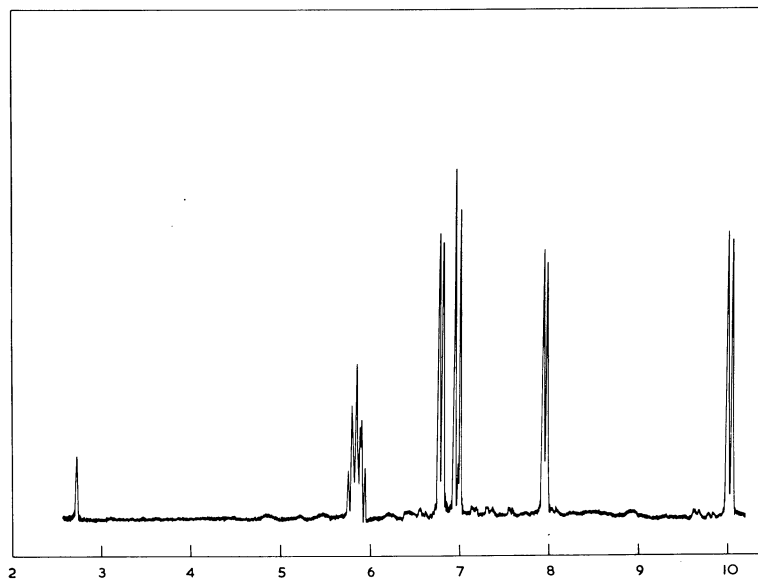


Figure 6. 220 MHz PMR spectrum of $\text{Mo}(\pi\text{-allyl})_4$ in perdeutero-benzene

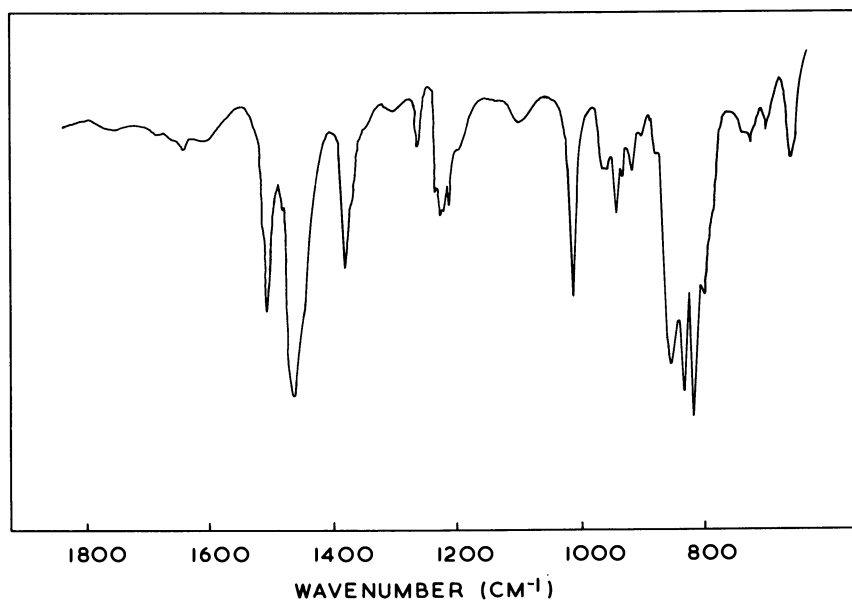


Figure 7. IR spectrum of $\text{Mo}_2(\pi\text{-allyl})_4$ in nujol

Tetra- π -allyldimolybdenum, $\text{Mo}_2(\pi\text{-C}_3\text{H}_5)_4$. A novel, straightforward route to $\text{Mo}_2(\pi\text{-allyl})_4$ exclusively, involves the reaction of a metal-metal bonded molybdenum(II) complex with $\text{C}_3\text{H}_5\text{MgX}$ with retention of the Mo-Mo bond (32, 33). Freshly prepared $\text{Mo}_2(\text{OCOCH}_3)_4$ (44) was added for 1 hr to a stirred $(\text{C}_2\text{H}_5)_2\text{O}$ solution containing 5 equivalents $\text{C}_3\text{H}_5\text{MgCl}$ at 0°C . The deep green solution was stirred at this temperature for 1 hr after which the ether solvent was removed *in vacuo* at 0°C . The residue was extracted with pentane at 0°C , and the extract quickly filtered through kieselguhr to yield a clear, green solution. Upon concentration of this filtrate and cooling to -80°C , deep green crystals separated out which were shown by IR (Figure 7) and PMR analysis to be pure $\text{Mo}_2(\pi\text{-allyl})_4$. Chemical analysis gave C, 38.82%; H, 5.66%; Mo, 53.90%. $\text{Mo}_2\text{C}_{12}\text{H}_{20}$ requires C, 40.43%; H, 5.11%; Mo, 54.38%. Typical yields were 40–50%.

Supports. The silica and alumina supports used in this work were standard commercial materials.

Stoichiometry of Reaction of Metal Hydrocarbyls with Supports. The reaction of $\text{Zr}(\pi\text{-allyl})_4$ and silica support surfaces was studied volumetrically using a conventional vacuum system fitted with a Topley pump and gas buret (45). Silica samples (Cabosil M5, Aerosil 380, or Manosil VN3) were weighed into a reaction vessel which could be attached to the vacuum system and dried and evacuated at 200°C to 650°C and at pressures less than 10^{-4} mm Hg. The dry support was allowed to cool and was slurried with a measured amount of toluene, the slurry being thoroughly degassed at -80°C . Solutions of known concentrations of $\text{Zr}(\pi\text{-allyl})_4$ in toluene and CH_3MgI in anisole were also thoroughly degassed at -80°C . To measure the total surface hydroxyl concentration, an excess of the organometallic reagent was run into the stirred silica slurry, and the C_3H_6 or CH_4 produced by reaction with the support was distilled from the solvent vapors and measured using a Topley pump and gas buret.

To study the stoichiometry of the reaction of $\text{Zr}(\pi\text{-allyl})_4$ with support surfaces, measured amounts of the reagent were run into the stirred silica slurry, and the produced C_3H_6 was measured as before. The unreacted π -allyl groups in the supported zirconium complex could be estimated by adding an excess of degassed *n*-butyl alcohol to the slurry and then measuring the resulting C_3H_6 in the gas buret.

The reaction of $\text{Zr}(\text{benzyl})_4$ with alumina support surfaces was studied by gas chromatographic analysis of the toluene produced in the reaction. Powdered alumina samples were weighed into a reaction vessel and dried *in vacuo* at 600° to 900°C . The dried support was allowed to cool and was slurried with a measured amount of benzene containing pure *m*-xylene as an internal standard for the gas chromatographic analysis. To study the reaction of $\text{Zr}(\text{benzyl})_4$ with support surfaces, measured amounts of a benzene solution of the reagent were run into the stirred alumina slurry, the suspension was allowed to settle, and small quantities of the supernatant were withdrawn for analysis. As described above, the residual benzyl groups in the supported zirconium complex could be estimated by adding excess *n*-butyl alcohol to the slurry. After prolonged stirring another sample of supernatant was removed for analysis.

ESR of Supported Nb(π -allyl)₄ (46). ESR studies of the reaction of the paramagnetic Nb(π -allyl)₄ with supports were made using a Varian V4500-10A spectrometer. Supports (0.1–0.2 gram) were dried and treated with pentane solutions of Nb(π -allyl)₄ in borosilicate glass vessels having ESR sample tubes glassblown onto them to ease sample handling. Silica (Manosil VN3) was dried *in vacuo* at 250° or 650°C for 2 hrs before use, and powdered alumina samples were dried at 250° to 750°C for 2 hrs. The dried supports were cooled in a nitrogen atmosphere, slurried with a small quantity of pentane, and treated with a known volume of a pentane solution of Nb(π -allyl)₄ which reacted immediately with the support. The support turned brown. This color appears to be typical of supported metal π -allyl complexes, irrespective of the color of the complex in solution. The pentane solvent could be removed under vacuum at room temperature, and the dry solid was transferred to the ESR tube by tilting the reaction vessel. ESR spectra could be obtained at temperatures from room temperature down to –180°C, solution spectra being studied below –40°C to prevent thermal decomposition of Nb(π -allyl)₄.

IR Studies of Surface Species. IR studies of the reaction between Zr(π -allyl)₄ and silica support surfaces have been described (41, 42, 43). A more detailed study, including the reaction of the supported species with C₂H₄ gas has been carried out using a modified Perkin Elmer model 257 IR spectrometer.

A self-supporting silica disc (~10 mg, grade 952) was initially dried by heating to 500°C under vacuum for 16 hrs. Upon cooling, an IR spectrum of the disc indicated only isolated hydroxyl (Type A) sites. The disc was then fitted against a calcium fluoride window and rapidly transferred to a high pressure IR cell, the details of which have been described previously (47). The brief exposure of the silica disc should not cause irreversible hydration of the siloxane bridge (48); an IR spectrum taken in the high pressure cell indicated that only Type A sites and physisorbed water were present. The adsorbed water was removed by heating to 150°C at 0.05 mm Hg.

This redried silica disc was treated with Zr(π -allyl)₄ (0.54 mmole in toluene 20 ml) for 30 min under nitrogen (~15 atm). The excess Zr(π -allyl)₄ solution was removed, and the disc was washed successively with toluene and hexane followed by drying under vacuum at room temperature. IR spectra of the supported zirconium species were recorded before and after exposure to various pressures of ethylene.

Catalytic Polymerization of Ethylene. Polymerization experiments were carried out in a conventional stirred reactor (43).

Catalytic Disproportionation of 1-Hexene. Silica and alumina supports were dried by heating *in vacuo* at 200° and 500°C at 10⁻⁴ mm Hg. The dried supports were cooled under nitrogen and treated for several hours with an excess of a pentane solution of the appropriate π -allyl compound at 0°C. The supports were washed several times by decantation with pentane and dried under vacuum at room temperature.

1-Hexene was added to a known weight of the supported π -allyl compound in a vessel fitted with an efficient reflux condenser, and the mixture was stirred at 20°–60°C. Ten-microliter samples were removed at intervals and analyzed by GLC using a 10% squalane/Embacel column.

Control experiments with the π -allyl compounds in the absence of silica or alumina supports and with the dried support materials themselves were carried out in an analogous manner.

Results

Reaction of Metal Hydrocarbyl Compounds with Support Surfaces.

Initial experiments in which 1-gram samples of silica were heated at 200°C under vacuum, slurried with 30 ml toluene, and treated with an excess of $\text{Zr}(\pi\text{-allyl})_4$ or CH_3MgI showed good agreement between the two reagents and good experimental reproducibility (Table I).

Table I. Surface Hydroxyl Content of Silica (41, 42, 43)

Reagent	Hydroxyl Content mmole/gram	Hydroxyl Content per 100 A^2
CH_3MgI	0.841	2.07
	0.889	
$\text{Zr}(\pi\text{-allyl})_4$	0.854	2.06
	0.897	
	0.821	

The effect of drying temperature on the surface hydroxyl concentration for Manosil VN3 slurried with 25 ml toluene and treated with excess $\text{Zr}(\pi\text{-allyl})_4$ is shown in Figure 8. The discrepancy between these results and literature determinations of surface hydroxyl concentrations (20, 49, 50) prompted an investigation of the experimental technique. It was found that the concentration of the silica slurry had a profound effect on the degree of reaction with the organometallic. The results for Aerosil 380 dried at 200°C for 2 hrs under vacuum, slurried with toluene, and allowed to react with excess $\text{Zr}(\pi\text{-allyl})_4$ or CH_3MgI are shown in Figure

Table II. Stoichiometry of Reaction of Metal Hydrocarbyls with Silica and Alumina Supports (41, 42, 43)

Support	Drying Temperature, °C	Reagent	Reaction with Support, moles RH/moles MR_n^a	Reaction with Butyl Alcohol, moles RH/moles MR_n^a
Silica	200	$\text{Cr}(\pi\text{-allyl})_3$	2.19	0.75
	200	$\text{Zr}(\pi\text{-allyl})_4$	2.16	2.19
Alumina	600	$\text{Zr}(\text{benzyl})_4$	1.97	2.07
	750		1.02	3.08
	^b 600		2.1	2.0

^a This indicates the moles of hydrocarbon (RH) liberated per mole of organometallic (MR_n) reacted.

^b This sample was annealed at 900°C for 15 hrs and rehydrated by boiling in water.

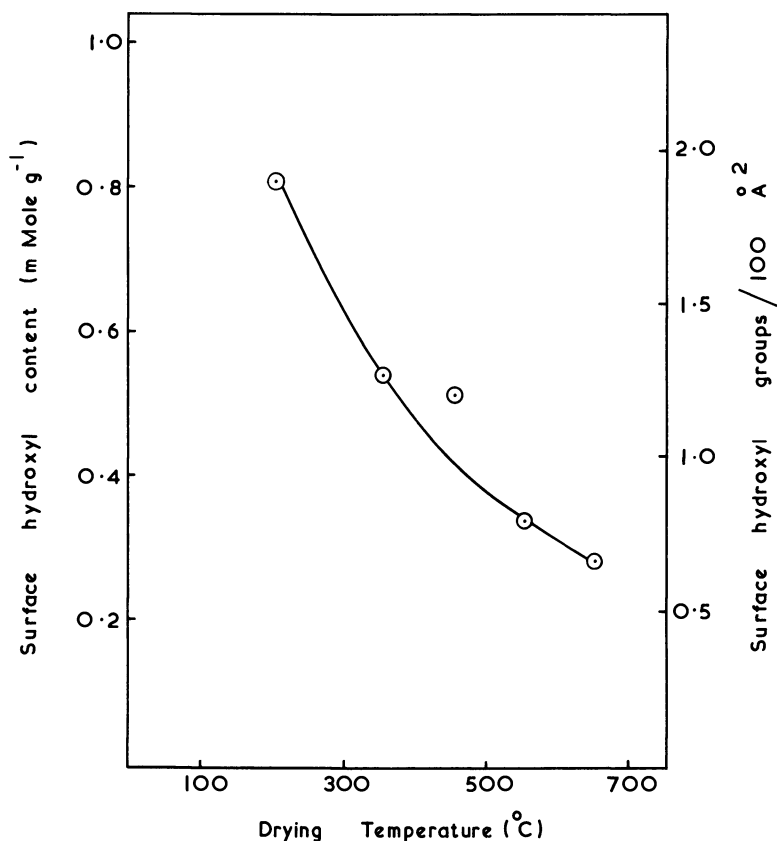


Figure 8. Variation of available surface hydroxyl content with drying temperature for 4% W/v slurry in toluene

9. At slurry concentrations below 0.01%, both reagents give similar values for surface hydroxyl concentration which are consistent with literature values (~ 4.6 hydroxyls/100 Å²).

Typical results for the reaction of measured amounts of metal hydrocarbyl with supports, followed by estimation of the unreacted hydrocarbyl groups by reaction with excess *n*-butyl alcohol, are shown in Table II.

ESR Studies. The isotropic ESR spectra of a solution of Nb(π -allyl)₄ in THF and the frozen solution are shown in Figure 10. The spectra at -180°C and room temperature of Nb(π -allyl)₄ after reaction with silica (Manosil VN3) dried at 650°C are shown in Figure 11; the corresponding spectra for silica dried at 250°C are in Figure 12.

Dehydration of powdered alumina at 250°C – 750°C followed by reaction with Nb(π -allyl)₄ gave, in all cases, spectra identical to Figure 13.

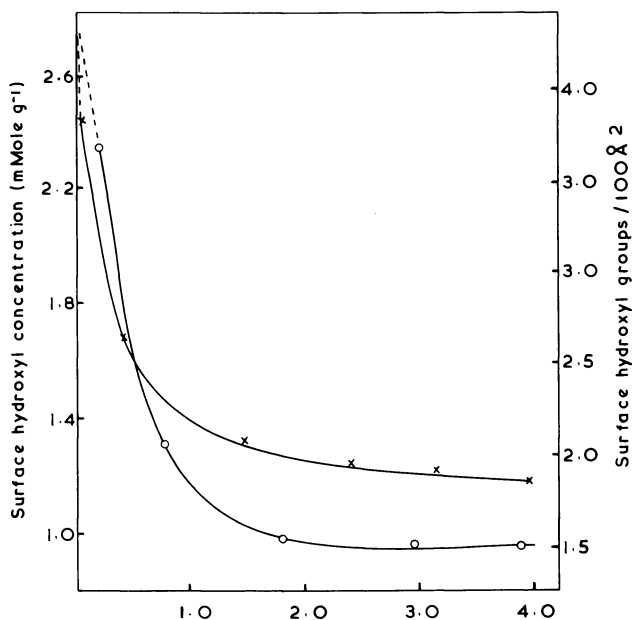


Figure 9. Apparent surface hydroxyl concentration as a function of slurry concentration: ○ Reaction with $Zr(\pi\text{-allyl})_4$, × Reaction with CH_3MgI

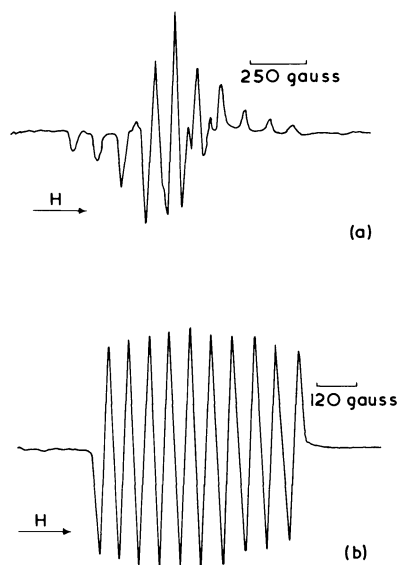


Figure 10. ESR spectra of $Nb(\pi\text{-allyl})_4$ in tetrahydrofuran: (a) at $-180^\circ C$, (b) at $-40^\circ C$

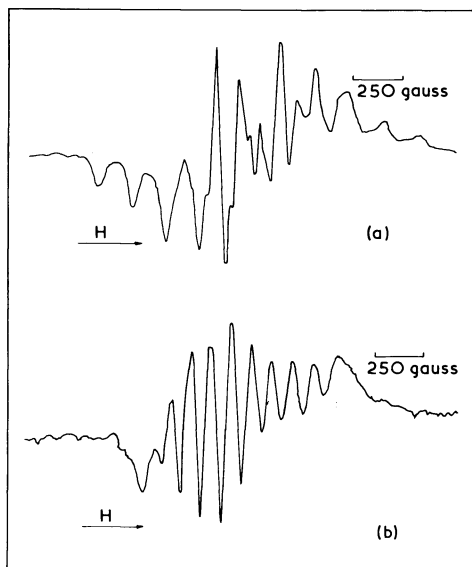


Figure 11. ESR spectra of $Nb(\pi\text{-allyl})_3$ after reaction with silica dried at 650°C : (a) at -180°C , (b) at room temperature

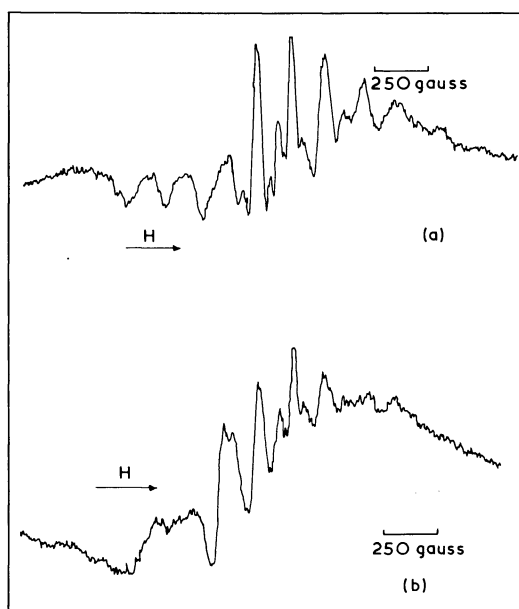


Figure 12. ESR spectra of $Nb(\pi\text{-allyl})_3$ after reaction with silica dried at 200°C : (a) at 180°C , (b) at room temperature

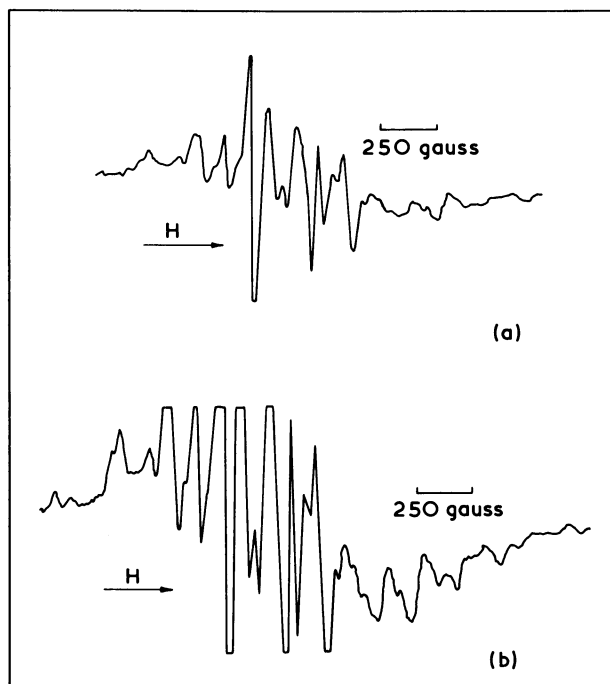


Figure 13. ESR spectra of $\text{Nb}(\pi\text{-allyl})_3$ after reaction with alumina: (a) low gain spectrum, (b) high gain spectrum

IR Studies. The IR spectra of the dried silica disc before and after treatment with $\text{Zr}(\pi\text{-allyl})_4$ and after subsequent exposure to ethylene are shown in Figure 14.

Polymerization of Ethylene. The initial investigations were carried out using homogeneous organometallic catalysts. The results are shown in Table III.

Polymerization activity was markedly enhanced when the catalysts were chemically grafted onto inorganic supports. Typical results are

Table III. Homogeneous Polymerization of Ethylene in Toluene, 500 ml (41, 42, 43)

Catalyst, mmole	Temperature, °C	Activity ^a
Zr ($\pi\text{-allyl}$) ₄ , 1.5	160	0.9
0.8	50	0.65
Nb ($\pi\text{-allyl}$) ₄ , 1.5	160	0.2
Cr (2-methallyl) ₃ , 3	160	0.4

^a Activity is expressed as gram polyethylene/mmole of catalyst/hr/atm of C_2H_4 .

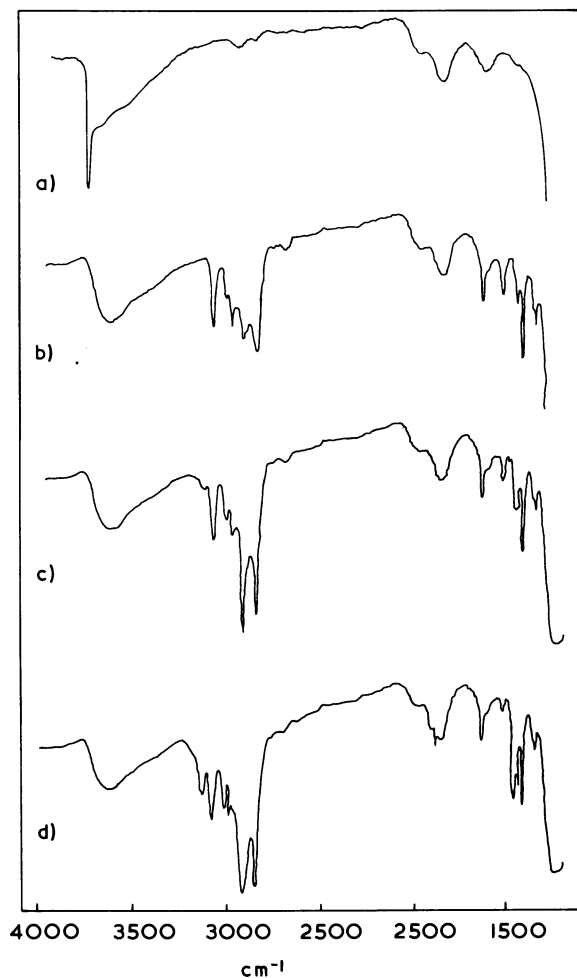


Figure 14. IR spectra of silica disc: (a) after drying at 500°C, (b) after reaction with $Zr(\pi\text{-allyl})_2$, (c) after admission of ethylene at 1.5 atms/25°C/30 min, and (d) after admission of ethylene at 3 atms/45°C/90 min

shown in Table IV. Typical results from the 1-hexene disproportionation experiments are summarized in Table V.

Disproportionation of 1-hexene did not occur with the above metal hydrocarbyl compounds in the absence of supports. Conditions for these experiments were ~ 24 hrs at room temperature followed by several hours at $\sim 68^\circ\text{C}$ (refluxing 1-hexene). The support materials themselves also failed to catalyze the disproportionation reaction.

Table IV. Heterogeneous Polymerization of Ethylene in Toluene, 500 ml (41, 42, 43)

<i>Catalyst, mmole</i>	<i>Support</i>	<i>Temperature, °C</i>	<i>Activity^a</i>
Zr (π -allyl) ₄ , 0.4	SiO ₂	80	38
0.2	Al ₂ O ₃	80	595
Zr (benzyl) ₄ , 0.2	Al ₂ O ₃	80	386
Cr (π -allyl) ₃ , 0.2	Al ₂ O ₃	80	194
Nb (π -allyl) ₄ , 0.5	Al ₂ O ₃	65	15
Mo (π -allyl) ₄ , 0.5	Al ₂ O ₃	65	0.5
Mo ₂ (π -allyl) ₄ , 0.5	Al ₂ O ₃	65	2

^a Activity is expressed as gram polyethylene/mmole of catalyst/hr/atm of C₂H₄.

Discussion

Surface Acidity of Silica and Alumina (51, 52, 53). The crystal lattices of many inorganic oxides are terminated by surface hydroxyl groups. Under ambient conditions these groups are covered by many layers of hydrogen-bonded water which may be removed by heating *in vacuo* or a stream of dry gas. In the case of silica, drying may also be effected by refluxing in xylene and removing the azeotropic mixture of water/xylene *via* a Dean-Stark apparatus.

The nature of the residual hydroxyl groups can vary considerably depending on the composition of the material and the drying procedure. With silica the type and concentration of the surface group can be altered progressively with higher drying temperature. Different crystalline modifications complicate the alumina system, but residual surface Al-OH groups are believed to exist on γ -alumina at temperatures up to 800°C.

The Bronsted or proton acidity of the surface hydroxyl groups on silica and alumina is weak (51, 52, 53). Evidence for this comes from IR studies of pyridine adsorption, no surface pyridinium species ($\text{py} \cdot \text{H}^+$)

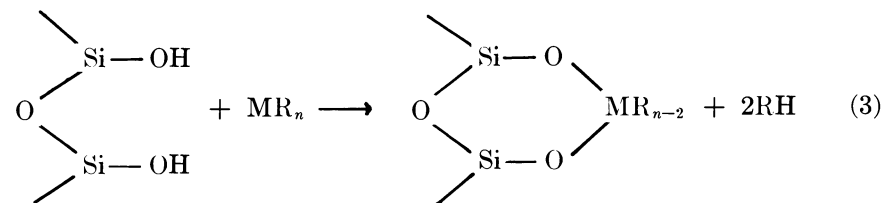
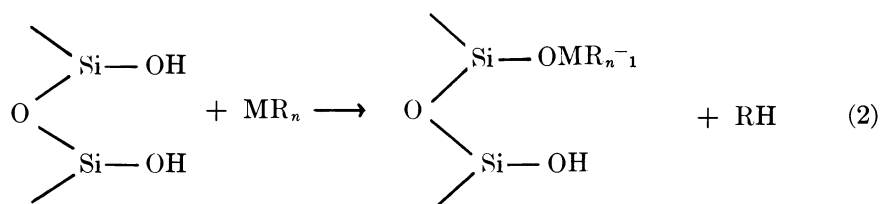
Table V. Heterogeneous

<i>Catalyst, mmole</i>	<i>Support, drying temperature, °C</i>	<i>1-Hexene, ml</i>
Mo (π -allyl) ₄ , 0.11	SiO ₂ , 500	20
0.11	500	20
0.26	200	32
Mo ₂ (π -allyl) ₄ , 0.46	SiO ₂ , 500	30
0.77	200	42
0.5	Al ₂ O ₃ , 500	15
0.5	500	15
W (π -allyl) ₄ , 0.21	SiO ₂ , 500	28
0.14	Al ₂ O ₃ , 500	15

being detected. Proton acidity can be enhanced by introducing electron withdrawing groups such as chloride or fluoride (54, 55, 56) onto the surface or by altering the matrix as in the mixed oxides $\text{SiO}_2/\text{Al}_2\text{O}_3$, $\text{Al}_2\text{O}_3/\text{B}_2\text{O}_3$ (51).

Lewis acidity, arising from electron deficient centers, does not exist in silica. In alumina this acidity is associated with surface aluminum ions which are coordinated in a tetrahedral manner. Such sites may be generated either by removal of water coordinated to an aluminum center or by dehydration of two adjacent hydroxyl groups above 500°C .

Interaction of Metal Hydrocarbyl with SiO_2 and Al_2O_3 . The extreme sensitivity of these organometallic compounds to hydrolysis by protonic acids is demonstrated by their instantaneous reaction with the surface hydroxyl groups of SiO_2 and Al_2O_3 . When the organometallic compounds have more than one reactive group (*e.g.*, $\text{Zr}(\pi\text{-allyl})_4$), the possibility of the following reactions arises (41, 42, 43)



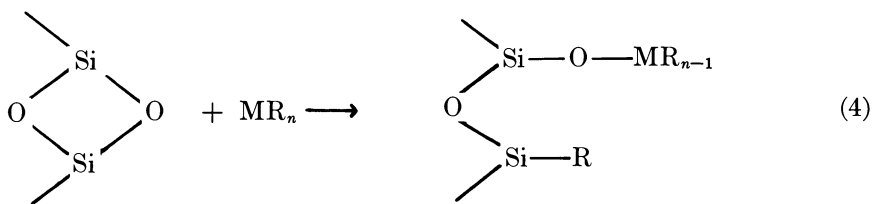
Disproportionation of 1-Hexene

Temp, $^\circ\text{C}$	Time, hrs	Products		
		C_6	$\text{C}_2 + \text{C}_{10}$	Others
20	4	80	20	trace
20	19	33	35	32
20	4	76	24	trace
60	4	77	21	~ 2
60	4	73	25	~ 2
30	4	84	16	trace
60	4	23	75	~ 2
20	24	99	1	—
35	8	74	25	~ 1

Claims of species containing more than two points of attachment to the surface postulated in early patent literature [MoCl_5 reacting with silica surface *via* five oxide bridges (57)] are probably unlikely considering both the stereochemical configuration and the accepted surface hydroxyl concentration on silica (4.6 hydroxyl/100 Å^2). The mode of interaction of the metal hydrocarbyl with the surface is confined to Reactions 2 and 3 with the remote possibility of a three-oxide attachment.

The overall mean stoichiometry can be obtained by measuring the amount of hydrocarbon (RH) liberated from Reactions 2 and 3. This technique has been employed previously for silica using TiCl_4 (58, 59) and VCl_4 (60). Using covalent halides for these determinations, however, requires elaborate experimental procedures to minimize problems caused by the reactive nature of the HCl produced. The advantage of metal hydrocarbyl compounds as reagents is apparent since the resulting product is an unreactive hydrocarbon. This technique is verified by comparing the determination of available hydroxyl on Manosil VN3 by the Zerewitinoff method using CH_3MgI (61) with that by $\text{Zr}(\pi\text{-allyl})_4$. The results, shown in Table I, show excellent agreement for the same slurry concentration of silica/solvent.

The effect of drying temperature on the available surface hydroxyl concentration of a silica is shown in Figure 8. A constant slurry concentration of 4% silica/toluene was used in these experiments. These results are comparable with other data (20, 62), and they indicate that the surface hydroxyl group concentration is reduced with increasing drying temperatures. The reaction of metal hydrocarbyl compounds with strained siloxane groups is illustrated in Reaction 4.



This reaction does not liberate RH and hence does not affect hydroxyl group determination shown in Figure 8.

The effect of varying slurry concentrations of silica/solvent on the available hydroxyl concentration per unit surface area is shown in Figure 9. This effect has not been observed previously, and it may be an artifact arising from the manner in which the experiments were performed. Many finely divided silicas occur as aggregates (48) which are unlikely to be broken up at higher slurry concentrations. Any reactive hydroxyl

groups in the center of the agglomerate will therefore be less accessible and hence may either not react with the organometallic reagent or may react more slowly because of the slow diffusion of the reagent into the agglomerate. Since many π -allyl compounds appear to react instantaneously with silica (visually observed), the results shown in Figure 9 are for data taken after approximately 30 min of reaction. The effect of stirring speed or reaction time on the stoichiometry of the reaction was not examined in detail. Perhaps with longer reaction times (*e.g.*, 24 hrs) the effect shown in Figure 9 may be less marked or may not be observed.

Table II indicates the stoichiometry of the reaction of metal hydrocarbyls with the surface of silicas and aluminas dried at various temperatures. The results indicate that at lower drying temperatures approximately 2 moles of hydrocarbon are liberated per mole of hydrocarbyl compound. Subsequent reaction with the proton source, *n*-butyl alcohol, generates 1 or 2 moles of hydrocarbon, depending on whether a tris- or tetrahydrocarbyl compound is used. The formation of 2 moles of hydrocarbon can arise as a fortuitous combination of metal species singly, doubly, and triply bonded to the support surface.

Experiments to determine the mode of bonding of the metal hydrocarbyl with silica dried above 200°C were not attempted because of Reaction 4. Strained siloxane bridges are not present on silicas dried below 200°C (63).

Drying alumina above 600°C removes surface groups such that at 750°C these groups are sufficiently dispersed that the metal hydrocarbyl reacts *via* a single oxide bond (Reaction 2). Heating alumina to 900°C, following with rehydration in boiling water for 60 mins, and subsequent drying at 600°C, regenerates a paired hydroxyl configuration.

ESR Studies of Surface Species. ESR has been applied widely in heterogeneous catalysis as a technique for examining the nature and concentration of possible catalytic sites when a material is activated either chemically or thermally (64, 65, 66). ESR studies on the Phillips polyethylene catalyst, $\text{CrO}_3/\text{SiO}_2$, are a classical example of this application (67). The interpretation of such ESR studies is questionable since the chemical changes during activation are not well understood, and the nature of the surface species may have to be assumed.

The ESR study of the interaction of VCl_4 with silica and alumina is a good example of the use of a paramagnetic probe to examine surface species (60). Information regarding the geometric distribution of hydroxyl groups on the surface of silica and alumina was obtained from these experiments. The work reported here using $\text{Nb}(\pi\text{-allyl})_4$ as a paramagnetic probe for surface studies was completed before the VCl_4 /surface study was reported. The present work using $\text{Nb}(\pi\text{-allyl})_4$ has the attrac-

tion that the generated niobium species are catalytically active for the polymerization of ethylene without any subsequent treatment.

$\text{Nb}(\pi\text{-allyl})_4$ has a 10-line ESR spectrum ($I = 9/2$) in THF solution with an isotropic coupling of 58 G and with $g = 2.005$ (Figure 10b). On cooling to -180°C , the solid state spectrum is observed (Figure 10a) giving $A(\text{parallel}) = 104$ G ($A(\text{perpendicular}) = 35$ G with $g(\text{parallel}) = 1.9895$ and $g(\text{perpendicular}) = 2.0060$, where A is the coupling constant measured from the ESR spectrum.

Figures 11a and 11b show the ESR spectra of $\text{Nb}(\pi\text{-allyl})_4$ at -180° and 25°C respectively, after reaction with silica previously dried at 650°C . Figure 11b shows a pseudoisotropic spectrum, indicating that a considerable degree of movement occurs in the supported species. This movement could be caused by rotation of a $\text{Nb}(\pi\text{-allyl})_3$ moiety around the Si-O-Nb bond formed by reaction with the support surface (*see* Reaction 2). At -180°C (Figure 11a) this rotation is frozen, and a typical powder spectrum is observed.

Figures 12a and 12b illustrate the ESR spectra at -180°C and 25°C , respectively, of $\text{Nb}(\pi\text{-allyl})_4$ after reaction with Manosil VN3 previously dried at 200°C . Figure 12b is complex and shows a mixture of at least two species present in the system. The major peaks are present in the system. The major peaks are also present in the frozen solution spectrum (Figure 10a) indicating that they arise from a rigidly held surface species. This species arises from the reaction of $\text{Nb}(\pi\text{-allyl})_4$ with two adjacent hydroxyl groups and is therefore the double oxide bridge configuration (Reaction 3). Upon further addition of $\text{Nb}(\pi\text{-allyl})_4$ to the silica, the pseudo isotropic spectrum (Figure 11b) becomes more evident. This suggests that $\text{Nb}(\pi\text{-allyl})_4$ reacts preferentially with the paired hydroxyl groups, an observation in accord with the literature (63).

Figures 13a and 13b are ESR spectra taken at 25°C of the reaction product obtained between $\text{Nb}(\pi\text{-allyl})_4$ and alumina. This same spectrum resulted irrespective of the grade of alumina, the particle size distribution, the crystalline form, or the pretreatment temperature in the $250^\circ\text{--}750^\circ\text{C}$ range. Cooling the reaction product down to -180°C does not affect the ESR spectrum. The spectrum identifies at least three types of bonded niobium species on the alumina surface, each rigidly held. Since the product of the reaction of $\text{Nb}(\pi\text{-allyl})_4$ with alumina dried at 750° fails to yield a pseudoisotropic ESR spectrum, it is evident that on alumina there is no species corresponding to the freely rotating species singly bonded to the surface that exists on silica (Figure 11b). The absence of such a freely rotating species could be the result of π -electron interaction between the allyl ligands and the Lewis acid centers on the surface, thus inhibiting free rotation around the Al-O-Nb bond. Attempts to neutralize the Lewis acid centers on alumina by prior reaction with

NaCl and subsequent heating (68) or by treating with acetonitrile (69) failed to alter the spectrum, but the rate of the reaction of $\text{Nb}(\pi\text{-allyl})_4$ with NaCl-treated alumina was markedly reduced. An alternative explanation for the spectrum (Figure 13) could be that all the niobium atoms are attached to the alumina surface by multiple oxide bridges, a conclusion which was also reached from the ESR spectrum of the VCl_4 /alumina reaction product (60). This is not confirmed by the stoichiometric results of the reaction of $\text{Zr}(\text{benzyl})_4$ with alumina previously dried at 750° (Table II).

When the surface of alumina had partially reacted (*i.e.*, below saturation loading) with diamagnetic $\text{Zr}(\pi\text{-allyl})_4$ and was then treated with $\text{Nb}(\pi\text{-allyl})_4$, a slight difference in the peak height ratios in the ESR spectrum of the product was observed when compared with the reaction product of alumina with $\text{Nb}(\pi\text{-allyl})_4$ alone. This is evidence of a difference in the reactivity of $\text{Zr}(\pi\text{-allyl})_4$ and $\text{Nb}(\pi\text{-allyl})_4$ with the alumina surface since it has been established that the ESR spectrum is not altered by successive additions of $\text{Nb}(\pi\text{-allyl})_4$ up to saturation of the alumina surface. The converse experiment of adding excess $\text{Zr}(\pi\text{-allyl})_4$ solution to a $\text{Nb}(\pi\text{-allyl})_4$ alumina surface did not alter the ESR spectrum (Figure 13), indicating no exchange between the surface species and that in solution.

Finally the ESR spectrum of $\text{Nb}(\pi\text{-allyl})_4$ /alumina was unaffected by the addition of ethylene gas to the ESR sample tube. It is assumed that polyethylene is produced in this process since polymer can be isolated from larger scale reactions under similar conditions. The accepted mechanism for the ethylene growth reaction postulates a steady-state concentration of a σ -bonded transition metal-hydrocarbon species which would be expected to modify the ESR spectrum of the supported complex. A possible explanation for the failure to detect a change in the ESR spectrum may be that only a small number of the niobium sites are active for polymerization. Although further experiments are needed to verify this proposition, it is consistent with IR data and radiochemical studies of similar catalyst systems (41, 42, 43).

IR Studies of the Interaction of $\text{Zr}(\pi\text{-allyl})_4$ with Silica. There has been substantial growth in the application of IR spectroscopy to the investigation of solid surfaces (17, 18, 19). Many studies of surface hydroxylation and of chemical reaction with surface groups are reported in the literature. Relatively little work, however, has been directed to the study of gas/solid reactions as they occur on support surfaces (70, 71).

Figure 14a shows the IR spectrum of a dried silica disc. The sharp band at 3755 cm^{-1} is consistent with the isolated hydroxyl groups (Type A sites) present, and the broad bands at ~ 1980 and 1860 cm^{-1} are overtones of the Si-O vibrations. Treatment of the disc with a toluene solu-

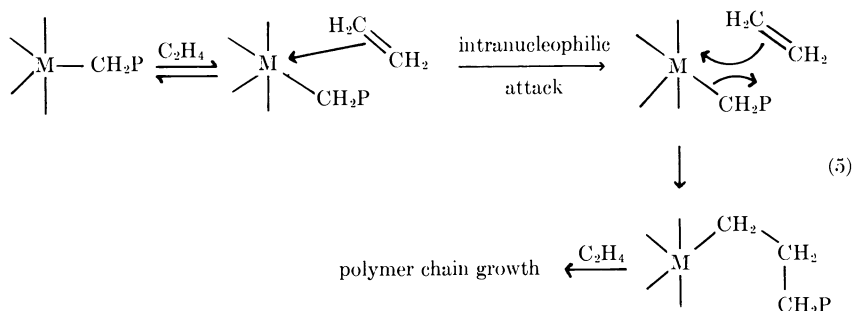
tion of $\text{Zr}(\pi\text{-allyl})_4$ followed by washing and drying gives the spectrum shown in Figure 14b. The most significant features of this spectrum are the disappearance of the band characteristic of Type A sites and the appearance of new bands at 1643 and 1535 cm^{-1} . The latter band corresponds to the stretching vibration of the π -allyl ligand, assigned by comparison with the solution spectrum of $\text{Zr}(\pi\text{-allyl})_4$ (37), and the band at 1643 cm^{-1} is probably attributable to a σ -allyl species of the type, $\text{M}-\text{CH}_2-\text{CH}=\text{CH}_2$ where M may be Zr or Si (the formation of the silicon- σ -allyl bond can occur by Reaction 4). The possibility that the absorption at 1643 cm^{-1} arises from 1,5-hexadiene, formed by the combination of two allyl groups, seems less likely since this species should be removed from the surface by evacuation. This spectrum indicates that the $\text{Zr}(\pi\text{-allyl})_4$ has reacted with surface hydroxyl groups and possibly with the siloxane bridges of silica dried at 500°C to give a species of the type $\text{Si}-\text{O}-\text{Zr}(\pi\text{-allyl})_{4-n}$ in which zirconium is chemically bonded to the silica support and which retains at least one π -allyl linkage.

Figure 14c illustrates the changes which occur on admitting a pressure of ethylene (~ 1.5 atm) to the disc at 25°C. Absorptions at 2925, 2855, and 1460 cm^{-1} increase markedly in intensity, and these are consistent with polymerization and polyethylene formation. The first two bands are antisymmetric and symmetric stretching vibrations, respectively, of the CH_2 groups in polyethylene (72). The 1535 cm^{-1} absorption attributable to the π -allyl species has decreased in relative intensity compared with the 1643 cm^{-1} band. This relative change is further accentuated when the ethylene is introduced at 3 atm and 45°C, resulting in increased polymer formation (Figure 14d). In later experiments performed using a thicker silica disc, the 1535 cm^{-1} absorption (arising from π -allyl ligands) remained for 24 hrs after admitting ethylene at 3 atm and 45°C. This could be an indication that not all the π -allyl groups were involved in the polymerization or merely that diffusion of the ethylene through the silica and/or polyethylene was slow.

Polymerization of Ethylene. Low pressure polymerization of ethylene using supported metal catalysts is not a recent development. Catalytic systems based on silica-chromia or silica-alumina (73) (Phillips Petroleum Co.) and molybdena-alumina (74, 75) (Standard Oil Co.) have been known for 20 years. In the past five years two novel, highly active catalyst systems have been described. These are the supported Ziegler systems using magnesium compounds as supports (76) (Solvay et Cie) and $(\pi\text{-C}_5\text{H}_5)_2\text{Cr}/\text{SiO}_2$ (3, 77, 78) (Union Carbide). Although mechanistic studies of the Phillips catalyst system have been widely reported in the literature (73, 79) very little information has been published regarding the other systems (80), resulting in imprecise definition

of the nature of the metal center and of the role of the support during the catalytic reaction.

A generally accepted mechanism for the polymerization of ethylene by typical Ziegler–Natta catalysts has been proposed by Cossee (81). More recently a mechanism for transition metal hydrocarbyl catalyzed polymerization of olefins has been discussed (41, 42, 43) which is essentially similar to that shown in Reaction 5.



The results shown in Tables III and IV illustrate the enhanced polymerization activity of all the metal hydrocarbyls when chemically grafted onto supports. Although the activity of the grafted molybdenum hydrocarbyls is low, these compounds possess no catalytic activity when studied homogeneously. The catalytic systems reported in Table IV have not been optimized, but initial observations suggest that the catalytic activities are higher on alumina supports than on silica. Increased thermal stability of the supported species is an additional advantage of grafted metal hydrocarbyl systems. $\text{Zr}(\pi\text{-allyl})_4$, for example, decomposes in about 30 min at room temperature whereas the silica-supported $\text{Zr}(\pi\text{-allyl})_4$ system is stable for weeks at this temperature.

In the other highly active catalyst systems, magnesia-supported Ziegler catalysts and $(\pi\text{-C}_5\text{H}_5)_2\text{Cr}/\text{SiO}_2$, where chemical interaction with the support is envisaged, the particular combination of organometallic and support is critical to produce an effective polymerization catalyst. In the present studies the choice of support material profoundly affects the activity of the grafted catalyst systems. In many of these polymerization systems the molecular weight distribution of the polyethylene produced is non-Gaussian, indicating a variety of different active sites in the material. Together with evidence that not all the metal centers in such systems are active polymerization sites (41, 42, 43), the conclusion is that chemical requirements for active polymerization sites are extremely stringent.

Heterogeneously Catalyzed Disproportionation of 1-Hexene. The disproportionation reaction of olefins can be described by the general equation:



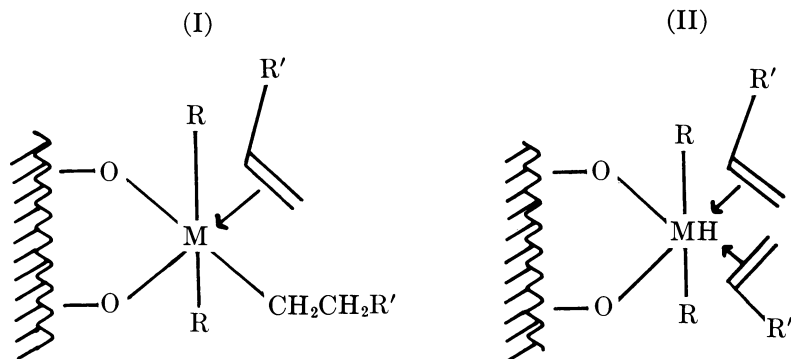
This reaction was one of the first examples of catalysis by a supported organometallic compound. In 1964 it was observed that $Mo(CO)_6/Al_2O_3$, after activation by heating in *vacuo* at 120°C, catalyzed the conversion of propylene into ethylene and 2-butene (82). The nature of the active site in this catalyst system is still not fully defined (83). Since the initial discovery many heterogeneous and homogeneous catalyst systems have been reported (84, 85), the latter being more amenable to kinetic and mechanistic studies.

The results in Table V show that active disproportionation catalysts are obtained when molybdenum and tungsten hydrocarbyls are supported on silica or alumina. These catalytic systems have not been optimized, and it is highly probable that more active catalysts based on these systems can be obtained. No obvious pattern emerges from the results; both silica and alumina supports confer activity on the organometallic compounds which are themselves inactive in homogeneous solution under similar conditions.

The disproportionation activity in the supported species is parallel to the increased activity of ethylene polymerization on supported catalysts. Many of the steps in the reaction may be identical; for example, the initial coordination of olefin to the metal center will be common to both systems. Indeed, some of these catalysts are also ethylene polymerization catalysts (*see* Table IV) although their activities are much less than the corresponding zirconium derivatives. A possible intermediate common to both disproportionation and polymerization could be the hydrocarbyl-olefin species (Structure I). Olefin disproportionation would result if the metal favored β -hydrogen elimination to give the diolefin intermediate (Structure II) which is thought to be necessary for olefin disproportionation. Thus, the similarity between the mechanism and activation of olefin disproportionation and polymerization is suggested.

An alternative effect, specific to π -allyl compounds, arises from the support promoting the conversion of the metal π -allyl into σ -allyl ligands, thereby exposing two further coordination sites on the metal.

Finally, just as in the case of polymerization, the particular active site may be a unique combination of organometallic compound and support with the added complication that all the sites catalyzing olefin disproportionation may not have the same activity.



Acknowledgments

We acknowledge our many colleagues who have contributed to this report. In particular we thank C. J. Joyce, J. Myatt, R. Whyman, E. Jones, C. J. Attridge, D. G. H. Ballard, J. Dewing, and R. J. Wyatt. We also thank the Directorate of the Corporate Laboratory for permission to publish this work.

Literature Cited

1. Candlin, J. P., Parkins, A. W., Randall, G. L. P., *Ann. Rep. Chem. Soc.* (1972) **69B**, 267.
2. Ballard, D. G. H., Jones, E., Pioli, A. J. P., Robinson, P. A., Wyatt, J., British Patent **1,314,828** (1973).
3. U.S. Patent **3,709,853** (1973).
4. Grubbs, R. H., Kroll, L. C., *J. Amer. Chem. Soc.* (1971) **93**, 3062.
5. Merrifield, R. B., *Advan. Enzymol. Relat. Areas Mol. Biol.* (1969) **32**, 221; *Chem. Abstr.* (1969) **71**, 67266.
6. Meienhoffer, J., *Chem. Tech.* (1973) **3**, 243.
7. Ragg, P. L., British Patent **1,239,812** (1971).
8. Allum, K. G., Hancock, R. D., Lawrenson, M. J., German Patent **2,022,710** (1971).
9. Haag, W. O., Whitehurst, D. D., *Abstr. 2nd Amer. Catal. Sect.*, Houston, Feb. 1971.
10. Grubbs, R. H., Gibbons, C., Kroll, L. C., Bonds, W. J., Brubaker, C. H., *J. Amer. Chem. Soc.* (1973) **95**, 2373.
11. Murrell, L. L., Oswald, A. A., "Chemistry of Covalent Anchoring of Phosphine Transition Metal Complex Catalysts," *Int. Conf. Organometal. Chem.*, 6th (Aug. 13-17, 1973), paper 50, Amherst, Mass.
12. Pittman, C. U., Jr., Evans, G. O., Jones, R. E., Felis, R. F., *Int. Conf. Organometal. Chem.*, 6th (Aug. 1973), Paper 51, Amherst, Mass.
13. Allum, K. G., Hancock, R. D., McKenzie, S., Pitkethly, R. C., *Intern. Cong. Catal.*, 5th, Prepr. (Aug. 1972) Miami.
14. Barnett, K. W., Glockner, P. W., British Patent **1,250,861** (1971).
15. Rony, P. R., Roth, J. F., British Patent **1,185,453** (1971).
16. Fox, D. B., Lee, E. H., *Chem. Tech.* (1973) **3**, 187.
17. Little, L. H., "Infra-red Spectra of Adsorbed Species," Academic, New York, 1966.

18. Hair, M. L., "Infra-red Spectroscopy in Surface Chemistry," Edward Arnold, London, 1967.
19. "Surface Chemistry of Oxides," *Discuss. Faraday Soc.* (1971) 52.
20. Armistead, C. G., Tyler, A. J., Hambleton, F. H., Mitchell, S. A., Hockey, J. A., *J. Phys. Chem.* (1969) 73, 3947.
21. Peri, J. B., *J. Phys. Chem.* (1965) 69, 211.
22. Jackson, P., Parfitt, G. D., *Trans. Faraday Soc.* (1971) 67, 2469.
23. Bruce, M. I., *Advan. Organometal. Chem.* (1972) 10, 273.
24. Mowat, W., Wilkinson, G., *J. Chem. Soc., Dalton Trans.* (1973) 1120.
25. Brateman, P. S., Cross, R. J., *J. Chem. Soc., Dalton Trans.* (1972) 657.
26. Carrick, W. L., Turbett, R. J., Karol, F. J., Karapinka, G. L., Fox, A. S., Johnson, R. N., *Amer. Chem. Soc., Div. Polym. Chem., Prepr.* (1972) 13 (2), 1084.
27. Davie, E. S., Whan, D. A., Kemball, C., *J. Catal.* (1972) 24, 272.
28. Wilke, G., Bogdanovic, B., Hardt, P., Heimbach, P., Keim, W., Kroner, M., Oberkirch, W., Tanaka, K., Steinrucke, E., Walter, D., Zimmermann, H., *Angew. Chem. Int. Ed.* (1966) 5, 151.
29. Becconsall, J. K., Job, B. E., O'Brien, S., *J. Chem. Soc. A* (1967) 423.
30. Ballard, D. G. H., Janes, W. H., Medinger, T., *J. Chem. Soc. B* (1968) 1168.
31. Cotton, F. A., Pipal, J. R., *J. Amer. Chem. Soc.* (1971) 93, 5441.
32. Candlin, J. P., Mawby, A. H., Thomas, H., British Patent Appl., 30266/71.
33. Holden, L. K., Mawby, A. H., Thomas, H., unpublished data.
34. Grummitt, O., Budewitz, E. P., Chudd, C. C., *Org. Synth.* (1963) 4, 751.
35. Eisch, J. J., Jacobs, A. M., *J. Org. Chem.* (1963) 28, 2145.
36. Gilman, H., Haubein, A. H., *J. Amer. Chem. Soc.* (1944) 66, 1515.
37. Steinrucke, E., Dissertation, Technische Hochschule Aachen (1966).
38. Oberkirch, W., Dissertation, Technische Hochschule Aachen (1963).
39. Zucchini, U., Albizzati, E., Giannini, U., *J. Organometal. Chem.* (1971) 26, 357.
40. Pioli, A. J. P., Hollyhead, W. B., Todd, P. F., British Patent 1,265,747 (1969).
41. Ballard, D. G. H., *Advan. Catal.* (1973) 23, 263.
42. Ballard, D. G. H., *Intern. Congr. Pure Appl. Chem., 23rd, London* (1971) • 6, 213.
43. Ballard, D. G. H., Jones, E., Medinger, T., Pioli, A. J. P., *Makromol. Chem.* (1971) 148, 176.
44. Stephenson, T. A., Bannister, E., Wilkinson, G., *J. Chem. Soc.* (1964) 2538.
45. Fripiat, J. J., Uytterhoeven, J., *J. Phys. Chem.* (1962) 66, 800.
46. Myatt, J., Ph.D. Thesis, University of Leicester (1972).
47. Rigby, W., Whyman, R., Wilding, K., *J. Phys. E* (1970) 3, 572.
48. Tyler, A. J., Hambleton, F. H., Hockey, J. A., *J. Catal.* (1969) 13, 35.
49. Peri, J. B., Hensley, A. L., *J. Phys. Chem.* (1968) 72, 2926.
50. DeBoer, J. H., Vleeskens, J. M., *Proc. Kon. Ned. Akad. Wetensch., Ser. B* (1958) 61, 2.
51. Tanable, K., "Solid Acids and Bases," Academic, New York, 1970.
52. Forri, L., *Catal. Rev.* (1973) 8, 65.
53. Linsen, B. G., Ed., "Physical and Chemical Aspects of Adsorbents and Catalysis," Academic, New York, 1970.
54. Antipina, T. V., *J. Catal.* (1968) 12, 108.
55. Gesser, H. D., Bader, L., Shimizu, M., *Chem. Ind.* (1972) 297.
56. Gati, G., Knozinger, H., *Z. Phys. Chem. Frankfurt am Main* (1972) 78, 243.
57. MacKenzie, J. C., Ovzechowski, A., British Patent 1,038,882 (1966).
58. Chien, J. C. W., *J. Catal.* (1971) 23, 71.
59. Kol'tsov, S. I., *J. Appl. Chem. USSR* (1969) 42, 975.
60. Chien, J. C. W., *J. Amer. Chem. Soc.* (1971) 93, 4675.
61. Uytterhoeven, J., Sleex, M., Fripiat, J. J., *Bull. Soc. Chim. Fr.* (1965) 1800.

62. Young, G. J., *J. Colloid Sci.* (1958) **13**, 67.
63. Kunawicz, J., Jones, P., Hockey, J. A., *Trans. Faraday Soc.* (1971) **67**, 848.
64. Seshadri, K. S., Petrakis, L., *J. Phys. Chem.* (1970) **74**, 4102.
65. Voorhoeve, R. J. H., *J. Catal.* (1971) **23**, 236.
66. Sancier, K. M., Dozono, T., Wise, H., *J. Catal.* (1971) **23**, 270.
67. Eley, D. D., Rochester, C. H., Scurrrell, M. S., *Proc. Roy. Soc.* (1972) **329A**, 361.
68. Pines, H., Haag, W. O., *J. Amer. Chem. Soc.* (1960) **82**, 2471.
69. Dewing, J., unpublished data.
70. Murray, J., Sharp, M. J., Hockey, J. A., *J. Catal.* (1970) **18**, 52.
71. Eley, D. D., Rochester, C. H., Scurrrell, M. S., *Proc. Roy. Soc.* (1972) **329A**, 375.
72. Kline, G. M., "High Polymers: Analytical Chemistry of Polymers," Interscience, New York (1962) **12** (2), 291.
73. Clark, A., *Catal. Rev.* (1969) **3**, 145.
74. Feller, M., Field, E., *Ind. Eng. Chem.* (1959) **51**, 155.
75. Juveland, O. D., Peters, E. F., Shepard, J. W., British Patent **1,045,178** (1966).
76. Forsman, J. P., *Hydrocarbon Proc.* (1972) **51** (11), 130.
77. Karapinka, G. L., British Patent **1,253,063** (1971).
78. Johnson, R. L., Karol, F. J., British Patent **1,298,220** (1972).
79. Spitz, R., Vuillaume, G., Revillon, A., Guyot, A., *J. Macromol. Sci.-Chem.* (1972) **A6**, 153, 169.
80. Karol, F. J., Karapinka, G. L., Wu, C., Dow, A. W., Johnson, R. N., Carrick, W. L., *J. Polym. Sci. Part A-1* (1972) **10**, 2621.
81. Cossee, P., *J. Catal.* (1964) **3**, 80.
82. Banks, R. L., Bailey, G. C., *Ind. Eng. Chem., Prod. Res. Develop.* (1964) **3**, 170.
83. Howe, R. F., Davidson, D. E., Whan, D. A., *J. Chem. Soc., Faraday Trans. I* (1972) 2266.
84. Calderon, N., *Accounts Chem. Res.* (1972) **5**, 127.
85. Banks, R. L., *Top. Current Chem.* (1972) **25**, 39.

RECEIVED August 21, 1973.

Hydroformylation with Rhodium–Amine Complexes

ANTHONY T. JUREWICZ, LOUIS D. ROLLMANN, and
D. DUAYNE WHITEHURST

Mobil Research and Development Corp., Central Research Division,
Princeton, N. J. 08540

Under mild conditions, hydroformylation of olefins with rhodium carbonyl complexes selectively produces aldehydes. A one-step synthesis of oxo alcohols is possible using monomeric or polymeric amines, such as dimethylbenzylamine or anion exchange resin analog to hydrogenate the aldehyde. The rate of aldehyde hydrogenation passes through a maximum as amine basicity and concentration increase. IR data of the reaction reveal that anionic rhodium carbonyl clusters, normally absent, are formed on addition of amine. Aldehyde hydrogenation is attributed to enhanced hydridic character of a Rh–H intermediate via amine coordination to rhodium.

Hydroformylation of olefins to aldehydes over cobalt carbonyl catalysts is the first step in the industrial synthesis of oxo alcohols (1, 2). Reaction conditions require temperatures above 150°C and pressures up to 3000 psig. Subsequent aldehyde hydrogenation occurs over supported cobalt or molybdenum disulfide catalysts.

Addition of modifying ligands such as tributyl phosphine affords a one-step, cobalt-catalyzed synthesis of alcohols (at lower pressure), but accompanying olefin hydrogenation reduces yields (3). With amine ligands, the effects are varied. Accelerated hydroformylation rates are possible with weak bases such as pyridine, but stronger bases (piperidine or triethylamine, for example) retard or completely inhibit the reaction (4, 5).

In comparison with their cobalt analogs, rhodium carbonyls are significantly more active catalysts (6). As with cobalt, aldehyde is the

principal product although some hydrogenation to alcohol has been reported at high temperature and pressure (7).

In contrast to cobalt, rhodium permits a one-step oxo alcohol synthesis in the presence of certain monomeric and polymeric amines (8, 9, 10). Included in this group are triethylamine, *N*-alkylpiperidines, *N*-methylpyrrolidine, and *N,N*-dimethylbenzylamine (DMBA). Initial kinetic data on this amine-promoted alcohol synthesis (under severe reaction conditions) have been reported by B. Fell and coworkers (11), but no attempt has been made to characterize the catalytic species in the reaction cycle.

Data are presented to identify some of the important factors in aldehyde hydrogenation and to characterize rhodium carbonyl chemistry under hydroformylation conditions. Comparison is made of the effects of monomeric and of polymeric amines, and a possible reaction mechanism is examined in the light of the data.

Experimental

Materials. Rhodium carbonyl chloride was prepared by heating $\text{RhCl}_3 \cdot 3\text{H}_2\text{O}$ (40.0% Rh, Matthey Bishop) in a CO stream (12). The cluster carbonyls, $\text{Rh}_4(\text{CO})_{12}$ and $\text{Rh}_6(\text{CO})_{16}$, were prepared according to Chini and Martinengo (13). Olefins (Humphrey, Aldrich) were percolated over alumina prior to use. Amines (Aldrich) were, on occasion, fractionally distilled under nitrogen but were typically used without further purification. Other materials were reagent grade.

The resins studied (Rohm and Haas and Ionac) were all functionalized, cross-linked, styrene polymers with the exception of poly(4-vinylpyridine). Porous, macroporous resins included the polymeric analogs of *N,N*-dimethylbenzylamine (A21 polyDMBA, Rohm and Haas), *N,N*-dimethylaniline, and 1-phenyl-2-(*N,N*-dimethylamino)ethane (poly-Alipham). The last two materials were prepared in this laboratory. Nitrogen content of the porous resins was 4.1, 2.5, and 2.6 mequiv/gram, respectively. Poly(4-vinylpyridine) (6.9 mequiv/gram) had a gel-type structure.

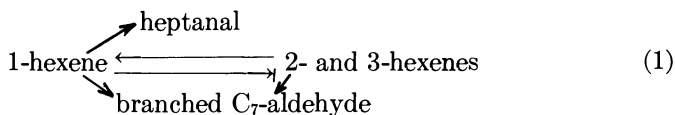
Procedures. Batch oxo experiments were performed in a 300cc autoclave. The autoclave and contents were flushed with CO and brought to reaction temperature at the beginning of a run. The vessel was then pressurized with the desired mixture of CO and hydrogen and the run commenced. Reaction was followed by monitoring hydrogen and CO consumption and by periodic sampling for GLC analysis on tricresylphosphate and Carbowax 1000 columns.

Rhodium carbonyl chemistry was monitored during the course of a run by attaching a high-pressure, heated IR cell to the autoclave. Cell design was similar to that reported by Noack (14). Sodium chloride plates were used.

Results

Catalysis. When 1-hexene reacts with CO and H_2 over rhodium carbonyls, the two competing reactions are the formation of aldehyde and

the olefin isomerization. The system is described schematically in Reaction 1 (9). Under mild conditions, the aldehyde formation dominates with no further hydrogenation to alcohol.



The plot of data for the carbonyl, $Rh_6(CO)_{16}$, (Figure 1) shows that the rate of 1-hexene isomerization exceeds that of hydroformylation. At olefin conversion in excess of 50%, little 1 isomer remains. An increase in branched aldehyde relative to linear aldehyde accompanies the change in isomer distribution. The absence of aldehyde hydrogenation is complete even at very high conversion levels using the conditions cited.

The effect of DMBA and polyDMBA on the hydroformylation of 1-hexene is shown in Table I. Product distributions are reported at 80% total olefin conversion for various rhodium sources and olefin concentrations. As shown, olefin isomerization is complete in all cases. In the presence of 2M DMBA, significant aldehyde hydrogenation occurred producing nearly 30% alcohol. With the exception of $RhCl_3 \cdot 3H_2O$ which is inactive, no differences were found between various rhodium sources.

The aldehyde hydrogenation reaction is strongly dependent on amine basicity. The data in Table I obtained with DMBA demonstrate

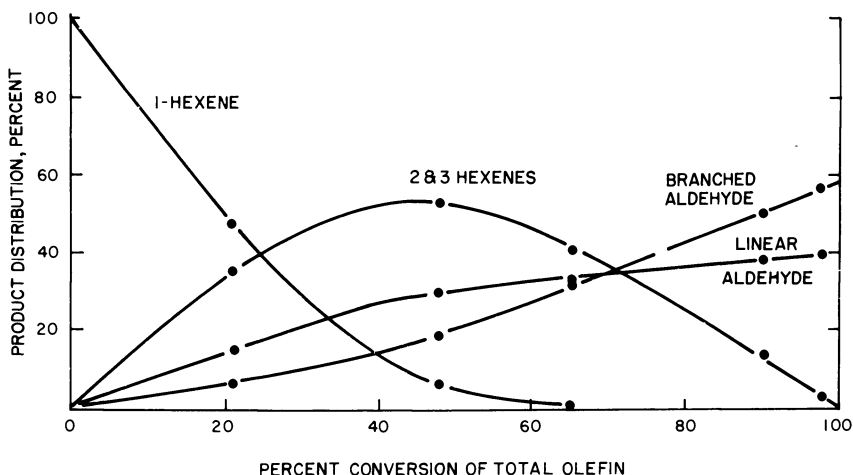


Figure 1. Hydroformylation of 1-hexene

100cc 0.8M 1-hexene in hexane, 60 mg $Rh_6(CO)_{16}$, 100°C, 1000 psig 1:1 $CO:H_2$

Table I. Effect of Amine on the Hydroformylation of 1-Hexene^a

Catalyst	Initial 1-Hexene Concen- tration, molar	Product Distribution ^b		
		2- and 3-Hexenes	C ₇ - Aldehyde	C ₇ -Alcohol
Rh ₆ (CO) ₁₆	0.8 ^c	20	80	<1
Rh ₆ (CO) ₁₆ + 2M DMBA	0.8	20	51	29
RhCl ₃ ·3H ₂ O	8 ^d	NR ^e	NR ^e	NR ^e
5% Rh on Charcoal	8	20	80	<1
RhCl ₃ ·3H ₂ O on polyDMBA	8	20	52	28

^a 100°C, 1000 psig 1:1 CO:H₂, 100cc solution containing 20–50 mg Rh.

^b At 80% total olefin conversion.

^c Hexane solvent.

^d No added solvent.

^e No reaction.

the effect of base. Table II shows the effect on alcohol production for 1-hexene hydroformylation using a series of tertiary amines. All monomers were at 1M concentration. The effective amine concentrations in resins were estimated to be 2.5–4M, based on nitrogen analyses, porosity data, and resin swelling characteristics.

Among the monomers, significant aldehyde hydrogenation was observed only for amines of pK_b between about 3 and 7, a range which includes triethylamine (TEA), methylpyrrolidine, and DMBA. At 1M concentration, TEA was the most effective (7% alcohol at 80% conver-

Table II. Effect of Amine Basicity on Product Distribution^a

Amine	pK _b	k _{hydrog} / k _{oxo} ^d	Product Distribution ^b		
			2- and 3-hexenes	C ₇ - aldehyde	C ₇ - alcohol
Pyridine	8.8	<0.5	20	80	<1
Dimethylaniline	8.9	<0.5	20	80	<1
Dimethylbenzylamine	5.1	3.5	20	75	5
Methylpyrrolidine	3.8	3.7	20	76	4
Triethylamine	3.2	3.6	20	73	7
1,4-Diazabicyclo[2.2.2] octane (dabco)					
	2.9	<0.5	20	80	<1
Polypyridine	(8.8) ^c	≤0.4	20	77	3
Polydimethylaniline	(8.9)	3.0	20	75	5
PolyDMBA	(5.1)	18.	20	52	28
PolyAlipham	(3.2)	1.6	20	78	2

^a 100°C, 1000 psig 1:1 CO:H₂, 100cc 1M 1-hexene/1M amine (3 gram in case of polymeric amines) in hexane, 5 × 10⁻⁴ moles RhCl₃·3H₂O.

^b At 80% total olefin conversion.

^c Estimates based on analogous monomer.

^d Relative rate constants for formation and hydrogenation of *n*-heptanal, × 10³.

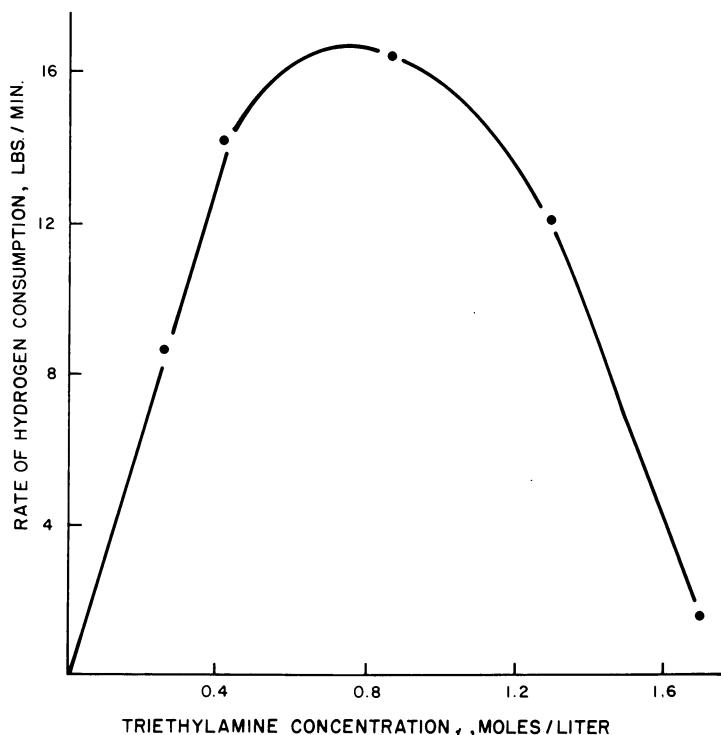


Figure 2. Effect of amine concentration on heptanal hydrogenation

100°C, 1000 psig 1:1 CO:H₂, 100cc aldehyde containing 40–50 mg Rh, 0–20% conversion

sion). No alcohol was found with the very weak (pyridine, dimethylaniline) or very strong amines (1,4-diazabicyclo[2.2.2]octane).

Of the polymers, polyDMBA was most effective, yielding 28% alcohol at 80% conversion. In contrast to the monomer, the polymeric analog of TEA exhibited the lowest hydrogenation activity.

Comparing Tables I and II reveals that amine concentration is the second important variable in the aldehyde hydrogenation reaction. For a given amine, selectivity to alcohol passes through a maximum with increasing concentration of N donor. Thus with DMBA, the alcohol present at 80% olefin conversion was 5, 29, and 28% at 1, 2, and ~3M (resin), respectively, suggesting an optimum DMBA concentration of about 2M.

This maximum in the aldehyde hydrogenation rate is most obvious for a stronger base such as TEA. Rates of hydrogen consumption, plotted against TEA concentration (Figure 2) show a rate initially first-

Table III. Effect of Olefin Structure^a

Olefin	k_{ozo}/k_{hydrog}	Product Distribution ^b	
		<i>C</i> ₇ -aldehyde	<i>C</i> ₇ -alcohol
1-Hexene	~6	51	29
2-Hexene	1.5	16	54
Cyclohexene	0.2	6	74

^a 100°C, 1000 psig 1:1 CO:H₂, 100cc olefin containing 40-50 mg Rh on polyDMBA (1%).

^b 80% total olefin conversion.

order in amine but passing through a maximum at ~0.8*M*. At very high concentrations, amine suppresses the hydrogenation reaction.

The TEA data provide an explanation for the apparent discrepancy between monomer and polymer behavior in Table II. A concentration of 1*M* was near optimum for TEA, the most effective of the monomers. The higher concentrations present within the polymers were near optimum for the weaker amines, and thus polyDMBA displayed the highest selectivity to alcohol among the resins. DMBA, the weaker base, is significantly more effective than TEA at their respective optimum concentrations.

The experiments in Tables I and II have dealt with the reactions of 1-hexene only. It is known that hydroformylation rates for various olefins are in the order, 1-hexene > 2-hexene > cyclohexene (15). Little dependence on structure would be expected in the aldehyde hydrogenation step, however.

Data in Table III reflect this decreasing ratio of hydroformylation/hydrogenation rates for this series of olefins. As expected in A → B → C reaction, maximum aldehyde(B) is observed where the initial hydroformylation rate is greatest, *i.e.*, with 1-hexene. Note that the rate constants for 1-hexene relate to the linear aldehyde only.

Rate differences are observed with aldehydes of varying electronic properties. To identify the rate-determining step in the alcohol formation, the hydrogenation rates for a series of para-substituted benzaldehydes were measured. These rates, shown in Table IV, increase markedly as the para substituent is varied in the order, CH₃O— < H— < CN—

Table IV. Para-Substituent Effects on Benzaldehyde Hydrogenation^a

Para Substituent	[RCHO], molar	<i>t</i> _{1/2} , min	Relative Rate Constant	σ ^{+b}
CH ₃ O	0.33	372	0.24	-0.78
H	0.33	88	1.0	0.0
CN	0.33	18	4.9	+0.66

^a 100°C, 1000 psig 1:1 CO:H₂, 100cc hexane solution containing 225 mg RhCl₃·3H₂O on 3 gram polyDMBA.

^b Ref. 21.

and show a good correlation between relative rate constants and Hammett σ^+ values (Figure 3). A ρ value of $+0.92$ is calculated from the data.

The hydrogenation of aldehydes in the absence of amines under more severe reaction conditions was studied extensively by Heil and Marko (16). They found that rates of alcohol formation passed through a maximum with increasing CO partial pressure (> 1000 psi), but at very low pressures CO was inhibiting.

In our experiments, no CO inhibition was observed, instead the rhodium-catalyzed hydrogenation of aldehydes in the presence of amines showed a first-order dependence on both CO and H₂ (Table V). The absence of any significant inhibition by CO is attributed to lower operating temperatures and lower H₂ pressures feasible in the presence of amine, relative to the earlier reports (16). Maxima in the rates are reported only at CO partial pressures exceeding 1000 psig (11, 16) and were neither expected nor observed in this investigation.

While Heil and Marko (16) reported linear plots of $\log[\text{aldehyde}]$ vs. time, indicating first-order dependence on aldehyde, the order in rhodium is more difficult to determine. With the resin catalysts, rates

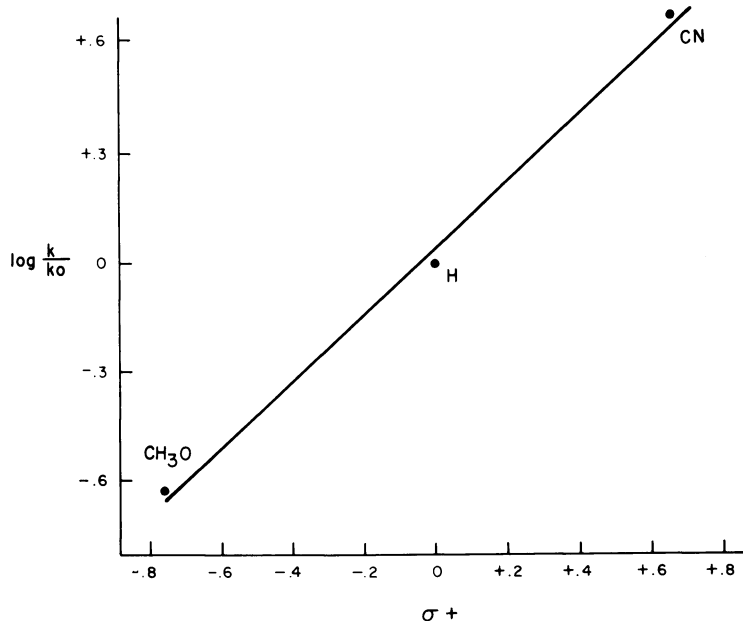


Figure 3. Relative rate constants for hydrogenation of *p*-substituted benzaldehydes vs. Hammett ρ^+ values

$\rho = 0.92$, 100°C , 100 psig, $1:1$ CO:H₂, RhCl₃ 3H₂O on polyDMBA

Table V. Effect of Hydrogen and Carbon Monoxide Pressure on the Hydrogenation of Heptanal^a

<i>Hydrogen, psia</i>	<i>Carbon Monoxide, psia</i>	<i>Rate of Hydrogen Consumption, lbs/min</i>
300	100	0.2
300	200	0.7
300	400	1.3
500	400	1.8
500	500	2.5
600	500	2.8

^a 100°C, 75cc heptanal containing 100 mg RhCl₃·3H₂O on 3 gram polyDMBA, 0–25% conversion.

appeared to be first order in rhodium. In the presence of monomer amine, deviation from first order behavior were observed when a precipitate formed at high rhodium levels. It is this deviation, already reported in rhodium systems (11, 16), which led to an IR study of the rhodium chemistry in these catalytic systems.

IR Data. Transformations of rhodium complexes under hydroformylation conditions were followed by attaching a heated, high-pressure IR cell to the autoclave and periodically sampling the reaction liquid. Solvents varied from pure hexane to actual reacting mixtures of olefin and aldehyde. The data are summarized in Table VI.

With rhodium trichloride, the only species observed in solution were Rh₂(CO)₄Cl₂ and HCl gas. As noted in Table I, no hydroformylation occurred in this reaction mixture. When the carbonyl chloride dimer was used as starting material, the clusters, Rh₄(CO)₁₂ and Rh₆(CO)₁₆, formed along with the anion, Rh(CO)₂Cl₂⁻. Aldehyde, but no alcohol, was produced. These IR data are in good agreement with earlier reports on amine-free systems (16), and they support the contention that a chloride-free carbonyl (or carbonyl hydride) is the active hydroformylation catalyst.

Amine profoundly alters the predominant rhodium carbonyl species in hydroformylation mixtures as shown in Table VI. At the higher

Table VI. IR Identification of Rhodium Complexes Under Hydroformylation Conditions^a

<i>Catalyst</i>	<i>Amine</i>	<i>Major Rhodium Species</i>
RhCl ₃ ·3H ₂ O	—	Rh ₂ (CO) ₄ Cl ₂
Rh ₂ (CO) ₄ Cl ₂	—	Rh ₄ (CO) ₁₂ , [Rh ₆ (CO) ₁₆ , Rh(CO) ₂ Cl ₂ ⁻]
Rh ₂ (CO) ₄ Cl ₂	2 <i>M</i> TEA	Rh ₁₂ (CO) ₃₀ ²⁻
Rh ₂ (CO) ₄ Cl ₂	2 <i>M</i> DMBA	Rh ₁₂ (CO) ₃₀ ²⁻
Rh ₂ (CO) ₄ Cl ₂	polyDMBA ^b	Rh ₁₂ (CO) ₃₀ ²⁻ , Rh ₃ (CO) ₁₀ ⁻ , Rh ₇ (CO) ₁₆ ³⁻

^a 100°C, 1000 psig 1:1 CO:H₂, 2–5 ± 10⁻³ *M* Rh, 1*M* 1-hexene/1*M* heptanal in hexane.

^b Nujol mull spectra, no liquid phase.

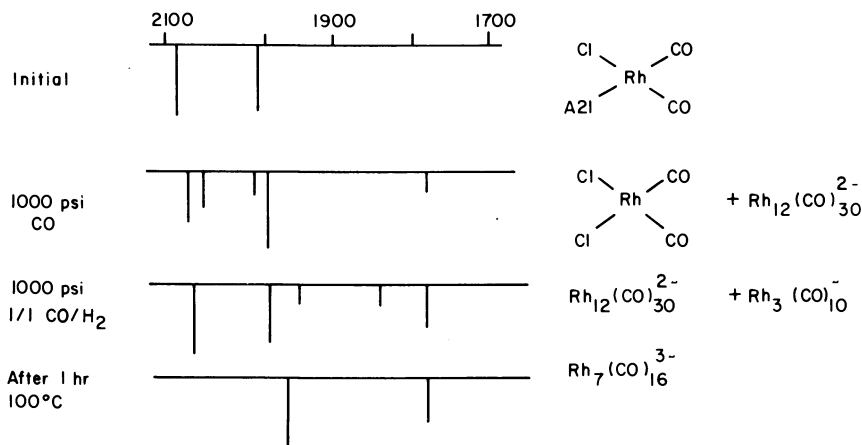


Figure 4. Transformation of Rh carbonyls on polyDMBA amine resins under oxo conditions

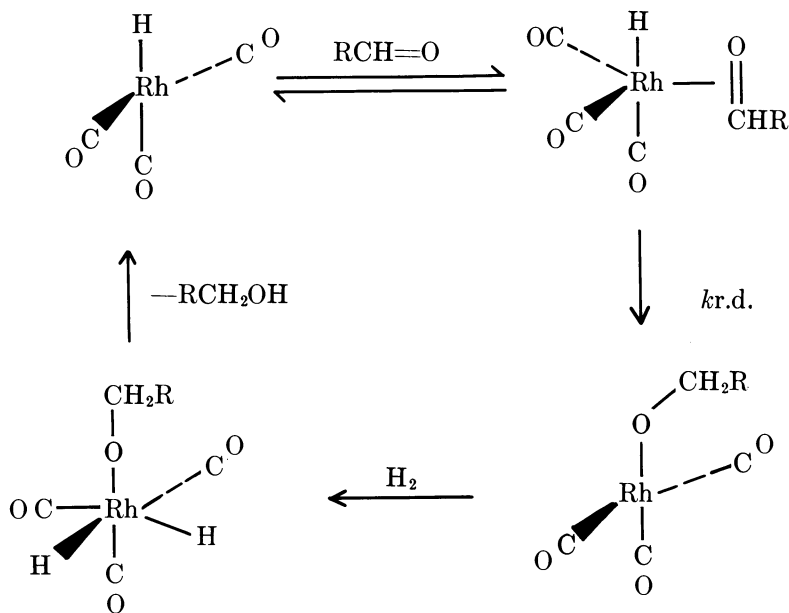
rhodium levels, precipitation occurs and detection of additional rhodium carbonyl clusters was not possible. In order to study the system at high rhodium levels, rhodium carbonyl chloride was deposited on an amine polymer (polyDMBA), and the effects of pressure and temperature were studied in the absence of solvent, *i.e.*, in Nujol and Fluorolube mulls. The data are presented in Figure 4.

Rhodium carbonyl chloride dimer undergoes a bridge-splitting reaction with polyDMBA to yield *cis*- $\text{Rh}(\text{CO})_2\text{Cl} \cdot \text{polyDMBA}$, the starting complex in this series of experiments. The polymer must be chloride-free to avoid initial formation of $\text{Rh}(\text{CO})_2\text{Cl}_2^-$ (17). On addition of CO, reduction of the amine complex occurs and yields the anions $\text{Rh}_{12}(\text{CO})_{30}^{2-}$ and $\text{Rh}(\text{CO})_2\text{Cl}_2^-$. The cation is taken to be $\text{polyDMBA} \cdot \text{H}^+$. In these polymer experiments, carried out in the absence of olefin or aldehyde, further reduction was observed on addition of hydrogen and also on heating to produce the clusters $\text{Rh}_3(\text{CO})_{10}^-$ and $\text{Rh}_7(\text{CO})_{16}^{3-}$.

IR data established a clear distinction between the predominant rhodium species in the absence and in the presence of amine, *i.e.*, in reaction systems producing aldehyde and alcohol, respectively. Rhodium carbonyl anions, normally absent, are formed on addition of amine. No significance is attached to the differences between monomer and polymer behavior since a facile interconversion among the various carbonyl anions is well established (18).

Discussion

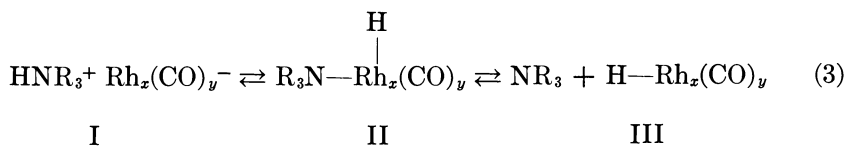
The kinetics of aldehyde hydrogenation over cobalt and rhodium carbonyl have been examined by Heil and Marko (16, 19) who proposed Mechanism 2.



Since the reaction was first order in aldehyde, the rate determining step was taken to be hydride transfer to the coordinated aldehyde. For simplicity, this reaction sequence has been used in the following discussion on amines. It is not known if the active species is monomeric nor is there IR evidence for any of the above intermediates. Heil and Marko explained the first-order dependence on CO (and H₂) to be linked to formation of a catalytically active HRh(CO)₃ complex from the CO- and H-deficient clusters discussed below.

IR data (Table VI) indicate that rhodium carbonyl chemistry in the presence of amines is very complex. The data are best represented by a facile equilibrium represented by Reaction 3, where *x* and *y* need not be constant across the series. The major carbonyl anions (I) are clearly identified in Table VI and in Figure 4.

Species II and III (Reaction 3) were postulated to account for the catalytic behavior of these systems; species II, for the amine-promoted hydrogenation activity, and species III, for continued hydroformylation activity in the presence of amine. In continuous flow experiments on polyDMBA catalysts, rhodium retention was reported to be good (9) with



rhodium concentrations in reactor effluents less than about 1 ppm. Thus species III (free hydrido carbonyl) is present in very minor amounts and contributes little to the hydroformylation activity which must then be attributed to species II. Other experiments with $(Et_4N)_2[Rh_{12}(CO)_{30}]$ confirmed the inactivity of the carbonyl anion clusters for aldehyde hydrogenation.

As amine concentration was increased, hydrogenation rates increased, passing through a maximum at 1–2*M*. This concentration dependence is readily understood in terms of a shift in Equilibrium 3 to favor the inactive ammonium carbonyl rhodate (I). In this equilibrium the concentration of active hydrogenation catalyst (II) passes through a maximum as the [amine] is increased. With stronger bases this maximum occurs at progressively lower concentration.

Catalyst activity at optimum amine level decreased with increasing basicity. This effect is also explained in terms of Reaction 3 where IR data indicate a pronounced shift to the left. If it is assumed that equilibrium increasingly favors the rhodate anion with the stronger bases, it can be readily shown that the maximum fraction of species II decreases with increasing basicity. In other words, the amount of species II present at optimum amine levels is lower for TEA than for DMBA.

The above discussion has shown that the effects of amine basicity and concentration on catalytic activity are consistent with Equilibrium 3. No explanation has been presented for the increased hydrogenation activity of species II as compared with the amine-free hydrido carbonyl (species III). The data in Table IV and the first-order dependence of aldehyde provide the basis for such an explanation.

As shown in Figure 3, a positive ρ -value (+0.92) was observed in the hydrogenation of substituted benzaldehydes, giving strong support to the postulation by Heil and Marko that the rate determining step in the formation of alcohol (Mechanism 2) is the hydride addition step. It is therefore suggested that coordination of amine to rhodium increases the hydridic character of the Rh–H bond, much the same as is postulated in cobalt–tributylphosphine complexation (20). The differing effect of amine on rhodium (promoter) and on cobalt (inhibitor) is attributed to the more hydridic nature of a Rh–H bond as compared with the very protonic $HCo(CO)_4$. Addition of amines to $HCo(CO)_4$ results in formation of inactive species similar to I.

Conclusions

In the hydroformylation of olefins over rhodium carbonyl catalysts, aldehyde hydrogenation was noted under mild conditions in the absence of amine. Rates of hydrogenation passed through a maximum with increasing amine basicity and concentration.

Particularly effective reaction mixtures contained tertiary amines of pK_b 3–7, present at about 0.5–3*M*. The optimum concentration for a given amine increased with decreasing basicity.

IR data supported the formation of rhodium carbonyl anions on addition of amine suggesting a mechanism in which these anions are in equilibrium with the active species, a hydrido rhodium carbonyl containing coordinated amine. Such a mechanism provides an explanation for the variation in catalyst activity with amine concentration and basicity and affords a method for predicting the effect of other amine ligands.

Acknowledgments

Helpful discussions with W. O. Haag and W. H. Lang of these laboratories are greatly appreciated.

Literature Cited

1. Denney, R. G., "Oxo Alcohols," Stanford Research Inst., Report No. 21, Menlo Park (1966).
2. Hatch, L. F., "Higher Oxo Alcohols," Wiley, New York, 1957.
3. Slaugh, L. H., Mullineaux, R. D., *J. Organometal. Chem.* (1968) **13**, 469.
4. Hasek, R. H., Wayman, C. W., U.S. Patent **2,820,059** (Jan. 14, 1958).
5. Iwanaga, R., *Bull. Chem. Soc. Jap.* (1962) **35**, 865.
6. Heil, B., Marko, L., *Chem. Ber.* (1968) **101**, 2209.
7. *Ibid.*, (1966) **99**, 1086.
8. Haag, W. O., Whitehurst, D. D., Belgian Patent **721,686** (1969).
9. Haag, W. O., Whitehurst, D. D., *Int. Congr. Catal. 5th*, Palm Beach, Fla., Aug. (1972).
10. Fell, B., Guerts, A., Müller, E., *Angew. Chem. Int. Ed. Engl.* (1971) **10**, 828.
11. Fell, B., Guerts, A., *Chem. Ing. Tech. Z.* (1972) **44**, 708.
12. McCleverty, J. A., Wilkinson, G., *Inorg. Synth.* (1966) **8**, 211.
13. Chini, P., Martinengo, S., *Inorg. Chim. Acta* (1969) **3**, 315.
14. Noack, K., *Spectrochim. Acta* (1968) **24A**, 1917.
15. Heil, B., Marko, L., *Chem. Ber.* (1969) **102**, 2238.
16. Heil, B., Marko, L., *Acta Chim. Acad. Sci. Hung.* (1968) **55**, 107.
17. Rollmann, L. D., *Inorg. Chim. Acta* (1972) **6**, 137.
18. Martinengo, S., Chini, P., *Gazz. Chim. Ital.* (1972) **102**, 344.
19. Marko, L., *Proc. Chem. Soc. London* (1962) 67.
20. Tucci, E. R., *Ind. Eng. Chem. Prod. Res. Devel.* (1970) **9**, 516.
21. Brown, H. C., Okamoto, Y., *J. Amer. Chem. Soc.* (1958) **80**, 4979.

RECEIVED July 30, 1973.

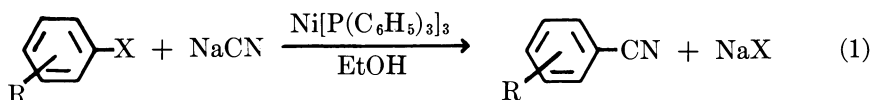
Nickel-Catalyzed Cyanation of Aromatic Halides

L. CASSAR, S. FERRARA, and M. FOÁ

Montedison, Centro Ricerche di Chimica Organica, 28100 Novara, Italy

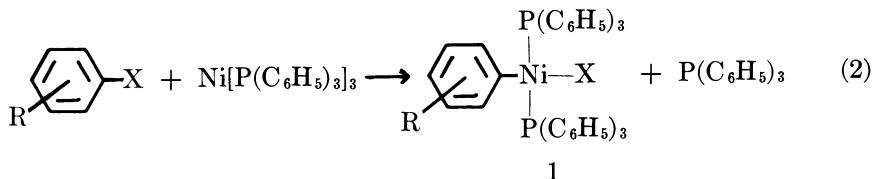
The nickel-catalyzed transformation of aromatic halides into the corresponding nitriles by reaction with cyanide ions is reported. Both tris(triarylphosphine)nickel(0) complexes and trans-chloro(aryl)bis(triarylphosphine)nickel(II) complexes catalyze the reaction. The influence of solvents, organophosphines, and substituents on the aromatic nucleus on catalytic cyanation is studied. A mechanism of the catalytic process is suggested based on the study of stoichiometric cyanation of trans-chloro(aryl)bis(triphenylphosphine)nickel(II) complexes with NaCN and the oxidative addition reaction of $Ni[P(C_6H_5)_3]_2$ with substituted aryl halides.

Conversion of aryl halides into the corresponding nitriles is usually effected by heating the halide with copper(I) cyanide (1, 2, 3, 4, 5) to 150°–240°C in solvents (or diluents) such as pyridine, quinoline, dimethylformamide, *N*-methylpyrrolidone, dimethylsulfoxide, or hexamethylphosphoramide. By using Group VIII metal complexes as catalysts the reaction temperature of this conversion can be reduced to as low as 30°C. Thus, an aromatic halide is transformed into the corresponding nitrile (7) by treating it with sodium cyanide in the presence of a catalytic quantity of tris(triphenylphosphine)nickel (Reaction 1). *trans*-Chloro(aryl)bis(triphenylphosphine)nickel(II) complexes 1 (8),



X = Cl, Br, J

easily obtained from aryl halides and $\text{Ni}[\text{P}(\text{C}_6\text{H}_5)_3]_3$ (Reaction 2), can also be used as catalysts.



The reaction can be carried out in solvents such as methanol, ethanol, acetone, etc. under conditions ($30^\circ\text{--}60^\circ\text{C}$) far milder than those of the previous methods.

This process is an example of the ability of nickel complexes to catalyze substitution reactions of aromatic halides under very mild conditions. A further example of their catalytic activity is the carbonylation of aromatic halides at the atmospheric pressure of carbon monoxide (6).

Experimental

All reagents were commercially available and used without further purification. The phosphine ligands were obtained commercially and recrystallized or distilled. Solvents were deoxygenated by vacuum-nitrogen technique.

$\text{Ni}[\text{P}(\text{C}_6\text{H}_5)_3]_3$, $\text{Ni}[\text{P}(\text{C}_6\text{H}_{11})_3]_3$, $\text{Ni}[\text{P}(p\text{-C}_6\text{H}_4\text{CH}_3)_3]_3$ and $\text{Ni}[(\text{C}_6\text{H}_5)_2\text{P}(\text{CH}_2)_4\text{P}(\text{C}_6\text{H}_5)_2]_2$ were prepared (9, 10) by adding phosphine to a stirred suspension of bis(cycloocta-1,5-diene)nickel in diethyl ether or by treating $\text{Ni}(\text{PR}_3)_2\text{C}_2\text{H}_4$ (11) with excess phosphine.

Preparations of $\text{Ni}[\text{P}(\text{C}_6\text{H}_5)_3]_3$ and *trans*-chloro(aryl)bis(triphenylphosphine)nickel from $\text{NiCl}_2[\text{P}(\text{C}_6\text{H}_5)_3]_2$ (12) are reported. Alternatively, the *trans*-chloro(aryl)bis(organophosphine)nickel complexes were prepared from $\text{Ni}(\text{PR}_3)_3$ (8, 13). Identical results were obtained from catalysts prepared in different ways. Because all the reactions involved in this work are sensitive to oxygen, all were carried out under N_2 .

All organic reaction products were identified by comparison with known samples using melting point, GLC, IR, and NMR. Yields were generally determined by GLC using an internal standard after treating the reaction mixture with water and extracting the organic compounds with diethyl ether. Hewlett-Packard model 7620 A (flame detector) gas chromatograph, equipped with a 2 meter stainless steel column packed with 10% Apiezon L or with 10% silicon rubber on Chromosorb was used.

IR spectra were recorded on a Perkin-Elmer model 125 spectrophotometer. Melting points were determined on a Kofler hot-stage apparatus and are not corrected.

Tris(triphenylphosphine)nickel. $\text{NiCl}_2[(\text{PC}_6\text{H}_5)_3]_2$ (5.0 grams), powdered manganese iron alloy (3.0 grams; Mn 79%, Fe 16%, C 1.45%, Si 0.8%, Ni 0.2%, particle size 0.025–0.040 mm), $\text{P}(\text{C}_6\text{H}_5)_3$ (4.5 grams),

and methanol (50 ml) were stirred at room temperature under nitrogen overnight. The solid remaining after filtration was dissolved in 60 ml of hot benzene (50°C). The hot solution was filtered and diethyl ether (120 ml) was added. The red solid crystallizing at -20°C was filtered, washed with cold diethyl ether, and dried for several hours under vacuum. Analysis calculated for $\text{Ni}[\text{P}(\text{C}_6\text{H}_5)_3]_3$: C, 76.7, H, 5.32%; found C, 76.2, H, 5.6%.

***trans*-Chloro(1-naphthyl)bis(triphenylphosphine)nickel.** $\text{NiCl}_2 \cdot [\text{P}(\text{C}_6\text{H}_5)_3]_2$ (10 grams), 1-chloronaphthalene (3.6 grams), manganese/iron alloy (5 grams), and dimethylformamide (100 ml) were stirred at room temperature under nitrogen overnight. Methanol (100 ml) was added, and the solid was filtered and washed with methanol. The solid was dissolved in hot benzene (300 ml; 50°C). The solution was filtered and reduced to 150 ml under vacuum. On addition of methanol (200 ml) an orange-yellow compound crystallized (10.4 grams, m.p. 172°C). Analysis calculated for $\text{C}_{10}\text{H}_7\text{NiCl}[\text{P}(\text{C}_6\text{H}_5)_3]_2$: C, 74.1, H, 4.97%; found C, 74.22, H, 4.98%. Other arylnickel(II) complexes (Reaction 2) were prepared in a similar way.

***trans*-Chloro(1-naphthyl)bis(tricyclohexylphosphine)nickel.** *trans*- $\text{C}_{10}\text{H}_7\text{NiCl}[\text{P}(\text{C}_6\text{H}_5)_3]_2$ (1.85 grams), tricyclohexylphosphine (2.1 grams), and acetone (30 ml) were stirred at 50°C for 3 hrs. The yellow solid was filtered, washed with acetone, and crystallized from benzene-methanol. The crystallized complex was filtered and dried under vacuum (1.6 gram, m.p. 190°C). Analysis calculated for $\text{C}_{10}\text{H}_7\text{NiCl}[\text{P}(\text{C}_6\text{H}_{11})_3]_2$: C, 70.7, H, 9.35%; found: C, 71.2, H, 9.45%.

***trans*-Cyano(*o*-chlorophenyl)bis(triphenylphosphine)nickel.** NaCN [0.06 gram in 5 ml acetone:water (80:20)] were added to a suspension of *o*- $\text{ClC}_6\text{H}_4\text{NiCl}[\text{P}(\text{C}_6\text{H}_5)_3]_2$ (0.75 gram), $\text{P}(\text{C}_6\text{H}_5)_3$ (1 gram), and acetone (30 ml). The solution was stirred for 3 hrs at room temperature, and filtered and evaporated to dryness under vacuum. The pale yellow solid was crystallized from benzene-hexane and dried under vacuum (0.4 gram; m.p. 142°-143°C). Analysis calculated for $\text{ClC}_6\text{H}_4\text{NiCN}[\text{P}(\text{C}_6\text{H}_5)_3]_2$: C, 71.6, H, 4.72, N, 1.94%; found: C, 71.3, H, 4.8, N, 1.70%.

A similar method was used to prepare *trans*-cyano(1-naphthyl)bis(tricyclohexylphosphine)nickel at 50°C (m.p. 157°-159°C, crystallized from benzene-hexane). Analysis calculated for $\text{C}_{10}\text{H}_7\text{NiCN}[\text{P}(\text{C}_6\text{H}_{11})_3]_2$: C, 73.0, H, 9.52, N, 1.81%; found: C, 72.7, H, 9.48, N, 2.02%.

The Cyanation Reaction. Three examples of the cyanation reaction and the general procedure for the determination of the relative rates are reported below.

CYANATION OF 1-CHLORONAPHTHALENE WITH A CATALYST PREPARED *in situ* FROM $\text{NiCl}_2[\text{P}(\text{C}_6\text{H}_5)_3]_2$. A 100-ml round-bottomed flask was equipped with a mechanical stirrer, a thermometer, and a water cooled condenser. The apparatus was swept out with nitrogen, and $\text{NiCl}_2[\text{P}(\text{C}_6\text{H}_5)_3]_2$ (0.7 gram, 0.93 mmole), powdered manganese-iron alloy (0.7 gram), $\text{P}(\text{C}_6\text{H}_5)_3$ (0.7 gram, 2.7 mmole), and ethanol (40 ml) were introduced. The mixture was stirred for 2 hrs at 30°C. 1-Chloronaphthalene (9.6 grams, 59 mmole) was added, and the temperature raised to 55°-60°C. After 2 hrs NaCN (2.9 grams) was added, and the mixture

was stirred for 7 hrs at 55°–60°C. The reaction mixture was poured into 300 ml of water, and the organic part was extracted with diethyl ether (3 × 50 ml). The ether extract was then dried and evaporated. 1-Cyanonaphthalene (8.1 grams, 53 mmole, 90%) was obtained by distillation under vacuum.

CYANATION OF 1-CHLORONAPHTHALENE IN THE PRESENCE OF TRIS(TRIPHENYLPHOSPHINE)NICKEL. 1-Chloronaphthalene (3.6 grams, 22.3 mmole), Ni[P(C₆H₅)₃]₃ (0.75 gram, 0.89 mmole), and ethanol (40 ml) were stirred and warmed up to 60°C. NaCN (1.1 grams, 22.3 mmole) was added, and the mixture was stirred for 3 hrs at 60°C. The reaction mixture was partitioned between water and diethyl ether. The ether extract contained 1-cyanonaphthalene (3.06 grams, 90%). The yield was determined by GLC with acetophenone as internal standard.

CYANATION OF BROMOBENZENE WITH ACETONE CYANOHYDRIN-TRIETHYLAMINE IN THE PRESENCE OF TRANS-CHLORO(1-NAPHTHYL)BIS(TRIPHENYLPHOSPHINE)NICKEL. Bromobenzene (7.85 grams, 50 mmole), C₁₀H₇NiCl[P(C₆H₅)₃]₂ (0.370 gram, 0.5 mmole), P(C₆H₅)₃ (0.130 gram, 0.5 mmole), and acetone (25 ml) were placed in a 100-ml flask equipped with two dropping funnels, magnetic stirrer, and thermometer under nitrogen. Triethylamine (5.6 grams, 50 mmole) and acetone cyanohydrin (4.5 grams, 50 mmole), respectively, were added to the reaction mixture in 7.5 ml of acetone at 35°C in 90 min. After 30 min the reaction mixture was poured into 300 ml of water, and the organic part was extracted with diethyl ether (3 × 50 ml). The ether extract contained benzonitrile (4.12 grams, 40 mmole, 80%) and bromobenzene (1.5 grams, 9.6 mmole, 19%). The yields were determined by GLC with naphthalene as the internal standard.

GENERAL PROCEDURE FOR DETERMINING THE RELATIVE RATES OF CYANATION IN THE PRESENCE OF TRANS-CHLORO(1-NAPHTHYL)BIS(TRIPHENYLPHOSPHINE)NICKEL. Ethanol (25 ml), C₁₀H₇NiCl[P(C₆H₅)₃]₂ (0.40 gram), P(C₆H₅)₃ (0.75 gram), and 5 mmole each of two aromatic halides were placed in a 50-ml round-bottomed flask (55°C) equipped with magnetic stirring bar and water cooled condenser. NaCN (0.05 gram, 1 mmole) was added, and the mixture was stirred for 60 min. The mixture was then partitioned between water and diethyl ether (3 × 20 ml). The relative quantity of nitriles formed was determined by GLC of the ether extract (The relative peaks area were always corrected with the response factor determined with pure nitriles.).

The following couples were tested: *p*-chlorobenzonitrile/*p*-chloroacetophenone, *p*-chloroacetophenone/*p*-chlorodiphenyl, *p*-chlorodiphenyl/chlorobenzene, *p*-chlorodiphenyl/*p*-chlorofluorobenzene, chlorobenzene/*p*-chlorotoluene, chlorobenzene/*p*-chloroanisole, *p*-chloroacetophenone/methyl ester of *m*-chlorobenzoic acid, chlorobenzene/*m*-chlorotoluene, *p*-chlorodiphenylether/*p*-chlorotoluene, *m*-chlorodiphenylether/chlorobenzene, *m*-chlorodiphenylether/*p*-chlorotoluene, chlorobenzene/methyl ester of *m*-chlorobenzoic acid, chlorobenzene/*p*-bromoanisole, *p*-bromoacetophenone/*p*-chlorobenzonitrile, *p*-bromobenzonitrile/*p*-chloroacetophenone, bromobenzene/*p*-chlorodiphenyl, *m*-bromotoluene/chlorobenzene, and *p*-chlorodiphenyl/*p*-bromotoluene.

Results

Catalyst of the Cyanation Reaction. The reaction was studied in the presence of Ni(0) complexes or aryl(chloro)nickel complexes. For a clearer interpretation the corresponding results are considered separately. A variant of the process consisting in the use of acetone cyanohydrin as source of cyanide ions is also reported.

Table I. Cyanation of 1-Chloronaphthalene^a Catalyzed by Nickel(0) Complexes in Ethanol^b at 60°C

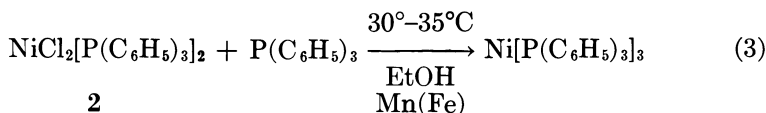
<i>Ni complex</i>	<i>ArX/Ni</i> <i>Molar</i> <i>Ratio</i>	<i>Time</i> <i>(hr)</i>	<i>1-Naphthonitrile</i> <i>Yield^b (%)</i>
Ni[P(C ₆ H ₅) ₃] ₃	25	3	90
Ni[P(<i>p</i> -C ₆ H ₄ CH ₃) ₃] ₃	20	4	90
Ni[(C ₆ H ₅) ₂ P(CH ₂) ₄ P(C ₆ H ₅) ₂] ₂	25	7	80
Ni[P(C ₆ H ₁₁) ₃] ₃	20	3	3
Ni(C ₈ H ₁₂) ₂	20	6	—

^a C₁₀H₇Cl 0.5M; the stoichiometric quantity of NaCN was added as soon as the reaction mixture reaches 60°C.

^b Yields are based on the halide used and were determined by GLC.

CYANATION CATALYZED BY NICKEL(0) COMPLEXES. Results of cyanation of 1-chloronaphthalene with NaCN in ethanol using various nickel(0) complexes as catalysts are shown in Table I.

Tris(triphenylphosphine)nickel, tris(tri-*p*-tolylphosphine)nickel, and bis(1,3-diphenylphosphinepropane)nickel proved to be good catalysts, the first being slightly more effective. The tricyclohexylphosphine complex was a very poor catalyst, and bis(cyclooctadiene)nickel did not catalyze cyanation. Cyanation of several substituted aromatic halides in the presence of Ni[P(C₆H₅)₃]₃ prepared by reducing dichlorobis(triphenylphosphine)nickel(II) **2** with a powdered manganese iron (80:20) alloy (Reaction 3) is reported in Table II.



Sodium cyanide was introduced after adding the aromatic halide because its presence inhibits the reduction of the nickel(II) complex **2** and promotes the decomposition of Ni[P(C₆H₅)₃]₃.

Aromatic nitriles were obtained in high yield when para and meta substituents were present on the aromatic nucleus. Among the para substituted aryl halides *p*-nitrochlorobenzene and *p*-bromoaniline did not

Table II. Cyanation^a of Aromatic Halides in the Presence of a Catalyst Prepared *in situ* from Nickel(II) Salt^b and Manganese-Iron Alloy

Aromatic halides	ArX/Ni		Product, Yield, ^c (%)
	Moles/ Liter	Molar Ratio	
Bromobenzene	2.0	125	benzonitrile ^f 90
	0.7	15 ^c	benzonitrile 95
	0.7	15 ^d	benzonitrile 93
<i>m</i> -Bromotoluene	0.5	20	<i>m</i> -tolunitrile 84
<i>p</i> -Bromo- <i>N,N</i> -dimethyl- aniline	0.7	20	<i>p</i> -cyanodimethylaniline 5
Bromomesitylene	0.7	30	2,4,6-trimethylbenzonitrile 5
Chlorobenzene	1.3	30	benzonitrile 95
1-Chloronaphthalene	1.5	60	1-cyanonaphthalene 90
2-Chloronaphthalene	0.5	20	2-cyanonaphthalene 91
<i>p</i> -Chlorobenzonitrile	1.5	40	terephthalonitrile 80
<i>p</i> -Chlorobenzophenone	0.5	20	<i>p</i> -cyanobenzophenone 83
<i>m</i> -Chlorofluorobenzene	0.5	20	<i>m</i> -fluorobenzonitrile 84
<i>p</i> -Chloroacetophenone	0.7	30	<i>p</i> -cyanoacetophenone 80
<i>m</i> -Chlorodiphenyl	0.7	30	<i>m</i> -cyanodiphenyl 85
<i>m</i> -Dichlorobenzene	1.0	30	isophthalonitrile 86
<i>p</i> -Dichlorobenzene	1.0	30	terephthalonitrile 91
<i>p</i> -Chloronitrobenzene	1.0	30	—
<i>o</i> -Dichlorobenzene	1.0	30	—
<i>o</i> -Chlorobenzonitrile	0.7	30	—
<i>o</i> -Chlorofluorobenzene	1.0	30	<i>o</i> -fluorobenzonitrile <3
Iodobenzene	0.7	20	benzonitrile 75

^a Solvent is anhydrous ethanol.

^b $NiCl_2[P(C_6H_5)_3]_2$ was always used except otherwise indicated. An additional quantity of $P(C_6H_5)_3$ (2 moles per mole of Ni complex) was added. Powdered Mn-Fe alloy (1 gram per gram of nickel(II) complex) was used. The reduction was completed in 2 hrs at 30°C; then the aryl halide was added, the temperature raised to 55°-60°C and the stoichiometric quantity of NaCN added. Reaction time, after the addition of NaCN, is between 3 and 12 hrs.

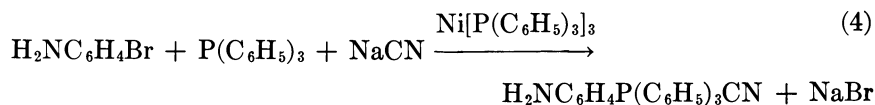
^c $NiBr_2[P(C_6H_5)_3]_2$.

^d $NiBr_2[P(p-C_6H_4CH_3)]_2$.

^e Yields were based on the aromatic halide used and were determined by GLC.

^f Yield was based on the bromobenzene used and was of isolated benzonitrile.

undergo cyanation. The former decomposed the catalyst while the latter yielded the phosphonium salt 3 (14).



Among the ortho substituted aryl halides, *o*-dichlorobenzene and *o*-chlorobenzonitrile did not react while *o*-fluorochlorobenzene and bromomesitylene gave the nitrile in poor yield. The highest catalytic efficiency obtained in the case of bromobenzene was about 110 moles of

Table III. Cyanation of Aromatic Halides in the Presence

<i>Aromatic halide</i>	<i>ArX/Ni</i>		<i>Temp., °C</i>
	<i>Moles/Liter</i>	<i>Molar Ratio</i>	
Bromobenzene	0.8	20	55
<i>p</i> -Bromoanisole	0.8	20	
Chlorobenzene	0.3	10	
1-Chloronaphthalene	0.3		
<i>p</i> -Chlorodiphenyl	0.3		
<i>m</i> -Chlorodiphenyl ether	0.8	20	
<i>p</i> -Chloroacetophenone	0.8	20	
<i>p</i> -Chloroaniline	0.8	20	
<i>o</i> -Dichlorobenzene	0.8	20	
<i>o</i> -Bromotoluene	0.3	10 ^{b, c}	50
<i>o</i> -Chlorofluorobenzene	0.8	10 ^{b, c}	55
<i>o</i> -Bromoanisole	0.5	10 ^{b, c}	20
<i>o</i> -Dichlorobenzene	0.5	10 ^{b, c}	80
<i>o</i> -Chlorobenzonitrile	0.5	10 ^{b, c}	

^a *trans*-Chloro(1-naphthyl)bis(triphenylphosphine)nickel was always used except otherwise indicated.

^b The complex obtained from the oxidative addition of the halide to the tris (triphenylphosphine)nickel was used.

nitrile per mole of nickel. No further attempts were made to improve this result.

Tris(*p*-tolylphosphine) was used successfully in place of triphenylphosphine. The cyanation reaction appears to be a substitutive reaction, the cyano group always occurring on the carbon originally bound to the halogen.

Table IV. Cyanation of Aromatic

<i>Aromatic halide</i>	<i>ArX/Ni</i>		<i>T, °C</i>	<i>Time, hrs</i>
	<i>(Moles/Liter)</i>	<i>Molar Ratio</i>		
Bromobenzene	(0.4)	10	55	1
				3
				1
				1
			50	0.4
			30	0.6
			20	0.6
Bromobenzene	(1.25)	100	50	1
			35	2
1-Chloronaphthalene	(0.4)	10	50	2
Bromomesitylene	(0.4)	10	50	2

^a The catalyst was *trans*-chloro(1-naphthyl)bis(triphenylphosphine)nickel. 0.08*M* of P(C₆H₅)₃ were added in each experiment.

of *trans*-Chloro(aryl) bis(triphenylphosphine) nickel(II)^a

<i>Time,</i> <i>hrs</i>	<i>Solvent</i>	<i>Product</i>	<i>Yield (%)^d</i>
1	Ethanol	benzonitrile	97
2		<i>p</i> -anisonitrile	97
1.5		benzonitrile	71
0.75		1-naphthonitrile	98
		<i>p</i> -cyanodiphenyl	94
6		<i>m</i> -cyanodiphenylether	98
1	DMF	<i>p</i> -cyanoacetophenone	93
6		<i>p</i> -cyanoaniline	30
12		<i>o</i> -chlorobenzonitrile	<2
1		<i>o</i> -tolunitrile	90
4		<i>o</i> -fluorobenzonitrile	5
16		<i>o</i> -anisonitrile	90
5		<i>o</i> -chlorobenzonitrile	<2
5		phthalonitrile	<2

^c A concentrated aqueous solution of NaCN was dropped.

^d Yields are based on the halide used and were determined by GLC.

CYANATION CATALYZED BY *trans*-CHLORO(ARYL)BIS(TRIPHENYLPHOSPHINE)NICKEL(II) COMPLEXES. In Table III cyanation of aryl halides catalyzed by the Ni(II) complexes obtained by reaction between aryl halides and Ni[P(C₆H₅)₃]₃ (Reaction 2) is shown. In general the *trans*-chloro(1-naphthyl)bis(triphenylphosphine)nickel(II) complex was used. Ortho substituted aryl halides were allowed to react in dimethylformamide

Halides with Acetone Cyanohydrin^a

<i>Amine</i>	<i>Solvent</i>	<i>Product</i>	<i>Yield (%)^c</i>
N(Et) ₃ ^b	benzene	benzonitrile	<2
N(Et) ₃			95
N(Et) ₃ ^b	DMF		90
N(Et) ₃ ^b			90
N(Et) ₃ ^b	ethanol		<2
N(Et) ₃			98
N(Et) ₃	acetone		98
N(Et) ₃			5
Pyridine			<1
N(Et) ₃			80
N(Et) ₃			90
		1-naphthonitrile	90
		cyanomesitylene	<1

^b Acetone cyanohydrin and N(Et)₃ were added all at once. In the other examples the two reagents were dropped in a time slightly inferior to the reported reaction time.

^c Yields are based on the halide used and were determined by GLC.

Table V. Influence of the Solvent in Cyanation of Bromobenzene^a with Sodium Cyanide

<i>Solvent</i>	<i>Time, hrs</i>	<i>Addition of NaCN</i>	<i>Benzonitrile Yield %^b</i>
Ethanol	1	in one batch	98
Methanol	1		<2
	1	water solution in 55 min	98
Dimethylformamide	4	in one batch	10
	1	water solution in 55 min	98
Benzene	1	in one batch	^c

^a Bromobenzene 0.8M; Catalyst: *trans*-chloro(1-naphthyl)bis(triphenylphosphine) nickel 0.08 M and P(C₆H₅)₃ 0.16 M.

^b Yields are based on the halide used and were determined by GLC.

^c Benzonitrile was not found.

in the presence of the complex between the corresponding halide and Ni[P(C₆H₅)₃]₃. Among the latter halides, *o*-chlorotoluene and *o*-bromoanisole gave the nitrile in good yield. *o*-Fluorochlorobenzene was less reactive while *o*-dichlorobenzene and *o*-chlorobenzonitrile reacted to a very low extent as shown in Table II.

CYANATION IN THE PRESENCE OF ACETONE CYANOHYDRIN. All the reactions described were carried out with sodium cyanide. Other cyanides such as potassium cyanide are also useful. The use of acetone cyanohydrin and triethylamine was very effective (Table IV).

By using this source of cyanide ions the reaction occurred in a variety of solvents and at very mild conditions. For example in acetone it was possible to observe a rapid reaction even at 30°C. A strong base, such as triethylamine, was necessary to induce the formation of cyanide ion (15). In the presence of weak bases such as pyridine, cyanation does not occur under the same reaction conditions. Ortho substituted aryl halides were

Table VI. Influence of Phosphorus Ligands

<i>Solvent</i>	<i>Cyanide source</i>	<i>Added ligand</i>
Ethanol	NaCN	P(C ₆ H ₅) ₃
	OH	
Acetone	CH ₃ —C—CH ₃ /NEt ₃ ^b	P(C ₆ H ₅) ₃
	CN	
		^b P(C ₆ H ₁₁) ₃
		^b P(C ₄ H ₆) ₃
Ethanol	NaCN	P(C ₆ H ₅)(OC ₆ H ₅) ₂
	NaCN	P(OC ₆ H ₅) ₃

^a 1-chloronaphthalene 0.3M; C₁₀H₆NiCl [P(C₆H₅)₃]₂ 0.03M Stoichiometric quantity of NaCN and acetone cyanohydrin-NEt₃ was added.

less reactive in these cases. High yields were generally obtained by slow addition of the mixture of acetone cyanohydrin with triethylamine to the solution containing the catalyst and the aromatic halide. Catalyst efficiency depends on reactivity of the aryl halide. Reaction temperature and feeding rate of the acetone cyanohydrin should be adjusted according to the reactivity of the aromatic halide.

Influence of Solvent, Ligand, and Substrate Substituents. These factors appear to play a very important role in the cyanation reaction.

INFLUENCE OF THE SOLVENT. Tables IV and V show the influence of the solvent on cyanation using both sodium cyanide and acetone cyanohydrin-triethylamine. The reaction can be carried out in a large number of solvents.

As reported before, the reaction can be carried out in ethanol by adding quickly a stoichiometric quantity of NaCN after the catalyst and aryl halide additions. In methanol or in dimethylformamide the catalytic cyanation occurs only if the sodium cyanide is added slowly. In benzene, always in the presence of NaCN, the reaction does not occur and complexes **1** can be isolated.

These results suggest that the concentration of cyanide ions must be very low, even less than the solubility of NaCN in anhydrous ethanol (0.1%). In fact by saturating ethanol with NaCN at 50°C and then adding the catalyst, the reaction occurred to a limited extent. Analogous conclusions can be drawn from the results of reactions carried out with acetone cyanohydrin (Table IV).

INFLUENCE OF PHOSPHORUS LIGANDS. In Table I, nickel(0) complexes with arylphosphines appear to be much more effective catalysts than those with alkylphosphines. The results of Table VI confirm this observation.

on Cyanation of 1-Chloronaphthalene^a

Moles/ Liter	T, °C	Time, hrs	1-Naphthonitrile Yield % ^c
0.09	55	1	98
0.09	50	1	96
0.09	50	6	<2
0.09	50	6	<2
0.09	55	1	<2
0.09	55	1	<2

^b Acetone cyanohydrin/NEt₃ solution was added in 55 min.

^c Yields are based upon the halide used and were determined by GLC.

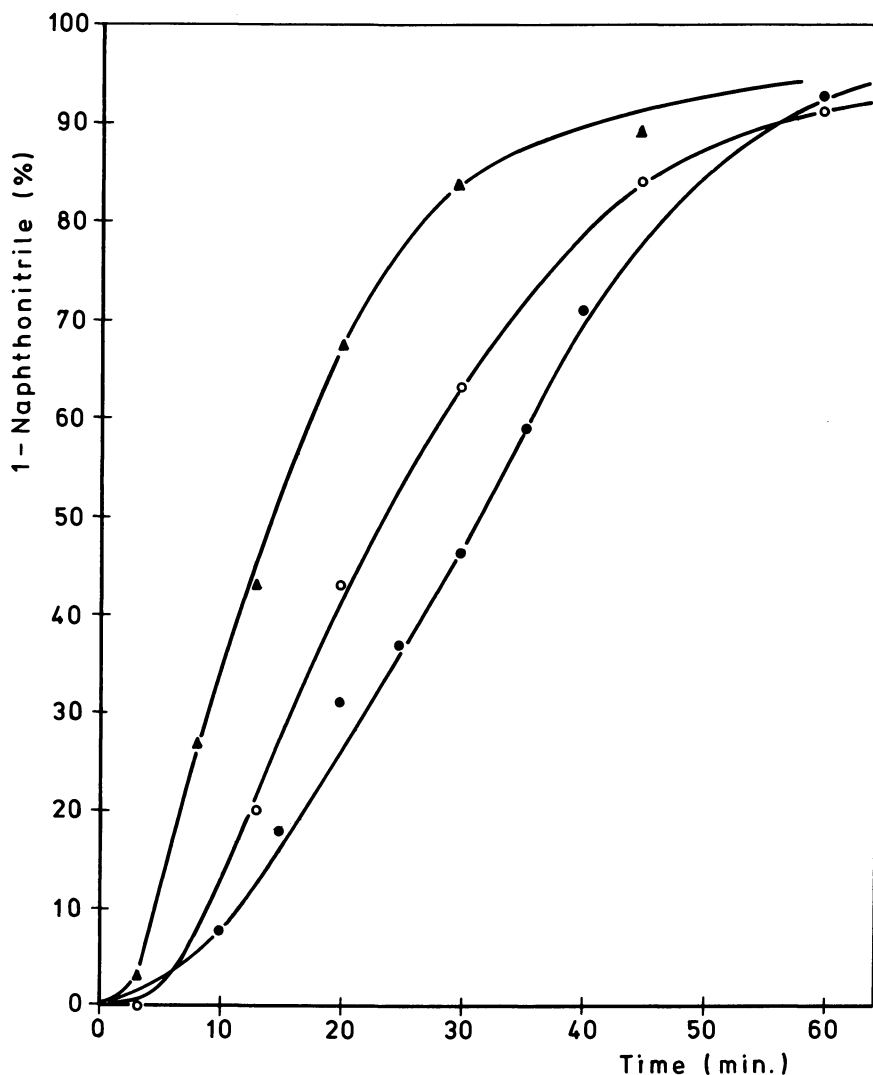


Figure 1. Influence of $P(C_6H_5)_3$ concentration on the cyanation of 1-chloronaphthalene in ethanol at $55^\circ C$ (see Table VI)
 Added $P(C_6H_5)_3$: \blacktriangle , 0.3M; \circ , 0.09M; \bullet , 0.03M

The reactions were carried out by using *trans*-chloro(1-naphthyl)-bis(triphenylphosphine)nickel(II) (1, Ar = $C_{10}H_7$) complex as catalyst in the presence of various phosphorus ligands. We observed that aromatic phosphines in arynickel(II) complexes 1 are easily replaced by aliphatic phosphines. In fact in the presence of alkylphosphines, such as $P(C_6H_{11})_3$ and $P(C_4H_9)_3$, cyanation did not occur. Moreover phosphites such as

$P(OC_6H_5)_3$ and $P(OC_6H_5)_2(C_6H_5)$ inhibited the reaction although $(C_6H_5)_2P(CH_2)_3P(C_6H_5)_2$ was effective. Finally, adding $P(C_6H_5)_3$ to the reaction mixture increased the reaction rate (Figure 1).

INFLUENCE OF THE SUBSTITUENT ON THE AROMATIC HALIDES ON THE RATE OF CYANATION. The experimental conditions of cyanation, the presence of a solid component slightly soluble (NaCN), or the need of a slow addition of the source of cyanide ion did not allow a rigorous kinetic study of the reaction. However we determined the influence of substituents on the aromatic halides on the rate of cyanation by competitive reactions. The rates relative to chlorobenzene are compared in Table VII.

Equimolar quantities of the reference halide (*e.g.* chlorobenzene) and the halide whose reactivity was to be established were mixed in the presence of the catalyst (1, Ar = $C_{10}H_7$) and a small quantity of NaCN which was necessary to avoid a change in the concentration of the two halides, especially when the difference in reactivity between the two

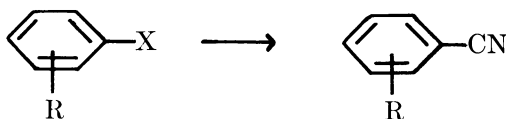


Table VII. Relative Rates of Cyanation of Aromatic Halides in Ethanol at 55°C^a

<i>R</i>	<i>X</i>	Relative Rate $\nu(ArX)/\nu(C_6H_5Cl)$
H	Cl	1
<i>p</i> -CH ₃	Cl	0.12
<i>p</i> -OCH ₃	Cl	0.52
<i>p</i> -OC ₆ H ₅	Cl	0.93
<i>p</i> -C ₆ H ₅	Cl	2.7
<i>p</i> -F	Cl	1.4
<i>p</i> -COCH ₃	Cl	$3.7 \cdot 10^2$
<i>p</i> -CN	Cl	$5.8 \cdot 10^2$
<i>m</i> -CH ₃	Cl	0.87
<i>m</i> -COOCH ₃	Cl	20
<i>m</i> -OC ₆ H ₅	Cl	5.0
H	Br	10
<i>p</i> -CH ₃	Br	0.08
<i>p</i> -OCH ₃	Br	0.37
<i>p</i> -COCH ₃	Br	$4.7 \cdot 10^3$
<i>p</i> -CN	Br	$5.2 \cdot 10^3$
<i>m</i> -CH ₃	Br	2.3

^a Five mmoles each of two aromatic halides were allowed to react in the presence of 0.5 mmoles of $C_{10}H_7NiCl [P(C_6H_5)_3]_2$ plus 0.15 mmoles of $P(C_6H_5)_3$ with 1.0 mmoles of NaCN in 25 ml of ethanol for 1 hr. The relative quantities of nitriles were determined by GLC.

Table VIII. Relative Rates of Cyanation of Aromatic Halides, Influence of the Concentration of the Aromatic Halide^a

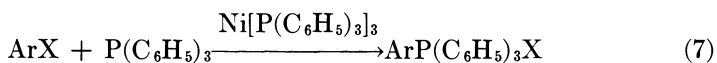
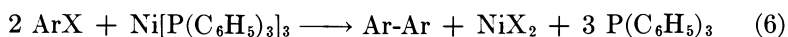
Chlorobenzene, M	<i>p</i> -Chlorodiphenyl, M	$\frac{\text{Relative Rate, } \nu(\text{C}_6\text{H}_5\text{C}_6\text{H}_4\text{Cl})}{\nu(\text{C}_6\text{H}_5\text{Cl})}$
0.2	0.2	3.0
0.4	0.2	1.3
0.8	0.1	0.33

^a Experimental conditions are similar to those of Table VII.

halides was large. Reaction rates are roughly first order in the aromatic halide as shown by the data in Table VIII.

The relative rates obtained for various para and meta substituents have been plotted against the values of Hammett's σ (Figure 2) (16). There is a good correlation for electron withdrawing substituents (*p*-F, *m*-OC₆H₅, *m*-COOCH₃, *m*-CN, *p*-COCH₃, *p*-CN; $\rho = 4.85$, $r = 0.965$) while electron releasing ones do not follow the same pattern. In fact *m*-chlorotoluene, *p*-chloroanisole, and *p*-chlorodiphenyl ether are only slightly less reactive than chlorobenzene. The data in Table VII permit derivation of the difference of reactivity between bromo and chloro derivatives. When electron-withdrawing groups are present on the aromatic nucleus, bromo derivatives are 10 times more reactive than chloro derivatives. On the contrary when electron-releasing groups are present, chloro are slightly more reactive than bromo derivatives.

Side Reactions. There are three secondary reactions which can be observed during cyanation: substitutive hydrogenation (Reaction 5) (8, 17, 18, 19) aryl dimerization (Reaction 6) (8, 17, 18, 19), and catalytic formation of phosphonium salts (Reaction 7) (14).



In general these reactions do not interfere with cyanation. Reaction 7 is a catalytic process (14) and is strongly favored by electron-releasing substituents on the aromatic halide. In fact in the case of *p*-aminochlorobenzene, formation of the phosphonium salt competes with the cyanation process.

Stoichiometric Cyanation Reaction. To elucidate the mechanism, the stoichiometric cyanation reaction of *trans*-chloro(aryl)bis(triphenylphosphine)nickel(II) complexes **1** was studied. Arylnickel(II) complexes

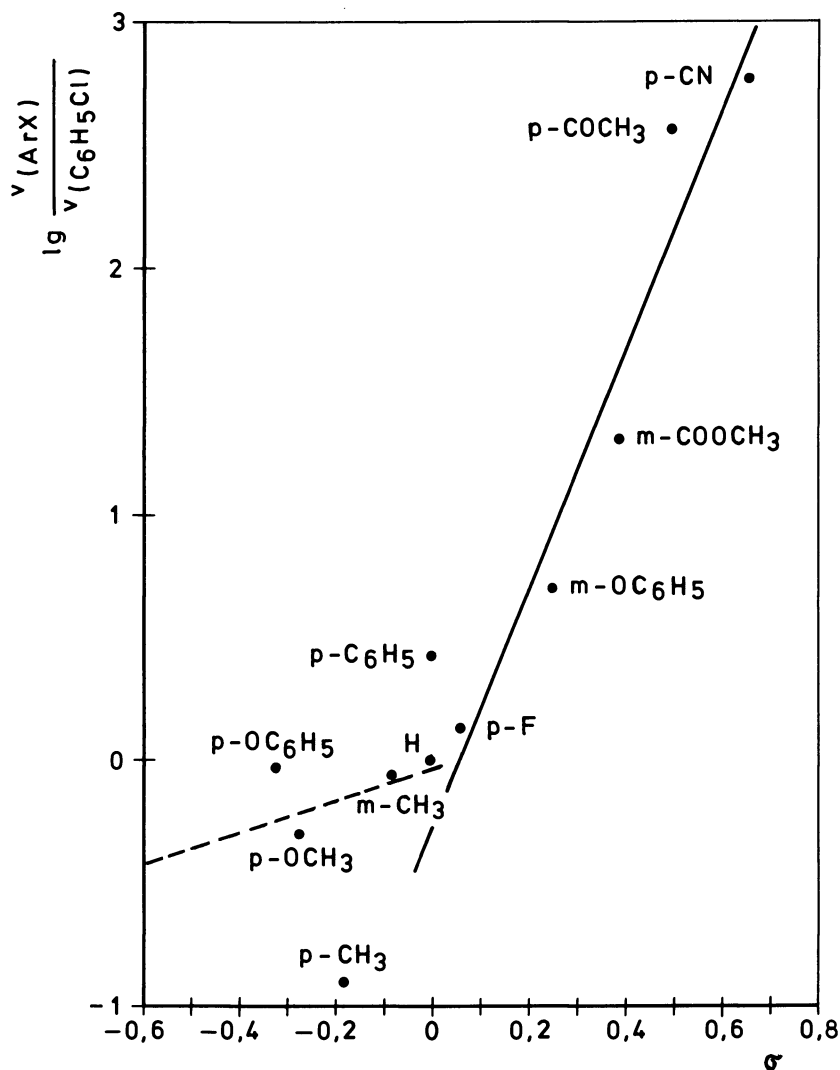
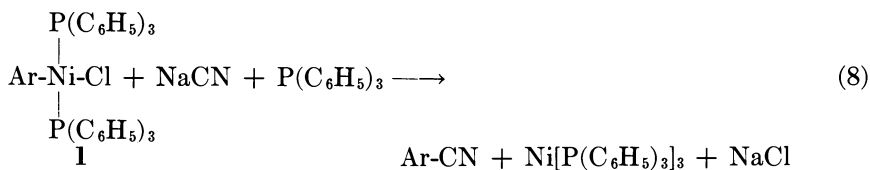


Figure 2. Correlation of relative rates of cyanation of substituted aromatic halides with σ constants (16) (see Table VII)

1 reacted with sodium cyanide in the presence of $\text{P}(\text{C}_6\text{H}_5)_3$ to give the aromatic nitriles and $\text{Ni}[\text{P}(\text{C}_6\text{H}_5)_3]_3$ according to Reaction 8. The reac-



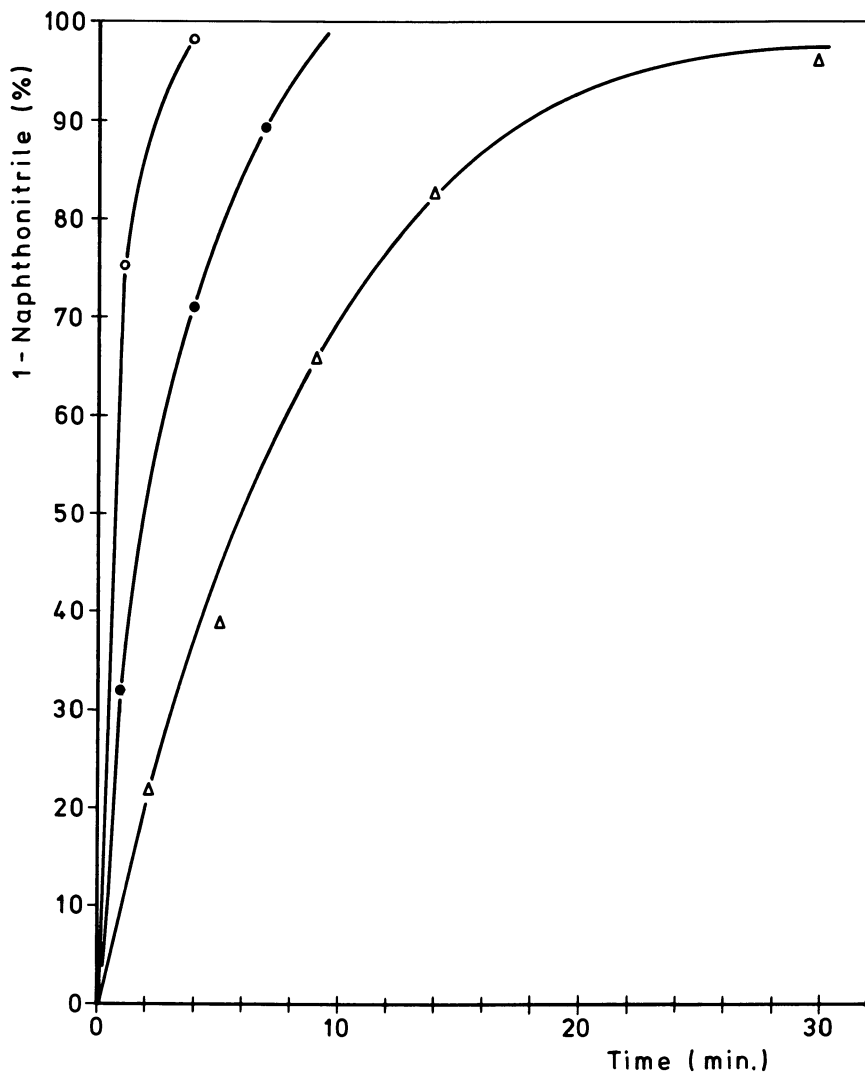


Figure 3. Cyanation of *trans-chloro(1-naphthyl)bis(triphenylphosphine)nickel* with NaCN in DMF at 20°C

Nickel complex, $2.7 \times 10^{-3}M$; NaCN: \circ $13.4 \times 10^{-3}M$; \bullet $8.0 \times 10^{-3}M$; \triangle $2.7 \times 10^{-3}M$. The formation of 1-naphthonitrile was determined by GLC.

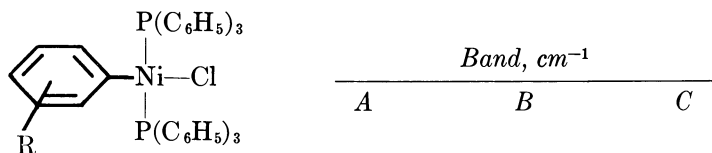
tion rate as determined by GLC increases with the concentration of sodium cyanide as shown in Figure 3. The progress of the reaction was followed also by IR.

The orange-yellow solution obtained by treating the complex of nickel(II) with NaCN in dimethylformamide was placed, under nitrogen, in an IR optical cell. Initially only a band at about 2123 cm^{-1} (Band

A) was observed. The intensity of this band decreases while two other bands at about 2225 (Band B) and 2150 cm^{-1} (Band C) increased gradually.

Three small bands at 2040, 2008, and 1970 cm^{-1} were also found along with a shoulder at about 2110 cm^{-1} which slowly disappeared as the reaction proceeded. This was more evident in the case of ortho derivatives, such as *o*-anisoylnickel(II) complex.

Table IX. Cyanation of *trans*-Chloro(aryl)bis(triphenylphosphine)-nickel(II) Complexes, IR Absorptions



R equal to:

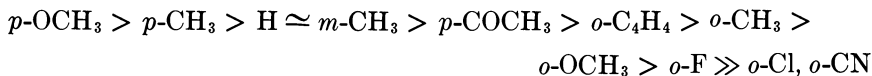
H	2121	2227	2154
<i>p</i> -OCH ₃	2123	2223	2159
<i>p</i> -CH ₃	2123	2228	2157
<i>p</i> -COCH ₃	2122	2217	2137
<i>m</i> -CH ₃	2123	2228	2155
<i>o</i> -CH ₃	2123	2225	2152
<i>o</i> -OCH ₃	2128	2236	2159
<i>o</i> -C ₄ H ₄	2126	2222	2142

^a Nickel II (complex) 0.1 mmoles, NaCN 0.2 mmoles, P(C₆H₅)₃ 0.2 mmoles, dimethylformamide 2 ml. After one minute stirring the solution was introduced in an NaCl optical cell (0.5 mm). Spectra were measured with a Perkin-Elmer Model 125 spectrophotometer.

The positions of the three principal bands (A, B, and C) are listed in Table IX for several complexes. B and C appeared when Ni[P(C₆H₅)₃]₃ was added to a solution of the nitrile (band B). Therefore it is reasonable to assign band B and C, respectively, to the free nitrile and to the nitrile coordinated on the nickel(0). A shift of ν (CN) to lower frequency on complexation of benzonitrile to Ni[P(O-*o*-C₆H₄CH₃)₃]₃ has been reported recently (20). A further proof that nickel(0) complex is responsible for band C is its disappearance on addition of an aromatic halide.

Band A is assigned to coordinated cyanide. The bands at 2040, 2008, and 1970 cm^{-1} were observed when NaCN was added to a dimethylformamide solution of Ni[P(C₆H₅)₃]₃ (21). The rate dependence of

nitrile formation on the aryl group substituent was found to be in the following order:



The $p\text{-OCH}_3$ is approximately four times more reactive than $p\text{-COCH}_3$. There is little difference in the reactivity of para- and meta-substituted aryl groups but ortho-substituted aryl groups are less reactive than the analogous meta and para substituted ones. For example $o\text{-CH}_3$ is about 12 times less reactive than $p\text{-CH}_3$. In the ortho series, $o\text{-CH}_3$ is about 15 times more reactive than $o\text{-F}$. Thus in both series the reactivity decreases on passing from electron-releasing to electron-withdrawing substituents.

Discussion

Aromatic halides react with nickel(0) phosphine complexes at room temperature to yield complexes **1** (8, 13) by oxidative addition. We observed that arylnickel complexes **1** react with sodium cyanide to produce aromatic nitriles and the phosphine nickel(0) complexes, thus closing the catalytic cycle.

Therefore it seems reasonable to assume that cyanation of aryl halides involves two fundamental processes: oxidative addition of the tris(triphenylphosphine)nickel complex on the aromatic halide (Reaction 2) and cyanation of the arylnickel(II) complex **1** (Reaction 8). A further proof of the validity of this scheme is that both $\text{Ni}[\text{P}(\text{C}_6\text{H}_5)_3]_3$ and arylnickel(II) complexes **1** have an equal catalytic activity, these latter being intermediates of the catalytic process. Recent studies (22) on the influence of substituents on the aromatic halide in the oxidative addition reaction with $\text{Ni}[\text{P}(\text{C}_6\text{H}_5)_3]_3$ have given the results shown in Figure 4.

A comparison of Figures 2 and 4 indicates that substituents have a qualitatively similar effect both on the oxidative addition reaction and on the catalytic cyanation. In both cases in fact there is a change in the slope on passing from electron-withdrawing to electron-releasing substituents. As to the effect of electron-withdrawing substituents, the sensitivity is lower in catalytic cyanation ($\rho = 4.8$) than in oxidative addition ($\rho = 8.8$) which is what is to be expected on the basis of the substituent effect in stoichiometric cyanation reaction of arylnickel complexes.

Furthermore the different halogen effect (Br/Cl) exerted by electron-withdrawing and electron-releasing substituents on the formation of nitriles parallels that observed in oxidative additions (22). The quanti-

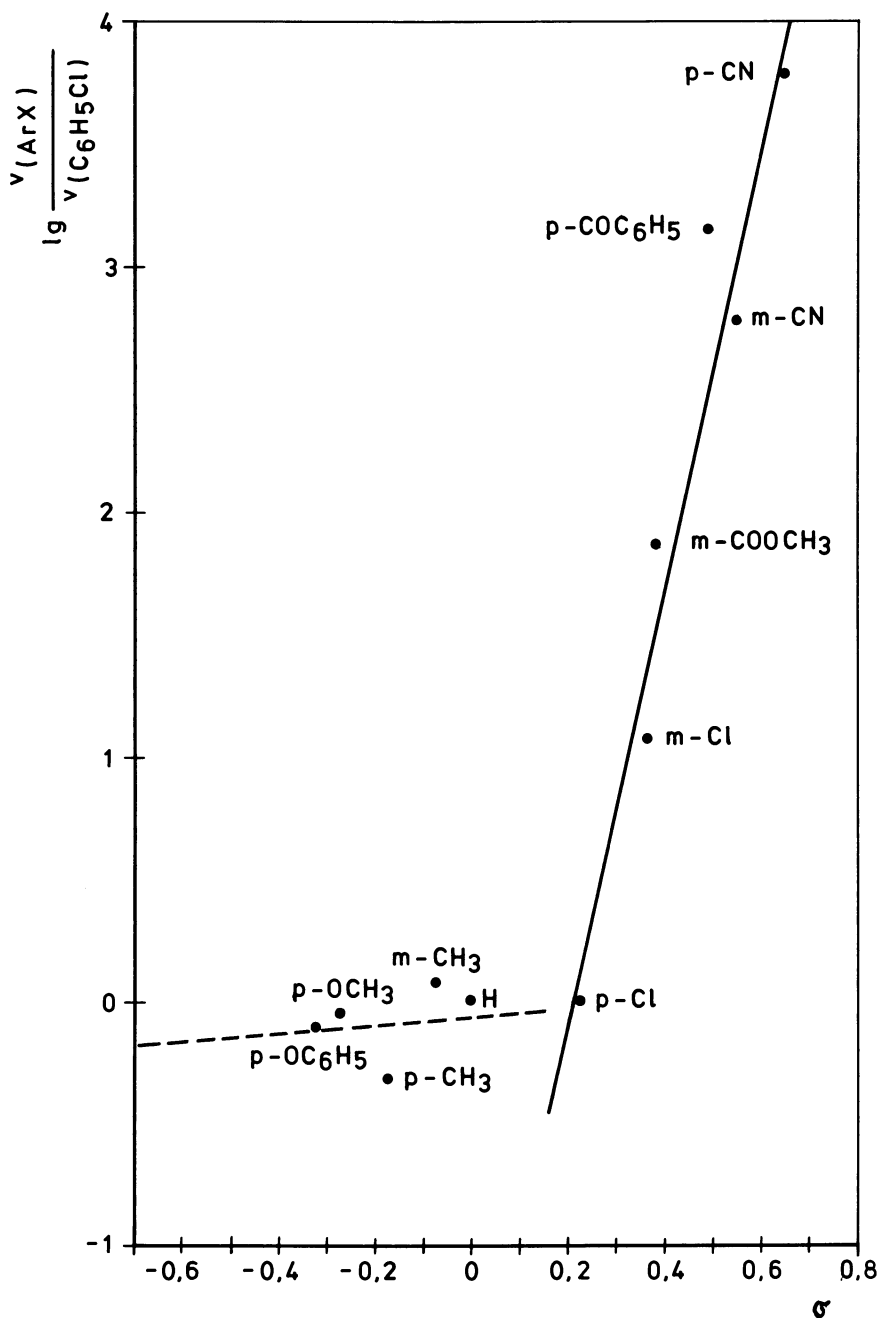
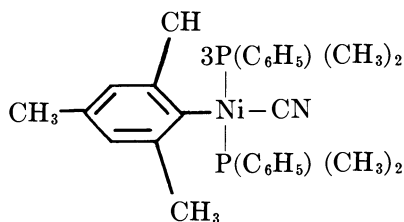


Figure 4. Correlation of relative rates of oxidative addition of $\text{Ni}[\text{P}(\text{C}_6\text{H}_5)_3]_3$ to substituted aromatic halides with σ constants (16, 22)

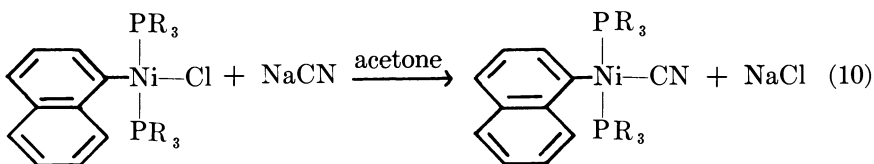
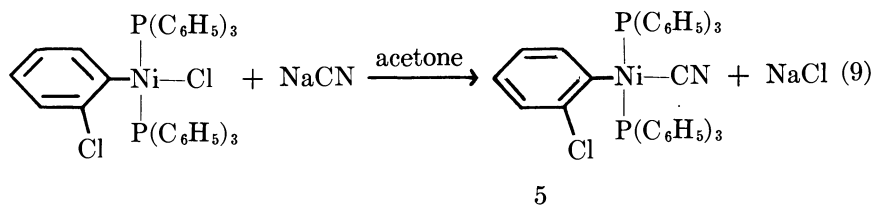
tative differences probably arise from differences in temperatures (50° and 20°) and solvents (ethanol and benzene) used in the two reactions.

The last aspect to be discussed is the pathway of nitrile formation from arynickel complexes **1** as suggested by IR evidence. The first band (A in Table IX) which is immediately formed on the reaction of NaCN and **1** has a frequency between 2120 and 2130 cm^{-1} .

During the reaction band A decreases in intensity while either bands B and C, characteristic of free and coordinated nitrile, or the band at 2110 cm^{-1} increase. The band at 2110 cm^{-1} is assigned to the product of metathetical replacement of the halogen, according to what has been reported (23) for complex **4** which has a CN stretching frequency at 2105 cm^{-1} in Nujol.



Moreover we isolated complexes resulting from metathetical replacement in those cases in which formation of nitriles (Reactions 9 and 10) was not observed.



a, R = C_6H_{11}
b, R = C_4H_9

The CN stretching frequency in dimethylformamide is at 2109 cm^{-1} for **5** and **6a** and at 2100 cm^{-1} for **6b**. The band between 2120 and 2130 cm^{-1} is assigned to an intermediate common to both processes, nitrile formation and metathetical replacement (Figure 5).

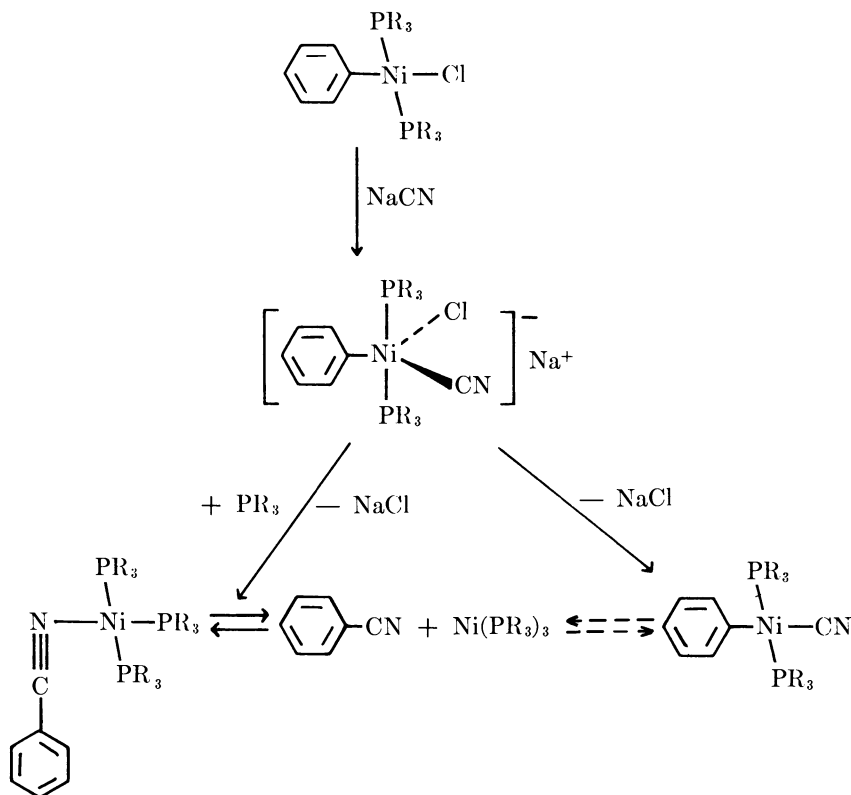


Figure 5. Nitrile formation and metathetical replacement

We believe that this intermediate is a five coordinated nickel complex. This is in agreement with the general finding that substitution reactions of d^8 square planar complexes take place *via* a five-coordinated intermediate (24, 25). During the formation of the nitrile there is a reductive elimination in which the oxidation state of nickel is reduced to zero. This process is obviously favored by electron-releasing substituents on the aryl group. This is exactly what has been observed.

Although we cannot exclude other mechanisms, we prefer to consider the reductive elimination leading to the product as resulting from aryl migration on the coordinated cyano group. This interpretation is supported by what is known about carbon monoxide insertion (26). Carbon monoxide insertion (27) is facilitated because of the greater ability of

this ligand to stabilize low oxidation states than the cyano group. As to the ortho derivatives, which are known to be more stable than the corresponding para and meta groups (8, 28), aryl migration will be more difficult and will take place at a reasonable rate only if electron-releasing substituents are present on the aryl group. Moreover the difficulty in obtaining nitriles with nickel(0) complexes and trialkylphosphine can be attributed to the higher stability of the corresponding nickel(II) complexes (19, 29) and therefore to the stability of the σ -aryl-nickel bond. This effect of alkylphosphines is so dramatic that the oxidative addition of aromatic nitriles to $\text{Ni}(\text{PR}_3)_4$ ($\text{R} = \text{alkyl}$) takes place under very mild conditions (30) to give a stable nickel(II) complex. We can then conclude that nitrile formation will be favored by a weak σ -aryl-nickel bond.

Literature Cited

1. Friedman, L., Shechter, H., *J. Org. Chem.* (1961) **26**, 2522.
2. Newman, M. S., Phillips, D. K., *J. Amer. Chem. Soc.* (1959) **81**, 3667, Newman, M. S., Boden, H., *J. Org. Chem.* (1961) **26**, 2525.
3. Bacon, R. G. R., Hill, H. A. Q., *J. Chem. Soc.* (1964) 1097.
4. Mowry, D. T., *Chem. Rev.* (1948) **42**, 189.
5. House, H. O., Fisher, W. F., *J. Org. Chem.* (1969) **34**, 3626.
6. Cassar, L., Foà, M., *J. Organometal. Chem.* (1973) **51**, 381.
7. Cassar, L., *J. Organometal. Chem.* (1973) **54**, C57.
8. Fahey, D. R., *Organometal. Chem. Rev.* (1972) **7**, 245.
9. Tolman, C. A., *J. Amer. Chem. Soc.* (1970) **92**, 2956.
10. Tolman, C. A., Siedel, W. C., Gerlach, D. H., *J. Amer. Chem. Soc.* (1972) **94**, 2669.
11. Heimbach, P., *Angew. Chem.* (1964) **76**, 586.
12. Venanzi, L. M., *J. Chem. Soc.* (1958) 719.
13. Hidai, M., Kashiwagi, T., Ikeuchi, T., Uchida, Y., *J. Organometal. Chem.* (1971) **30**, 279.
14. Cassar, L., Foà, M., *J. Organometal. Chem.*, in press.
15. Stewart, T. D., Fontana, B. J., *J. Amer. Chem. Soc.* (1940) **62**, 328.
16. McDaniel, D. H., Brown, H. C., *J. Org. Chem.* (1958) **23**, 420.
17. Semmelhack, M. F., Helquist, P. M., Jones, L. D., *J. Amer. Chem. Soc.* (1971) **93**, 5908.
18. Semmelhack, M. F., Helquist, P. M., Goraynski, J. D., *J. Amer. Chem. Soc.* (1972) **94**, 9234.
19. Cassar, L., Giarrusso, A., *Gazz. Chim. Ital.* (1973) **103**, 793.
20. Tolman, C. A., *Inorg. Chem.* (1971) **10**, 1540.
21. El-Sayed, M. F. A., Sheline, R. R., *J. Amer. Chem. Soc.* (1958) **80**, 2047.
22. Foà, M., Cassar, L., unpublished data.
23. Moss, J. R., Shaw, B. L., *J. Chem. Soc. A* (1966) 1793.
24. Basolo, F., Pearson, R. G., "Mechanism of Inorganic Reactions," 2nd ed., p. 375, John Wiley, New York, 1968.
25. Basolo, F., Chatt, J., Gray, H. B., Pearson, R. G., Shaw, B. L., *J. Chem. Soc.* (1967) 2207.
26. Noack, K., Calderazzo, F., *J. Organometal. Chem.* (1968) 101.
27. Hashimoto, I., Tsuruta, N., Ryang, M., Tsutsumi, S., *J. Org. Chem.* (1970) **35**, 3748.

28. Chatt, J., Shaw, B. L., *J. Chem. Soc.* (1960) 1718.
29. Miller, R. G., Fahey, D. R., Kuhlman, D. P., *J. Amer. Chem. Soc.* (1968) **90**, 6248.
30. Gerlach, D. H., Kane, A. R., Parshall, G. W., Jesson, J. P., Muettterties, E. L., *J. Amer. Chem. Soc.* (1971) **93**, 3543.

RECEIVED August 20, 1973.

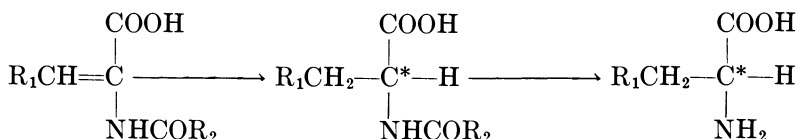
α -Amino Acids by Asymmetric Hydrogenation

W. S. KNOWLES, M. J. SABACKY, and B. D. VINEYARD

Monsanto Industrial Chemicals Co., St. Louis, Mo. 63166

An efficient asymmetric hydrogenation of α -acetamidocinnamic acids has been achieved using a rhodium-chiral phosphine catalyst. This paper describes the preparation of the catalyst and the hydrogenation procedure as well as studies on structure vs. activity.

Efficient catalytic asymmetric hydrogenations have been achieved using an optically active phosphine complexed with rhodium (1, 2, 3, 4, 5, 6, 7, 8). Through this process it is now possible to prepare a number of optically active α -amino acids from the corresponding unsaturated precursor without the usual resolution step by the following sequence.

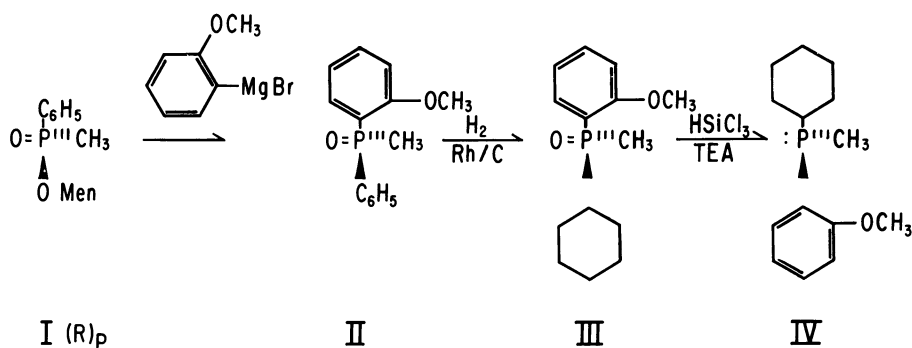


The generality of this approach is limited only by one's ability to obtain the starting prochiral olefin (9).

Preparation of the Catalyst

The most effective ligand in our work for complexing with rhodium was *o*-anisylcyclohexylmethylphosphine. This compound was made from the Mislow intermediate I (10) as shown in Figure 1. The (*R*)_P menthyl ester I gives a chiral phosphine by the sequence in Figure 1 which produces L amino acids while the (*S*)_P ester gives the D configuration. Starting with α -menthol the (*S*)_P menthyl ester was formed in excess and was easily separated. The (*R*)_P ester could be separated from the residual 50/50 mix of diastereoisomers by dissolving in α - or β -pinene and careful fortuitous selective seeding with (*R*)_P. The *o*-

anisylmagnesium bromide reacted with compound I to form the phosphine oxide II. Selective reduction of II to III was accomplished in about 60% yield using 5% rhodium on carbon (Rh/C). The menthyl function could not be displaced from the saturated menthyl ester, menthyl cyclohexylmethylphosphinate, with *o*-anisylmagnesium bromide because of the increased steric hindrance. Compound III can be reduced with either HSiCl₃ and triethylamine or Si₂Cl₆ (11) to give compound IV with inversion of configuration. Reduction of III with HSiCl₃ alone, which in other systems goes with retention (11) of configuration, gave extensive racemization.



Men = | - Menthol

Figure 1. Phosphine synthesis

The ligand IV could be used *in situ* with a soluble rhodium compound, but it was most conveniently converted to a complex of the type [L₂Rh (1,5-cyclooctadiene)]⁺ BF₄⁻ (V) (12, 13) which in the crystalline form was air stable and easy to introduce into hydrogenation batches either as a solid or in methanol solution. Other anions like Cl⁻ used *in situ* or the crystalline PF₆⁻ or B(C₆H₅)₄⁻ salts worked equally well. The catalyst used in some previous work (4, 6) may have been about 95% optically pure (4). The catalyst which gave 90% optical yield in our earlier hydrogenations was probably 98–99% pure since it was not possible to improve it by crystallization of the above complexes. Even purification of the phosphine ligand first as a *D*-camphor sulfonate or tetraphenyl borate salt followed by crystallization of the rhodium complex gave only about 1% improvement.

Study of Variables

These phosphine–rhodium catalyst systems are quite sensitive to variables and thus extreme caution must be used in comparing one ligand

Table I. Hydrogenation of Pro-Chiral Substrates' Enantiomeric Excess *vs.* Reaction Variables^a

<i>Catalyst Ligand</i>	<i>Substrate^b</i>	<i>Solvent</i>	<i>Temperature °C</i>	<i>Abs. Pres. Atm.</i>	<i>Ap-prox. Rel. Rate</i>	<i>ee of Satur. Product, %^c</i>	
IV	VI (free acid)	iso-PrOH (88%)	25	27	1.5	54 ^d	
					3.5	1.0	79 ^d
					0.7	.13	85.5 ^d
IV	VI (as anion)	MeOH	50	3.5	2.0	79 ^d	
			25		.3	79 ^d	
			0		.1	88 ^d	
			25	21	.5	71 ^d	
DIOP (7,8)	VII (free acid)	MeOH	25	3.5	1.0	80.5 ^d	
	VII (free acid)			27	3.0	60 ^e	
DIOP	VI (as anion)	MeOH	50	3.5	2.0	77 ^e	
			25		1.0	1.0	79 ^e
			0		3.5	4.0	76 ^e
DIOP	α -phenyl acrylic acid	MeOH	50	3.5	1.0	61 ^e	
			25		.5	76 ^e	
			0		.1	83 ^e	
IV	α -phenyl acrylic acid	MeOH	25	27	—	12	

^a All runs were made with 0.05% metal, based on substrate.

^b Substrates; VI, α -acetamidocinnamic acid; VII, 3-methoxy-4-hydroxy- α -acetamidocinnamic acid acetate; VIII, 3-methoxy-4-hydroxy- α -benzamidocinnamic acid.

^c The optical rotations of the respective products used for standards were, *N*-Acetyl-*L*-phenylalanine $[\alpha]_D^{20} + 47.2^\circ$ ($c = 1$ in 95% EtOH), 3-Methoxy-4-acetoxy-*N*-acetyl-*L*-phenylalanine $[\alpha]_D^{20} + 40.8^\circ$ ($c = 1$ in MeOH), all ee's were measured by dilution of reaction mixtures and comparison with standards. The correction for catalyst was only about 1%.

^d The ee was the isomer with *L* configuration.

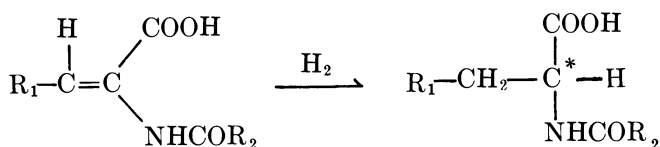
^e The ee was the isomer with *D* configuration.

with another. Generally speaking, the greatest stereoselectivity with the α -acylamidocinnamic acids was achieved with low pressures and low temperatures. The free acid is most responsive to pressure and the carboxylate anion more sensitive to temperature. Table I shows how optimum conditions can be obtained in a variety of ways. The Kagan catalyst (DIOP) (7, 8), though of different structure, behaves similarly; the main point of difference between the two catalysts is their behavior toward α -phenylacrylic acid where DIOP gives 60% optical yield and IV gives only 12%.

The sensitivity of these systems to oxygen or peroxide makes it difficult to draw conclusions from small rate differences, but it is evident that DIOP (7, 8) is somewhat faster. With both systems maximum yields are obtained at the expense of slower rates. In this study all alcohol solvents behave about the same. Small amounts of water are not harmful, but large amounts slow the rate.

The variation in efficiency with ligand structure has been studied, and Table II summarizes these results. In most cases only the best result obtained is given. Varying the large group on the phosphorus gives predictable results. A cyclohexyl is almost identical to an isopropyl. A

**Table II. Hydrogenation of Pro-Chiral Substrates
Phosphine *vs.* Enantiomeric Excess**



Run No.	Phosphine Ligand	Substrate ^a	Meth- od ^b	Pres- sure Atm	ee % ^c	
1	CH ₃ <i>n</i> -Pr	Ph	VIII	A	3.5	28
2	CH ₃ <i>iso</i> -Pr	Ph				28
3	CH ₃ <i>o</i> -anisyl	Ph		B		58
4	CH ₃ <i>o</i> -anisyl	C ₆ H ₁₁	VII	A	.7	88
5	CH ₃ <i>o</i> -anisyl	C ₆ H ₁₁	VIII			90
6	CH ₃ <i>o</i> -anisyl	<i>iso</i> -Pr	VII		3.5	85
7	Iso-Pr	Ph				1
8	CH ₃ <i>o</i> -anisyl	C ₆ H ₅ CH ₂				47
9	CH ₃ <i>o</i> -anisyl	(CH ₃) ₂ CHCH ₂				49
10	CH ₃ <i>o</i> - <i>iso</i> -PrO-Ph	C ₆ H ₁₁	VI		27	40 ^c
11	CH ₃ <i>o</i> - <i>iso</i> -PrO-Ph	C ₆ H ₁₁		B	3.5	46
12	CH ₃ <i>o</i> - <i>iso</i> -PrO-Ph	Ph	VII			37
13	CH ₃ <i>o</i> -BzO-Ph	C ₆ H ₁₁		A		49
14	CH ₃ <i>o</i> -BzO-Ph	C ₆ H ₁₁			27	3
15	CH ₃ <i>o</i> -EtO-Ph	C ₆ H ₁₁			3.5	71
16	CH ₃ <i>o</i> -EtO-Ph	C ₆ H ₁₁	VI	B		83
17	CH ₃ 2Me-4-Br-Ph	C ₆ H ₁₁	VII	A		74
18	CH ₃ <i>o</i> -anisyl	C ₆ H ₁₁	VI(amide)			70
19	CH ₃ <i>o</i> -anisyl	C ₆ H ₁₁	VI(Me ester)			60

^a Substrates; VI, α -acetamidocinnamic acid; VII 3-methoxy-4-hydroxy- α -acetamidocinnamic acid acetate; VIII, 3-methoxy-4-hydroxy- α -benzamidocinnamic acid.

^b A, Free acid procedure; B, Anion procedure; all runs at 25°C except run 16 at 0°C.

^c The ee was all of the L configuration, except run 10 which was D.

phenyl, isobutyl, or benzyl are all less hindered and inferior. Changing the ether group produces a large stereochemical effect which supports the contention that the ether plays a key role (4, 6). It is interesting that the isopropyl ether, under varying conditions, can go from 40% enantiomeric excess D to 46% excess of the L configuration; compare runs 10 and 11, Table II. Even though the best results were obtained with the free acid, the methyl esters and the amides worked reasonably well paralleling Kagan's experience (7, 8). The ethers were made by cleaving the methoxyl on III with BBr_3 by the procedure of McOmie (14) and then alkylating with the appropriate alkyl halide. The phosphines were prepared most conveniently by reducing the phosphine oxides with Si_2Cl_6 and then isolating them as air stable tetraphenylborate salts. These could be made into the cationic complex $[\text{L}_2\text{Rh}(\text{cyclooctadiene})]^+\text{B}(\text{C}_6\text{H}_5)_4^-$ directly using the calculated amount of NaOH to release the phosphine. By this means the ligands could be evaluated on a very small scale. The asymmetry's dependency on the ether structure offers an opportunity to optimize the system for other substrates by varying the advanced intermediate (III).

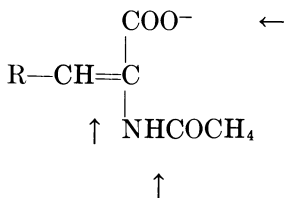
Table III. Hydrogenation Rates of Various Olefins

<i>Catalyst Ligand</i>	<i>Substrate</i>	<i>Approx. Rel. Rate</i>
IV	α -acetamidocinnamic acid	1
DIOP (7.8)	α -acetamidocinnamic acid	2
IV	cyclooctadiene	<.1
IV	norbomadiene	.5
IV	1-octene	.5
IV	α -phenylacrylic acid	<.1

When the catalyst was used for simple olefin systems, it was not as active as with the amino acid precursors. Table III shows the relative rates for a variety of substrates, special care being taken in each case to purge oxygen. The slow rate of α -phenylacrylic acid was unexpected, but, it may be the result of a stable olefin-rhodium complex similar to the one Wilkinson (15) experienced with ethylene. Such a contention is consistent with the increased speed of hydrogenation with increased pressure.

Discussion

Mechanistic details are still uncertain. Exactly two phosphine ligands are required, and these are probably *cis*. Enhanced rates as well as efficient stereochemistry can be explained by postulating that the α -acylamidocinnamic acid approaches the metal as a tridentate ligand (3).



We envision the double bond and the carboxylate anion as attached to the rhodium and the amide hydrogen bonding with one of the phosphine methoxyls (3). After hydrogen uptake the product is less firmly bound and is easily displaced by reactant making a rapid catalyst loop. Chelate ring formation involving two metal sites and a methoxyl would give the rigidity needed for efficient stereochemistry. Models support the hypothesis that the stereochemistry is controlled by the methoxyl on one of the two *cis*-phosphine ligands which hydrogen bonds with the amide, but it is difficult to predict from the models which is preferred. The above picture works best for the anion procedure B and applies to the free acid only if a charge difference is assumed between the free carboxyl and the amide. This interpretation does not provide a good explanation of the sensitivity of the anion system to temperature and the free acid to pressure. It also does not explain the similar behavior of the Kagan (7, 8) system where extra bonding sites like methoxyl are not present.

Experimental

All structures were confirmed by NMR. The rotations were run on a Perkin-Elmer 141 polarimeter.

(R)_P Menthyl Methylphenylphosphinate (I) (10). The (R)_P isomer was obtained from the Mislow diastereoisomeric mix (50/50) by selective seeding from a 50% solution in α - or β -pinene. The best procedure is to continue crystallizing several samples until light feathery crystals appear. Once separated, these feathery crystals are further purified by crystallization from hexane. Suitable material melted at 86°–87°C, $[\alpha]_{\text{D}}^{20} - 17.2$ ($c = 1$ in C₆H₆). [Mislow m.p. 89°C, $[\alpha]_{\text{D}}^{20} - 16$].

***o*-Anisylmethylphenylphosphine Oxide (II).** (R)_P menthyl methylphenylphosphinate I (27.1 grams, .092 mole) in 250 ml toluene was added to a solution of *o*-anisylmagnesium bromide (.295 mole) in 100 ml of tetrahydrofuran (THF). At 110°C the THF boiled off, and an equal volume of toluene was added. The batch was held for 24 hrs at 95°C, then cooled to 5°C; 300 ml of saturated NH₄Cl was slowly added followed by 50 ml H₂O. The two clear phases separated at 25°C. The organic phase dried over MgSO₄. The toluene was stripped off under vacuum, and the menthol and anisole were removed by distillation at 150°C and 1 mm Hg. The crude product contains up to 10% of starting ester by NMR. It may be purified by distillation at 190°–200°C at 0.5 mm. The pure product obtained in 70–90% yield melts at 70°–75°C, $[\alpha]_{\text{D}}^{20} + 25.9$ ($c = 1$ in MeOH). An alkali wash of the crude product removes a

small amount of *o*-hydroxyphenyl-methylphenylphosphine oxide, m.p. 177°–178°C, $[\alpha]_D^{20} + 60.0$ ($c = 1$ in MeOH).

***o*-Anisylcyclohexylmethylphosphine Oxide (III).** To 187 grams of molten II was added 13.7 grams of 5% Rh/C, and 350 ml of methanol was added to the thoroughly mixed slurry. This slurry was added to a 1-liter stainless steel autoclave and rinsed in with 30 ml more methanol. The batch was pressurized to 900 psig and heated with stirring to 75°C. The progress of the reaction was followed by hydrogen uptake, requiring 1800–1900 lbs using the autoclave as a reservoir. For more accurate monitoring the NMR in the methoxyl region can be used, II absorbs at 3.7 ppm and III at 3.9 ppm. If a single charge of catalyst does not achieve 95% completion, an additional 9 grams is added as a methanol slurry. The reaction usually takes 15–20 hrs.

The product is worked up by filtering the catalyst and evaporating the methanol at 110°C and 20 mm. The crude oil is dissolved in 280 ml of dibutyl ether, cooled to 0°C, and seeded. The crystals of III are filtered and washed with 100–200 ml hexane giving about 100 grams (52% yield) melting at 107°–109°C. An additional 15–20 grams can be obtained by removing the dibutyl ether from the filtrate, dissolving the 80–90 grams of oil residue in 80 ml of ether, and cooling to –10°C. Recrystallization of both crops from dibutyl ether (250 ml) gives 100 grams of III, m.p. 109°–111°C, $[\alpha]_D^{20} + 63.3$ ($c = 0.5$ in MeOH).

***o*-Anisylcyclohexylmethylphosphine (IV).** Triethylamine (81 grams, 0.8 mole) is added over 15 min to a solution of 108.6 grams (0.8 mole, 81.2 ml) of trichlorosilane in 1 liter of benzene at 25°C. The mixture is heated to reflux (76°C) for 1 hr under N₂. Then 50.4 grams of compound III (0.2 mole) in 200 ml of benzene is added in 1 hr at reflux. The batch is held at reflux for 0.5 hr and then cooled to 25°C. This mixture is quenched by adding carefully to a solution of 150 grams of NaOH in 450 ml of water at 25°C. The quench mixture is stirred for an additional hour at 25°C, and when settled the caustic layer is drawn off and discarded. The benzene layer is then evaporated *in vacuo* to give 47.2 grams of oil which, by GLC, contains less than 5% phosphine oxide. The crude product of compound IV, $[\alpha]_D^{20} + 98.5$ ($c = 1$ in MeOH) was used directly in the next step. It can be stored for long periods under N₂.

Cyclooctadiene-1,5-bis(*o*-anisylcyclohexylmethylphosphine) Rhodium Tetrafluoroborate (V) (12, 13). To a 1-liter flask purged with N₂ is added 300 ml of methanol and 15.4 grams (0.031 mole) of [Rh(cyclooctadiene)Cl]₂ making a thin slurry. Then 30.3 grams (0.12 mole, assay 98%) of IV is added and stirred 0.5 hr to give a red–orange solution. Then a solution of sodium tetrafluoroborate (13.7 grams, 0.12 mole) in 160 ml of water is added over 1 hr. Orange crystals separate, and they are collected and washed with two 30-ml portions of water. The product, dried *in vacuo* at 25°C, weighs 45 grams (95%), m.p. 170°–175°C dec. This material is about 96% optically pure and gives 77.5% enantiomeric excess (ee) on VI at 25°C, 40 psig in methanol. Recrystallized from ethanol gave an ee as high as 80.5%.

Hydrogenation Procedure A. To a 60 ml pressure bottle equipped with a magnetic stirrer was added 20 ml of methanol and 1.00 gram of α -benzamido-4-hydroxycinnamic acid and 0.0038 gram bis[(+)-*o*-anisylcyclohexylmethylphosphine]1,5-cyclooctadiene rhodium tetrafluorobo-

rate, V. The solution was purged by filling and evacuating with N_2 and finally H_2 . It was then agitated at $25^\circ C$ and 40 psig H_2 , the reaction being complete in less than 1 hr. The product was diluted to 50 ml with methanol and the optical yield checked on a polarimeter by comparison with a standard. It runs 78–80%. The DL form can be separated from the L by crystallization to give pure *N*-benzoyl-3(4-hydroxy-3-methoxy phenyl)-L-alanine.

This procedure can be varied widely with respect to temperature, pressure, and solvent. Highest yields were obtained in isopropyl alcohol and with low pressures. For larger runs less catalyst and longer times may be used. A 20–25% slurry of the less soluble α -acylamidocinnamics may be used without detriment. Care must be taken to purge these slurries thoroughly since oxygen destroys the catalyst. The solvent must be free of peroxides.

Hydrogenation Procedure B. To the 60 ml pressure bottle used in A is added to 1.0 gram of α -acetamidocinnamic acid, 0.0040 gram of catalyst V, 0.675 ml of triethylamine, and 25 ml of methanol. The solution is purged first with nitrogen, then hydrogen. It is finally pressured at 40 psig of H_2 and put in a $0^\circ C$ bath. Hydrogenation is complete in 3–4 hrs, the batch is diluted to 50 ml with methanol, and the rotation is compared with a known blank run in the same way. An optical yield of 85% resulted.

This procedure may be varied by using 0.9 equivalents of NaOH as the base or by using methanol containing as much as 40% water. Isolation of the product is accomplished by evaporating methanol, acidifying the water solution, and then crystallizing the excess enantiomer out of methanol.

Cyclohexylmethyl-*o*-hydroxyphenylphosphine Oxide. To a 500 ml flask was added 200 ml of CH_2Cl_2 under N_2 and 5.60 ml (15.0 gram) BBr_3 (Trona). Then 15 grams of III in 100 ml CH_2Cl_2 was added at $25^\circ C$, and the mixture was stirred at $25^\circ C$ for 18 hrs. Thirty ml of H_2O was cautiously added with cooling. The boric acid is filtered off, and the CH_2Cl_2 phase is washed with 5% NaOH to extract the phenol. The water phase is acidified with HCl, and the phenol is extracted with CH_2Cl_2 . After removing the solvent, the oily residue is crystallized from 50 ml acetone giving 11.7 grams (83%), m.p. 152° – $153^\circ C$, $[\alpha]_D^{20} + 60.8$ ($c = 0.5$ in MeOH). The other ethers in Table II were made by heating the sodium salt with the appropriate iodide or benzyl chloride in ethanol.

Reduction of the phosphine oxides to the phosphines may be performed in a procedure similar to the preparation of IV or more conveniently by refluxing 5 min in benzene with Si_2Cl_6 (II). For small quantities the tetraphenylborate salt of the phosphine is made and handled as an air-stable crystalline solid. *o*-Anisylcyclohexylmethylphosphine tetraphenylborate melts sharply at 131° – $132^\circ C$, $[\alpha]_D^{20} + 8.3$ ($c = 1$ in acetone).

Literature Cited

1. Knowles, W. S., Sabacky, M. J., *Chem. Commun.* (1969) 1445.
2. Knowles, W. S., Sabacky, M. J., Vineyard, B. D., *Ann. N.Y. Acad. Sci.* (1970) 172, 232.

3. *Ibid.*, (1973) **214**, 119.
4. Knowles, W. S., Sabacky, M. J., Vineyard, B. D., *Chem. Commun.* (1972) 10.
5. Belgian Patent **766,960**, 11-10-71, applied 6-11-70.
6. Knowles, W. S., Sabacky, M. J., Vineyard, B. D., *Chem. Tech.* (1972) 590.
7. Dang, T. P., Kagan, H. B., *Chem. Commun.* (1971) 481.
8. Dang, T. P., Kagan, H. B., *J. Amer. Chem. Soc.* (1972) **94**, 6429.
9. *Org. Synth. Coll.* Vol. 11 (1943), 1.
10. Korpiun, O., Lewis, R. A., Chickos, J., Mislow, K., *J. Amer. Chem. Soc.* (1968) **90**, 4842.
11. Nauman, K., Zon, G., Mislow, K., *J. Amer. Chem. Soc.* (1969) **91**, 7012.
12. Schrock, R. R., Osborn, J. A., *J. Amer. Chem. Soc.* (1971) **93**, 2397.
13. Green, M., Kue, T. A., Taylor, S. H., *Chem. Commun.* (1970) 1553.
14. McOmie, J. F. W., Watts, M. L., West, D. E., *Tetrahedron* (1968) **24**, 2289.
15. Osborn, J. A., Jardine, F. H., Young, J. F., Wilkinson, G., *J. Chem. Soc. (A)* (1966) 1711.

RECEIVED August 20, 1973.

Hydroformylation of Some Optically Active Olefins

F. PIACENTI, M. BIANCHI, and P. FREDIANI

Università di Firenze, Via Gino Capponi 9, Florence, ITALY

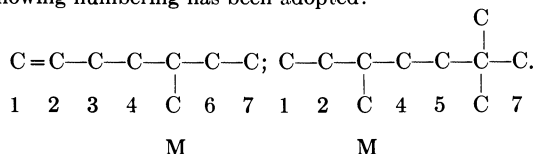
The hydroformylation of several olefins in the presence of $\text{Co}_2(\text{CO})_8$ under high carbon monoxide pressure is reported. (S)-5-Methylheptanal (75%) and (S)-3-ethylhexanal (4.8%) were products from (+)(S)-4-methyl-2-hexene with optical yields of 94 and 72%, respectively. The main products from (+)(S)-2,2,5-trimethyl-3-heptene were (S)-3-ethyl-6,6-dimethylheptanal (56.6%) and (R)-4,7,7-trimethyloctanal (41.2%) obtained with optical yields of 74 and 62%, respectively. (R)(S)-3-Ethyl-6,6-dimethylheptanal (3.5%) and (R)(S)-4,7,7-trimethyloctanal (93.5%) were formed from (R)(S)-3,6,6-trimethyl-1-heptene. (+)(S)-1-Phenyl-3-methyl-1-pentene, under oxo conditions, was almost completely hydrogenated to (+)(S)-1-phenyl-3-methylpentane with 100% optical yield. 3-(Methyl- d_3)-1-butene-4- d_3 gave 4-(methyl- d_3)pentanal-5- d_3 (92%), 2-methyl-3-(methyl- d_3)-butanal-4- d_3 (3.7%), 3-(methyl- d_3)pentanal-2- d_2 ,3- d_1 (4.3%) with practically 100% retention of deuterium. The reaction mechanism is discussed on the basis of these results.

The mechanism for forming isomeric aldehydes by hydroformylation of olefins has recently been given considerable attention. Different techniques have been used to gain more and better information (1, 2, 3, 4, 5, 6, 7, 8). The present investigation concerns the formation of aldehydes as a result of introducing a formyl group on a chain carbon atom other than at the double bond of the starting olefin when the reaction is carried out under a relatively high carbon monoxide pressure which suppresses olefin isomerization (4). The formation of the straight-chain and the α -methyl substituted aldehydes by hydroformylation of a linear α -olefin has been explained by Breslow and Heck (9), but the mechanism cannot be extended to the other isomers.

Table I. Hydroformylation of Some Olefins: Isomeric

Olefin	T, °C	P _{CO} , atm	P _{H₂} , atm
(+)(<i>S</i>)-3-Methyl-1-pentene	100	102	80
(+)(<i>S</i>)-3-Methyl-1-hexene	110	100	100
(-)(<i>S</i>)-4-Methyl-1-hexene	100	80	80
(+)(<i>S</i>)-4-Methyl-2-hexene	110	80	80
(+)(<i>S</i>)-5-Methyl-1-heptene	100	80	80
(+)(<i>S</i>)-2,2,5-Trimethyl-3-heptene	110	95	95
(<i>R</i>)-3,6,6-Trimethyl-1-heptene	110	95	95
(+)(<i>S</i>)-1-Phenyl-3-methyl-1-pentene ^c	150	115	145

^a The following numbering has been adopted:



The isomerization of the olefin prior to its hydroformylation has been the explanation of this question (3) and the formation of isomeric aldehydes was related to the presence of isomeric free olefins during the hydroformylation. This explanation, however, is being questioned in the literature. The formation of (+)(*S*)-4-methylhexanal with an optical yield of more than 98% by hydroformylation of (+)(*S*)-3-methyl-1-pentene (2, 6) is inconsistent with the olefin isomerization explanation. Another inconsistency has been the constance of the hydroformylation product composition and the contemporary absence of isomeric olefins throughout the whole reaction in hydroformylation experiments carried out with 4-methyl-1-pentene and 1-pentene under high carbon monoxide partial pressure. The data reported in Ref. 4 on the isomeric composition of the hydroformylation products of 1-pentene under high carbon monoxide pressure at different olefin conversions have recently been checked. The ratio of *n*-hexanal:2-methylpentanal:2-ethylbutanal was constant throughout the reaction and equal to 82:15.5:2.5 at 100°C and 90 atm carbon monoxide.

The hydroformylation of (+)(*S*)-3-methyl-1-hexene giving [besides (*S*)-4-methylheptanal] (*R*)-3-ethylhexanal with an optical yield of 70% gives further support to the argument that the olefin isomerizes only a small extent under oxo conditions (Table I). Different hypotheses have been made on the possible mechanism of formation of (*R*)-3-ethylhexanal from the original substrate without racemization. It was suggested by Piacenti *et al.* (5) that (*R*)-3-ethylhexanal could be formed with a high

Composition of Products and Optical Yields*Formyl Group Insertion on Carbon Atom of the Olefin^{a b}*

1		2	3	4	5	6	M		Ref.
Prod ^b , %	O.Y., ^b %	Prod., %						O.Y., %	
92.0	98	3.3	—	—	—	—	4.5	—	6
93.0	n.d.	3.1	—	—	—	—	3.1	70	5
88.0	95	10.2	—	—	—	—	1.7	72	12
75.3	94	16.6	—	—	—	3.2	4.8	72	—
77.0	94	18.9	2.4	—	—	—	1.3	77	12
41.2	62	1.8	—	0.43	—	—	56.6	74	—
93.5	—	2.4	—	0.6	—	—	3.5	—	—
—	—	—	—	—	—	—	—	—	—

^b Prod.: Product; O.Y.: Optical yield = $\frac{\text{optical purity of product}}{\text{optical purity of starting material}}$.

^c This olefin is almost completely hydrogenated with 100% optical yield.

optical yield by hydroformylation of (+)(*S*)-3-methyl-1-hexene through an oxidative addition of a C—H bond of the methyl group on the cobalt atom of the catalytically active species. This does not involve the asymmetric carbon atom and therefore does not affect its optical purity.

Casey and Cyr (7, 8) have repeated the experiment using 3-methyl-1-hexene-3-*d*₁ as substrate, and the results agreed with a 1,2 hydrogen shift in the complexed olefin. The expression, "olefin isomerization accompanying the hydroformylation," that Casey and Cyr used (8) to indicate the isomerization of the complex containing the olefin is misleading because, even according to them, free, isomerized olefins are not formed during the hydroformylation. The formation of isomeric aldehydes has been attributed to the presence of isomerized olefins in the substrate to react (3).

To determine if the presence of a hydrogen atom on the asymmetric carbon atom of the olefins mentioned above is essential to obtain the formylation of the methyl group, α -olefins containing a quaternary carbon atom were subjected to hydroformylation (10). 3,3-Dimethyl-1-butene, 2,3,3-trimethyl-1-butene, 3,3-dimethyl-1-hexene, and 4,4-dimethyl-1-hexene (Table II) all yielded more than 96% (and in one case nearly 100%) of the aldehyde deriving from the formylation of the carbon atom in position 1 while the remaining product was derived from formylation of the carbon atom in position 2. No product was detected from formylation of any of the carbon atoms belonging to the saturated alkyl substituents of the quaternary one. This implies strongly that at least one hydrogen atom must be present on each carbon atom of the olefinic chain to have

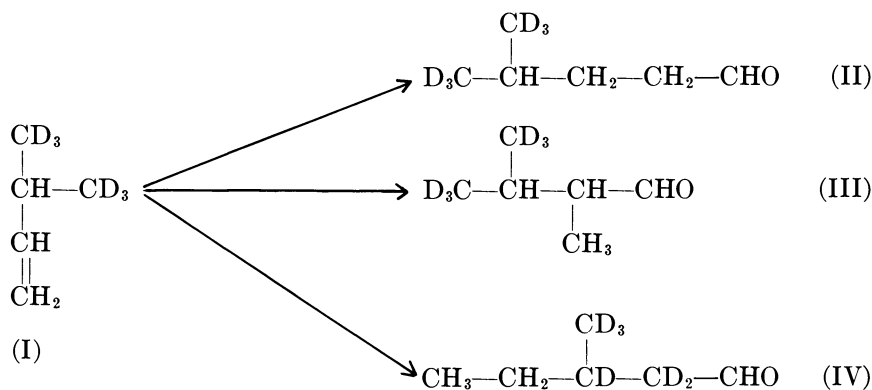
Table II. Composition of the Hydroformylation Products of Olefins Containing a Quaternary Carbon Atom^a

Olefin	Formyl Group Addition on Carbon Atoms of the Olefin	
	1, %	2, %
3,3-Dimethyl-1-butene	99.2	0.8
2,3,3-Trimethyl-1-butene	99.2	0.8
3,3-Dimethyl-1-hexene	100	trace
4,4-Dimethyl-1-hexene	96.6	3.4

^a Catalyst: $\text{Co}_2(\text{CO})_8$; solvent: benzene; T: 110°C ; p_{H_2} : 80 atm; p_{CO} : 80 atm.

the formylation of carbon atoms different from the originally unsaturated ones.

These data have been confirmed further by the results of the investigation of the hydroformylation of 3-(methyl- d_3)-1-butene-4- d_3 (I) under a high carbon monoxide partial pressure (125 atm) (II) (Scheme 1). 4-(Methyl- d_3)pentanal-5- d_3 (II) and 2-methyl-3-(methyl- d_3)butanal-4- d_3 (III) were obtained in the proportion of 92% and 3.7%, respectively, with almost 100% retention of deuterium in the original position of the chain. 3-(Methyl- d_3)pentanal-2- d_2 ,3- d_1 (IV) was 4.3% with practically 100% substitution of the hydrogen with deuterium on the tertiary carbon atom of the starting olefin (Scheme 1). These data are consistent with both Casey's and with our data for olefins with quaternary carbon atoms.



Scheme 1

The investigation on the hydroformylation of optically active olefins, started with 3-methyl-substituted α -olefins, has been extended to olefins

with different double bond positions and methyl branching positions (Table I).

(-)(*S*)-4-Methyl-1-hexene (12), (+)(*S*)-4-methyl-2-hexene, and (+)(*S*)-5-methyl-1-heptene (12) were synthesized and subjected to hydroformylation under a relatively high carbon monoxide pressure. The main product in all instances was the result of formylation of the terminal carbon atom on or next to the double bond of the starting olefin. The optical yields of these products were about 94% (Table I).

The other products formed in good yield are those resulting from formylation of the carbon atom in position 2. The formylation of the carbon atom of the methyl branching is rather small. It occurs to a greater extent (4.8%) in the case of the internal olefin tested, (+)(*S*)-4-methyl-2-hexene, than with α -olefins. In all cases the optical yield was 72–73%.

To demonstrate that optically active aldehydes from formylation of the methyl groups of optically active olefins can be obtained as main reaction products with good optical yields, we have studied the hydroformylation of (+)(*S*)-2,2,5-trimethyl-3-heptene. None of the methyl groups of the tertiary butyl group were carbonylated. Primarily the reaction product was from carbonylation of the other two methyl groups present in the molecule (Table 1). (*S*)-3-Ethyl-6,6-dimethylheptanal (56.6%) has been obtained with an optical yield of 74%, and (*R*)-4,7,7-trimethyloctanal (41.2%) with an optical yield of 62%. 2,3,6,6-Tetramethylheptanal and 2-(1-methylpropyl)-4,4-dimethylpentanal are 1.8% and 0.4%, respectively, of the total hydroformylation products.

(*R*)(*S*)-3,6,6-Trimethyl-1-heptene, an isomer of the above olefin, gave the same products although in different ratios: 4,7,7-trimethyloctanal is the main product. More 3-ethyl-6,6-dimethylheptanal than 2,3,6,6-tetramethylheptanal resulted indicating greater formylation of the carbon atom of the methyl substituent in position 3 (Table I). From Table I, the extent of formylation of the methyl branching of methyl substituted α -olefins decreases with increasing distance between the double bond and the methyl group.

(+)(*S*)-1-Phenyl-3-methyl-1-pentene, initially synthesized to extend the data obtained with (+)(*S*)-2,2,5-trimethyl-3-heptene, under usual oxo conditions is almost completely hydrogenated with an optical yield of practically 100% while the hydroformylation products are barely detectable.

The mechanism which allows the formylation of the saturated carbon atoms in the olefins in the present study may well be responsible for the prevalent formylation of terminal carbon atoms of internal olefins when the reaction is carried out under olefin isomerization-prohibiting conditions. All attempts to interpret the course of this reaction must consider

all the known data on carbonylation reactions carried out with the same catalytic system under analogous conditions.

The absence of free isomerized olefins, the constance of isomeric composition of the products throughout the whole reaction in hydroformylation experiments of 1-pentene and 4-methyl-1-pentene under high carbon monoxide pressure, the distribution of deuterium in the hydroformylation products of 3-methyl-1-hexene-3- d_1 and 3-(methyl- d_3)-1-butene-4- d_3 , and the results of carbonylation of olefins containing a quaternary carbon atom indicate initial formation of an olefin-cobaltcarbonyl complex. Isomerization of this complex, resulting in 1,2 hydrogen shifts in its organic moiety, can produce the necessary precursors of the various aldehydes that are formed.

Alkylcobalt carbonyl isomerization *via* the formation of olefincobaltcarbonyl hydride complexes with retention of the olefin attached to the cobalt atom has been suggested as the mechanism of formation, of the necessary precursors of the products with high stereospecificity.

Considering the results obtained in the reaction of orthoformic esters with CO and H₂ (13) and the postulated instability of secondary and tertiary alkylcobalt carbonyls, the suggested role of alkylcobalt carbonyls in the course of this reaction seems questionable. Although a small amount of olefin is detected among the reaction products of *sec*-butylorthoformate with CO and H₂, probably because of the low stability of secondary alkylcobalt carbonyls, and an 80:20 ratio is found between 2-methylbutanal and *n*-pentanal formed (13), it is still to be explained why the hydroformylation of 2-butene under the same conditions involving the same alkylcobalt intermediates gives a 29:71 ratio (4) of the same aldehydes.

Further investigation is necessary to elucidate the nature and behavior of the intermediate immediately preceding the formation of the alkyl derivative which is presumed to be a π -olefin-catalyst complex.

Experimental

All boiling points are uncorrected. GLC analysis was performed on a Perkin-Elmer model F 11 instrument equipped with a 50 mt capillary column coated with polypropylenglycol at 60°C. The isomeric esters were separated by a Perkin-Elmer model F 21 GLC preparative instrument.

IR spectra were recorded on a Perkin-Elmer model 225 spectrophotometer, and NMR spectra were recorded on a Varian T 60 spectrometer. Rotations were determined using a Perkin-Elmer model 141 polarimeter with a sensitivity of $\pm 0.005^\circ$, neat in a 1 dm tube. Elemental analyses were performed by a Perkin-Elmer model 140 elemental analyzer. The high pressure equipment used was the same as described in previous papers (4, 14).

The hydroformylation of the olefins, the treatment of the product, and the separation and identification of the various compounds were performed as described elsewhere (4, 6).

Materials. OCTACARBONYLDICOBALT. Prepared as described by Natta and Ercoli (15) had mp 51.5°C.

(-)(S)-2-METHYL-1-BUTANOL. Prepared by rectification of the commercial product had bp 129°C, n_D^{25} 1.4086, $[\alpha]_D^{25}$ -5.79, op 99.6% (16, 17).

HEXADEUTEROACETONE. Fluka A.G. product purissimum (deuteration 99.6%).

TRIS(DIPIVALOYLMETHANE)EUROPIUM(III) EU(DPM)₃. Fluka A.G. product purum.

(+)(S)-4-METHYL-2-HEXENE. A solution of *n*-butyllithium (0.2 mole) in *n*-heptane (70 ml) was slowly added under N₂ to a stirred suspension of triphenyl ethyl phosphonium bromide (74.2 grams, 0.2 mole) in ether (150 ml). After cooling (10°C), a solution of (+)(S)-2-methylbutanal (18) (18 grams, bp 92°C, n_D^{25} 1.3878, $[\alpha]_D^{25}$ +34.20, op 97.4%) in ethyl ether (200 ml) was added. After 30 min 400 ml of water was added, and two layers formed. The organic layer was separated. The aqueous layer was extracted three times with ether, and the extracts were added to the organic layer, dried, and rectified. (+)(S)-4-methyl-2-hexene was then recovered (30% yield) having bp 87°C, n_D^{25} 1.4002, d_4^{25} 0.6948, α_D^{25} +21.00°. The olefin thus recovered consisted of 21.1% trans isomer and 78.9% cis.

A portion of the olefin (2 grams) was treated with hydrogen under pressure (120 atm) in the presence of Raney Ni for 12 hrs and yielded (+)(S)-3-methylhexane [bp 91–92°C, n_D^{25} 1.3864, d_4^{25} 0.6826, $[\alpha]_D^{25}$ +9.1, op 92% (19)]. The optical purity of 92% is attributed to (+)(S)-4-methyl-2-hexene having α_D^{25} +21.00°.

(+)(S)-1-PHENYL-3-METHYL-1-PENTENE. Freshly distilled benzaldehyde (53 grams, 0.5 mole) was added slowly (2 hrs) at 0°C to a solution in ethyl ether (400 ml) of a Grignard reagent prepared from (+)(S)-1-bromo-2-methylbutane [75.5 grams, 0.5 mole] $[\alpha]_D^{25}$ +3.968, op 97.2% (20)] and Mg (12 grams).

The alcohol obtained after usual work up was heated at 170°C in the presence of CuSO₄ (40 grams) for 5 hrs. The crude olefin was recovered by distillation and then purified by rectification under reduced pressure. (+)(S)-1-Phenyl-3-methyl-1-pentene (trans) (40 grams) was thus obtained (bp 113°C at 18 mm Hg, n_D^{25} 1.5242, α_D^{25} +44.95°) (21).

A portion of the olefin (3.5 grams) dissolved in pentane (10 ml) was treated with ozone at -78°C for 8 hrs. The product was treated with excess LiAlH₄ in ether at 0°C and refluxed. After usual work up, benzyl alcohol (1.7 grams) and (-)(S)-2-methyl-1-butanol [1.1 grams $[\alpha]_D^{25}$ -5.50, op 94.5% (16, 17)] were recovered. An optical purity of 94.5% is attributed to (+)(S)-1-phenyl-3-methyl-1-pentene having α_D^{25} +44.95°.

(+)(S)-1-PHENYL-3-METHYLPENTANE. (+)(S)-1-Phenyl-3-methyl-1-pentene (2.2 grams, α_D^{25} +44.95°), Raney Ni (0.5 grams), and ethyl ether (5 ml) were placed in a high pressure reactor with hydrogen under pressure (130 atm) at 70°C for 12 hrs. (+)(S)-1-Phenyl-3-methylpentane (1.8 grams, bp 98.5°C at 18 mm Hg, α_D^{25} +14.46°) was recovered.

The optical purity of the product was assumed to be the same as the starting olefin (94.5%).

3-METHYL- d_3 -1-BUTENE-4- d_3 . Hexadeuteroacetone (88 grams) was reduced by the usual technique with LiAlH_4 (29 grams) to give isopropyl-1- d_3 ,3- d_3 alcohol (90 grams, bp 81°–82°C, n_D^{25} 1.3741).

Isopropyl-1- d_3 ,3- d_3 alcohol (46 grams) was treated at 0°C with PBr_3 (95 grams). After standing for 6 hrs at room temperature and 3 hrs at 60°C the solution was poured on ice and extracted with *n*-octane. This extract was washed with a saturated solution of NaHCO_3 , then water, and dried over CaCl_2 . By rectification isopropyl bromide-1- d_3 ,3- d_3 was recovered (42 grams, bp 59°C, n_D^{25} 1.4202).

By allowing isopropyl bromide-1- d_3 ,3- d_3 (41 grams) to react with diethyl malonate (53 grams), Na (8 grams) in ethyl alcohol (200 ml) and usual work up, diethyl(isopropyl-1- d_3 ,3- d_3) malonate (55 grams, bp 109°C at 19 mm Hg, n_D^{25} 1.4176) was produced and subsequently transformed into 3-(methyl- d_3)butanoic-4- d_3 acid (91% yield, bp 85°C at 22 mm Hg, n_D^{25} 1.4000). 3-(Methyl- d_3)butanoic-4- d_3 acid (18.5 grams) was reduced with LiAlH_4 (6.5 grams) in diethyl ether (100 ml) to 3-(methyl- d_3)-1-butanol-4- d_3 (14.5 grams, bp 132°C, n_D^{25} 1.4034).

3-(Methyl- d_3)-1-butanol-4- d_3 (12.4 grams) was allowed to react with acetic anhydride (18 grams) in the presence of AlCl_3 to give 3-(methyl- d_3)butyl-4- d_3 acetate (17.5 grams, bp 87°C at 128 mm Hg).

3-(Methyl- d_3)butyl-4- d_3 acetate (96.8 grams) was pyrolyzed in vapor phase at 470°C in a stream of nitrogen to give 3-(methyl- d_3)-1-butene-4- d_3 (25.5 grams) which was purified by rectification (bp 20°C).

(*R*)(*S*)-3,6,6-TRIMETHYL-1-HEPTENE. By allowing 5,5-dimethyl-2-hexanol (21) (70 grams, bp 77°C at 22 mm Hg, n_D^{25} 1.4227) to react with PBr_3 (37 grams) at 0°C for 2 hrs and then at 50°C for 2 more hrs and the usual work up, 2-bromo-5,5-dimethylhexane (91.5 grams, bp 64.5°C at 20 mm Hg, n_D^{25} 1.4464) was prepared.

2-Bromo-5,5-dimethylhexane (87 grams) was added to a solution of the sodium salt of diethyl malonate prepared from diethyl malonate (72 grams), sodium (10.4 grams), and ethyl alcohol (230 ml).

After refluxing for 20 hrs, diethyl (5,5-dimethylhex-2-yl)malonate (92.6 grams, bp 96.5°C at 0.4 mm Hg, n_D^{25} 1.4300) was recovered in the usual manner.

By saponification of the above ester (111.8 grams) the corresponding malonic acid was obtained (82 grams, mp 92.5°C, analysis for $\text{C}_{11}\text{H}_{20}\text{O}_4$; calculated: C 61.09; H 9.32%; found: C 60.79; H 9.20%). By pyrolysis of the above acid, 3,6,6-trimethylheptanoic acid was recovered (64 grams, bp 103°C at 1 mm Hg, n_D^{25} 1.4307, equivalent weight by neutralization for $\text{C}_{10}\text{H}_{20}\text{O}_2$ calculated: 172.26; found: 171.90). 3,6,6-Trimethylheptanoic acid (64 grams) was reduced with LiAlH_4 (14 grams) in diethyl ether (300 ml) to give 3,6,6-trimethyl-1-heptanol (57.3 grams, bp 103.5°C at 15 mm Hg, n_D^{25} 1.4326). This alcohol (75 grams), by reaction with acetic anhydrides (64 grams) in the presence of AlCl_3 (0.7 gram) at 100°C for 6 hrs, gave 3,6,6-trimethylheptyl acetate (91 grams, bp 106°C at 20 mm Hg, n_D^{25} 1.4237).

The above ester (91 grams) was pyrolyzed at 510°C in a stream of nitrogen and gave 3,6,6-trimethyl-1-heptene (30 grams, bp 146°C n_D^{25} 1.4144).

(+)(S)-2,2,5-TRIMETHYL-3-HEPTENE. (+)(S)-2,2,5-Trimethyl-3-heptene was synthesized as described elsewhere (23).

METHYL 4-METHYLPENTANOATE. From diethyl (2-methylpropyl)-malonate (24) by saponification followed by decarboxylation of the corresponding bicarboxylic acid, 4-methylpentanoic acid (25) was obtained (bp 66°–67°C at 1.5 mm Hg, n_D^{25} 1.4131). By treating this acid with CH_2N_2 in ether, methyl 4-methylpentanoate was formed (bp 142°C, n_D^{25} 1.4024). NMR $\delta_{\text{TMS}}^{\text{CCl}_4}$ 0.70–1.15 (d, 6 H, 2 CH_3), 1.15–1.90 (m, 3 H, CHCH_2), 2.10–2.50 (t, 2 H, $\text{CH}_2\text{CH}_2\text{COOCH}_3$), 3.60 (s, 3 H, COOCH_3).

METHYL 3-METHYLPENTANOATE. Prepared by esterification with CH_2N_2 of 3-methylpentanoic acid obtained according to Vliet *et al.* (26) (bp 141°C, n_D^{25} 1.4032). NMR $\delta_{\text{TMS}}^{\text{CCl}_4}$ 0.70–1.14 (m, 6 H, 2 CH_3), 1.14–2.50 (m, 5 H, 2 CH_2 , *tert*-CH), 3.64 (s, 3 H, COOCH_3); NMR $\delta_{\text{TMS}}^{\text{CCl}_4}$ (30 mole % $\text{Eu}(\text{DPM})_3$) 1.2–1.7 (t, 3 H, CH_3CH_2), 2.20–2.40 (d, 3 H, CH_3CH), 1.80–3.50 (m, 2 H, $\text{CH}_3\text{CH}_2\text{CH}$), 4.10–4.83 (m, 1 H, *tert*-CH), 5.00–5.65 (d of d, 2 H, $\text{CHCH}_2\text{COOCH}_3$), 6.55 (s, 3 H, COOCH_3).

METHYL 2,3-DIMETHYLBUTANOATE. Obtained by esterification with CH_2N_2 of the corresponding acid prepared according to Lardicci (27).

METHYL 2,3,6,6-TETRAMETHYLHEPTANOATE. By allowing 2-bromo-5,5-dimethylhexane (39 grams), prepared as described above, to react with the sodium salt of diethyl methylmalonate obtained from diethyl methylmalonate (35 grams) and sodium (4.6 grams) in ethyl alcohol (68 ml), diethyl methyl-(5,5-dimethyl-2-hexyl)malonate (24.5 grams, bp 134°C at 2 mm Hg, n_D^{25} 1.4325) was obtained. By saponification of the ester, methyl-(5,5-dimethyl-2-hexyl)malonic acid was recovered (14 grams, mp 147°C, analysis for $\text{C}_{12}\text{H}_{22}\text{O}_4$; calculated: C 62.58, H 9.63%; found: C 62.9, H 9.47%). By decarboxylation of the above acid (11.8 grams) 2,3,6,6-tetramethylheptanoic acid (9.4 grams, bp 148°C at 20 mm Hg, n_D^{25} 1.4345) was obtained. By esterification of the acid (4.3 grams) with CH_2N_2 the corresponding methyl ester was formed (4.0 grams, bp 99°C at 18 mm Hg, n_D^{25} 1.4249).

METHYL 2-(1-METHYLPROPYL)-4,4-DIMETHYLPENTANOATE. 4,4-Dimethylpentanoic acid (7.4 grams, bp 118°C at 17 mm Hg, n_D^{25} 1.4217) prepared according to Brändström (28) was allowed to react at 40°C with a THF solution of sodium naphthalene prepared from naphthalene (20 grams) and sodium (3.7 grams) in THF (127 ml). 2-Bromobutane (9 grams) was then added to the solution and stirred at 40°C for 2 days. After evaporation of the solvent, hydrolysis followed by extraction with ether, the aqueous solution of the sodium salt was acidified with H_2SO_4 , and the organic acid was recovered by ether extraction.

By treating the acid with CH_2N_2 , methyl 2-(1-methylpropyl)4,4-dimethylpentanoate was obtained in very small yield which was purified by preparative GLC (n_D^{25} 1.4258, analysis for $\text{C}_{12}\text{H}_{24}\text{O}_2$; calculated: C 71.95, H 12.08%; found: C 72.01, H 12.10%).

(+)(R)-METHYL-3-ETHYL-6,6-DIMETHYLHEPTANOATE, (+)(S)-METHYL 4,7,7-TRIMETHYLOCTONATE. These esters were synthesized as described elsewhere (23).

Hydroformylation of the Olefins and Identification of the Products

(+)(S)-4-METHYL-2-HEXENE. By hydroformylation of (+)(S)-4-methyl-2-hexene (36 grams, $\alpha_D^{25} +21.00^\circ$, op 92%) in benzene (50 ml) in the presence of $\text{Co}_2(\text{CO})_8$ (0.7 gram) at 110°C and a pressure of 160 atm of carbon monoxide and hydrogen (1:1), after usual work up of the products, 30 grams of methyl esters were obtained. By GLC analysis of the esters the hydroformylation product appeared to contain four compounds in the ratio 16.6/4.8/3.2/75.3. By rectification of the mixture, the product present in preponderant amount (75.3%) was recovered in the pure state (bp 69°C at 16 mm Hg, $\alpha_D^{25} +6.35^\circ$, n_D^{25} 1.4162). By saponification of a portion of this ester an acid was recovered (bp 131°C at 18 mm Hg, n_D^{25} 1.4273, $[\alpha]_D^{25} +7.60$) which had an IR spectrum of a known sample of (+)(S)-5-methylheptanoic acid. Its optical purity was 86.8% (29).

The other esters present in the original mixture were separated by preparative GLC using butandiol succinate on Chromosorb at 100°C and identified by comparing their IR spectra with those of known samples.

Methyl 2,4-dimethylhexanoate (diastereoisomeric mixture) was 16.6% of the original mixture. Methyl 4-methylheptanoate 3.2% of the original mixture was recovered in such a small quantity that its optical rotatory power could not be determined.

(+)(S)-2,2,5-TRIMETHYL-3-HEPTENE. By hydroformylation of (+)(S)-2,2,5-trimethyl-3-heptene (22.6 grams, $[\alpha]_D^{25} +38.09$, op 95.2%) in benzene (25 ml) in the presence of $\text{Co}_2(\text{CO})_8$ (0.5 gram) at 110°C and a pressure of 190 atm of carbon monoxide and hydrogen (1:1), after usual work up, a mixture of methyl esters was obtained (23 grams) which contained four products in the ratio 0.43/1.8/56.6/41.2. The esters were separated by GLC using Carbowax 1500 on Chromosorb W at 160°C and identified by comparing their IR spectra with those of known samples. (-)(R)-Methyl-4,7,7-trimethyloctanoate, 41.2% of the original product, had bp 111°C at 24 mm Hg, n_D^{25} 1.4284, $[\alpha]_D^{25} -0.324$, op 58.9%); (-)(S)-methyl-3-ethyl-6,6-dimethylheptanoate, 56.6% of the original product, had bp 110°C at 18 mm Hg, n_D^{25} 1.4255, $[\alpha]_D^{25} -2.33$, op 70.8%.

Methyl 2,3,6,6-tetramethylheptanoate was the compound present as 0.43% of the mixture while methyl 2-(1-methylpropyl)-4,4-dimethylpentanoate was the one present as 1.8%.

(R)(S)-3,6,6-TRIMETHYL-1-HEPTENE. (R)(S)-3,6,6-Trimethyl-1-heptene has been hydroformylated in exactly the same conditions adopted for the hydroformylation of its isomer 2,2,5-trimethyl-3-heptene. The separation and identification of the reaction products have been made using the technique previously described. The results are reported in Table I.

(+)(S)-1-PHENYL-3-METHYL-1-PENTENE. (+)(S)-1-Phenyl-3-methyl-1-pentene (4.5 grams, $\alpha_D^{25} +44.95^\circ$, op 94.5%) in benzene (15 ml) in the presence of $\text{Co}_2(\text{CO})_8$ (0.25 grams) under 115 atm of CO and 145 atm of H_2 was heated at 150°C for 4 hrs. The reaction product consisted practically of only one compound identified by its IR spectrum as (+)(S)-phenyl-3-methylpentane having $\alpha_D^{25} +14.46^\circ$, op 94.5%.

3-(METHYL- d_3)-1-BUTENE-4- d_3 . By hydroformylation of 3-(methyl- d_3)-1-butene-4- d_3 (20 grams) in toluene (90 ml), in the presence of $\text{Co}_2(\text{CO})_8$ (0.9 gram), under 250 atm of carbon monoxide and hydrogen

(1:1) at 100°C, and after working up the product as previously described, 25 grams of methyl esters were obtained. By GLC analysis the mixture consisted of three products in the ratio 3.7/4.3/92. The esters were separated by preparative GLC on diisodecyl phthalate on Chromosorb A at 80°C. The product present as 3.7% of the initial mixture had a retention time equal to that of methyl 2,3-dimethylbutanoate.

The product present as 4.3% of the mixture had a retention time equal to that of methyl 3-methylpentanoate. Its mass spectrum agreed with a $C_7D_6H_8O_2$ formulation, indicating an almost complete retention of the deuterium present in the original substrate. Its NMR spectrum showed $\delta_{TMS}^{CCl_4}$ 0.70–1.10 (m, 3 H, CH_3CH_2), 1.10–1.70 (m, 2 H, CH_3CH_2CD), 3.60 (s, 3 H, $COOCH_3$); $\delta_{TMS}^{CCl_4}$ [30% mol $Eu(DPM)_3$] 2.20–2.70 (t, 3 H, CH_3CH_2), 3.10–4.35 (m, 2 H, CH_3CH_2CD), 8.36 (s, 3 H, $COOCH_3$). On this basis its structure is assumed to be $CH_3CH_2CDCD_2COOCH_3$.



The main product (92%) had a retention time equal to that of methyl 4-methylpentanoate. Its mass spectrum indicated a $C_7D_6H_8O_2$ formulation. Its NMR spectrum showed $\delta_{TMS}^{CCl_4}$ 1.20–1.75 (m, 3 H, $CHCH_2$), 2.00–2.45 (t, 2 H, $CH_2CH_2COOCH_3$), 3.62 (s, 3 H, $COOCH_3$).

Acknowledgment

We thank Piero Pino for useful discussions and G. Bimbi and D. Pieraccioni for their collaboration.

Literature Cited

1. Pino, P., Piacenti, F., Neggiani, P. P., *Chem. Ind.* (1961) 1400.
2. Pino, P., Pucci, S., Piacenti, F., *Chem. Ind.* (1963) 294.
3. Johnson, M., *J. Chem. Soc.* (1963) 4859.
4. Piacenti, F., Pino, P., Lazzaroni, R., Bianchi, M., *J. Chem. Soc. C* (1966) 488.
5. Piacenti, F., Pucci, S., Bianchi, M., Lazzaroni, R., Pino, P., *J. Amer. Chem. Soc.* (1968) **90**, 6847.
6. Pino, P., Pucci, S., Piacenti, F., Dell'Amico, G., *J. Chem. Soc. C* (1971) 1640.
7. Casey, C. P., Cyr, C. R., *J. Amer. Chem. Soc.* (1971) **93**, 1280.
8. Casey, C. P., Cyr, C. R., *J. Amer. Chem. Soc.* (1973) **95**, 2240.
9. Heck, R. F., Breslow, D. S., *J. Amer. Chem. Soc.* (1961) **83**, 4023.
10. Bianchi, M., Frediani, P., Piacenti, F., *Chim. Ind. Milan* (1973) **55**, 798.
11. Keulemans, A. I. M., Kwantes, A., van Bavel, T., *Rec. Trav. Chim.* (1948) **67**, 298.
12. Piacenti, F., Bianchi, M., Frediani, P., *Chim. Ind. Milan* (1973) **55**, 262.
13. Piacenti, F., *Gazz. Chim. Ital.* (1962) **92**, 225.
14. Pino, P., Piacenti, F., Neggiani, P. P., *Chim. Ind. Milan* (1962) **44**, 1367.
15. Natta, G., Ercoli, R., *Chim. Ind. Milan* (1952) **34**, 503.
16. Rossi, R., Diversi, P., Ingrosso, G., *Gazz. Chim. Ital.* (1968) **98**, 1391.
17. Lardicci, L., Menicagli, R., *Atti Soc. Tosc. Sci. Natur., Pisa, Proc. Verb. Mem.* (1970) **77 A**, 25.

18. Lardicci, L., Rossi, R., *Atti Soc. Tosc. Sci. Natur., Pisa, Proc. Verb. Mem.* (1961) **68 A**, 23.
19. Lardicci, L., Salvadori, P., *Ann. Chim.* (1962) **52**, 652.
20. Salvadori, P., Lardicci, L., Stagi, M., *Gazz. Chim. Ital.* (1968) **98**, 1409.
21. Davis, D. D., Ansari, G. G., *J. Org. Chem.* (1970) **35**, 4285.
22. Whitmore, C., Whitmore, H. E., Cook, N. C., *J. Amer. Chem. Soc.* (1950) **72**, 51.
23. Bianchi, M., Frediani, P., Lardicci, L., Piacenti, F., *Gazz. Chim. Ital.*, in press.
24. Skinner, G. S., Mitchell Jr., J., *J. Amer. Chem. Soc.* (1945) **67**, 1252.
25. Papa, D., Schwenk, E., Ginsberg, H. F., *J. Org. Chem.* (1949) **14**, 723.
26. Vliet, E. B., Marvel, C. S., Hsueh, C. M., "Organic Syntheses, Coll.," Vol. 2, p. 416, J. Wiley, New York, 1943.
27. Lardicci, L., Menicagli, R., *Chim. Ind. Milan* (1969) **51**, 1387.
28. Brändström, A., *Acta Chem. Scand.* (1959) **13**, 612.
29. Lardicci, L., Conti, L., *Gazz. Chim. Ital.* (1962) **92**, 428.

RECEIVED August 20, 1973. This research was supported by Consiglio Nazionale delle Ricerche, Rome.

Asymmetric Hydroformylation.

Hydroformylation of Olefins in the Presence of Chiral Rhodium and Cobalt Catalysts

P. PINO, G. CONSIGLIO, C. BOTTEGHI, and C. SALOMON

Department of Industrial and Engineering Chemistry, Swiss Federal Institute of Technology, Zurich, Switzerland

Optical yields up to 17% and 25%, respectively, have been reached in the styrene hydroformylation in the presence of cobalt or rhodium catalysts using N-alkylsalicylaldimine or phosphines as asymmetric ligands. Furthermore the hydroformylation of aliphatic and internal olefins have been achieved using rhodium catalysts in the presence of optically active phosphines. With the same catalysts, cis-butene surprisingly undergoes asymmetric hydroformylation with optical yields up to 27%. On the basis of the results obtained for cis-butene and the asymmetric induction phenomena in dichlor(olefin)(amine)platinum(II) complexes, a simple model is proposed for the catalytic complex. The correlation among the prevailing chirality obtained in the asymmetric hydroformylation of vinyl, vinylidene, and internal olefins is discussed.

Although the hydroformylation of olefins has been known since 1938, the first successful attempts to synthesize optically active aldehydes by hydroformylation using optically active catalysts have been published only recently (1, 2, 3, 4). All the three possibilities to prepare optically active aldehydes (Scheme 1) have been successfully explored (5) using $\text{Co}(\text{R}^*-\text{Sal})_2$ or $[\text{Co}(\text{CO})_4]_2$ and R^*-SalH ($\text{R}^*-\text{SalH} = (S)-N-\alpha\text{-methylbenzylsalicylaldimine}$) as catalyst precursor, but the optical yields obtained were very poor. Much better results have been obtained

Table I. Asymmetric Hydroformylation

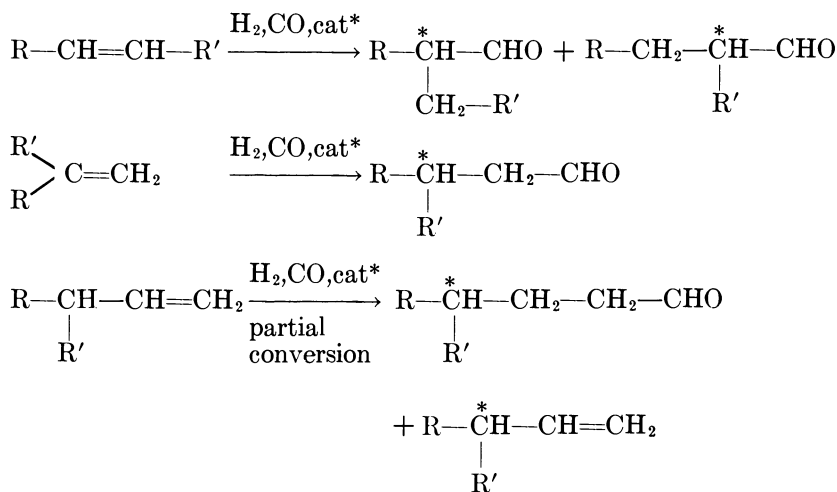
Olefin	$T, ^\circ\text{C}$
Styrene	120
Styrene ^{c, d, e}	90
Styrene ^c	90
α -Methylstyrene	120
α -Methylstyrene ^{c, d}	90
α -Ethylstyrene	120
1-Butene	120
3-Methyl-1-pentene	120

^a Catalyst: $[\text{Co}(\text{CO})_4]_2$. Asymmetric ligand: (*S*)-*N*- α -methylbenzylsalicylalimine. Co/Ligand = 1/4. Solvent: benzene when not otherwise indicated, initial $p_{\text{CO}} = p_{\text{H}_2} = 40$ atm.

^b The main reaction product is ethylbenzene (50–80%).

^c Ethanol as solvent.

using rhodium catalysts (6, 7); optical yields up to about 30% have been obtained in the case of vinyl or internal olefins whereas in the case of vinylidene olefins, the best optical yield is well below 5%. Besides the potential practical interest in synthesizing large quantities of optically active aldehydes using catalytic amounts of optically active ligands, the investigation of asymmetric hydroformylation contributes to a deeper insight into the hydroformylation mechanism and the nature of the catalytic species.



Scheme 1

in the Presence of Cobalt Catalysts^a*Optically Active Aldehyde*

	Yield, %	Optical Yield, %	Absolute Con- figuration
2-phenylpropanal ^b	24	1.9	S
2-phenylpropanaldiethylacetal ^b	15	15.2	R
2-phenylpropanal ^b	20	0.3	R
3-phenylbutanal ^f	11	2.5	S
3-phenylbutanaldiethylacetal ^f	5	0.6	R
3-phenylpentanal ^g	2.5	1.4	S
2-methylbutanal	15	<0.1	S
4-methylhexanal	44	<0.1	S

^a In the presence of ethyl orthoformate.

^b Initial $p_{\text{CO}} = p_{\text{H}_2} = 50$ atm.

^f The main reaction product is cumene (90–95%).

^g The main reaction product is 2-phenylbutane (94%). Optically active 4-phenylpentanal and 2-methyl-3-phenylbutanal (Scheme 2) are contemporaneously formed.

Cobalt Catalyzed Asymmetric Hydroformylation

The first attempts at asymmetric hydroformylation using

$[\text{Co}_2(\text{CO})_6(\text{P}^*(\text{C}_6\text{H}_5)_2\text{CH}_3)_2]$ ($\text{R} = \text{C}_2\text{H}_5-$ or C_3H_7-) as the catalyst precursor and aliphatic olefins as substrates were not encouraging (5). The first unequivocal result was obtained (1) using styrene as the substrate,

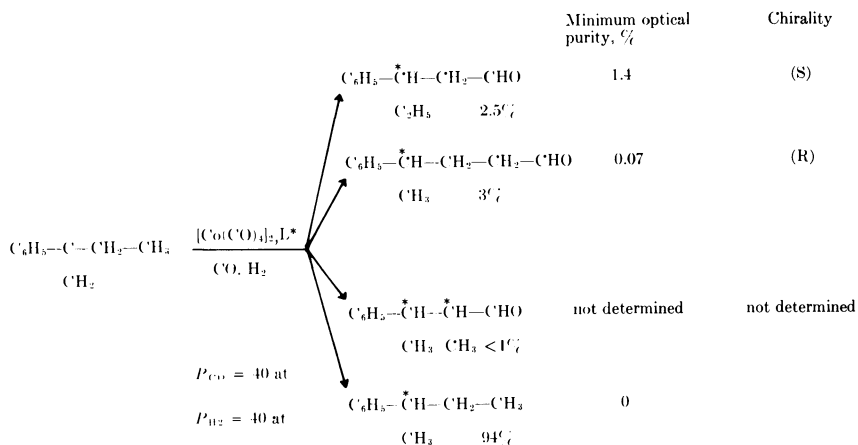
$[\text{Co}(\text{CO})_4]_2$ as the catalyst, and R^*-SalH as the asymmetric ligand. The optical yield was poor (Table I); however, this could be attributed to both intrinsically low asymmetric induction in the catalytic reaction and to racemization of 2-phenylpropanal in the rather drastic reaction conditions used.

Hydratropa aldehyde racemizes quickly even at room temperature (8). No reliable data have been found in the literature on the correlation between optical purity and rotatory power for this compound. We have estimated for the optically pure (*R*)-hydratropa aldehyde, $[\alpha]_{\text{D}}^{25} - 238^\circ$ (maximum value), by correlation to (+)(*R*)-hydratropa alcohol via (-)(*R*)-1-ethoxy-2-phenylpropane (9).

To avoid racemization of the reaction products the hydroformylation was carried out in the presence of ethyl orthoformate using absolute ethanol as solvent. Using the same (*S*) asymmetric ligand the sign of asymmetric induction was different, but the asymmetric induction was about 10 times greater. The change of the sign of the asymmetric induction was related to the change of solvent rather than to the presence of the orthoformic ester as another experiment carried out in ethanol without ethyl orthoformate showed. These results seem to indicate clearly that

hydratropa aldehyde racemizes in the hydroformylation conditions used, possibly because of the presence of cobalt tetracarbonyl hydride which is known to behave as a strong acid (10) in polar solvents.

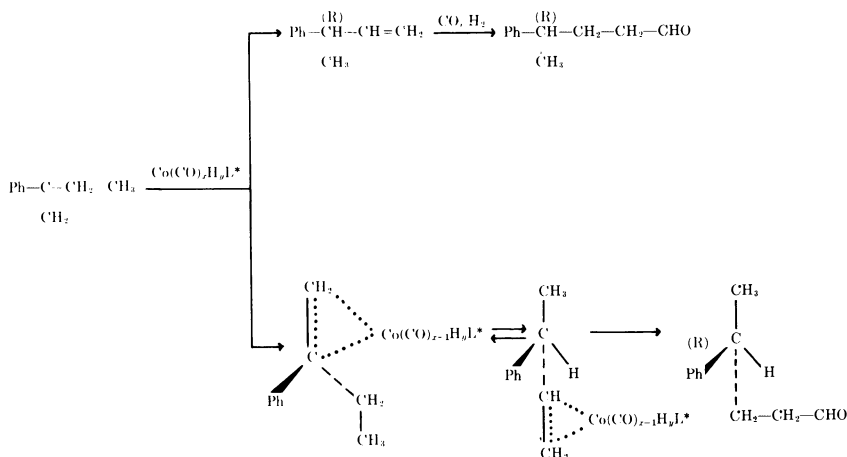
Experiments in progress show that using $[\text{Co}(\text{CO})_4]_2$ as catalyst precursor under typical oxo conditions (150 at CO:D₂ (2:1) and 100°C) the exchange between D₂ and the hydrogen atoms in the α position with respect to the carbonyl group (11) occurs even if benzene is used as solvent. Similar experiments using α -methylstyrene as substrate, resulted in hydrogenation more than hydroformylation, and a very low yield in aldehydic products was obtained. The chiral aldehyde (3-phenylbutanal) with the asymmetric carbon atom in the β position relative to the carbonyl was not expected to racemize. The optical purity obtained in the presence or absence of ethyl orthoformate was very low. As with styrene the prevailing chirality was opposite using benzene or ethanol as solvent.



L* = (S)-N- α -methylbenzylsalicylaldimine

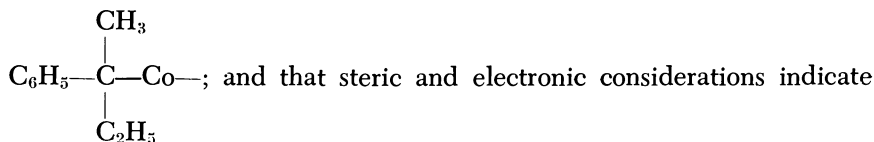
Scheme 2

To establish whether the olefin hydrogenation accompanying the hydroformylation is also asymmetric, α -ethylstyrene was used as substrate (12). The relative amount and the optical purity of the resulting aldehydes are shown in Scheme 2; the sign and the degree of asymmetric induction for the 3-phenylpentanal agree with the results obtained in the case of α -methylstyrene. As for the 4-phenylpentanal (Scheme 3) the observed chirality may be a result of asymmetric isomerization of the starting olefin (13) and/or the formation of 3- and 4-methylpentanal from the same olefin/asymmetric catalyst complex which undergoes hydroformylation with partial retention of configuration of the initially formed asymmetric carbon atom.



Scheme 3

The main reaction product, 2-phenylbutane, shows no detectable optical activity between 590 and 350 $m\mu$. The 2-phenylbutane does not arise from the alkylcobalt carbonyls as reported (10) since these give rise to the optically active 3-phenylpentanal or 4-phenylpentanal. Taking into account the peculiar behavior under oxo conditions of double bonds conjugated with phenyl rings (14), it might be assumed that: electronic effects produce predominately the disubstituted benzylcobalt complex



a labile configuration of the tertiary asymmetric carbon atom. Since the formation of the acyl compounds is not favored (15) in benzylcobalt complexes, hydrogenolysis and hence hydrogenation is favored over carbon monoxide insertion followed by hydroformylation when starting with tertiary alkylcobalt complex. Furthermore the configurational lability of the intermediate yields a racemic hydrogenation product. With the catalytic system $[\text{Co}(\text{CO})_4]_2/\text{R}^*-\text{SalH}$, hydroformylation of aliphatic substrates gave very poor results (5). With 1-butene the prevailing chirality [(S)] of the 2-methylbutanal formed has been established. In the case of partial hydroformylation of racemic 3-methyl-1-pentene, preferential reaction of the (S) antipode occurs. This is verified both from the prevailing chirality of the resulting aldehyde and from the prevailing chirality [(R)] of the recovered olefin. The partial asymmetric hydroformylation of (R)(S)-3-methyl-1-pentene can be considered as a typical kinetic resolution (16) on the basis of the unreacted olefin.

From the point of view of the formation of the optically active 4-methylhexanal, it has been defined as a stereoelective (17) hydroformylation (1).

Table II. Asymmetric Rhodium Catalyzed Hydroformylation of Aromatic Substrates

Olefin	Asymmetric Ligand	Chiral Aldehyde Product		Ref.
		α_D^{25} (l=1), °	Optical Purity, %	
α -Ethylstyrene	$\begin{array}{l} \text{Ph}^a \\ \diagdown \\ \text{P} \\ \diagup \\ \text{Ph} \\ \text{neo-Menthyl} \end{array}$	+0.070 ^b	1	2
Phenylvinyl ether		-0.051 ^c	0.3	2
Indene	$(-)-\text{P}^* \begin{array}{l} \text{Me}^a \\ \diagdown \\ \text{Pr} \\ \diagup \\ \text{Ph} \end{array}$	+0.25	^d	4
Isoeugenol		+0.25	^d	4
Cinnamic alcohol		-0.05	^d	4
Cinnamic aldehyde acetal		-0.10	^d	4
α -Methylstyrene	$(-)-\text{DIOP}^e$	-0.93	1.6	6
α -Ethylstyrene		-0.80	1.8	6
Allylbenzene		+1.89	15.5	6
<i>trans</i> - β -Methylstyrene		-13.80	14.4	6

^a The optical purity is not specified.

^b $t = 19^\circ\text{C}$.

^c $t = 18^\circ\text{C}$.

^d Not determined.

^e $(-)-\text{DIOP} = (-)-2,3\text{-O-isopropylidene-2,3-dihydroxy-1,4-bis(diphenylphosphino)-butane}$ (optical purity $\geq 90\%$).

Table III. Rhodium Catalyzed Styrene Hydroformylation

Catalyst	Asymmetric Ligand	Rh/P	T, °C
$[\text{Rh}(\text{CO})_2\text{Cl}]_2$	$(-)-\text{P}^* \begin{array}{l} \text{Ph}^a \\ \diagdown \\ \text{Pr} \\ \diagup \\ \text{Me} \end{array}$	1/2.7	80
$[\text{Rh}(\text{C}_6\text{H}_{10})\text{Cl}]_2$	$(+)-\text{P}^* \begin{array}{l} \text{Ph}^b \\ \diagdown \\ \text{CH}_2-\text{Ph} \\ \diagup \\ \text{Me} \end{array}$	1/10	120
$(+)-\text{RhCl}(\text{CO})\text{L}_2$	$\text{L} = \text{P} \begin{array}{l} \text{Ph}^a \\ \diagdown \\ \text{Ph} \\ \diagup \\ \text{neo-menthyl} \end{array}$	1/1	75
$\text{HRh}(\text{CO})(\text{Ph}_3)_3$	$(-)-\text{DIOP}^c$	1/2	25

^a The optical purity is not specified.

^b Optical purity $\sim 94\%$.

Rhodium Catalyzed Asymmetric Hydroformylation

The first successful experiments of asymmetric hydroformylation in the presence of rhodium catalysts and optically active phosphines as asymmetric ligands were carried out on olefinic substrates containing phenyl rings (2, 3, 4, 6, 18). Tables II and III show the most important results that have been previously reported. Optically active monophosphines containing optically active phosphorus atoms, chiral asymmetric alkyl or cycloalkyl groups, and chiral diphosphines were used as asymmetric ligands. The nature of the chiral ligand seems to have a remarkable influence on the optical yield as seen in Table III. At high temperature and pressure, an increase in optical yield was observed using a large excess of chiral ligand (3). Furthermore, the optical yields are definitely higher for vinyl than for vinylidene olefins, demonstrating that the type of substrate has a remarkable influence on the asymmetric induction.

The success achieved in the asymmetric hydroformylation of allylbenzene (6), the first olefin with a non-conjugated double bond used in such reactions, prompted an investigation of the asymmetric hydroformylation of aliphatic olefins using $\text{HRh}(\text{CO})(\text{PPh}_3)_3$ as the catalyst precursor and (–)-DIOP (see footnote ^a to Table II) as the asymmetric ligand (7). As shown in Table IV, an optical yield of 27% was obtained using *cis*-butene, but it was remarkably lower using the corresponding *trans*-olefin. The optical yields obtained using α -olefins are only slightly lower than those observed for styrene under similar conditions whereas only very low optical yields were obtained using vinylidene olefins.

The stereoelective hydroformylation of (*R*)(*S*)-3-methyl-1-pentene also has been achieved with rhodium catalysts; the optical purity of the

in Aromatic Solvents Using Different Asymmetric Ligands

P_{CO} , <i>atm</i>	P_{H_2} , <i>atm</i>	α -Phenylpropanal			Ref.
		Yield, %	Prevailing Chirality	Optical Purity, %	
100	100	^a	S	21.1	4
50	50	90	S	17.5	3
50	50	29	S	0.8	2
0.5	0.5	69	R	22.7	6

^c Optical purity \geq 90%.

^d Not determined.

**Table IV. Hydroformylation of Aliphatic Olefins with HRh(CO)
[Olefin/Rhodium = $3.0 \cdot 10^2$]**

Olefin	Total Pressure, atm ^a	T., °C	Isomeric Reaction Products Composition
1-Butene	1 ^b	25	12.5 ^c
1-Pentene	1	25	13.5 ^c
2-Ethyl-1-hexene	81	100	> 98% 3-ethylheptanal
3-Methyl-1-butene	1	25	13.5 ^d
1-Octene	1	25	9 ^c
<i>cis</i> -Butene	1 ^b	20	} > 98% 2-methylbutanal
<i>cis</i> -Butene	84	95	
<i>cis</i> -Butene ^e	86	95	
<i>trans</i> -Butene	84	98	
<i>cis</i> -2-Hexene	82	95	1.5 ^f
<i>trans</i> -2-Hexene	82	95	1.4 ^f
3-Methyl-1-pentene ^g	1	40	> 95% 4-methylhexanal

^a Starting pressure measured at room temperature.

^b Partial pressure of the olefin: 0.33 atm.

^c Straight chain aldehyde/Branched aldehyde.

^d 4-Methylpentanal/2.3-Dimethylbutanal ratio.

recovered aldehyde at 50% conversion being remarkably higher (4.6%) than with cobalt at high temperature and pressure. The influence of the different reaction variables (p_{CO} , p_{H_2} , temperature, catalyst concentration, etc.) on the optical yield has not been investigated systematically. It seems, however, that in the presence of the catalytic system (HRh(CO)(PPh₃)₃/(-)-DIOP), the optical yields are higher at lower carbon monoxide and hydrogen pressure and at lower temperature (Table V).

Table V. Influence of the Reaction Conditions on the Optical Yield in the Hydroformylation of Different Olefins with HRh(CO)(PPh₃)₃ and (-)-DIOP; $p_{H_2} = p_{CO}$

Olefin	Reaction Conditions		Optical Purity of the Obtained Aldehyde, %
	T., °C	Total Pressure, atm ^a	
1-Butene	100	80	3.8
1-Butene	25	1 ^b	18.8
<i>cis</i> -Butene	95	84	8.1
<i>cis</i> -Butene	20	1 ^b	27.0
1-Octene	95	84	2.5
1-Octene	25	1	16.5

^a Starting pressure measured at room temperature.

^b Partial pressure of the olefin = 0.33 atm.

**(PPh₃)₃ and (-)-DIOP (Molar Ratio 1/4) in Aromatic Solvents
— 1.6 · 10³; $p_{H_2}/P_{CO} = 1$]***Isolated Optically Active Compounds*

Compound	α_D^{25} ($l=1$) (neat)	Chirality	Optical Purity, %
2-methylbutanal	-5.27°	R	18.8
2-methylpentanoic acid	-3.62°	R	19.7
3-ethylheptanal	-0.02°	R	1.1
2,3-dimethylbutanal	-4.38°	R	15.2
2-methyloctanal	-4.91°	R	15.2
2-methylbutanal	+7.57°	S	27.0
2-methylbutanal	+2.28°	S	8.1
2-methylbutanal	+2.22°	S	7.9
2-methylbutanal	+0.89°	S	3.2
2-methylhexanoic acid	+1.68°	S	7.6
2-ethylpentanoic acid	-0.22°	R	5.8
2-methylhexanoic acid	+0.31°	S	1.4
2-ethylpentanoic acid	-0.11°	R	2.9
4-methylhexanal	-0.44°	R	4.6

* Rh₂O₃ as catalyst precursor.

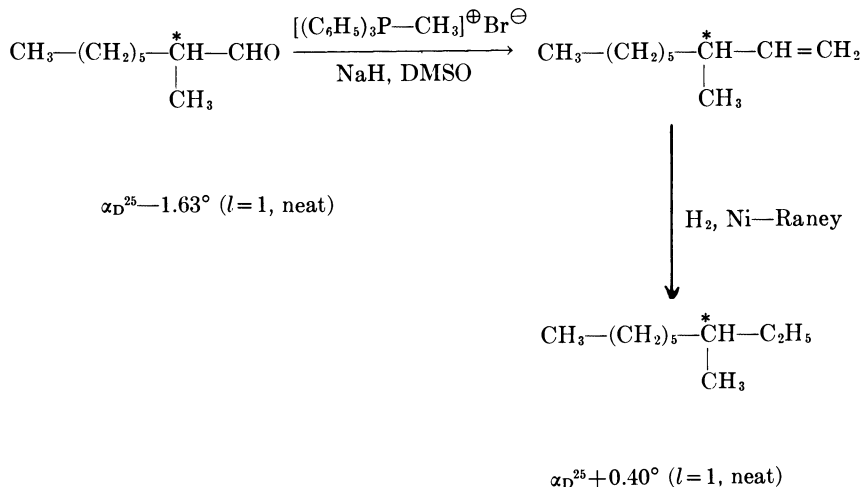
† 2-Methylhexanal/2-ethylpentanal ratio.

° The recovered olefin had $\alpha_D^{25} + 0.840$ (neat, $l=1$) (o.p.3,3%).

The relationship between sign of the optical activity and absolute configuration, and between values of the optical rotations and optical purity are known or easily calculated for all aldehydes synthesized in this investigation except 2-methyloctanal. To obtain the necessary data this aldehyde was converted, according to Scheme 4, into (+)(S)-3-methylnonane for which the relationship between optical rotation and optical purity (*l*₉) is known. As no appreciable racemization is expected in the reaction sequence (20), the calculated value for the optically pure (-)(R)-2-methyloctanal is $\alpha_D^{25} -29.9^\circ$ (neat, ($l = 1$); minimum value).

The prevailing chirality of the aldehyde produced using (-)-DIOP as the asymmetric ligand is [(R)] for vinyl olefins where the asymmetric carbon atom arises from the attack of carbon monoxide at the carbon atom in position 2. The same chirality [(R)] is found also for vinylidene olefins where the asymmetric carbon atom arises from the attack of a hydrogen atom on the same carbon atom.

Cis- and *trans*-butene under similar conditions yield 2-methylbutanal with prevailing [(S)] chirality. The same [(S)] prevailing chirality was found in the case of *cis*- and *trans*-2-hexene for the aldehydes arising from the attack of carbon monoxide at the carbon atom in position 2, accounting for 60% of the aldehydes formed. The opposite chirality



Scheme 4

[(R)] is found for the aldehydes arising from the attack of carbon monoxide at position 3. The above stereochemical relationships are summarized in Table VI. Finally in the stereoselective hydroformylation of racemic 3-methyl-1-pentene the (R) antipode is hydroformylated at a higher rate, yielding the (R)-4-methylhexanal; the ratio between the hydroformylation rate of the two antipodes is 1.1.

Experimental

Reactions at elevated temperature and pressure were carried out, unless specified otherwise, in a 150 ml stainless steel 18/8 M rocking autoclave heated with oil bath. The temperature was kept within $\pm 1^{\circ}\text{C}$ of that reported.

NMR spectra were determined using a Varian T 60 spectrometer. IR spectra were recorded on a Perkin-Elmer IR-221 spectrometer. Mass spectra were determined using a Hitachi-Perkin-Elmer RMU 6L mass spectrometer. GLC analyses were performed using a Perkin-Elmer F 11 or F 990 gas chromatographs with flame ionization detectors. The analyses of the reaction products were performed (unless otherwise stated) using a Silicon Oil GE SF 96 on Chromosorb G 2 m \times 1/8 inch column at the temperature specified and toluene as internal standard. For quantitative determinations of isomeric reaction mixture composition no calibration curves were used. In cases when the reaction mixture composition was checked by NMR, discrepancies not larger than 2% were found. Preparative gas chromatographic separations were accomplished with a Perkin-Elmer F 21 gas chromatograph using the columns and the temperatures specified. Rotations were taken on a Perkin-Elmer 141 digital polarimeter and with a Cary 60 spectropolarimeter, using 1-dm tubes.

Table VI. Stereochemical Relationships among the Aldehydes Produced by Asymmetric Hydroformylation

Olefin	Prevailing Chirality of the Resulting Asymmetric Carbon Atom	Group Attacking the Prochiral C-Atom to Form the Chiral Center	Prochiral Atom Considered	Prochiral Face Prevailing during the CO and H Reaction ^a
Styrene	(R)	CO	2	re-re
1-Butene	(R)	CO	2	re-re
3-Methyl-1-butene	(R)	CO	2	re-re
1-Pentene	(R)	CO	2	re-re
1-Octene	(R)	CO	2	re-re
Allylbenzene	(R)	CO	2	re-re
α -Methylstyrene	(R)	H	2	si-si
α -Ethylstyrene	(R)	H	2	re-re
2-Ethyl-1-hexene	(R)	H	2	si-si
<i>trans</i> - β -Methylstyrene	(R)	CO	3	re-si
<i>cis</i> -Butene	(S)	CO	2	re-si
<i>trans</i> -Butene	(S)	CO	2	si-si
	(S)	CO	2	re-si
<i>cis</i> -2-Hexene	(R)	CO	3	si-re
	(S)	CO	2	si-si
<i>trans</i> -2-Hexene	(R)	CO	3	si-si

^a The nomenclature proposed by Hanson (35) is used.

Hydroformylation yields are reported as moles of recovered aldehydes per 100 moles of starting olefin.

Materials. The gases used had a purity $\geq 99\%$; the carbon monoxide contained $< 1\%$ hydrogen by GLC silica gel, 4 m \times 1/8 inch, 70°C, Perkin-Elmer F 11 hot wire gas chromatograph and argon as carrier gas. All hydroformylation experiments were performed with a 1:1 mixture of carbon monoxide and hydrogen. The olefinic substrates were Fluka AG pure or very pure grade. α -Ethylstyrene, prepared according to Ref. 21, was $> 98\%$ pure by GLC.

Dicobalt octacarbonyl (22), (*S*)-*N*- α -methylbenzylsalicylaldimine (R^* -SalH) (1) ($[\alpha]_D^{25} + 183^\circ$) and (*-*)-2,3-*O*-isopropylidene-2,3-dihydroxy-1,4-bis(diphenylphosphino)butane (DIOP) (23) ($[\alpha]_D^{25} - 12.8^\circ$ (*c* 4.6, benzene), mp 82°C) were prepared as described in the literature. The optical purity of (*-*)-DIOP is not known. Comparison with highest optical purity obtained by Kagan and Dang (23) in the asymmetric hydrogenation with this chiral ligand, having the same optical activity, indicates that optical purity of (*-*)-DIOP must be higher than 90%.

Preparation of HRh(CO)(P ϕ_3)₃. The complex was prepared through Wilkinson's method (24) and modified according to Rehder-Stirnweis (25). It is important to prepare relatively large quantities (about 10 grams) because small batches gave impure products.

In a typical preparation carried out under argon, 10 grams (14.5 mmoles) of $\text{RhCl}(\text{CO})(\text{P}\phi_3)_2$, 50 grams (0.19 mole) of triphenylphosphine and 12.5 grams (0.33 mole) of sodium borohydride were heated under reflux in dry, degassed ethanol for four days. Every day 2.5 grams of sodium borohydride were added to the mixture. The suspension was then filtered under argon, and the residue taken up in 500 ml of dried and degassed hot benzene. The filtered benzene solution was reduced to about 60 ml and 500 ml of dry, degassed petroleum ether were added rapidly. The yellow precipitate, 13.1 grams (98%), was dried under high vacuum, mp 124°C ; found C, 72.6; H, 5.25%; calc. C, 71.9; H, 5.05%; IR ν_{max} 2016 s, 1931 m cm^{-1} (benzene solution).

Hydroformylations with Cobalt Chiral Catalysts. **STYRENE IN BENZENE SOLUTION.** In a 150-ml autoclave, flushed with nitrogen, was placed 0.715 mg (2.05 mmoles) of $[\text{Co}(\text{CO})_4]_2$. The autoclave was sealed and evacuated. A solution of 10.4 grams (0.1 mole) of freshly distilled styrene in 40 ml benzene was introduced by suction followed by carbon monoxide and hydrogen up to 80 atm. The autoclave was then placed in an oil bath at 120°C and rocked; as soon as the gas absorption began, 30 ml of a benzene solution containing 1.84 grams (8.2 mmoles) of (*S*)-*N*- α -methylbenzylsalicylaldehyde were pumped into the reaction vessel with a metering pump. The reaction was allowed to proceed until no further pressure drop was noted (2.5 hrs). After rapid cooling, the gases were discharged, and the reaction mixture was bulb-to-bulb distilled under vacuum. GLC analysis of the solution shows the following composition: 53% ethylbenzene, 27% 2-phenylpropanal, 19% 3-phenylpropanal, and 1% unreacted olefin. The hydroformylation yield on distilled products was 35%. The hydroformylation products were added dropwise to a LiAlH_4 suspension in diethyl ether, cooled at 0°C , and worked up in the usual way. The resulting (–)(*S*)-2-phenyl-1-propyl alcohol, purified through preparative gas chromatography (20% Carbowax 20 M on Chromosorb A, 2.7 m, 170°C) had bp 101°C (11 mm Hg), n_{D}^{25} 1.5239, $[\alpha]_{\text{D}}^{21}$ -0.33° (neat).

STYRENE IN ETHANOL SOLUTION. In a stainless steel 18/8 M 0.5-liter autoclave (equipped with a thermometer in a suitable sheath which is dipped into the reaction solution) flushed with nitrogen was placed 0.684 gram (2.0 mmoles) of $[\text{Co}(\text{CO})_4]_2$. The autoclave was sealed and evacuated. A solution of 41.6 grams (0.4 mole) of freshly distilled styrene in 150 ml of dry ethanol was introduced in the bomb by suction and the pressure was raised to 80 atm. The autoclave was then placed in a rocking heater and heated at 95°C . At the initiation of gas absorption 1.8 grams (8.0 mmoles) of R^* -SalH in 50 ml ethanol and 20 ml benzene were pumped into the reaction vessel with a metering pump. After 5.0 hrs no further pressure drop was observed. After rapid cooling, the gases were released and the reaction mixture was bulb-to-bulb distilled under vacuum. The hydroformylation yield determined by GLC was 25%. The solvent was evaporated under 100 mm Hg. The residue was distilled in vacuum to give (–)(*R*)-2-phenylpropanal which contains 9% (GLC) of the isomeric 3-phenylpropanal, bp $45^\circ\text{--}50^\circ\text{C}$ (1 mm Hg), $[\alpha]_{\text{D}}^{25}$ -0.53° .

STYRENE IN ETHANOL SOLUTION IN THE PRESENCE OF ETHYL ORTHOFORMATE. Using the same procedure and reaction conditions, 0.4 mole of styrene in 80 ml of dry ethanol and 90 grams of ethyl orthoformate were hydroformylated using 2.6 grams (7.6 mmoles) of $[\text{Co}(\text{CO})_4]_2$ and a solution of 6.84 grams (0.03 mole) of $\text{R}^*\text{-SalH}$, dissolved in 120 ml ethanol and 30 ml benzene.

The reaction time was 3.5 hrs. The composition of the mixture of the reaction products determined by GLC was 65% ethylbenzene, 19.5% 3-phenylpropanal diethylacetal, and 10.5% $(-)(R)$ -2-phenylpropanal diethylacetal. The yield of hydroformylation products was 32%. The optically active acetal purified by preparative GLC (9) and identified by comparison of GLC and mass spectroscopy with a known sample had $[\alpha]_{\text{D}}^{25} -0.52^\circ$ (neat).

α -ETHYLSTYRENE IN BENZENE SOLUTION. Following the procedure previously described, 0.1 mole of α -ethylstyrene in 40 ml of benzene were hydroformylated at 120°C and 100 atm total pressure using 0.342 gram (1 mmole) $[\text{Co}(\text{CO})_4]_2$ and a solution of 9.0 grams (40 mmoles) $\text{R}^*\text{-SalH}$ in 30 ml of benzene. The reaction time was 7.5 hrs. Distillation under reduced pressure of the reaction mixture gave 10.7 grams (84%) 2-phenylbutane which was purified ($\geq 99\%$ pure by GLC) through two-fold distillation and identified by NMR and mass spectroscopy. No optical activity was found between 590 and 350 $\text{m}\mu$. Distillation of the residue [bp $60^\circ\text{-}70^\circ\text{C}$ (0.01 mm Hg)] yielded 1.94 grams (12%) aldehydes.

The aldehyde mixture was added to a stirred suspension of 4.1 grams (0.018 mole) Ag_2O in 40 ml of water (26). After 16 hrs of stirring at room temperature and 3 hrs at 40°C , 0.72 gram (0.018 mole) of NaOH were added to the reaction mixture. Filtration, extraction with ether of the basic solution, acidification with concentrated H_2SO_4 , extraction with ether, drying (Na_2SO_4), esterification with diazomethane, and distillation gave 1.12 grams (53%) of a mixture of methyl esters. The mixture was analyzed by GLC (15% Carbowax 20M on Chromosorb G, 2 m \times 1/8 inch, 150°C) showing the composition reported in Scheme 2 and separated by preparative GLC (5% Carbowax 20 M on Chromosorb G, 4.5 m, 180°C). The identification of the methyl 3-phenylpentanoate was accomplished by comparing its retention time, NMR and mass spectrum with that of known sample. The $(+)(S)$ -3-phenylpentanoic acid obtained by saponification with NaOH solution of the corresponding methyl ester, had $[\alpha]_{\text{D}}^{25} + 0.730^\circ$ (*c* 17.5 benzene) (27). The other two methyl esters were identified by mass spectroscopy and NMR as:

$(-)(R)$ -Methyl 4-phenylpentanoate, $[\alpha]_{\text{D}}^{25} -0.024^\circ$ (*c* 33.0, ethanol) (28). $(-)$ -Methyl 2-methyl-3-phenylbutanoate, $[\alpha]_{\text{D}}^{25} -0.030^\circ$ (*c* 3.4, ethanol).

STEREOELECTIVE HYDROFORMYLATION OF $(R)(S)$ -3-METHYL-1-PENTENE. 15.0 grams (0.18 mole) of $(R)(S)$ -3-methyl-1-pentene in 80 ml of dry *m*-xylene were hydroformylated according to the usual procedure at 118°C and 80 atm using 0.156 grams of $[\text{Co}(\text{CO})_4]_2$ and a solution of 3.6 grams of $(-)(R)$ - $\text{R}^*\text{-SalH}$ in 30 ml benzene. After 24 hrs the conversion was 40%.

Careful rectification of the reaction mixture gave 4.2 grams of unreacted olefin, bp 53° – 54° C, n_D^{20} 1.3843, $[\alpha]_D^{17}$ $+0.015^{\circ}$, $[\alpha]_{365}^{17}$ $+0.045^{\circ}$. GLC analysis of the recovered olefin (Squalane, 90 m capillary column, 60° C) showed 10% isomeric products which obviously cannot be optically active. The hydroformylation products were oxidized with Ag_2O , according to the previously described procedure. The resulting acids were converted with diazomethane into the corresponding methyl esters. The mixture of the methyl esters had the following composition, determined by GLC (4% Polypropylenglycol on Chromosorb G, 2 m \times 1/8 inch, 120° C): 86% (–)(*R*)-methyl 4-methylhexanoate, 6.8% methyl 2,3-dimethylpentanoate, and 6.5% methyl 3-ethylpentanoate. The purified (–)(*R*)-4-methylhexanoic acid had $[\alpha]_{365}^{25}$ -0.015° (neat).

Hydroformylation with Rhodium Catalysts at Atmospheric Pressure. STYRENE. 230 mg (0.25 mmole) of $\text{HRh}(\text{CO})(\text{P}\phi_3)_3$ and 250 mg (0.5 mmole) of (–)-DIOP were placed in a 200-ml, two-necked flask. The stirrer was a Teflon coated magnet fitted with two Teflon flange discs. The flask was attached to a hydrogenation apparatus with storage bulbs, manometer, and gas burettes. The system was flushed three times with the gas mixture. 100 ml of dry, degassed benzene were introduced into the flask and the solution was brought to $40.0 \pm 0.1^{\circ}$ C. 9.22 grams (89 mmoles) of freshly distilled styrene were introduced with a syringe through a self-sealing rubber, and the flask was connected with the gas burette. After 48 hrs (25% conversion) the solvent was evaporated under reduced pressure, and the residue was distilled under high vacuum, yielding 2 ml of aldehyde mixture (69% of 2-phenylpropanal and 31% of 3-phenylpropanal). For the pure (–)(*R*)-2-phenylpropanal, α_D^{25} -44° was extrapolated from the above mixture composition.

OTHER SUBSTRATES. α -Methylstyrene, α -ethylstyrene, allylbenzene, *trans*- β -methylstyrene, 1-pentene, and 1-octene were hydroformylated as described for styrene, giving the results reported in Tables III and IV.

STEREOELECTIVE HYDROFORMYLATION OF 3-METHYL-1-PENTENE. The same apparatus and procedure as for styrene were used. 4.21 grams (0.05 moles) of 3-methyl-1-pentene were hydroformylated in 50 ml of dry, degassed mesitylene in the presence of 115 mg (0.125 mmole) of $\text{HRh}(\text{CO})(\text{P}\phi_3)_3$ and 249 mg (0.5 mmole) of (–)-DIOP. After 70 hrs the conversion was 51.1%. The unreacted olefin and the aldehydes were separated with a 1-m rectification column filled with Fenske rings. The pure olefin (GLC) had $[\alpha]_D^{17}$ $+1.25^{\circ}$ (neat). The aldehydes could not be completely separated from the solvent through rectification. A fraction containing 58% of (–)(*R*)-4-methylhexanal had α_D^{25} -0.26° .

1-BUTENE. In a 250-ml, three-necked flask were introduced under nitrogen 0.230 gram $\text{HRh}(\text{CO})(\text{P}\phi_3)_3$, 0.500 gram (–)-DIOP, 100 ml mesitylene, and 3 grams of 1-butene. The flask was cooled with liquid nitrogen, evacuated, and attached with rubber tubing to a gasometer containing a premixed mixture of carbon monoxide, hydrogen, and 1-butene (1:1:1). The mixture was allowed to react at room temperature with stirring for 26 days. The gas absorbed was 4 liters and the ratio of straight chain to branched aldehyde was 12.5. A rectified fraction containing 13% (–)(*R*)-2-methylbutanal and 87% *n*-pentanal had $[\alpha]_D^{25}$ -0.69° .

cis-BUTENE. The procedure was the same as for 1-butene, using the same quantities of catalyst, ligand, solvent, and olefin. The gas absorbed after 30 days was about 1 liter. A small amount of *n*-pentanal (~5%) was detected in the reaction mixture, probably deriving from ~1% of 1-butene contained in *cis*-butene. The (+)(*S*)-2-methylbutanal (1 ml) was isolated through rectification: $[\alpha]_D^{25} +9.47^\circ$ (neat).

Hydroformylation with Rhodium Catalysts at High Pressure. *cis*-BUTENE. The 150-ml autoclave was charged with 0.231 gram of $\text{HRh}(\text{CO})\text{-(P}\phi_3)_3$ and 0.504 gram of (-)-DIOP, evacuated and cooled. 10 grams of *cis*-butene in 70 ml of mesitylene were introduced by suction. The gas mixture was then admitted to 84 atm (room temperature). The autoclave was heated for 22 hrs at 95°C. The aldehyde was separated from the reaction solution by rectification; 4.5 grams of (+)(*S*)-2-methylbutanal, $[\alpha]_D^{25} + 2.85^\circ$ (neat) were obtained. The purity, checked by GLC (20% PPG on Chromosorb G, 2 m \times 1/8 inch, 90°C), was higher than 99%.

cis-BUTENE. The procedure was the same as described before. Rh_2O_3 (0.033 gram), (-)-DIOP (0.633 gram), and *cis*-butene (12 grams) in 80 ml *p*-xylene and 86 atm gas mixture (room temperature) were used. After 22 hrs at 95°C, the reaction was stopped. The resulting (+)(*S*)-2-methylbutanal (5.4 grams) was recovered through rectification: $[\alpha]_D^{25} +2.78^\circ$ (neat).

trans-BUTENE. The same procedure was used starting with 0.230 gram of $\text{HRh}(\text{CO})(\text{P}\phi_3)_3$, 0.5185 gram of (-)-DIOP, 20 grams *trans*-butene in 80 ml of mesitylene, and 84 atm gas mixture (room temperature). After 22 hrs at 98°C, 6.5 grams of (+)(*S*)-2-methylbutanal were recovered, having purity higher than 98% and $[\alpha]_D^{25} +1.11^\circ$ (neat).

1-BUTENE. Starting with 0.459 gram of $\text{HRh}(\text{CO})(\text{P}\phi_3)_3$ and 0.523 gram of (-)-DIOP, 9 grams of 1-butene in 80 ml mesitylene were hydroformylated at 90 atm and 95°C. The reaction time was 50 min. From the reaction mixture, containing 13% (-)(*R*)-2-methylbutanal and 87% *n*-pentanal (GLC), (-)(*R*)-2-methylbutanal was isolated through rectification: $[\alpha]_D^{25} -1.93^\circ$ (neat).

cis-2-HEXENE. The autoclave was charged with 0.230 gram of $\text{HRh}(\text{CO})(\text{P}\phi_3)_3$ and 0.490 gram of (-)-DIOP and evacuated. 17 grams of *cis*-2-hexene in 75 ml benzene were introduced by suction. The gas mixture was then admitted to 82 atm. The autoclave was heated during 95 hrs at 95°C with constant pressure. After distilling the solvent, the reaction mixture containing 40% 2-ethylpentanal and 60% 2-methylhexanal (66% yield) was oxidized with Ag_2O and esterified with CH_2N_2 as previously described (26). The two esters were separated by preparative GLC (20% PPG on Chromosorb A, 4.5 m, 150°C). The esters were identified through NMR and mass spectra. Saponification and distillation gave the (+)(*S*)-2-methylhexanoic acid, $\alpha_D^{25} +1.68^\circ$ (neat) and the (-)(*R*)-2-ethylpentanoic acid, $\alpha_D^{25} -0.22^\circ$ (neat).

trans-2-HEXENE. The same procedure and the same quantities as for *cis*-2-hexene were used. After 123 hrs the yield was 47%; the reaction mixture contained 58% 2-methylhexanal and 42% 2-ethylpentanal. After oxidation, esterification, separation, and saponification (+)(*S*)-2-

methylhexanoic acid, $\alpha_D^{25} +0.31^\circ$ (neat), and $(-)(R)$ -2-ethylpentanoic acid, $\alpha_D^{25} -0.11^\circ$ (neat) were recovered.

Conversion of $(-)(R)$ -2-methyloctanal in $(+)(S)$ -3-methylnonane. $(-)(R)$ -2-Methyloctanal, $\alpha_D^{25} -163^\circ$ (neat), (2.5 grams, 0.018 mole) was made to react with methylenetriphenylphosphorane according to the procedure of Corey *et al.* (29). The obtained $(-)(R)$ -3-methyl-1-nonene (1.4 grams, 0.01 mole, 50% yield), was hydrogenated to $(+)(S)$ -3-methylnonane (19) at 40 atm and room temperature using Raney nickel as catalyst. The reaction time was 17 hrs. The pure paraffin ($\geq 98\%$, GLC) had: bp 168°C , n_D^{20} 1.4125, $\alpha_D^{25} +0.40^\circ$ (neat).

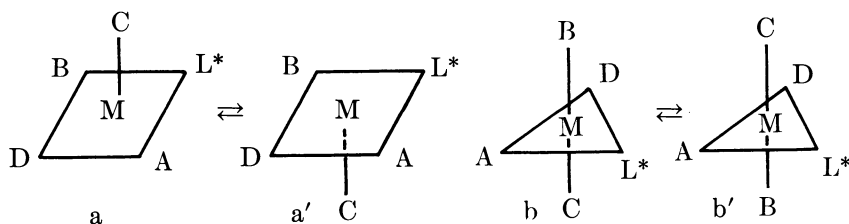
Discussion

The asymmetric hydroformylation gives some interesting insights into the reaction mechanism and, more generally, into the nature of the homogeneous catalysts. Some facts independent of the reaction mechanism are discussed along with some interesting aspects of the hydroformylation mechanism; aspects which, although very widely accepted, are not completely proved experimentally.

General Aspects of Asymmetric Hydroformylation. Asymmetric hydroformylation proves the presence of the asymmetric ligand in the catalytic complex or in at least one of the catalytic complexes if, as is probable, more than one active species are present. Diphosphines, monophosphines, and N-substituted salicylaldimine are then present in the catalytic complexes. As the optical yields, however, are in some cases very low, it is still an open question if the asymmetric induction by these ligands is intrinsically small or if it is large, but only one or some of the catalytic species contain the asymmetric ligand. Other catalytic species not containing the chiral ligand could catalyze a simultaneous hydroformylation yielding racemic aldehydes. In any case the use of chiral ligands seems very promising in the investigation of the nature of the active species in the hydroformylation and of the displacement equilibria of the ligands by carbon monoxide under the reaction conditions. The influence of alcohols on the sign (in the case of cobalt catalysts) and on the extent (~ 1 tenth the size) of asymmetric induction in the case of rhodium catalysts (30) does not necessarily mean that alcohols participate to the catalytic complexes since coordination compounds geometry may be different in polar or in hydrocarbon solvents (31).

The mechanism of the asymmetric induction in asymmetric catalysis by transition metal complexes is only speculation. In principle, the asymmetric induction can result from direct interaction between ligand and substrate as proposed, for instance, by McQuillin *et al.* (32) for the asymmetric hydrogenation. But it might take place simply by interaction between substrate and chiral transition metal atoms without

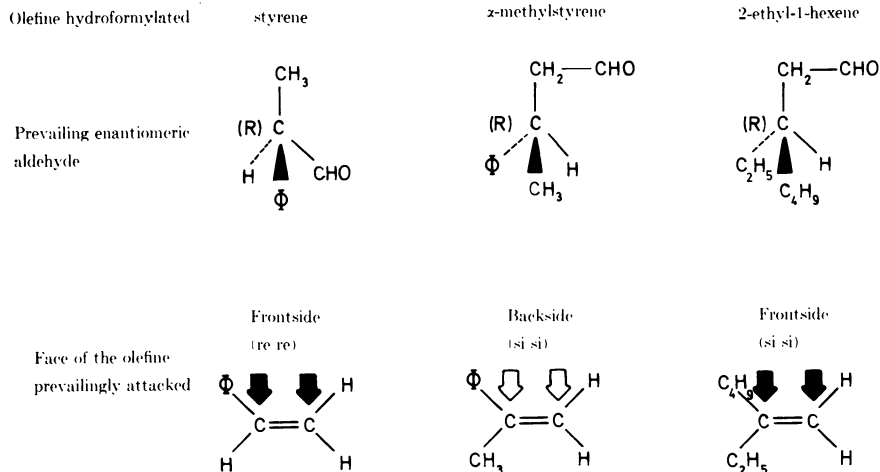
direct interaction between substrate and ligand. Asymmetric transition metal atoms are known to exist in the absence of chiral ligands, and they have been isolated when no rapid ligand exchange takes place (33). If chiral ligands are present in the complexes, and transition metal atoms (M) are chirality centers (23), for example in penta-coordinated complexes of the type a or b (Scheme 5), the complexes must exist in the most simple case (L^* contains only one chirality center and is optically pure) as two diastereomeric forms a, a' and b, b'. In this case, even if a rapid ligand exchange takes place, the thermodynamically more stable complex and hence metal atoms of one chirality must prevail, and the catalytic system can give rise by interaction with the nonchiral substrates to asymmetric induction phenomena.



Scheme 5

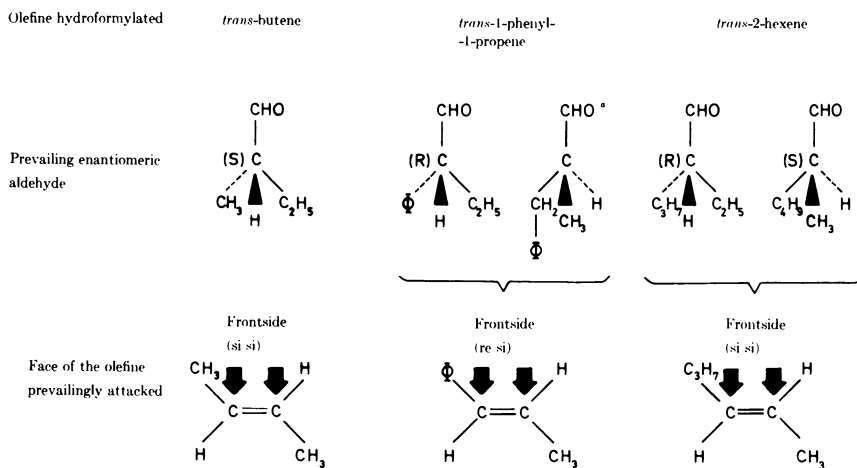
A further fact, from the asymmetric hydroformylation results concerns the face of olefin attacked by hydrogen and carbon monoxide and affects the prevailing chirality obtained with different substrates. The occurrence of a cis addition of carbon monoxide and hydrogen is proved beyond any doubt in the olefinic hydrocarbons hydroformylation by a rhodium catalyst (34) and for some special substrates in the cobalt catalyzed hydroformylation (10). Therefore the prevailing chirality of the aldehydes synthesized shows, in the case of prochiral olefins, which of the prochiral faces is prevailingly attacked by both hydrogen and carbon monoxide. Although it is generally assumed that the face of the olefin reacting with carbon monoxide and hydrogen is also the face interacting with the metal atom of the complex, this has never been experimentally proved. However, the only relevant fact is that in all cases investigated, the face interacting with the catalyst is the same, *i.e.*, either the face attacked by carbon monoxide and hydrogen or the opposite one.

For vinyl olefins the face prevailingly attacked by carbon monoxide and hydrogen is always the same and, as shown in Table VI, has the same name according to the Hanson's nomenclature (35). For vinylidene olefins, faces having different names according to Hanson are preferentially attacked (Table VI). As shown in the Scheme 6, if we equally



Scheme 6

orient the vinylidene olefins in the plane of the page (for instance with the bulkiest substituent on the left side up), it is easy to see that the same face of the vinylidene olefins is attacked in the case of α -substituted styrenes, but for 2-ethyl-1-hexene the opposite face is attacked. Furthermore, if we orient vinyl olefins in the same way and assume that methyl and ethyl groups are less bulky than phenyl group, the face attacked in



*product not isolated

Scheme 7

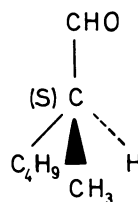
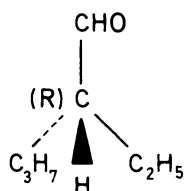
the case of vinyl olefins and 2-ethyl-1-hexene is the same but opposite to the face attacked in the α -substituted styrenes (Scheme 6).

For the three internal *trans*-olefins used, because of the Hanson nomenclature, prochiral faces with different names are attacked (Table VI). However, as shown in Scheme 7, the difference in this case is purely formal. In fact, by orienting equally the olefin in the plane of the sheet, with the bulkiest substituent on the left side up, the face of the olefin attacked is in all three cases the same and corresponds to the face attacked in the vinyl olefins.

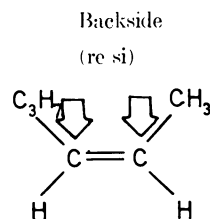
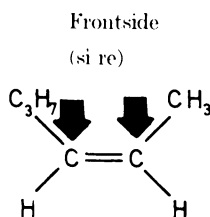
Olefine hydroformylated

cis-2-hexene

Prevailing enantiomeric aldehyde



Face of the olefin
prevalingly attacked

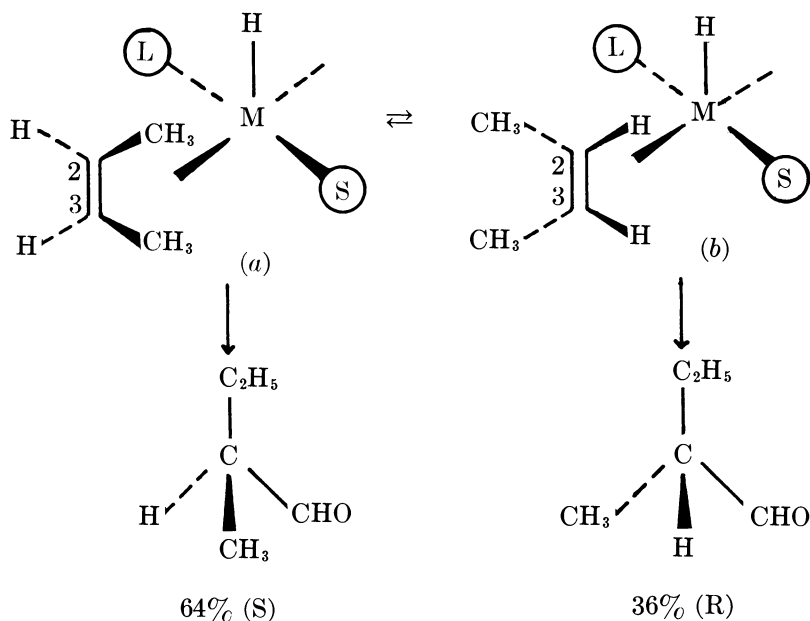


Scheme 8

Contrary to the *trans* olefins, the only *cis* olefin having different prochiral faces which has been examined, the *cis*-2-hexene, yields two aldehydes arising from the attack at the two opposite prochiral faces (Scheme 8).

Finally a very important fact arising from our results is the occurrence of the asymmetric hydroformylation in olefins having C_{2v} symmetry like *cis*-butene. In this case the two faces of the olefin are identical, and the catalyst is evidently able to dissymmetrize the double bond favoring the attack of hydrogen to the *re* carbon atom and of carbon monoxide to the *si* carbon atom. A very simple way of looking at this dissymmetrization of the double bond is to assume that the face of the olefin attacked

by carbon monoxide and hydrogen is the same face which interacts with the metal complex and, further, that a hydrogen atom and two other substituents of different size (for instance a carbon monoxide and a phosphine molecule) are located around the metal atom as in Scheme 9.



Scheme 9

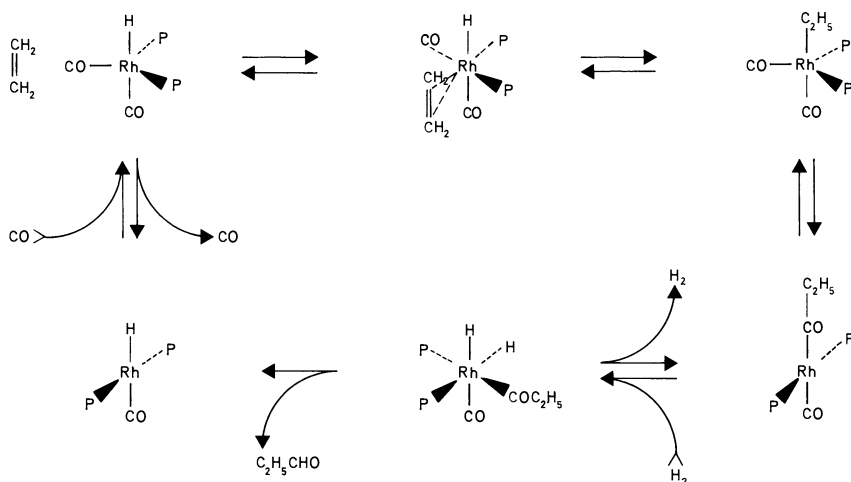
The interaction between olefin and catalytic complex can be investigated according to the above model by rotating the olefin around the axis joining the middle of the double bond with the metal atom. It appears that the (a) position is favored over the (b) position. The hydrogen would preferentially attack the *re* face of the carbon atom 2 and the carbon monoxide the *si* face of the carbon atom 3, yielding preferentially the (S)-2-methylbutanal.

This simple scheme permits a prediction of the prevailing chirality of the aldehydes obtained from all vinyl and *trans* or *cis* internal olefins when an additional group (larger than hydrogen) is bound to the metal in *trans* with respect to hydrogen.

The same simple model predicts in a qualitatively correct way the isomeric composition of the reaction products with the exception of styrene and *trans*- β -methylstyrene, in which the double bond is obviously conjugated with the phenyl ring. The predictions using the same model are contradictory for the vinylidene olefins. This is not surprising as the asymmetric induction in these olefins is always very small.

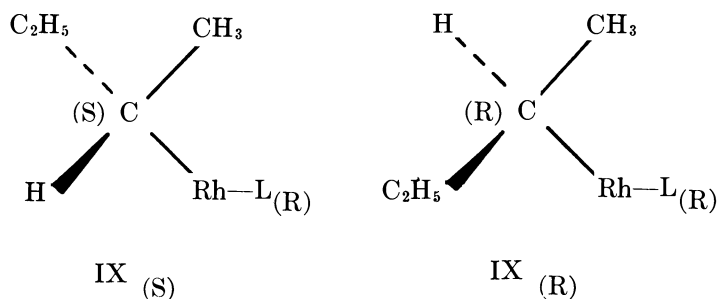
Its sign might be decided by factors which in the other cases play a secondary role.

Asymmetric Hydroformylation and Hydroformylation Mechanism. The present discussion is limited to the rhodium catalyzed hydroformylation. In the widely accepted mechanism proposed by Wilkinson *et al.* (36), on the basis of suggestions by Breslow and Heck (37) for the cobalt catalyzed hydroformylation, the reaction steps, with the exception of the hydrogenolysis of the acyl-rhodium complexes, correspond to equilibria (Scheme 10).



Scheme 10

To obtain information about the steps in which the asymmetric induction actually takes place, 1-butene, *cis*-butene, and *trans*-butene were hydroformylated using asymmetric rhodium catalyst. According to the Wilkinson mechanism, all three olefins yield a common intermediate, the *sec*-butyl-rhodium complex, which, if the asymmetric ligand contains one asymmetric center, must exist in the two diastereomeric forms, IX_(S) and IX_(R).



If no asymmetric induction takes place in the diastereomeric alkyls formation, the chiral aldehyde resulting from the three olefins must have the same chirality and the same optical purity. The experiments indicate (Table IV) the opposite result. Using the same chiral ligand [(−)-DIOP] the aldehyde obtained from 1-butene has prevailing [(R)] chirality while the same aldehyde arising from the two 2-butenes has prevailing [(S)] chirality. Furthermore, the two aldehydes obtained from *cis*-butene and *trans*-butene under the same reaction conditions have different optical purity (8.1 and 3.2% respectively). These results imply that the diastereomeric composition of the mixture $\text{IX}_{(S)} + \text{IX}_{(R)}$ depends on the type of the starting C_4 olefin and that for at least two of the olefins used the asymmetric induction occurs, at least in part, in the alkyl-rhodium complex formation.

For the reaction conditions used, substrates like *trans*-1-phenyl-1-propene, 2-hexene and 2-butene yield practically no isomeric aldehydes except that expected from the attack of carbon monoxide to one of the two carbon atoms originally linked by the double bond. This indicates that the formation of rhodium-alkyl complexes (Scheme 11) is not or is only very slowly reversible ($k_{\text{VI} \rightarrow \text{II}} \ll k_{\text{II} \rightarrow \text{VI}}$) in agreement with data of other authors (38, 39). As a consequence, in these conditions, the asymmetric induction should take place substantially only during the rhodium-alkyl formation. Since carbon monoxide insertion is more rapid than the rhodium-alkyl formation even if it occurs in the two diastereomeric alkyl-rhodium complexes with a remarkably different rate ($k_{\text{VI}_{(R)} \rightarrow \text{VII}_{(R)}} > k_{\text{VI}_{(S)} \rightarrow \text{VII}_{(S)}}$), the kinetic factor cannot give rise to relevant asymmetric induction. Disregarding the absence of other than the two predictable isomeric aldehydes, a second limit case can be considered which is in keeping with the results and gives the same conclusions: we can assume that the rhodium-alkyl formation is rapidly reversible and that the carbon monoxide insertion is much more rapid than the rhodium-alkyl decomposition ($k_{\text{VI} \rightarrow \text{VII}} \gg k_{\text{VII} \rightarrow \text{VI}}$), the reactivity of $\text{VI}_{(S)}$ and $\text{VI}_{(R)}$ in the insertion reaction being similar ($k_{\text{VI}_{(R)} \rightarrow \text{VII}_{(R)}} \sim k_{\text{VI}_{(S)} \rightarrow \text{VII}_{(S)}}$).

The results do not prove that in the reaction conditions used the alkyl formation is not reversible, but only that, if it is reversible, the carbon monoxide insertion on both diastereomeric rhodium-alkyls must be much faster than the rhodium-alkyls decomposition. Restricting this analysis of the asymmetric induction phenomena to the rhodium-alkyl complexes formation, two π -olefin complexes are possible for each diastereomer of the catalytic rhodium complex (*see* Scheme 11). The induction can take place in the π -olefin complexes formation ($\text{I} \rightarrow \text{II}_{(S)}$ or $\text{I} \rightarrow \text{II}_{(R)}$) or in the equilibrium between the diastereomeric π -olefin complexes ($\text{II}_{(R)}$ and

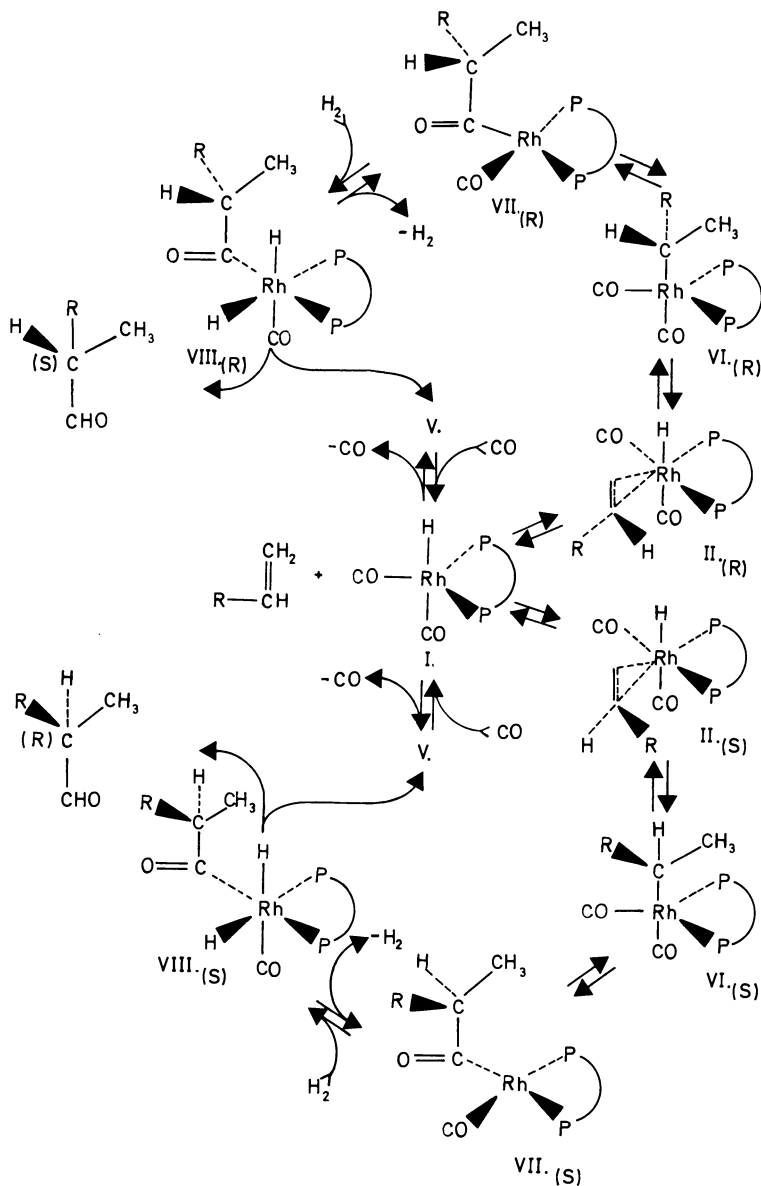
$\text{II}_{(\text{S})}$) and/or to a different reaction rate of the two diastereomeric π -olefin complexes to the corresponding diastereomeric alkyl-rhodium complexes ($\text{VI}_{(\text{S})}$ and $\text{VI}_{(\text{R})}$). For diastereomeric *cis*- or *trans*-[α -methylbenzyl]-[vinyl olefin]-dichloroplatinum(II) complexes, the diastereomeric equilibrium is very rapidly achieved in the presence of an excess of olefin even at room temperature (40). Therefore, it seems probable that asymmetric induction in π -olefin complexes formation ($\text{I} \rightarrow \text{II}$) cannot play a relevant role in determining the optical purity of the reaction products. On the other hand, both the free energy difference between the two π -olefin complexes ($\Delta G^\circ_{\text{II}_{(\text{S})}} - \Delta G^\circ_{\text{II}_{(\text{R})}} = \Delta G^\circ$) and the difference between the two free energies of activation for the isomerization of π -complexes $\text{II}_{(\text{S})}$ and $\text{II}_{(\text{R})}$ to the corresponding alkyl-rhodium complexes $\text{VI}_{(\text{S})}$ and $\text{VI}_{(\text{R})}$ ($\Delta G^\ddagger_{\text{II}_{(\text{R})}} - \Delta G^\ddagger_{\text{II}_{(\text{S})}} = \Delta \Delta G^\ddagger$) can control the overall difference in activation energy for the formation of the diastereomeric rhodium-alkyl complexes and hence the sign and extent of asymmetric induction.

A slightly different analysis of the origin of the asymmetric induction (Scheme 12) must be carried out for the hydroformylation of olefins having C_{2v} symmetry like *cis*-butene. In this case the two faces of the olefin being identical, only one π -olefin complex XII can exist for each diastereomer of the catalytic rhodium complex. For this complex, however, two allowed conformations, (XII a) and (XII b), having different energy are possible, and the conformational energy difference may well be of the same order of magnitude of that between diastereomers. Each of the conformers gives rise to only one diastereomeric alkyl-rhodium complex ($\text{XIII}_{(\text{S})}$ or $\text{XIII}_{(\text{R})}$), and the rate of conversion of each conformer to the corresponding diastereomer can also be different.

In this case a thermodynamic and/or a kinetic factor can control the overall difference in the activation energy and hence the diastereomeric composition of the alkyl-rhodium complexes and the asymmetric induction. The thermodynamic factor is the energy difference ΔG°_c between the two conformers (XII a) and (XII b); the kinetic factor is the difference between the free energy of activation $\Delta \Delta G^\ddagger_c$ of the reaction leading from each conformer to the corresponding alkyl-rhodium complex.

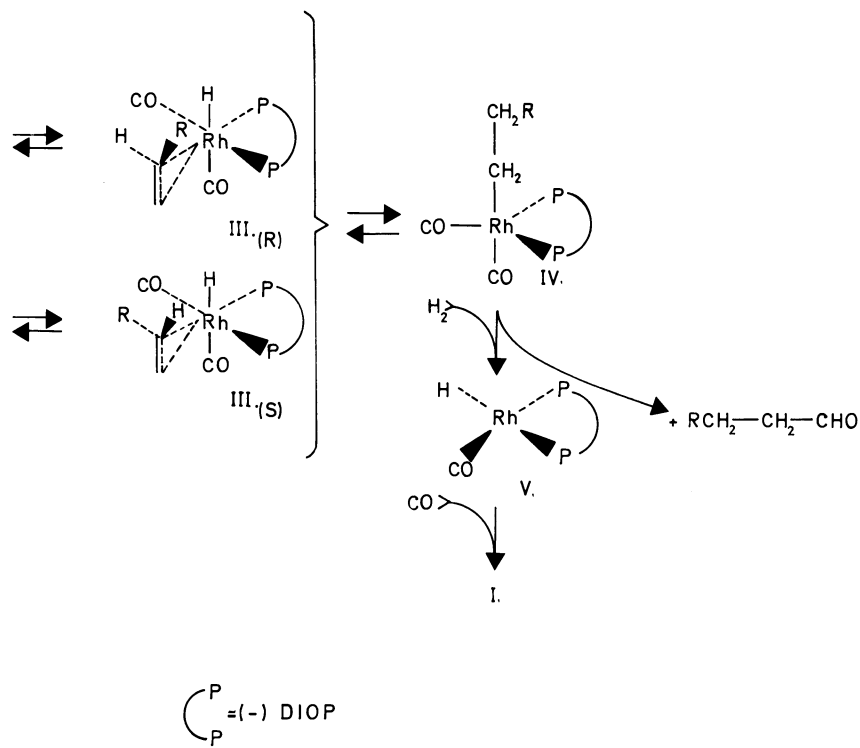
The experimental results do not permit us to establish the relative importance of the above thermodynamic and kinetic factors. Two arguments favor the hypothesis that thermodynamic factors ΔG° and ΔG°_c play a more important role than kinetic factors $\Delta \Delta G^\ddagger$ or $\Delta \Delta G^\ddagger_c$.

First, using the aforementioned very simple model of interaction between olefins and catalytic complexes most of the observed asymmetric induction phenomena can be explained without invoking kinetic effects.



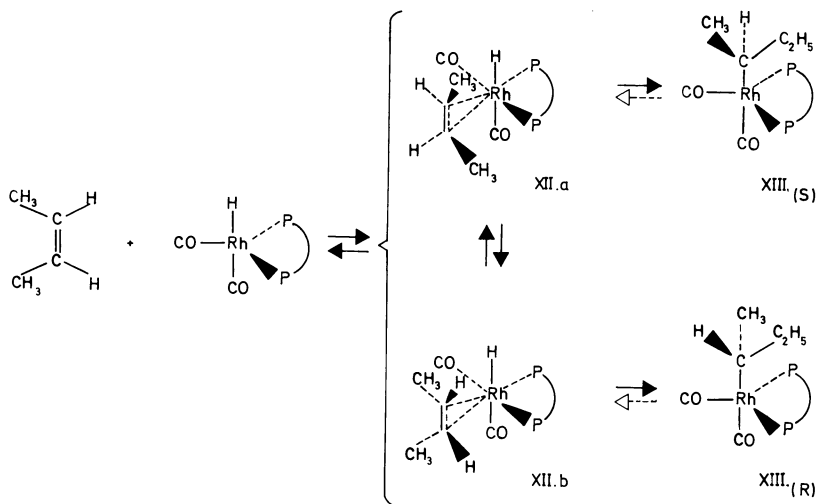
Scheme 11

The model can be identified with the diastereoisomeric π -olefin complexes, and thus ΔG° should, at least qualitatively, control the sign of the asymmetric induction. In this case, if $\Delta G^\ddagger_{\text{II}(S)} > \Delta G^\ddagger_{\text{II}(R)}$, ΔG° must be larger than $\Delta\Delta G^\ddagger$. If $\Delta G^\circ_{\text{II}(S)} < \Delta G^\circ_{\text{II}(R)}$ and $\Delta G^\ddagger_{\text{II}(S)} < \Delta G^\ddagger_{\text{II}(R)}$, which seems less probable, the sign of the asymmetric induction will correspond



to that determined by ΔG° , even if the asymmetric induction arises substantially from $\Delta\Delta G^\ddagger$.

Second, the asymmetric induction in hydroformylation at room temperature is in the range of that observed in the formation of *cis*- α -[methylbenzylamine]-[olefin]-dichloroplatinum(II) complexes after reaching



the epimerization equilibrium (40). The asymmetric induction is in both cases larger for styrene ($\sim 20\%$) than for other α -olefins (propylene $\sim 13\%$). Furthermore, as shown in Table VII, in the stereoselective hydroformylation of racemic 3-methyl-1-pentene the antipode preferentially hydroformylated is the one predicted from the epimerization equilibrium of *cis*-[benzylamine]-[(*S*)-3-methyl-1-pentene]-dichloroplatinum(II)

Table VII. Stereoselective Hydroformylation of (*R*)(*S*)-3-Methyl-1-pentene with $\text{HRh}(\text{CO})(\text{PPh}_3)_3/(-)\text{-DIOP}$ Catalytic System

Olefin	1-Butene	(<i>R</i>)(<i>S</i>)-3-methyl-1-pentene ^a
Chiral ligand considered	(-)-DIOP	(-)-DIOP
Chiral aldehyde considered	2-methylbutanal	4-methylhexanal
Aldehyde prevailing chirality	} predicted } found (R)	(R) ^b
Prevailing chirality at the C ₂ carbon atom bound to the metal		(S)
Prevailing chirality at the C ₃ carbon atom of the olefin	} predicted } found	(R) ^b (R)

^a Partial hydroformylation (conversion $\sim 50\%$).

^b On the basis of 1-butene asymmetric hydroformylation and of *cis*-[benzylamine]-[(*S*)-3-methyl-1-pentene]-dichloro-platinum(II) complexes epimerization (41).

^c On the basis of non chiral vinyl α -olefins asymmetric hydroformylation.

^d Not determined as the catalytic complex was not isolated.

complexes (41). Other experiments are in progress to determine if the facts reported here are merely coincidental or if platinum complexes really yield useful information in the interpretation of asymmetric hydroformylation.

Conclusions

The degree of asymmetric induction achieved in asymmetric hydroformylation may be important in synthetic chemistry as demonstrated by the preparation of optically active hydratropa aldehyde (9). No efforts have been made to date to optimize the process. The most hopeful steps in this direction are a thorough investigation of the reaction variables and the use of new asymmetric ligands.

In this respect the results achieved indicate that the asymmetric induction takes place largely by interaction of the olefin with a chiral metal atom while the direct interaction between olefin and ligand plays a less important role. An interesting direction for further investigation in this field is the study of the influence of the structure of chiral ligands on the diastereomeric equilibria between metal complexes containing a chiral metal atom and one or more chirality centers in the ligands. More effort is needed to clarify the steric structure of the catalytic complexes and the relative influence of thermodynamic equilibria between reaction intermediates and activation energies in the reaction steps in determining sign and extent of asymmetric induction. The research would not only help to clarify the origin of the asymmetric induction but would also improve the general knowledge of asymmetric catalysis by transition metal complexes.

The remarkable regularity observed in the asymmetric induction for a large number of substrates and for widely different reaction conditions is surprising in view of the relatively small overall activation energy difference involved for the formation of the two antipodes ($\sim 200 - 30$ cal/mole for vinyl and internal olefins). This fact shows that differences in solvation of the diastereomeric intermediates and transition states and differences in free energy of intermediates and of transition states arising from differences in substrates structure are relatively unimportant. Therefore speculations about the factors influencing qualitatively and quantitatively the asymmetric induction are worthwhile. The main contribution of the present research to the field of hydroformylation concerns the significance of the conformational equilibria in the π -olefin complexes. In fact the equilibrium between the allowed conformers, arising at least formally from the rotation of the olefin around the metal to olefin bond, might be relevant not only in determining

the asymmetric induction in *cis*-butene but also in determining the isomeric composition of the hydroformylation products.

It is probable that at least some of the above concepts developed for the rhodium catalysts are applicable also to cobalt-catalyzed hydroformylation.

Acknowledgment

The authors are grateful to A. Stefani, J. Halpern, and H. B. Kagan for reading and commenting on the manuscript.

Literature Cited

1. Botteghi, C., Consiglio, G., Pino, P., *Chimia* (1972) **26**, 141.
2. Tanaka, M., Watanabe, Y., Mitsudo, T., Yamamoto, K., Takegami, Y., *Chem. Lett.* (1972) 483.
3. Ogata, I., Ikeda, Y., *Chem. Lett.* (1972) 487.
4. Himmele, W., Siegel, H., Aquila, W., Müller, F. J., *Ger. Offen.* (1973) 2132, 414; *Chem. Abstr.* (1973) **78**, 97328.
5. Pino, P., Botteghi, C., Consiglio, G., Pucci, S., Proc. Chem. Hydroformylation Rel. React., Veszprém, Hungary, May-June 1972.
6. Salomon, C., Consiglio, G., Botteghi, C., Pino, P., *Chimia* (1973) **27**, 215.
7. Consiglio, G., Botteghi, C., Salomon, C., Pino, P., *Angew. Chem.* (1973) **85**, 663.
8. McKenzie, A., Luis, E. M., Mitchell, A. G., *Chem. Ber.* (1932) **65**, 798.
9. Botteghi, C., Consiglio, G., Pino, P., *Ann. Chem.*, in press.
10. Orchin, M., Rupilius, W., *Cat. Revs.* (1972) **6**, 85.
11. Stefani, A., Botteghi, C., Consiglio, G., unpublished data.
12. Pino, P., Salomon, C., Botteghi, C., Consiglio, G., *Chimia* (1972) **26**, 655.
13. Carlini, C., Politi, D., Ciardelli, F., *Chem. Commun.* (1970) 1260.
14. Lai, R., Ucciani, E., *C.R. Acad. Sci. Ser. C* (1971) **273**, 1368.
15. Nagy-Magos, Z., Bor, G., Markó, L., *J. Organometal. Chem.* (1968) **14**, 205.
16. Morrison, J. D., Mosher, H. S., "Asymmetric Organic Reactions," Prentice-Hall, Englewood Cliffs, 1971.
17. Pino, P., *Advan. Polym. Sci.* (1965) **4**, 393.
18. Stern, R., Hirschauer, A., Sajus, L., *Tetrahedron Lett.* (1973) 3247.
19. Lardicci, L., Botteghi, C., Benedetti, E., *J. Org. Chem.* (1966) **31**, 1534.
20. Clark, D. R., Mosher, H. S., *J. Org. Chem.* (1970) **35**, 1114.
21. Overberger, C. G., Tanner, D., *J. Amer. Chem. Soc.* (1955) **77**, 369.
22. Natta, G., Ercoli, R., *Chim. Ind. Milan* (1952) **34**, 503.
23. Kagan, H. B., Dang, T. P., *J. Amer. Chem. Soc.* (1972) **94**, 6429.
24. Evans, D., Yagupsky, G., Wilkinson, G., *J. Chem. Soc. A* (1968) 2660.
25. Rehder-Stirnweiss, W., private communication.
26. Pino, P., Pucci, S., Piacenti, F., Dell' Amico, G., *J. Chem. Soc. C* (1971) 1640.
27. Lardicci, L., Menicagli, R., Salvadori, P., *Gazz. Chim. Ital.* (1968) **98**, 738.
28. Mitsui, S., Imaizumi, S., *Nippon Kagaku Zasshi* (1965) **86**, 229; *Chem. Abstr.* (1965) **63**, 4134.
29. Greenwald, R., Chaykovsky, M., Corey, E. J., *J. Org. Chem.* (1963) **28**, 1128.
30. Botteghi, C., Consiglio, G., Pino, P., unpublished data.
31. Yamada, S., *Coord. Chem. Revs.* (1966) **1**, 415.

32. Abley, P., McQuillin, F. J., *J. Chem. Soc. C* (1971) 844.
33. Brunner, H., *Angew. Chem.* (1971) **83**, 274.
34. Stefani, A., Consiglio, G., Botteghi, C., Pino, P., *J. Amer. Chem. Soc.*, in press.
35. Hanson, K. R., *J. Amer. Chem. Soc.* (1966) **88**, 2731.
36. Evans, D., Osborn, J. A., Wilkinson, G., *J. Chem. Soc. A* (1968) 3133.
37. Heck, R. F., Breslow, D. S., *J. Amer. Chem. Soc.* (1961) **83**, 4023.
38. Brown, C. K., Wilkinson, G., *J. Chem. Soc. A* (1970) 2753.
39. Rupilius, W., Thesis, Technische Hochschule Aachen, 1969.
40. Paiaro, G., Panunzi, A., *J. Amer. Chem. Soc.* (1964) **86**, 5148.
41. Lazzaroni, R., Salvadori, P., Pino, P., *Chem. Commun.* (1970) 1164.

RECEIVED July 30, 1973.

INDEX

A	
Acetate	
-catalyzed reactions, palladium ..	50
catalyst system, bridged-	174
-catalyzed system	172
monomer, palladium	61
Acetic acid	34
Acetic acid, Pd(OAc ₂) system in ..	40
Acetophenone, effect of phosphine	
structure on the hydrogenation	
of	29
Acetoxypalladation	36
Acid chlorides, decarbonylation of	181
Acids, monocarboxy	156
Acidity of silica and alumina,	
surface	228
Active complexes, shift in the equi-	
librium between the catalyti-	
cally	138
Activation, entropies of	184
Acyl-alkyl rearrangements	189
α -acylamidocinnamic acids	276
Addition	
of alkyl chlorides to palla-	
dium(0), oxidative	101
Markovnikov	95
oxidative	97
reactions, halides used in	99
reaction, oxidative	268
Aldehydes, decarbonylation of	
chiral	185
Aldehydes, straight chain	20
Alkenylbenzenes, hydroformylation	
of	5
Alkyl	
intermediate	141
phosphines as ligands, tertiary ..	28
rearrangements, acyl-	189
-cobalt carbonyls	288
-rhodiumcarbonyl stability	12
Allyl propionate exchange	44
Alumina, surface acidity of silica	
and	228
Amine	
basicity on product distribution,	
effect of	243
carbonylation catalyzed by	
ruthenium complexes	166
complexes, hydroformylation	
with rhodium	240
on the hydroformylation of	
1-hexene, effect of	243
α -Amino acids by asymmetric	
hydrogenation	274
Aqueous solution, extraction	
catalyst from	21
Asymmetric	
induction	31, 298
hydroformylation	295
hydroformylation, general aspects	
of	310
Autoxidation of olefin	66
B	
Basicity on product distribution,	
effect of amine	243
Benzoquinone, oxidation by	58
Bridged-acetate catalyst system ..	174
<i>tert</i> -Butyl hydroperoxide, reactions	
of	70
C	
Carboalkoxylation	145
Carbon monoxide insertion	103
Carbon sigma-bonded complexes,	
palladium-	90
Carbonylation	92, 145
catalyzed by ruthenium	
complexes, amine	166
of cyclic olefins	97
Carbonyls, alkylcobalt	288
Catalyst(s)	
cobalt	295
formation, IR studies of	197
group VIII metals as	252
homogeneous hydrogenation ..	111
hydrogenation	125
Kagan	276
linoleate and conjugated linoleate	
palladium phosphine	159
olefin disproportionation	192
pre-formed homogeneous	23
rhodium chiral	295
ruthenium	167
supported organometallic	212
system, bridged-acetate	174
Wilkinson	121
Catalytic	
behavior of group VIa metals ..	208
cyanation	268
oxidation of	
3,3-dimethyl-1-butene	50
<i>cis</i> -2-hexene	50

Catalytic oxidation of (<i>Continued</i>)			
1-hexene	50		
process	91		
Catalyzed			
decarbonylations, rhodium-	181		
by hydridotetrakis(triphenylphosphine)rhodium(I), hydrogenation of hexene ..	134		
by ruthenium complexes, amine carbonylation	166		
system, acetate-	172		
Chiral aldehydes, decarbonylation of	185		
Chirality, loss of	185		
Chlorides to palladium(0), oxidative addition of alkyl	101		
Chloropalladation	37		
Chlororhodium complexes, triarylphosphine	116		
Complex(es)			
amine carbonylation catalyzed by ruthenium	166		
concentration, rate of hydrogenation as a function of	136		
hydroformylation with rhodium-amine	240		
hydrogenation catalyzed by transition metal	133		
molybdenum nitrosyl	195		
oxidized rhodium	111		
oxo	203		
oxotritruthenium cluster	174		
palladium-carbon sigma-bonded rhodium	90		
ruthenium	124		
shift in the equilibrium between the catalytically active ... transition metal	202		
transition metal	138		
triarylphosphine chlororhodium	64		
π -Complex formation, olefin	116		
π -Complex formation, olefin	42		
Compounds			
metal hydrocarbyl	215		
with support surfaces, reaction of metal hydrocarbyl	222		
water sensitive	213		
CO by PPh_3 , substituting	144		
Cobalt catalysts	295		
Cobalt catalyzed asymmetric hydroformylation	297		
Cobaltcarbonyls	1		
Concentration, dependence on olefin	139		
Cyanation			
of aromatic halides, nickel-catalyzed	252		
catalytic	268		
influence of solvent on	261		
reaction, stoichiometric	265		
Cycles, parallel hydrogenation ...	141		
Cyclic olefins, carbonylation of ...	97		
Cyclohexene, oxidation of	74		
Cyclohexene in the presence of cyclopentadienylmetalcarbonyl complexes, oxidation of	76		
D			
Decarbonylation			
of acid chlorides	181		
of chiral aldehydes	185		
rhodium catalyzed	181		
Decobaltation	25		
Diastereo, threo and erythro	15		
3,3-Dimethyl-1-butene, catalytic oxidation of	50		
Dioxygen ligand	115		
Diphenyl(<i>p</i> -dimethylaminophenyl)phosphine	125		
Disproportionation of 1-hexene, heterogeneously catalyzed ...	236		
Disproportionation catalysts, olefin	192		
Distribution, isomer	24		
(DMBA), <i>N,N</i> -dimethylbenzylamine	241		
E			
Elimination, β -hydride	188		
Entropies of activation	184		
Equilibrium between the catalytically active complexes, shift in the	138		
Erythro diastereoisomers, threo and	15		
ESR studies of surface species ...	231		
Ester(s)			
exchange, vinyl	43		
hydroformylation of α,β -unsaturated	2		
substituted succinic	93		
Ethylene, polymerization of	226		
Ethylene in toluene, homogeneous polymerization of	226		
Exchange			
allyl propionate	44		
reactions, palladium	102		
vinyl ester	43		
Extraction catalyst from aqueous solution	20		
F			
Free radical reactions, quinol as inhibitor of	52		
G			
Group VIII metals as catalysts	252		
H			
Halides used in addition reactions	99		
Hammett plots	183		
Hexene catalyzed by hydridotetrakis(triphenylphosphine)rhodium(I), hydrogenation of ..	134		

<i>cis</i> -2-Hexene, catalytic oxidation of	50
1-Hexene	
catalytic oxidation of	50
effect of amine on the hydroformylation of	243
heterogeneously catalyzed disproportionation of	236
oxidation of	52
Heterogeneously catalyzed disproportionation of 1-hexene	236
Homogeneous	
catalyst, pre-formed	23
hydrogenation	124
hydrogenation catalyst	111
polymerization of ethylene in toluene	226
HRh(PPh ₃) ₄	134
[HRu(CO) ₃] _n	167
β-hydride elimination	188
Hydride shifts, metal-assisted	178
Hydridopalladium species	59
Hydridotetrakis(triphenylphosphine)rhodium(I), hydrogenation of hexene catalyzed by	134
Hydrocarboxylation	145
Hydrocarbyl compounds with support surfaces, reaction of metal	222
Hydroformylation	
of alkenylbenzenes	5
asymmetric	295
cobalt catalyzed asymmetric	297
general aspects of asymmetric	310
of 1-hexene, effect of amine on the	243
of linear α-olefins	283
mechanism	215
of methyl crotonate	3
of methyl 3,3-dimethacrylate	3
of optically active olefins	283
reaction, stereospecificity in the with rhodium-amine complexes	14
rhodium catalyzed	240
of α,β-unsaturated esters	17
of 2	2
Hydrogenation	
of acetophenone, effect of phosphine structure on the	29
α-amino acids by asymmetric	274
catalysts	125
catalysts, homogeneous	111
catalyzed by transition metal complexes	133
cycles, parallel	141
effect of ligand-rhodium ratio	129
as a function of complex concentration, rate of	136
of hexene catalyzed by hydrotetrakis(triphenylphosphine)rhodium(I)	134
homogeneous	124
Hydroperoxide, reactions of <i>tert</i> -butyl	70
Hydroxyl content of silica, surface	222

I

Induction, asymmetric	31, 298
Initiator, radical	67
Insertion, carbon monoxide	103
Intermediate, alkyl	141
Investigations, kinetic	134
IR studies of catalyst formation	197
Isomer distribution	24
Isomerization	139
during oxidation, selectivity in	52

K

Kagan catalyst	276
Kinetic investigations	134
Kinetic isotope effect	141

L

Ligand(s)	
dioxygen	115
effects	200
tertiary alkyl phosphines as	28
-rhodium ratio on hydrogenation, effect of	129
Linoleate and conjugated linoleate palladium phosphine catalysts	158
Loss of chirality	185

M

Markovnikov addition	95
Material balance in oxidation	53
Metal	
-assisted hydride shifts	178
complexes, hydrogenation catalyzed by transition	133
complexes, transition	64
hydrocarbyl compounds	215
hydrocarbyl compounds with support surfaces, reaction of	222
Methoxypalladation	92
Methyl	
crotonate, hydroformylation of	3
3,3-dimethacrylate, hydroformylation of	3
linoleate, products from	149
linolenate, products from	154
linoleate, products from conjugated	153
Mislow intermediate	274
Molybdenum nitrosyl complexes	195
Monocarboxy acids	156
Monomer, palladium acetate	61

N

Nickel-catalyzed cyanation of aromatic halides	252
Nitrosyl complexes, molybdenum	195

O	
Olefin(s)	
autoxidation of	66
carbonylation of cyclic	97
π complex formation	42
concentration, dependence on	139
disproportionation catalysts	192
hydroformylation of optically active	283
oxidation of	44, 64
Organometallic catalysts, supported	212
Oxidation	39
by benzoquinone	58
olefin	44
PdCl ₂ -CuCl ₂ combined	47
material balance in	53
of	
cyclohexene	74
1-hexene	52
1-hexene, catalytic	50
olefins	64
styrene	82
tetramethylethylene	66
TME	85
Oxidative addition	97
of alkyl chlorides to palladium(0) reaction	101, 268
Oxidized rhodium complexes	111
Oxo complexes	203
Oxotriruthenium cluster complex	174
Oxypalladation	59
P	
Palladium	
acetate monomer	61
acetate, purification of	62
-(II) acetate trimer	41
acetate-catalyzed reactions	50
-carbon sigma-bonded complexes	90
-(II) chloride	34
-chloride-triphenylphosphine complex catalyst	145
exchange reactions	102
hydride, reversible elimination of oxidative addition of alkyl chlorides to	59, 101
phosphine catalysts, linoleate and conjugated linoleate	159
Parallel hydrogenation cycles	141
PdCl ₂ -CuCl ₂ combined oxidation	47
Pd(OAc) ₂ system in acetic acid	40
Phenylbis(<i>p</i> -dimethylaminophenyl) phosphine	126
Phosphine(s)	
catalysts, linoleate and conjugated linoleate palladium	159
as ligands, tertiary alkyl	28
structure on the hydrogenation of acetophenone, effect of	29
Polymerization of ethylene	226
PPh ₃ , substituting CO by	144
Pre-formed homogeneous catalyst	23
Process, catalytic	91
Propionate exchange, allyl	44
Q	
Quartz reactor	199
Quaternary alkylcobalt complex	299
Quinol as inhibitor of free radical reactions	52
R	
Rate of hydrogenation as a function of complex concentration	136
Reaction(s)	
halides used in addition	99
palladium acetate-catalyzed	50
of metal hydrocarbyl compounds with support surfaces	222
palladium exchange	102
Reactor, quartz	199
Rearrangements, acyl-alkyl	189
Reversible elimination of palladium hydride	59
Rhodium	
-amine complexes, hydroformylation with	240
catalyzed decarbonylations	181
catalyzed hydroformylation	17
complexes	124
oxidized	111
chiral catalysts	295
ratio on hydrogenation, effect of ligand-	129
Rhodiumcarbonyls	1
Ruthenium	
catalysts	167
complexes	202
amine carbonylation catalyzed by	166
[Ru(CO) ₂ (OCOCH ₃) ₂] _n	167
S	
Selectivity	139
in isomerization during oxidation	52
Shift in the equilibrium between the catalytically active complexes	138
Shifts, metal-assisted hydride	178
Sigma-bonded complexes, palladium-carbon	90
Silica and alumina, surface acidity of	228
Silica, surface hydroxyl content of	222
Solution, extraction catalyst from aqueous	21
Solvent on cyanation, influence of	261
Stereospecificity in the hydroformylation reaction	14
Stoichiometric cyanation reaction	265
Straight chain aldehydes	20

Styrene, oxidation of	82	Triarylphosphine chlororhodium complexes	116
Succinic esters, substituted	93	Trimer, palladium(II) acetate . . .	41
Support surfaces, reaction of metal hydrocarbyl compounds with	222	Tris(<i>p</i> -dimethylaminophenyl)-phosphine	125
Supported organometallic catalysts	212	Tris(triphenylphosphine)rhodium(I) chloride	124
Surface			
acidity of silica and alumina . .	228		
hydroxyl content of silica	222		
species, ESR studies of	231		
		U	
		Unsymmetrical π -allyl complex intermediate	146
T			
(TBM), 4- <i>tert</i> -butylmethylene-cyclohexene	113	V	
Temperature, rate constant independent of	136	Vanadylacetylacetonate	73
Tertiary alkyl phosphines as ligands	28	Vinyl ester exchange	43
Tetramethylethylene oxidation of . .	66	Vinyl acetates by oxidation, formation of	52
Threo and erythro diastereoisomers	15	Vinylidene olefins	296
TME, oxidation of	85		
Toluene, homogeneous polymerization of ethylene in	226	W	
Transition metal complexes	64	Water sensitive compound	213
hydrogenation catalyzed by	133	Wilkinson catalyst	121